Table of Contents (Continued)

2.6.5 Vibration 2.6-23
2.6.6 Water Spray 2.6-25
2.6.7 Free Drop (1-Foot): Cask Body Analysis 2.6-26
2.6.7.1 One-Foot End Drop 2.6-27
2.6.7.2 One-Foot Side Drop 2.6-40
2.6.7.3 One-Foot Corner Drop 2.6-47
2.6.7.4 One-Foot Oblique Drop 2.6-60
2.6.7.5 Impact Limiters 2.6-61
2.6.7.6 Closure Analysis 2.6-85
2.6.7.7 Neutron Shield Analysis 2.6-90
2.6.7.8 Upper Ring/Outer Shell Intersection Analysis 2.6-102
2.6.8 Corner Drop 2.6-106
2.6.9 Compression 2.6-106
2.6.10 Penetration 2.6-106
2.6.11 Fabrication Stresses 2.6-107
2.6.11.1 Lead Pour 2.6-108
2.6.11.2 Cooldown 2.6-109
2.6.11.3 Lead Creep 2.6-113
2.6.12 PWR Transportable Storage Canister Analysis - Normal Conditions of Transport 2.6-117
2.6.12.1 Analysis Description 2.6-117
2.6.12.2 Finite Element Model Description - PWR Canister 2.6-120
2.6.12.3 Thermal Expansion and Thermal Stresses Evaluation of Canister for PWR Fuel 2.6-129
2.6.12.4 Stress Evaluation of PWR Canister for 1-Foot End-Drop Load Condition 2.6-135
2.6.12.5 Stress Evaluation of PWR Canister for Combined Thermal and 1-Foot End Drop Load Condition 2.6-143
2.6.12.6 Stress Evaluation of PWR Canister for 1-Foot Side Drop Load Condition 2.6-149
2.6.12.7 Stress Evaluation of PWR Canister for Combined Thermal and 1-Foot Side Drop Load Condition 2.6-154

Table of Contents (Continued)

2.6.12.8 Stress Evaluation of PWR Canister for 1-Foot Corner Drop Load Condition 2.6-158
2.6.12.9 Stress Evaluation of PWR Canister for Combined Thermal and 1-Foot Corner Drop Load Conditions 2.6-164
2.6.12.10 Shear Stresses for 1-Foot Drops 2.6-170
2.6.12.11 Canister Bearing Stresses for 1-Foot Side Drop 2.6-170
2.6.12.12 Canister Buckling Evaluation for 1-Foot End Drop 2.6-172
2.6.13 PWR Basket Analysis - Normal Conditions of Transport 2.6-176
2.6.13.1 Analysis Description 2.6-180
2.6.13.2 Finite Element Model Description - PWR Basket 2.6-180
2.6.13.3 Thermal Conditions and Expansion Evaluation for PWR Support Disks 2.6-192
2.6.13.4 Stress Evaluation of PWR Support Disks for 1-Foot End-Drop Load Condition 2.6-193
2.6.13.5 Stress Evaluation of PWR Support Disks for Combined Thermal and 1-Foot End Drop Conditions 2.6-197
2.6.13.6 Stress Evaluation of PWR Support Disk for 1-Foot Side-Drop Load Conditions 2.6-200
2.6.13.7 Stress Evaluation of PWR Support Disk for Combined Thermal and 1-Foot Side-Drop Load Condition 2.6-223
2.6.13.8 Stress Evaluation of PWR Support Disk for 1-Foot Off-Angle Load Conditions 2.6-228
2.6.13.9 Stress Evaluation of Support Disk for Combined Thermal and 1-Foot Off-Angle Conditions 2.6-228
2.6.13.10 Stress Evaluation of Tie Rods and Spacers for 1-Foot End-Drop Load Condition 2.6-229
2.6.13.11 Support Disk Shear Stresses for 1-Foot Drops 2.6-230
2.6.13.12 Bearing Stress - Basket Contact with Canister Shell 2.6-231
2.6.13.13 Basket Weldment Analysis for 1-Foot End-Drop 2.6-231
2.6.13.14 Support Disk Buckling Evaluation 2.6-236

Table of Contents (Continued)

2.6.14 BWR Transportable Storage Canister Analysis - Normal Conditions of Transport 2.6-242
2.6.14.1 Analysis Description 2.6-245
2.6.14.2 Finite Element Model Description - BWR Canister 2.6-245
2.6.14.3 Thermal Expansion and Thermal Stress Evaluation of Canister for BWR Fuel 2.6-254
2.6.14.4 Stress Evaluation of BWR Canister for 1-Foot End-Drop Load Condition 2.6-259
2.6.14.5 Stress Evaluation of BWR Canister for Combined Thermal and 1-Foot End-Drop Load Condition 2.6-267
2.6.14.6 Stress Evaluation of the BWR Canister for 1-Foot Side-Drop Load Condition 2.6-273
2.6.14.7 Stress Evaluation of BWR Canister for Combined Thermal and 1-Foot Side-Drop Load Conditions 2.6-278
2.6.14.8 Stress Evaluation of BWR Canister for 1-Foot Corner-Drop Load Condition 2.6-282
2.6.14.9 Stress Evaluation of BWR Canister for Combined Thermal and 1-Foot Corner-Drop Load Conditions 2.6-288
2.6.14.10 Shear Stresses for 1-Foot Drops 2.6-294
2.6.14.11 Canister Bearing Stresses for 1-Foot Side-Drop 2.6-294
2.6.14.12 Canister Buckling Evaluation for 1-Foot End-Drop 2.6-294
2.6.15 BWR Basket Analysis - Normal Conditions of Transport 2.6-298
2.6.15.1 Analysis Description 2.6-303
2.6.15.2 Finite Element Model Description - BWR Basket 2.6-303
2.6.15.3 Thermal Condition and Expansion Evaluation of BWR Support-Disks 2.6-307
2.6.15.4 Stress Evaluation of BWR Support Disk for 1-Foot End-Drop Load Condition 2.6-308
2.6.15.5 Stress Evaluation of BWR Support Disk for Combined Thermal and 1-Foot End Drop Load Conditions 2.6-312

Table of Contents (Continued)

2.6.15.6 Stress Evaluation of BWR Support Disk for 1-Foot Side-Drop Load Condition 2.6-315
2.6.15.7 Stress Evaluation of BWR Support Disk for Combined Thermal and 1-Foot Side-Drop Load Conditions 2.6-356
2.6.15.8 Stress Evaluation of BWR Support Disk for 1-Foot Corner-Drop Load Conditions 2.6-362
2.6.15.9 Stress Evaluation of BWR Support Disk for Combined Thermal and 1-Foot Corner-Drop Load Conditions 2.6-362
2.6.15.10 Stress Evaluation of Tie Rods and Spacers for 1-Foot End-Drop Load Condition 2.6-362
2.6.15.11 Support Disk Shear Stresses for 1-Foot Drops 2.6-363
2.6.15.12 Bearing Stress - Basket Contact with Inner Shell 2.6-363
2.6.15.13 Basket Weldment Analysis for 1-Foot End-Drop 2.6-364
2.6.15.14 Support Disk Buckling Evaluation 2.6-368
2.6.16 Universal Transport Cask Cavity Spacers 2.6-377
2.6.16.1 PWR Cask Cavity Spacers 2.6-377
2.6.16.2 BWR Cask Cavity Spacers 2.6-381

2.7 Hypothetical Accident Conditions 2.7-1
2.7.1 Free Drop (30 ft) - Cask Body Analysis 2.7-1
2.7.1.1 30-Foot End Drop 2.7-3
2.7.1.2 30-Foot Side Drop 2.7-11
2.7.1.3 30-Foot Corner Drop 2.7-15
2.7.1.4 30-Foot Oblique Drop 2.7-22
2.7.1.5 Lead Slump Resulting from a Cask Drop Accident 2.7-29
2.7.1.6 Impact Limiter Analysis - Hypothetical Accident Conditions 2.7-30
2.7.1.7 Closure Analysis 2.7-33
2.7.2 Puncture 2.7-40
2.7.2.1 Puncture - Cask Side Midpoint 2.7-41
2.7.2.2 Puncture - Lid Center 2.7-48
2.7.2.3 Puncture - Center of Cask Bottom 2.7-52
2.7.2.4 Puncture - Port Cover 2.7-60

Table of Contents (Continued)

2.7.2.5 Puncture Accident - Shielding Consequences 2.7-61
2.7.3 Thermal 2.7-62
2.7.3.1 Summary of Pressures and Temperatures 2.7-62
2.7.3.2 Differential Thermal Expansion Stress 2-7-62
2.7.4 Crush 2.7-66
2.7.5 Immersion - Fissile Material 2.7-66
2.7.6 Immersion - All Packages 2.7-66
2.7.6.1 Membrane Stresses in Cask Outer Shell (away from ends) 2.7-69
2.7.6.2 Bending Stress in the Bottom Forging (at center) 2.7-69
2.7.6.3 Bending Stress in the Cask Lid (at center) 2.7-70
2.7.6.4 Bending Stress in the Cask Bottom (at center) 2.7-70
2.7.6.5 Bending Stress in the Port Cover Plate (at center) 2.7-71
2.7.7 PWR Transportable Storage Canister Analysis - Accident Conditions 2.7-73
2.7.7.1 Analysis Description 2.7-74
2.7.7.2 Analysis Results - PWR Canister 2.7-74
2.7.7.3 Canister Buckling Evaluation for 30-Foot End Drop 2.7-88
2.7.8 PWR Basket Analysis - Accident Conditions 2.7-91
2.7.8.1 Stress Evaluation of Support Disk 2.7-91
2.7.8.2 Stress Evaluation of Tie Rods and Spacers 2.7-116
2.7.8.3 Buckling Evaluation of Support Disk 2.7-119
2.7.8.4 Fuel Tube Analysis 2.7-125
2.7.8.5 Basket Weldment Analysis for 30-Foot End Drop 2.7-132
2.7.9 BWR Transportable Storage Canister Analysis - Accident Conditions 2.7-136
2.7.9.1 Analysis Description 2.7-137
2.7.9.2 Analysis Results - BWR Canister 2.7-137
2.7.9.3 Canister Buckling Evaluation for 30-Foot End Drop 2.7-151
2.7.10 BWR Basket Analysis - Accident Conditions 2.7-153
2.7.10.1 Stress Evaluation of Support Disk 2.7-154
2.7.10.2 Stress Evaluation of Tie Rods and Spacers 2.7-181
2.7.10.3 Buckling Evaluation of Support Disk 2.7-183
2.7.10.4 Fuel Tube Analysis 2.7-189
2.7.10.5 Basket Weldment Analysis for 30-Foot End-Drop 2.7-194

Table of Contents (Continued)

2.7.11 Summary of Damage to Cask Due to Hypothetical Accident Conditions .. 2.7-198
2.7.12 Cask Inner Shell Buckling Analysis 2.7-201
2.7.12.1 Analysis Methodology 2.7-201
2.7.12.2 Analysis Results 2.7-202
2.7.12.3 Detailed Code Case N-284-1 Buckling Evaluation 2.7-202

2.8 Special Form 2.8-1

2.9 Fuel Rods 2.9-1
2.9.1 PWR Fuel Rod Buckling Assessment 2.9-1
2.9.1.1 Overview of Analysis Methodology 2.9-1
2.9.1.2 Fuel Rod Mode Shapes and Buckling Evaluation 2.9-3
2.9.2 BWR Fuel Rod Buckling Assessment 2.9-4

2.10 Appendices 2.10-1
2.10.1 Computer Program Descriptions 2.10.1-1
2.10.1.1 ANSYS 2.10.1-1
2.10.1.2 LS-DYNA 2.10.1-2
2.10.2 Finite Element Model - Universal Transport Cask 2.10.2-1
2.10.2.1 Load Application and Boundary Conditions 2.10.2-5
2.10.2.2 Post-Processing of Results 2.10.2-13
2.10.3 Confirmatory Testing Program – UMS® Impact Limiters and Attachments 2.10.3-1
2.10.3.1 Confirmatory Testing Program Results Summary 2.10.3-1
2.10.3.2 Acceptance Criteria for Model Performance 2.10.3-3
2.10.3.3 30-Foot Top End Drop and 30-Foot Top Corner Drop Tests Performed at ORNL 2.10.3-4
2.10.3.4 30-Foot Side Drop Test Performed at SNL 2.10.3-19
2.10.3.5 Evaluation of the 30-Foot Oblique Drop 2.10.3-26
2.10.3.6 Scale Model Drawings 2.10.3-26
2.10.3.7 LS-DYNA Analyses of the UMS® Quarter-Scale Model 2.10.3-27

Table of Contents (Continued)

2.10.4 Dynamic Load Factor (DLF) Evaluation for PWR and BWR Support Disks 2.10.4-1
2.10.4.1 1-Foot End Drop Analysis 2.10.4-1
2.10.4.2 Side Drop Analysis 2.10.4-7

2.11 Site Specific Contents Structural Evaluations 2.11-1
2.11.1 Site Specific Spent Fuel 2.11-1
2.11.1.1 Maine Yankee Site Specific Spent Fuel 2.11.1-1
2.11.2 Site Specific Greater Than Class C Waste 2.11.2-1
2.11.2.1 Maine Yankee Greater Than Class C Waste 2.11.2-1

2.12 References 2.12-1

List of Figures

Figure 2.5.1.1-1 Primary Lifting Trunnion Geometry 2.5-27
Figure 2.5.1.1-2 Secondary Lifting Trunnion Geometry 2.5-28
Figure 2.5.2.1-1 Front Support and Tiedown Geometry 2.5-37
Figure 2.5.2.1-2 Shear Ring Geometry 2.5-38
Figure 2.5.2.1-3 Free-Body Diagram of Cask Subjected to Lateral Load 2.5-39
Figure 2.6.7.5-1 Universal Transport Cask with Impact Limiters 2.6-73
Figure 2.6.7.5-2 Cross-Section of Lower Impact Limiter 2.6-74
Figure 2.6.7.5-3 LS-DYNA Finite Element Model 2.6-75
Figure 2.6.7.5-4 Impact Limiter Shell LS-DYNA Finite Element Model 2.6-76
Figure 2.6.7.5-5 Acceleration Time History for the Cold Condition 30-Foot Top End Drop 2.6-77
Figure 2.6.7.5-6 Acceleration Time History for the Cold Condition 30-Foot Top Corner Drop 2.6-78
Figure 2.6.7.5-7 Acceleration Time History for the Cold Condition 30-Foot Side Drop 2.6-79
Figure 2.6.7.5-8 Impact Limiter Attachment Geometry 2.6-80
Figure 2.6.7.7-1 Neutron Shield Geometry 2.6-93
Figure 2.6.12-1 PWR Transportable Storage Canister 2.6-118
Figure 2.6.12-2 PWR Transportable Storage Canister Shell and Lids 2.6-119
Figure 2.6.12.2-1 PWR Canister Assembly Finite Element Model 2.6-124
Figure 2.6.12.2-2 Canister Structural and Shield Lid Finite Element Mesh 2.6-125
Figure 2.6.12.2-3 Structural and Shield Lid Weld Regions Finite Element Mesh 2.6-126
Figure 2.6.12.2-4 Canister Bottom Plate Finite Element Mesh 2.6-127
Figure 2.6.12.3-1 Identification of Sections for Evaluating Linearized Stresses in Canister 2.6-132
Figure 2.6.13-1 PWR Fuel Assembly Basket 2.6-177
Figure 2.6.13-2 Support Disk Cross Section Configuration 2.6-178
Figure 2.6.13-3 PWR Fuel Tube Configuration 2.6-179
Figure 2.6.13.2-1 PWR Basket Model for Side-Drop 2.6-185
Figure 2.6.13.2-2 Side Drop Orientation 2.6-186

List of Figures (Continued)

Figure 2.6.13.2-3 Location of the Section to Obtain Linearized Stresses (Left half of support disk) 2.6-187
Figure 2.6.13.2-4 Location of the Section to Obtain Linearized Stresses (Right half of support disk) 2.6-188
Figure 2.6.13.4-1 Locations of Maximum P_m+P_b Stresses —1-Foot End Drop, Thermal Case A 2.6-194
Figure 2.6.13.5-1 Locations of Maximum P+Q Stresses —1-Foot End Drop, Thermal Case A 2.6-198
Figure 2.6.13.6-1 Support Disk Side-Drop Orientations 2.6-202
Figure 2.6.13.6-2 Locations of Maximum P_m+P_b Intensities—0° Side Drop Orientation, Thermal Case A 2.6-203
Figure 2.6.13.6-3 Locations of Maximum P_m+P_b Stresses—18.22° Side Drop Orientation, Thermal Case A 2.6-204
Figure 2.6.13.6-4 Locations of Maximum P_m+P_b Stresses—26.28° Side Drop Orientation, Thermal Case A 2.6-205
Figure 2.6.13.6-5 Locations of Maximum P_m+P_b Stresses —45° Side Drop Orientation, Thermal Case A 2.6-206

Figure 2.6.13.13-1 Finite Element Model of the Top Weldment Plate 2.6-233
Figure 2.6.13.13-2 Finite Element Model of the Bottom Weldment Plate 2.6-234
Figure 2.6.14-1 BWR Transportable Storage Canister 2.6-243
Figure 2.6.14-2 BWR Transportable Storage Canister Shell and Lids 2.6-244
Figure 2.6.14.2-1 BWR Canister Assembly Finite Element Mesh (with 45° Basket orientation) 2.6-249
Figure 2.6.14.2-2 Canister Structural and Shield Lid Finite Element Mesh 2.6-250
Figure 2.6.14.2-3 Structural and Shield Lid Weld Regions Finite Element Mesh 2.6-251
Figure 2.6.14.2-4 Canister Bottom Plate Finite Element Mesh 2.6-252
Figure 2.6.14.3-1 Identification of the Sections for Evaluating the Linearized Stresses in the Canister 2.6-256

List of Figures (Continued)

Figure 2.6.15-1 BWR Fuel Assembly Basket 2.6-300
Figure 2.6.15-2 Support Disk Cross Section Configuration 2.6-301
Figure 2.6.15-3 BWR Fuel Tube Configuration 2.6-302
Figure 2.6.15.2-1 ANSYS Model of BWR Basket for Side-Drop 2.6-305
Figure 2.6.15.2-2 Close-up of the Ligaments and the Interface with the Canister Shell and the Cask Inner Shell 2.6-306
Figure 2.6.15.4-1 Locations of Maximum Primary Nodal Stress Intensities for 1-Foot End-Drop 2.6-309
Figure 2.6.15.5-1 Locations of Maximum Primary and Secondary Nodal Stress Intensities for 1-Foot End-Drop 2.6-313
Figure 2.6.15.6-1 Support Disk Side-Drop Orientations 2.6-318
Figure 2.6.15.6-2 Locations of the Sections Used to Obtain Linearized Stresses for the Support Disk for the 1st Quadrant (X>0,Y>0) 2.6-319
Figure 2.6.15.6-3 Locations of the Sections Used to Obtain Linearized Stresses for the Support Disk for the 2nd Quadrant (X<0,Y<0) 2.6-320
Figure 2.6.15.6-4 Locations of the Sections Used to Obtain Linearized Stresses for the Support Disk for the 3rd Quadrant (X<0,Y<0) 2.6-321
Figure 2.6.15.6-5 Locations of the Sections Used to Obtain Linearized Stresses for the Support Disk for the 4th Quadrant (X>0,Y<0) 2.6-322
Figure 2.6.15.6-6 Locations of Maximum Linearized Stress Intensities - 0° Drop Orientation 2.6-323
Figure 2.6.15.6-7 Locations of Maximum Linearized Stress Intensities - 31.82° Drop Orientation 2.6-324
Figure 2.6.15.6-8 Locations of Maximum Linearized Stress Intensities - 49.46° Drop Orientation 2.6-325
Figure 2.6.15.6-9 Locations of Maximum Linearized Stress Intensities - 77.92° Drop Orientation 2.6-326
Figure 2.6.15.6-10 Locations of Maximum Linearized Stress Intensities - 90° Drop Orientation 2.6-327

List of Figures (Continued)

Figure 2.6.15.13-1 Finite Element Model of the Top Weldment Plate 2.6-365
Figure 2.6.15.13-2 Finite Element Model of the Bottom Weldment Plate 2.6-366
Figure 2.7.1.5-1 Radial Lead Slump Model 2.7-31
Figure 2.7.2.1-1 Cask Body Model for Puncture Analysis 2.7-44
Figure 2.7.2.1-2 Location of Sections for Evaluation 2.7-45
Figure 2.7.2.2-1 ANSYS Model for Cask Lid 2.7-51
Figure 2.7.2.3-1 Bottom Puncture Finite Element Model and Boundary Conditions 2.7-56
Figure 2.7.2.3-2 Location of Sections for Evaluation 2.7-57
Figure 2.7.6-1 Cross Section of Cask Body 2.7-72
Figure 2.7.7.2-1 Identification of the Sections for Evaluating the Linearized Stresses in the PWR Canister 2.7-76
Figure 2.7.9.2-1 Identification of Sections for Evaluating Linearized Stresses in BWR Canister 2.7-139

Figure 2.9-1 Typical Fuel Rod Finite Element Model and Boundary Conditions 2.9-5
Figure 2.9-2 Typical First Lateral Mode Shape Plot for Fuel Rod 2.9-6
Figure 2.9-3 Typical First Buckling Mode Shape for Fuel Rod 2.9-7
Figure 2.10.2-1 Primary Components of the Universal Transport Cask 2.10.2-3
Figure 2.10.2-2 Universal Transport Cask 3-D Model 2.10.2-4
Figure 2.10.2.1-1 Cask Body Loading for Side-Drop Conditions 2.10.2-11
Figure 2.10.2.1-2 View of Cask Model Showing Pressure Distribution for Side-Drop Analysis 2.10.2-12
Figure 2.10.2.2-1 Lower Cask Body Section Locations 2.10.2-14
Figure 2.10.2.2-2 Sections Through Cask Body Ligaments 2.10.2-14
Figure 2.10.2.2-3 Cask Body Sections at Center 2.10.2-15
Figure 2.10.2.2-4 Cask Body Sections in Upper Cask 2.10.2-15
Figure 2.10.3-1 Typical Filtered Acceleration Time History for the Quarter- Scale Model Top End Drop, Overlayed with the Unfiltered Data 2.10.3-30

List of Figures (Continued)

Figure 2.10.3-2 Force-Deflection Curve for Static Test 1 (End Drop Orientation) for a 45° Section of the Quarter-Scale Model Upper Impact Limiter 2.10.3-31
Figure 2.10.3-3 Force-Deflection Curve for Static Test 2 (End Drop Orientation) for a 45° Section of the Quarter-Scale Model Upper Impact Limiter 2.10.3-32
Figure 2.10.3-4 Typical Filtered Acceleration Time History for the Quarter-Scale Model Top Corner Drop, Overlayed with the Unfiltered Data 2.10.3-33
Figure 2.10.3-5 UMS® Quarter-Scale Side Drop Accelerometer Locations 2.10.3-34
Figure 2.10.3-6 Typical Filtered Acceleration (Top Accelerometer) Time History for the Quarter-Scale Model Side Drop, Overlayed with the Unfiltered Data 2.10.3-35
Figure 2.10.3-7 Typical Filtered Acceleration (Bottom Accelerometer) Time History for the Quarter-Scale Model Side Drop, Overlayed with the Unfiltered Data 2.10.3-36
Figure 2.10.3-8 Comparison of Quarter-Scale Side Drop (LS-DYNA and Drop Test) Results (Upper Accelerometer) 2.10.3-37
Figure 2.10.3-9 Comparison of Quarter-Scale Side Drop (LS-DYNA and Drop Test) Results (Lower Accelerometer) 2.10.3-38
Figure 2.10.3-10 Quarter-Scale Side Drop Force-Displacement Curve 2.10.3-39
Figure 2.10.3-11 LS-DYNA Quarter-Scale Model 2.10.3-40
Figure 2.10.3-12 Comparison of Quarter-Scale Top End Drop (LS-DYNA and Drop Test) Results 2.10.3-41
Figure 2.10.3-13 Comparison of Quarter-Scale Top Corner Drop (LS-DYNA and Drop Test) Results 2.10.3-42
Figure 2.10.3-14 Comparison of Quarter-Scale Test Model and LS-DYNA Deformation During the Side Drop 2.10.3-43
Figure 2.10.4.1-1 ANSYS Finite Element Model of PWR Support Disk for End Drop Analysis 2.10.4-3
Figure 2.10.4.1-2 ANSYS Finite Element Model of BWR Support Disk for End Drop Analysis 2.10.4-3
Figure 2.10.4.1-3 1-Foot End-Drop Acceleration Time History 2.10.4-4
Figure 2.10.4.1-4 1-Foot End-Drop Frequency Response Spectrum 2.10.4-4

List of Figures (Continued)

Figure 2.10.4.2-1 ANSYS Finite Element Model of PWR Support Disk for Side Drop Analysis 2.10.4-9
Figure 2.10.4.2-2 ANSYS Finite Element Model of BWR Support Disk for Side Drop Analysis 2.10.4-9
Figure 2.10.4.2-3 LS-DYNA Finite Element Model for Side Drop Analysis 2.10.4-10
Figure 2.10.4.2-4 1-Foot Side-Drop Acceleration Time History 2.10.4-11
Figure 2.10.4.2-5 PWR Support Disk Acceleration Time History for 1-Foot Side-Drop 2.10.4-11
Figure 2.10.4.2-6 BWR Support Disk Acceleration Time History for 1-Foot Side-Drop 2.10.4-12
Figure 2.10.4.2-7 PWR Support Disk Frequency Response Spectrum for 1-Foot Side Drop 2.10.4-12
Figure 2.10.4.2-8 BWR Support Disk Frequency Response Spectrum for 1-Foot Side Drop 2.10.4-13
Figure 2.11.1.1-1 PWR Basket Drop Orientations and Case Study Loading Positions for Maine Yankee Consolidated Fuel 2.11.1-18
Figure 2.11.2.1-1 Maine Yankee GTCC Basket Finite Element Model 2.11.2-22
Figure 2.11.2.1-2 Maine Yankee GTCC Basket Finite Element Model Pressure Loading Locations 2.11.2-23
Figure 2.11.2.1-3 Maine Yankee GTCC Basket Finite Element Model Section Locations for Stress Evaluation 2.11.2-24
Figure 2.11.2.1-4 Finite Element Model for Maine Yankee GTCC Basket Support Wall 2.11.2-25
Figure 2.11.2.1-5 Finite Element Model for Maine Yankee GTCC Basket Separator Plate 2.11.2-26

List of Tables

Table 2.1.2-1 Exceptions to Codes and Standards 2.1-12
Table 2.1.2-2 Load Combinations: Normal and Hypothetical Accident Conditions 2.1-15
Table 2.1.2-3 Allowable Stress Limits for Containment Structures 2.1-16
Table 2.1.2-4 Allowable Stress Limits for Noncontainment Structures 2.1-17
Table 2.2-1 Calculated Weights and Centers of Gravity: Cask with Canister Containing PWR Fuel 2.2-2
Table 2.2-2 Calculated Weights and Centers of Gravity: Cask with Canister Containing BWR Fuel 2.2-3
Table 2.2-3 Calculated Weights and Centers of Gravity: Cask with Canister Containing Greater Than Class C (GTCC) Waste 2.2-4
Table 2.3.2-1 Mechanical Properties of SA-240, Type 304 Stainless Steel 2.3-4
Table 2.3.2-2 Mechanical Properties of SA-479, Type 304 Stainless Steel 2.3-5
Table 2.3.2-3 Mechanical Properties of SA-240, Type 304L Stainless Steel 2.3-6
Table 2.3.2-4 Mechanical Properties of SA-336, Type 304 Stainless Steel 2.3-7
Table 2.3.2-5 Mechanical Properties of Type XM-19 Stainless Steel 2.3-8
Table 2.3.3-1 Mechanical Properties of SA-564 and SA-693, Type 630, 17-4 PH Stainless Steel 2.3-10
Table 2.3.4-1 Mechanical Properties of SA-533, Type B, Class 2 Carbon Steel 2.3-12
Table 2.3.5-1 Mechanical Properties of SB-637, Grade N07718 Nickel Alloy Steel Bolting Material 2.3-14
Table 2.3.5-2 Mechanical Properties of SA-193, Grade B6, High Alloy Steel Bolting Material 2.3-15
Table 2.3.5-3 Mechanical Properties of SA-193, Grade B8S, High Alloy Steel Bolting Material 2.3-16
Table 2.3.6-1 Mechanical Properties of 6061-T651 Aluminum Alloy 2.3-18
Table 2.3.7-1 Static Mechanical Properties of Chemical Copper Lead 2.3-20
Table 2.3.7-2 Mechanical Properties of NS-4-FR 2.3-21
Table 2.4.4.2-1 Summary of Universal Transport Cask Materials Categories and Operating Environments 2.4-8
Table 2.5.1.1-1 Primary Trunnion/Top Forging Intersection Analysis Results 2.5-29
Table 2.5.2.1-1 Reactions Caused by Tiedown Devices (from 10 CFR 71.45(b)) 2.5-40
Table 2.5.2.1-2 Reactions Caused by Tiedown Devices (from AAR Field Manual Rule 88) 2.5-41

List of Tables (Continued)

Table 2.6.7.2-8 Critical $P_m + P_b + Q$ Stress Summary (ksi) - 1-Foot Side-Drop, Bolt Preload, Internal Pressure, Thermal Cold 2.6-46

Table 2.6.7.3-1 P_m Stresses - 1-Foot Top Corner-Drop, Bolt Preload, Internal Pressure 2.6-48

Table 2.6.7.3-2 $P_m + P_b$ Stresses - 1-Foot Top Corner-Drop Bolt Preload, Internal Pressure 2.6-49

Table 2.6.7.3-3 $P_m + P_b + Q$ Stresses - 1-Foot Top Corner-Drop, Bolt Preload, Internal Pressure, Thermal Hot 2.6-50

Table 2.6.7.3-4 $P_m + P_b + Q$ Stresses - 1-Foot Top Corner-Drop, Bolt Preload, Internal Pressure, Thermal Cold 2.6-51

Table 2.6.7.3-5 Critical P_m Stress Summary (ksi) - 1-Foot Top Corner-Drop, Bolt Preload, Internal Pressure 2.6-52

Table 2.6.7.3-6 Critical $P_m + P_b$ Stress Summary (ksi) - 1-Foot Top Corner-Drop, Bolt Preload, Internal Pressure 2.6-52

Table 2.6.7.3-7 Critical $P_m + P_b + Q$ Stress Summary (ksi) - 1-Foot Top Corner-Drop, Bolt Preload, Internal Pressure, Thermal Hot 2.6-53

Table 2.6.7.3-8 Critical $P_m + P_b + Q$ Stress Summary (ksi) - 1-Foot Top Corner-Drop, Bolt Preload, Internal Pressure, Thermal Cold 2.6-53

Table 2.6.7.3-9 P_m Stresses - 1-Foot Bottom Corner-Drop, Bolt Preload, Internal Pressure 2.6-54

Table 2.6.7.3-10 $P_m + P_b$ Stresses - 1-Foot Bottom Corner-Drop, Bolt Preload, Internal Pressure 2.6-55

Table 2.6.7.3-11 $P_m + P_b + Q$ Stresses - 1-Foot Bottom Corner-Drop, Bolt Preload, Internal Pressure, Thermal Hot 2.6-56

Table 2.6.7.3-12 $P_m + P_b + Q$ Stresses - 1-Foot Bottom Corner-Drop, Bolt Preload, Internal Pressure, Thermal Cold 2.6-57

Table 2.6.7.3-13 Critical P_m Stress Summary (ksi) - 1-Foot Bottom Corner-Drop, Bolt Preload, Internal Pressure 2.6-58

Table 2.6.7.3-14 Critical $P_m + P_b$ Stress Summary (ksi) - 1-Foot Bottom Corner-Drop Bolt Preload, Internal Pressure 2.6-58

List of Tables (Continued)

Table 2.6.7.3-15 Critical $P_m + P_b + Q$ Stress Summary (ksi) - 1-Foot Bottom Corner-Drop Bolt Preload, Internal Pressure, Thermal Hot 2.6-59
Table 2.6.7.3-16 Critical $P_m + P_b + Q$ Stress Summary (ksi) - 1-Foot Bottom Corner-Drop Bolt Preload, Internal Pressure, Thermal Cold 2.6-59
Table 2.6.7.5-1 Redwood Static Stress-Strain Properties 2.6-81
Table 2.6.7.5-2 Balsa Static Stress-Strain Properties 2.6-81
Table 2.6.7.5-3 Redwood Stress-Strain Properties (25 ε/sec) 2.6-82
Table 2.6.7.5-4 Balsa Stress-Strain Properties (25 ε/sec) 2.6-83
Table 2.6.7.5-5 Properties for the Impact Limiter Stainless Steel Shells 2.6-83
Table 2.6.7.5-6 Summary of Peak Accelerations and Maximum Crush Depths 2.6-84
Table 2.6.7-5-7 Quarter–Scale Model Impact Limiter Analysis Results Comparison to Drop Test Results 2.6-84
Table 2.6.7.8-1 Resultant Stress Intensity Values in the Equivalent Ring 2.6-105
Table 2.6.11.2-1 Stress Analysis Results for Uniform Pressure Loading of Inner Shell Due to Lead Pouring 2.6-114
Table 2.6.12.2-1 Gap and Element Type Definition - Canister Model 2.6-128
Table 2.6.12.2-2 Material Definition - Canister Model 2.6-128
Table 2.6.12.3-1 PWR Canister Linearized Q Stresses - Thermal Only (Hot 1) 2.6-133
Table 2.6.12.3-2 Linearized Stresses - Thermal Only (Cold 2) 2.6-134
Table 2.6.12.4-1 PWR Canister Critical Sections for the Pressure Only and 1-Foot End-Drop Load Condition 2.6-136
Table 2.6.12.4-2 PWR Canister P_m Stresses - Internal Pressure 2.6-137
Table 2.6.12.4-3 PWR Canister $P_m + P_b$ Stresses - Internal Pressure 2.6-138
Table 2.6.12.4-4 PWR Canister P_m Stresses - 1-Foot Top End Drop 2.6-139
Table 2.6.12.4-5 PWR Canister $P_m + P_b$ Stresses - 1-Foot Top End Drop 2.6-140
Table 2.6.12.4-6 PWR Canister P_m Stresses - 1-Foot Bottom End Drop, Internal Pressure 2.6-141
Table 2.6.12.4-7 PWR Canister $P_m + P_b$ Stresses - 1-Foot Bottom End Drop, Internal Pressure 2.6-142
Table 2.6.12.5-1 PWR Canister Critical Sections for the Combined 1-Foot End Drop and Thermal Load Condition 2.6-144

List of Tables (Continued)

Table 2.6.12.5-2 PWR Canister $P_m + P_b + Q$ Stresses - 1-Foot Top End Drop, Thermal Cold 2.6-145
Table 2.6.12.5-3 PWR Canister $P_m + P_b + Q$ Stresses - 1-Foot Top End Drop, Thermal Heat 2.6-146
Table 2.6.12.5-4 PWR Canister $P_m + P_b + Q$ Stresses - 1-Foot Bottom End Drop, Thermal Cold 2.6-147
Table 2.6.12.5-5 PWR Canister $P_m + P_b + Q$ Stresses - 1-Foot Bottom End Drop, Thermal Heat 2.6-148
Table 2.6.12.6-1 PWR Canister Critical Sections for the 1-Foot Side Drop Load Condition 2.6-151
Table 2.6.12.6-2 PWR Canister P_m Stresses - 1-Foot Side Drop 2.6-152
Table 2.6.12.6-3 PWR Canister $P_m + P_b$ Stresses - 1-Foot Side Drop, Internal Pressure 2.6-153
Table 2.6.12.7-1 PWR Canister Critical Sections for Combined 1-Foot Side Drop and Thermal Load Condition 2.6-155
Table 2.6.12.7-2 PWR Canister $P_m + P_b + Q$ Stresses - 1-Foot Side Drop, Thermal Cold 2.6-156
Table 2.6.12.7-3 PWR Canister $P_m + P_b + Q$ Stresses - 1-Foot Side Drop, Thermal Heat 2.6-157
Table 2.6.12.8-1 PWR Canister Critical Sections for the 1-Foot Corner Drop Load Condition 2.6-159
Table 2.6.12.8-2 PWR Canister P_m Stresses 1-Foot Top Corner Drop, Internal Pressure 2.6-160
Table 2.6.12.8-3 PWR Canister $P_m + P_b$ Stresses - 1-Foot Top Corner Drop 2.6-161
Table 2.6.12.8-4 PWR Canister P_m Stresses - 1-Foot Bottom Corner Drop 2.6-162
Table 2.6.12.8-5 PWR Canister $P_m + P_b$ Stresses - 1-Foot Bottom Corner Drop 2.6-163
Table 2.6.12.9-1 PWR Canister Critical Sections for the Combined 1-Foot Corner Drop and Thermal Load Condition 2.6-165
Table 2.6.12.9-2 PWR Canister $P_m + P_b + Q$ Stresses - 1-Foot Top Corner Drop, Thermal Cold 2.6-166
Table 2.6.12.9-3 PWR Canister $P_m + P_b + Q$ Stresses - 1-Foot Top Corner Drop, Thermal Heat 2.6-167
Table 2.6.12.9-4 PWR Canister $P_m + P_b + Q$ Stresses - 1-Foot Bottom Corner Drop, Internal Pressure, Thermal Cold 2.6-168

List of Tables (Continued)

Table 2.6.12.9-5 PWR Canister $P_m + P_b + Q$ Stresses - 1-Foot Bottom Corner Drop, Internal Pressure, Thermal Heat 2.6-169
Table 2.6.12.12-1 Geometry Parameters for the PWR Canister 2.6-174
Table 2.6.12.12-2 Buckling Evaluation Results for the PWR Canister for 1-Foot End Drop 2.6-175
Table 2.6.13.2-1 Listing of Cross Sections for Stress Evaluation of Support Disk 2.6-189
Table 2.6.13.4-1 $P_m + P_b$ Stresses for Support Disk -1-Foot End-Drop, Thermal Case A 2.6-195
Table 2.6.13.4-2 $P_m + P_b$ Stresses for Support Disk -1-Foot End-Drop, Thermal Case B 2.6-196
Table 2.6.13.5-1 $P_m + P_b + Q$ Stresses for Support Disk—1-Foot End-Drop, Thermal Case A 2.6-199
Table 2.6.13.6-2 P_m Stresses for Support Disk—1-Foot Side-Drop, 0° Orientation, Thermal Case A 2.6-207
Table 2.6.13.6-3 $P_m + P_b$ Stresses for Support Disk—1-Foot Side-Drop, 0° Orientation, Thermal Case A 2.6-208
Table 2.6.13.6-4 P_m Stresses for Support Disk—1-Foot Side-Drop, 0° Orientation, Thermal Case B 2.6-209
Table 2.6.13.6-5 $P_m + P_b$ Stresses for Support Disk—1-Foot Side-Drop, 0° Orientation, Thermal Case B 2.6-210
Table 2.6.13.6-6 P_m Stresses for Support Disk—1-Foot Side-Drop, 18.22° Orientation, Thermal Case A 2.6-211
Table 2.6.13.6-7 $P_m + P_b$ Stresses for Support Disk—1-Foot Side-Drop, 18.22° Orientation, Thermal Case A 2.6-212
Table 2.6.13.6-8 P_m Stresses for Support Disk—1-Foot Side-Drop, 18.22° Orientation, Thermal Case B 2.6-213
Table 2.6.13.6-9 $P_m + P_b$ Stresses for Support Disk—1-Foot Side-Drop, 18.22° Orientation, Thermal Case B 2.6-214
Table 2.6.13.6-10 P_m Stresses for Support Disk—1-Foot Side-Drop, 26.28° Orientation, Thermal Case A 2.6-215

List of Tables (Continued)

Table 2.6.13.6-11 $P_m + P_b$ Stresses for Support Disk—1-Foot Side-Drop, 26.28° Orientation, Thermal Case A 2.6-216
Table 2.6.13.6-12 P_m Stresses for Support Disk—1-Foot Side-Drop, 26.28° Orientation, Thermal Case B 2.6-217
Table 2.6.13.6-13 $P_m + P_b$ Stresses for Support Disk—1-Foot Side-Drop, 26.28° Orientation, Thermal Case B 2.6-218
Table 2.6.13.6-14 P_m Stresses for Support Disk—1-Foot Side-Drop, 45° Orientation, Thermal Case A 2.6-219
Table 2.6.13.6-15 $P_m + P_b$ Stresses for Support Disk—1-Foot Side-Drop, 45° Orientation, Thermal Case A 2.6-220
Table 2.6.13.6-16 P_m Stresses for Support Disk—1-Foot Side-Drop, 45° Orientation, Thermal Case B 2.6-221
Table 2.6.13.6-17 $P_m + P_b$ Stresses for Support Disk —1-Foot Side-Drop, 45° Orientation, Thermal Case B 2.6-222
Table 2.6.13.7-1 $P_m + P_b + Q$ Stresses for Support Disk—1-Foot Side-Drop, 0° Orientation, Thermal Case A 2.6-224
Table 2.6.13.7-2 $P_m + P_b + Q$ Stresses for Support Disk—1-Foot Side-Drop, 18.22° Orientation, Thermal Case A 2.6-225
Table 2.6.13.7-3 $P_m + P_b + Q$ Stresses for Support Disk—1-Foot Side-Drop, 26.28° Orientation, Thermal Case A 2.6-226
Table 2.6.13.7-4 $P_m + P_b + Q$ Stresses for Support Disk—1-Foot Side-Drop, 45° Orientation, Thermal Case A 2.6-227
Table 2.6.13.13-1 Minimum Margins of Safety for the Top/Bottom Weldments for 1-Foot End-Drop 2.6-235
Table 2.6.13.14-1 Minimum Margins of Safety from Buckling Evaluation of PWR Support Disk 2.6-241

Table 2.6.14.2-1 Real Constant Sets Defined in Canister Model 2.6-253
Table 2.6.14.2-2 Material Sets Defined in Canister Model 2.6-253
Table 2.6.14.3-1 BWR Canister Linearized Q Stresses - Thermal Only (Hot 1) 2.6-257
Table 2.6.14.3-2 BWR Canister Linearized Q Stresses - Thermal Only (Cold 2) 2.6-258
Table 2.6.14.4-1 BWR Canister Critical Sections for the 1-Foot End-Drop Condition . 2.6-260
Table 2.6.14.4-2 BWR Canister P_m Stresses - Internal Pressure 2.6-261

List of Tables (Continued)

Table 2.6.14.4-3 BWR Canister $P_m + P_b$ Stresses - Internal Pressure 2.6-262
Table 2.6.14.4-4 BWR Canister P_m Stresses - 1-Foot Top End-Drop..... 2.6-263
Table 2.6.14.4-5 BWR Canister $P_m + P_b$ Stresses - 1-Foot Top End-Drop..... 2.6-264
Table 2.6.14.4-6 BWR Canister P_m Stresses - 1-Foot Bottom End-Drop, Internal Pressure 2.6-265
Table 2.6.14.4-7 BWR Canister $P_m + P_b$ Stresses - 1-Foot Bottom End-Drop, Internal Pressure 2.6-266
Table 2.6.14.5-1 BWR Canister Critical Sections for the Combined 1-Foot End-Drop and Thermal Load Condition 2.6-268
Table 2.6.14.5-2 BWR Canister $P_m + P_b + Q$ Stresses - 1-Foot Top End-Drop, Thermal Cold 2.6-269
Table 2.6.14.5-3 BWR Canister $P_m + P_b + Q$ Stresses - 1-Foot Top End-Drop, Thermal Heat..... 2.6-270
Table 2.6.14.5-4 BWR Canister $P_m + P_b + Q$ Stresses - 1-Foot Bottom End-Drop, Thermal Cold 2.6-271
Table 2.6.14.5-5 BWR Canister $P_m + P_b + Q$ Stresses - 1-Foot Bottom End-Drop, Thermal Heat..... 2.6-272
Table 2.6.14.6-1 BWR Canister Critical Sections for the 1-Foot Side-Drop Load Condition 2.6-275
Table 2.6.14.6-2 BWR Canister P_m Stresses - 1-Foot Side-Drop 2.6-276
Table 2.6.14.6-3 BWR Canister $P_m + P_b$ Stresses - 1-Foot Side-Drop, Internal Pressure 2.6-277
Table 2.6.14.7-1 BWR Canister Critical Sections for the Combined 1-Foot Side-Drop and Thermal Load Condition 2.6-279
Table 2.6.14.7-2 BWR Canister $P_m + P_b + Q$ Stresses - 1-Foot Side-Drop, Thermal Cold 2.6-280
Table 2.6.14.7-3 BWR Canister $P_m + P_b + Q$ Stresses - 1-Foot Side-Drop, Thermal Heat..... 2.6-281
Table 2.6.14.8-1 BWR Canister Critical Sections for the 1-Foot Corner-Drop Load Condition 2.6-283
Table 2.6.14.8-2 BWR Canister P_m Stresses - 1-Foot Top Corner-Drop, Internal Pressure..... 2.6-284

List of Tables (Continued)

Table 2.6.14.8-3 BWR Canister $P_m + P_b$ Stresses - 1-Foot Top Corner Drop 2.6-285
Table 2.6.14.8-4 BWR Canister P_m Stresses - 1-Foot Bottom Corner-Drop, Internal Pressure 2.6-286
Table 2.6.14.8-5 BWR Canister $P_m + P_b$ Stresses - 1-Foot Bottom Corner-Drop..... 2.6-287
Table 2.6.14.9-1 BWR Canister Critical Sections for the Combined 1-Foot Corner-Drop and Thermal Load Condition 2.6-289
Table 2.6.14.9-2 BWR Canister $P_m + P_b + Q$ Stresses - 1-Foot Top Corner-Drop, Thermal Cold 2.6-290
Table 2.6.14.9-3 BWR Canister $P_m + P_b + Q$ Stresses - 1-Foot Top Corner-Drop, Thermal Heat..... 2.6-291
Table 2.6.14.9-4 BWR Canister $P_m + P_b + Q$ Stresses - 1-Foot Bottom Corner Drop, Internal Pressure, Thermal Cold 2.6-292
Table 2.6.14.9-5 BWR Canister $P_m + P_b + Q$ Stresses - 1-Foot Bottom Corner Drop, Thermal Heat..... 2.6-293
Table 2.6.14.12-1 Geometry Parameters for the BWR Canister 2.6-296
Table 2.6.14.12-2 Buckling Evaluation Results for the BWR Canister for 1-Foot End-Drop 2.6-297
Table 2.6.15.4-1 $P_m + P_b$ Stresses for Support Disk 1-Foot End-Drop, Thermal Case 1 ..... 2.6-310
Table 2.6.15.4-2 $P_m + P_b$ Stresses for Support Disk 1-Foot End-Drop, Thermal Case 4 ..... 2.6-311
Table 2.6.15.5-1 $P_m + P_b + Q$ Stresses for Support Disk 1-Foot End-Drop, Thermal Case 4 ..... 2.6-314
Table 2.6.15.6-1 Listing of Cross Sections for the Stress Evaluation of Support Disk 2.6-328
Table 2.6.15.6-2 P_m Stresses for Support Disk—1-Foot Side-Drop, 0° Orientation, Thermal Case 1 ..... 2.6-336
Table 2.6.15.6-3 $P_m + P_b$ Stresses for Support Disk—1-Foot Side-Drop, 0° Orientation, Thermal Case 1 ..... 2.6-337
Table 2.6.15.6-4 P_m Stresses for Support Disk—1-Foot Side-Drop, 0° Orientation, Thermal Case 2 ..... 2.6-338
Table 2.6.15.6-5 $P_m + P_b$ Stresses for Support Disk—1-Foot Side-Drop, 0° Orientation, Thermal Case 2 ..... 2.6-339

List of Tables (Continued)

Table 2.6.15.6-6 P_m Stresses for Support Disk—1-Foot Side-Drop, 31.82° Orientation, Thermal Case 1 ..... 2.6-340
Table 2.6.15.6-7 $P_m + P_b$ Stresses for Support Disk—1-Foot Side-Drop, 31.82° Orientation, Thermal Case 1 ..... 2.6-341
Table 2.6.15.6-8 P_m Stresses for Support Disk—1-Foot Side-Drop, 31.82° Orientation, Thermal Case 2 ..... 2.6-342
Table 2.6.15.6-9 $P_m + P_b$ Stresses for Support Disk—1-Foot Side-Drop, 31.82° Orientation, Thermal Case 2 ..... 2.6-343
Table 2.6.15.6-10 P_m Stresses for Support Disk—1-Foot Side-Drop, 49.46° Orientation, Thermal Case 1 ..... 2.6-344
Table 2.6.15.6-11 $P_m + P_b$ Stresses for Support Disk—1-Foot Side-Drop, 49.46° Orientation, Thermal Case 1 ..... 2.6-345
Table 2.6.15.6-12 P_m Stresses for Support Disk—1-Foot Side-Drop, 49.46° Orientation, Thermal Case 2 ..... 2.6-346
Table 2.6.15.6-13 $P_m + P_b$ Stresses for Support Disk—1-Foot Side-Drop, 49.46° Orientation, Thermal Case 2 ..... 2.6-347
Table 2.6.15.6-14 P_m Stresses for Support Disk—1-Foot Side-Drop, 77.92° Orientation, Thermal Case 1 ..... 2.6-348
Table 2.6.15.6-15 $P_m + P_b$ Stresses for Support Disk—1-Foot Side-Drop, 77.92° Orientation, Thermal Case 1 ..... 2.6-349
Table 2.6.15.6-16 P_m Stresses for Support Disk—1-Foot Side-Drop, 77.92° Orientation, Thermal Case 2 ..... 2.6-350
Table 2.6.15.6-17 $P_m + P_b$ Stresses for Support Disk—1-Foot Side-Drop, 77.92° Orientation, Thermal Case 2 ..... 2.6-351
Table 2.6.15.6-18 P_m Stresses for Support Disk—1-Foot Side-Drop, 90° Orientation, Thermal Case 1 ..... 2.6-352
Table 2.6.15.6-19 $P_m + P_b$ Stresses for Support Disk—1-Foot Side-Drop, 90° Orientation, Thermal Case 1 ..... 2.6-353
Table 2.6.15.6-20 P_m Stresses for Support Disk—1-Foot Side-Drop, 90° Orientation, Thermal Case 2 ..... 2.6-354
Table 2.6.15.6-21 $P_m + P_b$ Stresses for Support Disk—1-Foot Side-Drop, 90° Orientation, Thermal Case 2 ..... 2.6-355

List of Tables (Continued)

Table 2.6.15.7-1 $P_m + P_b + Q$ Stresses for Support Disk -1-Foot Side-Drop, 0° Orientation, Thermal Case 2 ..... 2.6-357
Table 2.6.15.7-2 $P_m + P_b + Q$ Stresses for Support Disk -1-Foot Side-Drop, 31.82° Orientation, Thermal Case 2 ..... 2.6-358
Table 2.6.15.7-3 $P_m + P_b + Q$ Stresses for Support Disk -1-Foot Side-Drop, 49.46° Orientation, Thermal Case 2 ..... 2.6-359
Table 2.6.15.7-4 $P_m + P_b + Q$ Stresses for Support Disk -1-Foot Side-Drop, 77.92° Orientation, Thermal Case 2 ..... 2.6-360
Table 2.6.15.7-5 $P_m + P_b + Q$ Stresses for Support Disk -1-Foot Side-Drop, 90° Orientation, Thermal Case 2 ..... 2.6-361
Table 2.6.15.13-1 Minimum Margins of Safety for the Top/Bottom Weldments for a 1-Foot End-Drop With and Without Thermal Stresses 2.6-367
Table 2.6.15.14-1 Minimum Margins of Safety from Buckling Evaluation of BWR Support Disk (Weak Axis) 2.6-375
Table 2.6.15.14-2 Minimum Margins of Safety from Buckling Evaluation of BWR Support Disk (Strong Axis) 2.6-376
Table 2.7.1.1-1 P_m Stresses—30-Foot Top End-Drop, Thermal Condition 1 ..... 2.7-5
Table 2.7.1.1-2 $P_m + P_b$ Stresses—30-Foot Top End-Drop, Thermal Condition 1 ..... 2.7-6
Table 2.7.1.1-3 Critical P_m Stress Summary—30-Foot Top End-Drop, Thermal Condition 1 ..... 2.7-7
Table 2.7.1.1-4 Critical $P_m + P_b$ Stress Summary—30-Foot Top End-Drop, Thermal Condition 1 ..... 2.7-7
Table 2.7.1.1-5 P_m Stresses—30-Foot Bottom End-Drop, Thermal Condition 1 ..... 2.7-8
Table 2.7.1.1-6 $P_m + P_b$ Stresses—30-Foot Bottom End-Drop, Thermal Condition 1 ..... 2.7-9
Table 2.7.1.1-7 Critical P_m Stress Summary—30-Foot Bottom End-Drop, Thermal Condition 1 ..... 2.7-10
Table 2.7.1.1-8 Critical $P_m + P_b$ Stress Summary—30-Foot Bottom End-Drop, Thermal Condition 1 ..... 2.7-10
Table 2.7.1.2-1 P_m Stresses—30-Foot Side-Drop, Thermal Condition 1 ..... 2.7-12
Table 2.7.1.2-2 $P_m + P_b$ Stresses—30-Foot Side-Drop, Thermal Condition 1 ..... 2.7-13
Table 2.7.1.2-3 Critical P_m Stress Summary—30-Foot Side-Drop, Thermal Condition 1 ..... 2.7-14

List of Tables (Continued)

Table 2.7.1.2-4 Critical $P_m + P_b$ Stress Summary—30-Foot Side-Drop, Thermal Condition 1 ..... 2.7-14
Table 2.7.1.3-1 P_m Stresses—30-Foot Top Corner-Drop, Thermal Condition 1 ..... 2.7-16
Table 2.7.1.3-2 $P_m + P_b$ Stresses—30-Foot Top Corner-Drop, Thermal Condition 1 ..... 2.7-17
Table 2.7.1.3-3 Critical P_m Stress Summary—30-Foot Top Corner-Drop, Thermal Condition 1 ..... 2.7-18
Table 2.7.1.3-4 Critical $P_m + P_b$ Stress Summary—30-Foot Top Corner-Drop, Thermal Condition 1 ..... 2.7-18
Table 2.7.1.3-5 P_m Stresses—30-Foot Bottom Corner-Drop, Thermal Condition 1 ..... 2.7-19
Table 2.7.1.3-6 $P_m + P_b$ Stresses—30-Foot Bottom Corner-Drop, Thermal Condition 1 ..... 2.7-20
Table 2.7.1.3-7 Critical P_m Stress Summary—30-Foot Bottom Corner-Drop, Thermal Condition 1 ..... 2.7-21
Table 2.7.1.3-8 Critical $P_m + P_b$ Stress Summary—30-Foot Bottom Corner-Drop, Thermal Condition 1 ..... 2.7-21
Table 2.7.1.4-1 P_m Stresses—30-Foot Top 75° Oblique-Drop, Thermal Condition 1 ... 2.7-23
Table 2.7.1.4-2 $P_m + P_b$ Stresses—30-Foot Top 75° Oblique-Drop, Thermal Condition 1 ..... 2.7-24
Table 2.7.1.4-3 Critical P_m Stress Summary—30-Foot Top 75° Oblique-Drop, Thermal Condition 1 ..... 2.7-25
Table 2.7.1.4-4 Critical $P_m + P_b$ Stress Summary—30-Foot Top 75° Oblique-Drop, Thermal Condition 1 ..... 2.7-25
Table 2.7.1.4-5 P_m Stresses—30-Foot Bottom 75° Oblique-Drop, Thermal Condition 1 ..... 2.7-26
Table 2.7.1.4-6 $P_m + P_b$ Stresses—30-Foot Bottom 75° Oblique-Drop, Thermal Condition 1 ..... 2.7-27
Table 2.7.1.4-7 Critical P_m Stress Summary—30-Foot Bottom 75° Oblique-Drop, Thermal Condition 1 ..... 2.7-28
Table 2.7.1.4-8 Critical $P_m + P_b$ Stress Summary—30-Foot Bottom 75° Oblique-Drop, Thermal Condition 1 ..... 2.7-28
Table 2.7.1.5-1 Lead Slump Calculation Parameters 2.7-32
Table 2.7.2.1-1 Local Membrane Stresses - Puncture Cask Side 2.7-46
Table 2.7.2.1-2 Stress Evaluation - Puncture Cask Side 2.7-47

List of Tables (Continued)

Table 2.7.10.1-21 $P_m + P_b$ Stresses for Support Disk 30-Foot Side-Drop, 90° Orientation, Thermal Case 2 ..... 2.7-177
Table 2.7.10.1-22 Summary of Stress Evaluation of Support Disk - 30-Foot End-Drop 2.7-178
Table 2.7.10.1-23 $P_m + P_b$ Stresses for Support Disk 30-Foot End-Drop, Thermal Case 1 ..... 2.7-179
Table 2.7.10.1-24 $P_m + P_b$ Stresses for Support Disk -30-Foot End-Drop, Thermal Case 4 ..... 2.7-180
Table 2.7.10.3-1 Minimum Margins of Safety from Buckling Evaluation of BWR Support Disk (Weak Axis) 2.7-187
Table 2.7.10.3-2 Minimum Margins of Safety from Buckling Evaluation of BWR Support Disk (Strong Axis) 2.7-188
Table 2.7.11-1 Summary of Maximum Calculated Stresses in Cask 30-Foot Free Drop 2.7-199
Table 2.7.11-2 Summary of Maximum Calculated Stresses in Cask—Puncture 2.7-200
Table 2.7.12-1 Buckling Evaluation Load Cases and Results for the Universal Transport Cask 2.7-210
Table 2.7.12-2 Geometry Parameters for the Universal Transport Cask 2.7-211
Table 2.9-1 Location of Lateral Constraints – PWR Fuel Rods 2.9-8
Table 2.9-2 PWR Fuel Rod Analysis Summary 2.9-8
Table 2.9-3 Location of Lateral Constraint for BWR Fuel Rods 2.9-9
Table 2.9-4 BWR Fuel Rod Analysis Summary 2.9-9
Table 2.10.2.2-1 Component Section and Temperature Definition 2.10.2-16
Table 2.10.2.2-2 Stress Section Locations 2.10.2-17
Table 2.10.4.1-1 Response Acceleration for PWR Support Disk for 1-Foot End Drop 2.10.4-5
Table 2.10.4.1-2 Response Acceleration for BWR Support Disk for 1-Foot End Drop 2.10.4-6
Table 2.10.4.2-1 Response Acceleration for PWR Support Disk for 1-Foot Side Drop 2.10.4-14
Table 2.10.4.2-2 Response Acceleration for BWR Support Disk for 1-Foot Side Drop 2.10.4-15

List of Tables (Continued)

Table 2.11.1.1-1 Normalized Stress Ratios – UMS® PWR Basket Support Disk Sectional Stresses Due to Maine Yankee Consolidated Fuel to the Design Basis PWR Fuel Basket Maximum Stresses (Base Case) 2.11.1-19

Table 2.11.1.1-2 P_m Stresses for Support Disk—1-Foot Side Drop, 45° Orientation, Thermal Case B, Structural Case 1 ..... 2.11.1-20

Table 2.11.1.1-3 $P_m + P_b$ Stresses for Support Disk—1-Foot Side Drop, 45° Orientation, Thermal Case B, Structural Case 1 ..... 2.11.1-21

Table 2.11.2.1-1 Maine Yankee GTCC Basket Weldment Sectional Stresses for Normal Condition Side Drop (ksi) 2.11.2-27

Table 2.11.2.1-2 Maine Yankee GTCC Basket Weldment Sectional Stresses for Accident Condition Side Drop (ksi) 2.11.2-27

Table 2.11.2.1-3 Summary of Maine Yankee GTCC Basket Weldment Side Drop Stress Evaluation 2.11.2-28

Table 2.11.2.1-4 Evaluation of the Weld Between the Shield Cylinder and Support Disk 2.11.2-28

$$I_{NA} = I_b + I_{cs} - I_h = 237.061 \text{ in}^4$$

The bolt (#1) most distant from the neutral axis is selected for calculation of stresses.

YIELD STRENGTH CRITERIA

Tension stress on bolt #1 due to the bending moment, M_{by}, is

$$\sigma_{bly} = \frac{M_{by} y_1'}{I_{NA}} = \frac{(1{,}600{,}000)(7.083)}{237.061} = 46{,}610.3 \text{ psi}$$

where $M_{by} = (F_y)_s \cdot D = (390{,}000)(1.5 + 2.5) = 1{,}560{,}000 \text{ in} \cdot \text{lb}.$

$$y_1' = 7.083 \text{ in.}$$

The bolt maximum pre-load torque (T_{max}) is 550(12) in-lb, which produces a tensile stress (σ_i) in addition to the bending stress:

$$\sigma_i = \frac{F_{imax}}{A_t} = \frac{39{,}111}{0.856} = 45{,}691 \text{ psi}$$

where:

At = 0.856 in.^{2} (1 1/8-in. bolt tensile area)

$$F_{imax} = \frac{T_{max}}{kd} = \frac{550(12)}{0.15(1.125)} = 39{,}111 \text{ lbs}$$

k = 0.15 for lubricated threads

d = 1.125 in. (nominal bolt diameter)

Shear stresses on the bolts do not show up due to the presence of the trunnion base plate. The total tensile stress (σ_T) in bolt #1 is then:

$$\sigma_T = \sigma_{bly} + \sigma_i = 46{,}610.3 + 45{,}691 \cong 92{,}301 \text{ psi}$$

The allowable stress, S_y, at 350°F is 139,500 psi.

The margin of safety is

$$M.S._Y = \frac{S_y}{\sigma_T} - 1 = \frac{139{,}500 \text{ psi}}{92{,}301 \text{ psi}} - 1 = +0.51$$

ULTIMATE STRENGTH CRITERIA

Tension stress on bolt #1 due to the bending moment, M_{bu}, is

$$\sigma_{blu} = \frac{M_{bu} y_1'}{I_{NA}} = \frac{(2{,}600{,}000)(7.083)}{237.061} = 77{,}684.0 \text{ psi}$$

where $M_{bu} = F_u \cdot D = (650{,}000)(1.5 + 2.5) = 2{,}600{,}000 \text{ in} \cdot \text{lb.}$

$y_1' = 7.083$ in.

The total tensile stress (σ_T) in bolt #1 is then

$$\sigma_T = \sigma_{blu} + \sigma_i = 77{,}684 + 45{,}691 = 123{,}375 \text{ psi}$$

The allowable stress, S_u, at 350°F is 172,100 psi.

The margin of safety is

$$M.S._u = \frac{S_u}{\sigma_T} - 1 = \frac{172{,}100 \text{ psi}}{123{,}375 \text{ psi}} - 1 = +0.39$$

In the upper bolts, where the trunnion flange is in compression, the bolt tensile load is the preload. The maximum tensile load (F_{imax}) is 39,111 pounds.

The minimum tensile load (F_{imin}) is

$$F_{imin} = \frac{T_{min}}{kd} = \frac{490(12)}{0.15(1.125)} = 34{,}844 \text{ lb}$$

2.6.7.5 Impact Limiters

The Universal Transport Cask design includes removable upper and lower impact limiters to ensure that the design impact loads on the cask are not exceeded for any of the defined load conditions. These impact load conditions include the cask falling 1-ft or 30-ft and landing: (1) horizontally on its side on both impact limiters, (2) vertically on one impact limiter at either end, or (3) obliquely (including C.G. over the corner) on one impact limiter at either end.

The impact limiters decelerate the cask by applying a force in the direction opposite to the motion of the cask. The deceleration force is generated by crushing the redwood and balsa wood materials of the impact limiter between the cask and the unyielding surface. The energy absorbed during crushing is net force, the vector sum of the cask weight (downward) and the deceleration force (upward) multiplied by the distance crushed. The amount of energy that an impact limiter absorbs is calculated for various cask impact orientations, from vertical (0°) to horizontal (90°).

The impact limiter analysis is based on the assumptions that the cask impacts upon an unyielding surface and that the impact limiter remains in position on the cask during all impact events (The qualification of the impact limiter attachment is presented in Section 2.6.7.5.7).

2.6.7.5.1 Description of Impact Limiters

Each of the impact limiters on the Universal Transport Cask consists of 2 energy-absorbing materials: (1) redwood and (2) balsa wood. The wood is enclosed in a thin stainless steel shell to maintain the wood orientation during an impact. Figures 2.6.7.5-1 and 2.6.7.5-2 show the locations on the cask and the primary cross-section dimensions of the impact limiters. The upper and lower impact limiters are configured similarly to each other, except that the upper limiter has pockets for the lifting trunnions and a larger inside diameter. The approximate radius used for the backed area of the bottom impact limiter is 41.3 inches. The approximate radius of the backed area of the top impact limiter is 42.6 inches.

The outside diameter of the Universal Transport Cask upper and lower impact limiters is 124.0 inches and the height is 43.0 inches. The overlap between the cask body and the impact limiters is 11.0 inches. Sixteen 1.25-inch diameter retaining rods, attach each impact limiter to the end of the cask. The attachments are described in detail in Section 2.6.7.5.7. The height of the redwood in the end section of the impact limiter is 30.0 inches. A ring of balsa wood forms part of the end section of the impact limiter. The balsa wood ring dimensions are: inside diameter = 99.2 inches, outside diameter = 123.75 inches, and height = 21.6 inches. The bottom region of the impact limiter is a 1.5-inch thick layer of balsa wood that absorbs most of the kinetic energy in a 1-ft end-drop impact and limits the impact force for normal conditions of transport (1-ft drop). The low crush strength balsa wood is necessary because the impact area is considerably greater in a flat end impact than in any other drop orientation. The redwood and the balsa wood side ring absorb most of the energy in a corner impact and all of the energy in a side impact.

The different segments and sections comprising each limiter are bonded to each other with DAP-Weldwood resorcinol adhesive.

For each of the impact load conditions in this analysis, the impact limiters remain in position on the cask and absorb the energy of the impact; thus, they limit the impact loads to the calculated values shown in Table 2.6.7.5-6.

2.6.7.5.2 Load Conditions

The specific loading conditions for the impact limiters are defined by 10 CFR 71.71(c)(7), 10 CFR 71.73(c)(1) and Regulatory Guide 7.8, as follows:

1. 1-ft drop of the cask impacting at any angle from vertical (flat end) to corner (cask center of gravity directly above point of impact).
2. 1-ft drop of the cask in a horizontal orientation (side impact).
3. 30-ft drop of the cask in an end, side, corner, or oblique orientation.

On the basis of these loading conditions, the Universal Transport Cask impact limiters are designed for the 30-ft cask drops but with consideration of the effects of the 1-ft drops. The maximum impact forces and the maximum crush depth for the 1-ft and 30-ft cask drops are

obtained from the LS-DYNA [33] analyses of the cask drops. LS-DYNA is an explicit finite element program capable of performing three-dimensional nonlinear analysis of structures containing nonlinear material behavior such as plastic deformation of steel or crushing of wood. LS-DYNA is described in Section 2.10.1.2.

2.6.7.5.3 Tests of Impact Limiter Specimens

A series of static and dynamic crush tests were performed to define the crush properties of the redwood and the balsa wood to be used in the impact limiters.

Static Tests

The static crush tests represent the crush strength of the wood for either static loading or low strain rate crush, which would be associated with the impact velocities for a 1-foot drop. The redwood force-deflection data was obtained at room temperature for the perpendicular to grain using 44 samples and parallel to grain crush direction using 44 samples and for the parallel to grain crush direction 45 samples. These crush tests were used to define an acceptable range for the density for redwood of 23.5 +/- 3.5 lb/ft^3. An average crush stress-strain curve was obtained for each direction of crush using a least squares straight line fit. To account for the effect of low temperatures (-20°F) for redwood as well for temperatures at 152°F, the test data was ratioed by the temperature effect shown in Figure 8 of NUREG/CR-0322 [34]. To account for fabrication tolerances and provide bounding maximum crush strength for the redwood, the cold properties are factored by 1.10. To obtain the bounding minimum crush strength, the hot properties are factored by 0.9. The static crush strength data for redwood is presented in Table 2.6.7.5-1.

For balsa wood (balsa) static properties, Figure 16 of JPL Technical Report No. 32-944 [35] shows the average crush strength of the balsa in the parallel to grain direction at room temperature to be 1,550 psi for a density of 10 lb/ft^3. The static balsa properties at -40°F and 152°F are obtained by factoring the room temperature crush stress-strain curve for balsa based on the temperature effect contained in Figure 15 of the JPL Technical Report. The static crush strength data for balsa is presented in Table 2.6.7.5-2.

Dynamic Tests

Dynamic crush tests are performed to establish the dynamic properties for the redwood and balsa. As in the static crush tests, the density of the redwood samples are restricted to be 23.5 +/- 3.5

lb/ft^3. While static testing was not performed for balsa by NAC, the density for balsa in the tests was restricted to 8.5 +/- 1.5 lb/ft^3.

The stress-strain curves for balsa and redwood are determined for two directions, perpendicular, and parallel to the grain. The test program conducted at room temperature was comprised of using 9 to 10 samples at each of five strain rates, which ranged from 25 strain/sec to 375 strain/sec. The force-deflection data for the samples having the same strain rate (for the same crush direction for the same wood) were averaged to produce a composite curve. The composite curve was reduced to a series of straight-line segments while retaining the maximum acceleration of the composite curve and the same area under the stress-strain curve. To account for the effect of temperatures, an additional series of tests was conducted at -40°F and at 200°F for three strain rates ranging over the same range employed for the room temperature evaluation. In performing the evaluation, the predominant strain rate is the 25 strain/sec for which the properties are presented in Tables 2.6.7.5-3 and 2.6.7.5-4 for the redwood and the balsa, respectively.

2.6.7.5.4 Specification for Universal Transport Cask Impact Limiters

The redwood material used for the Universal Transport Cask impact limiters must meet density, crush strength (converted from the force-deflection curve) and moisture content specifications. The density of any single redwood board shall be 23.5 ± 3.5 lb/ft^3. The density of any 15° or 30° pie-shaped section of redwood shall be 22.3 ± 1.2 lb/ft^3. Each 15°, pie-shaped section of redwood in the side segment of the impact limiter shall have an average static crush strength value (in the parallel-to-the-grain direction) of 5,898 ± 620 psi at 0.4 in./in. strain and 70°F. Each 30-degree, pie-shaped section of redwood in the end segment of the impact limiter shall have an average crush strength value (in the perpendicular-to-the-grain direction), of 1,190 ± 130 psi at 0.4 in./in. strain and 70°F. The moisture content of any single board shall be greater than 5% but less than 15%. The average moisture content for the lot of redwood shall be less than 12%.

The balsa wood to be used in the Universal Transport Cask impact limiters shall meet the specifications of MIL-S-7998A [38]: (1) density between 7 and 10 lb/ft^3, and (2) moisture content between 5 and 15% for any one piece with an average of not more than 12% for any lot of balsa wood.

2.6.7.5.5 Impact Limiter Analysis

The primary areas of analytical evaluation required in an impact limiter analysis are (1) crush depth, (2) maximum acceleration, and (3) attachment to the cask. The crush depth and maximum acceleration are dependent on the crush strength of the crushable material, the area engaged in crushing, the geometry of the impact limiter, and the energy to be dissipated.

The LS-DYNA general purpose explicit finite element computer program is used to analyze an impact limiter for an impact event to determine the dynamics of the event, the acceleration generated during that event, and the depth of crush. A detailed description of this program is provided in Section 2.10.1.2.

The impact limiter finite element model was built using the ANSYS pre-processor and LS-DYNA's Finite Element Model Builder. The impact analyses were performed using LS-DYNA. The model is constructed of 8-node brick and 4-node shell elements. Using the symmetry planes that exist for the various drop orientations, the model was simplified so that only a half model was necessary for the analyses. The finite element model used in the analyses corresponds to the full-scale cask body and impact limiters. The complete finite element model is shown in Figure 2.6.7.5-3. Figure 2.6.7.5-4 shows only the steel shells and gussets that contain the wood. The cask body section of the model consists of a single shell using an elastic material. The properties of the elastic modulus of the shell section of the cask body were adjusted so that the cross-sectional properties of the finite element model were equal to those of the full-scale design of the UMS transport cask. As shown in Figure 2.6.7.5-3, the model contains a detailed representation of the trunnion and the cut out in the top impact limiter. The impact limiters are attached to the cask ends by beam elements corresponding to the attachment bolts for the impact limiter. The redwood and the balsa wood are modeled as an isotropic foam material. The stress-strain curves used as input into the LS-DYNA model were obtained by dynamic crush testing of the wood specimens.

To account for the deformation of the Type 304 stainless steel shells and gussets, these components were modeled with an elasto-plastic material - LS-DYNA material Type 24 ("Piecewise_Linear_Plasticity"). The required input data for the stainless steel consists of the stress-strain data presented in Table 2.6.7.5-5.

Boundary Conditions and Initial Conditions

LS-DYNA "Surface_to_Surface" contact interfaces are employed between the cask body and the impact limiter shells. The unyielding surface is modeled as being flat using the "Rigidwall_Geometric_Flat" option in LS-DYNA. Symmetry boundary conditions are imposed on the nodes in the X-Z plane. Initial velocities of 96.3 in./sec and 527.4 in/sec were applied to the entire model to represent the 1-foot and 30-foot drops, respectively. A uniform gravitational field corresponding to 386.4 in/sec^2 is also applied in the direction of the drop.

There are three orientations considered in the evaluation of the 1-foot and the 30-foot drops: end drop, center of gravity (CG) over corner and side drop. The end drop results in the maximum axial accelerations. To establish the bounding axial accelerations, as well as the maximum axial crush depth, two end drop conditions are analyzed. To obtain the maximum acceleration, the top end drop is performed using –40°F material properties. This condition corresponds to the wood having maximum crush strength in conjunction with the largest backed area. To obtain the maximum crush depth for the end drop orientation, the bottom end drop is performed using the material properties at 200°F. The bottom end of the transport cask has a smaller area than the top end and the use of 200°F material properties corresponds to the minimum crush strength.

The corner drop (CG over corner) results in the largest crush depth of the limiter. The side drop results in the maximum acceleration in the lateral direction on the cask.

Based on the validation study provided in Section 2.6.7.5.8, the side drop condition bounds any slap down for cask designs in which $L/r < 2$. Therefore, only the side drop analysis is performed to determine the bounding lateral accelerations and crush depths. The bounding side drop accelerations are determined using the cold material properties (–40°F). The bounding side drop crush depths are determined using the 200°F material properties.

2.6.7.5.6 Analysis Results

To obtain results from LS-DYNA, nodes of interest are used to record output data. These nodes are located at the plane of symmetry on the outer surface of the cylinder at the end of the cask cavity. For the side drop, the nodes record the lateral acceleration, and for the end drop, the nodes record the axial acceleration. For the CG over corner orientation, the recorded acceleration corresponds to the direction of drop. The nodal output is in the form of displacement and acceleration time histories. However, the acceleration time histories contain high frequency

components, which do not represent the response of the cask to the external impact. Therefore, the time histories are filtered to obtain the true accelerations corresponding to the impact. For this evaluation, the Butterworth low-pass filter in LS-DYNA's post-processor is used with a filter frequency of 120 Hz. This filter frequency was used to filter the time histories of the impact tests for a steel billet in the side drop and end drop orientation (NUREG/CR-6608). The filter frequency was established by performing a modal analysis of the cask finite element model. The side drop modal analysis applied a simply supported condition in the direction of the drop at each of the cask ends, which resulted in a fundamental mode at 61 Hz. For the end drop modal analysis, an axial restraint is applied to the nodes at the end of the cask, which results in a fundamental mode at 129 Hz. A filter frequency of 120 Hz is used in the acceleration calculation.

The maximum accelerations for the 1-foot and the 30-foot drops are presented in Table 2.6.7.5-6. The filtered acceleration time histories for the conditions providing the maximum accelerations for the end drop, CG over corner and side drop are shown in Figure 2.6.7.5-5, Figure 2.6.7.5-6 and Figure 2.6.7.5-7, respectively.

2.6.7.5.7 Impact Limiter Attachment Analysis

The following design criteria apply to the method of attaching the impact limiters to the cask body.

1. The impact limiters must remain attached to the cask body during normal handling and transport. Satisfaction of this criterion ensures that the limiters will be in a proper position to perform their impact-limiting function in the event of a free drop (normal or accident).

2. In a free drop (normal or accident), the limiter (or limiters) making initial contact with the unyielding surface must remain in position on the cask for the full duration of the initial impact. Satisfaction of this criterion ensures that the limiter(s) will be able to properly perform the impact-limiting function.

3. In a free drop (normal or accident) involving an initial impact on a single impact limiter, the limiter on the opposite end of the cask must remain attached to the cask during the initial impact. Satisfaction of this criterion ensures that the limiter will be

in a proper position to perform its impact-limiting function in a subsequent secondary impact following the initial impact.

Sections 2.6.7.5.7.1 through 2.6.7.5.7.3 demonstrate that each of these criteria is satisfied.

2.6.7.5.7.1 Impact Limiter Attachment During Normal Handling and Transport

Attachment of the impact limiters to the cask body during normal handling and transport operations is ensured by demonstrating that the attachment hardware does not yield under normal handling and transport conditions. The worst-case loading associated with normal handling and transport is a 7.5 g-load corresponding to the peak longitudinal shock loading expected as the result of rail transport (as specified by the Field Manual of the AAR [31]).

The design load, P, on the attachment is P = (7.5)(8,846) = 66,345 lb, where 8,846 lb is the weight of each impact limiter.

Analysis of Retaining Rods

Sixteen 1.25-in. diameter retaining rods are equally spaced on a bolt circle diameter of 81.8 inches for the upper limiter and 71.1 inches for the lower limiter. The attachment geometry of the impact limiters is shown in Figure 2.6.7.5-8. The retaining rods are SA-193, Grade B8S stainless steel with a yield strength of 39.8 ksi and a design stress intensity (S_m) of 13.0 ksi at 200°F (Table 2.3.5-3).

The load on each retaining rod resulting from a longitudinal shock load of 7.5 g is given as

$$P = 66{,}345/16 = 4{,}147 \text{ lb per retaining rod.}$$

The retaining rod tensile area is 0.969 in^2 in the threaded region, resulting in a tensile stress of:

$$S_t = 4{,}147/0.969 = 4{,}275 \text{ psi}$$

Each retaining rod nut is torqued to 75 ± 5 ft-lbs, resulting in a preload of 2,560 lbs. Therefore, the preload stress is (2,560 lb/0.969 in^2 =) 2,642 psi. The total stress for the longitudinal shock load of 7.5g is, therefore, 4,275 + 2,642 = 6,920 psi (6.9 ksi). For the retaining rods, the allowable stress is twice S_m, or 2 x 13.0 = 26.0 ksi. The Margin of Safety (MS) is:

$$MS = (26/6.92) - 1 = +2.76$$

Analysis of Retaining Rod Anchorage

The nut of the retaining rod is bearing on a washer that has a diameter of 5.0 in. and a thickness of 0.50 in. The washer is bearing on the bearing plate portion of the impact limiter shell, which bears on the redwood material.

The load on each of the 16 retaining rods resulting during the normal transportation condition is 4,147 + 2,560 = 6,707 lb . The bearing area between the bearing plate and the redwood material is:

$$A = (\pi/4)(5.0^2 - 3.0^2) = 12.57 \text{ in}^2.$$

The bearing pressure is:

$$p = 6{,}707/12.57 = 534 \text{ psi}$$

The perpendicular-to-the-grain compressive stress in the redwood at 2.5% strain is 750 psi. The margin of safety for compression of the redwood is

$$MS = (750/534) - 1 = +0.41.$$

The washer is made of Type 304 stainless steel and has a 1.31-inch diameter hole in the center. It is analyzed by assuming that it is simply supported along a circle having a diameter equal to the edge of the hole in the bearing plate (3.00 in.). The total load of 6,707 lb is distributed along the edge of the nut, which has an average diameter of 1.939 in. From Roark, Table 24, Case 1a, [28], the stress on the washer is:

$$S_{max} = \left(\frac{12Wa^2}{\left(a - \frac{b^2}{a}\right)t^2}\right)\left[\frac{r_0}{a}\left\{\frac{1+\nu}{2}\ln\left(\frac{a}{r_o}\right) + \frac{1-\nu}{4}\left[1-\left(\frac{r_o}{a}\right)^2\right]\right\}\right] = 24.4 \text{ ksi}$$

where:

a = 1.50 in.	b = 0.655 in.
t = 0.50 in.	ν = 0.31
r_o = 0.9695 in.	W = (6,707/(2π x 0.9695)) = 1,101 lb/in.

The yield strength of Type 304 stainless steel is 25.0 ksi at 200°F. The margin of safety is calculated MS = 25.0/24.4 - 1 = + 0.02.

The positive margins of safety show that the attachment of the impact limiters is adequate during normal conditions of transport.

Evaluation of Impact Limiter Attachment for Vibration

During normal conditions of transport, the impact limiter attachment may be subjected to vibration induced from the combination of component natural frequency and a dynamic load forcing function dependent on the transport media. Design of the impact limiter attachment eliminates the potential for the postulated vibration loading to loosen the impact limiter attachment. Lock nuts are installed in back of each of the retaining rod attachment nuts to prevent them from becoming loose. Locking wires installed between sets of two retaining rods eliminate rotation of the impact limiter retaining rods relative to their anchorage. The combination of these two design features eliminates the potential for the impact limiter attachment to become loose as a result of postulated vibration loading during transport.

2.6.7.5.7.2 Response of Impacted Limiters During Initial Impact of Package with Ground

The second criterion applicable to the impact limiter attachments requires that the impact limiter making initial contact with the unyielding surface must remain in position on the cask for the full duration of the initial impact. To satisfy this criterion, the impact limiter(s) being crushed must not separate from the cask, although the attachment hardware (mounting plate and bolts) may fail during the impact event.

The ability of the NAC-STC impact limiter to remain in position during an impact was demonstrated with reference to several static compression tests of the NAC-STC, during which the only attachment mechanism was a strip of duct tape. All of the compression tests were performed by using eighth-scale models of the impact limiters. The results of these tests are applicable to the Universal Transport Cask.

Analytic evaluations are performed to further justify that the initially impacted Universal Transport Cask impact limiter remains in position during an impact event and properly perform its function. Results of evaluations indicate that the attachment hardware is not expected to fail

and that the cask and impact limiter do not separate even if the attachment does fail. A significant resistance to the applied separation moment exists as a result of a combination of crushing of the limiter at the cask interface and also as a result of frictional resistance that exists at the interface. This total resistance is calculated to be greater than the applied separation moment.

2.6.7.5.7.3 Response of Secondary Impact Limiter During Initial Impact of Package

The final criterion to be satisfied is that for a free drop (normal or accident) involving an initial impact on a single impact limiter. The limiter on the opposite end of the cask (secondary limiter) must remain attached to the cask during the initial impact, thus ensuring that the secondary limiter is in position to absorb the secondary impact. The secondary limiter remains in position for the full duration of the secondary impact and performs its impact-limiting function. Attachment is ensured by demonstrating that the attachment hardware (mounting plate and retaining rods) does not fail during the initial impact.

During a free drop of the cask (normal or accident) involving an initial impact on a single impact limiter, i.e., flat end, center of gravity over corner, or any oblique drop, the ground exerts an upward force on the impact limiter that strikes it. The impact limiter in turn exerts an upward force on the cask body, thus decelerating the cask body. The cask body exerts an upward force on the secondary impact limiter and decelerates it. This scenario is repeated during a rebound of the whole package: the ground exerts an upward force on the impact limiter that strikes it; the impact limiter that strikes the ground exerts an upward force on the cask body and the cask body exerts an upward force on the secondary impact limiter, thereby accelerating the whole package upwards. When the entire package is in the air, its components (the impact limiter, the cask body, and the secondary impact limiter) move with the same acceleration and velocity; no other force acts among them. Thus, it is evident that during a free-drop impact on the first impact limiter, no separation force exists between the cask body and the second impact limiter. The absence of separation forces ensures that the second impact limiter stays in position to absorb the second impact.

Analysis of the impact limiter mounting plate and retaining rods demonstrates that the impact limiter attachments provide significant resistance to any unspecified separation force on the impact limiter. This analysis provides further evidence that the secondary impact limiter will stay attached to the cask body to absorb the second impact.

2.6.7.5.8 Verification of LS-DYNA for Cask Drop Impact Limiter Evaluation

To confirm the adequacy of LS-DYNA for cask drop impact limiter analyses, a series of analyses were performed to compare analytical results to quarter-scale model tests for the NAC-STC transport cask. From the series of drop tests performed using the NAC-STC, four tests are compared to analytical calculations using LS-DYNA. The four-drop tests are: end drop, CG over corner drop, side drop and a 75° oblique drop (measured from the vertical). The modeling procedure and material properties described in Section 2.6.7.5.5 for the UMS full-scale cask model was employed in this evaluation to develop a quarter-scaled model of the NAC-STC cask. The filter frequency for the lateral drops and the end drops were selected to be 450 Hz and 550 Hz respectively. These were established by performing a modal analysis of the cask model. The results for the four drops are shown in Table 2.6.7.5-7. These results are compared to the NAC-STC results as shown in Table 2.6.7.5-7 and show that LS-DYNA adequately predicts the response of the wood impact limiters.

An additional analysis was performed using this model to determine the maximum accelerations for an 85° oblique drop orientation. The maximum accelerations were 201g and 195g for the cask top and cask bottom, respectively. The 75°, 85° and 90° results indicate that the side drop is bounding for this cask design in which the L/r (length to radius of gyration) is less than 2.

The oblique drop analyses for the 75° and 85° orientations used a coefficient of friction of 0.2, which is less than a typical value of 0.27 for steel-steel interface with an oxide film (Marks). An additional parametric study using the model described above showed that the bounding condition is the zero friction condition, which remains bounded by the side drop orientation.

Figure 2.6.7.5-1 Universal Transport Cask with Impact Limiters

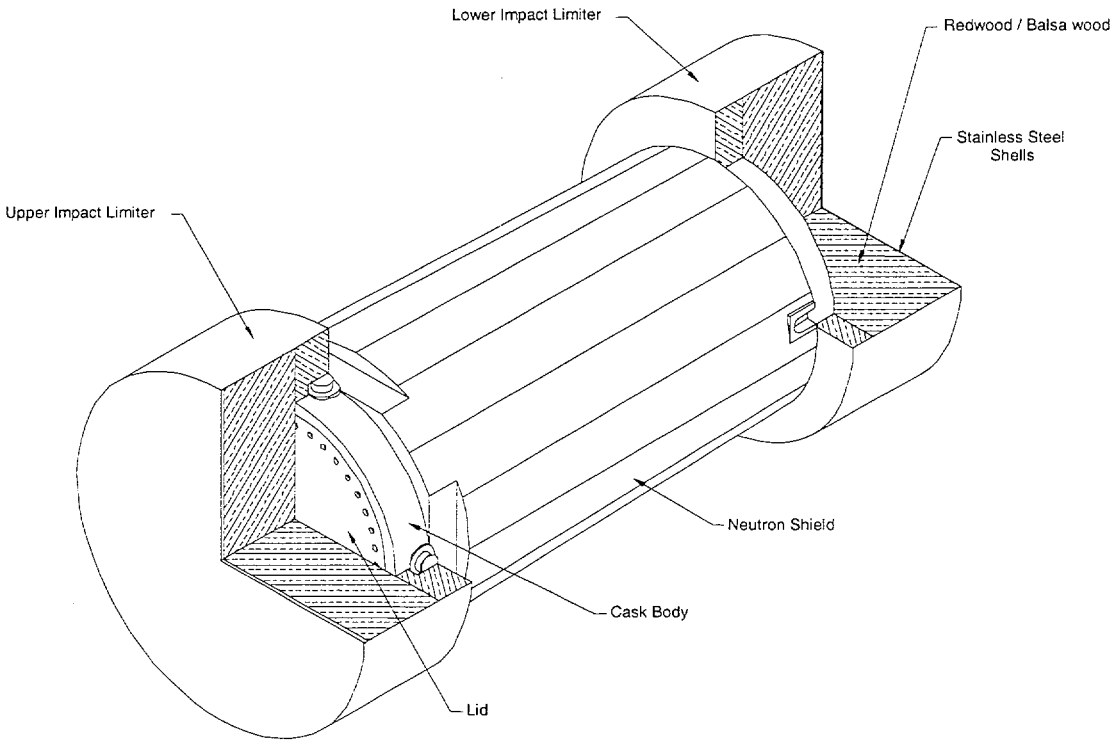

Figure 2.6.7.5-2 Cross-Section of Lower Impact Limiter

FIGURE WITHHELD UNDER 10 CFR 2.390

Figure 2.6.7.5-3 LS-DYNA Finite Element Model

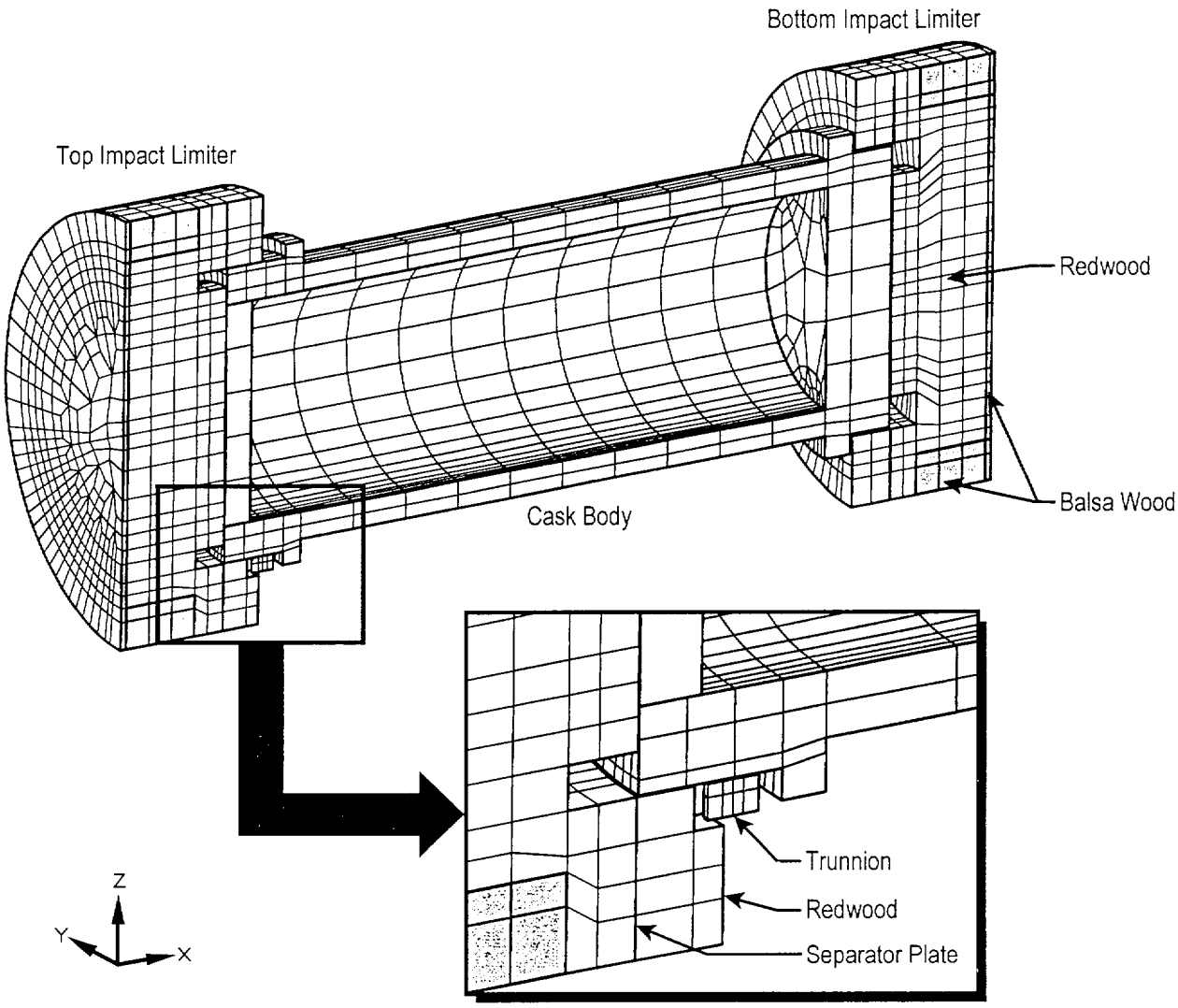

Figure 2.6.7.5-4 Impact Limiter Shell LS-DYNA Finite Element Model

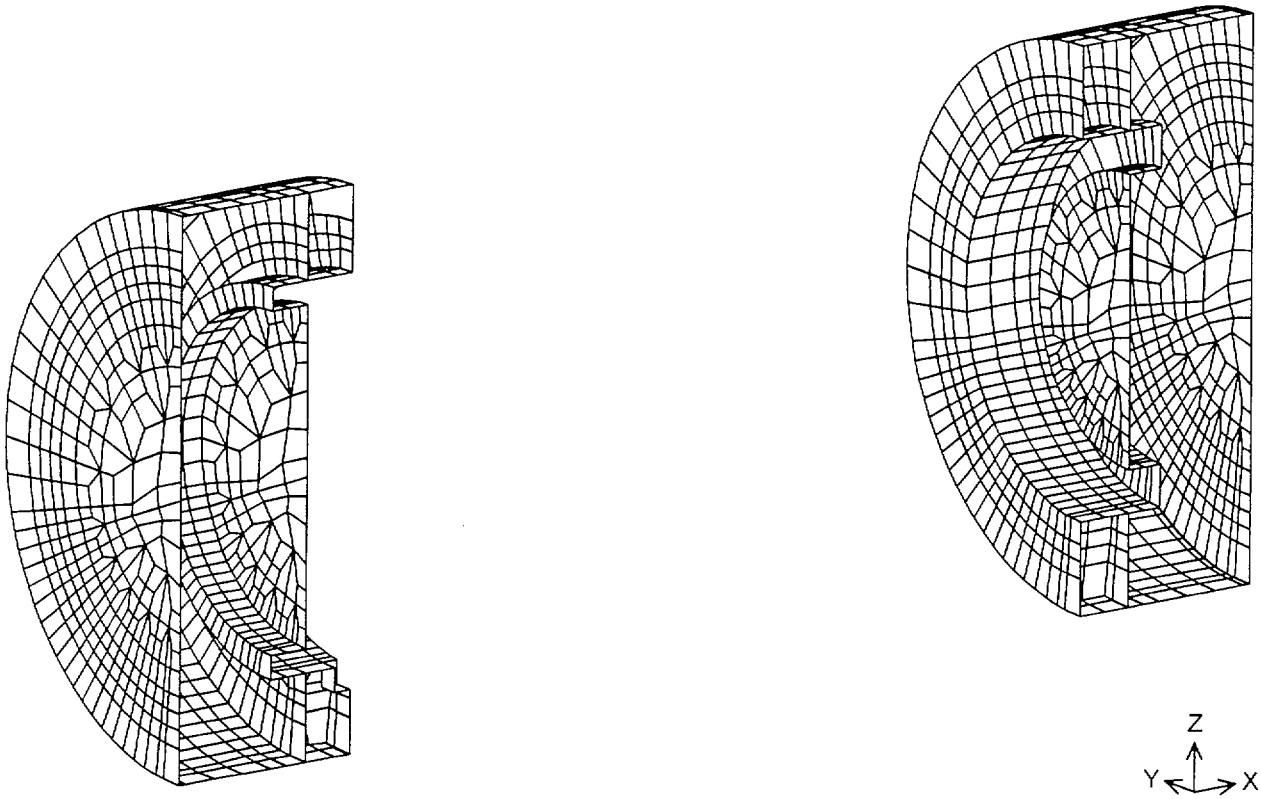

Figure 2.6.7.5-5 Acceleration Time History for the Cold Condition 30-Foot Top End Drop

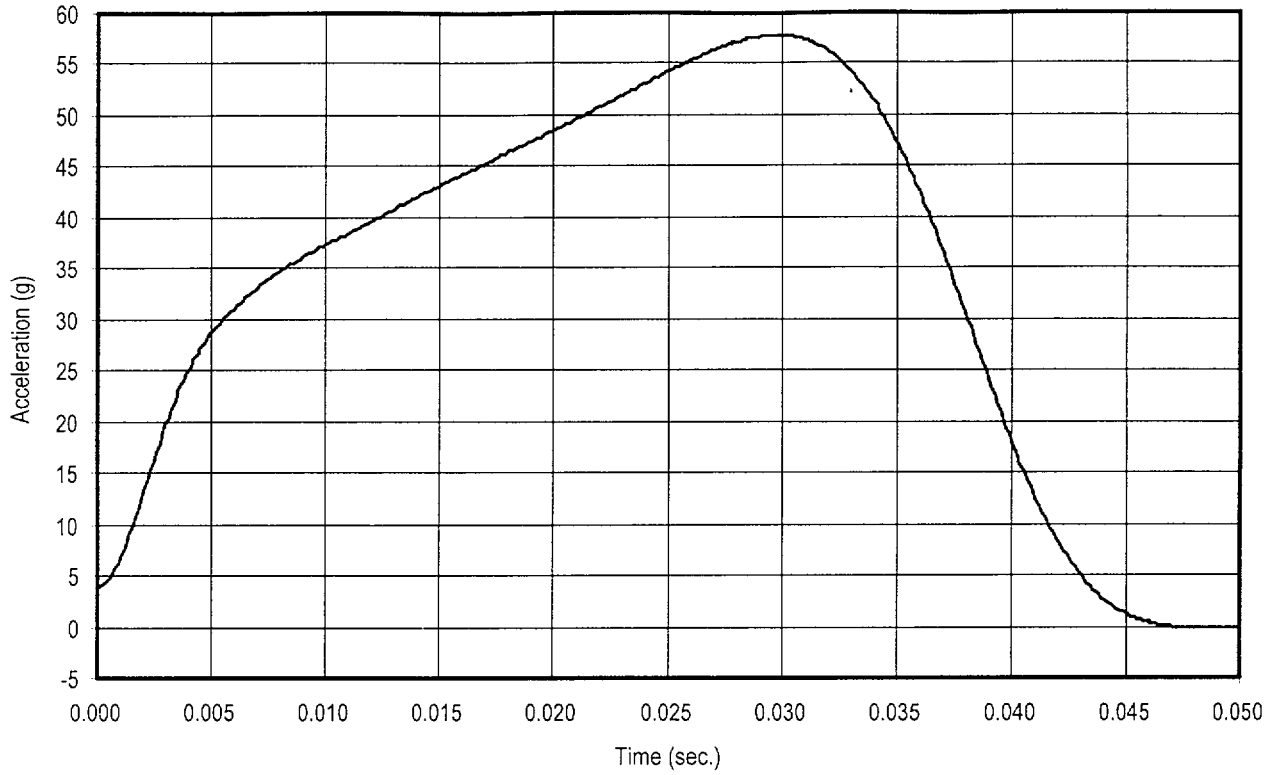

Figure 2.6.7.5-6 Acceleration Time History for the Cold Condition 30-Foot Top Corner Drop

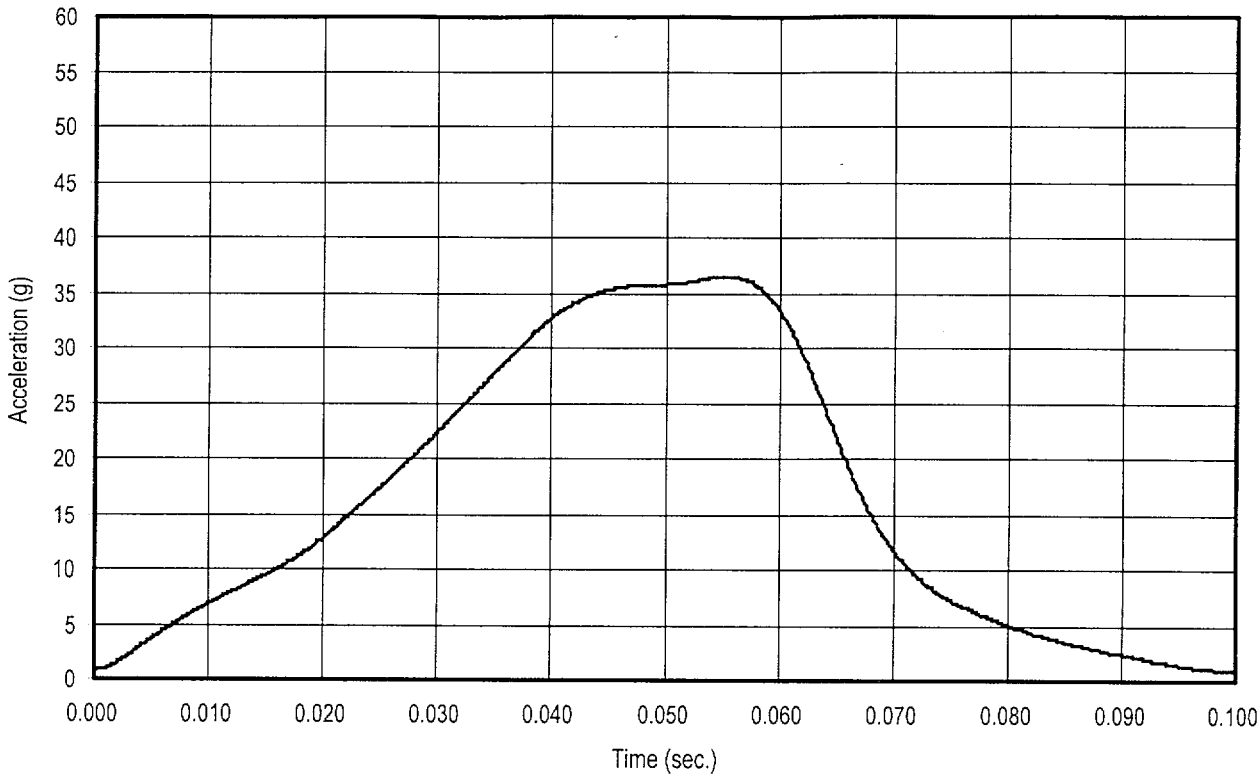

Figure 2.6.7.5-7 Acceleration Time History for the Cold Condition 30-Foot Side Drop

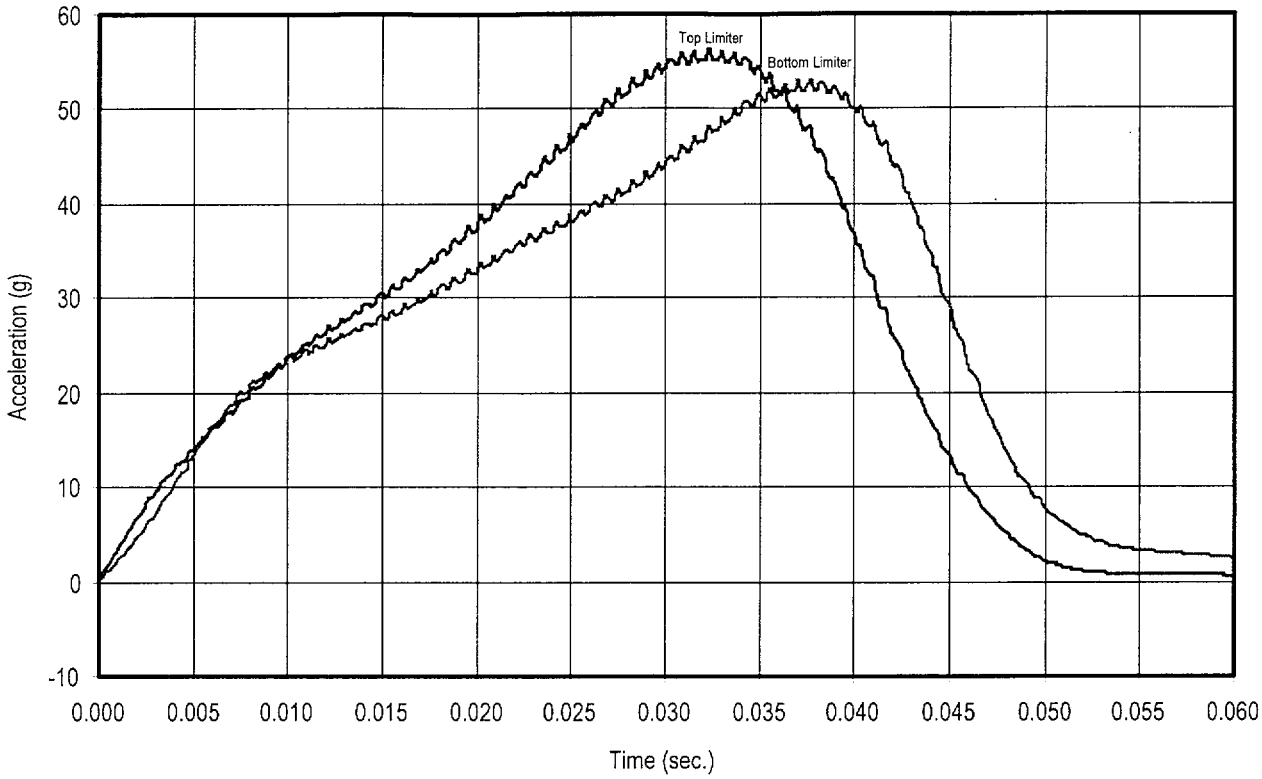

Figure 2.6.7.5-8 Impact Limiter Attachment Geometry

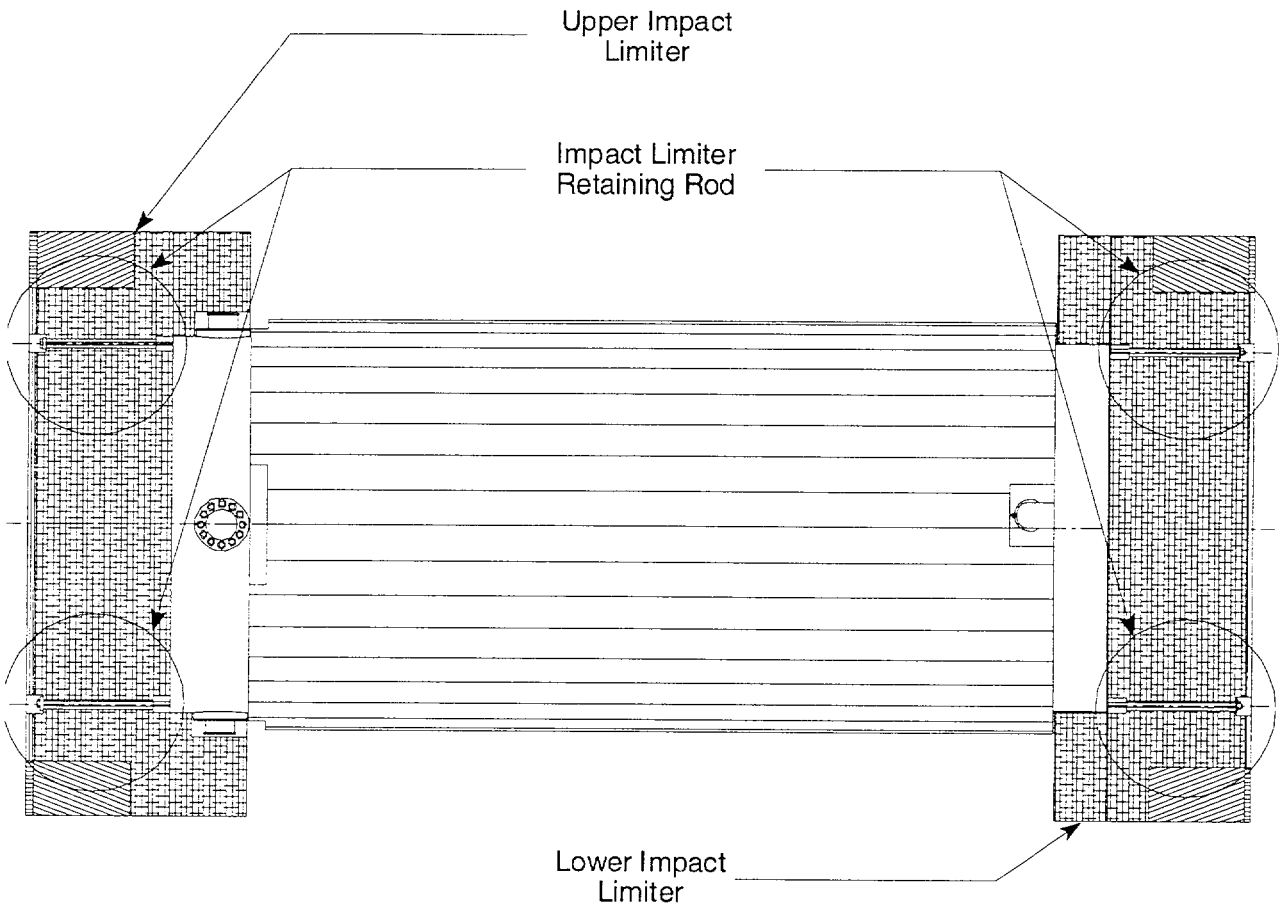

Table 2.6.7.5-1 Redwood Static Stress-Strain Properties

Strain (in/in)	Stress (psi)			
	Hot (Parallel to Grain)	Cold (Parallel to Grain)	Hot (Perpendicular to Grain)	Cold (Perpendicular to Grain)
0.000	0	0	0	0
0.025	7750	11310	750	1100
0.038	5990	8110	840	1190
0.250	6010	8420	1210	1800
0.440	5670	8160	1610	2450
0.500	5760	8310	2100	3210
0.630	6510	10430	5470	8760
0.690	11570	16780	10110	14660
1.000	33200	48150	30340	44010

Table 2.6.7.5-2 Balsa Static Stress-Strain Properties

Strain (in/in)	Stress (psi)			
	Hot (Parallel to Grain)	Cold (Parallel to Grain)	Hot (Perpendicular to Grain)	Cold (Perpendicular to Grain)
0.000	0	0	0	0
0.020	1850	2475	130	173
0.130	1676	2242	117	157
0.400	1550	2073	109	145
0.750	1550	2073	109	145
1.000	10000	13376	700	936

Table 2.6.7.5-3 Redwood Stress-Strain Properties (25 ε/sec)

Hot (Parallel to Grain)		Cold (Parallel to Grain)		Hot (Perpendicular to Grain)		Cold (Perpendicular to Grain)	
Strain (in/in)	**Stress (psi)**	**Strain (in/in)**	**Stress (psi)**	**Strain (in/in)**	**Stress (psi)**	**Strain (in/in)**	**Stress (psi)**
0.00	0	0.00	0	0.00	0	0.00	0
0.10	1109	0.10	1376	0.10	1318	0.10	1894
0.40	1506	0.40	1566	0.40	2168	0.40	3190
0.80	2497	0.80	3702	0.80	4249	0.80	6030

Table 2.6.7.5-4 Balsa Stress-Strain Properties (25 ε/sec)

Hot (Parallel to Grain)		Cold (Parallel to Grain)		Hot (Perpendicular to Grain)		Cold (Perpendicular to Grain)	
Strain (in/in)	**Stress (psi)**	**Strain (in/in)**	**Stress (psi)**	**Strain (in/in)**	**Stress (psi)**	**Strain (in/in)**	**Stress (psi)**
0.000	0	0.000	0	0.000	0	0.000	0
0.067	1398	0.224	2350	0.069	101	0.069	207
0.606	900	0.625	2116	0.630	270	0.630	550

Table 2.6.7.5-5 Properties for the Impact Limiter Stainless Steel Shells

Property	Value
Mass Density, ρ	7.51E-04 lb-sec^2/in^4
Modulus of Elasticity, E	27.9E6 psi
Poisson's Ratio, ν	0.30

Stress-Strain Curve for Type 304 Stainless Steel

STRESS (psi)	STRAIN (in/in)
23,809	0.000041
28,033	0.001180
29,500	0.003180
31,970	0.007180
36,900	0.015100
42,300	0.039200
85,080	0.230000

Table 2.6.7.5-6 Summary of Peak Accelerations and Maximum Crush Depths

Drop Orientation and Conditions		Peak Acceleration (g)		Design Basis Acceleration (g)	Maximum Crush (in)	
		Top Limiter	Bottom Limiter		Top Limiter	Bottom Limiter
1-Foot	Side Drop-Cold	13.5	13.2	20	1.1	1.4
	Side Drop-Hot	12.3	10.0	20	1.2	1.7
	Top End Drop-Cold	12.4	—	20	2.0	—
	Bottom End Drop Hot	—	9.6	20	—	2.0
	Corner Drop (24°) Cold	4.5	4.5	20	5.1	5.1
	Corner Drop (24°) Hot	3.9	3.9	20	6.1	6.1
30-Foot	Side Drop-Cold	56.2	53.1	60	10.7	13.4
	Side Drop-Hot	55.6	48.1	60	11.7	15.0
	Top End Drop-Cold	57.8	—	60	10.0	—
	Bottom End Drop Hot	—	40.7	60	—	11.0
	Corner Drop (24°) Cold	36.5	36.5	60	18.6	18.6
	Corner Drop (24°) Hot	35.3	35.3	60	20.2	20.2

Table 2.6.7.5-7 Quarter-Scale Model Impact Limiter Analysis Results Comparison to Drop Test Results

NAC-STC[1] Transport Cask Drop Orientation	Quarter-Scale Model Drop Test Accelerometer Filtered Results (g)		LS-DYNA Prediction for Accelerations Filtered Results (g)		Design Basis Accelerations (g)
	Top	Bottom	Top	Bottom	
End Drop	222	N/A	222	N/A	224.4
Side Drop	205	204	211	216	220.0
Corner Drop	117	N/A	130	N/A	220.0
Slap-down (75°)	181	180	188	181	220.0

1. NAC Storable Transport Cask (NAC-STC), NRC Docket 71-9235.

2.6.7.6 Closure Analysis

The Universal Transport Cask closure lid and the bolts are required to satisfy two criteria: (1) calculated maximum stresses must be less than the allowable stress limit (the material yield strength is conservatively selected), and (2) lid deformation or rotation at the O-rings must be less than the elastic rebound of the O-rings. Using consistently conservative assumptions, the NUREG/CR6007 [9] analysis of the cask closure system demonstrates that the cask closure assembly satisfies the performance and structural integrity requirements of 10 CFR 71.71(c)(7) for normal conditions of transport. The NUREG/CR-6007 analysis is summarized in the following paragraphs.

NUREG/CR-6007 provides formulas for calculating bolt forces generated by all regulatory (normal and hypothetical accident) transportation loading. Specifically, the report deals with the bolt stress analysis of a circular, cylindrical cask with a flat, circular, closure lid.

To ensure positive closure, the cask has 48 bolts 2–8 UN–2A socket head cap screws fabricated from SB-637, grade N07718. Material properties are taken at 275°F for the cask lid, closure bolts, and cask wall. A maximum temperature gradient of 3°F through the thickness of the cask lid is used as well. For evaluation purposes, a maximum internal pressure of 80 psi is used.

Accelerations are based on the impact limiter analysis for normal conditions of transport. Therefore, an acceleration of 20 g (1-foot drop) is taken to be the worst case. The 20 g load is also used for the vibration case. A factor of 1.1 is used for the dynamic load. The following calculations are a summary of the NUREG/CR-6007 evaluation based on the calculated preload of 111,680 lb/bolt.

The preload on the cask lid closure bolts considers the following factors: (1) an internal pressure force on the inner lid of 80 psi; (2) the O-ring compression force; and (3) the inertial weight of the lid, canister, basket, and fuel due to the 30-ft accident corner drop conditions. Based on the above considerations, a preload of 111,680 pounds/bolt is conservatively selected for the cask lid closure bolts. A minimum torque value of 3,738 foot-pounds, develops a tensile preload force of 111,680 pounds/bolt based on the following relationship:

$$T = F\left[\frac{L}{2\pi} + \frac{d_m \mu}{2\cos\alpha} + \frac{(d+b)\mu}{4}\right] \qquad [46]$$

where:

T = applied torque in inch-pounds
F = preload force in pounds
d = bolt diameter = 2.0 in
b = bolt head diameter = 3.75 in. (at the bottom of the bolt head)
d_m = mean diameter of threads = 1.9188 in
α = one-half the thread angle = 30°
μ = coefficient of friction = 0.15
N = 8 threads per inch
L = 1/N

Therefore, the minimum torque, T, required to develop the preload of 111,680 pounds/bolt is determined as:

$$T = F(0.4017) \div 12$$

$$T = 3{,}738 \text{ foot-pounds}$$

An installation torque of 3,900 ±100 foot-pounds is specified to ensure that the minimum required torque of 3,739 foot-pounds is achieved.

Maximum stresses in the closure bolt result during the top-end corner drop (23.35° from axial plane of cask) assuming the closure bolts support the full weight of the cask lid and contents. This is conservative since during a top-end drop, the cask lid is fully supported by the impact limiter; thus, the closure bolts do not carry any weight. For the following evaluation, only worst case forces and stresses are reported.

The tensile force per bolt, F_{a_pt}, due to preload and thermal is:

$$F_{a_pt} = P_L + P_{th} = 134{,}877 \text{ pounds}$$

where P_L = 111,680 pounds, preload

P_{th} = 23,197 pounds resulting from thermal expansion

The tensile force per bolt, F_{a_al}, from all other credible loads is:

$$F_{a_al} = P_o + P_i + P_{20} + P_v = 59{,}573 \text{ pounds}$$

where P_o = 667 pounds, load resulting from O-ring compression and operation

P_i = 6,549 lb, load resulting from internal pressure

P_{20} = 48,662 lb, load due to 20 *g* top-end corner impact.

P_v = 3,695 pounds, load resulting from 20 g vibration.

Since F_{a_pt} is greater than F_{a_al}, the total tensile bolt load, F_a, is equal to F_{a_pt}:

$$F_a = 134{,}877 \text{ pounds}$$

The shear load is

$$F_s = |P_i + P_{th} + P_{20} + P_v| = 37{,}242 \text{ pounds}$$

where P_i = 15,245 pounds, load resulting from internal pressure

P_{th}= -57,647 pounds, load resulting from temperature difference between the cask lid and upper forging

P_{20} = 1,465 pounds, load resulting from 20 g top-end corner drop

P_v = 3,695 pounds, load resulting from 20 g side vibration load

The bending moment is

M_b = -675 inch-pounds, due to thermal load (other loads do not contribute due to cask lid design).

and the load resulting from torsion is

M_t = 22,440 inch-pounds.

These loads and moments translate into the following stresses:

The tensile stress in the bolt is:

$$\sigma_a = \frac{1.2732 F_a}{D^2} = 48{,}679 \text{ psi}$$

where D = 1.878 in., minimum bolt diameter. The shear stress is

$$\tau = \frac{1.2732 F_s}{D^2} = 13{,}441 \text{ psi}$$

Where D = 1.878 in., minimum bolt diameter.

The bending stress is

$$\sigma_b = \frac{10.186 M_b}{D^3} = 1{,}038 \text{ psi}$$

where D = 1.878 in., minimum bolt diameter.

The stress resulting from torsion is

$$\tau_t = \frac{5.093 M_t}{D^3} = 17{,}249 \text{ psi}$$

where D = 1.878 in., minimum bolt diameter.

For normal conditions, Table 6.1 of NUREG/CR-6007 requires that the average tensile stress is less than S_m (where $S_m = 2/3\ S_y$), or

$$\sigma_{t(ave)} = \sigma_a = 48{,}679 \text{ psi} < S_m = 94{,}350 \text{ psi.}$$

Table 6.1 also requires that the average shear, which is comprised of the average direct shear (τ) be less than 0.6 S_m. This is expressed as

$$\sigma_{s(ave)} = \tau = 13{,}441 \text{ psi} < 0.6\ S_m = 56{,}610 \text{ psi.}$$

For the combined state of stress that includes tension plus shear, the square of the computed average tensile stress divided by the allowable tensile stress plus the square of the average shear stress divided by the allowable shear stress must be less than 1. This is expressed as

$$\left(\frac{48{,}679}{94{,}350}\right)^2 + \left(\frac{13{,}441}{56{,}610}\right)^2 = 0.33 < 1.$$

For the combined state of stress that includes tensile, shear, and bending; the bolts must have a maximum stress intensity less than 1.35 S_m (when the minimum tensile strength is greater than 100,000 psi). Therefore, the maximum stress intensity is

$$\sigma_{total} = \sqrt{\left[\left(\sigma_a + \sigma_b\right)^2 + 4\left(\tau_t + \tau\right)^2\right]} = 78{,}989 \text{ psi} < 1.35\ S_m = 127{,}372 \text{ psi.}$$

The margin of safety for ASME SB-637, Grade N07718 closure bolts is 0.61.

2.6.7.6.1 Bolt Fatigue Evaluation

For the 2.00-inch closure bolts the fatigue life of 944 cycles is obtained from ASME Code Section III, Appendix I, Table I-9.1, Figure I-9.4 [17].

The maximum stress, S, on the cask closure bolts is:

$$S = \frac{4.0F}{A} = \frac{4.0(142{,}691)}{2.77} = 206{,}053 \text{ psi} \quad (206.053 \text{ ksi})$$

where:

$F = F_i + F_{th} = 119{,}494 + 23{,}197 = 142{,}691$ lb

$$F_i = \frac{12T}{\left(\frac{L}{2\pi} + \frac{d_2\mu_1}{2\cos\alpha} + \frac{(d+b)\mu_2}{4}\right)} = 119{,}494 \text{ lb (maximum preload force)}$$

T = 4,000 ft-lb (maximum initial torque, see Section 2.6.7.6)
F_{th} = 23,197 lb (thermal load, see Section 2.6.7.6)
A = 2.77 in^2, the cross-sectional tensile area of the bolt
4.0 = the stress reduction factor per NB-3232.3(c)

The number of cycles (N) is ([17], Table I-9.1):

$$N = N_i\left(\frac{N_j}{N_i}\right)^{\log\left(\frac{Si}{S}\right)\Big/\log\left(\frac{Si}{Sj}\right)} \text{ or } N = 500\left(\frac{1000}{500}\right)^{\log\left(\frac{143}{103.03}\right)\Big/\log\left(\frac{143}{100}\right)} = 944 \text{ cycles}$$

where

the maximum nominal stress (206.053 ksi) < $2.7S_m$ = 254.7 ksi, and the alternating stress (S_{alt}) is: (206.053 – 0)(0.5) = 103.027 ksi
N_i = 500 cycles
N_j = 1000 cycles
S_i = 143 ksi
S_j = 100 ksi

2.6.7.7 Neutron Shield Analysis

The Universal Transport Cask neutron shield is evaluated for two distributed-load conditions: a 1-foot end-drop event and a 1-foot side-drop event. For each of these conditions, the solid neutron shielding material applies a load on the neutron shield shell. The weights of the neutron shield shell and fins are included in the analysis. The neutron shield geometry is shown in Figure 2.6.7.7-1.

2.6.7.7.1 End Plate 1-Foot End-Drop Analysis

The primary loading on the neutron shield shell and end plates is the weight of the NS-4-FR neutron shielding material. The neutron shield is also evaluated for the impact loading of the NS-4-FR during a 1-foot bottom-end-drop event.

$$p = d_B L + d_p t, = 11 \text{ psi}$$

where:

d_B = 0.0607 lb/in^3, the density of NS-4-FR
L = 178.56 in, height of NS-4-FR material
d_p = 0.291 lb/in^3, density of Type 304 stainless steel
t = 0.5 in, plate thickness

The deceleration of the package during a 1-foot end-drop event is 20g. The impact load on the plate is calculated as PI = p(20) = 220 psi.

The material properties (conservatively taken at 300°F) for the Type 304 stainless steel shell, fins and bottom plate are:

S_u = 66,000 psi
S_y = 22,500 psi
$S_s = (0.5)S_y$ = 11,250 psi

Allowable Stresses

The allowable stress intensity for normal condition loading is (Regulatory Guide 7.6):

$$S_{allow} = \text{Axial} + \text{Bending} = 1.5\ S_m = 30{,}000 \text{ psi},$$

Where S_m is equal to 20,000 psi for Type 304 stainless steel.

Calculated Stresses

From Table 26, Case 1 [28]:

$$S_s = \frac{\beta P b^2}{t^2} = 12{,}028 \text{ psi}$$

where:

$P = P_I$ = 220 psi
a = 11.49 inch and b = 4.5 inch
t = 0.5 inch
β= 0.675

The margin of safety is:

$$MS = \frac{30{,}000}{12{,}028} - 1 = +1.49$$

For the reaction in the welds, conservatively assuming all welds are quarter-inch fillets:

$$q_w = \frac{(P)(b)(a)}{(2)(b+a)} = \frac{(220)(4.5)(11.49)}{(2)(4.5+11.49)} = 356\,\text{lb/in}$$

The allowable shear/inch is (0.707)(0.25)(Ss), or 1,988 lb/in. Therefore the Margin of Safety is:

$$MS = \frac{1{,}988}{356} - 1 = 4.58$$

Figure 2.6.7.7-1 Neutron Shield Geometry

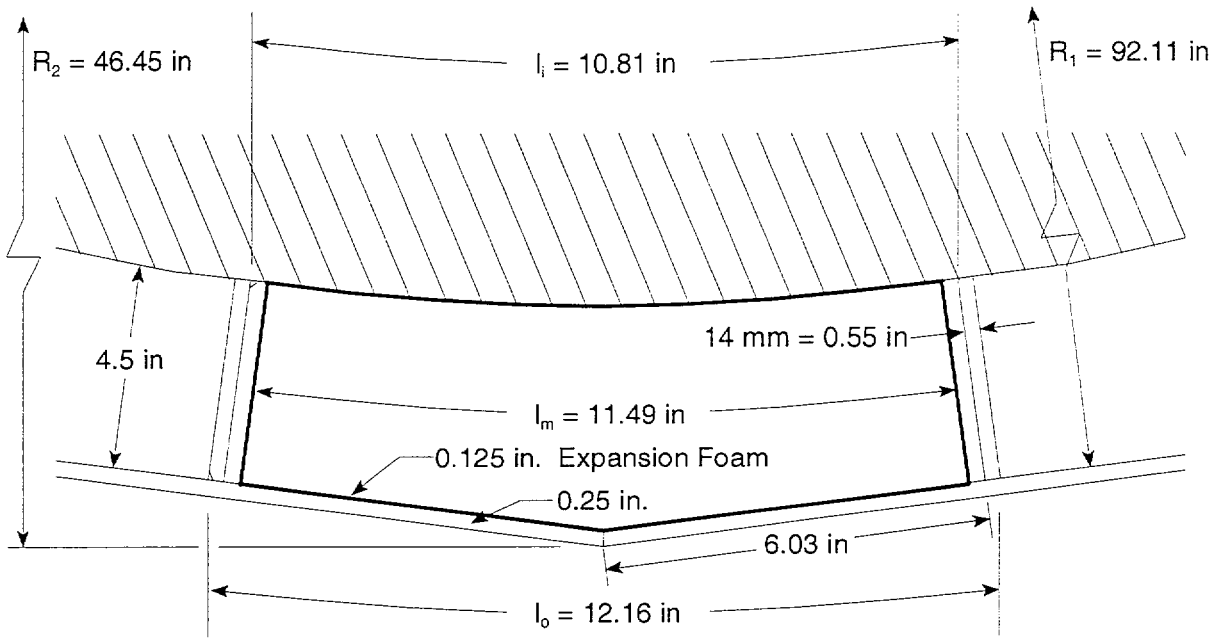

Neutron Shield Bottom Plate Attachment

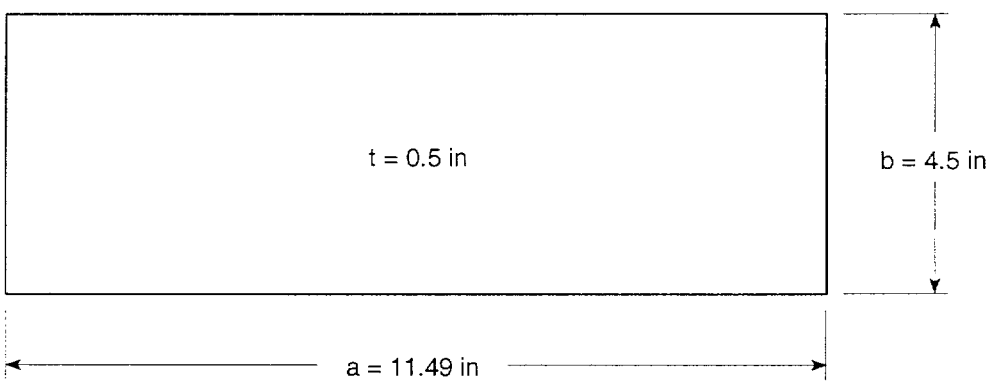

Equivalent Flat Plate Simply Supported

2.6.7.7.2 Side-Drop Analysis

This analysis assumes that the cask is subjected to a 1-foot side-drop event. The side-drop impact force is limited by the upper and lower impact limiters. For this analysis, an impact force equivalent to a 20-*g* side impact is used. The cask is stopped by the impact limiter before the neutron shield contacts the impacted surface. Therefore, the impact force is distributed through the cask body from the impact limiters. The impact deceleration force of the weight of the neutron shielding material is reacted by the neutron shield shell and fins, which transfer the load to the cask body. The NS-4-FR neutron shielding material is assumed to act as an internal pressure on the shell.

Because the structural function of the neutron shield shell and radial heat transfer fins is to support the NS-4-FR radial neutron shield, ASME Code Section III, Subsection NF [19] is used as the governing structural criterion for the evaluation of the welds connecting the radial heat transfer fins to the neutron shield shell and cask outer shell.

In addition to assuming the conservative load combination resulting from cold impact loads and discontinuity thermal expansion between the NS-4-FR and radial fin from hot, steady-state conditions, an additional 3-psi pressure is assumed to have been created from potential gas loss from the NS-4-FR subjected to extended service in a high end temperature environment.

Following the methodology of the ASME Code, Section III criteria and cask design practice, the load on the weld joints has been categorized into the following service-level conditions

Service Level B

1. Pressure developed on the neutron shield shell from differential radial thermal expansion of the NS-4-FR neutron shield is relative to the Type 304 stainless steel radial heat transfer fin. The thermal expansion is

$$T_E = (\alpha \times L \times \Delta T)_{NS-4-FR} - (\alpha \times L \times \Delta T)_{304SS}$$
$$= (4.72 \times 10^{-5})(11.49)(75) - (8.79 \times 10^{-6})(11.49)(75)$$
$$= 0.033 \text{ in.}$$

where

$\alpha_{NS\text{-}4\text{-}FR}$ = 4.72×10^{-5} in/in/°F, coefficient of thermal expansion at 158°F

α_{304SS} = 8.79×10^{-6} in/in/°F, coefficient of thermal expansion at 200°F

L = Length of the section

ΔT = 150 - 75 = 75°F, average temperature differential

Considering differential thermal expansion and 3% initial compression of the HT800 expansion foam on the inside surface of the neutron shield shell, a compressive load develops. The total compression is

$$\text{Compression} = 3\% \, (0.125) + 0.033 = 0.037 \text{ in}$$

The equivalent compression of the foam is

$$\%\ \text{Compression} = \frac{0.037}{0.125} \times 100 = 29.6\% \, .$$

Interpolating the manufacturer design information presented in Table 4.2-1, the equivalent pressure load developed on the neutron shield shell is 12.1 psi.

2. Potential pressure developed from extended service of the NS-4-FR neutron shield at high-end temperatures is defined as 3 psi for this evaluation.

Service Level C

1. Service Level B loads plus dynamic induced load from a postulated one foot side impact (20 *g*).

   Considering the mass of the neutron shield shell and NS-4-FR, the effective pressure load becomes

$$P = MA = (0.346)(20) = 6.9 \text{ psi}$$

where, from the dimensions provided in Fig. 2.6.7.7-1

M= [(4.5)(0.0607) + (0.25)(0.291)] x 1 = .346 lb, the mass of a 1 in^2 unit area,

A= 20 g, the acceleration during a side drop.

Service Level D

1. Service Level B loads plus dynamic induced load from a postulated 30-foot side impact (60 g). Considering the mass of the neutron shield shell and the NS-4-FR, the effective pressure load becomes

$$P = (0.346)(60) = 20.8 \text{ psi.}$$

The following evaluation is presented for two different load orientations of the fin welds. Case 1 represents the loads induced as a result of loading applied to the neutron shield and Case 2 represents loading applied to the radial heat transfer fin.

Case 1—Neutron Shield Shell Loading

Implementing the design criteria for noncontainment support structures presented in NF-3250, normal operation load service level stress in the weld region connecting the neutron shield shell to the radial heat transfer fin is evaluated using a conservative simplification of the plate and shell structure to that of a uniformly loaded beam having unit depth.

The maximum tension stress from Service Level B is:

$$S = \frac{6m}{t^2} \; 17{,}867 \text{ psi}$$

where $m = \frac{wl^2}{12} = 186.1 \text{ in.} - \text{lb}$

$t = 0.25 \text{ in.}$

and $w = 12.1 + 3 = 15.1 \text{ psi}$

$l = 12.16 \text{ in.}$

Allowable stress limits defined in NF-3256.2 and Table NF-3522 (b)-1 for full penetration groove welds define acceptable stress for this condition load as

$$S_{all} = 1.33 \times 1.5 \times 17{,}200 = 34{,}314 \text{ psi}$$

Thus, the margin of safety is

$$MS = \frac{34{,}314}{17{,}867} - 1 = +92.$$

The maximum tension stress for Service Level C load is:

$$S = \frac{6m}{t^2} \; 26{,}024 \text{ psi}$$

where $m = \frac{wl^2}{12} = 271.1 \text{ in.} - \text{lb}$

$t = 0.25 \text{ in.}$

and $w = 15.3 + 6.9 = 22.0 \text{ psi}$

$l = 12.16 \text{ in.}$

Allowable membrane plus bending stress limits defined in NF-3256.2 for Service Level C limits is

$$S_{all} = 1.5 \times 1.5 \times 17{,}200 = 38{,}700 \text{ psi}$$

Thus, the margin of safety is

$$MS = \frac{38{,}700}{26{,}024} - 1 = +0.49.$$

The maximum tension stress for Service Level D load is

$$S = \frac{6m}{t^2} = 31{,}850 \text{ psi}$$

As directed by NE-3256.2 for Service Level D, qualification of the structure is based on ASME Code Section III, Appendix F, [17] Paragraph F-1340, "Acceptance Criteria Using Plastic System Analysis."

Considering plastic failure of fixed-end beams with uniformly distributed load, the plastic moment then becomes (from [28] Table 15, Case 2d):

$$m = \frac{wl^2}{16} = 331.8 \text{ in.-lb}$$

where $w = 15.1 + 20.8 = 35.9$ psi

$l = 12.16$ inch

$t = 0.25$ inch

Paragraph F-1340 defines the allowable primary membrane plus primary bending stress intensity as the lesser of 1.5 ($2.4S_m$) and 1.5 ($0.7S_u$). Implementation of this criterion limits Service Level D stress to 68.8 ksi.

$$MS = \frac{68{,}800}{31{,}850.3} - 1 = +1.16 .$$

In addition to the evaluation of the maximum local bending stress in the weld region, shear stress is evaluated as follows:

Service Level	w (psi)	$S_s = \frac{wl}{2t}$ (psi)	Allowable Stress (psi)	MS
B	15.10	367	1.33 (.4S_y) = 12,700	+ Large
C	22.00	535	1.5 (.4S_y) = 14,000	+ Large
D	36.10	878	0.42 (S_u) = 28,900	+ Large

where $l = 12.16$

$t = 0.25$

Case 2—Heat Transfer Fin Loading

Following a similar method as used in the evaluation of the neutron shield shell, the heat transfer fin is evaluated by using a uniformly loaded beam with a fixed end at the cask outer shell surface and a simple support at the neutron shield shell. Because Level B load is developed from radial thermal growth of the NS-4-FR and postulated off gas pressure, Service Level B does not load the fin in the lateral direction. Tension stress developed in the fin from these radial loads is 70 psi, which is insignificant.

Lateral load from Service Level C produces the following stress:

$$S = \frac{6m}{t^2} = 2{,}135 \text{ psi}$$

where $m_{max} = \frac{wl^2}{8} = 35.3$ in.-lb

$w = (0.0607)(11.49)(20) = 13.95$ lb

$$l = \frac{92.11 - 82.61}{2} - 0.25 = 4.5 \text{ in.}$$

$$t = 0.315 \text{ in. (8 mm)}$$

From the preceding evaluation of the neutron shield shell, the service level C allowable is 38,925 psi. Therefore,

$$MS = \frac{38{,}925}{2{,}135} - 1 = \text{Large}.$$

Lateral load for Service Level D produces the following stress:

$$S = \frac{6m}{t^2} = 8{,}540 \text{ psi}$$

where $m_{max} = \frac{wl^2}{6} = 141.23$ in.-lb

$$w = (0.0607)(11.49)(60) = 41.85 \text{ lb}$$

$$l = 4.5 \text{ in.}$$

$$t = 0.315 \text{ in. (8 mm).}$$

Using the acceptance criteria for an elastic system analysis provided in the ASME Code Section III, Appendix F, Paragraph F-1332.2, ($1.5 \times 1.2S_y$ or $1.5 \times 1.55S_m < 1.5 \times .7S_u$).

$$S_{All} = 45{,}000 \text{ psi}$$

$$MS = \frac{45{,}000}{8{,}540} - 1 = 4.27$$

In addition to the evaluation of the maximum local bending stress in the weld region, shear stress is evaluated as follows:

Service Level	w (psi)	$S_s = \frac{wl}{2t}$ (psi)	Allowable Stress (psi)	MS
C	13.95	6,126	14,400	+ Large
D	41.85	377	28,900	+ Large

where $l = 4.5$ in.

$t = 0.25$ in.

Therefore, the heat transfer load path through the welds connecting the neutron shield skin to the radial heat transfer fins is maintained for all transport package normal and accident condition loads.

2.6.7.8 Upper Ring/Outer Shell Intersection Analysis

When the cask is lifted at the lifting trunnions bending stresses are induced in the upper ring and outer shell intersection region of the cask body. These stresses are evaluated by means of a closed-form ring solution (from [29], pp. 390-393). The support provided by the bolted cask lid is conservatively neglected in this analysis.

The geometry and loading of the equivalent ring are defined as follows:

F = lifting force (not including weight of impact limiter)

$$= \frac{260{,}000}{2} = 130{,}000 \text{ lb}$$

q = dead weight load per unit length

W = width of equivalent ring = 3.45 in.

r = mean radius of the equivalent ring = 40.905 in.

$$a = \text{moment arm for the equivalent ring} = 45.63 - 40.905 = 4.725 \text{ in.}$$

On the basis of a total weight of 260,000 lb, q is calculated as:

$$q\,(\pi)(40.905)(2) = 260{,}000 \;\Rightarrow\; q = 1{,}011.6 \text{ lb/in.}$$

The moment and torque on the equivalent ring are given by

$$M = \frac{T_o \sin\theta}{2} - qr^2\left(1 - \frac{\pi}{2}\sin\theta\right)$$

$$T = \frac{T_o \cos\theta}{2} - qr^2\left(\theta + \frac{\pi}{2}\cos\theta - \frac{\pi}{2}\right)$$

where theta, θ, is measured from the trunnion ($\theta = 0$) in plane perpendicular to the centerline of the cask ($0 \le \theta \le 180$).

$$T_o = (F)(a) = (130{,}000)(4.725) = 611{,}997 \text{ in-lb.}$$

Substituting for T_o, q, and r,

$$M = 3.06 \times 10^5 \sin\theta - 1.693 \times 10^6\left(1 - \frac{\pi}{2}\sin\theta\right)$$

$$T = 3.06 \times 10^5 \cos\theta + 1.693 \times 10^6\left(\theta + \frac{\pi}{2}\cos\theta - \frac{\pi}{2}\right).$$

The normal stress is treated as bending resulting from the moment acting over a cross section.

$$\sigma = \frac{M(h/2)}{I} = 0.00511M$$

where $h = 18.44$ in

$$I = \frac{Wh^3}{12} = \frac{3.45 \times 18.44^3}{12} 14 = 1802.7 \text{ in}^4$$

The shear stress is (Roark's, 6th Edition, Table 20, Case 4)

$$\tau = \frac{3T}{8ab^2}\left[1 + 0.6095\frac{b}{a} + 0.8865\left(\frac{b}{a}\right)^2 - 1.8023\left(\frac{b}{a}\right)^3 + 0.9100\left(\frac{b}{a}\right)^4\right] = 0.0176T$$

where $a = \frac{h}{2} = \frac{18.44}{2} = 8.22$ in, length of longer side,

$b = \frac{w}{2} = \frac{3.45}{2} = 1.725$ in, length of shorter side.

The maximum stress intensity, where the moment and torque are functions of s, is calculated as

$$SI = 2\sqrt{\frac{\sigma^2}{4} + \tau^2} = 2\sqrt{(6.528 \times 10^{-6})M^2 + (3.10 \times 10^{-4})T^2}\,.$$

Resultant values of the stress intensity are evaluated in Table 2.6.7.8-1. The minimum margin of safety is

$$MS = \frac{30{,}000}{28{,}309} - 1 = +0.06$$

where $S_m = 20{,}000$ psi

$S_{allow} = 1.5\, S_m = 30{,}000$ psi.

Table 2.6.7.8-1 Resultant Stress Intensity Values in the Equivalent Ring

Angle [1] (degrees)	Moment (in-lb)	Torque (in-lb)	SI (psi)
0.0	$-1.693(10)^6$	$3.060(10)^5$	13,819
5.0	$-1.435(10)^6$	$4.425(10)^5$	17,219
10.0	$-1.178(10)^6$	$5.564(10)^5$	20,498
15.0	$-9.255(10)^5$	$6.482(10)^5$	23,310
20.0	$-6.788(10)^5$	$7.181(10)^5$	25,525
25.0	$-4.398(10)^5$	$7.669(10)^5$	27,098
30.0	$-2.103(10)^5$	$7.952(10)^5$	28,021
35.0	$7.860(10)^3$	$8.039(10)^5$	28,309
40.0	$2.131(10)^5$	$7.942(10)^5$	27,987
45.0	$4.038(10)^5$	$7.671(10)^5$	27,093
50.0	$5.786(10)^5$	$7.242(10)^5$	25,671
55.0	$7.361(10)^5$	$6.667(10)^5$	23,775
60.0	$8.751(10)^5$	$5.962(10)^5$	21,466
65.0	$9.945(10)^5$	$5.145(10)^5$	18,817
70.0	$1.094(10)^6$	$4.232(10)^5$	15,917
75.0	$1.171(10)^6$	$3.243(10)^5$	12,892
80.0	$1.227(10)^6$	$2.194(10)^5$	9,952
85.0	$1.261(10)^6$	$1.107(10)^5$	7,531
90.0	$1.272(10)^6$	0.0000	6,502

[1] The Angle is measured from the centerline of the trunnion.

2.6.8 Corner Drop

The Universal Transport Cask is composed of materials other than fiberboard or wood, and the weight of the package exceeds 220 lb (100 kg). Therefore, according to 10 CFR 71.71(c)(8), this test is not applicable to the Universal Transport Cask.

2.6.9 Compression

According to 10 CFR 71.71(c)(9), this test is not applicable to the Universal Transport Cask because the package weight is greater than 11,000 lb (5,000 kg).

2.6.10 Penetration

According to 10 CFR 71.71(c)(10), a penetration test involving a 13-lb (6-kg) penetration cylinder dropped from a height of 1 m is required for evaluation of packages during normal conditions of transport. However, Regulatory Guide 7.8 states that "the penetration test of 71.71 is not considered by the NRC staff to have structural significance for large shipping casks (except for unprotected valves and rupture disks) and will not be considered as a general requirement." Because the Universal Transport Cask has no unprotected valves or rupture disks that could be affected by normal conditions of transport, a penetration test is not performed.

2.6.11 Fabrication Stresses

The process of manufacturing the Universal Transport Cask can introduce thermal stresses in the inner and outer shells as a result of pouring molten lead between them. These thermal stresses are evaluated in this section to provide assurance that the manufacturing process does not adversely affect the normal operation of the cask or its ability to survive an accident. According to Regulatory Position 7 of Regulatory Guide 7.6, any residual stresses in the containment vessel shell resulting from inelastic strain associated with the secondary local bending stresses, which are due to the lead pour thermal gradient, must be considered in the total stress range for normal and accident load conditions. Residual stresses in the containment vessel and the outer shell induced by shrinkage of the lead shielding after the lead pouring operation are relieved early in the life of the cask because of the low creep strength of lead.

For the lead pour process, the initial temperature of the cask shells is controlled between 550°F and 650°F, and the lead temperature before pouring is between 698°F and 790°F. The cask is initially heated, at a rate not to exceed 90°F/hour, by using heaters inside the inner shell and heating rings around the outside of the outer shell. Heat-up is time-controlled consistent with uniform increases in shell temperatures. The heating procedures ensure that the cask surface temperature does not exceed 800°F during the molten lead pouring process. The shell temperatures are measured by thermocouples attached to the shell surfaces. A portable thermometer is also used to measure temperature at any location. To minimize the time that the cask is at elevated temperatures, cask heating begins only after all preparations have been completed.

The lead is poured after the cask reaches the specified temperatures. Molten lead is poured continuously through a filling tube with its open end maintained under the lead surface. The pouring time is kept as short as possible. During pouring, the interior heaters and exterior heating rings are continuously energized.

The cooling process consists of sequentially turning the exterior heating rings and interior heaters off, starting from the lowest point, and of spraying the cask with water from the outside. A layer of molten lead is maintained until the upper surface starts to solidify. This process allows the molten lead to fill the open space below it created by the lead shrinkage as it cools. The basic requirements and procedures for the Universal Transport Cask lead pour operations are described in Section 8.3.3.

2.6.11.1 Lead Pour

2.6.11.1.1 Cask Shell Geometry

At 70°F, the Type 304 stainless steel shell geometry is:

Inner Shell

Inside Diameter ($d_{i\text{-}70}$) = 67.61 in.

Outside Diameter ($d_{o\text{-}70}$) = 71.61 in.

Shell Thickness (t_i) = 2 in.

Outer Shell

Inside Diameter ($D_{i\text{-}70}$) = 77.11 in.

Outside Diameter ($D_{o\text{-}70}$) = 82.61 in.

Shell Thickness ($T_{o\text{-}70}$) = 2.75 in.

2.6.11.1.2 Stresses Resulting from Lead Pour

The hydrostatic pressure produced by the column of lead is:

$$q = \rho h = 73.8 \text{ psi}$$

where $\rho = 0.41 \text{ lb/in}^3$ (lead density)

$h = 180$ in (maximum height of lead column)

For this analysis, it is assumed that the lead at a maximum temperature of 790°F, and the shell initially at 650°F, reach an equilibrium temperature of 750°F. At 750°F, key shell geometric dimensions are:

$$d_{o\text{-}750} = d_{o\text{-}70}\left(1 + \alpha \ \Delta T\right) = 72.09 \text{ in.}$$

$$D_{i\text{-}750} = D_{i\text{-}70}\left(1 + \alpha \ \Delta T\right) = 77.62 \text{ in.}$$

$$t_{i\text{-}750} = t_{i\text{-}70}\left(1 + \alpha \ \Delta T\right) = 2.01 \text{ in.}$$

where $\alpha = 9.76 \times 10^{-6}$ in/in/°F at 750°F (stainless steel)

$\Delta T = 750 - 70 = 680°F.$

The hydrostatic pressure of the molten lead subjects the inner shell to an external hydrostatic pressure, and the outer shell to an internal hydrostatic pressure. The hydrostatic pressure will vary from a maximum of 73.8 psi at the bottom of the inner shell to 0 psi at the top of the lead cylinder.

Using Reference [28] Table 29, Case 6, the deformation at the bottom of the inner shell, y_B, is found to be -1.955×10^{-3} in.

The maximum circumferential membrane stress in the inner shell is:

$$S_{\theta_{max}} = \frac{y_B E}{R} = -1323 \text{ psi}$$

where $E = 24.4\times10^{6}$ psi at 750°F

$R = 72.09/2 = 36.045$ in.

This stress will exist only as long as the lead is molten and will produce no plastic deformation of the inner shell. When the lead solidifies and begins to cool, it will shrink and exert a uniform external pressure on the inner shell because lead's coefficient of expansion is larger than that of stainless steel.

2.6.11.2 Cooldown

2.6.11.2.1 Hoop (Circumferential) Stresses

Lead decreases in volume during solidification. As the lower lead region solidifies, the molten lead above fills the shrinkage void between the solidifying lead and the inner and outer shells.

Using the coefficients of expansion for stainless steel and lead, the outer diameter of the steel shell and the inner diameter of the lead cylinder (assuming it is free to shrink) can be determined at 620°F (the melting point of lead) and at 70°F (normal conditions). Because the lead has a higher coefficient of expansion than stainless steel, a shrinkage force will develop between the steel shell outer surface and the lead inner surface. At 620°F, the outside diameter of the inner shell, and the inside diameter of the lead as it begins to solidify is:

$$d_{oshell620} = d_{oshell70}\left(1 + \alpha\ \Delta T\right) = 71.61\left(1 + 9.56 \times 10^{-6}(620 - 70)\right) = 71.98 \text{ in.}$$

where $d_{oshell70} = 71.61$ in.

$\alpha_{shell} = 9.56 \times 10^{-6}$ in./in./ °F (at 620°F)

If the lead were cooled without restraint to 70°F, the inner diameter of the lead cylinder would shrink to:

$$d_{ilead\,70} = d_{ilead\,620}\left(1 - \alpha\ \Delta T\right) = 71.98\left(1 - 20.2 \times 10^{-6}(620 - 70)\right) = 71.18 \text{ in.}$$

where

$d_{ilead620} = d_{oshell620} = 71.98$ in.

$\alpha_{lead} = 20.2 \times 10^{-6}$ in./in./°F

The interference between the lead cylinder and the inner shell is (71.61-71.18)/2 = 0.215 in. To fully accommodate this interference, the lead must be deformed 0.215 in.

For $\delta = 0.215$ in., the maximum circumferential stress, $S_{\theta max}$, in the inner shell is:

$$S_{\theta max} = \frac{\delta\,(E)}{R} = 13.8 \text{ psi}$$

where $R = 71.18/2 = 35.6$ in.

$E = E_{lead70} = 2.28 \times 10^3$ psi

From Reference [28], Table 29, Case 12, the radial deformation of the inner shell under a uniform external radial pressure of 13.8 psi is determined for values of x, the distance from the open end of the inner shell, at 0.15 ft increments and the results are tabulated in Table 2.6.11.2-1. Examination of the data in Table 2.6.11.2-1 shows that the maximum radial deformation and circumferential stress, S_θ, occur at x = 13.65 ft.

The maximum circumferential membrane stress in the inner shell is:

$$S_{\theta_{max}} = \frac{yE}{R} = -255.3 \text{ psi}$$

where y = the radial deformation, -3.299×10^{-4} in.

$E = 28.3\times10^{6}$ psi

$R = 71.61/2 = 35.805$ in.

Axial Stresses

Axial stresses also develop in the lead shell and inner shell during fabrication as a result of the unequal shrinkage of the lead and steel shells. Assuming that the lead bonds to the inner shell during the cooldown process after completion of lead pouring, the strain in the lead, when cooled to 70°F, is:

$$M_{lead} = (\alpha_{lead} - \alpha_{shell})\Delta T = 0.0060 \text{ in/in.}$$

where $\alpha_{lead} = 20.2 \times 10^{-6}$ in/in/°F

$\alpha_{shell} = 9.56 \times 10^{-6}$ in/in/°F

$\Delta T = 620 - 70 = 550$°F

$$S_{lead} = \varepsilon E = 0.006 \times 2.28\times10^{6} = 13{,}680 \text{ psi}$$

The calculated stress is above the yield point of lead (ranging from 20 psi at 620°F to 640 psi at 70°F). The axial load placed on the steel inner shell by shrinkage of the lead is therefore limited by the yield strength of lead. The maximum load is:

$$P_{lead} = 640 \times (38.56^2 - 35.805^2)\pi = 411{,}930 \text{ lb.}$$

The corresponding compression stress in the inner shell to maintain equilibrium is:

$$S_{shell} = \frac{P}{A} = \frac{-411{,}930}{\pi\left((35.805)^2 - (33.805)^2\right)} = -942 \text{ psi}$$

This value is conservative because the yield strength of lead is very low at elevated temperatures (505 psi at 200°F; 380 psi at 300°F), therefore, the creep rate is high. Also, complete bonding of

the lead to the stainless steel inner shell is not expected to occur. Because it is based on the yield strength of lead at 70°F, this case bounds all others to be considered for axial loading.

2.6.11.2.3 Effects of Temperature Differential During Cooldown

The preceding analyses assume that the inner and outer shells and the lead are always at the same temperature at any time during the cooldown process. This assumption may not be true under actual conditions. However, because of the high thermal conductivity of the stainless steel and the lead, and because of the time-controlled cooldown process, the temperature differential between any two of the above shells is kept to a minimum. To determine the effect of temperature differential on the stresses in the shells, a temperature differential of 100°F is used.

If the inner shell is cooler than the lead, the interference between them as well as the corresponding interface pressure and hoop stresses are less than for the case of equal temperatures. Hence, the preceding analysis is conservative.

If the inner shell is hotter than the lead shell, an analysis is required. Assume the temperature of the inner shell to be 170°F and that of the lead to be 70°F. The inner radius of the stress-free lead shell at 70°F is 35.59 in.; the outer radius of the inner shell at 170°F is:

$$r_o = 35.805\,[1 + (8.54 \times 10^{-6})(100)] = 35.836 \text{ in.}$$

The interference between the inner shell and the lead is 35.836 - 35.59 = 0.246 in. To fully accommodate this interference, the lead must undergo a deformation of 0.246 in.

For $\delta = 0.246$ in., $S = \dfrac{\delta(E)}{R} = 15.6$ psi

where $R = 71.18/2$ in. $= 35.59$ in.

$E = 2.28\times10^3$ psi (at 70°F)

Using the same method as in the previous section, the radial deformation of the inner shell at x = 13.65 ft., the point of maximum deflection, is found to be -3.293×10^{-4} in.

The maximum circumferential membrane stress in the inner shell is:

$$S_{\theta_{max}} = \frac{yE}{R} = \frac{-3.293\times10^{-4}\left(27.8\times10^{6}\right)}{35.836} = -255.5 \text{ psi}$$

The axial stress in the inner shell also increases when the inner shell is 100°F hotter than the lead shell. As shown previously, the axial load on the inner shell is limited by the yield strength of the lead. Therefore, the previously computed axial load is the bounding case for this analysis.

Temperature differentials between the inner and outer shells are of no consequence, because the axial restraint between them is welded in place after cooldown, when the cask is at a uniform ambient temperature. Welding of the outer shell and the bottom inner forging to the bottom outer forging after cooldown is, therefore, a necessary fabrication step.

2.6.11.3 Lead Creep

As discussed in Section 2.6.11, cooling of the lead shell and inner shell introduces acceptably low hoop and axial stresses in the inner shell. Because lead demonstrates a significant creep rate at both room and elevated temperatures, these small stresses will be relieved early in the life of the cask, and will be further relieved during the thermal test of the cask.

Table 2.6.11.2-1 Stress Analysis Results for Uniform Pressure Loading of Inner Shell Due to Lead Pouring

X (ft)	Hoop stress, σ_2 (psi)	Radial Deflection, y (in.)
0.00	-247.1	-0.00031
0.15	-247.1	-0.00031
0.30	-247.1	-0.00031
0.45	-247.1	-0.00031
0.60	-247.1	-0.00031
0.75	-247.1	-0.00031
0.90	-247.1	-0.00031
1.05	-247.1	-0.00031
1.20	-247.1	-0.00031
1.35	-247.1	-0.00031
1.50	-247.1	-0.00031
1.65	-247.1	-0.00031
1.80	-247.1	-0.00031
1.95	-247.1	-0.00031
2.10	-247.1	-0.00031
2.25	-247.1	-0.00031
2.40	-247.1	-0.00031
2.55	-247.1	-0.00031
2.70	-247.1	-0.00031
2.85	-247.1	-0.00031
3.00	-247.1	-0.00031
3.15	-247.1	-0.00031
3.30	-247.1	-0.00031
3.45	-247.1	-0.00031
3.60	-247.1	-0.00031
3.75	-247.1	-0.00031
3.90	-247.1	-0.00031
4.05	-247.1	-0.00031
4.20	-247.1	-0.00031
4.35	-247.1	-0.00031
4.50	-247.1	-0.00031
4.65	-247.1	-0.00031
4.80	-247.1	-0.00031

Table 2.6.11.2-1 Stress Analysis Results for Uniform Pressure Loading of Inner Shell Due to Lead Pouring (Continued)

X (ft)	Hoop stress, σ_2 (psi)	Radial Deflection, y (in.)
4.95	-247.1	-0.00031
5.10	-247.1	-0.00031
5.25	-247.1	-0.00031
5.40	-247.1	-0.00031
5.55	-247.1	-0.00031
5.70	-247.1	-0.00031
5.85	-247.1	-0.00031
6.00	-247.1	-0.00031
6.15	-247.1	-0.00031
6.30	-247.1	-0.00031
6.45	-247.1	-0.00031
6.60	-247.1	-0.00031
6.75	-247.1	-0.00031
6.90	-247.1	-0.00031
7.05	-247.1	-0.00031
7.20	-247.1	-0.00031
7.35	-247.1	-0.00031
7.50	-247.1	-0.00031
7.65	-247.1	-0.00031
7.80	-247.1	-0.00031
7.95	-247.1	-0.00031
8.10	-247.1	-0.00031
8.25	-247.1	-0.00031
8.40	-247.1	-0.00031
8.55	-247.1	-0.00031
8.70	-247.1	-0.00031
8.85	-247.1	-0.00031
9.00	-247.1	-0.00031
9.15	-247.1	-0.00031
9.30	-247.1	-0.00031
9.45	-247.1	-0.00031
9.60	-247.1	-0.00031
9.75	-247.1	-0.00031

Table 2.6.11.2-1 Stress Analysis Results for Uniform Pressure Loading of Inner Shell Due to Lead Pouring (Continued)

X (ft)	Hoop stress, σ_2 (psi)	Radial Deflection, y (in.)
9.90	-247.1	-0.00031
10.05	-247.1	-0.00031
10.20	-247.1	-0.00031
10.35	-247.1	-0.00031
10.50	-247.1	-0.00031
10.65	-247.1	-0.00031
10.80	-247.1	-0.00031
10.95	-246.9	-0.00031
11.10	-246.9	-0.00031
11.25	-246.9	-0.00031
11.40	-246.9	-0.00031
11.55	-246.9	-0.00031
11.70	-246.7	-0.00031
11.85	-246.7	-0.00031
12.00	-246.7	-0.00031
12.15	-246.7	-0.00031
12.30	-246.9	-0.00031
12.45	-247.1	-0.00031
12.60	-247.6	-0.00031
12.75	-248.2	-0.00031
12.90	-249.1	-0.00032
13.05	-250.4	-0.00032
13.20	-251.7	-0.00032
13.35	-253.2	-0.00032
13.50	-254.5	-0.00032
13.65	-255.3	-0.00032
13.80	-255.1	-0.00032
13.95	-253.2	-0.00032
14.10	-248.6	-0.00031
14.25	-240.7	-0.0003
14.40	-227.9	-0.00029
14.55	-209.9	-0.00027
14.70	-185.9	-0.00024
14.85	-156.5	-0.0002
15.00	-123.5	-0.00016

2.6.12 PWR Transportable Storage Canister Analysis - Normal Conditions of Transport

In this section, the Transportable Storage Canister assembly containing PWR fuel is evaluated for the normal conditions of transport. The principal components of the canister assembly are the canister, the fuel basket assembly, the shield lid, and the structural lid. The canister and the canister shell, bottom plate, and lids are shown in Figures 2.6.12-1 and 2.6.12-2.

Spacers are used to properly locate the canisters containing Class 1 and 2 PWR fuel in the cask cavity. The analysis of the spacers is presented in Section 2.6.16. The geometries and materials of construction of the canister, baskets, and spacers are described in Section 1.2.1.2.

2.6.12.1 Analysis Description

The Transportable Storage Canister contains and confines the spent fuel in the fuel basket. The canister is the defined confinement boundary for its contents during transport and storage operations, but the canister is not considered to provide containment during transport operation; the Universal Transport Cask provides the containment boundary for transport. The canister in the transfer cask serves as the handling component for its basket and contents during loading, closure, and transfer from the pool to storage or to the transport vehicle.

Three canisters of varying lengths are designed to accommodate the three classes of PWR fuel. The design parameters of the canisters are provided in Table 1.2-3. For this analysis, the canister is modeled with the heaviest fuel (Class 2).

The structural design criteria for the canister is from the ASME Code Section III, Subsection NB. Consistent with this criterion, the structural components of the canister are shown to satisfy the allowable stress limits presented in Tables 2.1.2-2 and 2.1.2-3 as applicable. The allowable stresses used in this analysis are based on a temperature of 380°F for all locations in the canister, unless otherwise indicated. These allowables are conservative for all sections in the canister with the exception of Sections 5 and 6 (see Figure 2.6.12.3-1 for section locations).

For the canister structural lid weld (Section 13, Figure 2.6.12.3-1), base metal properties are used to define the allowable stress limits since the weld filler rod tensile properties are greater than the base metal. Also, the allowable stress is multiplied by a stress reduction factor of 0.8 per ISG-4 [49].

Figure 2.6.12-1 PWR Transportable Storage Canister

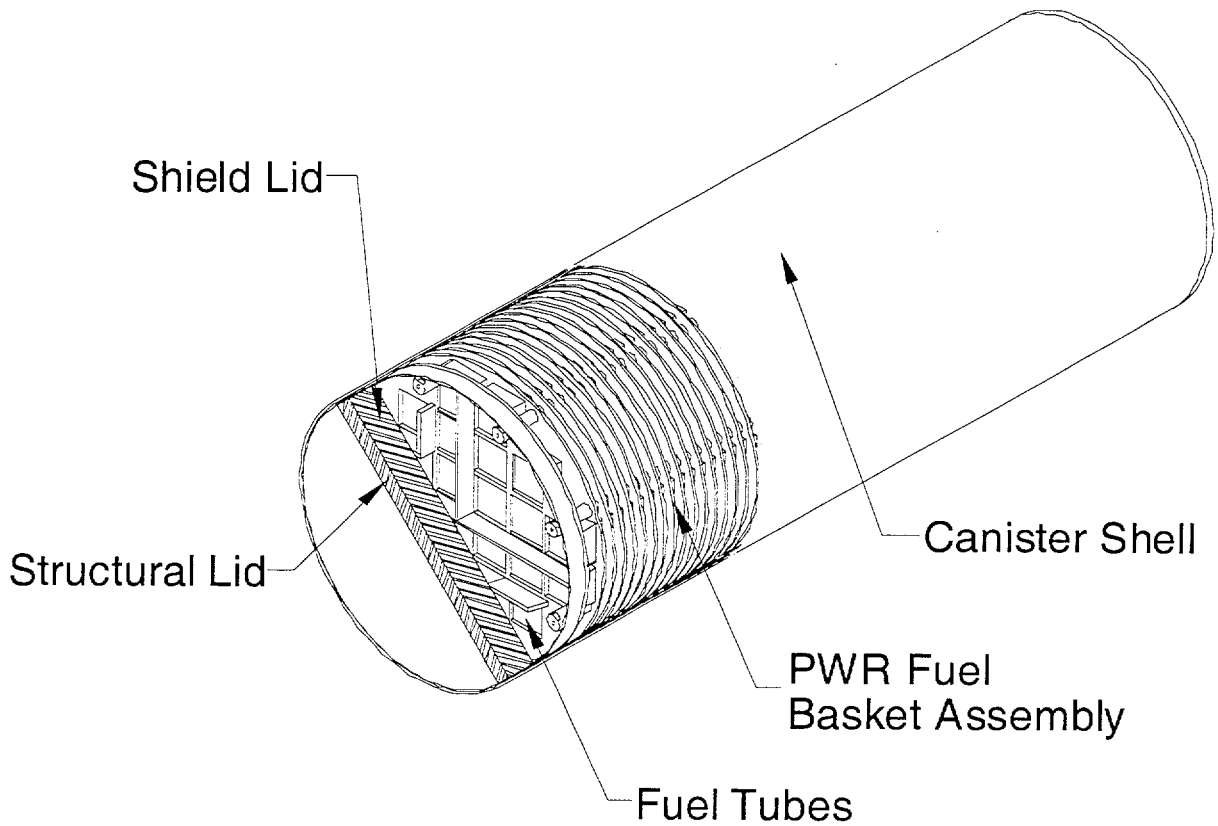

Figure 2.6.12-2 PWR Transportable Storage Canister Shell and Lids

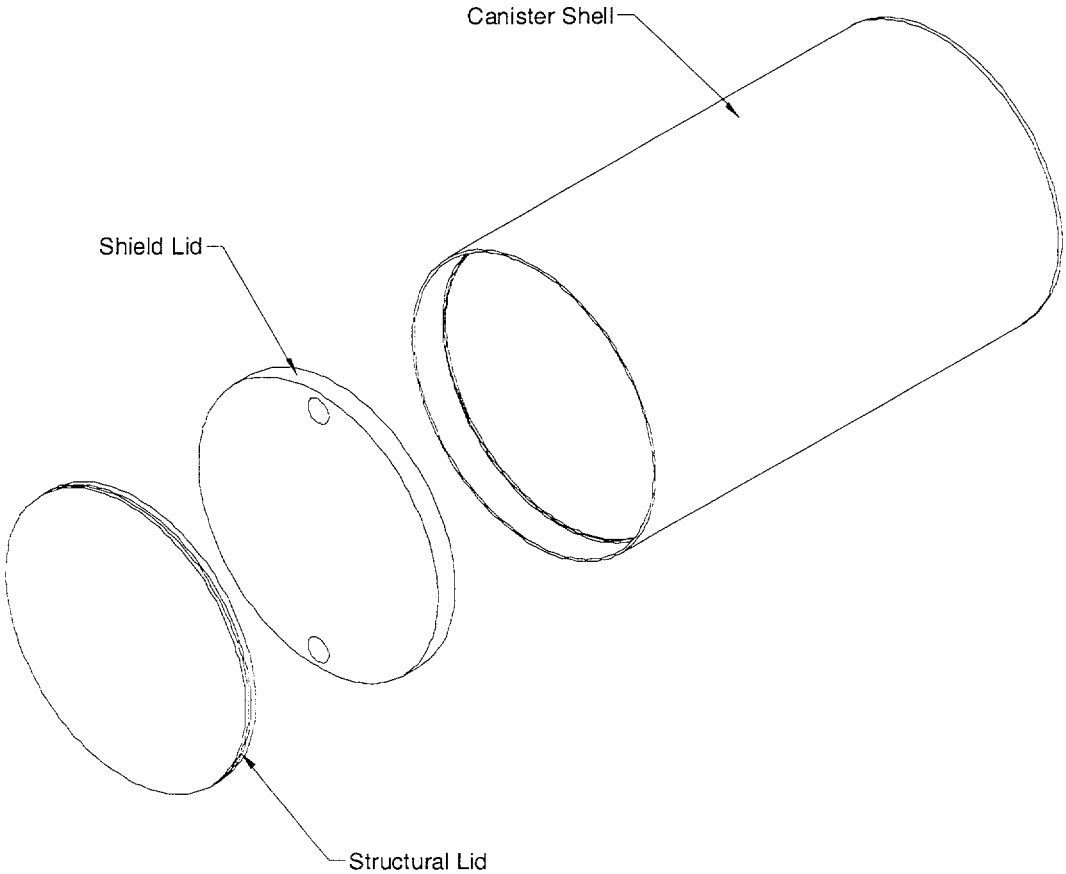

The maximum temperature in the canister shell central region is 399°F as determined in the thermal analysis presented in Section 3.4.2. This increase in temperature reduces the allowable S_m for Type 304L stainless steel from 16.0 ksi to 15.8 ksi. A review of the margins of safety for all cases evaluated indicates that the minimum margin for Sections 5 or 6 is 4.3 for the side-drop with pressure (Table 2.6.12.6-3). Using the allowable stress based on a temperature of 399°F reduces this minimum margin of safety to 4.23. Because this change in margin of safety is small, the increased peak temperature in the center of the canister has a negligible impact on the presented minimum margins.

The canister is analyzed by using the ANSYS [32] finite element computer program for the 1-ft free-drop condition in the top and bottom end, side, and top and bottom corner impact orientations. In addition, the effects of normal operating internal pressure and thermal stresses resulting from exposure of the cask to the hot (100°F ambient and solar insolance) and cold (-40°F ambient) normal conditions are evaluated. The worst-case stresses from these analyses are presented in Section 2.6.12.4.

2.6.12.2 Finite Element Model Description - PWR Canister

To evaluate the PWR Transportable Storage Canister for normal conditions of transport, ANSYS is used to construct and analyze a finite element model of the canister and its contents. The contents modeled consist of the fuel basket support disks and weldments. The fuel assemblies, fuel tubes, aluminum heat transfer disks, tie-rods, and related hardware are not explicitly modeled but rather are accounted for by applying pressure loads to the support disk slots as appropriate.

The finite element model of the canister is constructed by using ANSYS solid (SOLID45) elements. The model represents a one-half (180°) section of the canister and fuel basket. The basket support disks are modeled with three-dimensional shell (SHELL63) elements. The model uses gap-spring elements to simulate contact between adjacent components. Interaction between the basket and canister is accomplished by using three-dimensional gap elements (CONTAC52) along the periphery of the support disks. Contact between the canister and the cask inner shell is also modeled by using CONTAC52 gap elements. Contact between the canister structural lid and shield lid is modeled by using COMBIN40 combination elements in the axial degree of freedom. Simulation of the backing ring is accomplished by using a ring of COMBIN40 spring

gap elements connecting the shield lid and the canister in the axial direction at the lid lower outside radius. In addition, CONTAC52 elements are used to model interaction between the structural lid and canister shell and the shield lid and canister shell just below the respective lid weld joints. The size of the CONTAC52 gaps are determined from the nominal dimensions of contacting components. The COMBIN40 elements used between the structural and shield lids and for the backing ring are assigned small gap sizes of $1(10)^{-8}$ in. All gap-spring elements are assigned a stiffness of $1(10^{8})$ lb/in. Table 2.6.12.2-1 lists the element types assigned to specific gaps of the model. Table 2.6.12.2-2 lists the material properties used for the model.

Boundary conditions are applied to enforce symmetry at the cut boundary of the model. All nodes on the cask shell side of the canister-to-cask gap elements are fixed in all degrees of freedom. In addition, the axial and in-plane rotational degrees of freedom of the basket nodes are fixed.

Figure 2.6.12.2-1 is a plot of the entire canister finite element model including the support disks. An isolated view of the canister shield and structural lids portion of the model is presented in Figure 2.6.12.2-2, and an enlarged view of the model in the structural lid and shield lid weld regions is shown in Figure 2.6.12.2-3. The canister bottom plate portion of the model is shown in Figure 2.6.12.2-4.

The loading for the normal operating condition is based on 1-ft drops in conjunction with the internal pressure loading (to the canister). Drop orientations considered are the top and bottom end, side, and top and bottom corner-drops. In the end-drop orientation, the fuel contents load is transferred to the canister end and directly to the transport cask end through the cavity spacer. This corresponds to a compressive stress in the canister ends that is present in the finite element model. The canister shell is designed to be flush with the top surface of the structural lid with the worse case tolerance stack-up. This ensures that the content weight will be transferred through the lids to the transport cask during a top end or top corner drop condition. For the side-drop condition, the loads from the canister contents weight are transferred through the support disks into the canister wall, which is backed by the cask inner shell. Because the canister wall and the inner shell have different radii, a gap exists between the two surfaces. This gap results in the load passing only through regions in which the canister shell deflects to contact the inner shell. This load pattern is reflected in the side-drop analysis. For the corner-drop orientation, both the end-and side-load reactions with the cask inner shell are present.

The modeled contents weight includes 37,080 lb for all fuel assemblies (24 Class 1 PWR fuel assemblies), the fuel tube weight (3,417 lb), the aluminum heat transfer disk weight (1,946 lb), the disk spacer weight (1,879 lb), and the tie rod and nut and washer weights (783 + 94 lb). The weight of the support disks and weldments is accounted for by their being physically modeled. The PWR Class 1 configuration results in the largest load per support disk. The modeled canister length is 173.75 inches.

For the side and corner-drops, the weights of the fuel assemblies (W_{fuel}), aluminum heat transfer disks ($W_{ht\ disks}$), fuel tubes (W_{tubes}), tie rods (W_{rods}), nuts/washers (W_{nuts}), and spacers ($W_{spacers}$) are included in the model by applying a pressure load (F_{slot}) to the slot openings of the modeled support/weldment disks. This pressure load is calculated according to the following equation:

$$F_{slot} = \frac{W_{fuel} + W_{ht\ disks} + W_{tubes} + W_{rods} + W_{nuts} + W_{spacers}}{N_{slots} \times w_{slot} \times N_{disks}} \times g$$

where,

N_{slots} = number of slot openings in each support/weldment disk,
w_{slot} = width of each slot opening in each support/weldment disk,
N_{disks} = number of support/weldment disks, and
g = the associated g-loading for the drop height of interest.

For basket orientations other than 0°, the components of this resulting pressure load are applied to two faces of the slot opening. Additionally, for the corner-drops, the component resulting from accounting for the drop angle is used as the pressure load on the disk slot openings. For the PWR canister drop analyses, with 24 slot openings, a slot opening width of 9.272 inches, and a total of 34 support/weldment disks (32 support disks and 2 weldment disks), the resulting base pressure load used is:

$$F_{slot} = \frac{37{,}080 + 1{,}946 + 3{,}417 + 783 + 94 + 1{,}879}{24 \times 9.272 \times 34} \times g = 5.974 \times g$$

For the end drops, a uniform pressure representing the total weight of the fuel and fuel basket (52,369 lb) is applied to the canister shield lid (for top end-drop) or canister bottom plate (for

bottom end-drop). For the corner-drops, the component of this uniform pressure resulting from accounting for the drop angle is applied to the appropriate elements.

Changes were made to the fuel and fuel basket weight calculations after the finite element analyses were performed. These changes resulted in a total fuel and fuel basket weight of 52,565 lb. The total weight of the fuel and fuel basket analyzed in the PWR canister models is 52,369 lb. The revised calculations result in an increase in fuel and fuel basket weight of less than 1%; therefore, the modeled configuration will provide adequate stress results. Additionally, the length of the PWR Class 1 canister length was increased from 173.75 in. to 175.05 in. This is an increase of less than 1% and would also not sufficiently affect the results presented from these analyses.

The operational conditions also contain loads developed from the temperature distribution in the canister. These are included in the canister model analyses. The thermal analyses are described in Section 3.4.

The canister is analyzed for basket orientations of 0° and 45°. The angles describe the orientation of the basket elements with respect to the symmetry plane of the model. A value of 0° orients the ligaments in the basket elements parallel and perpendicular to the symmetry plane; a value of 45° orients the basket ligaments at +/- 45° from the symmetry plane. To accurately predict the canister response to impact, both orientations are run for the side, top-over-center-of-gravity, and bottom-over-center-of-gravity drop orientations. Top-end and bottom-end drops with varying basket orientations are not required since the basket disks are not included in these runs (their presence is accounted for by using applied pressure loads to the inner surface of the top or bottom).

Figure 2.6.12.2-1 PWR Canister Assembly Finite Element Model

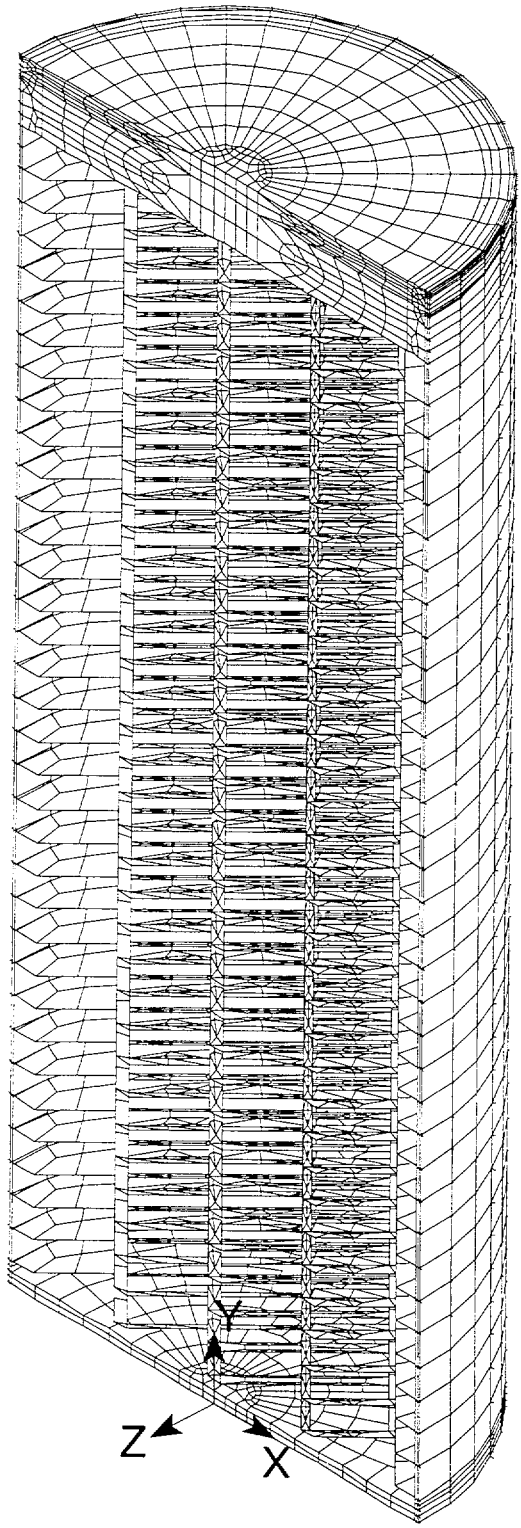

Figure 2.6.12.2-2 Canister Structural and Shield Lid Finite Element Mesh

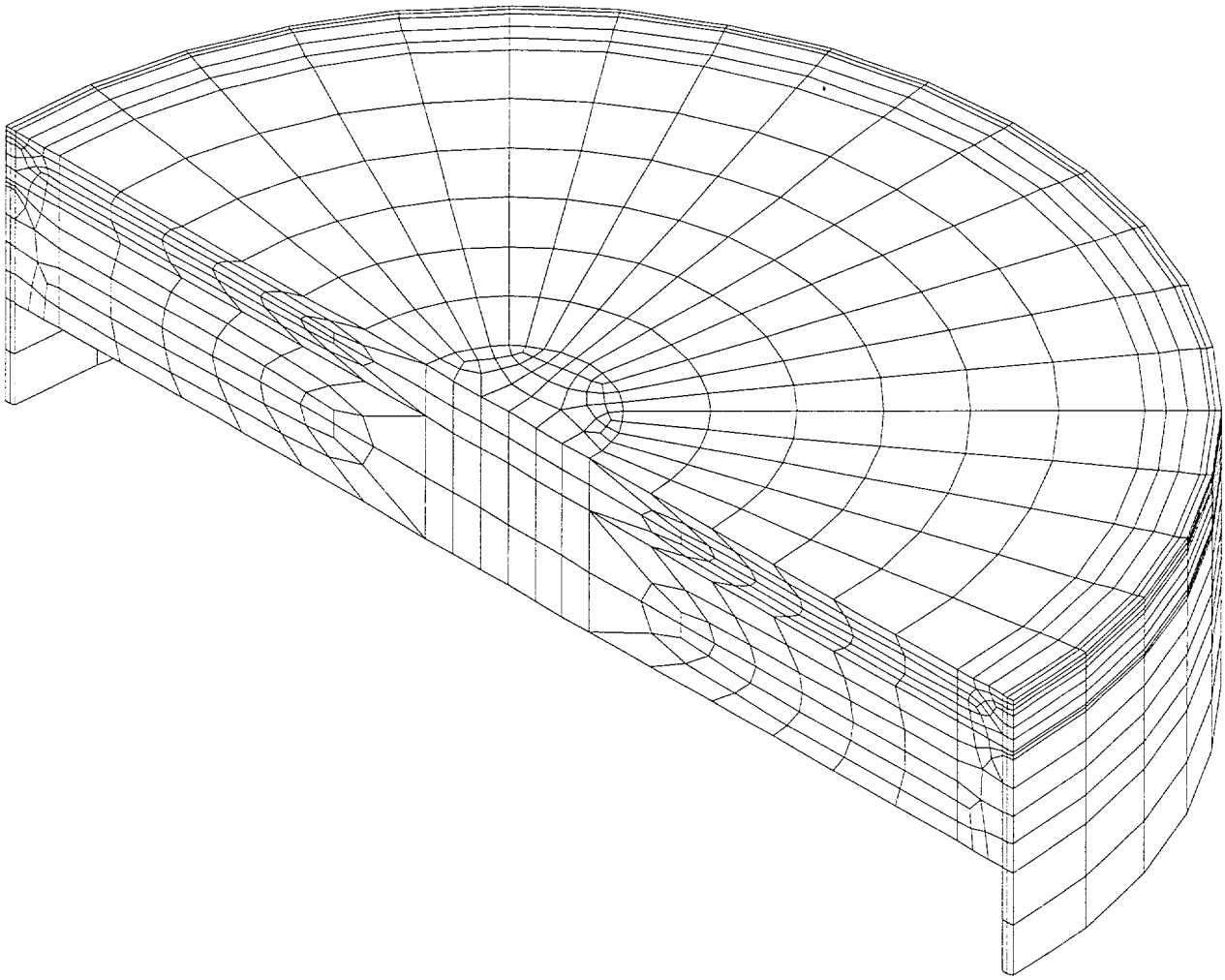

Figure 2.6.12.2-3 Structural and Shield Lid Weld Regions Finite Element Mesh

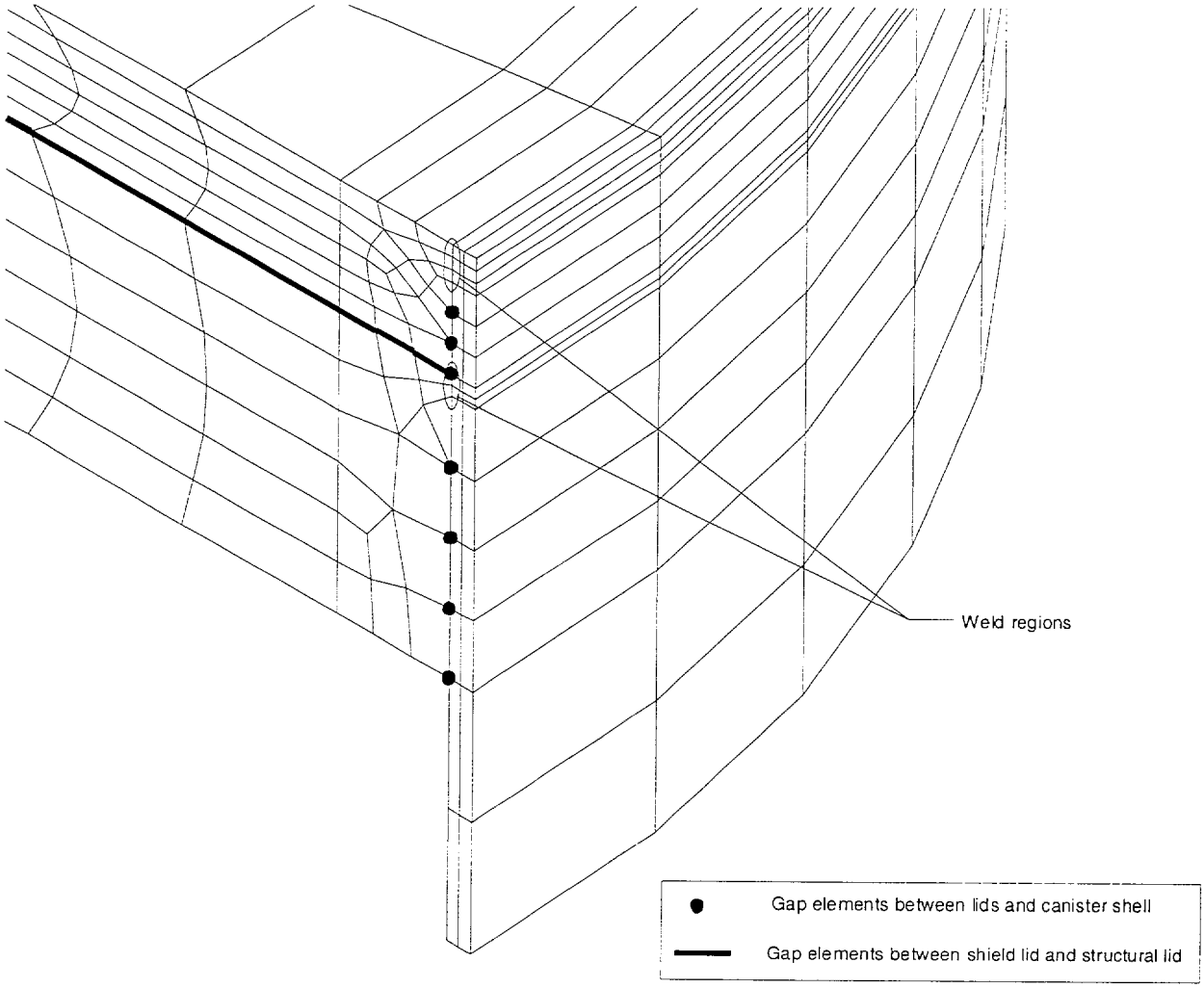

Figure 2.6.12.2-4 Canister Bottom Plate Finite Element Mesh

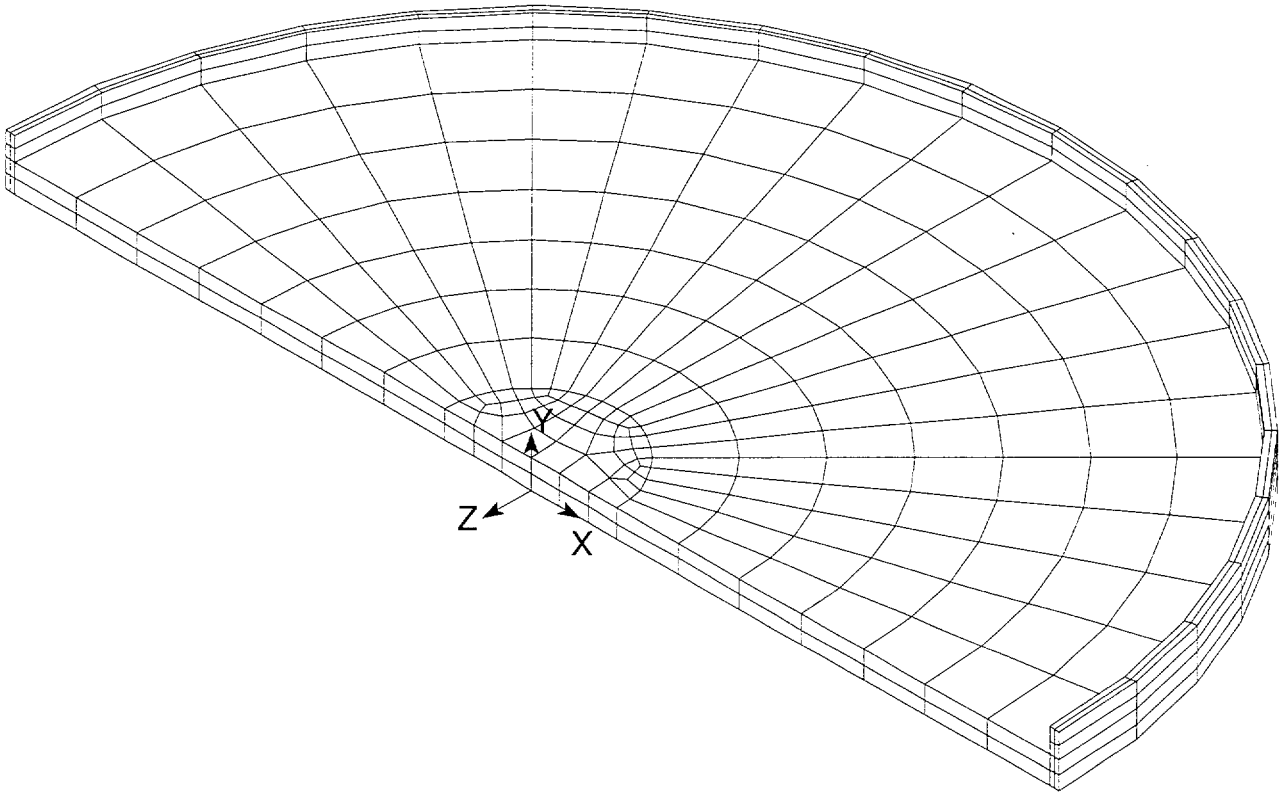

Table 2.6.12.2-1 Gap and Element Type Definition - Canister Model

Component
Axial Gaps from Canister Bottom Plate to Cask Shell (CONTAC52)
Radial Gaps from Canister Side to Cask Shell (CONTAC52)
Axial Gaps from Structural Lid Top to Cask Shell (CONTAC52)
Axial Gaps Between Structural and Shield Lid (COMBIN40)
Radial Gaps Between Shield Lid and Canister Inner Surface (CONTAC40)
Radial Gaps Between Shield Lid and Canister Inner Radius (CONTAC52)
Axial Gaps Between Shield Lid and Canister Wall to Simulate Backing Ring (COMBIN40)
Radial Gaps Between Basket and Canister Inner Surface (CONTAC52)

Table 2.6.12.2-2 Material Definition - Canister Model

Component	Material
Canister Shell and Structural Lid	304L Stainless Steel; ASME SA240
Top and Bottom Weldments	304 Stainless Steel; ASME SA240
Shield Lid	304 Stainless Steel; ASME SA240
Support disk	17-4 PH, ASME SA693 Type 630 Stainless Steel

2.6.12.3 Thermal Expansion and Thermal Stresses Evaluation of Canister for PWR Fuel

A thermal stress evaluation performed by using ANSYS determines the differential thermal expansion and the associated thermal stresses that result from a heat load of 20 kW. In assessing the thermal stresses, the following three extreme conditions are possible:

Condition	Ambient Temperature	Solar Insolance Applied to Cask Surface	20 kW Fuel Load
1	100°F	Yes	Yes
2	-40°F	No	Yes
3	-40°F	No	No

The temperatures employed in the thermal stress analysis are obtained by applying temperatures at 36 key locations on the canister shell and ends as thermal boundary conditions to the thermal equivalent model of the structural canister model. These temperatures are taken from the thermal evaluation described in Section 3.4. The structural finite element model described in Section 2.6.12.2 is used in this analysis. The equivalent thermal model is obtained by changing the structural element (SOLID45, which has three global displacements for degrees of freedom) to a SOLID70, which has temperature degrees of freedom at the individual nodes. The temperature-dependent thermal conductivity for the canister material is employed in the thermal conduction analysis. The temperatures generated in this analysis are used in the thermal stress analysis to evaluate the properties at temperature, as well as the stresses resulting from thermal expansion. Using this method, two separate cases: (Conditions 1 and 2) are evaluated: a hot case (100°F ambient with solar heat load and maximum decay heat) and a cold case (-40°F ambient and maximum decay heat). Condition 3 is not evaluated because the entire assembly would be at -40°F for the conditions described.

According to the ASME Code, Section III, Subsection NB, the allowable stress criteria are based on the evaluation of linearized stresses across critical cross sections through the canister wall. For the evaluation of the thermal stresses, the criteria for the stresses is based on peak stresses. The stress values taken from the analyses are the nodal stresses at the surface. The sections used in this evaluation are shown in Figure 2.6.12.3-1. Sections are evaluated every 9° around the circumference for each of the locations shown. The thermal stresses reported in Tables

2.6.12.3-1 and 2.6.12.3-2 correspond to the maximum stresses for any circumferential section, for each of the locations shown in Figure 2.6.12.3-1.

For Condition 1 or 2, the canister is hotter than the cask body and will undergo more thermal expansion than the cask body. To conservatively determine the minimum gap between the canister and the cask body resulting from thermal expansion, only expansion of the canister is considered. The canister is considered to be at 399°F (maximum shell temperature for thermal heat condition) and the cask inner shell temperature is assumed to be 70°F. Using the outer diameter of the canister of 67.06 in. and the coefficient of expansion for Type 304L stainless steel of 9.19 $(10)^{-6}$ at 400°F, the canister inner shell gap is reduced by (9.19 $(10)^{-6}$)(67.06 in.)(329°F) = 0.203 in. Because the nominal diametrical canister-inner shell gap is 67.61-67.06 = 0.55 in., the canister shell does not bind with the inner shell as a result of thermal expansion.

The maximum canister shell temperature is 399°F. This temperature is conservative to use for the axial expansion since a temperature gradient exists along the length of the canisters (i.e., the canister is cooler on the ends). The thermal expansion coefficient of Type 304L stainless steel at 400°F is 9.19 $(10)^{-6}$ in/in-°F. The longest canister configuration is PWR Class 3 with a length of 191.95 in. The increase in length of the canister is then

$$l = l_0 \, \alpha \, \Delta T$$

$$\Delta l = 191.95 \, (9.19 \, (10)^{-6} \text{ in/in-°F}) \, (399 - 70) = 0.58 \text{ in.}$$

The canister length increases to 191.95 + 0.58 = 192.53 in.

The minimum cask shell temperature is conservatively assumed to be 150°F (the peak inner shell temperature is 367.7°F; the upper forging minimum temperature is 237.5°F). The thermal expansion coefficient of Type 304 stainless steel at 70°F is conservatively used since the expansion coefficient increases with temperature 8.46 $(10)^{-6}$ in/in-°F. The cask cavity nominal length is 192.5 in. The increase in length of the cask cavity is then

$$\Delta l = 192.5 \, (8.46 \, (10)^{-6} \text{ in/in-°F}) \, (150 - 70) = 0.13 \text{ in.}$$

The cask cavity length increases to 192.5 + 0.13 = 192.63 in. The resulting axial gap is 192.63 - 192.53 = 0.1 in. Therefore, the canister and cask will expand axially and not bind during normal transport conditions.

Figure 2.6.12.3-1 Identification of Sections for Evaluating Linearized Stresses in Canister

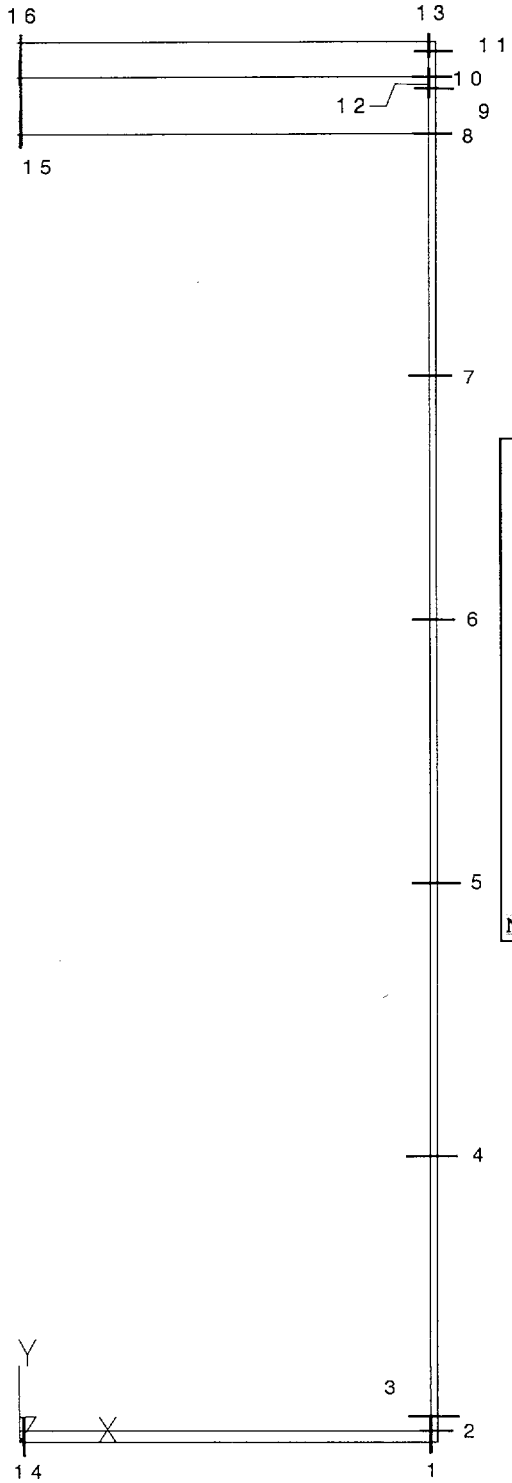

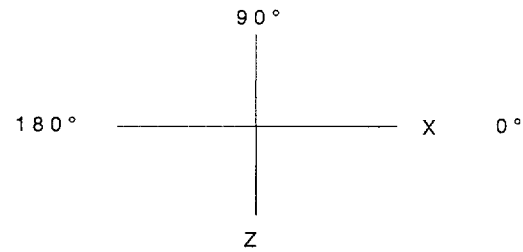

Top View of Axis

Section Coordinates at Z = 0

Axial Section	Node 1		Node 2	
	x	y	x	y
1	32.905	0.0	32.905	1.75
2	32.905	1.75	33.53	1.75
3	32.905	2.25	33.53	2.25
4	32.905	34.15	33.53	34.15
5	32.905	66.55	33.53	66.55
6	32.905	98.95	33.53	98.95
7	32.905	131.35	33.53	131.35
8	32.905	163.75	33.53	163.75
9	32.905	170.25	33.53	170.25
10	32.905	170.75	33.53	170.75
11	32.905	172.87	33.53	172.87
12	32.905	170.25	32.905	170.75
13	32.905	172.87	32.905	173.75
14	0.1	0.0	0.1	1.75
15	0.1	163.75	0.1	170.73
16	0.1	170.75	0.1	173.75

Note: Dimensions in inches.

Table 2.6.12.3-1 PWR Canister Linearized Q Stresses - Thermal Only (Hot 1)

Section Location	Angle of Peak Stress Location	Q Stresses (ksi)						SI (ksi)		
		Sx	Sy	Sz	Sxy	Syz	Sxz			
1	180	0.2	0.1	2.1	-0.1	0	-0.1	2.2		
2	9	-0.3	-1.2	0.7	-0.1	0	0.2	1.9		
3	9	-0.1	-1.1	0.9	-0.1	0	0.2	1.9		
4	0	0	-0.2	0.1	0	0	0	0.3		
5	0	0	-0.8	0.7	0	-0.2	0	1.5		
6	0	0	-0.6	0.3	0	0.1	0	0.9		
7	0	0	-0.6	0.1	0	0	0	0.6		
8	90	1	1.6	0	0	0	0	1.6		
9	162	0.1	-1.6	-0.5	-0.1	0	0.2	1.7		
10	90	0.3	1.7	-0.2	-0.2	0	0	1.9		
11	81	-0.5	-1.4	0.2	-0.1	-0.1	-0.1	1.6		
12	162	-0.3	0.6	-0.1	-0.1	0.1	-0.2	1.1		
13	81	-0.4	0.1	-0.7	0	-0.1	0	0.8		
14	0	-8.1	-1.4	-7.9	0.8	0.8	0.5	7.3		
15	180	0.4	0	-0.1	-0.8	0	1.7	3.8		
16	180	-0.2	0	0.1	-0.7	0	-1.2	2.7		

Table 2.6.12.3-2 Linearized Stresses - Thermal Only (Cold 2)

Section Location	Angle of peak stress location	Q Stresses (ksi)						SI (ksi)		
		Sx	Sy	Sz	Sxy	Syz	Sxz			
1	180	0.2	0.1	2.4	-0.1	0	-0.2	2.4		
2	9	-0.3	-1.2	0.9	-0.1	0	0.2	2.1		
3	9	-0.1	-1.1	1	-0.1	0	0.2	2.1		
4	0	0	-0.3	0.1	0	0	0	0.4		
5	0	0	-0.9	0.8	0	-0.2	0	1.7		
6	0	0	-0.7	0.4	0	0.1	0	1.1		
7	0	0	-0.7	0.1	0	0	0	0.8		
8	90	1.1	1.8	0	0	0	0	1.8		
9	162	0.1	-1.6	-0.5	-0.1	0	0.2	1.7		
10	90	0.4	2	-0.2	-0.2	0	0	2.2		
11	81	-0.6	-1.5	0.2	-0.1	-0.1	-0.1	1.8		
12	162	-0.3	0.6	-0.1	-0.1	0.2	-0.2	1.1		
13	81	-0.5	0.1	-0.8	0	-0.1	0	0.9		
14	0	-9.1	-1.7	-8.8	0.7	0.9	0.5	8		
15	180	0.4	0	-0.1	-0.7	0	1.5	3.4		
16	180	-0.2	0	0.1	-0.6	0	-1	2.4		

2.6.12.4 Stress Evaluation of PWR Canister for 1-Foot End-Drop Load Condition

A structural analysis performed by using ANSYS evaluates the effect of a 1-ft end-drop impact for both the bottom and top-end orientations of the PWR canister. The ASME Code, Section III, Subsection NB requires that stresses arising from operational loads be assessed on the basis of the primary loads. The primary loads for the 1-ft drop result from the deceleration of the canister and its contents and the 25-psig pressure load internal to the canister. The applied deceleration is 20 *g* for both orientations. The inertial load of the canister is addressed by the deceleration factor applied to the canister density. The weight of the contents is represented by a pressure load on the inner end surface of the canister. Displacement constraints are applied to the plane of symmetry and the gap elements attached at the canister end to represent the top or bottom of the transport cask.

To determine the effect of the 25-psig pressure load, the top-end and bottom-end orientations with and without the pressure load are analyzed.

The locations of the linearized stresses are shown in Figure 2.6.12.3-1. The summary for P_m and $P_m + P_b$ stresses due to the internal pressure of 25 psig are summarized in Table 2.6.12.4-2 and 2.6.12.4-3, respectively. Results from the end-drops are summarized in Tables 2.6.12.4-4 through 2.6.12.4-7 for the conditions that produce the minimum margin of safety. Table 2.6.12.4-1 provides a summary of critical section stresses for the top and bottom end-drop conditions. The margins of safety in these tables are calculated as:

MS = (allowable stress/SI) -1.

Table 2.6.12.4-1 PWR Canister Critical Sections for the Pressure Only and 1-Foot End-Drop Load Condition

Condition	Stress	Critical Section	Table	Minimum Margin of Safety
Pressure (only)	P_m	2	2.6.12.4-2	+ 3.32
Pressure (only)	$P_m + P_b$	3	2.6.12.4-3	+ 0.71
Top-End Drop Inertia	P_m	2	2.6.12.4-4	+ 4.04
Top-End Drop Inertia	$P_m + P_b$	3	2.6.12.4-5	+ 1.1
Bottom-End Drop + Pressure	P_m	4	2.6.12.4-6	+ 4.33
Bottom-End Drop + Pressure	$P_m + P_b$	2	2.6.12.4-7	+ 5.71

Table 2.6.12.4-2 PWR Canister P_m Stresses - Internal Pressure

Section Location	Angle of Peak Stress Location	P_m Stresses (ksi)						SI (ksi)	Allowable Stress (ksi)	Margin of Safety
		Sx	Sy	Sz	Sxy	Syz	Sxz			
1	0	0.2	2.4	1	-0.3	0	0.1	2.4	16	5.75
2	0	1.6	-1.6	-2	-0.3	0	-0.2	3.7	16	3.32
3	0	0.3	0	-2.7	0.3	0	-0.2	3.3	16	3.83
4	0	0	0.6	1.3	0	0	0.1	1.3	16	10.98
5	0	0	0.6	1.3	0	0	0.1	1.3	16	11.02
6	0	0	0.6	1.3	0	0	0.1	1.3	16	11.02
7	0	0	0.6	1.3	0	0	0.1	1.3	16	11.02
8	0	0	0.6	0.7	0	0	0.1	0.7	16	22.64
9	180	0	0.5	0.3	-0.1	0	0	0.5	16	33.63
10	180	-0.3	0.3	0.2	0.1	0	0	0.6	16	25.71
11	0	0.3	-0.1	0.2	0	0	0	0.4	16	37.08
12	0	-0.1	-0.4	0	-0.1	0	0	0.5	16	33.99
13	9	0	0.3	0.2	0	0	0	0.3	12.8*	41.67
14	90	0.2	-0.2	0.2	-0.1	0.2	0	0.6	16	23.81
15	90	0	0	0	0	0	0	0	16	1025.99
16	0	0	0	0	0	0	0	0	16	365.18

* Allowable stress includes a stress reduction factor for weld: 0.8 x allowable stress.

Note: All of the allowable stress values presented in this table are based on SA240, Type 304L stainless steel at a temperature of 380°F unless otherwise stated. Localized peak temperatures in the central portion of the canister shell reach 399°F—resulting in slightly lower allowable stress values and subsequently slightly lower margins of safety for sections 5 and 6 than those presented in the table. However, this difference is negligible as discussed in Section 2.6.12.1.

Table 2.6.12.4-3 PWR Canister $P_m + P_b$ Stresses - Internal Pressure

Section Location	Angle of Peak Stress Location	$P_m + P_b$ Stresses (ksi)						SI (ksi)	Allowable Stress (ksi)	Margin of Safety
		Sx	Sy	Sz	Sxy	Syz	Sxz			
1	0	1.9	5.9	0.2	0	0	-0.1	5.7	24	3.24
2	0	0.8	-11.2	-5.1	-0.8	0	-0.4	12.2	24	0.97
3	0	0.7	-13.3	-6.5	0.1	0	-0.5	14	24	0.71
4	0	0	0.6	1.3	0	0	0.1	1.4	24	16.74
5	0	0	0.7	1.3	0	0	0.1	1.4	24	16.73
6	0	0	0.7	1.3	0	0	0.1	1.4	24	16.73
7	0	0	0.6	1.3	0	0	0.1	1.4	24	16.73
8	180	0	0.7	0.7	0	0	-0.1	0.7	24	31.59
9	180	0.1	0.9	0.5	-0.1	0	0	0.9	24	26.24
10	180	-0.1	1.4	0.6	0	0	-0.1	1.5	24	14.58
11	0	0.2	-1	-0.1	0.1	0	0	1.2	24	19.74
12	0	-0.4	-0.8	-0.1	-0.2	0	0	0.7	24	34.13
13	180	-0.4	0	0	-0.1	0	0	0.4	19.2*	47.00
14	90	7.6	-0.2	7.6	-0.1	0.2	0	7.8	24	2.06
15	90	-0.6	0	-0.6	0	0	0	0.6	24	40.86
16	81	0.3	0	0.3	0	0	0	0.3	24	74.05

* Allowable stress includes a stress reduction factor for weld: 0.8 x allowable stress.

Note: All of the allowable stress values presented in this table are based on SA240, Type 304L stainless steel at a temperature of 380°F unless otherwise stated. Localized peak temperatures in the central portion of the canister shell reach 399°F—resulting in slightly lower allowable stress values and subsequently slightly lower margins of safety for sections 5 and 6 than those presented in the table. However, this difference is negligible as discussed in Section 2.6.12.1.

Table 2.6.12.4-4 PWR Canister P_m Stresses - 1-Foot Top End Drop

Section Location	Angle of Peak Stress Location	P_m Stresses (ksi)						SI (ksi)	Allowable Stress (ksi)	Margin of Safety
		Sx	Sy	Sz	Sxy	Syz	Sxz			
1	0	-0.1	-2	-0.7	0.3	0	0	1.9	16	7.31
2	0	-1.3	1.2	1.8	0.3	0	0.2	3.2	16	4.04
3	0	-0.3	0	2.5	-0.2	0	0.2	3	16	4.38
4	144	0	-0.7	0	0	0	0	0.7	16	20.58
5	153	0	-0.9	0	0	0	0	0.9	16	16.18
6	162	0	-1.1	0	0	0	0	1.1	16	13.28
7	180	0	-1.3	0	0	0	0	1.3	16	11.21
8	180	0	-1.2	0	0	0	0	1.3	16	11.57
9	180	0	-0.9	-0.2	0	0	0	1	16	15.82
10	144	-0.1	-0.9	-0.1	0	0	0.1	0.9	16	17.09
11	135	-0.1	-0.9	-0.1	0	0	0.1	0.9	16	17.3
12	144	0	-0.7	-0.1	0	0	0	0.7	16	21.43
13	180	0	-0.7	-0.1	0	0	0	0.7	12.8*	17.29
14	90	-0.2	0	-0.2	0.1	-0.1	0	0.4	16	44.06
15	144	0	-0.3	0	0	0	0	0.4	16	44.54
16	0	0	-0.4	0	0	0	0	0.4	16	40.07

* Allowable stress includes a stress reduction factor for weld: 0.8 x allowable stress.

Note: All of the allowable stress values presented in this table are based on SA240, Type 304L stainless steel at a temperature of 380°F unless otherwise stated. Localized peak temperatures in the central portion of the canister shell reach 399°F—resulting in slightly lower allowable stress values and subsequently slightly lower margins of safety for sections 5 and 6 than those presented in the table. However, this difference is negligible as discussed in Section 2.6.12.1.

Table 2.6.12.4-5 PWR Canister $P_m + P_b$ Stresses - 1-Foot Top End Drop

Section Location	Angle of Peak Stress Location	$P_m + P_b$ Stresses (ksi)						SI (ksi)	Allowable Stress (ksi)	Margin of Safety
		Sx	Sy	Sz	Sxy	Syz	Sxz			
1	0	-1.4	-4.7	0.1	0	0	0.1	4.8	24	3.99
2	0	-0.6	9	4.3	0.7	0	0.4	9.8	24	1.45
3	0	-0.5	10.8	5.6	0	0	0.5	11.4	24	1.1
4	162	0	-0.8	0	0	0	0	0.8	24	30.8
5	162	0	-0.9	0	0	0	0	0.9	24	24.77
6	144	0	-1.1	0	0	0	0	1.1	24	20.42
7	171	0	-1.3	0	0	0	0	1.3	24	17.3
8	180	0.1	-1.2	0	-0.1	0	0	1.3	24	17.37
9	45	-0.1	-1.1	-0.1	0	0	-0.1	1.1	24	21.59
10	180	0	-1	-0.2	0	0	0	1	24	22.45
11	135	-0.1	-1	-0.1	0	0	0.1	1	24	23.42
12	180	0	-0.7	-0.1	-0.1	0	0	0.7	24	31.5
13	180	0	-0.8	-0.1	0	0	0	0.7	19.2*	26.43
14	90	-6.8	-0.1	-6.8	0.1	-0.1	0	6.7	24	2.57
15	81	0.1	-0.3	0.1	0	0	0	0.4	24	55.49
16	0	0	-0.4	0	0	0	0	0.4	24	59.08

* Allowable stress includes a stress reduction factor for weld: 0.8 x allowable stress.

Note: All of the allowable stress values presented in this table are based on SA240, Type 304L stainless steel at a temperature of 380°F unless otherwise stated. Localized peak temperatures in the central portion of the canister shell reach 399°F—resulting in slightly lower allowable stress values and subsequently slightly lower margins of safety for sections 5 and 6 than those presented in the table. However, this difference is negligible as discussed in Section 2.6.12.1.

Table 2.6.12.4-6 PWR Canister P_m Stresses - 1-Foot Bottom End Drop, Internal Pressure

Section Location	Angle of Peak Stress Location	P_m Stresses (ksi)						SI (ksi)	Allowable Stress (ksi)	Margin of Safety
		Sx	Sy	Sz	Sxy	Syz	Sxz			
1	180	0	-0.6	0	0.1	0	0	0.6	16	24.4
2	180	0.3	-1.9	-0.3	0.1	0	0	2.2	16	6.24
3	180	0.1	-1.9	-0.3	-0.1	0	0	2	16	7.08
4	180	0	-1.7	1.3	0	0	-0.1	3	16	4.33
5	180	0	-1.5	1.3	0	0	-0.1	2.8	16	4.69
6	180	0	-1.3	1.3	0	0	-0.1	2.6	16	5.11
7	180	0	-1.1	1.3	0	0	-0.1	2.4	16	5.58
8	180	0	-0.7	0.7	0	0	-0.1	1.4	16	10.31
9	18	-0.1	-0.5	-0.4	-0.1	0	-0.1	0.4	16	36.52
10	180	0.4	-0.3	-0.2	-0.1	0	0	0.7	16	21.21
11	0	-0.5	0.1	-0.2	0	0	0	0.6	16	27.29
12	99	-0.1	0.5	0.1	0	-0.1	0	0.6	16	27.09
13	0	0	-0.5	-0.3	0	0	0	0.4	12.8*	31.00
14	0	0.1	-0.4	0.1	0	0	0	0.4	16	34.57
15	108	0	0	0	0	0	0	0.1	16	302.05
16	0	0	0	0	0	0	0	0.1	16	286.36

* Allowable stress includes a stress reduction factor for weld: 0.8 x allowable stress.

Note: All of the allowable stress values presented in this table are based on SA240, Type 304L stainless steel at a temperature of 380°F unless otherwise stated. Localized peak temperatures in the central portion of the canister shell reach 399°F—resulting in slightly lower allowable stress values and subsequently slightly lower margins of safety for sections 5 and 6 than those presented in the table. However, this difference is negligible as discussed in Section 2.6.12.1.

Table 2.6.12.4-7 PWR Canister $P_m + P_b$ Stresses - 1 Foot Bottom End Drop, Internal Pressure

Section Location	Angle of Peak Stress Location	$P_m + P_b$ Stresses (ksi)						SI (ksi)	Allowable Stress (ksi)	Margin of Safety
		Sx	Sy	Sz	Sxy	Syz	Sxz			
1	180	0.2	-0.4	0.1	0.1	0	0	0.7	24	34.19
2	180	0.2	-3.4	-0.7	0.1	0	0.1	3.6	24	5.71
3	180	0.1	-3.3	-0.6	-0.1	0	0	3.3	24	6.16
4	0	0	-1.7	1.3	0	0	0.1	3	24	6.95
5	0	0	-1.5	1.3	0	0	0.1	2.8	24	7.5
6	0	0	-1.3	1.3	0	0	0.1	2.6	24	8.11
7	0	0	-1.1	1.3	0	0	0.1	2.4	24	8.82
8	27	0.2	-0.9	0.5	0	0	0.2	1.5	24	14.94
9	108	-0.5	-1.1	-0.1	0	0.1	0.1	1.1	24	21.15
10	99	-0.7	-1.6	0.1	0	0	0.1	1.8	24	12.44
11	0	-0.2	1.3	0.2	-0.1	0	0	1.5	24	14.78
12	99	0.2	0.9	0.5	0	-0.2	0.1	0.8	24	29.14
13	0	0.5	0	0	-0.1	0	0	0.5	19.2*	37.40
14	0	0.1	-0.4	0.1	0	0	0	0.5	24	49.26
15	90	0.8	0	0.8	0	0	0	0.8	24	28.07
16	0	-0.4	0	-0.4	0	0	0	0.4	24	56.39

* Allowable stress includes a stress reduction factor for weld: 0.8 x allowable stress.

Note: All of the allowable stress values presented in this table are based on SA240, Type 304L stainless steel at a temperature of 380°F unless otherwise stated. Localized peak temperatures in the central portion of the canister shell reach 399°F—resulting in slightly lower allowable stress values and subsequently slightly lower margins of safety for sections 5 and 6 than those presented in the table. However, this difference is negligible as discussed in Section 2.6.12.1.

2.6.12.5 Stress Evaluation of PWR Canister for Combined Thermal and 1-Foot End Drop Load Condition

The thermal stress loads described in Section 2.6.12.3 are applied in conjunction with the primary loads in Section 2.6.12.4 to produce a combined thermal stress plus end-impact loading. The stress evaluation is performed according to the ASME Code, Section III, Subsection NB. The most critical sections are listed in Table 2.6.12.5-1. The stresses reported in this table correspond to the nodal stress at the surface. The minimum margin of safety is +2.44 when 3 S_m is used as the stress criterion. Tables 2.6.12.5-2 through 2.6.12.5-5 tabulate the peak stresses for both the hot and cold conditions for both the top-and bottom-end-drop cases for the conditions that result in the minimum margin of safety. For both top and bottom orientations, the minimum margins occur without the addition of pressure. The margins of safety are calculated as:

MS = (allowable stress/SI) -1.

Table 2.6.12.5-1 PWR Canister Critical Sections for the Combined 1-Foot End Drop and Thermal Load Condition

Condition	Stress	Critical Section	Table	Minimum Margin of Safety
Top-End Drop + Thermal (cold)	P + Q	14	2.6.12.5-2	+ 2.44
Top-End Drop + Thermal (hot)	P + Q	3	2.6.12.5-3	+ 2.6
Bottom-End Drop + Thermal (cold)	P + Q	14	2.6.12.5-4	+ 7.47
Bottom-End Drop + Thermal (hot)	P + Q	14	2.6.12.5-5	+ 8.44

Table 2.6.12.5-2 PWR Canister $P_m + P_b + Q$ Stresses - 1-Foot Top End Drop, Thermal Cold

Section Location	Angle of Peak Stress Location	$P_m + P_b + Q$ Stresses (ksi)						SI (ksi)	Allowable Stress (ksi)	Margin of Safety
		Sx	Sy	Sz	Sxy	Syz	Sxz			
1	90	1.3	-5.8	-1.8	0	0	0	7.2	47.9	5.67
2	45	3.4	10.6	3.4	0.4	-0.6	3.5	10.8	47.9	3.46
3	9	-0.1	-10.9	0.8	-0.6	0	0.2	11.8	47.9	3.08
4	0	0	-1.2	0	0	0	0	1.2	47.9	37.94
5	0	0	-2.1	0.6	0	-0.2	0	2.8	47.9	16.12
6	0	0	-2.3	0.2	0	0	0	2.5	47.9	18.39
7	0	0	-2.6	0	0	0	0	2.6	47.9	17.46
8	9	-0.2	-3.4	-0.3	0	0.1	0	3.3	47.9	13.67
9	162	0.1	-3.1	-0.7	-0.2	-0.1	0.3	3.3	47.9	13.63
10	0	-0.1	-2	-0.5	0.1	0	0	1.8	47.9	25.05
11	171	0	-3.3	-0.8	0	0	0.1	3.3	47.9	13.51
12	0	0.4	-0.9	0	0.2	0	0	1.3	47.9	35.99
13	0	0.2	-1	-0.1	0	0	0	1.2	38.32*	30.93
14	0	-15.7	-1.8	-15.4	0.1	-1	0.1	14	47.9	2.44
15	81	0.1	-0.3	0.1	0	0	0	0.4	47.9	116.3
16	0	0.1	-0.5	0.1	0	0	0	0.6	47.9	85.61

* Allowable stress includes a stress reduction factor for weld: 0.8 x allowable stress.

Note: All of the allowable stress values presented in this table are based on SA240, Type 304L stainless steel at a temperature of 380°F unless otherwise stated. Localized peak temperatures in the central portion of the canister shell reach 399°F—resulting in slightly lower allowable stress values and subsequently slightly lower margins of safety for sections 5 and 6 than those presented in the table. However, this difference is negligible as discussed in Section 2.6.12.1.

Table 2.6.12.5-3 PWR Canister $P_m + P_b + Q$ Stresses-1-Foot Top End Drop, Thermal Heat

Section Location	Angle of Peak Stress Location	$P_m + P_b + Q$ Stresses (ksi)						SI (ksi)	Allowable Stress (ksi)	Margin of Safety
		Sx	Sy	Sz	Sxy	Syz	Sxz			
1	90	1.2	-5.9	-1.8	0	0	0	7.1	47.9	5.77
2	45	3.3	10.5	3.3	0.4	-0.6	3.5	10.8	47.9	3.44
3	9	-0.1	-11	0.7	-0.6	0.1	0.1	11.8	47.9	3.08
4	0	0	-1.1	0	0	0	0	1.2	47.9	40.01
5	0	0	-2	0.5	0	-0.2	0	2.5	47.9	17.84
6	0	0	-2.1	0.2	0	0	0	2.3	47.9	20.04
7	0	0	-2.4	0	0	0	0	2.4	47.9	19.03
8	9	-0.2	-3.2	-0.3	0	0.1	0	3	47.9	14.85
9	162	0.1	-3	-0.7	-0.1	-0.1	0.3	3.2	47.9	14.01
10	162	-0.3	-2	-0.5	-0.2	-0.1	0.1	1.8	47.9	26.36
11	171	0	-3	-0.7	0	0	0.1	3	47.9	14.76
12	0	0.3	-0.9	-0.1	0.2	0	0	1.2	47.9	37.66
13	0	0.2	-0.9	-0.1	0	0	0	1.1	38.32*	33.84
14	0	-14.8	-1.6	-14.6	0.1	-0.9	0	13.3	47.9	2.6
15	81	0.1	-0.3	0.1	0	0	0	0.4	47.9	116.41
16	0	0.1	-0.5	0.1	0	0	0	0.5	47.9	87.74

* Allowable stress includes a stress reduction factor for weld: 0.8 x allowable stress.

Note: All of the allowable stress values presented in this table are based on SA240, Type 304L stainless steel at a temperature of 380°F unless otherwise stated. Localized peak temperatures in the central portion of the canister shell reach 399°F—resulting in slightly lower allowable stress values and subsequently slightly lower margins of safety for sections 5 and 6 than those presented in the table. However, this difference is negligible as discussed in Section 2.6.12.1.

Table 2.6.12.5-4 PWR Canister $P_m + P_b + Q$ Stresses -1-Foot Bottom End Drop, Thermal Cold

Section Location	Angle of Peak Stress Location	$P_m + P_b + Q$ Stresses (ksi)						SI (ksi)	Allowable Stress (ksi)	Margin of Safety
		Sx	Sy	Sz	Sxy	Syz	Sxz			
1	9	0.1	-2.1	1.2	-0.3	0.1	0.2	3.4	47.9	13.23
2	9	-0.3	-4.5	0.3	-0.1	0.1	0.1	4.8	47.9	9.04
3	9	-0.1	-4	0.6	0	0.1	0.1	4.6	47.9	9.38
4	0	0	-3.2	0	0	0	0	3.2	47.9	14.02
5	0	0	-3.5	0.6	0	-0.2	0	4.1	47.9	10.6
6	0	0	-3	0.2	0	0.1	0	3.2	47.9	13.91
7	0	0	-2.6	0	0	0	0	2.7	47.9	17.02
8	9	-0.2	-2.7	-0.2	0	0.2	0	2.6	47.9	17.55
9	162	-0.2	-3.3	-1.4	0.1	0.1	0.4	3.3	47.9	13.69
10	0	0.4	-3.9	-1.5	0	0.1	-0.1	4.3	47.9	10.22
11	0	-0.5	2.7	0.7	-0.1	0.1	0.1	3.2	47.9	13.86
12	18	1.1	1.7	0.3	0.4	0.1	-0.1	1.6	47.9	28.65
13	0	-1.4	-2	-1	0.3	0	0	1.2	38.32*	30.93
14	0	-11.2	-5.5	-10.9	0	0.1	0.1	5.7	47.9	7.47
15	81	1.7	0	1.4	0	0	0	1.7	47.9	27.66
16	72	-0.7	0	-0.6	0	0	0	0.7	47.9	68.32

* Allowable stress includes a stress reduction factor for weld: 0.8 x allowable stress.

Note: All of the allowable stress values presented in this table are based on SA240, Type 304L stainless steel at a temperature of 380°F unless otherwise stated. Localized peak temperatures in the central portion of the canister shell reach 399°F—resulting in slightly lower allowable stress values and subsequently slightly lower margins of safety for sections 5 and 6 than those presented in the table. However, this difference is negligible as discussed in Section 2.6.12.1.

Table 2.6.12.5-5 PWR Canister $P_m + P_b + Q$ Stresses - 1-Foot Bottom End Drop, Thermal Heat

Section Location	Angle of Peak Stress Location	$P_m + P_b + Q$ Stresses (ksi)						SI (ksi)	Allowable Stress (ksi)	Margin of Safety
		Sx	Sy	Sz	Sxy	Syz	Sxz			
1	9	0.1	-1.9	1.1	-0.3	0.1	0.2	3.1	47.9	14.36
2	9	-0.3	-4.5	0.1	-0.1	0.1	0.1	4.6	47.9	9.45
3	9	-0.1	-4	0.4	0	0.1	0.1	4.4	47.9	9.79
4	0	0	-3.1	0	0	0	0	3.1	47.9	14.64
5	0	0	-3.3	0.6	0	-0.2	0	3.9	47.9	11.41
6	0	0	-2.8	0.2	0	0.1	0	3	47.9	14.76
7	0	0	-2.5	0	0	0	0	2.5	47.9	17.96
8	9	-0.2	-2.6	-0.2	0	0.2	0	2.4	47.9	18.74
9	162	-0.2	-3.2	-1.3	0.1	0.1	0.4	3.1	47.9	14.46
10	162	0	-3.8	-1.4	-0.1	0.1	0.5	4	47.9	10.93
11	9	-0.5	2.5	0.5	-0.1	0.1	0.1	3.1	47.9	14.68
12	162	0.6	1.9	0.2	-0.4	0	0.1	1.8	47.9	25.24
13	0	1	-0.2	0.2	-0.1	0	-0.1	1.2	38.32*	30.93
14	0	-10	-4.9	-9.7	0	0.1	0	5.1	47.9	8.44
15	72	1.7	0	1.4	0	0	0	1.6	47.9	28.14
16	72	-0.7	-0.1	-0.6	0	0	0	0.7	47.9	68.12

* Allowable stress includes a stress reduction factor for weld: 0.8 x allowable stress.

Note: All of the allowable stress values presented in this table are based on SA240, Type 304L stainless steel at a temperature of 380°F unless otherwise stated. Localized peak temperatures in the central portion of the canister shell reach 399°F—resulting in slightly lower allowable stress values and subsequently slightly lower margins of safety for sections 5 and 6 than those presented in the table. However, this difference is negligible as discussed in Section 2.6.12.1.

2.6.12.6 Stress Evaluation of PWR Canister for 1-Foot Side Drop Load Condition

The stresses in the PWR canister that result from a 1-ft side-drop are determined by using ANSYS. In the local regions of the lids and bottom plate, the loads are transmitted through the canister shell into the cask body inner shell. Outside of the lid and bottom plate regions, stress develops in the canister shell as a result of the basket loading the canister wall. The difference in the radii of the basket, canister, and cask body implies that the contact angle between the components is dependent on the loading. For this reason, the finite element model described in Section 2.6.12.2 contains a half model of the basket. Gap elements between the basket and the canister allow the interface to be dependent on the loading. The interface between the canister and the cask body inner shell is also represented by gap elements.

The load resulting from the contents is applied to the basket by means of pressure acting in the plane of the disks. The weight is assumed to act over the effective width of 9.272 in., in which the disk is 0.5 in. thick. This weight is distributed over the 32 support disks plus two end weldments. A deceleration factor of 20 *g* applied to the weights provides the loading for the basket assembly. In addition to the contents load, a 25-psig pressure is applied to the inner surface of the canister.

Analyses of the canister are performed for basket orientations of 0° and 45°. The angles describe the orientation of the basket elements with respect to the symmetry plane of the model. A value of 0° orients the ligaments in the basket elements parallel and perpendicular to the symmetry plane, a value of 45°orients the basket ligaments at +/- 45° from the symmetry plane. To assess the impact of the basket orientation on the canister response during impact, both basket orientations are run for the side-impact loading.

The methodology used to evaluate the stresses for the side-drop are similar to that used for the end-drop (Section 2.6.12.4) with following exceptions. Sections 9, 10, and 11 at the 0° circumferential position (see Figure 2.6.12.3-1) are not included in the evaluation. These regions are characterized as a bearing stress since they result from the canister shell bearing against the cask inner shell. Section 2.6.12.11 provides an assessment of the canister shell bearing stresses. Sections 9, 10, and 11 at all other angular locations are included in the evaluation. Also, Sections 12 and 13 at 0° are treated as local membrane stresses. According to the ASME Code Section III, Paragraph NB-3213.10, a stressed region may be considered local if the distance over which the membrane stress intensity exceeds 1.1 S_m does not extend more than 1.0 times the

square root of RT in the meridional direction, where R is the minimum midsurface radius of curvature and T is the minimum thickness in the region considered. For Section 13, the minimum thickness is that of the canister shell (0.625 in.) and the midsurface radius of the shell is 33.2175 in. The resulting distance is 4.56 in. A section located 4.56 in. from Section 13 in the meridional direction results in a membrane stress intensity of 6.7 ksi, which is below S_m. This section conservatively encompasses Section 12 since it is located 1.56 in. from this section. The stresses at adjacent circumferential sections (i.e., at 9°) for Sections 12 and 13 are also included in the tables for comparison. The critical section stresses are reported in Table 2.6.12.6-1 for the P_m and $P_m + P_b$ stresses.

Results are calculated for 1-ft side-drop with internal pressure both the 0° and 45° basket orientations. Tables 2.6.12.6-2 and 2.6.12.6-3 present the worst-case margins for the side-drop which occurs with the conditions noted. The minimum margin occurs for membrane without pressure and with pressure for membrane plus bending. The minimum margin of safety for the PWR canister in the side-drop is +0.02, which occurs at Section 12 in Table 2.6.12.3-1. The margins of safety are calculated as:

$$MS = (\text{allowable stress}/SI) - 1.$$

Table 2.6.12.6-1 PWR Canister Critical Sections for the 1-Foot Side Drop Load Condition

Condition	Stress	Critical Section	Table	Minimum Factor of Safety
Side Drop	Pm	1	2.6.12.6-2	+ 0.07
Side Drop + Pressure	$P_m + P_b$	12	2.6.12.6-3	+ 0.02

Table 2.6.12.6-2 PWR Canister: P_m Stresses - 1 Foot Side Drop

Section Location	Angle of Peak Stress Location	P_m Stresses (ksi)						SI (ksi)	Allowable Stress (ksi)	Margin of Safety
		Sx	Sy	Sz	Sxy	Syz	Sxz			
1	0	-14.7	-0.2	-5.2	-0.4	-0.1	-2	14.9	16	0.07
2	0	-13	-0.8	-6.4	-0.8	-0.4	-1.2	12.5	16	0.28
3	0	-3.8	-0.6	-3.3	-0.3	-0.6	-1.3	4.5	16	2.55
4	81	0	-0.2	0	0.8	0.1	0	1.5	16	9.39
5	9	-0.7	0.9	0.2	0	0	0.2	1.6	16	9.23
6	9	-0.7	1	0.2	0	0	0.2	1.7	16	8.19
7	9	-0.8	1.1	0.3	0	-0.1	0.2	2	16	7.18
8	0	-0.7	2.5	-1.1	-0.1	0.5	-0.1	3.7	16	3.34
9	9	-0.4	2.6	-2.1	0.05	1.3	-1.0	5.8	16	1.76
10	9	1.5	1.7	-2.1	-0.3	1.0	-0.6	4.6	16	2.48
11	9	3.7	1.8	-1.2	0.7	1.2	-1.6	6.4	16	1.5
12***	0	-24.4	-5.4	-6.7	-4.5	1.2	-1	21.7	24***	0.11
12	9	-0.5	-0.1	-3.5	0.1	0.6	-1.9	4.9	16	2.27
13*	0-7.5	-11.66	-3.42	-4.02	0.05	1.1	-2.33	9.99	12.8**	0.28
14	0	-0.9	-0.1	0.3	0	0	0	1.2	16	11.92
15	0	-0.3	0	0.1	0	0	0	0.4	16	35.79
16	0	-0.5	0.1	0.2	0	0	0	0.7	16	22.61

* Stress evaluated over weld compression region

** Allowable stress includes a stress reduction factor for weld: 0.8 x allowable stress.

*** Stresses treated as a local membrane stress. Allowable for normal conditions is $1.5S_m = 24$ ksi for P_L and $P_L = P_B$

Note: All of the allowable stress values presented in this table are based on SA240, Type 304L stainless steel at a temperature of 380°F unless otherwise stated. Localized peak temperatures in the central portion of the canister shell reach 399°F—resulting in slightly lower allowable stress values and subsequently slightly lower margins of safety for sections 5 and 6 than those presented in the table. However, this difference is negligible as discussed in Section 2.6.12.1.

Table 2.6.12.6-3 PWR Canister $P_m + P_b$ Stresses - 1-Foot Side Drop, Internal Pressure

Section Location	Angle of Peak Stress Location	$P_m + P_b$ Stresses (ksi)						SI (ksi)	Allowable Stress (ksi)	Margin of Safety
		Sx	Sy	Sz	Sxy	Syz	Sxz			
1	0	-23	-0.9	-7.6	0.6	0	-2	22.5	24	0.07
2	18	0.5	-12.7	-3.1	-0.2	0.2	-1.5	13.7	24	0.74
3	27	-0.6	-12.5	-4.6	0.1	-0.6	-2.3	13	24	0.85
4	9	-0.8	1.9	3.9	0	0.1	0.7	4.8	24	3.95
5	9	-0.6	2.3	3.7	0	0	0.7	4.5	24	4.3
6	9	-0.6	2.4	3.7	0	-0.1	0.7	4.5	24	4.33
7	9	-0.7	2.4	3.7	0	-0.1	0.7	4.7	24	4.12
8	0	-0.4	2.7	-2.4	-0.2	0.4	-0.2	5.1	24	3.66
9	9	1.2	6.3	-0.4	-0.1	1.5	0.1	7.4	24	2.24
10	0	-18.9	-2	-4.5	-5.3	1	-1.1	20.3	24	0.18
11	9	4.0	0.9	-1.4	0.8	1.3	2.7	8.2	24	1.93
12*	0	-28.6	-6.6	-8.2	-4.3	1.5	-0.7	24.5	25	0.02
13**	0-7.9	-16.65	-6.26	-6.48	-0.11	1.66	-1.98	12.49	20***	0.60
14	90	-0.8	0	0.4	0	0	0	1.2	24	18.27
15	90	-0.6	0	-0.2	0	0	0	0.6	24	39.77
16	0	-0.4	0	0.3	0	0	0	0.7	24	33.98

* The peak temperature as calculated in Section 3.4 is 265°F in the region of Sections 12 and 13. There the allowable stress for Type 304L stainless steel is 1.5 (16.7) = 25.05 ksi.

** The peak temperature as calculated in Section 3.4 is 265°F in the region of Sections 12 and 13. There the allowable stress for 304L stainless steel is 1.5 (16.7) = 25.05 ksi. Stress evaluated over weld compressing region.

*** Allowable stress includes a stress reduction factor for weld: 0.8 x allowable stress.

Note: All of the allowable stress values presented in this table are based on SA240, Type 304L stainless steel at a temperature of 380°F unless otherwise stated. Localized peak temperatures in the central portion of the canister shell reach 399°F—resulting in slightly lower allowable stress values and subsequently slightly lower margins of safety for sections 5 and 6 than those presented in the table. However, this difference is negligible as discussed in Section 2.6.12.1.

2.6.12.7 Stress Evaluation of PWR Canister for Combined Thermal and 1-Foot Side Drop Load Condition

The thermal stress loads described in Section 2.6.12.3 are applied in conjunction with the primary loads in Section 2.6.12.6 to produce a combined thermal stress plus 1-ft side-drop loading. The stress evaluation is performed according to the ASME Code, Section III, Subsection NB. The most critical sections are listed in Table 2.6.12.7-1. Results from the side-drop plus thermal load cases for the configurations that result in the minimum margins are presented in Tables 2.6.12.7-2 and 2.6.12.7-3. The stresses reported in this table correspond to the nodal stress at the surface. The minimum margin is +0.41 at Section 9 (see Table 2.6.12.7-1) when 3 S_m is used as the stress criteria. The margins of safety are calculated as:

MS = (allowable stress/SI) -1.

Table 2.6.12.7-1 PWR Canister Critical Sections for Combined 1-Foot Side Drop and Thermal Load Condition

Condition	Stress	Critical Section	Table	Minimum Margin of Safety
Side Drop + Thermal (cold)	$P_m + P_b + Q$	9	2.6.12.7-2	+ 0.41
Side Drop + Thermal (hot)	$P_m + P_b + Q$	9	2.6.12.7-3	+ 0.59

Table 2.6.12.7-2 PWR Canister $P_m + P_b + Q$ Stresses - 1-Foot Side Drop, Thermal Cold

Section Location	Angle of Peak Stress Location	$P_m + P_b + Q$ Stresses (ksi)						SI (ksi)	Allowable Stress (ksi)	Margin of Safety
		Sx	Sy	Sz	Sxy	Syz	Sxz			
1	0	-15.3	-0.4	-4	-0.1	0.1	-1.7	15.1	47.9	2.17
2	0	-11.7	-0.2	-2.2	-1.2	-0.4	-1.7	12.1	47.9	2.97
3	27	0.7	5.2	1.3	1.2	1.6	1.2	6.4	47.9	6.46
4	0	-0.4	1.1	2.9	0	-0.1	0.6	3.5	47.9	12.73
5	45	-1.2	1.5	-1.2	-0.4	-0.4	-1.3	4.2	47.9	10.41
6	45	-1	1.2	-1.1	0.3	0.3	-1.2	3.5	47.9	12.51
7	0	-0.4	1.1	2.6	0	0	0.5	3.1	47.9	14.33
8	0	0	2.7	-1.5	-0.1	0.6	-0.1	4.3	47.9	10.04
9	0	-26.6	6.9	-9.1	-2.1	1.7	0.2	34	47.9	0.41
10	0	-18.8	-2.6	-5	-4.5	0.9	-1.1	18.9	47.9	1.54
11	0	-26.3	3.3	-8.7	-0.3	1.8	-0.1	29.9	47.9	0.6
12	0	-26.4	-4.8	-7.9	-3.7	1.7	-0.6	23.5	47.9	1.04
13	0	-32.5	-9.8	-10.6	-1.2	2	-1.4	24.5	38.32*	0.56
14	180	-9.3	-2.5	-7.6	0.1	1.2	-0.1	7	47.9	5.8
15	0	-0.7	0	-0.1	0	0	0	0.7	47.9	69.76
16	0	-0.6	0.1	0.1	0	0	0	0.7	47.9	63.87

* Allowable stress includes a stress reduction factor for weld: 0.8 x allowable stress.

Note: All of the allowable stress values presented in this table are based on SA240, Type 304L stainless steel at a temperature of 380°F unless otherwise stated. Localized peak temperatures in the central portion of the canister shell reach 399°F—resulting in slightly lower allowable stress values and subsequently slightly lower margins of safety for sections 5 and 6 than those presented in the table. However, this difference is negligible as discussed in Section 2.6.12.1.

Table 2.6.12.7-3 PWR Canister $P_m + P_b + Q$ Stresses - 1-Foot Side Drop, Thermal Heat

Section Location	Angle of Peak Stress Location	$P_m + P_b + Q$ Stresses (ksi)						SI (ksi)	Allowable Stress (ksi)	Margin of Safety
		Sx	Sy	Sz	Sxy	Syz	Sxz			
1	0	-13.4	-0.3	-3.8	-0.1	0.1	-1.4	13.2	47.9	2.62
2	0	-9.8	0	-2	-1	-0.3	-1.4	10.2	47.9	3.7
3	27	0.6	4.6	1.1	1	1.3	1	5.5	47.9	7.65
4	0	-0.4	0.8	2.4	0	-0.1	0.5	3	47.9	15.13
5	45	-1	1.2	-1.1	-0.4	-0.4	-1.2	3.6	47.9	12.17
6	45	-0.9	1.1	-0.9	0.3	0.3	-1	3.1	47.9	14.39
7	0	-0.4	1	2.1	0	0	0.4	2.7	47.9	16.98
8	0	0	2.6	-1.2	-0.1	0.5	-0.1	4	47.9	11.05
9	0	-23.3	6.4	-8.2	-1.8	1.4	0.3	30.1	47.9	0.59
10	0	-16.5	-2.1	-4.8	-3.9	0.8	-0.8	16.6	47.9	1.88
11	0	-22.8	3.2	-7.8	-0.2	1.5	0	26.1	47.9	0.83
12	0	-23.3	-4.1	-7.4	-3.2	1.5	-0.4	20.8	47.9	1.31
13	0	-28.2	-8.5	-9.6	-1	1.6	-1.1	21.1	38.32*	0.82
14	180	-8.8	-1.6	-7.1	0.1	0.8	-0.1	7.4	47.9	5.51
15	0	-0.6	0	0.1	0	0	0	0.7	47.9	69.62
16	0	-0.7	0	-0.1	0	0	0	0.8	47.9	61.85

* Allowable stress includes a stress reduction factor for weld: 0.8 x allowable stress.

Note: All of the allowable stress values presented in this table are based on SA240, Type 304L stainless steel at a temperature of 380°F unless otherwise stated. Localized peak temperatures in the central portion of the canister shell reach 399°F—resulting in slightly lower allowable stress values and subsequently slightly lower margins of safety for sections 5 and 6 than those presented in the table. However, this difference is negligible as discussed in Section 2.6.12.1.

2.6.12.8 Stress Evaluation of PWR Canister for 1-Foot Corner Drop Load Condition

A structural analysis performed by using ANSYS to evaluate the effect of a 1-ft end-drop impact for both the top-and bottom-corner orientations of the PWR canister. The ASME Code, Section III, Subsection NB, requires that stresses arising from operational loads be assessed on the basis of the primary loads. The primary loads for the 1-ft corner-drop result from the deceleration of the canister and its contents and the 25-psig pressure load internal to the canister. The applied deceleration is 20 *g* for both orientations (Note—the actual deceleration is 5.6 *g*; therefore, the results presented in this section are conservative). The inertial load of the canister is addressed by the deceleration factor applied to the canister density. The contents weight is represented by a pressure load on the inner end surface of the canister and a pressure applied to the basket by means of pressure acting in the plane of the disks. Displacement constraints are applied to the plane of symmetry and the gap elements attached at the canister end to represent the top or bottom of the transport cask.

The locations of the linearized stresses are shown in Figure 2.6.12.3-1. The maximum stresses for P_m and $P_m + P_b$ are tabulated in Tables 2.6.12.8-2 through 2.6.12.8-5 for the conditions that result in the worst-case stresses. The critical sections for the pressure and the pressure plus the deceleration load, with reference to the section and the appropriate tables, are shown in Table 2.6.12.8-1. The margins of safety in these tables are calculated as:

$$MS = (\text{allowable stress}/SI)-1.$$

Table 2.6.12.8-1 PWR Canister Critical Sections for the 1-Foot Corner Drop Load Condition

Condition	Stress	Critical Section	Table	Margin of Safety*
Top Corner Drop + Pressure	P_m	9	2.6.12.8-2	+ 0.08
Top Corner Drop Inertia	$P_m + P_b$	2	2.6.12.8-3	+ 0.02
Bottom Corner Drop + Pressure	P_m	9	2.6.12.8-4	+ 0.02
Bottom Corner Drop + Inertia	$P_m + P_b$	11	2.6.12.8-5	+0.26

* Note: These margins of safety are based on stresses calculated for corner drops with a 20 g deceleration load. The actual deceleration load is 5.6 g; therefore, these margins of safety are conservative.

Table 2.6.12.8-2 PWR Canister P_m Stresses 1-Foot Top Corner Drop, Internal Pressure

Section Location	Angle of Peak Stress Location	P_m Stresses (ksi)						SI (ksi)	Allowable Stress (ksi)	Margin of Safety
		Sx	Sy	Sz	Sxy	Syz	Sxz			
1	0	-5.9	0.3	-1.7	0.2	-0.1	-0.8	6.4	16	1.5
2	0	-1.6	0.3	-1.5	-0.1	-0.3	-0.4	2.4	16	5.75
3	0	-0.5	0.5	-0.9	0.2	-0.3	-0.3	1.7	16	8.18
4	0	-1.2	-0.1	1.5	0	0	0	2.7	16	4.89
5	0	-1.2	-0.2	1.4	0	0	0	2.6	16	5.14
6	0	-1.2	-0.4	1.4	0	0	0	2.6	16	5.12
7	0	-1.2	-0.8	1.5	0	-0.1	0	2.7	16	4.91
8	45	0.4	-0.8	0.3	-0.4	-0.4	0.4	1.9	16	7.39
9	0	-16.1	-2	-4.4	-1.8	0.5	-0.4	14.7	16	0.08
10	0	-11.1	-4.3	-3.3	-1.9	0.2	-0.8	8.6	16	0.86
11	0	-15.1	-6.6	-5.4	-0.7	0.4	-0.4	9.9	16	0.61
12	0	-14.1	-6.2	-3.3	-2.9	0.2	-1	12	16	0.33
13	0	-13.2	-8	-4	-0.8	0.2	-1	9.5	12.8*	0.35
14	0	-0.2	0	0.2	0	0	0	0.4	16	37.89
15	171	-0.1	-0.3	0	0	0	0	0.4	16	40.38
16	0	-0.2	-0.4	0.1	0	0	0	0.5	16	34.04

* Allowable stress includes a stress reduction factor for weld: 0.8 x allowable stress.

Note: All of the allowable stress values presented in this table are based on SA240, Type 304L stainless steel at a temperature of 380°F unless otherwise stated. Localized peak temperatures in the central portion of the canister shell reach 399°F—resulting in slightly lower allowable stress values and subsequently slightly lower margins of safety for sections 5 and 6 than those presented in the table. However, this difference is negligible as discussed in Section 2.6.12.1.

Table 2.6.12.8-3 PWR Canister $P_m + P_b$ Stresses - 1-Foot Top Corner Drop

Section Location	Angle of Peak Stress Location	$P_m + P_b$ Stresses (ksi)						SI (ksi)	Allowable Stress (ksi)	Margin of Safety
		Sx	Sy	Sz	Sxy	Syz	Sxz			
1	0	-15.3	-6.5	-4.5	-3.9	-0.2	-1	12.4	24	0.93
2	0	-19.4	3.9	-4.4	-0.7	1.2	-0.1	23.5	24	0.02
3	180	-0.5	9.9	5.3	0	0	-0.4	10.4	24	1.3
4	0	-1.4	0	2.5	0	0	0.1	4	24	5.04
5	0	-1.4	-0.1	2.4	0	0	0.1	3.8	24	5.37
6	0	-1.4	-0.4	2.4	0	0	0.1	3.8	24	5.35
7	0	-1.4	-0.7	2.5	0	-0.1	0.1	3.9	24	5.09
8	36	0.1	-1.4	0.1	-0.4	-0.7	0.1	2.2	24	9.92
9	0	-16.9	0.2	-5.4	-1.3	0.5	-0.2	17.3	24	0.38
10	0	-11.9	-5.7	-2.9	-3.4	0.1	-1.1	10.9	24	1.21
11	0	-17	-8.9	-5.6	-1.2	0.5	-0.7	11.8	24	1.03
12	0	-15.4	-6.1	-3.7	-2.4	0.4	-0.9	12.6	24	0.91
13	0	-15.7	-10.2	-5.4	-1.4	0.4	-1	10.8	19.2*	0.78
14	90	-6.4	-0.1	-5.9	0.1	-0.1	0	6.3	24	2.78
15	81	0	-0.3	0.1	0	0	0	0.4	24	54.38
16	0	-0.2	-0.3	0.1	0	0	0	0.4	24	53.04

* Allowable stress includes a stress reduction factor for weld: 0.8 x allowable stress.

Note: All of the allowable stress values presented in this table are based on SA240, Type 304L stainless steel at a temperature of 380°F unless otherwise stated. Localized peak temperatures in the central portion of the canister shell reach 399°F—resulting in slightly lower allowable stress values and subsequently slightly lower margins of safety for sections 5 and 6 than those presented in the table. However, this difference is negligible as discussed in Section 2.6.12.1.

Table 2.6.12.8-4 PWR Canister P_m Stresses - 1-Foot Bottom Corner Drop

Section Location	Angle of Peak Stress Location	P_m Stresses (ksi)						SI (ksi)	Allowable Stress (ksi)	Margin of Safety
		Sx	Sy	Sz	Sxy	Syz	Sxz			
1	0	-7	-1.9	-2.4	-0.3	0	-1	6	16	1.67
2	18	0.6	-3.3	-0.6	0.1	-0.1	-0.5	4	16	2.95
3	18	0	-3.1	-0.9	0.1	-0.2	-0.4	3.3	16	3.84
4	0	-1.2	-2.3	0.2	0	0	-0.1	2.8	16	4.75
5	180	0	-2.2	-0.1	0	0	0	2.3	16	6.07
6	180	0	-2.2	-0.1	0	0	0	2.2	16	6.36
7	180	0	-1.9	-0.1	0	0	0	1.9	16	7.27
8	45	0.1	-1.1	0	-0.3	-0.3	0	1.5	16	10.29
9	0	-15	0.2	-4.5	-1.4	0.9	-0.3	15.6	16	0.02
10	0	-7.5	-0.4	-2.5	-1.4	0.7	-0.7	7.9	16	1.03
11**	0	-17.6	-1.1	-5.1	-0.2	1.1	-0.3	16.8	24	0.43**
11	9	2.9	1.3	-0.5	0.3	0.6	-1.0	4.1	16	2.90
12	0	-11.7	-2.7	-2.8	-2	0.6	-0.8	10.5	16	0.53
13	0	-11.8	-3.4	-3.1	0.1	0.8	-1.2	9.6	12.8*	0.33
14	0	-0.4	-0.3	0.2	0	0	0	0.5	16	28.96
15	0	-0.1	0	0.1	0	0	0	0.2	16	104.27
16	0	-0.3	0	0	0	0	0	0.3	16	50.45

* Allowable stress includes a stress reduction factor for weld: 0.8 x allowable stress.

** Stresses treated as local membrane stress. Allowable for normal conditons is 1.5 S_m = 24 ksi for P_L and $P_L + P_B$.

Note: All of the allowable stress values presented in this table are based on SA240, Type 304L stainless steel at a temperature of 380°F unless otherwise stated. Localized peak temperatures in the central portion of the canister shell reach 399°F—resulting in slightly lower allowable stress values and subsequently slightly lower margins of safety for sections 5 and 6 than those presented in the table. However, this difference is negligible as discussed in Section 2.6.12.1.

Table 2.6.12.8-5 PWR Canister $P_m + P_b$ Stresses - 1-Foot Bottom Corner Drop

Section Location	Angle of Peak Stress Location	$P_m + P_b$ Stresses (ksi)						SI (ksi)	Allowable Stress (ksi)	Margin of Safety
		Sx	Sy	Sz	Sxy	Syz	Sxz			
1	0	-7.5	-0.8	-2.5	0.3	0.1	-1	7	24	2.44
2	18	-0.2	-6.9	-1.4	-0.1	0	-0.5	6.9	24	2.46
3	18	-0.3	-6.1	-1.3	0.2	0	-0.5	6	24	3.02
4	0	-1.4	-1.9	2.5	0	0	0.1	4.4	24	4.39
5	0	-1.3	-1.4	2.4	0	0	0.1	3.9	24	5.21
6	0	-1.3	-1.1	2.4	0	0	0.1	3.7	24	5.4
7	0	-1.4	-0.8	2.4	0	0	0.1	3.8	24	5.27
8	18	0.3	-1.1	-0.9	0.3	0.4	-0.4	2	24	11.1
9	0	-15.2	2.9	-5	-1.2	0.9	-0.1	18.3	24	0.31
10	0	-7.9	-0.8	-1.5	-2.3	0.5	-0.9	8.9	24	1.7
11	0	-15.9	2.9	-4.4	-0.1	1	0	18.9	24	0.26
12	0	-14.6	-3.7	-3.9	-1.8	0.8	-0.7	12.2	24	0.96
13	0	-18	-6.8	-5.9	-0.2	1.1	-0.9	13	19.2*	0.48
14	0	-0.4	-0.3	0.2	0	0	0	0.5	24	43.89
15	72	1.3	0	1.4	0	0	0	1.4	24	15.9
16	18	-0.9	0	-0.6	0	0	0	0.9	24	25.01

* Allowable stress includes a stress reduction factor for weld: 0.8 x allowable stress.

Note: All of the allowable stress values presented in this table are based on SA240, Type 304L stainless steel at a temperature of 380°F unless otherwise stated. Localized peak temperatures in the central portion of the canister shell reach 399°F—resulting in slightly lower allowable stress values and subsequently slightly lower margins of safety for sections 5 and 6 than those presented in the table. However, this difference is negligible as discussed in Section 2.6.12.1.

2.6.12.9 Stress Evaluation of PWR Canister for Combined Thermal and 1-Foot Corner Drop Load Conditions

The thermal stress loads described in Section 2.6.12.3 are applied in conjunction with the primary loads in Section 2.6.12.8 to produce a combined thermal stress plus corner impact loading. The stress evaluation is performed according to the ASME Code, Section III, Subsection NB. On the basis of the results in Section 2.6.12.8, the most critical sections are identified in Table 2.6.12.9-1. The stresses reported in this table correspond to the nodal stress at the surface. The minimum margin of safety is +1.14 when 3 S_m is used as the stress criterion. Tables 2.6.12.9-2 through 2.6.12.9-5 tabulate the results for top and bottom corner-drop with thermal results for the conditions that result in the minimum margins of safety. The stress intensity criterion of 3.0 S_m is satisfied. The margins of safety are calculated as:

MS = (allowable stress/SI)-1.

Table 2.6.12.9-1 PWR Canister Critical Sections for the Combined 1-Foot Corner Drop and Thermal Load Condition

Condition	Stress	Critical Section	Table	Minimum Margin of Safety
Top Corner Drop + Thermal (cold)	$P_m + P_b + Q$	2	2.6.12.9-2	+ 1.14
Top Corner Drop + Thermal (hot)	$P_m + P_b + Q$	2	2.6.12.9-3	+ 1.24
Bottom Corner Drop + Pressure + Thermal (cold)	$P_m + P_b + Q$	9	2.6.12.9-4	+1.96
Bottom Corner Drop + Pressure + Thermal (hot)	$P_m + P_b + Q$	9	2.6.12.9-5	+1.37

Table 2.6.12.9-2 PWR Canister $P_m + P_b + Q$ Stresses - 1-Foot Top Corner Drop, Thermal Cold

Section Location	Angle of Peak Stress Location	$P_m + P_b + Q$ Stresses (ksi)						SI (ksi)	Allowable Stress (ksi)	Margin of Safety
		Sx	Sy	Sz	Sxy	Syz	Sxz			
1	0	-19.5	-7.1	-4.4	-3.7	-0.2	-1	16.3	47.9	1.95
2	0	-19.9	2.3	-3.3	-0.6	1.2	-0.3	22.4	47.9	1.14
3	126	0.4	-10.3	0.3	0.7	0.1	-0.5	11.2	47.9	3.3
4	0	-1.4	-0.6	2.4	0	-0.1	0	3.7	47.9	11.79
5	0	-0.8	-2.9	1.7	0	-0.4	-0.2	4.8	47.9	9.08
6	0	-1.1	-1.9	2.1	0	0.2	-0.2	4.1	47.9	10.72
7	0	-1.3	-0.7	2.3	0	0	0	3.5	47.9	12.54
8	171	-0.2	-3.6	-0.4	0	0.2	0	3.5	47.9	12.78
9	0	-12.6	0.1	-3.8	-1.1	0.5	-0.2	12.9	47.9	2.71
10	0	-10	-4.8	-2.4	-2.5	0.1	-1	9	47.9	4.35
11	0	-11.8	-6.9	-3.9	-0.9	0.4	-0.6	8.2	47.9	4.85
12	0	-11.8	-4.2	-2.8	-1.9	0.4	-0.7	9.8	47.9	3.87
13	0	-11.8	-6.9	-3.9	-0.9	0.4	-0.6	8.2	38.32*	3.67
14	0	-15.3	-1.8	-14.4	0	-1	0	13.6	47.9	2.52
15	81	-0.1	-0.3	0.1	0	0	0	0.4	47.9	116.04
16	0	-0.1	-0.4	0.1	0	0	0	0.6	47.9	82.56

* Allowable stress includes a stress reduction factor for weld: 0.8 x allowable stress.

Note: All of the allowable stress values presented in this table are based on SA240, Type 304L stainless steel at a temperature of 380°F unless otherwise stated. Localized peak temperatures in the central portion of the canister shell reach 399°F—resulting in slightly lower allowable stress values and subsequently slightly lower margins of safety for sections 5 and 6 than those presented in the table. However, this difference is negligible as discussed in Section 2.6.12.1.

Table 2.6.12.9-3 PWR Canister $P_m + P_b + Q$ Stresses - 1-Foot Top Corner Drop, Thermal Heat

Section Location	Angle of Peak Stress Location	$P_m + P_b + Q$ Stresses (ksi)						SI (ksi)	Allowable Stress (ksi)	Margin of Safety
		Sx	Sy	Sz	Sxy	Syz	Sxz			
1	0	-18.3	-6.7	-4.4	-3.4	-0.2	-0.9	14.9	47.9	2.22
2	0	-18.7	2.5	-3.1	-0.7	1	-0.3	21.4	47.9	1.24
3	126	0.4	-10.2	0.2	0.7	0.1	-0.4	11	47.9	3.35
4	0	-1.1	-0.5	2	0	-0.1	0.1	3.1	47.9	14.7
5	0	-0.5	-2.4	1.7	0	-0.3	0.1	4.2	47.9	10.38
6	0	-0.6	-1.5	2.1	0	0.2	0.3	3.7	47.9	12.08
7	180	0	-2.9	0	0	0	0	2.9	47.9	15.69
8	171	-0.1	-3.6	-0.4	0	0.2	0	3.5	47.9	12.78
9	0	-12.8	0.4	-3.8	-1.1	0.5	-0.2	13.5	47.9	2.56
10	0	-10.2	-4.8	-2.4	-2.6	0.1	-1	9.1	47.9	4.27
11	0	-12	-6.9	-4	-1	0.4	-0.6	8.4	47.9	4.73
12	0	-11.9	-4.1	-2.8	-2.1	0.4	-0.7	10	47.9	3.81
13	0	-12	-6.9	-4	-1	0.4	-0.6	8.4	38.32*	3.56
14	0	-14.5	-1.6	-13.6	0.1	-0.9	0	13	47.9	2.69
15	90	-0.1	-0.3	0.1	0	0	0	0.4	47.9	116.24
16	0	-0.1	-0.4	0.1	0	0	0	0.6	47.9	84.45

* Allowable stress includes a stress reduction factor for weld: 0.8 x allowable stress.

Note: All of the allowable stress values presented in this table are based on SA240, Type 304L stainless steel at a temperature of 380°F unless otherwise stated. Localized peak temperatures in the central portion of the canister shell reach 399°F—resulting in slightly lower allowable stress values and subsequently slightly lower margins of safety for sections 5 and 6 than those presented in the table. However, this difference is negligible as discussed in Section 2.6.12.1.

Table 2.6.12.9-4 PWR Canister $P_m + P_b + Q$ Stresses - 1-Foot Bottom Corner Drop, Internal Pressure, Thermal Cold

Section Location	Angle of Peak Stress Location	$P_m + P_b + Q$ Stresses (ksi)						SI (ksi)	Allowable Stress (ksi)	Margin of Safety
		Sx	Sy	Sz	Sxy	Syz	Sxz			
1	0	-6.3	-0.9	-1.9	0.1	0	-0.8	5.6	47.9	7.53
2	27	-0.2	-5	-1.4	-0.2	-0.1	-0.8	5.2	47.9	8.15
3	27	-0.2	-5.1	-1.3	0	-0.3	-0.6	5.2	47.9	8.20
4	0	-1	-1.5	2.8	0	0	-0.2	4.3	47.9	10.03
5	0	-1	-1.1	2.8	0	0	0.2	3.9	47.9	11.33
6	0	-0.9	-0.8	2.8	0	0	0.2	3.8	47.9	11.75
7	0	-0.9	-0.6	2.8	-0.2	0	0.2	3.7	47.9	11.81
8	0	-0.6	0.2	1.2	-1.1	0.4	0.1	2	47.9	22.65
9	0	-14.3	2.2	-4.5	-1.1	0.9	-0.2	16.7	47.9	1.86
10	0	-9	-1.5	-1.7	-2.2	0.5	-1	9.2	47.9	4.23
11	0	-14.2	1.1	-4.5	-0.2	1.9	-0.1	15.4	47.9	2.11
12	0	-13.6	-2.9	-3.5	-1.8	9	-0.7	11.9	47.9	3.02
13	0	-17.3	-5.6	-5.5	-0.5	1	-0.8	12.9	38.32*	1.97
14	0	-0.3	-0.4	0.2	0	0	0	0.6	47.9	85.16
15	81	0.7	0	0.9	0	0	0	0.9	47.9	51.95
16	45	-0.6	-0.1	-0.4	0	0	0	0.6	47.9	82.75

* Allowable stress includes a stress reduction factor for weld: 0.8 x allowable stress.

Note: All of the allowable stress values presented in this table are based on SA240, Type 304L stainless steel at a temperature of 380°F unless otherwise stated. Localized peak temperatures in the central portion of the canister shell reach 399°F—resulting in slightly lower allowable stress values and subsequently slightly lower margins of safety for sections 5 and 6 than those presented in the table. However, this difference is negligible as discussed in Section 2.6.12.1.

Table 2.6.12.9-5 PWR Canister $P_m + P_b + Q$ Stresses - 1-Foot Bottom Corner Drop, Internal Pressure, Thermal Heat

Section Location	Angle of Peak Stress Location	$P_m + P_b + Q$ Stresses (ksi)						SI (ksi)	Allowable Stress (ksi)	Margin of Safety
		Sx	Sy	Sz	Sxy	Syz	Sxz			
1	0	-2.1	0	1.3	0	0.1	-0.1	3.5	47.9	12.79
2	162	0.1	-5.1	0.3	0.1	0	-0.1	5.4	47.9	7.87
3	162	0.1	-4.9	0.4	0	-0.1	-0.1	5.3	47.9	8.12
4	180	0	-3.7	1.2	0	0	-0.1	4.9	47.9	8.76
5	180	0	-3.8	1.5	0	-0.2	0	5.3	47.9	8.06
6	0	-0.5	-1.6	3.5	0	0.1	0.2	5.1	47.9	8.34
7	0	-0.9	-0.6	3.2	0	-0.1	0.3	4.1	47.9	10.82
8	0	-0.6	0.8	2	-0.1	0.6	0.3	2.9	47.9	15.7
9	0	-17	2.9	-5.3	-1.3	1.2	-0.3	20.2	47.9	1.37
10	0	-11.5	-1.9	-2.4	-2.7	0.6	-1.2	11.6	47.9	3.13
11	0	-16.7	1.4	-5.5	-0.2	1.1	-0.2	18.4	47.9	1.61
12	0	-16	-3.2	-4	-2.2	1	-0.9	14.3	47.9	2.36
13	0	-20.5	-6.3	-6.5	-0.7	1.3	-1	15.6	38.3*	1.46
14	0	-10	-4.9	-9.7	0	0.1	0	5.1	47.9	8.33
15	90	0.8	0	1	0	0	0	1	47.9	47.69
16	27	-0.6	-0.1	-0.3	0	0	0	0.6	47.9	79.93

* Allowable stress includes a stress reduction factor for weld: 0.8 x allowable stress.

Note: All of the allowable stress values presented in this table are based on SA240, Type 304L stainless steel at a temperature of 380°F unless otherwise stated. Localized peak temperatures in the central portion of the canister shell reach 399°F—resulting in slightly lower allowable stress values and subsequently slightly lower margins of safety for sections 5 and 6 than those presented in the table. However, this difference is negligible as discussed in Section 2.6.12.1.

2.6.12.10 Shear Stresses for 1-Foot Drops

The primary mechanism for shear loading in the canister drop analyses occurs for the bottom end-drop in the canister structural and shield lid welds. The maximum stress intensity for either Sections 12 or 13 during the bottom end-drop is 1.8 ksi for the bottom end-drop with thermal heat (Table 2.6.12.5-5). The maximum shear is 1.8/2 = 0.9 ksi. The allowable shear is 0.6 S_m per the ASME Code, Section III, Subsection NB-3227.2 for pure shear loading. The maximum canister shell temperature is 399°F and the margin of safety for pure shear is

$$MS = 0.6 \times 15.8 / 0.9 - 1 = 9.53$$

2.6.12.11 Canister Bearing Stresses for 1-Foot Side Drop

The average bearing stress on the canister wall is computed for the side-drop using the smallest length of canister and the maximum mass for either the PWR or BWR canisters. This results in a conservatively bounding value of the average bearing stress. The maximum canister plus contents mass is for the BWR Class 5 with a weight of 75,896 lb. For contact of the canister wall with the inner shell over an 18° arc (conservative), the projected bearing width is 10.54 in. The length of the shortest canister is 175.25 in. (PWR Class 1). The average bearing stress is

$$\text{Bearing Stress} = 75{,}896 \text{ lb} \times 20g/(175.25 \text{ in.} \times 10.54 \text{ in.}) = 822 \text{ psi}$$

Based on a yield strength of 17.5 ksi at 400°F, the margin of safety is

$$MS = (17.5 / 0.822) - 1 = +\text{Large}$$

Next, the bearing stress evaluation is presented in the regions under the shield lid and structural lid welds for the normal conditions side-drop (see Sections 9, 10, and 11 in Figure 2.6.12.3-1). Three separate regions are considered for the bearing evaluation; (1) the area beneath the structural lid weld from 0° to 9°, (2) area between the structural lid weld and shield lid weld from 0° to 9°, and (3) area below shield lid weld between 0° and 9°.

In order to calculate the bearing stresses in these regions, forces from the gap elements between the canister shell and the cask inner shell in these regions are examined. The forces from the gap elements act normal to the surface of the shell (i.e., radially), but are conservatively summed for each of the three regions described above. The following enveloping force summations are obtained from the PWR and BWR analysis results for each of the regions. The governing load case is also noted.

Region 1:	-45,373 lb	PWR Side Drop with no Internal Pressure
Region 2:	-43,935 lb	PWR Side Drop With Internal Pressure
Region 3:	-78,640 lb	BWR Side Drop with Internal Pressure

Gaps at both 0° and 9° are closed. Gaps at angular locations greater than 9° remain open in the regions of interest. The projected width conservatively based on 9° contact is 5.27 for the three regions. Region 1 has a length equal to the weld thickness (0.88 in.), Region 2 has a length of (3 - 0.88) 2.12 in., and Region 3 has a length of 0.5 in. equal to length of the shield lid weld. The corresponding bearing stresses for each region are

Region 1: 45,373/(5.27 x 0.88) = 9,784 psi

Region 2: 43,935/(5.27 x 2.12) = 3,932 psi

Region 3: 78,640/(5.27 x 0.5) = 29,844 psi

The peak temperature in the canister shell in the region of the lids is 266°F for the PWR canister (see Section 3.4). The yield strength is 19,950 psi based on this temperature for 304L stainless steel. The margins of safety for each region are presented below.

Region 1: 19.950 / 9.784 - 1 = 1.04

Region 2: 19.950 / 3.918 - 1 = 4.09

Region 3 is allowed 1.5 S_y since the width of application of the load is less than the distance to the free edge (0.5 < 3.0) and

Region 3: 1.5 x 19.950 / 29.844 - 1 = 0.0026

2.6.12.12 Canister Buckling Evaluation for 1-Foot End Drop

Code Case N-284-1 [12] of the ASME Boiler and Pressure Vessel Code is used to analyze the PWR canister for the normal condition 1-foot end drop (both top and bottom end drops). The evaluation requirements of Regulatory Guide 7.6, Paragraph C.5, are shown to be satisfied by the results of the buckling interaction equation calculations of Code Case N-284-1. The canister buckling design criteria are described in Section 2.1.2.5.3.

The data considered for the buckling evaluation includes shell geometry parameters, shell fabrication tolerances, shell material properties, theoretical elastic buckling stress values for the shell, and membrane stress components in the shell. The internal stress field that controls the buckling of a cylindrical shell consists of the longitudinal (axial) membrane, circumferential (hoop) membrane, and in-plane shear stresses. These stresses may exist singly or in combination, depending on the applied loading. Only these three stress components are considered in the buckling analysis.

A 20 g deceleration load was used for all the 1-ft drop canister analyses that are presented in Sections 2.6.12.4 through 2.6.12.9. The 20 g-load bounds all 1-ft deceleration loads for all other drop angles. The top- and bottom-end drops result in the largest potential for canister shell buckling and, therefore, are the two load cases presented here. The side drop load case is not considered a credible buckling mode of the canister shell and is, therefore, not presented here.

The stress results from the canister analysis are screened for the maximum values of the longitudinal compression, circumferential compression, or in-plane shear stresses for the 1-ft drop cases (top- and bottom-end drops) with and without pressure. For each loading case, the largest of each of the three stress components anywhere regardless of location within the PWR canister shell are combined. To these maximum stress components are added the maximum

stresses from the hot and cold thermal cases (Tables 2.6.12.3-1 and 2.6.12.3-2). Combining the maximum stress components in this way produces a conservative, bounding-case buckling evaluation of the PWR canister, one which envelopes all 1-ft PWR canister drop cases including those presented in Tables 2.6.12.4-4 and 2.6.12.4-6.

Consistent with the Code Case, the following are used:

- The symbols ϕ, θ, or $\phi\theta$ correspond to the longitudinal (axial) direction or stress component, circumferential (hoop) direction or stress component, and in-plane shear stress component, respectively.
- The formulas in the Code Case for cylindrical shells (unstiffened) are used.
- The factor of safety is 2.0 for Normal Conditions.

The analytical process used for the PWR canister is the same as that described in a step-by-step example presented in Section 2.7.12.3 (for the cask inner shell).

The geometry parameters used in the PWR canister evaluation are presented in Table 2.6.12.12-1.

The maximum stress components used in the evaluation and the buckling interaction ratios for the top- and bottom-end drop cases are provided in Table 2.6.12.12-2. The results of the buckling analysis show that all interaction equation ratios are less than 1.0. Therefore, the buckling criteria of Code Case N-284-1 are satisfied, thus demonstrating that buckling of the PWR canister does not occur.

Table 2.6.12.12-1 Geometry Parameters for the PWR Canister

Parameter	Value
t = thickness (in)	0.625
ID = inside diameter (in)	65.81
R = radius (in) = (ID+t)/2	33.22
R/t	53.15
$(Rt)^{0.5}$	4.56
Overall Length (in)	191.95
Bottom Thickness (in)	1.75
Structural Lid Thickness (in)	3.0
L_ϕ = Length used in evaluation (in)*	187.2
$L_\theta = 2\pi R$ = circumference (in)	208.7
ν = Poisson's Ratio	0.275

L_ϕ = Overall canister length - Bottom thickness - Structural lid thickness.

Table 2.6.12.12-2 Buckling Evaluation Results for the PWR Canister for 1-Foot End Drop

Load Condition	Longitudinal (Axial) Stress* S_ϕ (psi)	Circumferential (Hoop) Stress* S_θ (psi)	In-plane Shear Stress $S_{\phi\theta}$ (psi)	Elastic Buckling Interaction Equations				Plastic Buckling Interaction Equations			
				Q1	Q2	Q3	Q4	Q5	Q6	Q7	Q8
1-Ft Top End Drop	2400	300	400	.009	.077	.066	.009	.077	.065	.077	.066
1-Ft Bottom End Drop	3600	600	300	.063	.115	.131	.064	.115	.131	.115	.131

Component stresses include thermal stresses.

* Compressive stresses

2.6.13 PWR Basket Analysis - Normal Conditions of Transport

The Universal Transport Cask PWR basket is a right-cylinder structure fabricated with 24 square fuel tubes, a number of circular support disks, a number of heat transfer disks, eight tie rods with spacers, and two end weldment plates. The number of support disks and heat transfer disks varies depending upon the class of PWR fuel the basket is designed to contain. The basket components and their geometry are illustrated in Figure 2.6.13-1 and Figure 2.6.13-2. Figure 2.6.13-3 shows the details of the fuel tube with the encasing BORAL. The fuel tubes are open at each end; therefore, longitudinal fuel assembly loads are imparted to the canister shield lid or the bottom plate, and not the fuel basket structure. The fuel basket contains the fuel and is laterally supported by the canister shell.

The fuel assemblies together with the tubes are laterally supported in the holes in the stainless steel support disks. The aluminum heat transfer disks are located throughout the cavity to fully optimize the passive heat rejection from the package. They serve no structural function other than supporting their own weight. The dimensional differences between the heat transfer disk and the support disk accommodate the different rate of thermal growth between aluminum and stainless steel, thereby preventing interference between the tube, support disk, and heat transfer disks.

The primary function of the spacers and the threaded top nut is to locate and structurally assemble the support disks, heat transfer disks, and top and bottom weldment plates into an integral assembly. The spacers carry the inertial weight of the support disks, heat transfer disks, one end plate, and their own inertial weight for a normal transport condition 1-ft end-drop. The end-drop loading of the split spacers and tie rods represents a classical, closed-form structural analysis. The support disk requires a detailed finite element analysis for side-drop, end-drop, and oblique drops. The stainless steel fuel tubes are not considered to be a structural component with respect to the disks other than consideration of their mass contribution to loading.

The PWR fuel basket is evaluated for the normal transport loads in this section. End-drop, side-drop, oblique drop orientations are evaluated. The basket is evaluated for the hypothetical accident condition in Section 2.7.8.

Figure 2.6.13-1 PWR Fuel Assembly Basket

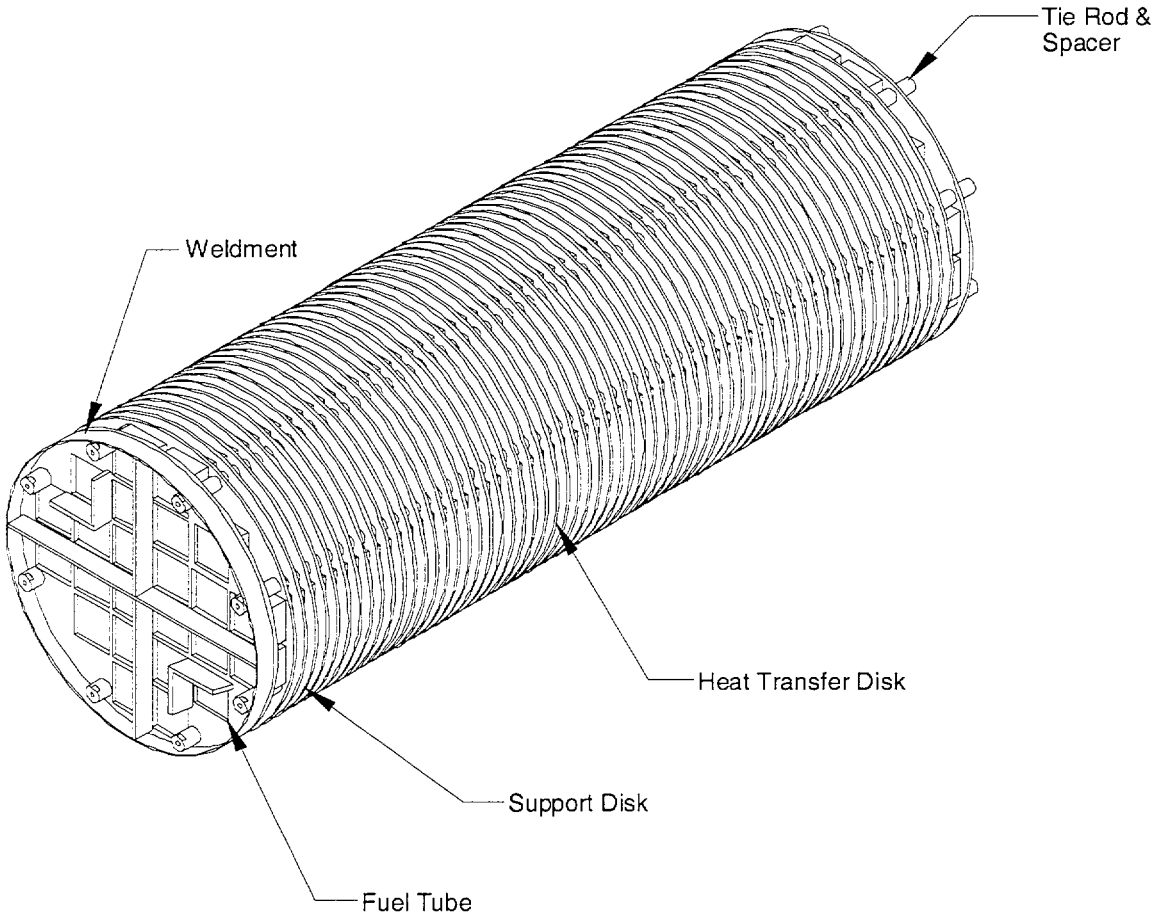

Figure 2.6.13-2 Support Disk Cross Section Configuration

FIGURE WITHHELD UNDER 10 CFR 2.390

Note:

Engineering drawings provide appropriate tolerances for dimensions shown.

Figure 2.6.13-3 PWR Fuel Tube Configuration

FIGURE WITHHELD UNDER 10 CFR 2.390

2.6.13.1 Analysis Description

On the basis of criticality control requirements, the PWR fuel basket design criteria require the maintenance of fuel support and control of spacing of the fuel assemblies for all load conditions. The structural design criteria for the structural components in the fuel basket is the ASME Code, Section III, Division 1, Subsection NG [15]. Consistent with this criterion, for any normal condition load and position orientation, the main structural component in the fuel basket, the stainless steel support disk, is shown to have a maximum primary membrane stress intensity and a primary membrane plus bending stress intensity in any disk. These are less than the design stress intensity value S_m and $1.5S_m$, respectively. The value of S_m is defined at the temperatures for the component being analyzed.

In the side-drop, the loads of the fuel assemblies are transferred into the plane of the support disks, from which they are transmitted to the canister shell. For the end-drop, the fuel basket components are loaded by their own inertial weight and do not experience load from the guided but freestanding fuel assemblies. Various cask drop angles and radial impact orientations of the support disk are evaluated. In addition to the load from inertial weight, the differential thermal expansion of the support disk is also evaluated.

2.6.13.2 Finite Element Model Description - PWR Basket

Two finite element models are generated to analyze the PWR fuel basket for the normal operating conditions: one for the end-drop, in which the loads are perpendicular to the plane of the disk, and one for the side-drop, in which the loads act in the plane of the disk. Both models accommodate thermal expansion effects by using the temperature distribution from the thermal analysis and the coefficient of thermal expansion. Off-angle (ϕ) drop results are calculated based on the component stresses from the end and side drop evaluation.

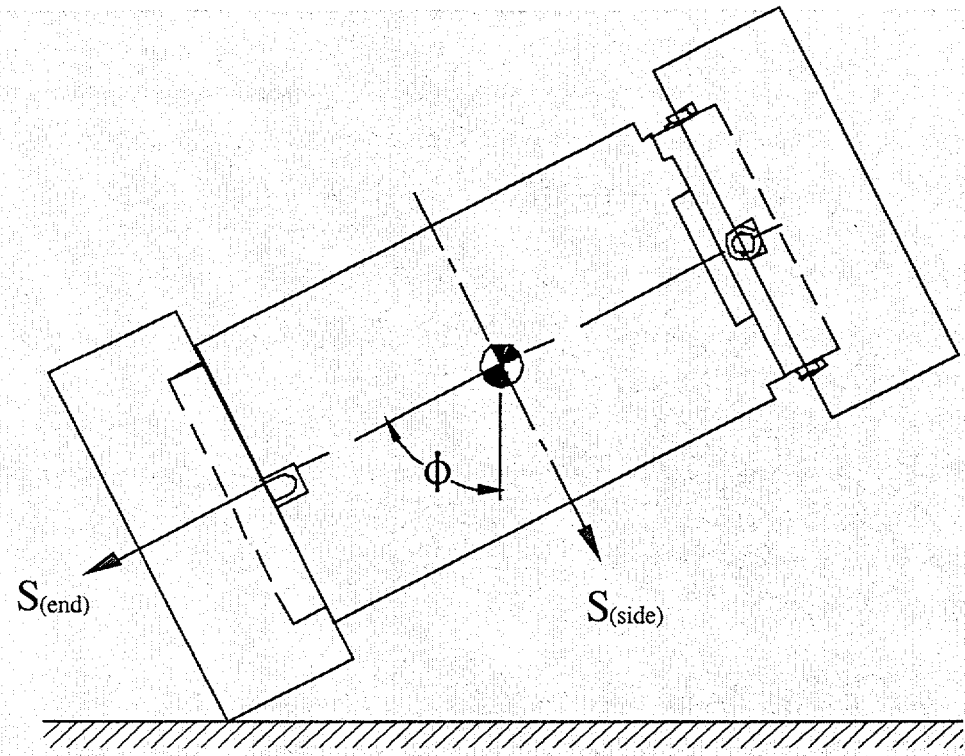

Oblique Drop

The finite element model for the side-drop is a two-dimensional model that includes the cross section of the canister shell. A complete basket support disk is modeled for the side impact evaluation (see Figure 2.6.13.2-1). ANSYS PLANE42 elements are used to model the support disk and canister. The PLANE42 is a two-dimensional element with four nodes. The PLANE42 elements correspond to plane stress and the thickness of the model for the disk is input as 0.5 in., which corresponds to the thickness of the support disk. For the canister shell, a thickness of 4 inches is used to approximate the center to center distance of support disks. For the end-drop, the PLANE42 elements are replaced with the SHELL63 elements and elements for canister shell are deleted. The nodal-element relationship is the same; with the exception of the change in the stiffness-displacement degree of freedoms. The shell elements accommodate the out-of-plane bending, which is present in the end-drop condition. The only loading in the out-of-plane direction is the inertial weight of the support disk.

In the model for side drop, compressive loads are transmitted from the basket support disks to the canister shell. The interface between the support disk and canister is modeled by using the ANSYS CONTAC52 element, which permits the support disk model nodes to interface with the canister elements. The interface between the canister shell and the inner radius of the transport cask inner shell is also modeled with CONTAC52 elements, which act as a compression-only element. The deformed shape of the transport cask inner shell is applied to the outer nodes of the CONTAC52 elements as boundary conditions. Contact elements are also modeled in the gap created by the slit located at the support rod hole. For all CONTAC52 elements the gap stiffness is set to 1.00E+06 lb/in. Because all contact interfaces are circular, additional rotational stiffness is added to the model by including weak beams between the support disk and the canister shell, and between the canister and cask inner shell.

The loads from the fuel assembly are modeled as a pressure loading at the inner surface of each support disk slot opening. The surface pressure loads are determined by performing a comparison analysis of all relevant PWR assemblies. For the PWR support disk the worst case loading is (PWR Class #1):

$$\text{Weight of single fuel assembly + fuel tube} = \frac{37608\,\text{lb}}{24\,\text{slots}} + \frac{3285\,\text{lb}}{24\,\text{slots}} \approx 1{,}705\,\text{lb}$$

$$\text{Pressure applied to web slot} = (1705\ \text{lb}/(9.272\ \text{in} \times 0.5\ \text{in}))/30 = 12.26\ \text{psi},$$

where, the slot size is 9.272 in., the thickness of the disk is 0.5 in, and the number of disks[1] is 30.

The weight of the tie-rods and split spacers is accounted for by multiplying the density of the support disk material by a factor of 1.373 as shown below.

$$\text{Ratio} = \frac{\text{Disk Weight + Rods and Spacers}}{\text{Disk Weight}} = \frac{186.4 + 69.4}{186.4} = 1.373$$

[1] No credit is taken for the top and bottom weldments when calculating the pressure load. Only the 30 support disks are used.

$$\text{Density} = 0.291 \times 1.373 = 0.3997 \text{ lb/in}^3$$

Inertial loads applied to the support disk include 20 *g* for normal and 60 *g* for accident conditions. The pressure load is also multiplied by the appropriate acceleration.

For the side drop, pressure loads are applied to the ligament based on the impact angle. The PWR fuel assembly basket with 24 slots exhibits one-eighth symmetry. A minimum perimeter radial thickness occurs between the corner of the fuel assembly slot in the basket and the outer radius at three locations: 18.22°, 26.28°, and 45° measured counterclockwise from the Y-axis (see Fig. 2.6.13.2-2). Therefore, to ensure that the bounding basket orientation is evaluated, drop orientations of 0°, 18.22°, 26.28°, and 45° are considered. To simulate end drop loading, pressure loads are set to zero and the acceleration is applied in the axial direction of the cask.

To evaluate oblique impacts, the stress components (i.e. S_x, S_y, S_{xy}) are calculated based on the stress results of the side and end drop cases. These stress combinations are accomplished with the use of an ANSYS macro. The macro extracts the component stresses based on the basket drop orientation for the side and end drop cases. Once the stress data is stored in an array, the macro cycles through the cask drop angles (0°, 23°, 30°, 40°, 45°, 50°, 60°, 70°, 75°, 80°, 85°, 88°, and 90°), as well as the basket drop orientation (0°, 18.22°, 26.28°, and 45°) and calculates the stresses. Finally, the macro then sorts the data to determine the worst case stresses and the drop orientations where the stress occurs.

To determine the most critical cross sections, a series of cross sections are considered. To aid in the identification of these sections, Figures 2.6.13.2-3 and 2.6.13.2-4 show the locations on a support disk. Table 2.6.13.2-1 lists the cross sections versus Point 1 and Point 2, which spans the cross section of the web in the plane of the support disk. Points 1 and 2 for each cross section are shown in Figures 2.6.13.2-3 and 2.6.13.2-4. For example, Section 3 from Table 2.6.13.2-1 refers to Points 5 and 6 shown in Figure 2.6.13.2-3 (just to the left of the center-line of the support disk). From the corresponding nodal coordinates given in Table 2.6.13.2-1, point 5 (x=-0.75, y=0.75) and point 6 (x=-0.75, y=-0.75), it is known that the section is taken across the vertical ligament.

The stress evaluation for the support disk is performed according to the ASME Code, Section III, Subsection NG [15]. According to this subsection, linearized stresses of cross sections of the

structure are to be compared against the allowable stresses. The allowable stresses for normal and accident conditions are taken from Subsection NG as shown below.

	Normal (Level A)	Accident (Level D)
P_m	1.0 Sm	0.7 Su
P_m+P_b	1.5 Sm	1.0 Su
P+Q	3.0 Sm	N/A

The following table summarizes the side, end, and off-angle stresses in the PWR support disk for normal conditions (1-Foot drop). The minimum margin of safety is +0.18.

Stress State	Thermal Case[1]	Section	Drop Angle[2]	Basket Angle[3]	Sx (ksi)	Sy (ksi)	Sxy (ksi)	Stress Intensity (ksi)	Allowable Stress (ksi)	Margin of Safety
P_m	B	120	90.0	45.0	9.6	-9.8	8.0	25.2	45.0	0.79
P_m+P_b	B	21	85.0	45.0	-46.8	-41.5	12.5	57.0	67.5	0.18
P+Q	B	21	88.0	45.0	-48.7	-45.2	15.6	62.7	135.0	1.15
P_m	A	120	90.0	45.0	9.1	-9.1	7.6	23.7	44.3	0.86
P_m+P_b	A	21	90.0	45.0	-42.8	-39.0	11.6	52.7	64.5	0.22
P+Q	A	4	85.0	26.3	-41.3	-43.6	14.9	57.4	125.9	1.19

[1] See Section 2.6.13.3 for definition of thermal cases.
[2] Cask drop angle, see figure shown on previous page.
[3] Basket angle (orientation), see Figure 2.6.13.2-2.

Figure 2.6.13.2-1 PWR Basket Model for Side-Drop

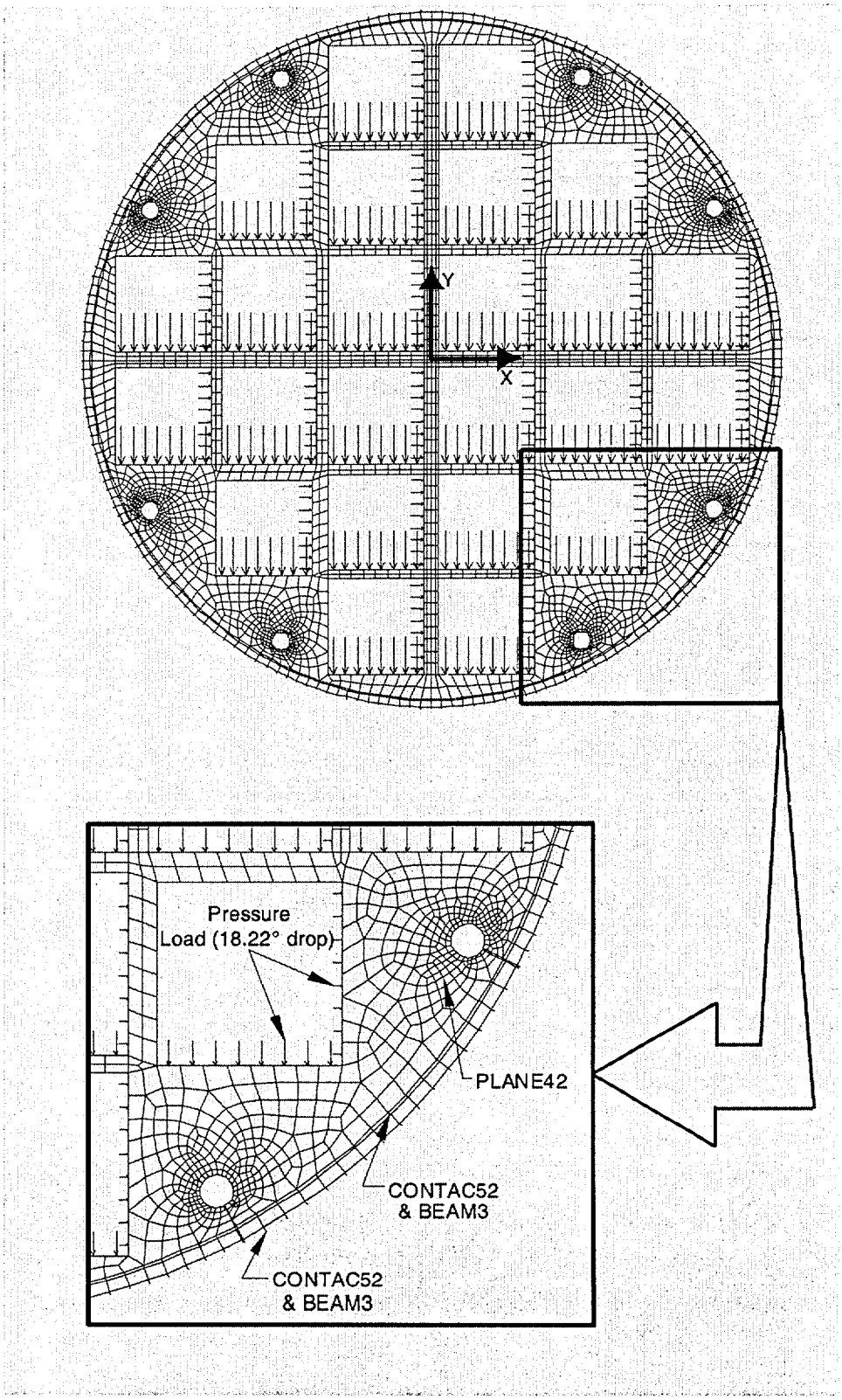

Figure 2.6.13.2-2 Side Drop Orientation

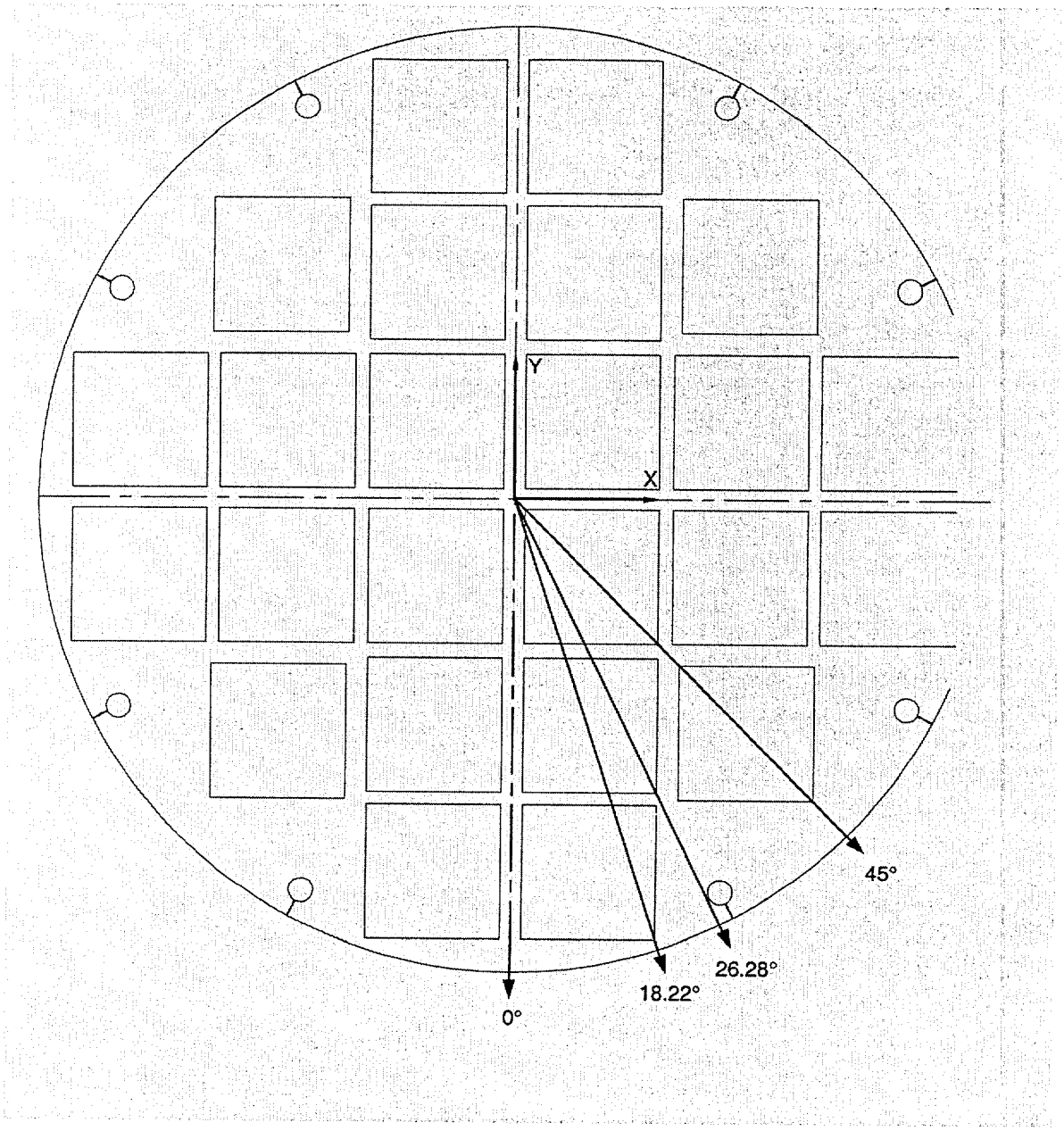

Figure 2.6.13.2-3 Location of the Section to Obtain Linearized Stresses (Left half of support disk)

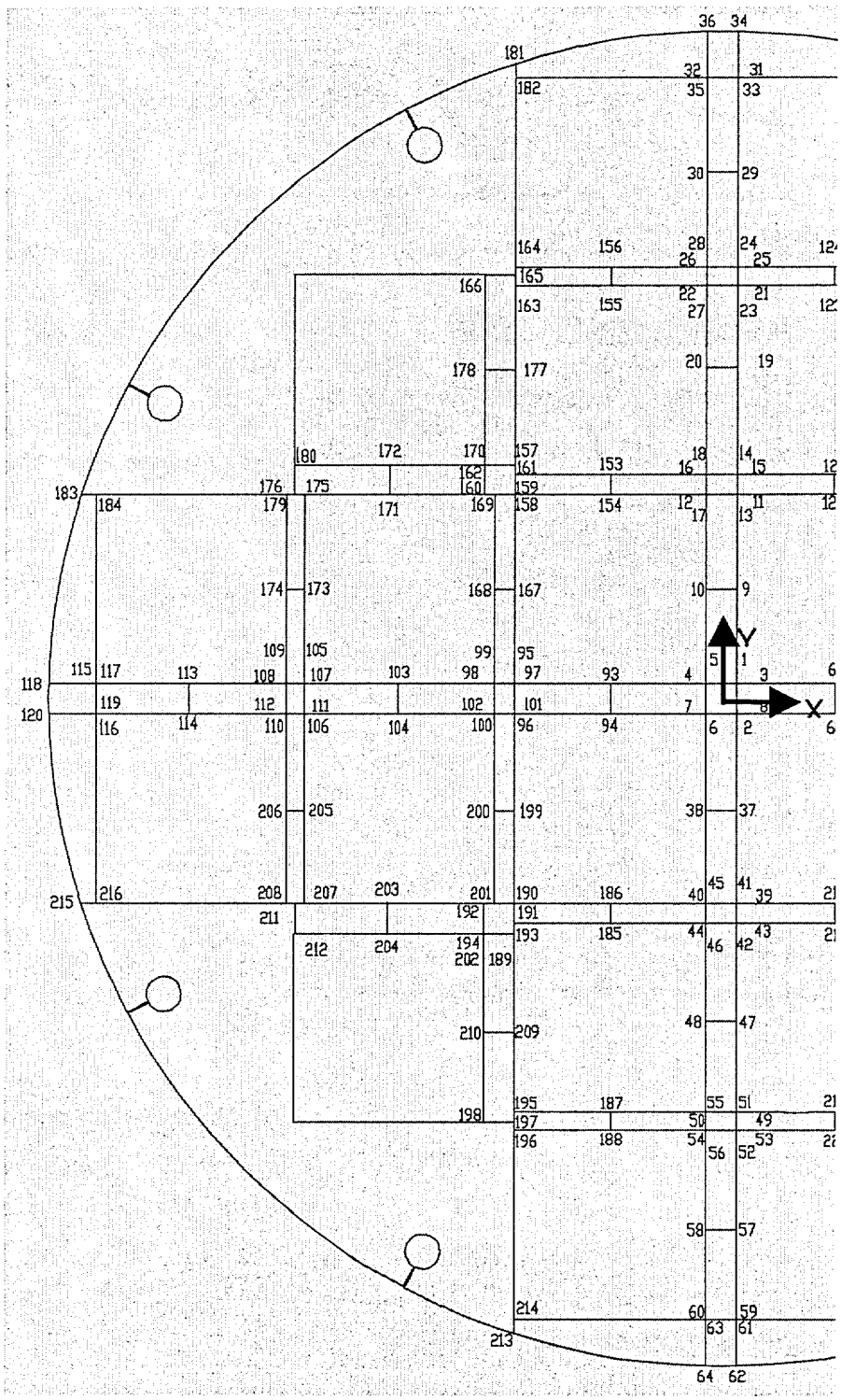

Figure 2.6.13.2-4 Location of the Section to Obtain Linearized Stresses (Right half of support disk)

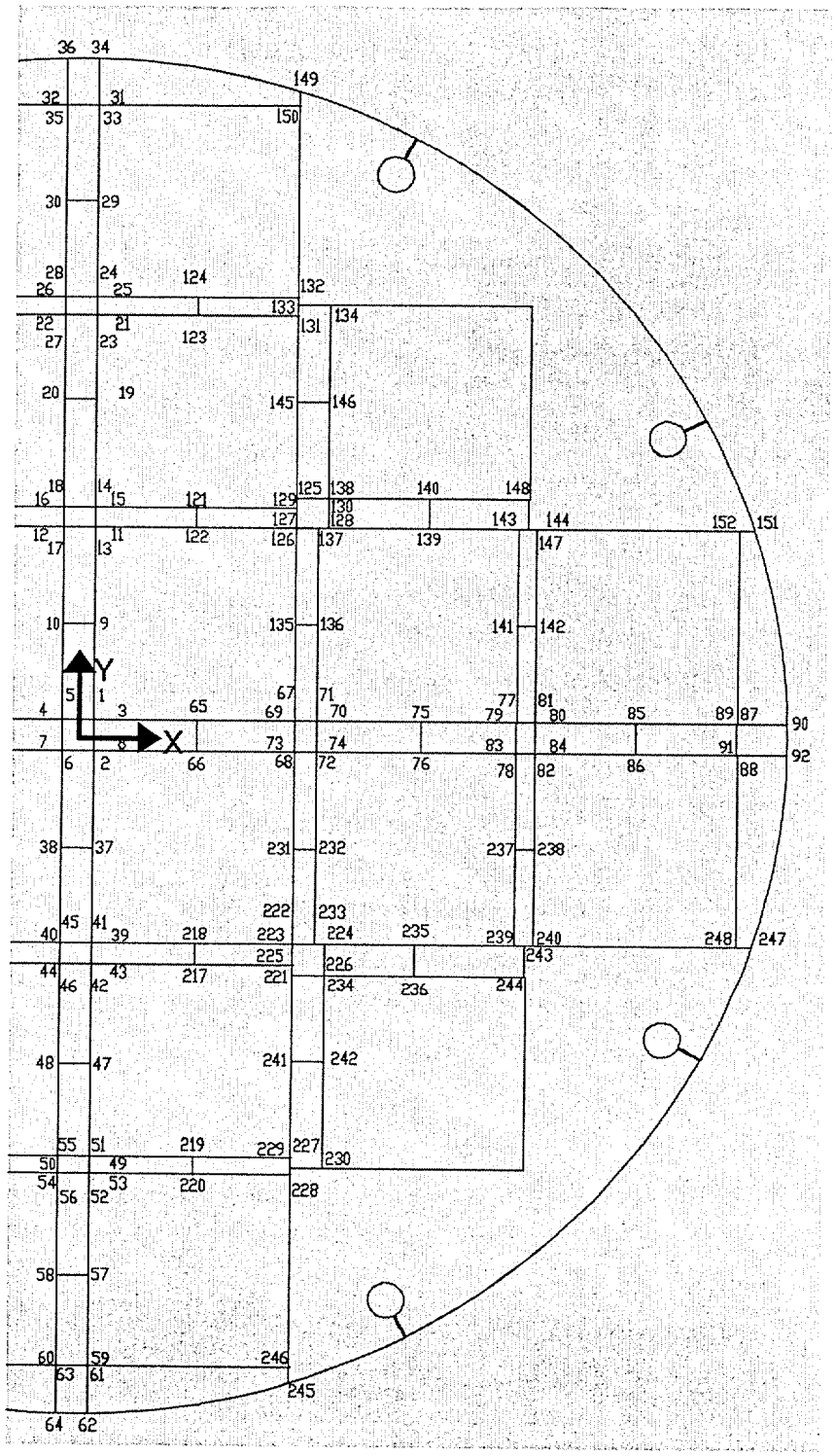

Table 2.6.13.2-1 Listing of Cross Sections for Stress Evaluation of Support Disk

Section & Line#	Point 1	Point 2	X 1	Y 1	X 2	Y 2
1	1	2	0.75	0.75	0.75	-0.75
2	3	4	0.75	0.75	-0.75	0.75
3	5	6	-0.75	0.75	-0.75	-0.75
4	7	8	-0.75	-0.75	0.75	-0.75
5	9	10	0.75	5.39	-0.75	5.39
6	11	12	0.75	10.02	-0.75	10.02
7	13	14	0.75	10.02	0.75	11.02
8	15	16	0.75	11.02	-0.75	11.02
9	17	18	-0.75	10.02	-0.75	11.02
10	19	20	0.75	15.66	-0.75	15.66
11	21	22	0.75	20.29	-0.75	20.29
12	23	24	0.75	20.29	0.75	21.17
13	25	26	0.75	21.17	-0.75	21.17
14	27	28	-0.75	20.29	-0.75	21.17
15	29	30	0.75	25.81	-0.75	25.81
16	31	32	0.75	30.44	-0.75	30.44
17	33	34	0.75	30.44	0.75	32.74
18	35	36	-0.75	30.44	-0.75	32.74
19	37	38	0.75	-5.39	-0.75	-5.39
20	39	40	0.75	-10.02	-0.75	-10.02
21	41	42	0.75	-10.02	0.75	-11.02
22	43	44	0.75	-11.02	-0.75	-11.02
23	45	46	-0.75	-10.02	-0.75	-11.02
24	47	48	0.75	-15.66	-0.75	-15.66
25	49	50	0.75	-20.29	-0.75	-20.29
26	51	52	0.75	-20.29	0.75	-21.17
27	53	54	0.75	-21.17	-0.75	-21.17
28	55	56	-0.75	-20.29	-0.75	-21.17
29	57	58	0.75	-25.81	-0.75	-25.81
30	59	60	0.75	-30.44	-0.75	-30.44
31	61	62	0.75	-30.44	0.75	-32.74
32	63	64	-0.75	-30.44	-0.75	-32.74
33	65	66	5.39	0.75	5.39	-0.75
34	67	68	10.02	0.75	10.02	-0.75
35	69	70	10.02	0.75	11.02	0.75
36	71	72	11.02	0.75	11.02	-0.75
37	73	74	10.02	-0.75	11.02	-0.75
38	75	76	15.66	0.75	15.66	-0.75
39	77	78	20.29	0.75	20.29	-0.75
40	79	80	20.29	0.75	21.17	0.75
41	81	82	21.17	0.75	21.17	-0.75

Table 2.6.13.2-1 Listing of Cross Sections for Stress Evaluation of Support Disk (Continued)

Section & Line#	Point 1	Point 2	X 1	Y 1	X 2	Y 2
42	83	84	20.29	-0.75	21.17	-0.75
43	85	86	25.81	0.75	25.81	-0.75
44	87	88	30.44	0.75	30.44	-0.75
45	89	90	30.44	0.75	32.74	0.75
46	91	92	30.44	-0.75	32.74	-0.75
47	93	94	-5.39	0.75	-5.39	-0.75
48	95	96	-10.02	0.75	-10.02	-0.75
49	97	98	-10.02	0.75	-11.02	0.75
50	99	100	-11.02	0.75	-11.02	-0.75
51	101	102	-10.02	-0.75	-11.02	-0.75
52	103	104	-15.66	0.75	-15.66	-0.75
53	105	106	-20.29	0.75	-20.29	-0.75
54	107	108	-20.29	0.75	-21.17	0.75
55	109	110	-21.17	0.75	-21.17	-0.75
56	111	112	-20.29	-0.75	-21.17	-0.75
57	113	114	-25.81	0.75	-25.81	-0.75
58	115	116	-30.44	0.75	-30.44	-0.75
59	117	118	-30.44	0.75	-32.74	0.75
60	119	120	-30.44	-0.75	-32.74	-0.75
61	121	122	5.39	11.02	5.39	10.02
62	123	124	5.39	20.29	5.39	21.17
63	125	126	10.02	11.02	10.02	10.02
64	127	128	10.02	10.02	11.02	10.02
65	129	130	10.02	11.52	11.52	11.52
66	131	132	10.02	20.29	10.02	21.17
67	133	134	10.02	20.29	11.52	20.29
68	135	136	10.02	5.39	11.02	5.39
69	137	138	11.52	10.02	11.52	11.52
70	139	140	16.16	10.02	16.16	11.52
71	141	142	20.29	5.39	21.17	5.39
72	143	144	20.29	10.02	21.17	10.02
73	145	146	10.02	16.16	11.52	16.16
74	147	148	20.29	10.02	20.29	11.52
75	149	150	10.02	31.18	10.02	30.44
76	151	152	31.18	10.02	30.44	10.02
77	153	154	-5.39	11.02	-5.39	10.02
78	155	156	-5.39	20.29	-5.39	21.17
79	157	158	-10.02	11.02	-10.02	10.02
80	159	160	-10.02	10.02	-11.02	10.02
81	161	162	-10.02	11.52	-11.52	11.52
82	163	164	-10.02	20.29	-10.02	21.17
83	165	166	-10.02	20.29	-11.52	20.29
84	167	168	-10.02	5.39	-11.02	5.39

Table 2.6.13.2-1 Listing of Cross Sections for Stress Evaluation of Support Disk (Continued)

Section & Line#	Point 1	Point 2	X 1	Y 1	X 2	Y 2
85	169	170	-11.52	10.02	-11.52	11.52
86	171	172	-16.16	10.02	-16.16	11.52
87	173	174	-20.29	5.39	-21.17	5.39
88	175	176	-20.29	10.02	-21.17	10.02
89	177	178	-10.02	16.16	-11.52	16.16
90	179	180	-20.29	10.02	-20.29	11.52
91	181	182	-10.02	31.18	-10.02	30.44
92	183	184	-31.18	10.02	-30.44	10.02
93	185	186	-5.39	-11.02	-5.39	-10.02
94	187	188	-5.39	-20.29	-5.39	-21.17
95	189	190	-10.02	-11.02	-10.02	-10.02
96	191	192	-10.02	-10.02	-11.02	-10.02
97	193	194	-10.02	-11.52	-11.52	-11.52
98	195	196	-10.02	-20.29	-10.02	-21.17
99	197	198	-10.02	-20.29	-11.52	-20.29
100	199	200	-10.02	-5.39	-11.02	-5.39
101	201	202	-11.52	-10.02	-11.52	-11.52
102	203	204	-16.16	-10.02	-16.16	-11.52
103	205	206	-20.29	-5.39	-21.17	-5.39
104	207	208	-20.29	-10.02	-21.17	-10.02
105	209	210	-10.02	-16.16	-11.52	-16.16
106	211	212	-20.29	-10.02	-20.29	-11.52
107	213	214	-10.02	-31.18	-10.02	-30.44
108	215	216	-31.18	-10.02	-30.44	-10.02
109	217	218	5.39	-11.02	5.39	-10.02
110	219	220	5.39	-20.29	5.39	-21.17
111	221	222	10.02	-11.02	10.02	-10.02
112	223	224	10.02	-10.02	11.02	-10.02
113	225	226	10.02	-11.52	11.52	-11.52
114	227	228	10.02	-20.29	10.02	-21.17
115	229	230	10.02	-20.29	11.52	-20.29
116	231	232	10.02	-5.39	11.02	-5.39
117	233	234	11.52	-10.02	11.52	-11.52
118	235	236	16.16	-10.02	16.16	-11.52
119	237	238	20.29	-5.39	21.17	-5.39
120	239	240	20.29	-10.02	21.17	-10.02
121	241	242	10.02	-16.16	11.52	-16.16
122	243	244	20.29	-10.02	20.29	-11.52
123	245	246	10.02	-31.18	10.02	-30.44
124	247	248	31.18	-10.02	30.44	-10.02

2.6.13.3 Thermal Conditions and Expansion Evaluation for PWR Support Disks

Three thermal conditions are considered when evaluating the PWR support disk evaluation.

Condition 1: 100°F ambient temperature with maximum decay heat load and maximum solar insolation.
Condition 2: -40°F ambient temperature with maximum decay heat load and no insolation.
Condition 3: -40°F ambient temperature, no decay heat load, and no solar insolation.

Temperatures of the support disk for each heat condition are as follows:

Heat Condition	T_{max} (°F)	T_{min} (°F)	ΔT (°F)
1	686	366	320
2	600	255	345
3	-40	-40	0

Two thermal cases (A and B) are considered in the analysis. As shown in the following table, Thermal case A bounds heat condition 1 (maximum temperature) and heat condition 2 (maximum temperature gradient) while thermal case B represents heat condition 3.

Thermal Case	Heat Condition	T_{max} (°F)	T_{min} (°F)	ΔT (°F)
A	1 & 2	686	341	345
B	3	-40	-40	0

The allowable stresses are calculated by using the temperature distribution based on the results of a steady-state conduction analysis performed by using temperature boundary conditions.

Temperatures are applied to the PWR support disk model to simulate worst-case temperature conditions. The maximum temperature is applied to the center of the support disk model and the minimum temperature is applied to the outer edge. A thermal conduction analysis (with all planar elements temporarily changed to ANSYS SHELL57 thermal elements) then determines the temperature distribution across the disk. The temperature data is then read back into the structural model so that material properties can be taken at temperature. For each basket angle, two analyses are prepared. The first run analyzes the support disk without thermal stresses and

the second run accounts for thermal stresses. Although thermal stress evaluations are not required for Level D conditions, combinations of impact and thermal stresses are calculated for both Level A and Level D as input to the buckling evaluations presented in Section 2.6.13.14.

The thermal stress at the outer radius of the basket is tension, whereas the interior thermal stress is compression. With the application of the primary loads, the area in contact with the shell is in compression, thus reducing the combined stresses. During the 1-ft drop impact, the support disk deflects so as to maximize the contact region with the canister. The result is tension stresses at the outer radius of the support disk and compression of the interior ligaments. For this reason, the primary + secondary stress intensity range evaluation is considered to envelope the evaluation for the thermal-stress-only condition.

2.6.13.4 Stress Evaluation of PWR Support Disks for 1-Foot End-Drop Load Condition

The support disks of the basket are located by eight tie rods with spacers. A structural analysis is performed by using ANSYS to evaluate the effect of a 1-ft end-drop impact that corresponds to the most severe out-of-plane loading. The finite element model described in Section 2.6.13.2 is used in conjunction with a 20 g deceleration.

The calculated values of maximum primary membrane and bending stresses for thermal cases A and B are provided in Tables 2.6.13.4-1 and 2.6.13.4-2. The membrane stresses for the 1-ft end drop conditions is effectively zero.

The maximum primary membrane plus bending stress intensity is 7.8 ksi (thermal case A), which results in a margin of safety of +7.44. The location of the top ten maximum primary membrane plus bending stresses, Thermal Case A, are presented in Figure 2.6.13.4-1.

Figure 2.6.13.4-1 Locations of Maximum P_m+P_b Stresses—1-Foot End Drop, Thermal Case A

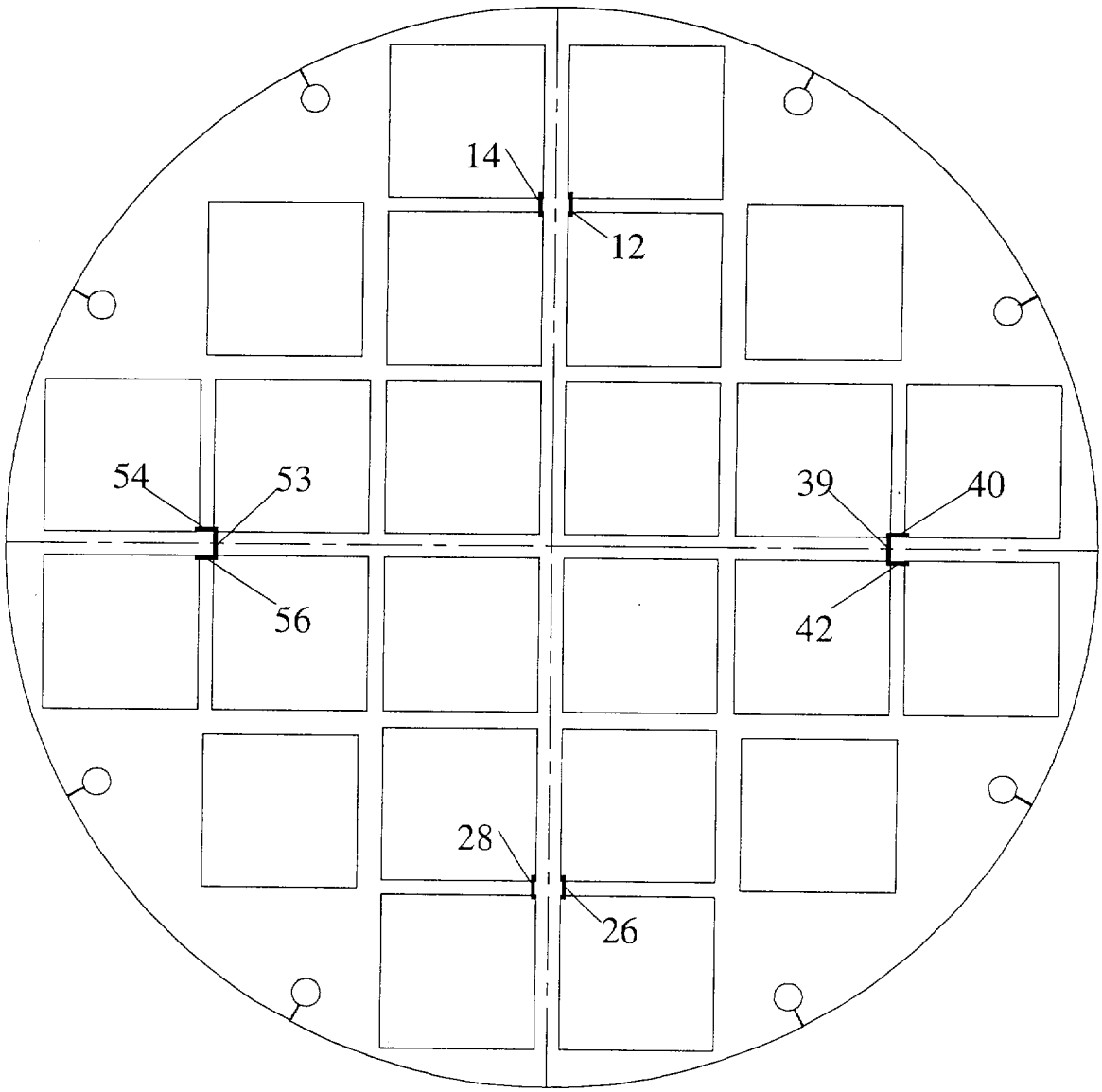

Table 2.6.13.4-1 $P_m + P_b$ Stresses for Support Disk—1-Foot End-Drop, Thermal Case A

Section	Sx (ksi)	Sy (ksi)	Sxy (ksi)	Stress Intensity (ksi)	Allowable Stress (ksi)	Margin of Safety
40	2.0	-5.8	0.2	7.8	65.8	7.44
42	2.0	-5.8	-0.2	7.8	65.8	7.44
54	2.0	-5.8	-0.2	7.8	65.8	7.44
56	2.0	-5.8	0.2	7.8	65.8	7.44
12	-5.7	2.0	0.2	7.8	65.8	7.45
14	-5.7	2.0	-0.2	7.8	65.8	7.45
26	-5.7	2.0	-0.2	7.8	65.8	7.45
28	-5.7	2.0	0.2	7.8	65.8	7.45
39	2.6	-3.7	0.0	6.4	65.8	9.36
53	2.6	-3.7	0.0	6.4	65.8	9.36
11	-3.7	2.6	0.0	6.3	65.8	9.37
25	-3.7	2.6	0.0	6.3	65.8	9.37
67	1.7	5.1	2.3	6.2	66.4	9.63
83	1.7	5.1	-2.3	6.2	66.4	9.63
99	1.7	5.1	2.3	6.2	66.4	9.63
115	1.7	5.1	-2.3	6.2	66.4	9.63
74	5.0	1.6	2.3	6.2	66.4	9.73
106	5.0	1.6	2.3	6.2	66.4	9.73
90	5.0	1.6	-2.3	6.2	66.4	9.73
122	5.0	1.6	-2.3	6.2	66.4	9.73
55	2.2	-3.5	0.0	5.7	65.9	10.55
41	2.2	-3.5	0.0	5.7	65.9	10.55
27	-3.5	2.2	0.0	5.7	65.9	10.57
13	-3.5	2.2	0.0	5.7	65.9	10.57
82	3.4	3.2	-2.0	5.3	66.4	11.46
114	3.4	3.2	-2.0	5.3	66.4	11.46
98	3.4	3.2	2.0	5.3	66.4	11.46
66	3.4	3.2	2.0	5.3	66.4	11.46
72	3.2	3.4	2.0	5.3	66.4	11.52
104	3.2	3.4	2.0	5.3	66.4	11.52
120	3.2	3.4	-2.0	5.3	66.4	11.52
88	3.2	3.4	-2.0	5.3	66.4	11.52
5	0.0	-5.1	0.0	5.1	63.6	11.58
19	0.0	-5.1	0.0	5.1	63.6	11.58
33	-5.1	0.0	0.0	5.1	63.6	11.58
47	-5.1	0.0	0.0	5.1	63.6	11.58
2	-3.0	-4.9	0.0	4.9	63.0	11.91
4	-3.0	-4.9	0.0	4.9	63.0	11.91
3	-4.9	-3.0	0.0	4.9	63.0	11.92
1	-4.9	-3.0	0.0	4.9	63.0	11.92

Table 2.6.13.4-2 $P_m + P_b$ Stresses for Support Disk—1-Foot End-Drop, Thermal Case B

Section	Sx (ksi)	Sy (ksi)	Sxy (ksi)	Stress Intensity (ksi)	Allowable Stress (ksi)	Margin of Safety
40	2.0	-5.8	0.2	7.8	67.5	7.67
42	2.0	-5.8	-0.2	7.8	67.5	7.67
54	2.0	-5.8	-0.2	7.8	67.5	7.67
56	2.0	-5.8	0.2	7.8	67.5	7.67
12	-5.8	2.0	0.2	7.8	67.5	7.68
14	-5.8	2.0	-0.2	7.8	67.5	7.68
26	-5.8	2.0	-0.2	7.8	67.5	7.68
28	-5.8	2.0	0.2	7.8	67.5	7.68
39	2.6	-3.7	0.0	6.3	67.5	9.69
53	2.6	-3.7	0.0	6.3	67.5	9.69
11	-3.7	2.6	0.0	6.3	67.5	9.70
25	-3.7	2.6	0.0	6.3	67.5	9.70
67	1.7	5.1	2.2	6.2	67.5	9.89
83	1.7	5.1	-2.2	6.2	67.5	9.89
99	1.7	5.1	2.2	6.2	67.5	9.89
115	1.7	5.1	-2.2	6.2	67.5	9.89
74	5.0	1.5	2.3	6.1	67.5	10.00
106	5.0	1.5	2.3	6.1	67.5	10.00
90	5.0	1.5	-2.3	6.1	67.5	10.00
122	5.0	1.5	-2.3	6.1	67.5	10.00
55	2.2	-3.5	0.0	5.7	67.5	10.86
41	2.2	-3.5	0.0	5.7	67.5	10.86
27	-3.5	2.2	0.0	5.7	67.5	10.89
13	-3.5	2.2	0.0	5.7	67.5	10.89
82	3.4	3.2	-2.0	5.3	67.5	11.76
114	3.4	3.2	-2.0	5.3	67.5	11.76
98	3.4	3.2	2.0	5.3	67.5	11.76
66	3.4	3.2	2.0	5.3	67.5	11.76
72	3.2	3.4	2.0	5.3	67.5	11.82
104	3.2	3.4	2.0	5.3	67.5	11.82
120	3.2	3.4	-2.0	5.3	67.5	11.82
88	3.2	3.4	-2.0	5.3	67.5	11.82
5	0.0	-5.2	0.0	5.2	67.5	11.95
19	0.0	-5.2	0.0	5.2	67.5	11.95
33	-5.2	0.0	0.0	5.2	67.5	11.96
47	-5.2	0.0	0.0	5.2	67.5	11.96
2	-3.1	-5.0	0.0	5.0	67.5	12.50
4	-3.1	-5.0	0.0	5.0	67.5	12.50
3	-5.0	-3.1	0.0	5.0	67.5	12.50
1	-5.0	-3.1	0.0	5.0	67.5	12.50

2.6.13.5 Stress Evaluation of PWR Support Disks for Combined Thermal and 1-Foot End Drop Conditions

The thermal expansion loading described in Section 2.6.13.3 are applied to the finite element model simultaneously with the 20 *g* end-drop loads described in Section 2.6.13.4 to produce a combined thermal expansion plus end-impact loading. The stress evaluation is performed according to the ASME Code, Section III, Subsection NG [15]. The stress intensity attains its maximum value at the surface of the extreme fiber.

Thermal case A is used for this evaluation. The top ten maximum sectional stress locations for the combined thermal and 1-ft end-drop condition are shown in Figure 2.6.13.5-1. The maximum stress intensity is 9.5 ksi and the $3S_m$ allowable limit at temperature for 17-4 PH [21] is 133.5 ksi, which results in a margin of safety of +13.07. Results of the combined thermal and 1-ft end-drop condition are presented in Table 2.6.13.5-1.

Figure 2.6.13.5-1 Locations of Maximum P+Q Stresses—1-Foot End Drop, Thermal Case A

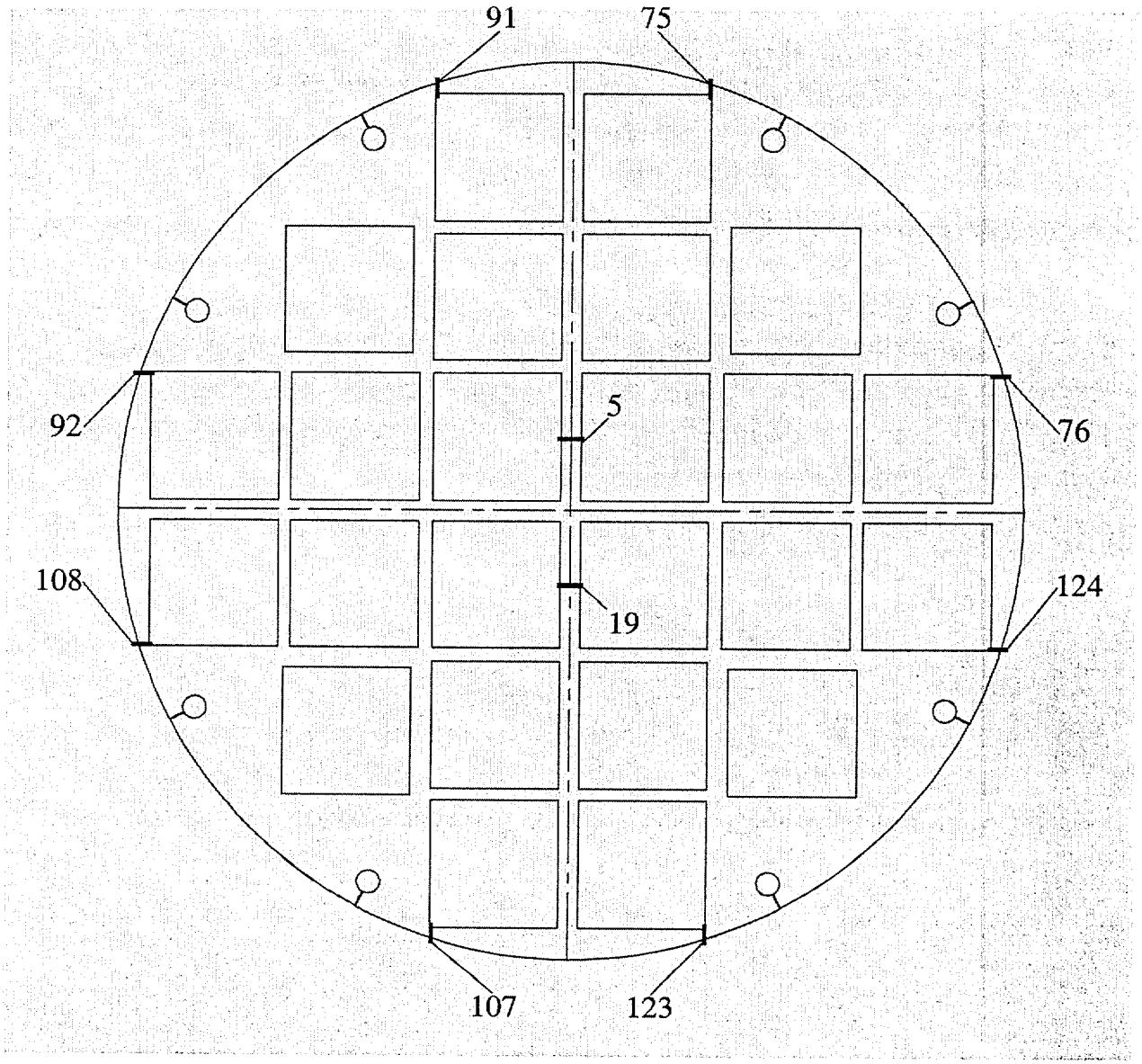

Table 2.6.13.5-1 $P_m + P_b + Q$ Stresses for Support Disk—1-Foot End-Drop, Thermal Case A

Section	Sx (ksi)	Sy (ksi)	Sxy (ksi)	Stress Intensity (ksi)	Allowable Stress (ksi)	Margin of Safety
76	1.0	9.0	-2.0	9.5	133.5	13.07
92	1.0	9.0	2.0	9.5	133.5	13.07
108	1.0	9.0	-2.0	9.5	133.5	13.07
124	1.0	9.0	2.0	9.5	133.5	13.07
5	0.0	-8.9	0.0	8.9	127.3	13.23
19	0.0	-8.9	0.0	8.9	127.3	13.23
107	8.3	1.3	-3.0	9.4	133.5	13.25
91	8.3	1.3	3.0	9.4	133.5	13.25
123	8.3	1.3	3.0	9.4	133.5	13.25
75	8.3	1.3	-3.0	9.4	133.5	13.25
33	-8.9	0.0	0.0	8.9	127.3	13.26
47	-8.9	0.0	0.0	8.9	127.3	13.26
84	0.0	-9.1	-0.1	9.1	130.1	13.30
116	0.0	-9.1	-0.1	9.1	130.1	13.30
100	0.0	-9.1	0.1	9.1	130.1	13.30
68	0.0	-9.1	0.1	9.1	130.1	13.30
109	-9.1	0.0	-0.1	9.1	130.1	13.30
77	-9.1	0.0	-0.1	9.1	130.1	13.30
61	-9.1	0.0	0.1	9.1	130.1	13.30
93	-9.1	0.0	0.1	9.1	130.1	13.30
2	-4.9	-8.7	0.0	8.7	125.9	13.48
4	-4.9	-8.7	0.0	8.7	125.9	13.48
3	-8.7	-4.9	0.0	8.7	125.9	13.50
1	-8.7	-4.9	0.0	8.7	125.9	13.50
21	-8.3	-3.9	0.9	8.5	129.0	14.12
23	-8.3	-3.9	-0.9	8.5	129.0	14.12
9	-8.3	-3.9	0.9	8.5	129.0	14.12
7	-8.3	-3.9	-0.9	8.5	129.0	14.12
37	-3.9	-8.3	0.9	8.5	129.0	14.12
35	-3.9	-8.3	-0.9	8.5	129.0	14.12
49	-3.9	-8.3	0.9	8.5	129.0	14.12
51	-3.9	-8.3	-0.9	8.5	129.0	14.12
34	-5.5	-8.0	0.0	8.0	129.0	15.08
48	-5.5	-8.0	0.0	8.0	129.0	15.08
6	-8.0	-5.6	0.0	8.0	129.0	15.08
20	-8.0	-5.6	0.0	8.0	129.0	15.08
44	-1.7	-8.0	0.0	8.0	133.4	15.58
58	-1.7	-8.0	0.0	8.0	133.4	15.58
16	-8.0	-1.9	0.0	8.0	133.4	15.63
30	-8.0	-1.9	0.0	8.0	133.4	15.63

2.6.13.6 Stress Evaluation of PWR Support Disk for 1-Foot Side-Drop Load Conditions

To determine the structural adequacy of the PWR fuel basket support disk for the 1-ft side-drop impact load condition, a quasi-static impact load equal to the weight of the fuel and fuel tubes multiplied by a 20 *g* amplification factor is applied to the support disk structure. The inertial loading of the support disk is also included by means of the density input for the 17-4 PH stainless steel. The value of 20 *g* is conservative because the Universal Transport Cask impact limiter design deceleration for a 1-ft side-drop is 16.4 *g*. The fuel assembly load is transmitted in direct compression through the tube wall to the web structure of the support disk. A conservative number of disks is assumed to transmit the load to the canister shell (see Section 2.6.13.2). The maximum in-plane loading occurs in the side-drop, which requires a detailed structural evaluation. A finite element analysis is performed by using ANSYS and the finite element model described in Section 2.6.13.2.

2.6.13.6.1 Drop Orientations

For the side drop, pressure loads are applied to the ligament based on the impact angle. The PWR fuel assembly basket with 24 slots exhibits one-eighth symmetry. A minimum perimeter radial thickness occurs between the corner of the fuel assembly slot in the basket and the outer radius at four locations: 0°, 18.22°, 26.28°, and 45° measured counterclockwise from the Y-axis (see Fig. 2.6.13.6-1). Therefore, to ensure that the bounding basket orientation is evaluated, drop orientations of 0°, 18.22°, 26.28°, and 45° are considered. The material properties and stress allowables are taken at temperature for both thermal cases A and B.

2.6.13.6.2 Analysis Results for the 1-Foot Side-Drop

Finite element analyses are performed for the 1-ft side-drop load Conditions for the four different radial basket orientations (0°, 18.2°, 26.28°, and 45°) and for two thermal cases that would result in the use of different moduli of elasticity throughout the basket. Locations of maximum nodal SI stresses for the four orientations are shown in Figures 2.6.13.6-2 through 2.6.13.6-5.

For normal conditions of transport, the allowable stress limit for the support disk primary membrane stress (P_m) is S_m. For primary membrane + bending stress (P_m+P_b), the allowable stress is $1.5S_m$.

The cross sections with the 40 minimum margins of safety are presented in Tables 2.6.13.6-2 through 2.6.13.6-17. The tables are identified below:

Table Number	Basket Orientation (°)	Thermal Case	Stress Evaluation	Minimum Margin of Safety
2.6.13.6-2	0	A	P_m	+1.17
2.6.13.6-3	0	A	$P_m + P_b$	+0.53
2.6.13.6-4	0	B	P_m	+1.16
2.6.13.6-5	0	B	$P_m + P_b$	+0.50
2.6.13.6-6	18.22	A	P_m	+1.15
2.6.13.6-7	18.22	A	$P_m + P_b$	+0.27
2.6.13.6-8	18.22	B	P_m	+1.11
2.6.13.6-9	18.22	B	$P_m + P_b$	+0.31
2.6.13.6-10	26.28	A	P_m	+1.04
2.6.13.6-11	26.28	A	$P_m + P_b$	+0.40
2.6.13.6-12	26.28	B	P_m	+1.10
2.6.13.6-13	26.28	B	$P_m + P_b$	+0.41
2.6.13.6-14	45	A	P_m	+0.86
2.6.13.6-15	45	A	$P_m + P_b$	+0.22
2.6.13.6-16	45	B	P_m	+0.79
2.6.13.6-17	45	B	$P_m + P_b$	+0.19

The minimum margin of safety of +0.19 for the side-drop occurs in the 45°, Thermal Case B, no-thermal-stresses. This margin of safety is produced by a primary membrane plus bending stress of 56.9 ksi.

Figure 2.6.13.6-1 Support Disk Side-Drop Orientations

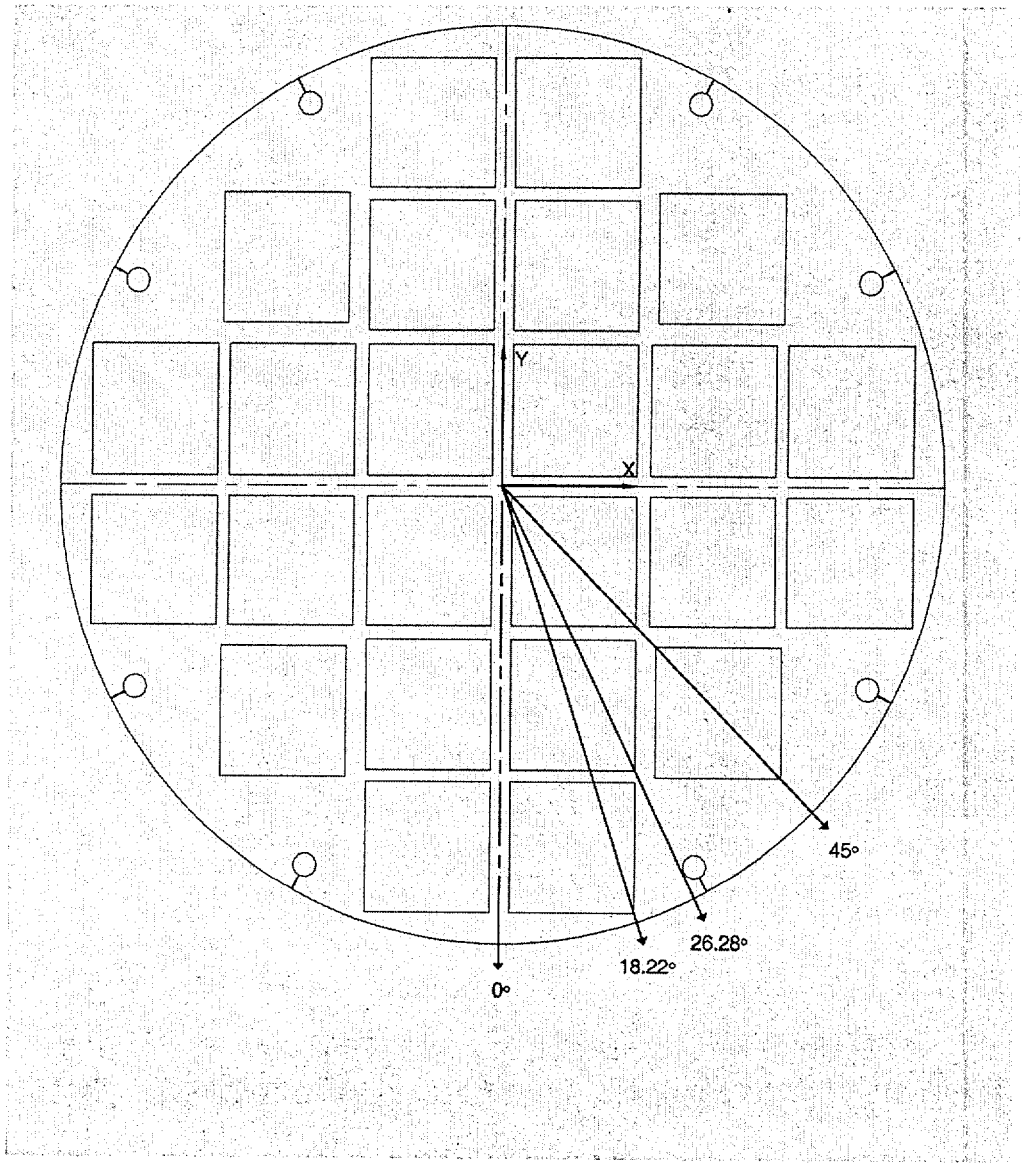

Figure 2.6.13.6-2 Locations of Maximum P_m+P_b Intensities—0° Side Drop Orientation, Thermal Case A

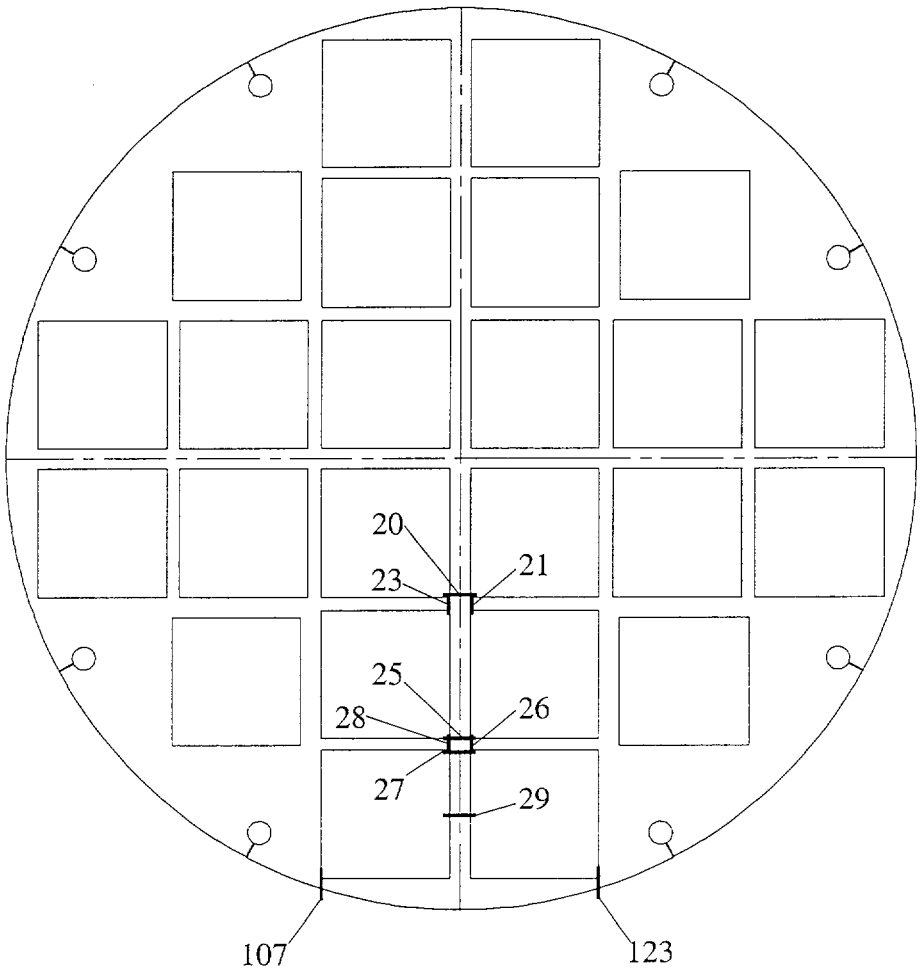

Figure 2.6.13.6-3 Locations of Maximum P_m+P_b Stresses—18.22° Side Drop Orientation, Thermal Case A

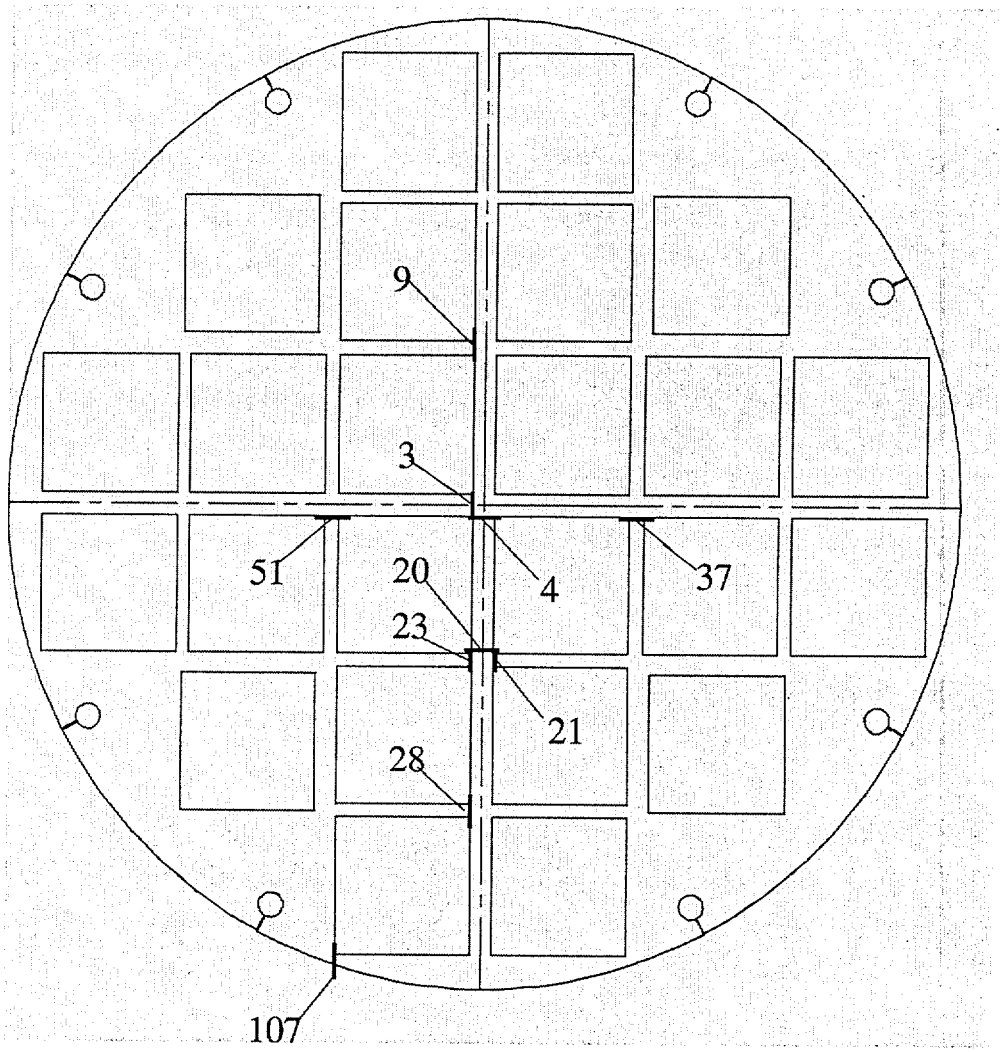

Figure 2.6.13.6-4 Locations of Maximum P_m+P_b Stresses—26.28° Side Drop Orientation, Thermal Case A

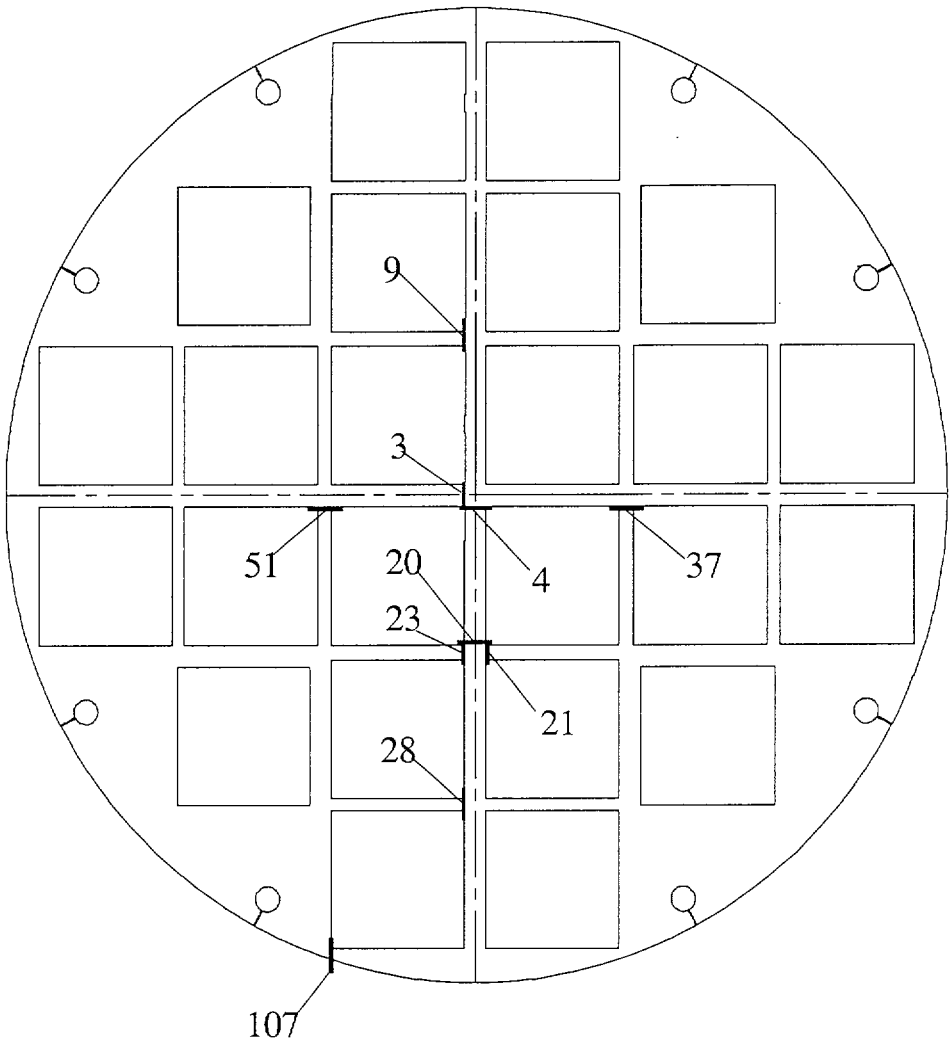

Figure 2.6.13.6-5 Locations of Maximum P_m+P_b Stresses—45° Side Drop Orientation, Thermal Case A

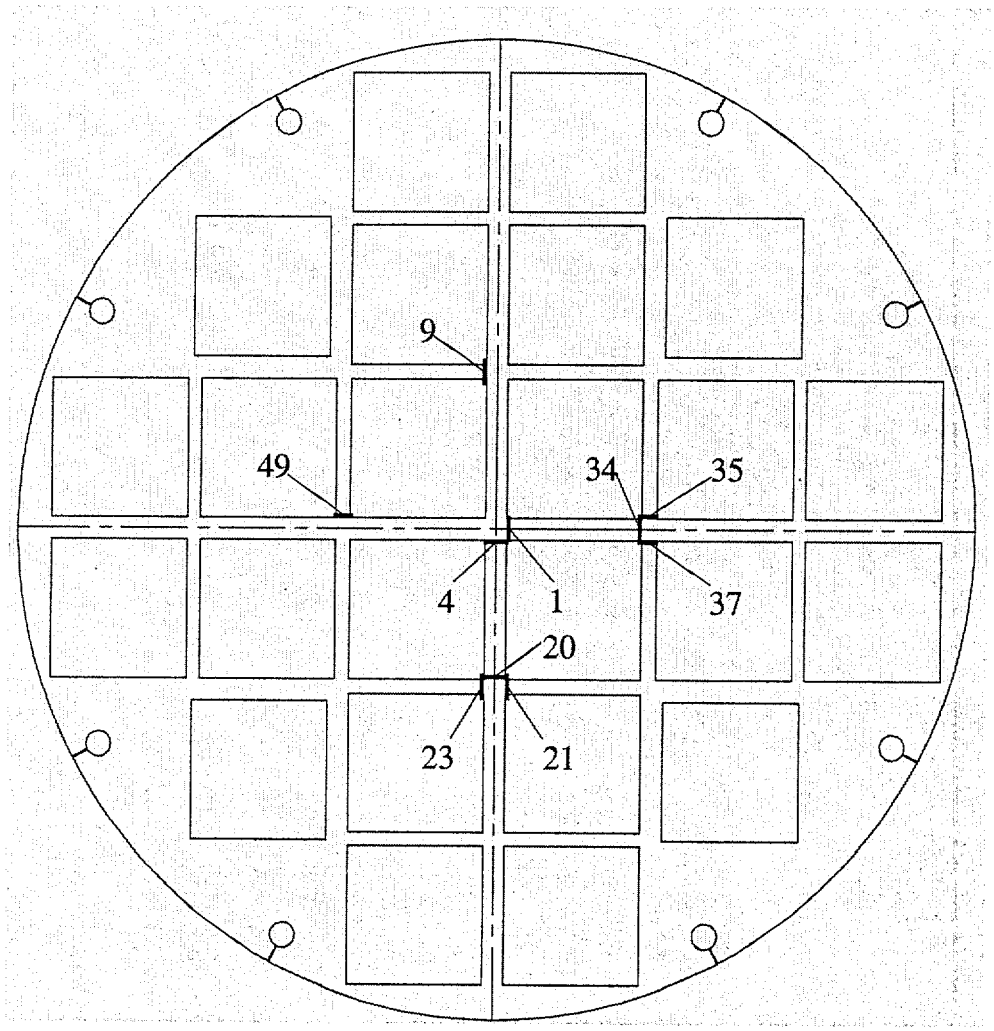

THIS PAGE INTENTIONALLY LEFT BLANK

FOR THE READER'S INFORMATION, TABLE 2.6.13.6-1 HAS BEEN DELETED

Table 2.6.13.6-2 P_m Stresses for Support Disk—1-Foot Side-Drop, 0° Orientation, Thermal Case A

Section	Sx (ksi)	Sy (ksi)	Sxy (ksi)	Stress Intensity (ksi)	Allowable Stress (ksi)	Margin of Safety
25	11.0	-9.2	0.0	20.2	43.9	1.17
107	-10.6	-13.2	8.1	20.1	44.5	1.21
123	-10.6	-13.2	-8.1	20.1	44.5	1.21
20	8.7	-7.3	0.0	16.0	43.0	1.70
29	0.0	-13.7	0.0	13.7	44.2	2.22
28	4.8	-6.9	3.2	13.4	43.9	2.28
26	4.8	-6.9	-3.2	13.4	43.9	2.28
27	-4.4	-12.5	0.0	12.5	43.9	2.51
2	6.1	-5.2	0.0	11.4	42.0	2.70
24	0.0	-11.4	0.0	11.4	43.5	2.81
22	-4.9	-10.4	0.0	10.4	43.1	3.16
21	2.8	-5.9	-2.6	10.1	43.0	3.25
23	2.8	-5.9	2.6	10.1	43.0	3.25
114	4.8	-5.3	-0.5	10.2	44.3	3.34
98	4.8	-5.3	0.5	10.2	44.3	3.34
30	-4.7	-9.6	0.0	9.6	44.5	3.63
19	0.0	-9.1	0.0	9.1	42.4	3.67
8	5.5	-3.1	0.0	8.6	43.1	3.99
4	-6.4	-7.9	0.0	7.9	42.0	4.30
31	-6.7	-6.2	1.7	8.2	44.5	4.45
32	-6.7	-6.2	-1.7	8.2	44.5	4.45
115	2.7	-5.2	-0.5	7.9	44.3	4.60
99	2.7	-5.2	0.5	7.9	44.3	4.60
112	2.7	-4.4	0.0	7.1	43.7	5.13
96	2.7	-4.4	0.0	7.1	43.7	5.13
95	2.5	-4.4	-0.2	6.9	43.7	5.32
111	2.5	-4.4	0.2	6.9	43.7	5.32
11	-6.9	-4.0	0.0	6.9	43.9	5.32
13	5.3	-1.3	0.0	6.6	43.9	5.64
6	-6.4	-5.9	0.0	6.4	43.0	5.74
5	0.0	-6.3	0.0	6.3	42.4	5.77
1	0.3	-4.5	-1.9	6.1	42.0	5.89
3	0.3	-4.5	1.9	6.1	42.0	5.89
110	6.2	-0.1	0.1	6.3	44.1	5.96
94	6.2	-0.1	-0.1	6.3	44.1	5.96
116	0.0	-6.1	0.0	6.1	43.4	6.16
100	0.0	-6.1	0.0	6.1	43.4	6.16
121	0.0	-5.9	-0.1	5.9	44.0	6.47
105	0.0	-5.9	0.1	5.9	44.0	6.47
7	-0.6	-3.2	-2.3	5.3	43.0	7.09

Table 2.6.13.6-3 $P_m + P_b$ Stresses for Support Disk—1-Foot Side-Drop, 0° Orientation, Thermal Case A

Section	Sx (ksi)	Sy (ksi)	Sxy (ksi)	Stress Intensity (ksi)	Allowable Stress (ksi)	Margin of Safety
107	-23.6	-30.9	15.9	43.6	66.8	0.53
123	-23.6	-30.9	-15.9	43.6	66.8	0.53
25	11.0	-9.2	-1.1	20.3	65.8	2.24
26	15.5	-3.5	-2.4	19.6	65.8	2.36
28	15.5	-3.5	2.4	19.6	65.8	2.36
20	8.7	-7.3	-0.7	16.0	64.5	3.03
23	12.0	-2.9	1.7	15.2	64.5	3.23
21	12.0	-2.9	-1.7	15.2	64.5	3.23
27	-4.4	-12.5	-3.2	13.7	65.9	3.82
29	0.0	-13.7	0.0	13.7	66.3	3.83
114	7.1	-5.5	-0.3	12.6	66.4	4.29
98	7.1	-5.5	0.3	12.6	66.4	4.29
2	6.1	-5.2	-0.8	11.5	63.0	4.50
22	-4.9	-10.4	-3.0	11.7	64.6	4.52
30	-4.7	-9.6	4.2	12.0	66.7	4.54
1	8.9	-1.9	-1.0	11.1	63.0	4.70
3	8.9	-1.9	1.0	11.1	63.0	4.70
24	0.0	-11.4	0.0	11.4	65.2	4.72
14	-9.6	-4.7	3.1	11.1	65.8	4.91
12	-9.6	-4.7	-3.1	11.1	65.8	4.91
4	-6.4	-7.9	3.3	10.6	63.0	4.96
94	10.9	0.6	-0.1	10.9	66.1	5.07
110	10.9	0.6	0.1	10.9	66.1	5.07
9	-8.6	-5.9	3.1	10.6	64.5	5.07
7	-8.6	-5.9	-3.1	10.6	64.5	5.07
75	6.7	6.8	-3.6	10.4	66.8	5.44
91	6.7	6.8	3.6	10.4	66.8	5.44
31	-4.9	-7.9	3.3	10.0	66.7	5.65
32	-4.9	-7.9	-3.3	10.0	66.7	5.65
19	0.0	-9.1	0.0	9.1	63.6	6.01
8	5.5	-3.1	-0.9	8.8	64.6	6.35
6	-6.4	-5.9	-2.5	8.7	64.5	6.44
17	8.9	1.4	-0.7	9.0	66.7	6.45
18	8.9	1.4	0.7	9.0	66.7	6.45
115	2.2	-6.4	-0.6	8.7	66.4	6.63
99	2.2	-6.4	0.6	8.7	66.4	6.63
11	-6.9	-4.0	-2.4	8.3	65.8	6.96
37	-1.7	-7.8	-1.2	8.1	64.5	6.99
51	-1.7	-7.8	1.2	8.1	64.5	6.99
113	-2.6	-7.1	-1.4	7.5	65.6	7.79

Table 2.6.13.6-4 P_m Stresses for Support Disk—1-Foot Side-Drop, 0° Orientation, Thermal Case B

Section	Sx (ksi)	Sy (ksi)	Sxy (ksi)	Stress Intensity (ksi)	Allowable Stress (ksi)	Margin of Safety
25	11.3	-9.5	0.0	20.8	45.0	1.16
107	-10.3	-13.3	8.3	20.2	45.0	1.22
123	-10.3	-13.3	-8.3	20.2	45.0	1.22
20	9.0	-7.5	0.0	16.5	45.0	1.73
29	0.0	-14.1	0.0	14.1	45.0	2.18
28	4.9	-7.2	3.3	13.7	45.0	2.28
26	4.9	-7.2	-3.3	13.7	45.0	2.28
27	-4.6	-12.9	0.0	12.9	45.0	2.49
2	6.7	-5.4	0.0	12.0	45.0	2.74
24	0.0	-11.8	0.0	11.8	45.0	2.83
22	-5.2	-10.7	0.0	10.7	45.0	3.20
21	2.8	-6.1	-2.7	10.4	45.0	3.33
23	2.8	-6.1	2.7	10.4	45.0	3.33
114	4.9	-5.2	-0.6	10.2	45.0	3.43
98	4.9	-5.2	0.6	10.2	45.0	3.43
30	-4.6	-9.8	0.0	9.8	45.0	3.57
19	0.0	-9.4	0.0	9.4	45.0	3.79
8	5.8	-3.2	0.0	9.0	45.0	4.01
31	-6.7	-6.3	1.7	8.3	45.0	4.44
32	-6.7	-6.3	-1.7	8.3	45.0	4.44
4	-7.0	-8.2	0.0	8.2	45.0	4.48
115	2.6	-5.1	-0.5	7.7	45.0	4.85
99	2.6	-5.1	0.5	7.7	45.0	4.85
11	-7.2	-4.2	0.0	7.2	45.0	5.28
13	5.5	-1.3	0.0	6.8	45.0	5.57
111	2.5	-4.3	0.2	6.8	45.0	5.61
95	2.5	-4.3	-0.2	6.8	45.0	5.61
112	2.5	-4.3	0.0	6.8	45.0	5.63
96	2.5	-4.3	0.0	6.8	45.0	5.63
6	-6.7	-6.0	0.0	6.7	45.0	5.74
5	0.0	-6.4	0.0	6.4	45.0	5.98
110	6.3	-0.1	0.1	6.4	45.0	6.01
94	6.3	-0.1	-0.1	6.4	45.0	6.01
1	0.2	-4.6	-2.1	6.4	45.0	6.05
3	0.2	-4.6	2.1	6.4	45.0	6.05
116	0.0	-5.9	0.0	5.9	45.0	6.66
100	0.0	-5.9	0.0	5.9	45.0	6.66
121	0.0	-5.7	-0.1	5.7	45.0	6.84
105	0.0	-5.7	0.1	5.7	45.0	6.84
7	-0.6	-3.3	-2.4	5.5	45.0	7.12

Table 2.6.13.6-5 $P_m + P_b$ Stresses for Support Disk—1-Foot Side-Drop, 0° Orientation, Thermal Case B

Section	Sx (ksi)	Sy (ksi)	Sxy (ksi)	Stress Intensity (ksi)	Allowable Stress (ksi)	Margin of Safety
107	-24.1	-31.9	16.5	44.9	67.5	0.50
123	-24.1	-31.9	-16.5	44.9	67.5	0.50
25	11.3	-9.5	-1.2	20.9	67.5	2.22
26	15.9	-3.6	-2.5	20.2	67.5	2.34
28	15.9	-3.6	2.5	20.2	67.5	2.34
20	9.0	-7.5	-0.8	16.6	67.5	3.07
23	12.4	-3.0	1.8	15.8	67.5	3.27
21	12.4	-3.0	-1.8	15.8	67.5	3.27
29	0.0	-14.1	0.0	14.1	67.5	3.78
27	-4.6	-12.9	-3.4	14.1	67.5	3.79
114	7.5	-5.2	-0.5	12.7	67.5	4.30
98	7.5	-5.2	0.5	12.7	67.5	4.30
30	-4.6	-9.8	4.3	12.3	67.5	4.50
22	-5.2	-10.7	-3.2	12.2	67.5	4.55
2	6.7	-5.4	-0.9	12.1	67.5	4.56
1	9.7	-1.9	-1.1	11.8	67.5	4.71
3	9.7	-1.9	1.1	11.8	67.5	4.71
24	0.0	-11.8	0.0	11.8	67.5	4.74
14	-9.9	-4.9	3.2	11.5	67.5	4.86
12	-9.9	-4.9	-3.2	11.5	67.5	4.86
4	-7.0	-8.2	3.5	11.1	67.5	5.06
9	-9.1	-6.1	3.2	11.1	67.5	5.07
7	-9.1	-6.1	-3.2	11.1	67.5	5.07
94	11.0	0.6	-0.1	11.0	67.5	5.14
110	11.0	0.6	0.1	11.0	67.5	5.14
75	7.1	7.2	-3.8	11.0	67.5	5.16
91	7.1	7.2	3.8	11.0	67.5	5.16
31	-4.7	-8.1	3.4	10.2	67.5	5.62
32	-4.7	-8.1	-3.4	10.2	67.5	5.62
18	9.4	1.5	0.8	9.4	67.5	6.15
17	9.4	1.5	-0.8	9.4	67.5	6.15
19	0.0	-9.4	0.0	9.4	67.5	6.19
8	5.8	-3.2	-0.9	9.2	67.5	6.36
6	-6.7	-6.0	-2.6	9.0	67.5	6.49
11	-7.2	-4.2	-2.4	8.5	67.5	6.91
115	2.0	-6.3	-0.6	8.4	67.5	7.00
99	2.0	-6.3	0.6	8.4	67.5	7.00
37	-1.6	-7.9	-1.2	8.1	67.5	7.31
51	-1.6	-7.9	1.2	8.1	67.5	7.31
113	-2.5	-7.0	-1.3	7.4	67.5	8.10

Table 2.6.13.6-6 P_m Stresses for Support Disk—1-Foot Side-Drop, 18.22° Orientation, Thermal Case A

Section	Sx (ksi)	Sy (ksi)	Sxy (ksi)	Stress Intensity (ksi)	Allowable Stress (ksi)	Margin of Safety
112	11.6	-7.8	3.0	20.3	43.7	1.15
35	11.4	-4.8	3.1	17.3	43.0	1.48
107	0.6	-6.7	7.3	16.4	44.5	1.72
37	-12.4	-10.1	3.3	14.8	43.0	1.92
120	6.7	-6.9	3.4	15.2	44.3	1.92
23	2.6	1.8	6.8	13.7	43.0	2.13
9	-1.0	-7.9	5.9	13.6	43.0	2.17
114	-3.8	2.8	6.0	13.6	44.3	2.25
51	11.8	1.8	3.9	13.2	43.0	2.27
28	-3.4	-2.9	6.6	13.3	43.9	2.30
21	-0.3	-11.3	3.0	12.5	43.0	2.44
49	-11.0	-1.2	3.7	12.3	43.0	2.50
116	0.0	-12.3	0.0	12.3	43.4	2.53
115	3.4	-7.8	2.5	12.2	44.3	2.62
64	-11.3	-6.4	1.9	11.9	43.7	2.67
20	5.6	-5.8	0.7	11.5	43.0	2.73
98	-3.9	-8.7	4.9	11.8	44.3	2.76
14	0.5	-1.2	5.6	11.3	43.9	2.88
31	-4.3	-10.9	1.8	11.3	44.5	2.92
63	0.6	-6.1	4.4	11.0	43.7	2.96
29	0.0	-11.0	0.7	11.0	44.2	3.00
95	2.0	-5.4	4.0	10.9	43.7	3.03
121	-0.4	-10.8	0.8	10.9	44.0	3.04
27	-8.1	-9.9	-1.5	10.8	43.9	3.08
113	-5.6	-10.1	1.4	10.5	43.8	3.17
25	2.9	-7.4	-0.1	10.4	43.9	3.24
66	-1.1	-4.3	4.9	10.3	44.3	3.29
26	-4.1	-9.5	2.0	10.2	43.9	3.32
123	-9.7	-0.7	-2.2	10.2	44.5	3.37
96	-7.9	-0.1	3.1	10.0	43.7	3.38
111	-0.4	-3.3	4.8	10.0	43.7	3.39
22	-4.1	-8.2	-2.6	9.4	43.1	3.57
2	4.3	-4.1	1.4	8.9	42.0	3.74
24	0.0	-9.1	0.6	9.1	43.5	3.77
119	0.0	-9.0	-0.2	9.0	44.1	3.91
36	0.2	-4.7	-3.6	8.8	43.1	3.92
80	8.2	0.7	2.3	8.9	43.7	3.92
82	0.8	4.7	3.9	8.7	44.3	4.09
40	2.9	-5.0	1.6	8.5	43.9	4.18
3	0.3	-4.6	3.1	7.9	42.0	4.33

Table 2.6.13.6-7 $P_m + P_b$ Stresses for Support Disk—1-Foot Side-Drop, 18.22° Orientation, Thermal Case A

Section	Sx (ksi)	Sy (ksi)	Sxy (ksi)	Stress Intensity (ksi)	Allowable Stress (ksi)	Margin of Safety
107	-28.5	-37.9	18.7	52.4	66.8	0.27
23	36.6	21.3	8.0	40.0	64.5	0.61
4	-28.2	-34.0	4.3	36.3	63.0	0.74
3	-31.2	-30.3	4.0	34.8	63.0	0.81
9	-29.7	-24.4	8.0	35.4	64.5	0.82
37	-23.8	-29.1	8.2	35.0	64.5	0.84
28	-31.7	-17.3	7.6	35.0	65.8	0.88
20	32.7	18.8	1.1	32.8	64.5	0.97
51	25.2	23.9	7.3	31.9	64.5	1.02
21	-21.1	-26.4	5.9	30.2	64.5	1.14
49	-24.2	-21.6	6.8	29.8	64.5	1.17
2	-19.1	-28.3	0.9	28.4	63.0	1.22
34	-25.3	-25.7	3.4	28.9	64.5	1.23
6	-26.8	-25.2	2.4	28.5	64.5	1.26
48	27.7	22.6	2.0	28.4	64.5	1.27
111	-27.1	-19.1	4.0	28.8	65.5	1.28
30	-7.5	-27.5	5.7	29.0	66.7	1.30
98	-23.1	-16.5	8.2	28.6	66.4	1.32
95	-23.3	-21.1	5.8	28.1	65.5	1.33
22	-27.6	-16.6	-0.1	27.6	64.6	1.34
96	-23.8	-20.1	5.6	27.8	65.5	1.36
27	-26.8	-16.8	2.0	27.2	65.9	1.42
63	-22.5	-19.0	6.0	27.0	65.5	1.43
112	25.6	8.9	5.0	26.9	65.5	1.43
64	-22.2	-19.1	5.7	26.6	65.5	1.47
91	14.5	20.3	9.1	26.9	66.8	1.48
14	24.1	10.9	5.5	26.1	65.8	1.52
35	22.6	12.5	5.7	25.2	64.5	1.56
1	-19.4	-24.4	0.7	24.4	63.0	1.57
8	24.1	4.6	-1.3	24.2	64.6	1.67
115	-7.1	-24.6	-0.8	24.6	66.4	1.70
114	-23.3	-5.3	4.7	24.4	66.4	1.72
99	-19.8	-15.8	6.2	24.4	66.4	1.72
79	20.5	16.5	4.8	23.7	65.5	1.76
113	-16.0	-23.0	1.6	23.4	65.6	1.81
36	4.0	-18.2	-2.7	22.9	64.6	1.82
80	20.3	15.8	4.6	23.2	65.5	1.83
26	-17.5	-18.9	4.7	23.0	65.8	1.87
25	-16.9	-22.8	0.2	22.8	65.8	1.88
50	2.5	-17.7	-3.3	21.3	64.6	2.03

Table 2.6.13.6-8 P_m Stresses for Support Disk—1-Foot Side-Drop, 18.22° Orientation, Thermal Case B

Section	Sx (ksi)	Sy (ksi)	Sxy (ksi)	Stress Intensity (ksi)	Allowable Stress (ksi)	Margin of Safety
112	12.3	-8.2	3.0	21.3	45.0	1.11
35	12.1	-5.1	3.1	18.3	45.0	1.46
37	-13.2	-10.7	3.4	15.5	45.0	1.90
107	0.5	-6.3	7.0	15.5	45.0	1.91
120	6.3	-6.7	3.2	14.5	45.0	2.09
23	2.7	1.7	7.1	14.2	45.0	2.18
51	12.7	2.2	4.0	14.1	45.0	2.20
9	-1.1	-8.0	6.1	13.9	45.0	2.23
28	-3.3	-3.3	6.9	13.7	45.0	2.28
114	-3.7	2.2	6.2	13.7	45.0	2.29
49	-11.9	-1.1	3.8	13.1	45.0	2.42
115	3.8	-8.2	2.4	13.0	45.0	2.47
116	0.0	-12.9	0.0	12.9	45.0	2.48
21	-0.3	-11.4	3.1	12.8	45.0	2.52
64	-11.8	-6.8	1.8	12.4	45.0	2.64
31	-4.4	-11.4	1.8	11.8	45.0	2.81
20	5.8	-5.9	0.7	11.8	45.0	2.81
98	-3.9	-8.4	5.2	11.8	45.0	2.83
14	0.4	-1.2	5.7	11.6	45.0	2.88
121	-0.4	-11.4	0.8	11.5	45.0	2.93
63	0.6	-6.1	4.6	11.3	45.0	2.98
29	0.0	-11.2	0.7	11.2	45.0	3.01
113	-6.0	-10.7	1.4	11.1	45.0	3.07
95	2.2	-4.9	4.2	11.0	45.0	3.11
27	-8.0	-10.1	-1.5	10.8	45.0	3.15
96	-8.5	0.1	3.1	10.6	45.0	3.24
25	3.0	-7.6	-0.2	10.6	45.0	3.26
111	-0.4	-4.0	5.0	10.5	45.0	3.28
66	-1.1	-4.3	5.0	10.5	45.0	3.29
123	-9.8	-0.7	-2.2	10.3	45.0	3.36
26	-4.0	-9.3	2.2	10.1	45.0	3.46
22	-4.2	-8.3	-2.6	9.6	45.0	3.69
80	8.7	0.9	2.3	9.3	45.0	3.82
24	0.0	-9.2	0.6	9.3	45.0	3.85
36	0.2	-5.0	-3.8	9.2	45.0	3.88
2	4.5	-4.2	1.5	9.2	45.0	3.91
82	0.8	4.8	4.0	9.0	45.0	3.99
119	0.0	-8.7	-0.2	8.7	45.0	4.17
79	-0.6	4.0	3.5	8.4	45.0	4.36
30	-1.0	-7.4	2.6	8.3	45.0	4.39

Table 2.6.13.6-9 $P_m + P_b$ Stresses for Support Disk—1-Foot Side-Drop, 18.22° Orientation, Thermal Case B

Section	Sx (ksi)	Sy (ksi)	Sxy (ksi)	Stress Intensity (ksi)	Allowable Stress (ksi)	Margin of Safety
107	-29.1	-37.1	18.2	51.7	67.5	0.31
23	37.8	22.0	8.2	41.3	67.5	0.63
4	-29.7	-35.6	4.5	38.0	67.5	0.78
9	-30.8	-25.1	8.2	36.7	67.5	0.84
3	-32.9	-31.8	4.2	36.5	67.5	0.85
28	-32.7	-18.2	7.9	36.2	67.5	0.87
37	-24.7	-29.7	8.5	36.0	67.5	0.87
20	33.8	19.3	1.1	33.9	67.5	0.99
51	26.3	24.8	7.7	33.3	67.5	1.03
21	-22.0	-27.1	6.1	31.1	67.5	1.17
49	-25.2	-21.9	7.1	30.8	67.5	1.19
30	-7.7	-29.0	5.9	30.5	67.5	1.21
111	-28.0	-20.0	4.3	29.9	67.5	1.26
34	-26.3	-26.3	3.6	29.9	67.5	1.26
2	-20.1	-29.7	0.9	29.8	67.5	1.26
48	29.0	23.3	2.2	29.8	67.5	1.27
6	-27.8	-25.9	2.4	29.4	67.5	1.29
98	-23.9	-16.5	8.4	29.3	67.5	1.30
95	28.5	11.2	2.4	28.8	67.5	1.34
22	-28.6	-17.3	-0.1	28.6	67.5	1.36
96	-24.5	-19.8	5.7	28.3	67.5	1.39
27	-27.8	-17.7	2.1	28.2	67.5	1.40
91	15.0	20.9	9.4	27.8	67.5	1.43
63	-23.1	-19.1	6.2	27.6	67.5	1.45
112	26.3	8.3	5.0	27.6	67.5	1.45
64	-22.8	-19.3	5.8	27.1	67.5	1.49
14	24.8	11.2	5.7	26.8	67.5	1.52
35	23.4	12.3	5.9	26.0	67.5	1.60
1	-20.5	-25.6	0.7	25.7	67.5	1.63
114	-23.9	-6.2	4.9	25.2	67.5	1.68
8	25.0	5.0	-1.4	25.1	67.5	1.69
115	-7.0	-25.0	-1.0	25.0	67.5	1.70
99	-20.5	-15.6	6.3	24.9	67.5	1.72
79	21.2	16.8	5.0	24.5	67.5	1.76
113	-16.4	-23.8	1.8	24.3	67.5	1.78
36	5.0	-18.4	-2.8	24.1	67.5	1.81
80	21.1	16.0	4.7	23.9	67.5	1.83
25	23.7	8.0	-0.5	23.7	67.5	1.85
26	-18.2	-19.2	4.8	23.6	67.5	1.86
50	3.4	-17.7	-3.6	22.3	67.5	2.03

Table 2.6.13.6-10 P_m Stresses for Support Disk—1-Foot Side-Drop, 26.28° Orientation, Thermal Case A

Section	Sx (ksi)	Sy (ksi)	Sxy (ksi)	Stress Intensity (ksi)	Allowable Stress (ksi)	Margin of Safety
120	9.4	-9.2	5.6	21.7	44.3	1.04
112	10.0	-7.2	4.4	19.3	43.7	1.26
114	-6.7	6.9	6.8	19.3	44.3	1.30
35	12.6	-3.5	4.5	18.5	43.0	1.33
37	-13.5	-9.2	5.0	16.8	43.0	1.57
21	-3.2	-14.8	4.3	16.2	43.0	1.66
23	1.4	6.2	7.7	16.1	43.0	1.67
9	-0.9	-9.9	6.5	15.8	43.0	1.72
51	13.7	2.9	5.1	15.7	43.0	1.74
49	-12.7	-0.8	4.7	15.2	43.0	1.83
28	-6.1	-1.6	6.8	14.4	43.9	2.06
96	-10.2	0.9	4.5	14.2	43.7	2.07
98	-6.7	-9.9	5.4	13.9	44.3	2.19
63	0.9	-7.6	5.0	13.2	43.7	2.31
64	-11.8	-5.3	2.8	12.9	43.7	2.40
95	0.2	-8.0	4.7	12.6	43.7	2.48
40	3.9	-7.2	2.7	12.4	43.9	2.54
66	-0.8	-5.7	5.7	12.4	44.3	2.58
119	0.0	-12.1	-0.3	12.1	44.1	2.65
14	1.2	-0.9	5.8	11.8	43.9	2.72
107	2.6	-4.4	4.9	12.0	44.5	2.72
26	-7.1	-9.8	2.8	11.5	43.9	2.81
111	-2.4	1.2	5.4	11.4	43.7	2.84
42	-5.6	-9.4	3.2	11.2	43.9	2.90
116	0.0	-11.1	0.0	11.1	43.4	2.91
31	-3.2	-11.0	1.6	11.3	44.5	2.92
80	9.8	1.2	3.1	10.8	43.7	3.06
27	-9.3	-8.6	-1.8	10.8	43.9	3.07
115	1.9	-6.5	3.4	10.9	44.3	3.08
72	-8.7	-7.6	2.4	10.6	44.3	3.16
104	-5.6	-0.1	4.5	10.6	44.3	3.18
79	0.0	6.4	4.0	10.2	43.7	3.28
22	-4.9	-7.1	-3.8	9.9	43.1	3.36
121	-0.5	-9.7	1.0	9.8	44.0	3.51
71	0.0	-9.7	-0.2	9.7	44.1	3.55
82	1.7	5.9	4.4	9.7	44.3	3.56
99	-9.3	-0.7	1.9	9.7	44.3	3.56
29	-0.1	-9.6	0.7	9.7	44.2	3.57
113	-5.8	-8.8	1.6	9.5	43.8	3.61
36	0.2	-3.5	-4.2	9.1	43.1	3.71

Table 2.6.13.6-11 $P_m + P_b$ Stresses for Support Disk—1-Foot Side-Drop, 26.28° Orientation, Thermal Case A

Section	Sx (ksi)	Sy (ksi)	Sxy (ksi)	Stress Intensity (ksi)	Allowable Stress (ksi)	Margin of Safety
23	40.4	29.3	9.9	46.2	64.5	0.40
4	-34.3	-41.3	4.5	43.5	63.0	0.45
37	-30.3	-37.2	10.0	44.3	64.5	0.46
3	-37.5	-36.8	4.3	41.4	63.0	0.52
107	-24.6	-31.3	14.6	42.9	66.8	0.56
21	-31.0	-33.9	8.6	41.2	64.5	0.57
9	-33.7	-29.3	9.2	41.0	64.5	0.57
51	31.1	31.8	9.2	40.6	64.5	0.59
20	-30.2	-38.1	1.4	38.3	64.5	0.68
28	-35.7	-17.1	7.8	38.6	65.8	0.71
49	-29.7	-27.0	8.2	36.7	64.5	0.76
34	-31.8	-33.4	3.3	36.0	64.5	0.79
95	-29.7	-27.5	7.6	36.2	65.5	0.81
96	-30.1	-26.3	7.4	35.9	65.5	0.83
2	33.5	27.0	2.2	34.2	63.0	0.84
48	33.8	29.6	2.3	34.8	64.5	0.85
111	-33.9	-19.5	3.8	34.8	65.5	0.88
35	29.0	21.3	7.6	33.6	64.5	0.92
6	-31.0	-30.7	2.4	33.3	64.5	0.94
22	-33.0	-14.1	-1.4	33.1	64.6	0.95
112	-9.6	-33.2	2.1	33.4	65.5	0.96
98	-27.7	-18.8	9.5	33.8	66.4	0.97
63	-26.7	-24.4	7.2	32.8	65.5	1.00
64	-26.8	-24.3	6.9	32.5	65.5	1.02
1	-27.8	-30.1	1.1	30.5	63.0	1.06
120	3.1	-27.1	3.9	31.2	66.4	1.13
27	-30.0	-15.8	1.7	30.2	65.9	1.18
79	24.9	21.9	6.1	29.7	65.5	1.20
30	-6.3	-28.8	5.5	30.0	66.7	1.22
114	-28.9	-2.1	4.8	29.7	66.4	1.23
7	24.5	22.0	5.5	28.8	64.5	1.24
80	24.9	21.3	5.9	29.3	65.5	1.24
8	28.0	5.0	-2.0	28.1	64.6	1.30
99	-23.9	-17.9	7.4	28.8	66.4	1.30
26	-23.8	-20.9	6.0	28.5	65.8	1.31
14	26.3	12.3	5.9	28.5	65.8	1.31
42	-14.3	-25.3	6.0	28.0	65.8	1.35
115	-10.1	-27.6	-0.5	27.7	66.4	1.40
91	13.9	21.0	9.1	27.3	66.8	1.45
36	0.5	-24.4	-3.5	25.9	64.6	1.50

Table 2.6.13.6-12 P_m Stresses for Support Disk—1-Foot Side-Drop, 26.28° Orientation, Thermal Case B

Section	Sx (ksi)	Sy (ksi)	Sxy (ksi)	Stress Intensity (ksi)	Allowable Stress (ksi)	Margin of Safety
120	9.5	-9.1	5.4	21.5	45.0	1.10
112	11.0	-7.6	4.4	20.6	45.0	1.19
114	-6.8	6.7	7.1	19.7	45.0	1.28
35	13.6	-3.8	4.5	19.7	45.0	1.29
37	-14.5	-9.9	5.0	17.8	45.0	1.54
51	14.5	3.4	5.2	16.6	45.0	1.72
23	1.6	6.3	7.9	16.4	45.0	1.74
21	-2.9	-14.7	4.6	16.3	45.0	1.77
9	-1.0	-10.0	6.7	16.1	45.0	1.79
49	-13.5	-0.7	4.8	16.0	45.0	1.81
28	-6.3	-1.6	7.0	14.7	45.0	2.05
96	-10.5	1.1	4.5	14.7	45.0	2.07
98	-7.0	-9.8	5.5	14.1	45.0	2.19
63	1.0	-7.6	5.2	13.6	45.0	2.32
64	-12.5	-5.7	2.8	13.5	45.0	2.34
66	-0.8	-5.8	5.8	12.7	45.0	2.54
95	0.6	-7.5	4.9	12.7	45.0	2.54
40	3.9	-7.2	2.5	12.2	45.0	2.68
14	1.2	-0.9	5.9	12.0	45.0	2.74
119	0.0	-12.0	-0.3	12.0	45.0	2.75
116	0.0	-11.9	0.0	11.9	45.0	2.78
31	-3.2	-11.5	1.6	11.8	45.0	2.82
26	-7.2	-9.7	3.1	11.8	45.0	2.83
111	-2.3	0.3	5.6	11.6	45.0	2.88
115	2.2	-7.0	3.5	11.6	45.0	2.89
80	10.2	1.5	3.0	11.2	45.0	3.02
107	2.5	-3.9	4.5	11.0	45.0	3.08
42	-5.6	-9.3	3.0	11.0	45.0	3.09
27	-9.2	-8.5	-1.8	10.7	45.0	3.20
79	-0.2	6.3	4.1	10.5	45.0	3.28
121	-0.5	-10.3	1.0	10.4	45.0	3.31
72	-8.7	-7.6	2.2	10.4	45.0	3.32
104	-5.6	0.0	4.4	10.3	45.0	3.35
113	-6.2	-9.5	1.7	10.2	45.0	3.40
99	-9.7	-0.4	1.9	10.0	45.0	3.48
82	1.7	6.0	4.5	10.0	45.0	3.50
22	-4.6	-7.0	-3.8	9.8	45.0	3.60
36	0.2	-3.9	-4.4	9.8	45.0	3.61
71	0.0	-9.6	-0.2	9.6	45.0	3.67
29	-0.1	-9.5	0.8	9.6	45.0	3.68

Table 2.6.13.6-13 $P_m + P_b$ Stresses for Support Disk—1-Foot Side-Drop, 26.28° Orientation, Thermal Case B

Section	Sx (ksi)	Sy (ksi)	Sxy (ksi)	Stress Intensity (ksi)	Allowable Stress (ksi)	Margin of Safety
23	41.9	30.1	10.2	47.7	67.5	0.41
37	-31.5	-38.2	10.4	45.8	67.5	0.47
4	-35.9	-43.1	4.6	45.4	67.5	0.49
3	-39.2	-38.5	4.4	43.2	67.5	0.56
21	-32.3	-34.7	8.9	42.4	67.5	0.59
9	-34.8	-30.1	9.4	42.2	67.5	0.60
51	32.1	32.6	9.5	41.9	67.5	0.61
107	-24.4	-29.9	13.9	41.3	67.5	0.63
28	-36.9	-17.7	8.0	39.8	67.5	0.70
20	-31.3	-38.8	1.3	39.0	67.5	0.73
49	-30.8	-27.3	8.5	37.8	67.5	0.79
34	-33.3	-34.2	3.6	37.4	67.5	0.81
95	-30.3	-27.3	7.7	36.6	67.5	0.84
111	-35.2	-20.9	4.1	36.3	67.5	0.86
48	35.0	30.4	2.6	36.1	67.5	0.87
96	-30.7	-25.9	7.5	36.1	67.5	0.87
2	35.1	28.7	2.2	35.8	67.5	0.89
35	30.1	21.4	7.9	34.8	67.5	0.94
98	-28.6	-19.0	9.8	34.7	67.5	0.94
6	-32.0	-31.4	2.4	34.1	67.5	0.98
22	-33.9	-14.9	-1.5	34.0	67.5	0.98
112	30.9	18.1	6.8	33.9	67.5	0.99
63	-27.6	-24.7	7.4	33.7	67.5	1.00
64	-27.6	-24.6	7.1	33.4	67.5	1.02
1	-29.5	-31.6	1.1	32.1	67.5	1.10
30	-6.6	-30.3	5.6	31.6	67.5	1.14
27	-31.1	-16.4	1.7	31.3	67.5	1.16
114	-30.2	-2.7	5.2	31.2	67.5	1.17
120	3.5	-26.2	3.7	30.6	67.5	1.21
79	25.7	22.1	6.3	30.4	67.5	1.22
7	25.7	22.8	5.7	30.1	67.5	1.24
26	-25.4	-21.5	6.3	30.0	67.5	1.25
80	25.6	21.4	6.1	29.9	67.5	1.26
99	-24.6	-18.0	7.6	29.6	67.5	1.28
14	26.9	12.6	6.0	29.1	67.5	1.32
8	28.8	5.5	-2.1	29.0	67.5	1.33
115	-10.4	-28.7	-0.6	28.7	67.5	1.35
91	14.2	21.4	9.3	27.8	67.5	1.43
36	1.7	-24.8	-3.7	27.5	67.5	1.46
42	-13.8	-24.3	5.8	26.9	67.5	1.51

Table 2.6.13.6-14 P_m Stresses for Support Disk—1-Foot Side-Drop, 45° Orientation, Thermal Case A

Section	Sx (ksi)	Sy (ksi)	Sxy (ksi)	Stress Intensity (ksi)	Allowable Stress (ksi)	Margin of Safety
120	9.1	-9.1	7.6	23.7	44.3	0.86
114	-9.0	9.1	7.6	23.7	44.3	0.87
35	12.7	-1.4	7.0	19.8	43.0	1.17
23	-1.4	12.7	7.0	19.8	43.0	1.17
37	-16.8	-7.7	6.0	19.8	43.0	1.17
21	-7.7	-16.8	6.0	19.8	43.0	1.18
49	-12.9	-0.6	6.4	17.7	43.0	1.44
9	-0.6	-12.9	6.4	17.6	43.0	1.44
112	7.1	-5.8	6.1	17.7	43.7	1.47
111	-5.8	7.0	6.1	17.7	43.7	1.47
96	-10.7	1.5	5.7	16.7	43.7	1.61
63	1.5	-10.6	5.7	16.7	43.7	1.61
51	12.0	3.1	5.4	14.5	43.0	1.96
7	3.1	12.0	5.4	14.5	43.0	1.96
28	-8.3	0.9	5.4	14.2	43.9	2.10
40	0.9	-8.3	5.4	14.2	43.9	2.10
98	-8.9	-10.3	4.6	14.3	44.3	2.11
72	-10.4	-8.8	4.5	14.1	44.3	2.14
66	-0.3	-6.7	6.2	13.9	44.3	2.18
104	-6.6	-0.1	6.1	13.9	44.3	2.19
64	-11.7	-3.2	4.5	13.6	43.7	2.21
95	-3.2	-11.6	4.5	13.6	43.7	2.21
42	-6.9	-9.4	4.2	12.5	43.9	2.51
26	-9.4	-6.9	4.2	12.5	43.9	2.51
80	9.8	1.1	4.1	12.0	43.7	2.63
79	1.1	9.8	4.1	12.0	43.7	2.64
119	-0.1	-12.1	-0.5	12.1	44.1	2.65
110	-12.1	-0.1	-0.5	12.1	44.1	2.65
94	-11.1	-0.1	-0.4	11.2	44.1	2.95
71	-0.1	-11.1	-0.4	11.1	44.1	2.96
46	-9.8	-1.0	2.0	10.3	44.5	3.33
36	-2.8	-4.1	-4.9	9.9	43.1	3.34
22	-4.1	-2.8	-4.9	9.9	43.1	3.34
74	-0.2	-9.5	2.0	10.1	44.3	3.37
99	-9.5	-0.3	2.0	10.1	44.3	3.38
14	2.5	0.6	4.8	9.8	43.9	3.47
54	0.5	2.5	4.8	9.8	43.9	3.49
31	-1.0	-9.4	1.9	9.8	44.5	3.53
122	-4.9	1.1	3.7	9.6	44.3	3.62
115	1.1	-4.7	3.8	9.5	44.3	3.65

Table 2.6.13.6-15 $P_m + P_b$ Stresses for Support Disk—1-Foot Side-Drop, 45° Orientation, Thermal Case A

Section	Sx (ksi)	Sy (ksi)	Sxy (ksi)	Stress Intensity (ksi)	Allowable Stress (ksi)	Margin of Safety
21	-42.8	-39.0	11.6	52.7	64.5	0.22
37	-39.0	-42.8	11.6	52.7	64.5	0.22
35	36.1	35.8	10.5	46.4	64.5	0.39
23	35.8	36.1	10.5	46.4	64.5	0.39
1	-41.9	-37.5	3.0	43.4	63.0	0.45
4	-37.5	-41.9	3.0	43.4	63.0	0.45
49	-34.1	-34.4	9.9	44.1	64.5	0.46
9	-34.4	-34.1	9.8	44.1	64.5	0.46
34	-42.0	-39.6	3.0	44.1	64.5	0.46
20	-39.6	-42.0	3.0	44.1	64.5	0.46
3	-40.8	-38.0	3.1	42.8	63.0	0.47
2	-38.0	-40.8	3.1	42.8	63.0	0.47
7	34.8	32.0	9.1	42.6	64.5	0.52
51	32.0	34.8	9.1	42.6	64.5	0.52
111	-41.3	-17.6	3.7	41.8	65.5	0.57
112	-17.6	-41.2	3.7	41.8	65.5	0.57
95	-32.2	-32.1	8.6	40.7	65.5	0.61
64	-32.1	-32.1	8.6	40.7	65.5	0.61
96	-32.4	-31.3	8.7	40.6	65.5	0.62
63	-31.3	-32.4	8.7	40.5	65.5	0.62
48	-36.6	-32.9	2.1	37.5	64.5	0.72
6	-32.9	-36.6	2.1	37.5	64.5	0.72
120	-0.3	-34.1	5.5	35.6	66.4	0.87
114	-34.0	-0.6	5.5	35.2	66.4	0.89
79	27.4	27.6	7.2	34.7	65.5	0.89
80	27.6	27.3	7.2	34.6	65.5	0.89
22	-33.6	-6.2	-3.5	34.0	64.6	0.90
36	-6.2	-33.6	-3.5	34.0	64.6	0.90
28	-32.9	-13.1	6.2	34.7	65.8	0.90
40	-13.0	-32.8	6.1	34.6	65.8	0.91
26	-31.1	-19.5	7.2	34.5	65.8	0.91
42	-19.5	-31.1	7.2	34.5	65.8	0.91
98	-27.1	-18.5	9.3	33.0	66.4	1.01
72	-18.6	-27.1	9.3	33.0	66.4	1.01
8	29.4	3.6	-3.4	29.8	64.6	1.17
50	3.5	29.3	-3.4	29.8	64.6	1.17
30	-9.2	-28.4	4.8	29.5	66.7	1.26
44	-28.2	-9.5	4.7	29.3	66.7	1.28
75	-16.2	-21.3	9.7	28.8	66.8	1.32
99	-23.4	-17.7	7.4	28.5	66.4	1.33

Table 2.6.13.6-16 P_m Stresses for Support Disk—1-Foot Side-Drop, 45° Orientation, Thermal Case B

Section	Sx (ksi)	Sy (ksi)	Sxy (ksi)	Stress Intensity (ksi)	Allowable Stress (ksi)	Margin of Safety
120	9.6	-9.8	8.0	25.2	45.0	0.79
114	-9.7	9.6	8.0	25.1	45.0	0.79
35	14.3	-1.4	7.1	21.2	45.0	1.12
23	-1.4	14.3	7.1	21.2	45.0	1.12
37	-17.7	-8.2	6.6	21.1	45.0	1.13
21	-8.2	-17.7	6.6	21.1	45.0	1.13
112	7.6	-6.2	6.5	18.9	45.0	1.38
111	-6.2	7.5	6.5	18.9	45.0	1.38
49	-13.1	-0.6	6.4	17.9	45.0	1.51
9	-0.6	-13.1	6.4	17.9	45.0	1.51
96	-10.8	1.7	6.0	17.4	45.0	1.59
63	1.7	-10.8	6.0	17.4	45.0	1.59
51	12.7	3.3	5.8	15.4	45.0	1.92
7	3.3	12.7	5.8	15.4	45.0	1.92
28	-8.9	1.6	5.2	14.9	45.0	2.03
40	1.7	-8.9	5.2	14.8	45.0	2.03
98	-9.6	-10.8	4.4	14.7	45.0	2.06
66	-0.1	-7.0	6.5	14.7	45.0	2.07
104	-7.0	0.0	6.4	14.6	45.0	2.08
72	-10.8	-9.4	4.4	14.6	45.0	2.09
64	-12.3	-3.3	4.6	14.3	45.0	2.16
95	-3.3	-12.3	4.6	14.2	45.0	2.16
42	-6.9	-10.1	4.5	13.3	45.0	2.38
26	-10.1	-6.9	4.6	13.3	45.0	2.38
119	-0.1	-13.0	-0.5	13.0	45.0	2.46
110	-13.0	-0.1	-0.5	13.0	45.0	2.46
80	9.9	1.1	4.2	12.2	45.0	2.68
79	1.1	9.9	4.2	12.2	45.0	2.69
94	-12.0	-0.1	-0.4	12.0	45.0	2.75
71	-0.1	-12.0	-0.4	12.0	45.0	2.75
36	-2.1	-3.7	-5.3	10.7	45.0	3.21
22	-3.7	-2.1	-5.3	10.7	45.0	3.22
74	-0.1	-9.7	2.1	10.5	45.0	3.30
99	-9.7	-0.2	2.1	10.5	45.0	3.30
122	-5.2	1.0	4.0	10.0	45.0	3.48
115	1.0	-5.0	4.0	10.0	45.0	3.51
14	2.7	0.6	4.8	9.8	45.0	3.61
54	0.6	2.7	4.7	9.7	45.0	3.63
116	-0.1	-9.6	0.0	9.6	45.0	3.70
109	-9.6	-0.1	0.0	9.6	45.0	3.70

Table 2.6.13.6-17 $P_m + P_b$ Stresses for Support Disk—1-Foot Side-Drop, 45° Orientation, Thermal Case B

Section	Sx (ksi)	Sy (ksi)	Sxy (ksi)	Stress Intensity (ksi)	Allowable Stress (ksi)	Margin of Safety
21	-46.6	-41.5	12.6	56.9	67.5	0.19
37	-41.5	-46.5	12.6	56.9	67.5	0.19
23	37.2	38.8	11.1	49.1	67.5	0.38
35	38.8	37.1	11.1	49.1	67.5	0.38
20	-42.8	-44.4	3.4	47.1	67.5	0.43
34	-44.4	-42.8	3.4	47.1	67.5	0.43
4	-39.5	-45.5	3.1	46.8	67.5	0.44
1	-45.5	-39.5	3.0	46.8	67.5	0.44
51	33.7	37.0	9.7	45.2	67.5	0.49
7	37.0	33.7	9.7	45.2	67.5	0.49
49	-35.0	-35.1	10.0	45.1	67.5	0.50
9	-35.1	-35.0	10.0	45.1	67.5	0.50
3	-42.5	-41.0	3.1	44.9	67.5	0.50
2	-41.0	-42.5	3.1	44.9	67.5	0.50
111	-44.0	-18.8	3.9	44.6	67.5	0.51
112	-18.7	-44.0	3.9	44.5	67.5	0.52
95	-33.2	-33.5	8.9	42.3	67.5	0.60
64	-33.5	-33.1	8.9	42.3	67.5	0.60
96	-33.5	-32.7	9.0	42.1	67.5	0.60
63	-32.7	-33.4	9.0	42.1	67.5	0.60
48	-37.6	-33.8	2.0	38.4	67.5	0.76
6	-33.8	-37.6	1.9	38.4	67.5	0.76
120	-0.3	-36.1	5.8	37.7	67.5	0.79
114	-36.1	-0.6	5.8	37.3	67.5	0.81
26	-33.4	-20.1	7.6	36.9	67.5	0.83
42	-20.1	-33.3	7.6	36.8	67.5	0.83
22	-34.9	-5.3	-4.1	35.5	67.5	0.90
36	-5.3	-34.9	-4.1	35.5	67.5	0.90
79	27.8	28.1	7.3	35.3	67.5	0.91
80	28.1	27.8	7.3	35.3	67.5	0.91
28	-33.1	-12.4	5.9	34.7	67.5	0.95
40	-12.4	-33.0	5.9	34.5	67.5	0.95
98	-27.5	-19.0	9.4	33.6	67.5	1.01
72	-19.0	-27.4	9.4	33.5	67.5	1.01
8	30.1	4.1	-3.6	30.6	67.5	1.21
75	-17.3	-22.6	10.3	30.6	67.5	1.21
50	4.0	30.1	-3.6	30.6	67.5	1.21
122	-29.2	-13.0	-0.5	29.2	67.5	1.31
30	-10.7	-28.1	4.5	29.2	67.5	1.31
99	-23.8	-18.2	7.6	29.1	67.5	1.32

2.6.13.7 Stress Evaluation of PWR Support Disk for Combined Thermal and 1-Foot Side-Drop Load Condition

The inertial loading for the 1-ft side-drop is combined with the thermal loading for Thermal Case A to produce the largest stress intensities. The allowable stress intensity 3 S_m, is evaluated at the section temperature.

The 40 sections with the smallest margins of safety are presented in Tables 2.6.13.7-1 through 2.6.13.7-4. The tables are identified here:

Table Number	Basket Orientation (°)	Thermal Case	Stress Evaluation	Minimum Margin of Safety
2.6.13.7-1	0	A	$P_m + P_b + Q$	+3.75
2.6.13.7-2	18.22	A	$P_m + P_b + Q$	+1.59
2.6.13.7-3	26.28	A	$P_m + P_b + Q$	+1.21
2.6.13.7-4	45	A	$P_m + P_b + Q$	+1.46

The minimum margin of safety is +1.21.

Table 2.6.13.7-1 $P_m + P_b + Q$ Stresses for Support Disk—1-Foot Side-Drop, 0°, Orientation, Thermal Case A

Section	Sx (ksi)	Sy (ksi)	Sxy (ksi)	Stress Intensity (ksi)	Allowable Stress (ksi)	Margin of Safety
75	21.2	17.5	-8.5	28.1	133.5	3.75
91	21.2	17.5	8.5	28.1	133.5	3.75
107	-11.3	-21.2	9.3	26.7	133.5	3.99
123	-11.3	-21.2	-9.3	26.7	133.5	3.99
17	25.3	2.9	-2.0	25.4	133.4	4.24
18	25.3	2.9	2.0	25.4	133.4	4.24
26	12.7	-8.5	-1.3	21.3	131.6	5.17
28	12.7	-8.5	1.3	21.3	131.6	5.17
25	12.7	-8.5	-1.3	21.3	131.6	5.17
6	-16.8	-10.8	-5.4	20.0	129.0	5.46
7	-16.8	-10.8	-5.4	20.0	129.0	5.46
9	-16.8	-10.8	5.4	20.0	129.0	5.46
1	-13.0	-12.2	-4.9	17.5	125.9	6.19
3	-13.0	-12.2	4.9	17.5	125.9	6.19
4	-13.0	-12.2	4.9	17.5	125.9	6.19
29	0.0	-18.3	0.1	18.3	132.6	6.26
12	-14.8	-8.9	-5.0	17.6	131.6	6.48
14	-14.8	-8.9	5.0	17.6	131.6	6.48
11	-14.8	-8.9	-5.0	17.6	131.6	6.48
24	0.0	-16.1	0.1	16.1	130.4	7.09
23	-8.2	-13.4	4.2	15.7	129.0	7.22
21	-8.2	-13.4	-4.2	15.7	129.0	7.22
22	-8.2	-13.4	-4.2	15.7	129.2	7.23
27	-4.3	-14.4	-3.9	15.8	131.8	7.36
34	-7.4	-13.6	-3.5	15.2	129.0	7.46
35	-7.4	-13.6	-3.5	15.2	129.0	7.46
48	-7.4	-13.6	3.5	15.2	129.0	7.46
49	-7.4	-13.6	3.5	15.2	129.0	7.46
32	-7.4	-12.4	-5.1	15.6	133.4	7.54
30	-7.4	-12.4	5.1	15.6	133.4	7.54
31	-7.4	-12.4	5.1	15.6	133.4	7.54
16	-14.6	-10.2	-1.7	15.1	133.4	7.82
20	6.4	-7.9	0.0	14.3	129.0	8.00
19	0.0	-14.0	0.2	14.0	127.3	8.07
76	5.5	14.5	-1.3	14.7	133.5	8.08
92	5.5	14.5	1.3	14.7	133.5	8.08
13	12.5	-0.7	-3.0	14.4	131.8	8.12
2	7.4	-5.8	-1.2	13.4	125.9	8.38
46	1.4	13.6	0.9	13.6	133.4	8.80
60	1.4	13.6	-0.9	13.6	133.4	8.80

Table 2.6.13.7-2 $P_m + P_b + Q$ Stresses for Support Disk—1-Foot Side-Drop Orientation, 18.22°, Thermal Case A

Section	Sx (ksi)	Sy (ksi)	Sxy (ksi)	Stress Intensity (ksi)	Allowable Stress (ksi)	Margin of Safety
3	-35.1	-36.6	12.8	48.7	125.9	1.59
4	-35.1	-36.6	12.8	48.7	125.9	1.59
6	-36.3	-29.0	11.5	44.7	129.0	1.89
9	-36.3	-29.0	11.5	44.7	129.0	1.89
34	-25.3	-33.1	10.1	40.0	129.0	2.23
37	-25.3	-33.1	10.1	40.0	129.0	2.23
48	-29.4	-29.7	10.2	39.6	129.0	2.25
49	-29.4	-29.7	10.2	39.6	129.0	2.25
91	26.4	28.5	11.8	39.3	133.5	2.40
21	-24.8	-31.2	9.1	37.6	129.0	2.43
20	-24.8	-31.2	9.1	37.6	129.0	2.43
2	29.2	17.4	8.9	34.0	125.9	2.71
23	-30.5	-18.9	7.7	34.4	129.0	2.75
22	-30.5	-18.9	7.7	34.4	129.2	2.76
1	-18.7	-27.9	7.2	31.8	125.9	2.96
107	-12.0	-27.8	10.4	32.9	133.5	3.06
96	-24.3	-22.0	7.3	30.5	131.0	3.29
95	-24.3	-22.0	7.3	30.5	131.0	3.29
11	-26.3	-16.2	7.9	30.6	131.6	3.30
14	-26.3	-16.2	7.9	30.6	131.6	3.30
28	-25.5	-18.5	7.7	30.5	131.6	3.32
27	-25.5	-18.5	7.7	30.5	131.8	3.32
111	-27.1	-19.5	5.3	29.8	131.0	3.39
13	26.9	7.9	6.8	29.1	131.8	3.52
51	23.4	18.1	6.8	28.0	129.0	3.60
8	26.9	3.6	5.1	28.0	129.2	3.61
30	-9.2	-24.8	7.8	28.0	133.4	3.76
31	-9.2	-24.8	7.8	28.0	133.4	3.76
112	-7.9	-26.6	4.2	27.5	131.0	3.77
26	-15.4	-22.6	6.1	26.1	131.6	4.05
25	-15.4	-22.6	6.1	26.1	131.6	4.05
79	-24.8	-11.3	3.9	25.8	131.0	4.07
80	21.3	17.6	6.0	25.7	131.0	4.11
115	-4.8	-25.1	0.8	25.2	132.8	4.28
39	-13.9	-21.2	6.3	24.8	131.6	4.30
42	-13.9	-21.2	6.3	24.8	131.6	4.30
64	-19.5	-17.6	6.0	24.6	131.0	4.32
63	-19.5	-17.6	6.0	24.6	131.0	4.32
16	-17.6	-22.2	4.5	25.0	133.4	4.33
18	-17.6	-22.2	4.5	25.0	133.4	4.33

Table 2.6.13.7-3 $P_m + P_b + Q$ Stresses for Support Disk—1-Foot Side-Drop, 26.28°, Orientation, Thermal Case A

Section	Sx (ksi)	Sy (ksi)	Sxy (ksi)	Stress Intensity (ksi)	Allowable Stress (ksi)	Margin of Safety
3	-41.1	-43.0	15.0	57.0	125.9	1.21
4	-41.1	-43.0	15.0	57.0	125.9	1.21
6	-39.8	-33.9	12.9	50.1	129.0	1.57
9	-39.8	-33.9	12.9	50.1	129.0	1.57
34	-31.1	-40.5	12.2	48.8	129.0	1.64
37	-31.1	-40.5	12.2	48.8	129.0	1.64
20	-33.6	-39.0	12.0	48.6	129.0	1.66
21	-33.6	-39.0	12.0	48.6	129.0	1.66
48	-34.6	-35.0	11.9	46.7	129.0	1.76
49	-34.6	-35.0	11.9	46.7	129.0	1.76
2	34.6	23.4	10.9	41.3	125.9	2.05
1	-25.9	-33.1	9.4	39.6	125.9	2.18
23	31.9	24.7	9.8	38.8	129.0	2.32
95	-30.1	-28.4	9.3	38.7	131.0	2.39
96	-30.1	-28.4	9.3	38.7	131.0	2.39
22	-35.5	-15.9	7.6	38.1	129.2	2.39
91	25.7	28.8	11.7	39.0	133.5	2.43
112	-15.4	-34.9	5.9	36.6	131.0	2.58
51	28.7	25.1	8.8	35.8	129.0	2.60
42	-18.7	-29.6	8.5	34.2	131.6	2.85
39	-18.7	-29.6	8.5	34.2	131.6	2.85
111	-31.8	-17.4	5.6	33.7	131.0	2.88
28	-27.4	-18.5	8.0	32.1	131.6	3.10
27	-27.4	-18.5	8.0	32.1	131.8	3.10
8	30.2	3.5	5.3	31.2	129.2	3.14
80	25.3	22.8	7.4	31.6	131.0	3.15
79	25.3	22.8	7.4	31.6	131.0	3.15
107	28.3	16.9	-7.5	32.0	133.5	3.17
14	-26.5	-16.6	7.9	30.9	131.6	3.26
11	-26.5	-16.6	7.9	30.9	131.6	3.26
13	28.3	9.0	7.2	30.7	131.8	3.30
63	-23.0	-22.6	7.4	30.2	131.0	3.34
64	-23.0	-22.6	7.4	30.2	131.0	3.34
120	-0.6	-28.7	5.5	30.2	132.8	3.40
124	19.7	29.1	-0.1	29.1	133.5	3.59
31	-8.3	-25.8	7.8	28.8	133.4	3.64
30	-8.3	-25.8	7.8	28.8	133.4	3.64
26	-18.7	-22.9	6.7	27.8	131.6	3.73
25	-18.7	-22.9	6.7	27.8	131.6	3.73
35	22.7	14.9	6.4	26.3	129.0	3.91

Table 2.6.13.7-4 $P_m + P_b + Q$ Stresses for Support Disk—1-Foot Side-Drop, 45° Orientation, Thermal Case A

Section	Sx (ksi)	Sy (ksi)	Sxy (ksi)	Stress Intensity (ksi)	Allowable Stress (ksi)	Margin of Safety
1	-35.6	-40.3	13.0	51.1	125.9	1.46
2	-35.6	-40.3	13.0	51.1	125.9	1.46
6	-40.2	-37.4	13.5	52.4	129.0	1.46
9	-40.2	-37.4	13.5	52.4	129.0	1.46
48	-37.4	-40.2	13.5	52.4	129.0	1.46
49	-37.4	-40.2	13.5	52.4	129.0	1.46
3	-40.2	-35.6	13.0	51.1	125.9	1.46
4	-40.2	-35.6	13.0	51.1	125.9	1.46
34	-36.1	-36.5	12.1	48.4	129.0	1.67
37	-36.1	-36.5	12.1	48.4	129.0	1.67
20	-36.5	-36.1	12.1	48.4	129.0	1.67
21	-36.5	-36.1	12.1	48.4	129.0	1.67
63	-26.3	-28.3	8.8	36.1	131.0	2.63
64	-26.3	-28.3	8.8	36.1	131.0	2.63
95	-28.3	-26.2	8.8	36.1	131.0	2.63
96	-28.3	-26.2	8.8	36.1	131.0	2.63
111	-33.4	-16.4	5.9	35.2	131.0	2.72
112	-16.3	-33.3	5.9	35.1	131.0	2.73
79	26.5	26.5	8.2	34.7	131.0	2.78
80	26.5	26.5	8.2	34.7	131.0	2.78
35	-12.4	-31.7	6.2	33.5	129.0	2.85
23	-31.7	-12.4	6.2	33.5	129.0	2.85
36	-12.4	-31.7	6.2	33.5	129.2	2.85
22	-31.7	-12.4	6.2	33.5	129.2	2.85
91	22.8	25.3	10.2	34.3	133.5	2.90
8	29.8	1.6	4.6	30.5	129.2	3.23
50	1.6	29.8	4.6	30.5	129.2	3.23
44	-27.8	-10.5	8.4	31.2	133.4	3.28
46	-27.8	-10.5	8.4	31.2	133.4	3.28
30	-10.1	-27.6	8.2	30.9	133.4	3.32
31	-10.1	-27.6	8.2	30.9	133.4	3.32
7	20.5	24.4	7.0	29.7	129.0	3.34
51	24.4	20.4	7.0	29.7	129.0	3.35
26	-23.3	-20.6	7.3	29.4	131.6	3.48
25	-23.3	-20.6	7.3	29.4	131.6	3.48
42	-20.6	-23.3	7.3	29.3	131.6	3.49
39	-20.6	-23.3	7.3	29.3	131.6	3.49
14	26.0	9.6	6.8	28.4	131.6	3.64
13	26.0	9.6	6.8	28.4	131.8	3.64
54	9.5	25.9	6.8	28.3	131.6	3.65

2.6.13.8 Stress Evaluation of PWR Support Disk for 1-Foot Off-Angle Load Conditions

As previously discussed, the evaluation of off-angle impacts is accomplished by using the stress results from the side and end-drop evaluations. To evaluate oblique impacts, the stress components (i.e. S_x, S_y, S_{xy}) are combined from the side and end drop cases. The evaluatation considers various cask drop angles (ϕ = 0°, 23°, 30°, 45°, 60°, 70°, 75°, 80°, 85°, 88°, and 90°), as well as the basket drop orientation (0°, 18.22°, 26.28°, and 45°). Note that the end drop (ϕ = 0°) and side drop (ϕ = 90°) are included in the evaluation so that the results envelope all cask drop angles. The normal stresses (S_x and S_y) and the shear stress (S_{xy}) for an off-angle (ϕ) drop are calculated by the following equations,

$$S_{x(\phi)} = S_{x(end)}\mathrm{Cos}\phi + S_{x(side)}\mathrm{Sin}\phi\,,$$

$$S_{y(\phi)} = S_{y(end)}\mathrm{Cos}\phi + S_{y(side)}\mathrm{Sin}\phi\,,$$

$$S_{xy(\phi)} = S_{xy(end)}\mathrm{Cos}\phi + S_{xy(side)}\mathrm{Sin}\phi\,,$$

where,

$S_{x(side)}$, $S_{y(side)}$, and $S_{xy(side)}$ are the section stresses calculated by the ANSYS analysis for the side drop conditions. $S_{x(end)}$, $S_{y(end)}$, and $S_{xy(end)}$ are the sectional stresses calculated by the ANSYS analysis for the end drop. The principal stresses and the stress intensity are then determined based on the stress components. The orientations where the maximums occur for each loading condition are then determined. A summary of the evaluation is presented in Section 2.6.13.2.

2.6.13.9 Stress Evaluation of Support Disk for Combined Thermal and 1-Foot Off-Angle Conditions

The stress evaluation for the combined thermal and oblique condition is performed using the same methodology discussed in Section 2.6.13.8. The summary of the maximum P+Q stresses is also presented Section 2.6.13.2.

2.6.13.10 Stress Evaluation of Tie Rods and Spacers for 1-Foot End-Drop Load Condition

The PWR basket support disks are connected by eight tie rods with spacers to maintain spacing of the support disks and heat transfer disk. The tie rods and spacers are constructed from Type 304 stainless steel. The tie rods are threaded only at the upper end so that the top nut can provide rigidity of the basket assembly. The tie rods do not transmit any load other than their own weight. In a side-drop, the load resulting from the disks and the fuel is transmitted directly into the canister wall by the support disks. In an end-drop, the spacers transmit the load resulting from the weight of the support disks, aluminum heat transfer disks, one end weldment, and spacers to either the lid or bottom depending on the orientation of the drop. The weight of the fuel assemblies is transmitted directly into the canister lid or bottom, because the fuel tubes in the basket are open at both ends. In drop orientations other than on the end, the spacers experience only a portion of the weight of the support disks, heat transfer disks, one end weldment, and the spacers that act along the centerline axis of the cask. Thus, the end-drop is the critical loading condition.

During an end-drop, the weight of the support disks, end weldment, aluminum heat transfer disks, and spacers and end nuts is supported by the spacers on the 8 tie rods, thereby resulting in compressive stress over the cross-sectional area of the spacers. Taking the largest weight of all three PWR fuel classes, the total weight of the basket is 16,489 lb. Because the weights of the bottom end weldment (527 lb) and the fuel tubes (3,676 lb) are transmitted directly into the end of the canister, the remaining load acting over the area of the spacers is 12,286 lb. For the 1-ft end-drop, the deceleration is 20 *g*, which results in a total end-drop load of 245,720 lb. The area in compression is $\pi(3.0^2 - 1.75^2)/4 = 4.66$ in^2. The compressive stress, is 245,720/(8 x 4.66) = 6,591 psi, and is considered to be a membrane stress.

Based on the ASME Code, Section III, Subsection NG, the allowable membrane stress is 1.0 S_m. Using a conservative material temperature for the outer edge of the support disk of 500°F, S_m = 17.5 ksi. The corresponding margin of safety is

$$MS = (17{,}500/6{,}591) - 1 = +1.66.$$

Therefore, structural adequacy of the tie rod/spacer assemblies is demonstrated.

2.6.13.11 Support Disk Shear Stresses for 1-Foot Drops

The ASME Code, Section III, Division 1, Subsection NG, criteria define the Level A allowable for shear stress to be 0.6 S_m. The extrapolated design stress intensity for 17-4 PH at a bounding temperature of 750°F is 41.9 ksi. The maximum stress intensity across any section (membrane stress) for the 1-ft side-drop is 31.4 ksi for the 45° drop orientation at Case 1. Similarly, for the end-drop, a maximum membrane stress across a section is 0 ksi for the 1-ft drop. Therefore, the maximum shear stress for any normal loading condition is 31.4/2 or 15.7 ksi.

Using the allowable stresses as stated previously, the minimum margin of safety for shear is

$$\begin{aligned} MS &= [2(0.6)S_m / SI] - 1 \\ &= [2(0.6)(41.9) / 31.4] - 1 \\ &= +0.60 \end{aligned}$$

Therefore, structural adequacy of the PWR fuel basket support disk design for the normal conditions of transport, 1-ft side and end-drops is demonstrated for shear stress criteria.

2.6.13.12 Bearing Stress - Basket Contact with Canister Shell

For the bearing stress (S_{br}) acting along the basket support disk-canister shell interface, an angular contact of 18° is considered on the basis of ANSYS gap element status (at a radius of 32.75 in). The load considered to be acting on the support disks is the total contents weight (55,810 lb), times the deceleration value of 20 g, divided among 30 support disks in the basket. The bearing area is considered to be the 0.5-in. thick disk over an 18° contact area.

$$S_{br} = (55{,}810)(20)/[(0.5)(30)(\pi)(65.5)/(360/18)] = 7{,}233 \text{ psi}$$

The allowable bearing stress is the yield stress, which is 89.8 ksi for SA-693, Type 630, 17-4 PH stainless steel at a temperature of 400°F. The margin of safety for the support disk (not the canister) is computed as

$$MS = 89.8/ S_{br} - 1 = +11.41.$$

2.6.13.13 Basket Weldment Analysis for 1-Foot End-Drop

The responses of the top and bottom weldment plates of the fuel assembly to a 1-ft end-drop in conjunction with the thermal expansion stress are evaluated in this section. The top and bottom weldment plates are 1.25-in.-thick and 1.0-in.-thick plates of Type 304 stainless steel, respectively. The weldments support their own weight plus the weight of 24 PWR fuel assembly tubes. A finite element analysis is performed for both plates, because the support for each weldment is different as a result of the location of the welded ribs for each. Both models use the SHELL63 element, which permits out-of-plane loading. Figures 2.6.13.13-1 and 2.6.13.13-2 show the finite element models for the top and bottom weldments, respectively. The load from the fuel tube is represented as point forces applied to the nodes at the periphery of the fuel assembly slots. An average point force is applied. The application of the nodal loads at the slot periphery is accurate because the tube weight is transmitted to the edge of the slot, which provides support to the fuel tubes in the end-drop condition. The analysis using the applied nodal forces demonstrates that the weldment design satisfies the primary membrane (P_m) and the primary membrane plus bending (P_m+P_b) stress criteria. Thermal expansion stresses are also analyzed. The determination of the weldment temperatures is discussed in Chapter 3.0.

The margins of safety are calculated as

$$MS = [(P_m + P_b) / 1.5\ S_m] - 1$$

or

$$MS = [(P_m + P_b + Q) / 3\ S_m] - 1$$

The margins of safety evaluated for the weldments are shown in Table 2.6.13.13-1. The weldments are shown to satisfy the stress criteria in the ASME Code, Section III, Division I, Subsection NG.

Figure 2.6.13.13-1 Finite Element Model of the Top Weldment Plate

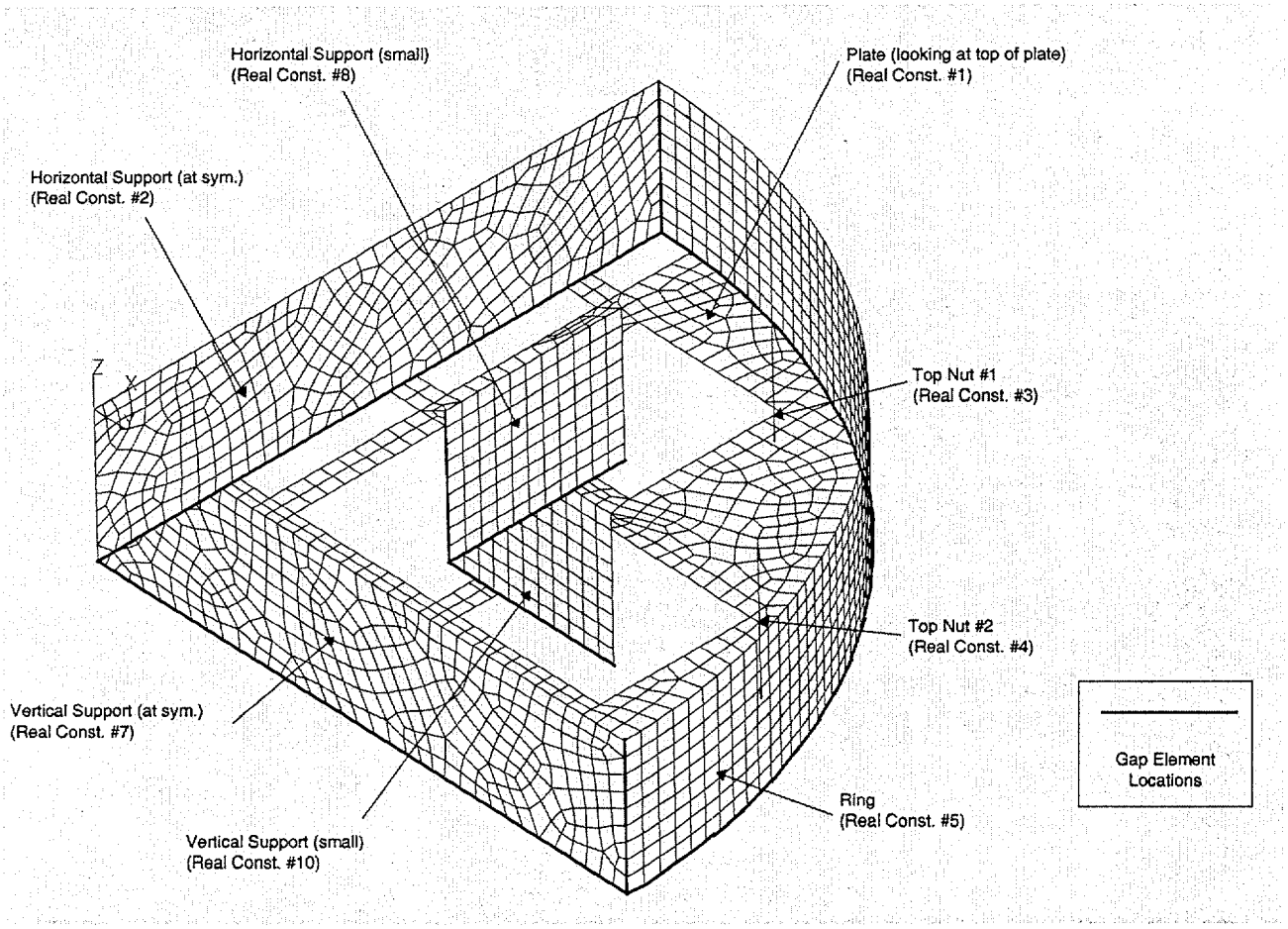

Figure 2.6.13.13-2 Finite Element Model of the Bottom Weldment Plate

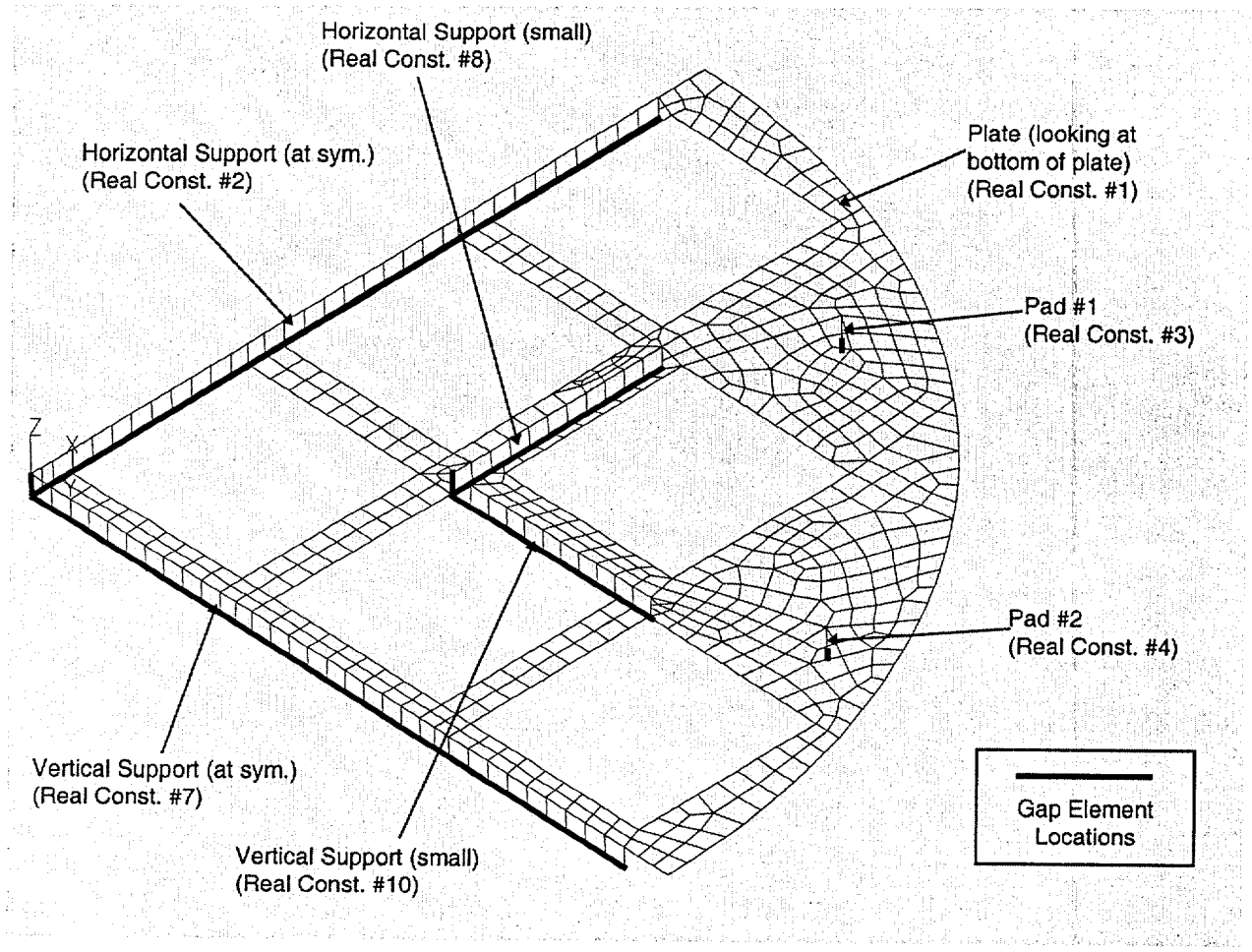

Table 2.6.13.13-1 Minimum Margins of Safety for the Top/Bottom Weldments for 1-Foot End-Drop

Component/Condition	P_m (ksi)	Allowable S_m (ksi)	MS
Top Weldment/1-ft End-Drop	5.86	17.38	+1.97
Bottom Weldment/1-ft End-Drop	6.13	17.56	+1.86
Component/Condition	$P_m + P_b$ (ksi)	Allowable $1.5S_m$ (ksi)	MS
Top Weldment/1-ft End-Drop	2.54	26.07	+9.26
Bottom Weldment/1-ft End-Drop	4.33	26.34	+5.08
Component/Condition	$P_m + P_b + Q$ (ksi)	Allowable $3S_m$ (ksi)	MS
Top Weldment/1-ft End-Drop + Thermal	35.41	52.14	+0.47
Bottom Weldment/1-ft End-Drop + Thermal	35.27	52.68	+0.49

2.6.13.14 Support Disk Buckling Evaluation

The PWR fuel basket support disks are subjected to compressive and inertial loads during impact conditions. Depending on the cask orientation for the impact, both in-plane and out-of-plane loads are applied to the support disk. The in-plane loads (basket side impact component) apply compressive forces and in-plane (strong axis) bending moments on the support disk and the out-of-plane inertial loads (basket end-impact component) produce out-of-plane (weak axis) bending moments on the support disk.

Buckling of the support disk is evaluated in accordance with the methods and acceptance criteria of NUREG/CR-6322. The support disk buckling evaluation for the hypothetical accident conditions is presented in Section 2.7.8.3.

2.6.13.14.1 Support Disk Buckling Evaluation Input Data

The support disk is constructed of SA-693, Type 630, 17-4 PH stainless steel plate. The properties are evaluated at the actual temperature of the locations where buckling evaluations are performed.

2.6.13.14.2 Detailed Support Disk Buckling Evaluation

Methodology

The buckling evaluation of the support disk web is based on the Interaction Equations 31 and 32 in NUREG/CR-6322. These two equations adopt the "Limit Analysis Design" approach for structural members subjected to stresses beyond the yield limit of the material, i.e., for members deformed elastically as a result of both axial load and bending moment. Other equations applicable to the calculations are listed later in this section.

The maximum forces and moments are determined for the end-drop condition and for four different radial orientations of the support disk for the side-drop condition based on the stress results of the finite element analysis (Sections 2.6.13.4 through 2.6.13.7). The forces and

moments for the cask off-angle drop conditions are determined from the end and side drop results based on the drop angle. The buckling evaluations account for both in-plane (about the strong axis of the web) and out-of-plane (about the weak axis of the web) buckling modes. Evaluation for strong axis buckling is performed only for the side drop condition since it is the governing case. Evaluation for weak axis buckling is performed for all end drops and off-angle drops (0°, 23°, 30°, 40°, 45°, 50°, 60°, 70°, 75°, 80°, 85°, and 88°).

Detailed buckling calculations are performed using ANSYS macros. The methodology and equations used in the calculations are those from NUREG/CR-6322. The load amplification factors used are 20 *g* for 1-ft end-drop, 1-ft side-drop, and off-angle drop conditions. The buckling evaluation is performed for each of the sections identified in Figures 2.6.13.2-3 and 2.6.13.2-4.

The buckling evaluation methodology/equations are summarized as follows:

Symbols and Units

P = applied compressive axial load, kips

M = moment, kips-in.

P_a = allowable axial compressive load, kips

P_{cr} = critical axial compression load, kips

P_e = Euler buckling loads, kips

P_y = plastic axial load, equal to profile area times specified minimum yield stress, kips (for normal operating condition)

C_c = column slenderness ratio separating elastic and inelastic buckling

C_m = coefficient applied to bending term in interaction equation

M_m = critical moment that can be resisted by a plastically designed member in the absence of axial load, kip-in.

M_p = plastic moment, kip-in.

F_a = axial compressive stress permitted, ksi

F_e = Euler stress for a prismatic member divided by factor of safety, ksi

k = ratio of effective column length to actual unbraced length

l = unbraced length of member, in.

r = radius of gyration, in.

S_y = yield stress allowable, ksi

A = area of the ligament, in^2

Z_x = plastic section modulus with respect to the major axis, in^3

Σ = allowable reduction factor, dimensionless.

From NUREG/CR-6322, the following equations are used to evaluate the support disk for normal conditions:

$$\frac{P}{P_{cr}} + \frac{C_m M}{M_m\left[1-\frac{P}{P_e}\right]} \leq 1.0$$

$$\frac{P}{P_y} + \frac{M}{1.18\,M_p} \leq 1.0$$

where: $P_{cr} = 1.7 \times A \times F_a$

$$F_a = \frac{\left[1-\frac{1}{2}\left(\frac{k\cdot l}{r\cdot C_c}\right)^2\right]\cdot S_y}{\frac{5}{3}+\frac{3}{8}\left(\frac{k\cdot l}{r\cdot C_c}\right)-\frac{1}{8}\left(\frac{k\cdot l}{r\cdot C_c}\right)^3} \quad \text{for} \quad \frac{k\cdot l}{r} < C_c = \sqrt{2\cdot\pi^2\frac{E}{S_y}}$$

$P_e = 1.92 \times A \times F_e$

$$F_e = \frac{\pi^2\cdot E}{1.92\left(\frac{k\cdot l}{r}\right)^2} \text{ (non-austenitic)}$$

$$F_e = \frac{\pi^2\cdot E}{1.3\left(\frac{k\cdot l^2}{r}\right)} \text{ (austenitic)}$$

$P_y = S_y \times A$

$C_m = 0.85$ for members with joint translation (sideways).

$M_p = S_y \times Z_x$

$$M_m = M_p \cdot \left(1.07 - \frac{\left(\frac{1}{r}\right) \cdot \sqrt{S_y}}{3160}\right) \leq M_p$$

Buckling evaluation is performed at all sections defined in Figures 2.6.13.2-3 and 2.6.13.2-4. Using the cross-sectional stresses calculated at each of the section located in the web for each loading condition the corresponding compressive forces (P) and bending moment (M) are determined as follows,

$P = \sigma_m A$,

$M = \sigma_b S$,

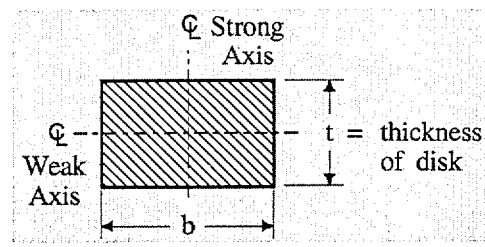

where, σ_m is the membrane stress, σ_b is the strong axis bending stress or weak axis bending stress, A is the area ($b \times t$), and S is the section modulus ($tb^2/6$ for strong axis bending and $bt^2/6$ for weak axis bending).

Support disk buckling evaluation results

The equations used in the buckling analysis are:

$$P_1 = P/P_{cr} \qquad M_1 = \frac{C_m M}{\left(1 - P/P_e\right) M_m} \quad (P_1 + M_1 \leq 1) \quad \text{(Eq. 31, NUREG/CR-6322)}$$

and $$P_2 = P/P_y \qquad M_2 = \frac{M}{1.18\, M_p} \quad (P_1 + M_1 \leq 1) \quad \text{(Eq. 32, NUREG/CR-6322)}$$

The margins of safety are calculated as:

$$MS1 = \frac{1}{P_1 + M_1} - 1$$ (based on Eq. 31, NUREG/CR-6322)

and $$MS2 = \frac{1}{P_2 + M_2} - 1$$ (based on Eq. 32, NUREG/CR-6322)

Table 2.6.13.14-1 summarizes the worst buckling margins of safety for each stress category and thermal case for normal conditions of transport. As the results demonstrate, the PWR support disks meet the requirements of NUREG/CR-6322.

Table 2.6.13.14-1 Minimum Margins of Safety from Buckling Evaluation of PWR Support Disk

Loading Condition	Stress State*	Thermal Case	Section Number	Drop Angle	Basket Angle	P (kip)	P_{cr} (kip)	M (in-kip)	M_p (in-kip)	M_m (in-kip)	MS1	MS2
Strong Axis Buckling												
Normal	P	A	21	90.00	45.00	3.8	39.3	2.9	10.9	10.7	1.97	2.18
	P+Q	A	4	90.00	26.28	7.8	59.6	6.2	23.6	23.6	1.80	1.88
	P	B	21	90.00	45.00	4.1	46.7	3.2	13.1	12.7	2.26	2.51
	P+Q	B	21	90.00	45.00	4.2	46.7	3.3	13.1	12.7	2.20	2.45
Weak Axis Buckling												
Normal	P	A	29	85.00	0.00	10.3	47.5	0.0	8.5	7.4	3.59	5.57
	P+Q	A	29	90.00	0.00	13.7	47.5	0.0	8.5	7.4	2.47	3.97
	P	B	29	85.00	0.00	10.6	53.4	0.0	9.8	8.5	4.02	6.40
	P+Q	B	29	85.00	0.00	10.6	53.4	0.0	9.8	8.5	3.98	6.33

* P = Primary Stress, P+Q = Primary + Secondary Stresses.

2.6.14 BWR Transportable Storage Canister Analysis - Normal Conditions of Transport

In this section, the Transportable Storage Canister Assembly containing BWR fuel is evaluated for the normal conditions of transport. The principal components of the canister assembly are the canister, fuel basket assembly, shield lid, and structural lid. The canister and the canister shell, bottom plate, and lids are shown in Figures 2.6.14-1 and 2.6.14-2.

Spacers are used to properly locate the canisters containing Class 4 and 5 BWR fuel in the cask cavity. The analysis of the spacers is presented in Section 2.6.16. The geometries and materials of construction of the canister, baskets, and spacers are described in Section 1.2.1.2.

Figure 2.6.14-1 BWR Transportable Storage Canister

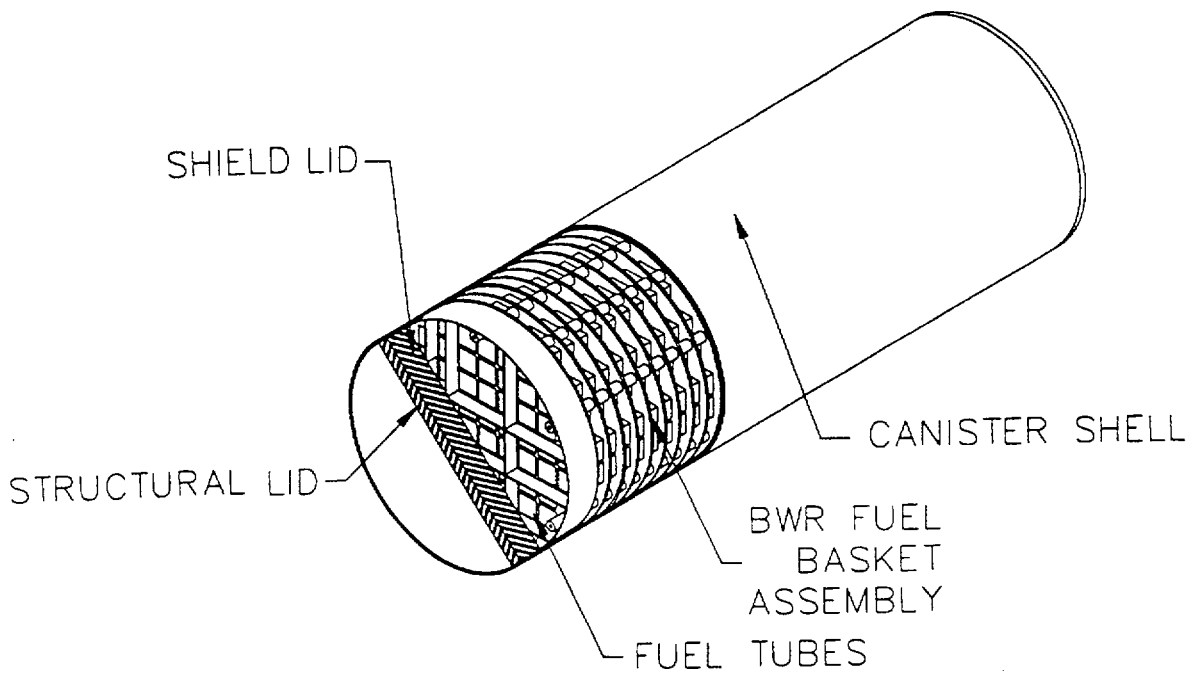

Figure 2.6.14-2 BWR Transportable Storage Canister Shell and Lids

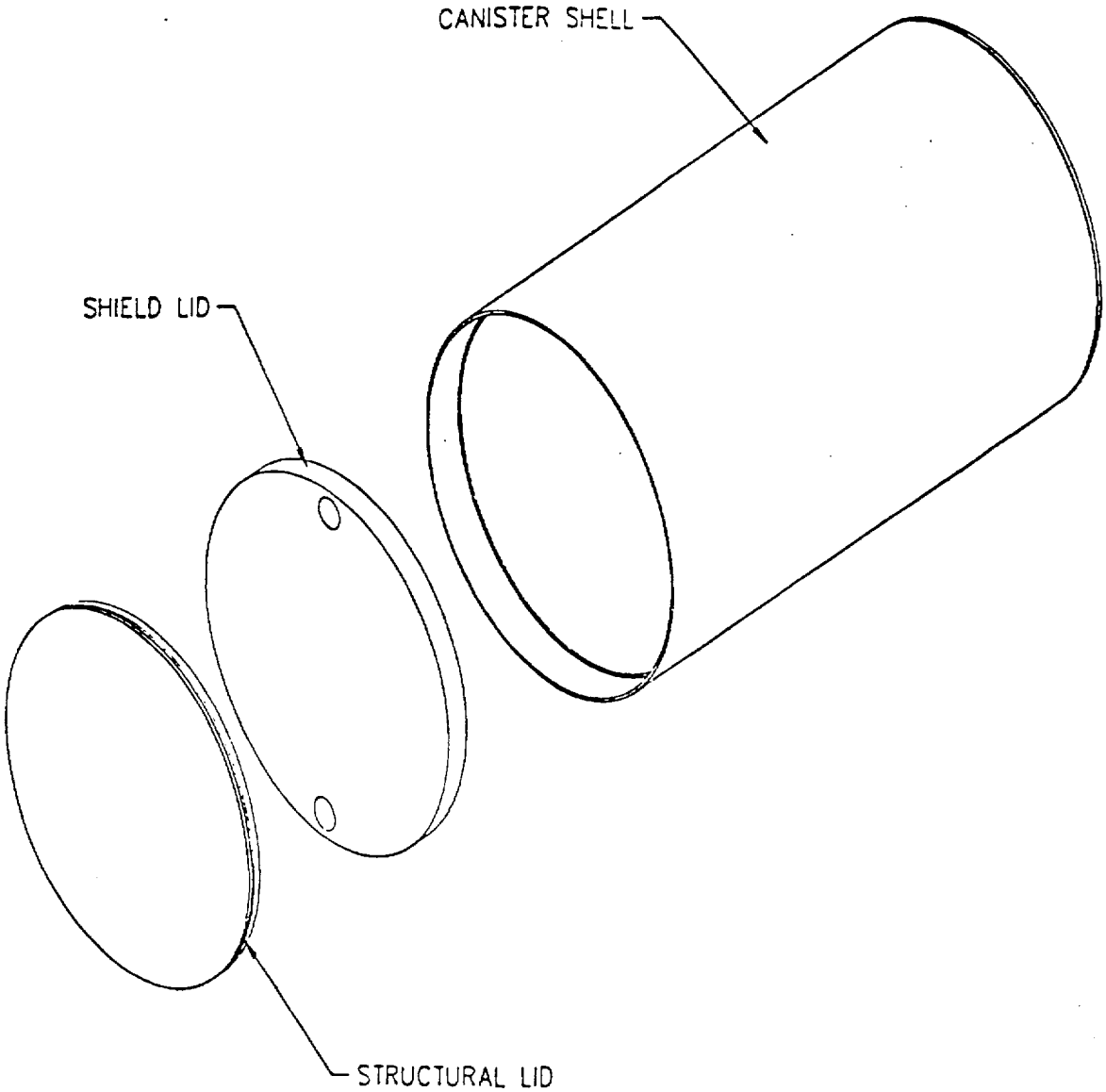

2.6.14.1 Analysis Description

Two canisters of different lengths are designed to accommodate the two classes of BWR fuel. The overall lengths of the two BWR canisters are 185.75 in and 190.55 in. Other design parameters of the canisters are provided in Table 1.2-3. For this analysis, the largest load per disk configuration (BWR Class 4) is modeled with the longest canister of 191.95 in.

As is the case for the PWR canister, the structural design criteria for the BWR canister is the ASME Code, Section III, Subsection NB. Consistent with this criterion, the structural components of the canister are shown to satisfy the allowable stress limits presented in Tables 2.1.2-3 and 2.1.2-4 as applicable. The allowable stresses used in this analysis are based on a maximum material temperature of 380°F for all locations in the canister, unless otherwise indicated. These allowables are conservative for all sections because the maximum temperature in the canister shell central region is determined to be 372°F in the thermal analysis presented in Section 3.4.2. For the canister structural lid weld (Section 13, Figure 2.6.12.3-1), base metal properties are used to define the allowable stress limits since the weld filler rod tensile properties are greater than the base metal. Also, the allowable stress is multiplied by a stress reduction factor of 0.8 per ISG-4.

The ANSYS finite element computer program is used to analyze the canister for the 1-ft free-drop condition in the top and bottom end, side, and top and bottom corner-impact orientations. In addition, the effects of normal operating internal pressure and thermal stresses resulting from exposure of the cask to the hot (100°F ambient and solar insolance) and cold (-40°F ambient) normal conditions are evaluated. The worst-case stresses from these analyses are presented in Section 2.6.14.4.

2.6.14.2 Finite Element Model Description - BWR Canister

To evaluate the BWR Transportable Storage Canister for normal conditions of transport, ANSYS is used to construct and analyze a finite element model of the canister and its contents. The contents modeled consist of the fuel basket support disks and weldments. The fuel assemblies, fuel tubes, tie-rods, and related hardware are not explicitly modeled but are accounted for by applying pressure loads to the support disk slots as appropriate.

The maximum unit load per length results in the largest bearing stresses. Stresses in the top and bottom of the canister are not affected by its length. Moreover, distortion in the shell is not affected by the 6-in differential of the longest canister and the shortest canister.

The finite element model of the BWR canister is similar to the model for the PWR canister. A detailed description of the PWR model is provided in Section 2.6.12.2. Table 2.6.14.2-1 lists the real constants assigned to specific components of the model. Table 2.6.14.2-2 lists the material properties used for the model.

Figure 2.6.14.2-1 is a plot of the entire canister finite element model. An isolated view of the canister shield and structural lids portion of the model is presented in Figure 2.6.14.2-2, and an enlarged view of the model in the structural lid and shield lid weld regions is shown in Figure 2.6.14.2-3. The canister bottom plate portion of the model is shown in Figure 2.6.14.2-4.

The loading for the normal operating condition is based on 1-ft drops in conjunction with the internal pressure loading (to the canister). Drop orientations considered are the top and bottom end, side, and top and bottom corner-drops. The transfer of loads due to the drop orientations and the resulting stresses are similar to the PWR canister case discussed in Section 2.6.12.2. The contents weight analyzed includes 38,920 lb for all fuel assemblies (56 fuel assemblies), the fuel tubes weight (4,034 lb), the disk spacer weight (1,060 lb), and the tie rods and nuts weights (586 + 116 lb). The actual bounding fuel assembly weight is 38,976 lb. The effect of the increased contents weight is discussed below.

For the side and corner-drops, the weights of the fuel assemblies (W_{tubes}), fuel tubes (W_{tubes}), tie rods (W_{rods}), nuts/washers (W_{nuts}), and spacers ($W_{spacers}$) are included in the model by applying a pressure load (F_{slot}) to the slot openings of the support/weldment disks. This pressure load is:

$$F_{slot} = \frac{W_{fuel} + W_{tubes} + W_{rods} + W_{nuts} + W_{spacers}}{N_{slots} \times w_{slot} \times N_{disks}} \times g$$

where,

N_{slots} = number of slot openings in each support/weldment disk,
w_{slot} = width of each slot opening in each support/weldment disk,
N_{disks} = number of support/weldment disks, and
g = the associated g-loading for the drop height of interest.

For basket orientations other than 0°, the components of this pressure load are applied to two faces of the slot opening. For corner-drops, the component resulting from accounting for the drop angle is used as the pressure load on the disk slot openings. For the BWR canister drop analyses, with 56 slot openings, a slot opening width of 6.278 inches, and a total of 35 support/weldment disks (33 support disks and 2 weldment disks), the base pressure load is:

$$F_{slot} = \frac{38{,}920 + 4{,}034 + 586 + 116 + 1{,}060}{56 \times 6.278 \times 35} \times g = 3.634 \times g$$

For the end drops, a uniform pressure representing the total weight of the fuel and fuel basket (54,351 lb) is applied to the canister shield lid (for top end-drop) or canister bottom plate (for bottom end-drop). For the corner-drops, the component of this uniform pressure resulting from accounting for the drop angle is applied to the appropriate elements.

Design changes were made to the BWR basket after the finite element analyses of the canister were performed. The effects of the design changes are evaluated as follows. The support disks were changed from thirty-three (33) 0.75-inch thick disks to forty (40) 0.625-inch thick disks. Reducing the thickness of the support disks makes them more similar to the PWR support disks (0.5-inch thick). Increasing the number of disks distributes the internal load more uniformly on the canister shell. Also, seventeen (17) aluminum heat transfer disks were added to the BWR basket design. The heat transfer disks do not provide structural support, but their addition along with the associated spacers does add weight that must be considered.

The increase in the number of support disks has a minimal effect on the stress results presented in this section since this change helps to distribute the load to the canister shell more evenly. In addition, the design changes and bounding fuel assembly weight results in a total fuel and fuel basket weight of 56,821 lb. This is an increase in weight of 2,471 lb (a 4.5% increase) over the total fuel and fuel basket weight (54,351 lb) used in the BWR canister analyses. Therefore, the stress intensities presented in the following tables for the BWR canister are conservatively ratioed up according to the following: Sections 3 through 8 (see Figure 2.6.14.3-1) are increased by 5% for the side and corner-drops to account for the additional contents weight on the canister shell. Sections 1 and 14 stress intensities are increased by 5% for the bottom end and bottom corner-drops to account for the additional load on the canister bottom end. Sections 12, 13, 15,

and 16 stress intensities are increased by 5% for the top end and top corner-drops to account for the additional load on the canister shield lid.

The operational conditions also contain loads developed from the temperature distribution in the canister. The temperature distributions used for the BWR canister analysis are obtained from the PWR thermal evaluation since this resulted in conservative values of the temperatures and temperature gradients in the canister. These are included in the canister model analyses. The thermal analyses are described in Section 3.4.

The BWR canister is analyzed for basket orientations of 0° and 45°. To accurately predict the canister response to impact, both orientations are run for these drop orientations: side, top corner, and bottom corner. Top- and bottom-end-drops are not required because the basket disks are not included in these runs (their presence is accounted for by using applied pressure loads to the inner surface of the top or bottom).

Figure 2.6.14.2-1 BWR Canister Assembly Finite Element Mesh (with 45° Basket orientation)

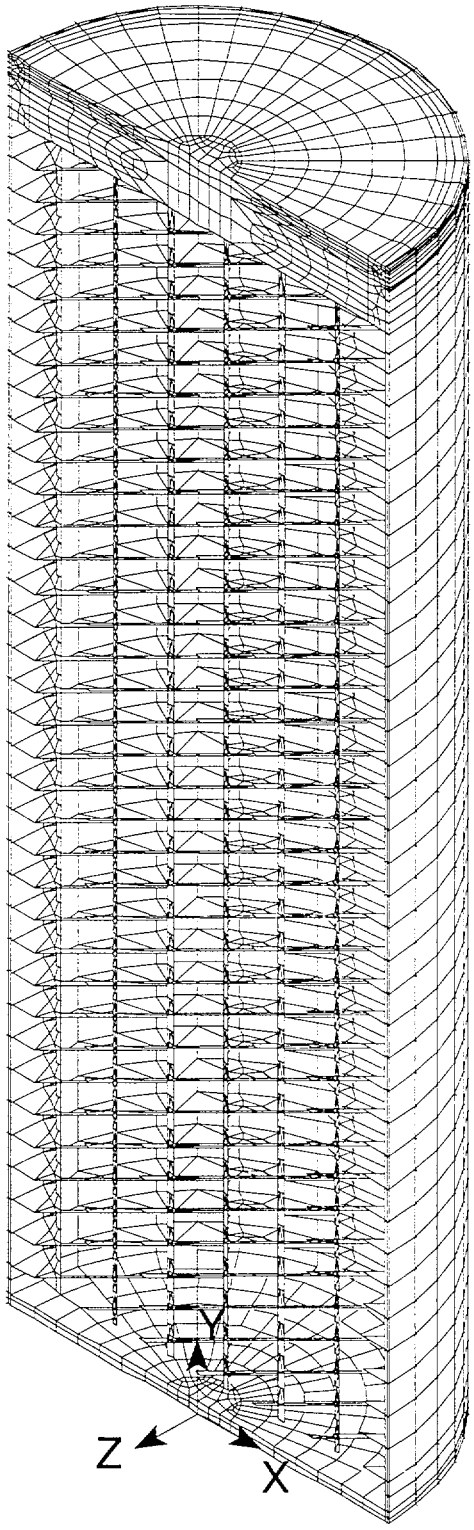

Figure 2.6.14.2-2 Canister Structural and Shield Lid Finite Element Mesh

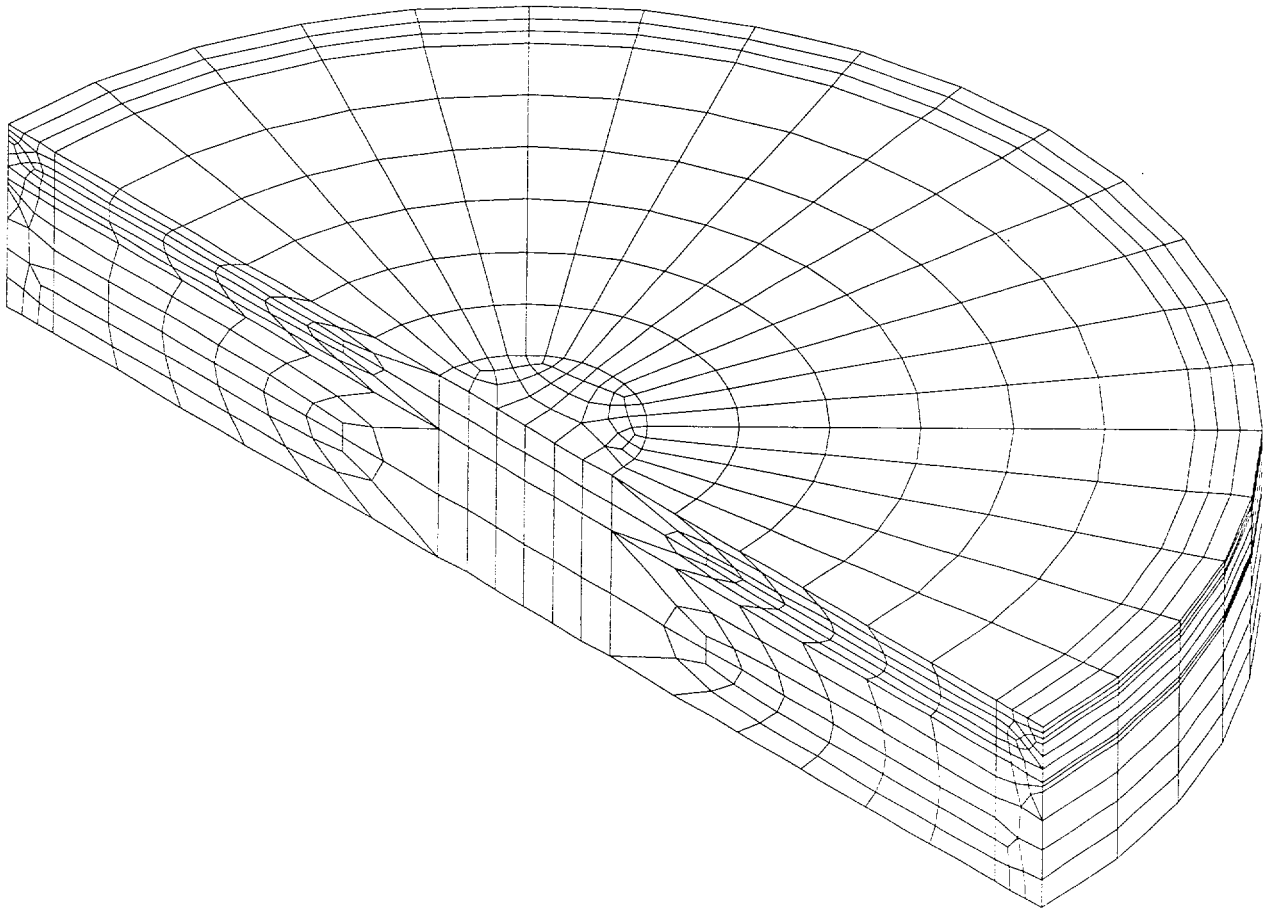

Figure 2.6.14.2-3 Structural and Shield Lid Weld Regions Finite Element Mesh

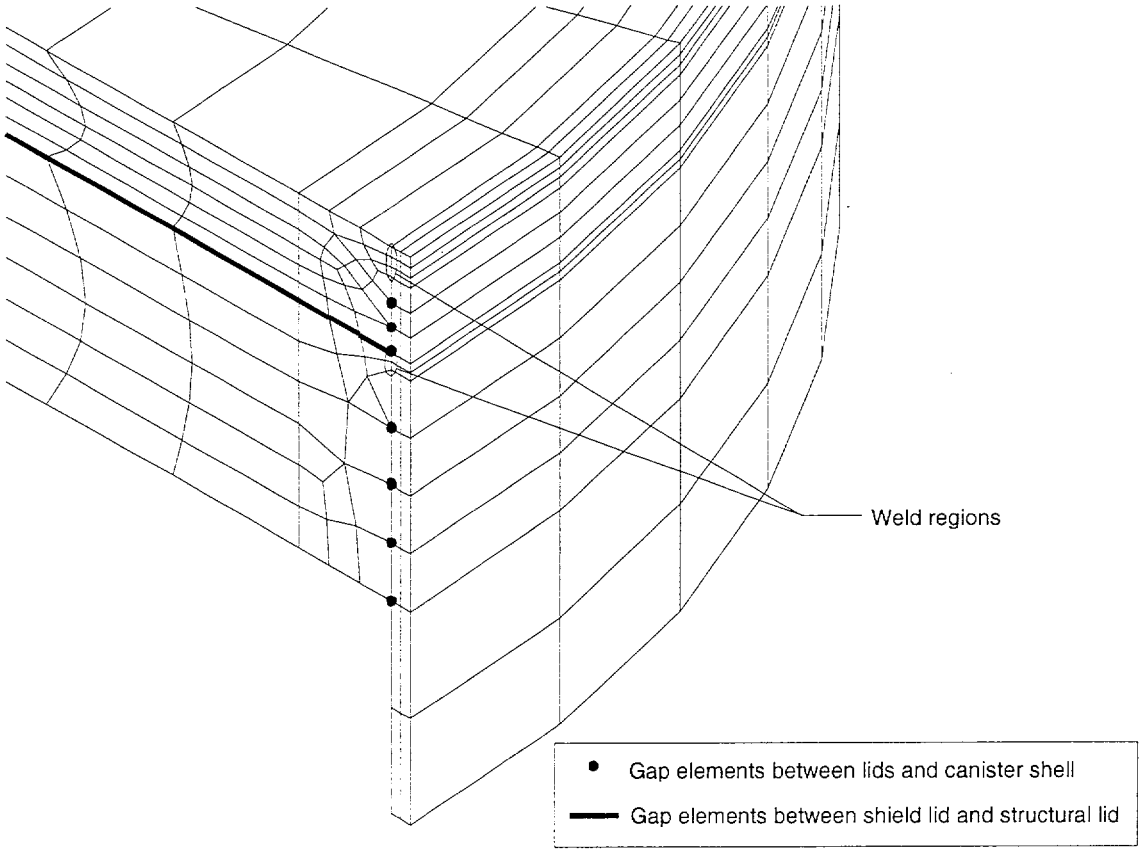

Figure 2.6.14.2-4 Canister Bottom Plate Finite Element Mesh

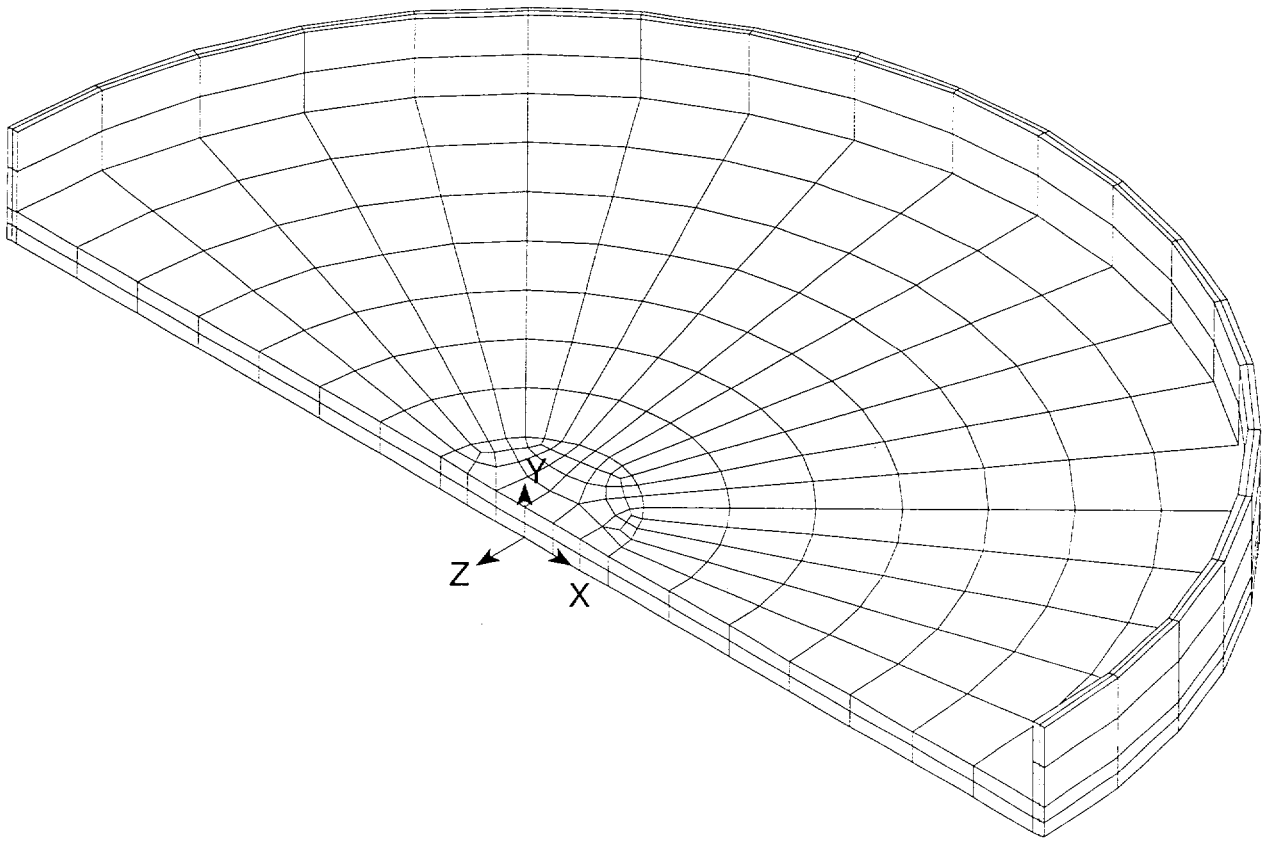

Table 2.6.14.2-1 Real Constant Sets Defined in Canister Model

Real Constant Set	Component
1	Canister Bottom Plate (SOLID45)
2-9	Canister Shell (SOLID45)
10-11	Shield Lid (SOLID45)
12-13	Structural Lid (SOLID45)
100	Axial Gaps from Canister Bottom Plate to Cask Shell (CONTAC52)
200	Radial Gaps from Canister Side to Cask Shell (CONTAC52)
300	Axial Gaps from Structural Lid Top to Cask Shell (CONTAC52)
400	Axial Gaps Between Structural and Shield Lid (COMBIN40)
500	Radial Gaps Between Shield Lid and Canister Inner Surface (CONTAC40)
600	Radial Gaps Between Shield Lid and Canister Inner Radius (CONTAC52)
700	Axial Gaps Between Shield Lid and Canister Wall to Simulate Backing Ring (COMBIN40)
800	Radial Gaps Between Basket and Canister Inner Surface (CONTAC52)
1000	Intermediate Basket Thickness Real Constant
1100	End Basket Thickness Real Constant
1200	Weak Spring Real Constant

Table 2.6.14.2-2 Material Sets Defined in Canister Model

Material Property Set	Component	Material
1	Canister Shell and Structural Lid	304L Stainless Steel; ASME SA240
2	Top and Bottom End Basket Disk	304 Stainless Steel; ASME SA240
3	Shield Lid	304 Stainless Steel; ASME SA240
4	Support disk	ASME SA-533, Type B Class 2 Carbon Steel

2.6.14.3 Thermal Expansion and Thermal Stress Evaluation of Canister for BWR Fuel

A thermal stress evaluation is performed by using ANSYS to determine the differential thermal expansion and the associated thermal stresses that result from a heat load of 16 kW. In assessing the thermal stresses, the following three extreme conditions are considered:

Condition	Ambient Temperature	Solar Insolance Applied to Cask Surface	16 kW Fuel Load
1	100°F	Yes	Yes
2	-40°F	No	Yes
3	-40°F	No	No

The temperatures employed in the thermal stress analysis are obtained by applying temperatures at 36 key locations on the canister shell and ends to the thermal equivalent model of the structural canister model as thermal boundary conditions. These temperatures are taken from the thermal evaluation described in Section 3.4. The temperature distribution of the PWR canister is conservatively used in the BWR canister analyses since this produces the peak temperatures and temperature gradients. The structural finite element model is described in Section 2.6.14.2 and 2.6.12.2. The equivalent thermal model is obtained by changing the structural element SOLID45, which has three global displacements for degrees of freedom, to a SOLID70, which has temperature degrees of freedom at the individual nodes.

The temperature-dependent thermal conductivity for the canister material is employed in the thermal conduction analysis. The temperatures generated in this analysis are used in the thermal stress analysis to evaluate the properties at temperature as well as the stresses resulting from thermal expansion. Using this method, two separate cases are evaluated: a hot case (100°F ambient with solar heat load and maximum decay heat) and a cold case (-40°F ambient and maximum decay heat). Condition 3 is not evaluated because the entire assembly would be at -40°F for the conditions described.

According to the ASME Code, Section III, Subsection NB, the allowable stress criteria are based on the evaluation of linearized stresses across critical cross sections through the canister wall. For the evaluation of the thermal stresses, the criteria for the stresses are based on peak stresses. The stress values taken from the analyses are the nodal stresses at the surface. The sections used in this evaluation are shown in Figure 2.6.14.3-1. The thermal stresses reported in Tables 2.6.14.3-1 and 2.6.14.3-2 correspond to the maximum stresses for any circumferential section for the locations shown in Figure 2.6.14.3-1.

For Conditions 1 or 2, the canister is hotter than the cask body and will undergo more thermal expansion than the cask body. To conservatively determine the minimum gap between the canister and the cask body results from thermal expansion, only expansion of the canister is considered as is the case in the analysis of the PWR canister. The canister is considered to be at 380°F (the maximum shell temperature for Condition 1 is 372°F) and the cask inner shell temperature is assumed to be 70°F. These conditions are conservatively bounded by the analysis presented in Section 2.6.12.3. Section 2.6.12.3 also provides a conservative evaluation of the axial thermal growth.

Figure 2.6.14.3-1 Identification of the Sections for Evaluating the Linearized Stresses in the Canister

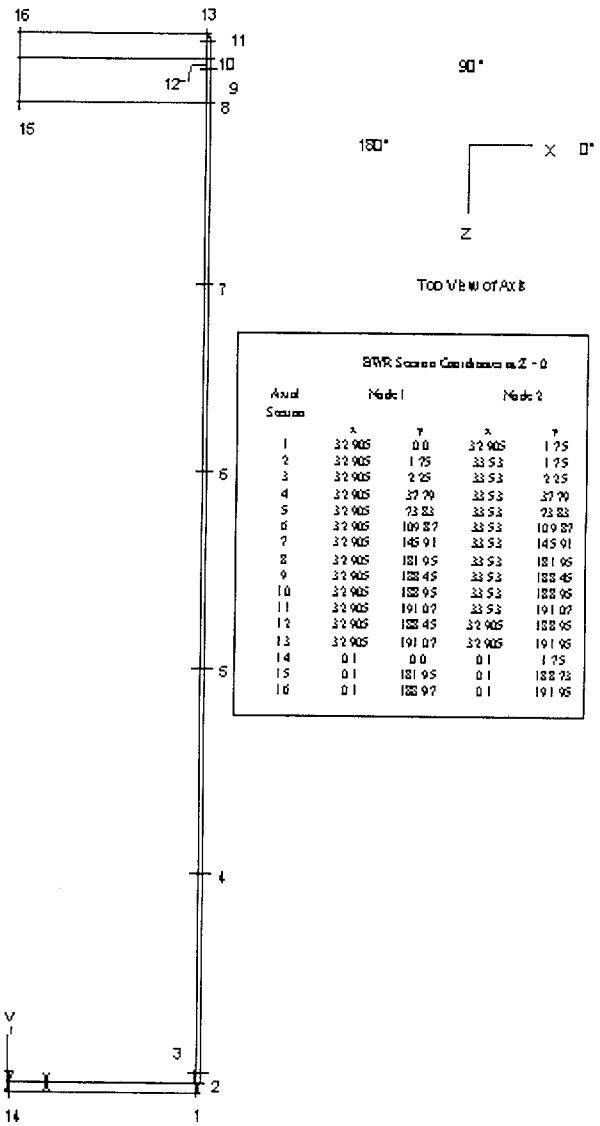

BWR Section Coordinates in Z = 0

Axial Section	Node 1 X	Node 1 Y	Node 2 X	Node 2 Y
1	32.905	0.0	32.905	1.75
2	32.905	1.75	33.53	1.75
3	32.905	2.25	33.53	2.25
4	32.905	37.79	33.53	37.79
5	32.905	73.33	33.53	73.33
6	32.905	109.87	33.53	109.87
7	32.905	145.91	33.53	145.91
8	32.905	181.95	33.53	181.95
9	32.905	188.45	33.53	188.45
10	32.905	188.95	33.53	188.95
11	32.905	191.07	33.53	191.07
12	32.905	188.45	32.905	188.95
13	32.905	191.07	32.905	191.95
14	0.1	0.0	0.1	1.75
15	0.1	181.95	0.1	188.73
16	0.1	188.97	0.1	191.95

Table 2.6.14.3-1 BWR Canister Linearized Q Stresses—Thermal Only (Hot 1)

Section Location	Angle of Peak Stress Location	Q Stresses (ksi)						Stress Intensity (ksi)	Allowable Stress (ksi)	Margin of Safety
		Sx	Sy	Sz	Sxy	Syz	Sxz			
1	180	-0.5	0	2.3	-0.1	0	-0.2	2.8	47.9	16.29
2	9	0	-0.6	1.3	0	0	0.2	1.9	47.9	23.99
3	9	0	-0.6	1.2	0	0	0.2	1.8	47.9	25.87
4	0	0	-0.2	0.1	0	0	0	0.2	47.9	193.56
5	0	0	-0.5	0.3	0	0	0	0.8	47.9	59.35
6	0	0	-0.8	0.5	0	0.1	0	1.3	47.9	36.13
7	0	0	-0.5	0.1	0	0	0	0.6	47.9	76.09
8	90	1.1	1.6	0	0	0	0	1.6	47.9	28.39
9	162	0	-1.4	-0.4	-0.1	0	0.1	1.5	47.9	30.75
10	90	0.3	1.5	-0.1	-0.2	0	0.1	1.6	47.9	28.3
11	81	-0.4	-1	0.2	-0.1	-0.1	-0.1	1.3	47.9	36.48
12	162	-0.2	0.7	0	-0.1	0.1	-0.2	1	47.9	46.99
13	81	-0.3	0.4	-0.6	0	-0.1	0	1	38.32	37.32
14	0	-9	-1.1	-8.9	0.6	0.7	0.7	8.6	47.9	4.54
15	180	0.3	0	0	-0.8	0	2	4.2	47.9	10.33
16	180	-0.2	0	0.2	-0.6	0	-1.2	2.7	47.9	16.45

* Allowable stress includes a stress reduction factor for the weld: 0.8 x allowable stress.

Table 2.6.14.3-2 BWR Canister Linearized Q Stresses—Thermal Only (Cold 2)

Section Location	Angle of Peak Stress Location	Q Stresses (ksi)						Stress Intensity (ksi)	Allowable Stress (ksi)	Margin of Safety
		Sx	Sy	Sz	Sxy	Syz	Sxz			
1	180	-0.5	0	2.5	-0.1	0	-0.2	3.1	47.9	14.55
2	45	1.3	0.5	1.3	0	0	1	2.1	47.9	21.79
3	9	0	-0.6	1.4	0	0	0.2	1.9	47.9	23.64
4	0	0	-0.2	0.1	0	0	0	0.3	47.9	159.33
5	0	0	-0.6	0.4	0	-0.1	0	0.9	47.9	49.66
6	0	0	-1	0.5	0	0.1	0	1.5	47.9	30.31
7	0	0	-0.7	0.1	0	0	0	0.8	47.9	60.83
8	90	1.2	1.8	0	0	0	0	1.8	47.9	25.66
9	162	0.1	-1.4	-0.4	-0.1	0	0.1	1.5	47.9	30.23
10	90	0.4	1.7	-0.1	-0.2	0	0.1	1.8	47.9	24.97
11	81	-0.5	-1.1	0.2	-0.1	-0.1	-0.2	1.4	47.9	32.93
12	162	-0.2	0.7	0	-0.1	0.2	-0.2	1	47.9	44.7
13	81	-0.4	0.4	-0.7	0	-0.1	0	1.1	38.32*	33.84
14	0	-10.1	-1.3	-9.9	0.6	0.8	0.7	9.5	47.9	4.04
15	180	0.3	0	-0.1	-0.7	0	1.7	3.7	47.9	11.83
16	180	-0.2	0	0.2	-0.6	0	-1.1	2.4	47.9	18.7

* Allowable stress includes a stress reduction factor for the weld: 0.8 x allowable stress.

2.6.14.4 Stress Evaluation of BWR Canister for 1-Foot End-Drop Load Condition

A structural analysis is performed using ANSYS to evaluate the effect of a 1-ft end-drop impact for both the bottom and top end orientations of the BWR canister. The ASME Code, Section III, Subsection NB requires that the stresses from operational loads be assessed on the basis of the primary loads. The primary loads for the 1-ft drop are due to the deceleration of the canister and its contents and the 25 psig pressure load internal to the canister. The applied deceleration is 20 *g* for both orientations. The inertial load of the canister is addressed by the deceleration factor applied to the canister density. The contents weight is represented by a pressure load on the inner end surface of the canister. Displacement constraints are applied to the plane of symmetry and the gap elements attached at the canister end to represent the top or bottom of the transport cask.

To determine the effect of the 25 psig pressure load, the top-end and bottom-end orientations with and without the pressure load are analyzed.

The locations of the linearized stresses are shown in Figure 2.6.14.3-1. The maximum stresses for P_m and $P_m + P_b$ are tabulated in Tables 2.6.14.4-2 through 2.6.14.4-7. Results from the end-drop analyses are presented for the cases that result in the minimum margins of safety. The critical sections for the pressure and the pressure plus the deceleration load, with reference to the section and the appropriate tables, are shown in Table 2.6.14.4-1. The margins of safety in these tables are calculated as:

$$MS = (\text{allowable stress}/SI) - 1.$$

Table 2.6.14.4-1 BWR Canister Critical Sections for the 1-Foot End-Drop Condition

Condition	Stress	Critical Section	Table	Minimum Margin of Safety
Pressure (only)	P_m	2	2.6.14.4-2	+ 4.04
Pressure (only)	$P_m + P_b$	3	2.6.14.4-3	+ 1.28
Top End-Drop Inertia	P_m	3	2.6.14.4-4	+ 4.15
Top End-Drop Inertia	$P_m + P_b$	2	2.6.14.4-5	+ 1.65
Bottom End-Drop + Pressure	P_m	4	2.6.14.4-6	+ 4.18
Bottom End-Drop + Pressure	$P_m + P_b$	2	2.6.14.4-7	+ 6.13

Table 2.6.14.4-2 BWR Canister P_m Stresses - Internal Pressure

Section Location	Angle of Peak Stress Location	P_m Stresses (ksi)						Stress Intensity (ksi)	Allowable Stress (ksi)	Margin of Safety
		Sx	Sy	Sz	Sxy	Syz	Sxz			
1	0	-0.1	2	0.7	-0.4	0	0.1	2.2	16	6.12
2	0	0.9	-1.4	-2.2	-0.4	0	-0.2	3.2	16	4.04
3	0	0.6	-0.9	-2.6	-0.2	0	-0.2	3.2	16	3.94
4	180	0	0.7	1.3	0	0	-0.1	1.3	16	10.95
5	0	0	0.7	1.3	0	0	0.1	1.3	16	11.02
6	0	0	0.7	1.3	0	0	0.1	1.3	16	11.02
7	0	0	0.7	1.3	0	0	0.1	1.3	16	11.02
8	0	0	0.7	0.7	0	0	0.1	0.7	16	22.62
9	0	0	0.5	0.3	0.1	0	0	0.5	16	33.49
10	0	-0.3	0.3	0.2	-0.1	0	0	0.6	16	25.64
11	18	0.3	-0.1	0.2	0	0	-0.1	0.4	16	38.49
12	0	-0.1	-0.4	0	-0.1	0	0	0.5	16	34.2
13	180	0	0.3	0.2	0	0	0	0.3	12.8*	41.67
14	90	0.3	0	0.3	-0.1	0.1	0	0.4	16	35.12
15	180	0	0	0	0	0	0	0	16	1809.97
16	90	0	0	0	0	0	0	0	16	378.21

* Allowable stress includes a stress reduction factor for the weld: 0.8 x allowable stress.

Table 2.6.14.4-3 BWR Canister $P_m + P_b$ Stresses - Internal Pressure

Section Location	Angle of Peak Stress Location	$P_m + P_b$ Stresses (ksi)						Stress Intensity (ksi)	Allowable Stress (ksi)	Margin of Safety
		Sx	Sy	Sz	Sxy	Syz	Sxz			
1	0	0.9	4.5	-0.5	-0.2	0	-0.1	5	24	3.77
2	0	0.8	-9.5	-4.6	-0.7	0	-0.4	10.5	24	1.28
3	0	0.7	-9.1	-5	-0.4	0	-0.4	9.8	24	1.44
4	0	0	0.7	1.3	0	0	0.1	1.4	24	16.64
5	0	0	0.7	1.3	0	0	0.1	1.4	24	16.74
6	0	0	0.7	1.3	0	0	0.1	1.3	24	16.77
7	180	0	0.7	1.3	0	0	-0.1	1.4	24	16.76
8	0	0	0.7	0.7	0	0	0.1	0.7	24	31.43
9	0	0.1	0.9	0.5	0.1	0	0	0.9	24	26.1
10	180	-0.1	1.4	0.6	0	0	-0.1	1.5	24	14.52
11	18	0.2	-0.9	-0.1	0.1	0	-0.1	1.1	24	20.14
12	135	-0.2	-0.8	-0.2	0.1	0.1	-0.1	0.7	24	34.23
13	0	-0.4	0	0	0.1	0	0	0.4	19.2*	47.00
14	90	8.1	0.1	8.1	-0.1	0.1	0	8.1	24	1.97
15	90	-0.6	0	-0.6	0	0	0	0.6	24	39.21
16	90	0.3	0	0.3	0	0	0	0.3	24	73.72

* Allowable stress includes a stress reduction factor for the weld: 0.8 x allowable stress.

Table 2.6.14.4-4 BWR Canister P_m Stresses - 1-Foot Top End-Drop

Section Location	Angle of Peak Stress Location	P_m Stresses (ksi)						Stress Intensity (ksi)	Allowable Stress (ksi)	Margin of Safety
		Sx	Sy	Sz	Sxy	Syz	Sxz			
1	0	0.1	-1.7	-0.6	0.3	0	-0.1	2	16	7.19
2	0	-0.7	1.2	2.1	0.4	0	0.2	2.9	16	4.46
3	0	-0.5	0.8	2.6	0.2	0	0.2	3.1	16	4.15
4	171	0	-0.8	0	0	0	0	0.8	16	18.84
5	36	0	-1	0	0	0	0	1	16	14.77
6	144	0	-1.2	0	0	0	0	1.2	16	12.07
7	171	0	-1.4	0	0	0	0	1.4	16	10.13
8	180	0	-1.3	0	0	0	0	1.4	16	10.52
9	135	-0.1	-1	-0.1	0	0	0.1	1	16	14.79
10	144	-0.1	-1	-0.1	0	0	0.1	0.9	16	16.12
11	135	-0.1	-0.9	-0.1	0	0	0.1	0.9	16	16.62
12*	144	0	-0.7	-0.1	0	0	0	0.8	16	19.77
13*	180	0	-0.8	-0.1	0	0	0	0.8	12.8**	15.00
14	90	-0.2	0	-0.2	0.1	-0.1	0	0.4	16	41.06
15*	144	0	-0.3	0	0	0	0	0.4	16	43.07
16*	0	0	-0.4	0	0	0	0	0.4	16	38.68

* Stresses at these locations are increased by 5% to account for the heavier BWR fuel basket/fuel assemblies.

** Allowable stress includes a stress reduction factor for the weld: 0.8 x allowable stress.

Table 2.6.14.4-5 BWR Canister $P_m + P_b$ Stresses - 1-Foot Top End-Drop

Section Location	Angle of Peak Stress Location	$P_m + P_b$ Stresses (ksi)						Stress Intensity (ksi)	Allowable Stress (ksi)	Margin of Safety
		Sx	Sy	Sz	Sxy	Syz	Sxz			
1	0	-0.7	-4	0.6	0.1	0	0.1	4.6	24	4.2
2	0	-0.7	8.2	4.2	0.6	0	0.4	9	24	1.65
3	0	-0.6	7.9	4.6	0.4	0	0.4	8.5	24	1.81
4	180	0	-0.8	0	0	0	0	0.8	24	28.6
5	153	0	-1	0	0	0	0	1	24	22.64
6	162	0	-1.2	0	0	0	0	1.2	24	18.58
7	180	0	-1.4	0	0	0	0	1.4	24	15.68
8	180	0.1	-1.3	0	-0.1	0	0	1.4	24	15.81
9	135	-0.1	-1.2	-0.1	0	0	0.1	1.1	24	20.03
10	180	0	-1.1	-0.2	0	0	0	1.1	24	20.69
11	45	-0.1	-1	-0.1	0	0	-0.1	1	24	22.71
12*	180	0.1	-0.7	-0.1	-0.1	0	0	0.8	24	28.62
13*	180	0	-0.8	-0.1	0	0	0	0.8	19.2**	23.00
14	90	-7.3	-0.1	-7.3	0.1	-0.1	0	7.2	24	2.32
15*	81	0.1	-0.3	0.1	0	0	0	0.4	24	53.27
16*	0	0	-0.4	0	0	0	0	0.4	24	57.08

* Stresses at these locations are increased by 5% to account for the heavier BWR fuel basket/fuel assemblies.

** Allowable stress includes a stress reduction factor for the weld: 0.8 x allowable stress.

Table 2.6.14.4-6 BWR Canister P_m Stresses - 1-Foot Bottom End-Drop, Internal Pressure

Section Location	Angle of Peak Stress Location	P_m Stresses (ksi)						Stress Intensity (ksi)	Allowable Stress (ksi)	Margin of Safety
		Sx	Sy	Sz	Sxy	Syz	Sxz			
1*	180	0	-0.7	-0.1	0.1	0	0	0.7	16	21.2
2	180	0.2	-1.9	-0.3	0.1	0	0	2.2	16	6.41
3	180	0.1	-2	-0.2	0.1	0	0	2.1	16	6.58
4	180	0	-1.8	1.3	0	0	-0.1	3.1	16	4.18
5	180	0	-1.6	1.3	0	0	-0.1	2.9	16	4.57
6	0	0	-1.3	1.3	0	0	0.1	2.7	16	5.01
7	180	0	-1.1	1.3	0	0	-0.1	2.5	16	5.52
8	180	0	-0.7	0.7	0	0	-0.1	1.4	16	10.31
9	72	-0.4	-0.5	-0.1	0	0.1	-0.1	0.4	16	36.29
10	180	0.4	-0.3	-0.2	-0.1	0	0	0.7	16	21.41
11	0	-0.5	0.1	-0.2	0	0	0	0.6	16	27.65
12	0	0.1	0.5	-0.1	0.1	0	0	0.5	16	28.25
13	180	0	-0.5	-0.3	0	0	0	0.4	12.8**	31.00
14*	0	0.1	-0.4	0.1	0	0	0	0.5	16	33.31
15	180	0	0	0	0	0	0	0.1	16	271.79
16	90	0	0	0	0	0	0	0	16	423.44

* Stresses at these locations are increased by 5% to account for the heavier BWR fuel basket/fuel assemblies.

** Allowable stress includes a stress reduction factor for the weld: 0.8 x allowable stress.

Table 2.6.14.4-7 BWR Canister $P_m + P_b$ Stresses - 1-Foot Bottom End-Drop, Internal Pressure

Section Location	Angle of Peak Stress Location	$P_m + P_b$ Stresses (ksi)						Stress Intensity (ksi)	Allowable Stress (ksi)	Margin of Safety
		Sx	Sy	Sz	Sxy	Syz	Sxz			
1*	180	0.1	-0.7	0	0.1	0	0	0.8	24	27.93
2	180	0.1	-3.2	-0.7	0.1	0	0.1	3.4	24	6.13
3	180	0.1	-3	-0.5	0.1	0	0	3.1	24	6.68
4	0	0	-1.8	1.3	0	0	0.1	3.1	24	6.74
5	0	0	-1.6	1.3	0	0	0.1	2.9	24	7.31
6	0	0	-1.3	1.3	0	0	0.1	2.7	24	7.97
7	0	0	-1.1	1.3	0	0	0.1	2.5	24	8.74
8	45	0.3	-0.9	0.3	0	0	0.3	1.5	24	14.93
9	72	-0.5	-1.1	-0.1	0	0.1	-0.1	1.1	24	21.24
10	90	-0.7	-1.6	0.1	0	0	0	1.8	24	12.59
11	0	-0.2	1.3	0.2	-0.1	0	0	1.5	24	14.87
12	90	0.1	0.8	0.5	0	-0.2	0	0.8	24	29.83
13	180	0.5	0	0	0.1	0	0	0.5	19.2**	37.4
14*	0	0.1	-0.4	0.1	0	0	0	0.5	24	47.50
15	90	0.8	0	0.8	0	0	0	0.8	24	28.02
16	90	-0.4	0	-0.4	0	0	0	0.4	24	59.45

* Stresses at these locations are increased by 5% to account for the heavier BWR fuel basket/fuel assemblies.

** Allowable stress includes a stress reduction factor for the weld: 0.8 x allowable stress.

2.6.14.5 Stress Evaluation of BWR Canister for Combined Thermal and 1-Foot End-Drop Load Condition

The stress evaluation of the BWR canister is performed by applying the thermal stress loads described in Section 2.6.14.3 in conjunction with the primary loads in Section 2.6.14.4 to produce a combined thermal stress plus end-impact loading. The evaluation is in accordance with the ASME Code, Section III, Subsection NB. The most critical sections are listed in Table 2.6.14.5-1. The stresses reported in this table correspond to the nodal stress at the surface. When 3 S_m is used as the stress criteria, the minimum margin of safety is +2.27. Tables 2.6.14.5-2 through 2.6.14.5-5 present the peak stresses for the hot and cold conditions for both the top and bottom end-drop cases for the loading conditions that result in the minimum margin of safety. The margins of safety are calculated as:

$$MS = (\text{allowable stress}/SI) - 1.$$

Table 2.6.14.5-1 BWR Canister Critical Sections for the Combined 1-Foot End-Drop and Thermal Load Condition

Condition	Stress	Critical Section	Table	Minimum Margin of Safety
Top-End-Drop + Thermal (cold)	$P_m + P_b + Q$	14	2.6.14.5-2	+ 2.27
Top-End-Drop + Thermal (hot)	$P_m + P_b + Q$	14	2.6.14.5-3	+ 2.42
Bottom-End-Drop + Thermal (cold)	$P_m + P_b + Q$	14	2.6.14.5-4	+ 6.04
Bottom-End-Drop + Thermal (hot)	$P_m + P_b + Q$	14	2.6.14.5-5	+ 7.85

Table 2.6.14.5-2 BWR Canister $P_m + P_b + Q$ Stresses - 1-Foot Top End-Drop, Thermal Cold

Section Location	Angle of Peak Stress Location	$P_m + P_b + Q$ Stresses (ksi)						Stress Intensity (ksi)	Allowable Stress (ksi)	Margin of Safety
		Sx	Sy	Sz	Sxy	Syz	Sxz			
1	162	-0.8	-5.1	1.6	0	0	-0.9	7.1	47.9	5.78
2	171	-0.5	10	6.5	-0.5	-0.2	-1.1	10.7	47.9	3.5
3	171	-0.3	9.2	6.6	-0.3	-0.2	-1.1	9.7	47.9	3.94
4	0	0	-1.2	0	0	0	0	1.2	47.9	39.52
5	0	0	-1.9	0.2	0	-0.1	0	2.1	47.9	21.85
6	0	0	-2.6	0.4	0	0.1	0	3	47.9	14.95
7	0	0	-2.7	-0.1	0	0	0	2.7	47.9	16.85
8	9	-0.1	-3.3	0	0	0.1	0	3.3	47.9	13.41
9	162	0.1	-3.1	-0.7	-0.1	-0.1	0.3	3.3	47.9	13.55
10	0	-0.1	-2	-0.5	0.1	0	0	1.9	47.9	23.64
11	171	0	-3.2	-0.8	0	0	0.1	3.2	47.9	13.85
12*	0	0.3	-0.9	-0.1	0.2	0	0	1.4	47.9	33.21
13*	0	0.1	-1.1	-0.2	0.1	0	0	1.3	38.32**	28.48
14	0	-15.9	-1.3	-15.1	0.1	-0.8	0	14.7	47.9	2.27
15*	90	0.1	-0.3	0.1	0	0	0	0.4	47.9	112.07
16*	0	0.1	-0.5	0.1	0	0	0	0.6	47.9	84.16

* Stresses at these locations are increased by 5% to account for the heavier BWR fuel basket/fuel assemblies.

** Allowable stress includes a stress reduction factor for the weld: 0.8 x allowable stress.

Table 2.6.14.5-3 BWR Canister $P_m + P_b + Q$ Stresses - 1-Foot Top End-Drop, Thermal Heat

Section Location	Angle of Peak Stress Location	$P_m + P_b + Q$ Stresses (ksi)						Stress Intensity (ksi)	Allowable Stress (ksi)	Margin of Safety
		Sx	Sy	Sz	Sxy	Syz	Sxz			
1	9	-1	-5.1	1.8	0	0	0.5	6.9	47.9	5.9
2	171	-0.5	9.9	6.3	-0.5	-0.2	-1.1	10.7	47.9	3.49
3	171	-0.4	9.2	6.4	-0.3	-0.1	-1.1	9.7	47.9	3.92
4	0	0	-1.1	0	0	0	0	1.1	47.9	40.91
5	0	0	-1.8	0.2	0	-0.1	0	1.9	47.9	23.6
6	0	0	-2.4	0.3	0	0.1	0	2.8	47.9	16.39
7	0	0	-2.5	0	0	0	0	2.5	47.9	18.26
8	9	-0.1	-3.1	0	0	0.1	0	3.1	47.9	14.54
9	162	0.1	-3	-0.7	-0.1	-0.1	0.3	3.2	47.9	13.92
10	162	-0.3	-2.1	-0.6	-0.2	-0.1	0.1	1.8	47.9	25
11	171	0	-2.9	-0.7	0	0	0.1	3	47.9	15.12
12*	0	0.3	-0.9	-0.1	0.2	0	0	1.3	47.9	35.24
13*	0	0.1	-1	-0.1	0	0	0	1.2	38.32**	30.93
14	0	-15.1	-1.1	-14.4	0.1	-0.7	0	14	47.9	2.42
15*	90	0.1	-0.3	0.1	0	0	0	0.4	47.9	112.18
16*	0	0.1	-0.5	0.1	0	0	0	0.5	47.9	86.30

* Stresses at these locations are increased by 5% to account for the heavier BWR fuel basket/fuel assemblies.

** Allowable stress includes a stress reduction factor for the weld: 0.8 x allowable stress.

Table 2.6.14.5-4 BWR Canister $P_m + P_b + Q$ Stresses - 1-Foot Bottom End-Drop, Thermal Cold

Section Location	Angle of Peak Stress Location	$P_m + P_b + Q$ Stresses (ksi)						Stress Intensity (ksi)	Allowable Stress (ksi)	Margin of Safety
		Sx	Sy	Sz	Sxy	Syz	Sxz			
1*	162	0.3	-2.1	1.3	0.2	0	-0.4	3.8	47.9	11.61
2	9	0	-3.5	1.1	-0.1	0.1	0.2	4.6	47.9	9.48
3	9	0	-3.5	1	0	0.1	0.1	4.5	47.9	9.69
4	0	0	-3.1	0	0	0	0	3.1	47.9	14.61
5	0	0	-3.1	0.3	0	-0.1	0	3.4	47.9	13.21
6	0	0	-3.2	0.5	0	0.1	0	3.7	47.9	12.02
7	0	0	-2.6	0	0	0	0	2.7	47.9	17.02
8	9	-0.1	-2.6	0	0	0.2	0	2.6	47.9	17.59
9	162	-0.2	-3.3	-1.3	0.1	0.1	0.4	3.3	47.9	13.64
10	0	0.4	-4	-1.5	0	0.1	-0.1	4.4	47.9	9.98
11	0	-0.5	2.8	0.7	-0.1	0.1	0.1	3.3	47.9	13.37
12	18	1.2	1.7	0.4	0.5	0.1	-0.1	1.6	47.9	28.13
13	0	-1.4	-2.1	-1	0.3	0	0	1.2	38.32**	30.93
14*	0	-10.8	-4.4	-10	0	0.2	0	6.7	47.9	6.15
15	72	1.7	0	1.4	0	0	0	1.7	47.9	27.57
16	81	-0.7	0	-0.6	0	0	0	0.7	47.9	67.25

* Stresses at these locations are increased by 5% to account for the heavier BWR fuel basket/fuel assemblies.

** Allowable stress includes a stress reduction factor for the weld: 0.8 x allowable stress.

Table 2.6.14.5-5 BWR Canister $P_m + P_b + Q$ Stresses - 1-Foot Bottom End-Drop, Thermal Heat

Section Location	Angle of Peak Stress Location	$P_m + P_b + Q$ Stresses (ksi)						Stress Intensity (ksi)	Allowable Stress (ksi)	Margin of Safety
		Sx	Sy	Sz	Sxy	Syz	Sxz			
1*	162	0.3	-2	1.2	0.2	0	-0.4	3.5	47.9	12.69
2	9	0	-3.5	0.9	-0.1	0.1	0.1	4.4	47.9	9.89
3	9	0	-3.5	0.8	0	0.1	0.1	4.3	47.9	10.12
4	0	0	-3	0	0	0	0	3	47.9	15.16
5	0	0	-3	0.2	0	-0.1	0	3.2	47.9	13.91
6	0	0	-3	0.4	0	0.1	0	3.5	47.9	12.89
7	0	0	-2.5	0	0	0	0	2.5	47.9	17.93
8	9	-0.1	-2.4	0	0	0.2	0	2.4	47.9	18.79
9	162	-0.2	-3.2	-1.3	0.1	0.1	0.4	3.1	47.9	14.42
10	162	0.1	-3.8	-1.4	-0.1	0.1	0.5	4.1	47.9	10.79
11	9	-0.5	2.6	0.6	-0.1	0.1	0.2	3.2	47.9	14.15
12	162	0.7	1.9	0.2	-0.4	0	0.1	1.8	47.9	25.33
13	0	1	-0.2	0.2	-0.1	0	-0.1	1.2	38.32**	30.93
14*	0	-9.7	-3.9	-9	0	0.2	0	6.1	47.9	6.87
15	81	1.7	0	1.4	0	0	0	1.7	47.9	28.04
16	72	-0.8	-0.1	-0.6	0	0	0	0.7	47.9	67.46

* Stresses at these locations are increased by 5% to account for the heavier BWR fuel basket/fuel assemblies.

** Allowable stress includes a stress reduction factor for the weld: 0.8 x allowable stress.

2.6.14.6 Stress Evaluation of the BWR Canister for 1-Foot Side-Drop Load Condition

ANSYS is used to determine the stresses in the BWR canister resulting from a 1-ft side-drop. The finite element model of the BWR canister is similar to the model for the PWR canister. A detailed description of the PWR canister model is provided in Section 2.6.12.2.

The load resulting from the contents is applied to the basket by means of pressure acting in the plane of the disks. The weight is assumed to act over the effective width of 6.428 in. (for 33 support disks) in which each disk is 0.75 in. thick. This weight is distributed over the 33 support disks plus two end weldments. A deceleration factor of 20 *g* is applied to the weights to provide the loading for the basket assembly. In addition to the contents load, a 25 psig pressure is applied to the inner surface of the canister. The canister is analyzed for basket orientations of 0° and 45°. As discussed in Section 2.6.14.2, the actual design uses 40 support disks of 0.625 in. thickness. The impact of these differences are also discussed in Section 2.6.14.2.

The methodology used to evaluate the stresses for the side-drop are identical to that used for the PWR side-drop (Section 2.6.12.6). Sections 9, 10, and 11 at the 0° circumferential position (see Figure 2.6.12.3-1) are not included in the evaluation. These regions are characterized as a bearing stress since they result from the canister shell bearing against cask inner shell. Section 2.6.14.11 provides an assessment of the bearing stresses. Sections 9, 10, and 11 at all other angular locations are included in the evaluation. Also, Sections 12 and 13 at 0° are treated as local membrane stresses. According to the ASME Code, Section III, Subsection NB-3213.10, a stressed region may be considered local if the distance over which the membrane stress intensity exceeds 1.1 S_m does not extend more than 1.0 times the square root of RT in the meridional direction, where R is the minimum midsurface radius of curvature and T is the minimum thickness in the region considered. For Section 13, the minimum thickness is that of the canister shell (0.625 in.) and the midsurface radius of the shell is 33.2175 in. The resulting distance is 4.56 in. A section located 4.56 in. from Section 13 in the meridional direction results in a membrane stress intensity of 6.44 ksi, which is below S_m. This section conservatively encompasses Section 12 since it is located 1.56 in. from this section. The stresses at adjacent circumferential sections (i.e., at 9°) for Sections 12 and 13 are also included in the tables for comparison. The critical sections stresses are reported in Table 2.6.14.6-1 for the P_m and $P_m + P_b$ stresses.

Results are calculated for 1-ft side-drop with internal pressure for both the 0° and 45° basket orientations. Tables 2.6.14.6-2 and 2.6.14.6-3 present the worst-case margins of safety for the side-drop with the conditions noted. The minimum margin of safety occurs for primary membrane without pressure and with pressure for primary membrane plus primary bending. The minimum margin of safety for the BWR canister for the side-drop is +0.02, which occurs at Section 12 in Figure 2.6.14.3-1. The margins of safety are calculated as:

MS = (allowable stress/SI) -1.

Table 2.6.14.6-1 BWR Canister Critical Sections for the 1-Foot Side-Drop Load Condition

Condition	Stress	Critical Section	Table	Minimum Margin of Safety
Side-Drop	P_m	1	2.6.14.6-2	+ 0.11
Side-Drop + Pressure	$P_m + P_b$	12	2.6.14.6-3	+ 0.02

Table 2.6.14.6-2 BWR Canister P_m Stresses - 1-Foot Side-Drop

Section Location	Angle of Peak Stress Location	P_m Stresses (ksi)						Stress Intensity (ksi)	Allowable Stress (ksi)	Margin of Safety
		Sx	Sy	Sz	Sxy	Syz	Sxz			
1	0	-13.3	0.1	-4.2	-0.3	-0.1	-2	13.8	16	0.16
2	0	-8.5	-0.3	-4.6	-0.4	-0.3	-1.4	8.7	16	0.83
3**	0	-6.1	-0.3	-3.6	-0.3	-0.3	-1.3	6.75	16	1.37
4**	0	-2.3	-0.5	0.2	0	0	0.1	2.65	16	5.05
5**	0	-2.3	0.1	0.2	0	0	0.1	2.65	16	5.03
6**	0	-2.4	0.3	0.2	0	-0.1	0.1	2.88	16	4.56
7**	0	-2.4	0.3	0.1	0	-0.1	0.1	2.96	16	4.40
8**	0	-0.8	2.1	-1.1	-0.2	0.5	-0.1	3.56	16	3.50
9	9	-0.24	2.56	-1.99	0.05	1.35	-1.06	5.73	16	1.8
10	9	1.45	1.67	-2.09	-0.3	0.99	-0.65	4.6	16	2.48
11	9	4.17	1.8	-1.1	0.7	1.2	-1.7	6.75	16	1.37
12*	0	-24.3	-5.4	-6.6	-4.5	1.2	-1	21.6	24	0.11
12	9	-0.42	-0.18	-3.42	0.15	0.55	-1.9	4.97	16	2.22
13†	0-7.4	-11.61	-3.40	-4.00	0.05	1.10	-2.23	9.96	12.8***	0.29
14	0	-0.8	0	0.3	0	0	0	1.1	16	13.12
15	0	-0.3	0	0.1	0	0	0	0.4	16	35.05
16	0	-0.5	0	0.1	0	0	0	0.6	16	24.17

* Treated as a local membrane stress . Allowable for normal conditions is 1.5 S_m = 24 ksi for P_L and P_L+P_B.

** Stresses at these locations are increased by 5% to account for the heavier BWR fuel basket/fuel assemblies.

*** Allowable stress includes a stress reduction factor for the weld: 0.8 x allowable stress.

† Stress evaluated over weld compression region.

Table 2.6.14.6-3 BWR Canister $P_m + P_b$ Stresses - 1-Foot Side-Drop, Internal Pressure

Section Location	Angle of Peak Stress Location	$P_m + P_b$ Stresses (ksi)						Stress Intensity (ksi)	Allowable Stress (ksi)	Margin of Safety
		Sx	Sy	Sz	Sxy	Syz	Sxz			
1	0	-17.1	-0.9	-5.3	0.2	-0.1	-2	16.5	24	0.46
2	0	-8	0.8	-2.5	-0.6	-0.3	-1.7	9.4	24	1.55
3**	0	-5.8	0.9	-1.5	-0.4	-0.3	-1.5	7.7	24	2.12
4**	0	-2.4	1	3.3	0	0	0.4	6.1	24	2.93
5**	0	-2.4	1.6	3.6	0	-0.1	0.4	6.4	24	2.75
6**	0	-2.5	1.8	3.7	0	-0.1	0.4	6.6	24	2.64
7**	0	-2.5	1.7	3.7	0	-0.1	0.4	6.5	24	2.69
8**	0	-0.6	2.5	-2.4	-0.2	0.4	-0.2	5.2	24	3.61
9	9	1.1	6.4	-0.3	-0.08	1.6	0.1	7.44	24	2.22
10	0	-18.9	-2.1	-4.5	-5.3	1	-1.1	20.3	24	0.18
11	9	4.3	0.9	-1.4	0.8	1.3	2.7	8.4	24	1.86
12†	0	-28.6	-6.6	-8.2	-4.3	1.6	-0.7	24.5	25	0.02
13†*	0-7.8	-16.57	-6.23	-6.42	-0.09	1.68	-2	12.49	20***	0.60
14	0	-0.7	0	0.3	0	0	0	1.1	24	21.32
15	90	-0.7	0	-0.1	0	0	0	0.7	24	34.37
16	0	-0.6	0	0.1	0	0	0	0.7	24	34.67

† The peak temperature as calculated in Section 3.4 is 265°F in the region of Sections 12 and 13. The allowable stress is 1.5 (16.7 ksi) = 25.05 ksi based on this temperature.

* Stress evaluated over weld compression region.

** Stresses at these locations are increased by 5% to account for the heavier BWR fuel basket/fuel assemblies.

*** Allowable stress includes a stress reduction factor for the weld: 0.8 x allowable stress.

2.6.14.7 Stress Evaluation of BWR Canister for Combined Thermal and 1-Foot Side-Drop Load Conditions

The BWR canister is evaluated by applying the thermal stress loads described in Section 2.6.14.3 in conjunction with the primary loads in Section 2.6.14.6 to produce a combined thermal stress plus 1-ft side-drop loading. The stress evaluation is performed according to the ASME Code, Section III, Subsection NB. The most critical sections are listed in Table 2.6.14.7-1. The stresses reported in this table correspond to the nodal stress at the surface. Results from the side-drop plus thermal load cases for the configurations that result in the minimum margins of safety are presented in Tables 2.6.14.7-2 and 2.6.14.7-3. The minimum margin of safety is +0.42 at Section 9 (see Figure 2.6.14.3-1) when 3 S_m is used as the stress criterion. The margins of safety are calculated as:

$$MS = (\text{allowable stress}/SI) - 1.$$

Table 2.6.14.7-1 BWR Canister Critical Sections for the Combined 1-Foot Side-Drop and Thermal Load Condition

Condition	Stress	Critical Section	Table	Minimum Margin of Safety
Side-Drop + Thermal (cold)	P + Q	9	2.6.14.7-2	+ 0.42
Side-Drop + Thermal (hot)	P + Q	9	2.6.14.7-3	+ 0.60

Table 2.6.14.7-2 BWR Canister $P_m + P_b + Q$ - 1-Foot Side-Drop, Thermal Cold

Section Location	Angle of Peak Stress Location	$P_m + P_b + Q$ Stresses (ksi)						Stress Intensity (ksi)	Allowable Stress (ksi)	Margin of Safety
		Sx	Sy	Sz	Sxy	Syz	Sxz			
1	0	-16.4	-1.3	-3	0.3	0	-1.7	15.4	47.9	2.12
2	0	-6.4	1.5	-0.4	0	-0.2	-1.6	8.3	47.9	4.77
3**	0	-4.6	1.6	0.2	-0.1	-0.1	-1.3	6.8	47.9	6.04
4**	0	-2.4	0.8	2.1	0	-0.1	0.3	4.7	47.9	9.19
5**	0	-2.1	-0.4	2.4	0	-0.3	0.4	4.8	47.9	8.98
6**	0	-1.9	-1.4	2.1	0	0.2	0.4	4.4	47.9	9.89
7**	0	-2.3	0.3	2.2	0	-0.1	0.3	4.8	47.9	8.98
8**	0	-0.3	2.2	-1.7	-0.2	0.6	-0.1	4.3	47.9	10.1
9	0	-26.6	6.7	-9	-2.1	1.7	0.1	33.7	47.9	0.42
10	0	-18.8	-2.8	-5	-4.5	0.9	-1.1	18.8	47.9	1.54
11	0	-26.3	3	-8.8	-0.3	1.8	-0.1	29.6	47.9	0.62
12	0	-26.3	-4.9	-7.9	-3.7	1.7	-0.7	23.4	47.9	1.05
13	0	-32.4	-9.9	-10.6	-1.2	1.9	-1.4	24.4	38.32*	0.57
14	0	-11.2	-3.3	-9.4	0	0	0	7.9	47.9	5.07
15	9	-0.7	0	-0.3	0	0	0	0.7	47.9	72.63
16	0	-0.6	0	0	0	0	0	0.7	47.9	69.59

* Allowable stress includes a stress reduction factor for the weld: 0.8 x allowable stress.

** Stresses at these locations are increased by 5% to account for the heavier BWR fuel basket/fuel assemblies.

Table 2.6.14.7-3 BWR Canister $P_m + P_b + Q$ Stresses - 1-Foot Side-Drop, Thermal Heat

Section Location	Angle of Peak Stress Location	$P_m + P_b + Q$ Stresses (ksi)						Stress Intensity (ksi)	Allowable Stress (ksi)	Margin of Safety
		Sx	Sy	Sz	Sxy	Syz	Sxz			
1	0	-14.5	-0.3	-3	0.2	0	-1.5	14.3	47.9	2.35
2	0	-6	0.9	-0.6	-0.3	-0.1	-1.4	7.3	47.9	5.59
3**	0	-4.3	1	0	-0.3	-0.1	-1.2	5.9	47.9	7.12
4**	0	-2.3	0.2	1.5	0	0	0.3	4.1	47.9	10.68
5**	0	-2.1	-0.5	2.1	0	-0.2	0.4	4.4	47.9	9.89
6**	0	-2	-1.3	1.7	0	0.2	0.4	4.0	47.9	10.98
7**	0	-2.2	0.3	1.9	0	-0.1	0.3	4.3	47.9	10.14
8**	0	-0.3	2.2	-1.4	-0.1	0.5	-0.1	4.0	47.9	10.98
9	0	-23.4	6.3	-8.3	-1.9	1.5	0.3	30	47.9	0.6
10	0	-16.6	-2.2	-4.9	-3.9	0.8	-0.8	16.6	47.9	1.88
11	0	-22.8	2.8	-7.9	-0.2	1.5	0	25.9	47.9	0.85
12	0	-23.4	-4.2	-7.4	-3.2	1.5	-0.4	20.7	47.9	1.31
13	0	-28.2	-8.6	-9.7	-1	1.6	-1.1	21	38.32*	0.82
14	0	-9.7	-2.5	-8	0.1	-0.2	0	7.2	47.9	5.63
15	27	-0.6	0	-0.3	0	0	0	0.6	47.9	75.57
16	0	-0.6	0	0.1	0	0	0	0.7	47.9	65.48

* Allowable stress includes a stress reduction factor for the weld: 0.8 x allowable stress.

** Stresses at these locations are increased by 5% to account for the heavier BWR fuel basket/fuel assemblies.

2.6.14.8 Stress Evaluation of BWR Canister for 1-Foot Corner-Drop Load Condition

ANSYS is used to perform a structural analysis to evaluate the effect of a 1-ft end-drop impact for both the top and bottom corner orientations of the BWR canister. The ASME Code, Section III, Subsection NB requires that the stresses arising from operational loads be assessed on the basis of the primary loads. The primary loads for the 1-ft corner-drop result from the deceleration of the BWR canister and its contents and the 25-psig pressure load internal to the canister. The applied deceleration is 20 *g* for both orientations. The inertial load of the canister is addressed by the deceleration factor applied to the canister density. The contents weight is represented by a pressure load on the inner end surface of the canister and a pressure applied to the basket by means of pressure acting in the plane of the disks. Displacement constraints are applied to the plane of symmetry and the gap elements attached at the canister end to represent the top or bottom of the transport cask.

The locations of the linearized stresses are shown in Figure 2.6.14.3-1. The maximum stresses for P_m and $P_m + P_b$ are presented in Tables 2.6.14.8-2 through 2.6.14.8-5 for the conditions that result in the worst case stresses. The critical sections for the pressure and the pressure plus the deceleration load, with reference to the section and the appropriate tables, are shown in Table 2.6.14.8-1. The margins of safety in these tables are calculated as:

$$MS = (\text{allowable stress}/SI) - 1.$$

Table 2.6.14.8-1 BWR Canister Critical Sections for the 1-Foot Corner-Drop Load Condition

Condition	Stress	Critical Section	Table	Minimum Margin of Safety
Top Corner-Drop + Pressure	P_m	9	2.6.14.8-2	+ 0.18
Top Corner-Drop Inertia	$P_m + P_b$	9	2.6.14.8-3	+ 0.52
Bottom Corner-Drop + Pressure	P_m	11	2.6.14.8-4	+ 0.12
Bottom Corner-Drop +Inertia	$P_m + P_b$	11	2.6.14.8-5	+0.41

Table 2.6.14.8-2 BWR Canister P_m Stresses - 1-Foot Top Corner-Drop, Internal Pressure

Section Location	Angle of Peak Stress Location	P_m Stresses (ksi)						Stress Intensity (ksi)	Allowable Stress (ksi)	Margin of Safety
		Sx	Sy	Sz	Sxy	Syz	Sxz			
1	0	-4.5	0.1	-1.2	0.3	-0.1	-0.6	4.8	16	2.32
2	0	-0.9	0.4	-0.9	0	-0.2	-0.3	1.7	16	8.54
3**	0	-0.6	0.4	-0.7	0	-0.2	-0.2	1.4	16	10.37
4**	0	-0.9	-0.3	1.4	0	0	0.2	2.4	16	5.66
5**	0	-0.9	-0.3	1.4	0	0	0.2	2.4	16	5.70
6**	0	-0.9	-0.5	1.4	0	0	0.2	2.4	16	5.68
7**	0	-0.9	-0.9	1.4	0	-0.1	0.2	2.4	16	5.65
8**	54	0.5	-1.1	0.2	-0.3	-0.2	0.3	2.0	16	7.04
9	0	-14.8	-1.8	-4	-1.6	0.5	-0.4	13.6	16	0.18
10	0	-10.2	-4	-3	-1.7	0.2	-0.7	8	16	1
11	0	-13.9	-6.1	-4.9	-0.6	0.4	-0.4	9.2	16	0.74
12**	0	-12.9	-5.7	-2.9	-2.7	0.2	-1	11.7	16	0.37
13**	0	-12.2	-7.3	-3.7	-0.7	0.2	-1	9.3	12.8*	0.38
14	0	-0.2	0	0.2	0	0	0	0.4	16	44.29
15**	0	-0.1	-0.3	0	0	0	0	0.4	16	38.74
16**	0	-0.2	-0.4	0.1	0	0	0	0.5	16	32.99

* Allowable stress includes a stress reduction factor for the weld: 0.8 x allowable stress.

** Stresses at these locations are increased by 5% to account for the heavier BWR fuel basket/fuel assemblies.

Table 2.6.14.8-3 BWR Canister $P_m + P_b$ Stresses - 1-Foot Top Corner Drop

Section Location	Angle of Peak Stress Location	$P_m + P_b$ Stresses (ksi)						Stress Intensity (ksi)	Allowable Stress (ksi)	Margin of Safety
		Sx	Sy	Sz	Sxy	Syz	Sxz			
1	0	-9.2	-4.4	-2.2	-1.9	-0.1	-0.6	7.8	24	2.06
2	0	-8.9	4.9	-1.1	0.9	0.8	0.2	14	24	0.72
3**	0	-6.9	3.6	-0.6	0.5	0.7	-0.2	11.1	24	1.16
4**	0	-0.9	-0.7	0.5	0	0	0.1	1.5	24	15.00
5**	0	-0.9	-0.7	0.7	0	0	0.1	1.7	24	13.12
6**	0	-0.9	-0.9	0.7	0	0	0.1	1.8	24	12.33
7**	0	-0.9	-1.3	0.8	0	-0.1	0.1	2.2	24	9.91
8**	54	0.1	-1.4	0.1	-0.3	-0.3	0	1.8	24	12.27
9	0	-15.3	0.2	-4.7	-1.2	0.5	-0.2	15.8	24	0.52
10	0	-10.8	-5.2	-2.6	-3.1	0.1	-1	9.9	24	1.42
11	0	-15.5	-8.1	-5	-1.1	0.5	-0.7	10.8	24	1.23
12**	0	-13.9	-5.5	-3.3	-2.2	0.4	-0.8	12.1	24	0.98
13**	0	-14.2	-9.3	-4.8	-1.2	0.4	-0.9	10.4	19.2*	0.85
14	90	-6.9	-0.1	-6.4	0.1	-0.1	0	6.8	24	2.52
15**	90	0	-0.3	0.1	0	0	0	0.5	24	51.78
16**	0	-0.2	-0.3	0.1	0	0	0	0.5	24	51.61

* Allowable stress includes a stress reduction factor for the weld: 0.8 x allowable stress.

** Stresses at these locations are increased by 5% to account for the heavier BWR fuel basket/fuel assemblies.

Table 2.6.14.8-4 BWR Canister P_m Stresses - 1-Foot Bottom Corner-Drop, Internal Pressure

Section Location	Angle of Peak Stress Location	P_m Stresses (ksi)						Stress Intensity (ksi)	Allowable Stress (ksi)	Margin of Safety
		Sx	Sy	Sz	Sxy	Syz	Sxz			
1**	0	-5.1	-0.8	-1.5	-0.1	0	-0.7	4.7	16	2.40
2	36	0	-2.4	-0.3	-0.1	0.1	-0.5	2.8	16	4.77
3**	36	0	-2.4	-0.3	0	0.1	-0.4	2.8	16	4.71
4**	0	-0.9	-2	1.3	0	0	0.2	3.6	16	3.44
5**	0	-0.9	-1.6	1.4	0	0	0.2	3.2	16	4.00
6**	180	0	-1.6	1.2	0	0	-0.1	2.9	16	4.52
7**	180	0	-1.3	1.2	0	0	-0.1	2.7	16	4.88
8**	63	0.5	-0.7	0.2	-0.2	-0.1	0.3	1.6	16	9.02
9	0	-13.4	0.4	-3.7	-1.3	0.8	-0.3	14.2	16	0.12
10	0	-7.3	-0.4	-2.1	-1.2	0.6	-0.6	7.6	16	1.09
11	0	-14.6	-0.9	-4.3	-0.2	1	-0.3	14	16	0.15
12	0	-10.7	-2.5	-2.4	-1.9	0.6	-0.8	9.7	16	0.65
13	0	-10.2	-2.7	-2.6	0	0.7	-1	8.4	12.8*	0.52
14**	0	-0.3	-0.4	0.2	0	0	0	0.6	16	27.64
15	0	-0.1	0	0.1	0	0	0	0.1	16	111.46
16	90	-0.2	0	0	0	0	0	0.3	16	61.79

* Allowable stress includes a stress reduction factor for the weld: 0.8 x allowable stress.

** Stresses at these locations are increased by 5% to account for the heavier BWR fuel basket/fuel assemblies.

Table 2.6.14.8-5 BWR Canister $P_m + P_b$ Stresses - 1-Foot Bottom Corner-Drop

Section Location	Angle of Peak Stress Location	$P_m + P_b$ Stresses (ksi)						Stress Intensity (ksi)	Allowable Stress (ksi)	Margin of Safety
		Sx	Sy	Sz	Sxy	Syz	Sxz			
1**	0	-6.3	-0.8	-2	0.2	0	-0.8	6.0	24	3.00
2	27	-0.2	-4.2	-1.2	-0.1	-0.1	-0.6	4.3	24	4.57
3**	27	-0.2	-4	-1.1	-0.1	-0.1	-0.5	4.4	24	4.45
4**	0	-0.9	-2.4	0.8	0	0	0.1	3.5	24	5.86
5**	0	-0.9	-2	0.8	0	0	0.1	2.9	24	7.28
6**	0	-0.9	-1.7	0.9	0	0	0.1	2.6	24	8.23
7**	0	-0.9	-1.4	0.9	0	-0.1	0.1	2.4	24	9.00
8**	18	0.3	-1.1	-0.6	0.3	0.5	-0.2	1.9	24	11.63
9	0	-13.5	2.5	-4.4	-1	0.8	-0.1	16.2	24	0.48
10	0	-6.9	-0.7	-1.3	-2	0.5	-0.8	7.8	24	2.07
11	0	-14.2	2.6	-4	-0.1	0.9	0	17	24	0.41
12	0	-12.9	-3.3	-3.5	-1.6	0.7	-0.6	10.8	24	1.22
13	0	-16.1	-6.1	-5.3	-0.2	1	-0.8	11.6	19.2*	0.66
14**	0	-0.3	-0.3	0.1	0	0	0	0.5	24	47.00
15	45	1.3	0	1.5	0	0	0	1.5	24	15.49
16	9	-0.9	0	-0.7	0	0	0	0.9	24	26.14

* Allowable stress includes a stress reduction factor for the weld: 0.8 x allowable stress.

** Stresses at these locations are increased by 5% to account for the heavier BWR fuel basket/fuel assemblies.

2.6.14.9 Stress Evaluation of BWR Canister for Combined Thermal and 1-Foot Corner-Drop Load Conditions

The thermal stress loads described in Section 2.6.14.3 are applied in conjunction with the primary loads in Section 2.6.14.8 to produce a combined thermal stress plus corner impact loading. The stress evaluation is performed according to the ASME Code, Section III, Subsection NB. On the basis of results in Section 2.6.14.8, the most critical sections are listed in Table 2.6.14.9-1. The stresses reported in this table correspond to the nodal stress at the surface. The minimum margin of safety is +1.57 when 3 S_m is used as the stress criterion. Tables 2.6.14.9-2 through 2.6.14.9-5 present the results for top and bottom corner-drop with thermal results for the loading conditions that result in the minimum margins of safety. The margins of safety are calculated as:

MS = (allowable stress/SI) -1.

Table 2.6.14.9-1 BWR Canister Critical Sections for the Combined 1-Foot Corner-Drop and Thermal Load Condition

Condition	**Stress**	**Critical Section**	**Table No.**	**Minimum Margin of Safety**
Top Corner-Drop + Thermal (cold)	$P_m + P_b + Q$	2	2.6.14.9-2	+ 2.02
Top Corner-Drop + Thermal (hot)	$P_m + P_b + Q$	2	2.6.14.9-3	+ 2.05
Bottom Corner-Drop + Pressure + Thermal (cold), 45° Basket	$P_m + P_b + Q$	9	2.6.14.9-4	+ 1.54
Bottom Corner-Drop + Thermal (hot)	$P_m + P_b + Q$	11	2.6.14.9-5	+1.62

Table 2.6.14.9-2 BWR Canister $P_m + P_b + Q$ Stresses - 1-Foot Top Corner-Drop, Thermal Cold

Section Location	Angle of Peak Stress Location	$P_m + P_b + Q$ Stresses (ksi)						Stress Intensity (ksi)	Allowable Stress (ksi)	Margin of Safety
		Sx	Sy	Sz	Sxy	Syz	Sxz			
1	0	-14.1	-4.7	-2	-2.5	0	-1.1	12.8	47.9	2.73
2	0	-14.3	1.3	-2.4	-0.1	1	-0.5	15.9	47.9	2.02
3**	0	-10.7	0.6	-1.4	-0.3	0.8	-0.7	12.4	47.9	2.86
4**	0	-0.9	-0.7	1.1	0	-0.1	0.1	2.1	47.9	21.81
5**	0	-0.8	-1.4	2.8	0	-0.2	0.4	4.4	47.9	9.89
6**	0	-0.6	-2.3	2.2	0	0.3	0.1	4.8	47.9	8.98
7**	180	0	-2.9	0	0	0	0	3.1	47.9	14.45
8**	171	-0.1	-3.6	-0.2	0	0.2	0	3.7	47.9	11.95
9	0	-12.6	0.1	-3.8	-1.1	0.5	-0.2	13	47.9	2.68
10	0	-10	-4.8	-2.4	-2.6	0.1	-1	9	47.9	4.35
11	0	-12	-7	-4	-1	0.4	-0.6	8.3	47.9	4.77
12**	0	-11.7	-4.2	-2.7	-2	0.4	-0.7	10.3	47.9	3.65
13**	0	-12	-7	-4	-1	0.4	-0.6	8.7	38.32*	3.40
14	0	-15.6	-1.2	-14.1	0.1	-0.8	0	14.4	47.9	2.34
15**	72	-0.1	-0.3	0.1	0	0	0	0.4	47.9	110.66
16**	0	-0.1	-0.4	0.1	0	0	0	0.6	47.9	80.29

* Allowable stress includes a stress reduction factor for the weld: 0.8 x allowable stress.

** Stresses at these locations are increased by 5% to account for the heavier BWR fuel basket/fuel assemblies.

Table 2.6.14.9-3 BWR Canister $P_m + P_b + Q$ - 1-Foot Top Corner-Drop, Thermal Heat

		$P_m + P_b + Q$ Stresses (ksi)								
Section Location	**Angle of Peak Stress Location**	**Sx**	**Sy**	**Sz**	**Sxy**	**Syz**	**Sxz**	**Stress Intensity (ksi)**	**Allowable Stress (ksi)**	**Margin of Safety**
1	0	-13.7	-4.6	-2.1	-2.4	0	-1.1	12.4	47.9	2.88
2	0	-13.9	1.6	-2.3	-0.2	0.9	-0.6	15.7	47.9	2.05
3**	0	-10.4	0.9	-1.3	-0.4	0.7	-0.7	12.2	47.9	2.93
4**	0	-0.8	-0.8	0.8	0	0	0.1	1.8	47.9	25.61
5**	0	-0.9	-1.5	2	0	-0.2	0.1	3.6	47.9	12.31
6**	0	-0.7	-2.1	1.8	0	0.2	0.2	4.2	47.9	10.40
7**	180	0	-3	0	0	0	0	3.2	47.9	13.97
8**	171	-0.1	-3.6	-0.2	0	0.2	0	3.7	47.9	11.95
9	0	-12.1	0.4	-3.5	-1	0.5	-0.2	12.7	47.9	2.78
10	0	-9.5	-4.5	-2.2	-2.5	0.1	-0.9	8.6	47.9	4.59
11	0	-11.4	-6.5	-3.7	-0.9	0.4	-0.6	8	47.9	5.03
12**	0	-11.1	-3.9	-2.6	-1.9	0.4	-0.7	9.9	47.9	3.84
13**	0	-11.4	-6.5	-3.7	-0.9	0.4	-0.6	8.4	38.32*	3.56
14	0	-14.8	-1.1	-13.5	0.1	-0.7	0	14.4	47.9	2.50
15**	90	0	-0.3	0.1	0	0	0	0.4	47.9	111.90
16**	0	-0.1	-0.4	0.1	0	0	0	0.5	47.9	82.69

* Allowable stress includes a stress reduction factor for the weld: 0.8 x allowable stress.

** Stresses at these locations are increased by 5% to account for the heavier BWR fuel basket/fuel assemblies.

Table 2.6.14.9-4 BWR Canister $P_m + P_b + Q$ Stresses - 1 Foot Bottom Corner-Drop, Internal Pressure, Thermal Cold

Section Location	Angle of Peak Stress Location	$P_m + P_b + Q$ Stresses (ksi)						Stress Intensity (ksi)	Allowable Stress (ksi)	Margin of Safety
		Sx	Sy	Sz	Sxy	Syz	Sxz			
1**	0	-2	0.1	1.7	0.2	0	-0.2	4.0	47.9	10.98
2	162	0.1	-4.5	0.8	0	0	-0.3	5.4	47.9	7.93
3**	162	0.1	-4.4	0.8	0	0	-0.3	5.6	47.9	7.55
4**	180	0	-3.7	1.3	0	0	-0.1	5.3	47.9	8.04
5**	0	-0.6	-1.4	3.9	0	-0.3	0.2	5.6	47.9	7.55
6**	0	-0.7	-2.4	3.4	0	0.2	0.1	6.2	47.9	6.73
7**	0	-1	-0.6	3.5	0	-0.1	0.3	4.7	47.9	9.19
8**	0	-0.6	0.6	2	-0.1	0.6	0.3	3.0	47.9	14.97
9	0	-15.6	2.7	-4.9	-1.2	1.1	-0.2	18.7	47.9	1.57
10	0	-10.4	-1.7	-2.1	-2.5	0.6	-1.1	10.6	47.9	3.54
11	0	-15.5	1.4	-5.1	-0.2	1	-0.1	17.1	47.9	1.81
12	0	-14.8	-3	-3.8	-2	1	-0.8	13.1	47.9	2.65
13	0	-19	-5.9	-6	-0.6	1.2	-0.9	14.4	38.32*	1.66
14**	0	-10.9	-4.4	-9.9	0	0.2	0	6.8	47.9	6.04
15	90	0.9	0	0.9	0	0	0	1	47.9	49.23
16	18	-0.6	0	-0.3	0	0	0	0.6	47.9	78.82

* Allowable stress includes a stress reduction factor for the weld: 0.8 x allowable stress.

** Stresses at these locations are increased by 5% to account for the heavier BWR fuel basket/fuel assemblies.

Table 2.6.14.9-5 BWR Canister $P_m + P_b + Q$ Stresses – 1-Foot Bottom Corner-Drop, Thermal Heat

		$P_m + P_b + Q$ Stresses (ksi)								
Section Location	**Angle of Peak Stress Location**	**Sx**	**Sy**	**Sz**	**Sxy**	**Syz**	**Sxz**	**Stress Intensity (ksi)**	**Allowable Stress (ksi)**	**Margin of Safety**
1**	162	0.4	-2.7	1.2	0.2	0.1	-0.3	4.2	47.9	10.40
2	162	0	-4.3	0.6	0	0	-0.3	5	47.9	8.57
3**	162	0	-4.3	0.6	0	0	-0.3	5.3	47.9	8.04
4**	180	0	-4.4	0	0	0	0	4.6	47.9	9.41
5**	180	0	-4	0	0	0	0	4.2	47.9	10.40
6**	0	-0.7	-2.9	1.8	0	0.2	0.2	5.0	47.9	8.58
7**	0	-0.9	-1.4	1.5	0	0	0.2	3.2	47.9	13.97
8**	171	-0.1	-2.4	-0.1	0	0.2	0	2.5	47.9	18.16
9	0	-15.4	2.3	-5.2	-1.2	1	-0.3	18	47.9	1.66
10	0	-9.6	-1.4	-2.1	-2.3	0.5	-1	9.9	47.9	3.85
11	0	-16.6	1.6	-5.4	-0.2	1.1	-0.1	18.3	47.9	1.62
12	0	-14.6	-3	-4	-1.8	1	-0.8	12.8	47.9	2.75
13	0	-20.2	-6.4	-6.6	-0.7	1.2	-1	15.1	38.32*	1.54
14**	0	-9.8	-3.9	-8.9	0	0.2	0	6.2	47.9	6.73
15	81	1.4	0	1.6	0	0	0	1.6	47.9	29.36
16	45	-1	-0.1	-0.6	0	0	0	0.9	47.9	52.33

* Allowable stress includes a stress reduction factor for the weld: 0.8 x allowable stress.

** Stresses at these locations are increased by 5% to account for the heavier BWR fuel basket/fuel assemblies.

2.6.14.10 Shear Stresses for 1-Foot Drops

The primary mechanism for shear loading in the canister drop analyses occurs for the bottom end-drop in the canister structural and shield lid welds. The maximum stress intensity for either sections 12 or 13 during any bottom end-drop is 1.8 ksi for the bottom end-drop with thermal heat (Table 2.6.14.5-5). The maximum shear is 1.8/2 = 0.9 ksi. The allowable shear is $0.6S_m$ per the ASME Code, Section III, Subsection NB-3227.2 for pure shear loading. The maximum canister shell temperature is 380°F and the margin of safety for pure shear is

$$MS = 0.6 \times 16.0 / 0.9 - 1 = 9.66$$

2.6.14.11 Canister Bearing Stresses for 1-Foot Side-Drop

The bearing stress evaluation presented in section 2.6.12.11 conservatively encompasses bounding values for both the BWR and PWR canisters.

2.6.14.12 Canister Buckling Evaluation for 1-Foot End-Drop

Code Case N-284-1 of the ASME Boiler and Pressure Vessel Code is used to analyze the BWR canister for the normal condition 1-ft end-drop (both top and bottom end-drops). The evaluation requirements of Regulatory Guide 7.6, Paragraph C.5, are shown to be satisfied by the results of the buckling interaction equation calculations of Code Case N-284-1.

The canister buckling design criteria are described in Section 2.1.2.5.3.

A 20 g deceleration load was used for all the 1-ft drop canister analyses that are presented in Sections 2.6.14.4 through 2.6.14.9. The 20 g-load bounds all 1-ft deceleration loads for all other drop angles. The top- and bottom-end drops result in the largest potential for canister shell buckling and, therefore, are the two load cases presented here. The side drop load case is not considered a credible buckling mode of the canister shell and is, therefore, not presented here.

The BWR canister is evaluated for buckling in the same manner as the PWR canister (see Section 2.6.12.12). The analytical process used for the BWR canister is the same as that described in a step-by-step example presented in Section 2.7.12.3 (for the cask inner shell).

The stress results from the canister analyses are screened for the maximum values of the longitudinal compression, circumferential compression, or in-plane shear stresses for the 1-ft drop cases (top- and bottom-end drops) with and without pressure. For each loading case, the largest of each of the three stress components anywhere regardless of location within the BWR canister shell are combined. To these maximum stress components are added the maximum stresses from the hot and cold thermal cases (Tables 2.6.14.3-1 and 2.6.14.3-2). Combining the maximum stress components in this way produces a conservative, bounding-case buckling evaluation of the BWR canister, one which envelopes all 1-ft BWR canister drop cases including those presented in Tables 2.6.14.4-4 and 2.6.14.4-6.

The geometry parameters used in the BWR canister evaluation are presented in Table 2.6.14.12-1.

The maximum stress components used in the evaluation and the buckling interaction equation ratios for the BWR canister top- and bottom-end drop cases are provided in Table 2.6.14.12-2. The results of the buckling evaluation show that all interaction equation ratios are less than 1.0. Therefore, the buckling criteria of Code Case N-284-1 are satisfied, thus demonstrating that buckling of the BWR canister does not occur.

Table 2.6.14.12-1 Geometry Parameters for the BWR Canister

Parameter	Value
t = thickness (in)	0.625
ID = inside diameter (in)	65.81
R = radius (in) = (ID+t)/2	33.22
R/t	53.15
$(Rt)^{0.5}$	4.56
Overall Length (in)	190.55
Bottom Thickness (in)	1.75
Structural Lid Thickness (in)	3.0
L_ϕ = Length used in evaluation (in)*	185.8
$L_\theta = 2\pi R$ = circumference (in)	218.7
ν = Poisson's Ratio	0.275

* L_ϕ = Overall canister length - Bottom thickness - Structural lid thickness.

Table 2.6.14.12-2 Buckling Evaluation Results for the BWR Canister for 1-Foot End-Drop

Load Case	Load Condition	Longitudinal (Axial) Stress* S_ϕ (psi)	Circumferential (Hoop) Stress* S_θ (psi)	In-plane Shear Stress $S_{\phi\theta}$ (psi)	Elastic Buckling Interaction Equations				Plastic Buckling Interaction Equations			
					Q1	Q2	Q3	Q4	Q5	Q6	Q7	Q8
A	1-Ft Top End-Drop	2100	200	400	0.0	.068	.043	0.0	.067	.043	.068	.043
B	1-Ft Bottom End-Drop	3100	500	300	.040	.099	.108	.040	.099	.108	.099	.108

Component stresses include thermal stresses.

* Compressive stresses.

2.6.15 BWR Basket Analysis—Normal Conditions of Transport

The Universal Transport Cask BWR basket is similar in design to the PWR basket. It is a right-cylinder structure fabricated with 56 square fuel tubes, a number of circular support disks, a number of heat transfer disks, six tie rods with split spacers, and two end weldment plates. The number of support disks and heat transfer disks varies depending upon the class of BWR fuel the basket is designed to contain. The basket components and their geometry are illustrated in Figure 2.6.15-1 and Figure 2.6.15-2. Figure 2.6.15-3 shows the details of the fuel tube with the encasing BORAL on two sides. The fuel tubes are open at each end; therefore, longitudinal fuel assembly loads are imparted to the canister shield lid or bottom plate, and not the fuel basket structure. The fuel basket contains the fuel and is laterally supported by the canister shell.

In the BWR basket, the fuel assemblies, together with the tubes, are laterally supported in the holes in the carbon steel support disks. The aluminum heat transfer disks located at the mid section of the cavity are used to fully optimize the passive heat rejection from the package and are self-supporting. The dimensional differences between the heat transfer disk and the support disk accommodate the different rate of thermal growth between aluminum and stainless steel, thereby preventing interference between the tube, support disk, and heat transfer disks.

The primary function of the spacers and the threaded top nut is the same as those in the PWR basket described in Section 2.6.13. As described in that section, the only component that requires a detailed finite element analysis is the support disk. The stainless steel fuel tubes are not considered to be structural components with respect to the disks other than consideration of their mass contribution to loading.

The basket support disk is designed to restrain 56 fuel assemblies, which would nominally fit into a 6.278 inch square slot. Since a populace of BWR fuel assemblies are not expected to fit into the 6.278 inch square, four oversized fuel assemblies slots are specified as 6.478 inch squares. This will reduce the thickness of the ligament at the outer most corner. However, the size of the web (.65 inch) is not changed. Therefore, the oversized slots will not affect the buckling calculations, since they pertain to the in-plane and out of plane buckling of the webs. In an inspection of the maximum stresses of the BWR basket, the ligament that contains the reduction due to the oversized slots, does not appear in the maximum stress summaries. The smallest ligament at the corner is still significantly controlled by the .8 inch ligament. Therefore,

the use of oversized holes is not considered to alter the model of the BWR basket, which employs a slot size of 6.278 inches.

In this section, the BWR fuel basket is evaluated for the normal transport loads. As discussed in Section 2.6.13, the g-loads produced by the corner-drops are bounded by the g-loads produced by the end and side-drops. Therefore, only the end-drop and side-drop orientations are evaluated. The basket is evaluated for the hypothetical accident condition in Section 2.7.10.

Figure 2.6.15-1 BWR Fuel Assembly Basket

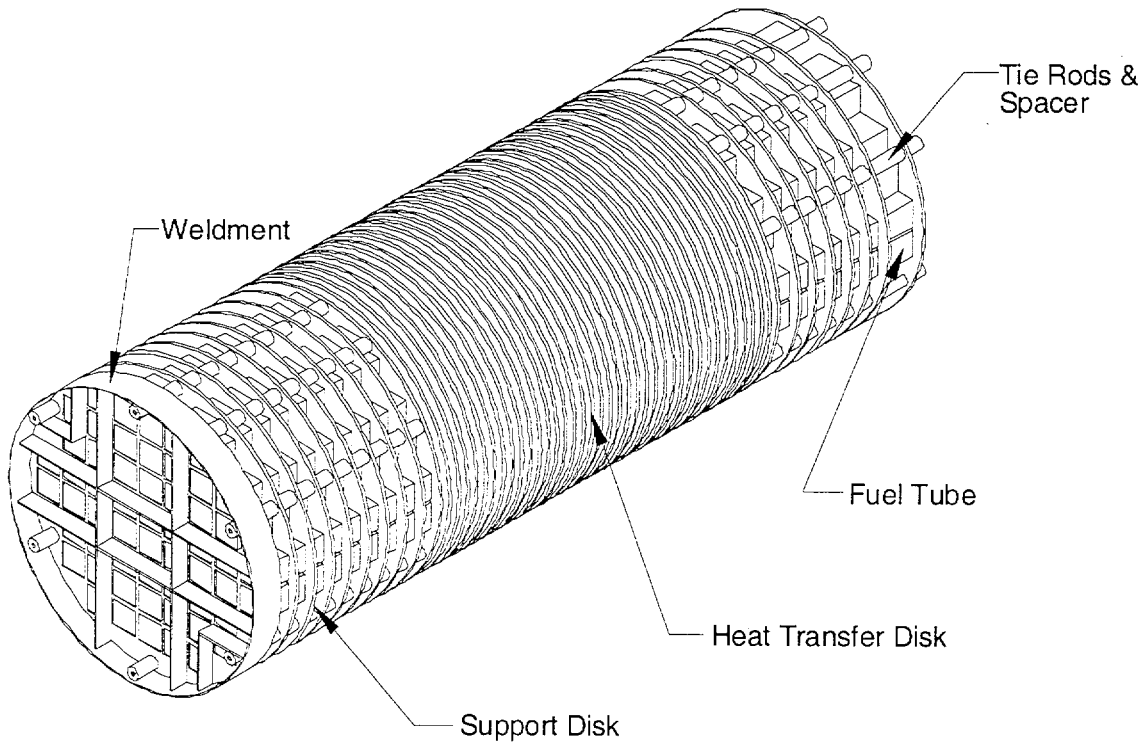

Figure 2.6.15-2 Support Disk Cross Section Configuration

FIGURE WITHHELD UNDER 10 CFR 2.390

Note:

Engineering drawings provide appropriate tolerances for dimensions shown.

Figure 2.6.15-3 BWR Fuel Tube Configuration

FIGURE WITHHELD UNDER 10 CFR 2.390

2.6.15.1 Analysis Description

The criticality and structural design criteria for the BWR basket are similar to those for the PWR basket discussed in Section 2.6.13.1. Consistent with the structural design criteria, the main structural component in the fuel basket—the stainless steel support disk—is shown to have (in any disk for any normal-condition load and position orientation) a maximum primary membrane stress intensity and primary membrane plus bending stress intensity that are less than the design stress intensity values S_m and $1.5S_m$, respectively. The value of S_m is defined at the temperatures for the component being analyzed.

In the side-drop, the loads of the fuel assemblies are transferred into the plane of the support disks, from which they are transmitted to the canister shell. In the vertical orientation, the fuel basket components are loaded by their own inertial weight and do not experience load from the guided but freestanding fuel assemblies. Various radial impact orientations of the support disk are evaluated. In addition to the load from inertial weight, the differential thermal expansion of the support disk is also evaluated.

2.6.15.2 Finite Element Model Description - BWR Basket

As is the case for the analysis of the PWR basket, two finite element models are generated to analyze the BWR fuel basket for the normal operating conditions: one for the end-drop, in which the loads are perpendicular to the plane of the disk, and one for the side-drop, in which the loads act in the plane of the disk. Both models accommodate thermal expansion effects by using the temperature distribution from the thermal analysis and the coefficient of thermal expansion.

A complete basket support disk is modeled for the side impact evaluation because planes of symmetry are not present when the impact can be at an arbitrary angle. The basket model for the side-drop is shown in Figure 2.6.15.2-1. Although the end-drop orientation exhibits a quarter symmetry, the model conversion is simplified by using the same nodal pattern as that for the side-drop model.

The finite element model for the side-drop evaluation of the BWR basket is similar to that used for the evaluation of the PWR basket. A detailed description of the model for the side-drop of the PWR basket is provided in Section 2.6.13.2. Figure 2.6.15.2-2 shows the ligaments and the

interface with the BWR canister shell and the cask inner shell. The loads from the fuel assembly are modeled as a pressure loading at the inner surface of each support disk slot opening. The surface pressure loads applied to the support disk slot opening to represent fuel assemblies are determined by performing a comparison analysis of all relevant BWR assemblies. A comparison is performed to determine the highest load per disk. The load is then divided by the fuel tube's width and the disk thickness to result in a worst case scenario pressure loading. The pressure loading applied to each slot opening is calculated as follows.

Load per disk = (Max. fuel assembly weight + max. fuel tube weight) / No. of loaded disk

Max. fuel assembly weight = 821.3 lbs (very conservative based on actual max fuel assembly weight of 696 lbs [GE BWR/2-3 & 4-6])

Max. fuel tube weight = 83

Number of loaded disks= 37

Load per disk = (821.3 lbs + 83 lbs)/37 disks = 24.4 lbs/disk

Therefore, the pressure loading applied to each slot opening is (24.4 lbs)(0.625)/ 6.278 = 6.2 psi). The loading is multiplied by a *g* load factor based on the drop condition being analyzed:

1. Normal condition - 20 *g*
2. Accident condition - 60 *g*

The PLANE42 element used in the model corresponds to plane stress and the thickness of the model is input as 0.625 in., which corresponds to the thickness of the support disk in the BWR basket.

Figure 2.6.15.2-1 ANSYS Model of BWR Basket for Side-Drop

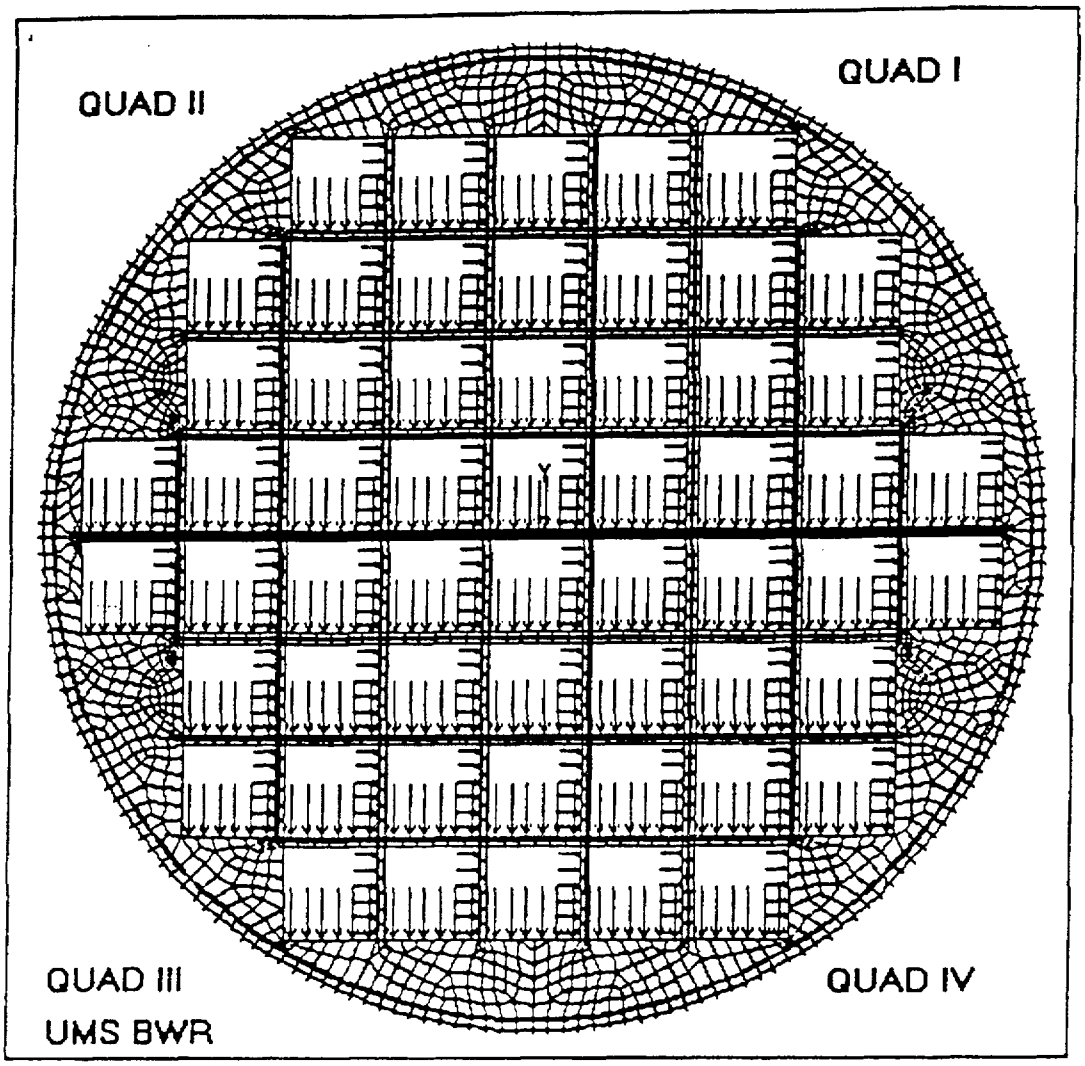

Figure 2.6.15.2-2 Close-up of the Ligaments and the Interface with the Canister Shell and the Cask Inner Shell

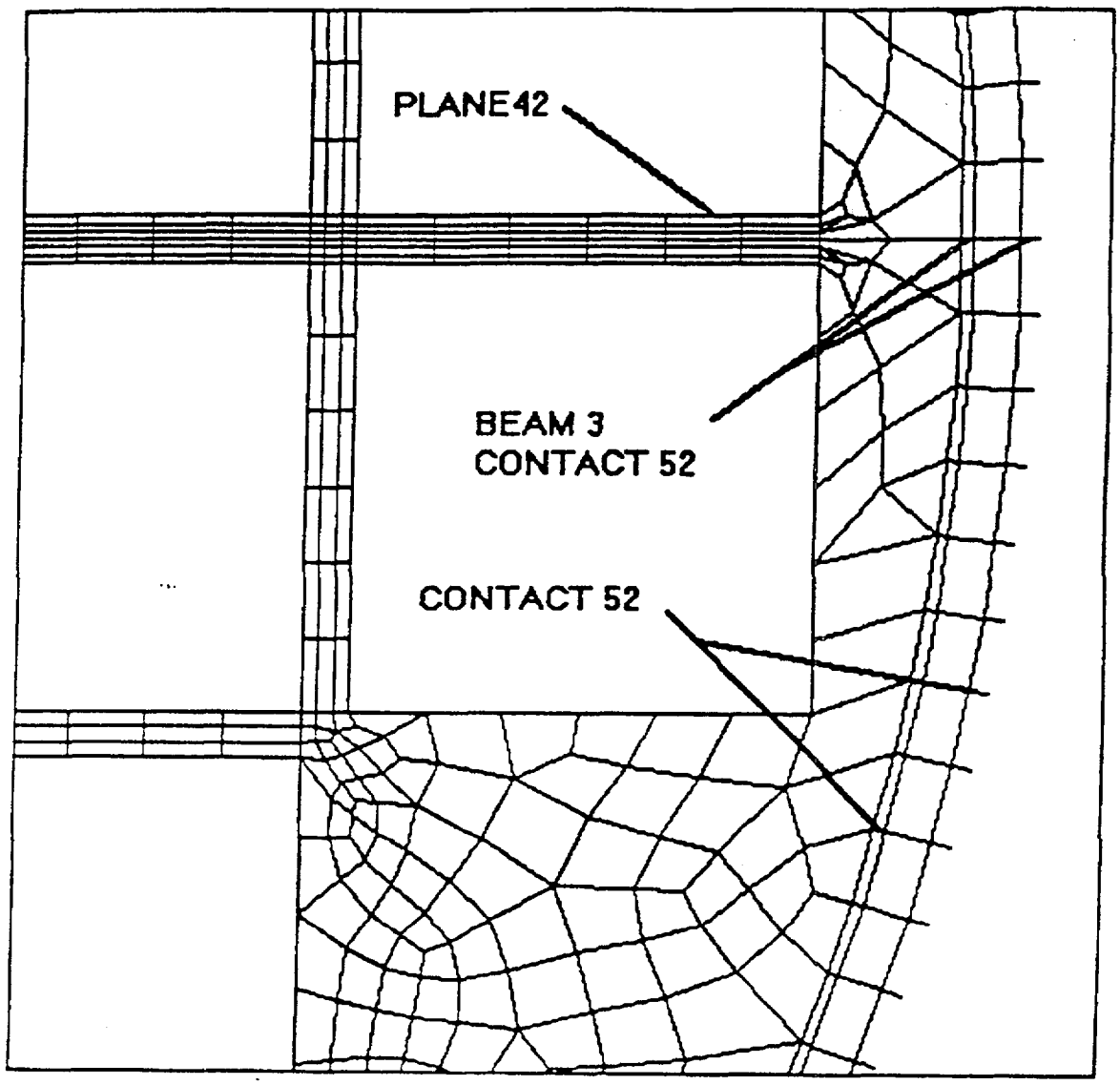

2.6.15.3 Thermal Condition and Expansion Evaluation of BWR Support-Disks

The three thermal conditions evaluated for the support disk analysis are as follows:

Thermal Condition	Ambient Temperature	Solar Insolance Applied to Cask Surface	16 kW Fuel Load
1	-40°F	No	No
2	-40°F	No	Yes
3	100°F	Yes	Yes

The table below reflects the maximum and minimum temperatures required for the support disk evaluation. These temperatures were obtained from the thermal analysis of the BWR configuration as contained in Section 3.4.2.

Case No.	T_{max}	T_{min}	Condition No.	α*	E*	Eα*
1	-40°F	-40°F	1	NC**	NC**	NC**
3	616°F	296°F	3	7.598E-6	27.34E3	.2077
5	524°F	349°F	2	7.433E-6	27.988E3	.2080

In the structural evaluation of the support disk, the table below shows the temperatures cases employed.

Case No.	T_{max}	T_{min}	Condition No.	α*	E*	Eα*
1	-40°F	-40°F	1	NC**	NC**	NC**
2	600°F	150°F	3	7.5425E-6	27.550E3	.2078
4	516°F	106°F	2	7.4465E-6	27.934E3	.2080

* Evaluated at average of T_{max} and T_{min} (α = thermal expansion coefficient, in/in/°F; E = modulus of elasticity, ksi)

** NC denotes Not Compared because of uniform temperature.

The thermal stress is dependent on the Eα as well as the overall temperature change along the basket radius. Consequently, Cases 2 and 4 are enveloping as compared to Cases 3 and 5, which are the results of the thermal analysis for the BWR configuration. In comparing Case 2 and 4,

the larger temperature change occurs for Case 2, and since the Eα's are approximately equal, the enveloping thermal stress would be developed in Case 4. To compute the margin of safety, the allowables are derived from Case 3 since it corresponds to the maximum temperatures which would result in the lowest stress allowables. Thermal condition 1 is also analyzed, since it generated the maximum modulus of elasticity, even though stresses arising a thermal gradient are zero.

2.6.15.4 Stress Evaluation of BWR Support Disks for 1-Foot End-Drop Load Condition

The BWR basket support disks are located by six tie rods with spacers. An ANSYS structural analysis evaluates the effect of a 1-ft-end-drop impact that corresponds to the most severe out of plane loading. The finite element model described in Section 2.6.15.2 (and Section 2.6.13.2) is used in conjunction with a 20 *g* deceleration. Because shell elements are employed for the analysis, the nodal stress for the midplane of the plate or the outer fiber stress can be reported at each node. Maximum nodal stresses for the midplane (which correspond to the primary membrane stress) and the outer fiber (which correspond to primary membrane plus bending) are shown in Figure 2.6.15.4-1.

The calculated values of maximum primary membrane and bending stresses are provided in Table 2.6.15.4-2. The membrane stresses for the 1-ft end drop condition is effectively zero.

The minimum margin of safety corresponding to a maximum primary membrane plus bending stress of 32.5 ksi is

$$MS\ (P_m+P_b) = (45.0/32.5) - 1 \qquad (1.5\ S_m \text{ at } 500°F = 45.00 \text{ ksi for SA533 carbon steel})$$

$$= +0.39.$$

Results of the 1-ft end-drop condition are presented in Tables 2.6.15.4-1 and 2.6.15.4-2.

Figure 2.6.15.4-1 Locations of Maximum Primary Nodal Stress Intensities for 1-Foot End-Drop

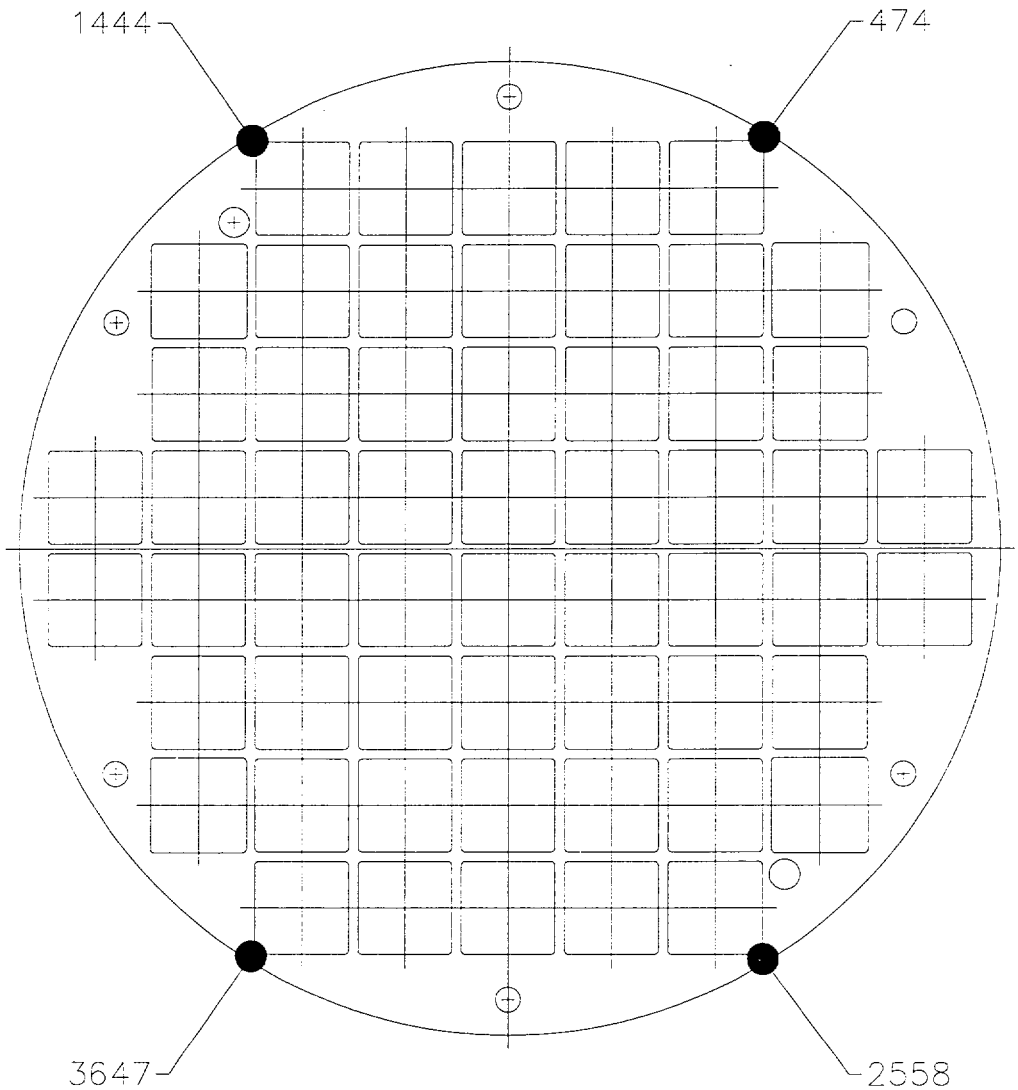

Table 2.6.15.4-1 $P_m + P_b$ Stresses for Support Disk 1-Foot End-Drop, Thermal Case 1

Node	Principal Stresses (ksi)			Stress Intensity (ksi)	Allowable Stress (ksi)*	Margin of Safety
	S1	S2	S3			
86	25.3	0.0	-1.0	26.3	45.0	0.71
474	32.2	2.1	0.0	32.2	45.0	0.40
1129	29.6	1.5	0.0	29.6	45.0	0.52
1444	32.2	2.1	0.0	32.2	45.0	0.40
1564	25.3	0.0	-1.0	26.3	45.0	0.71
2236	29.6	1.5	0.0	29.6	45.0	0.52
2558	32.2	2.1	0.0	32.2	45.0	0.40
2680	25.3	0.0	-1.0	26.3	45.0	0.71
3332	29.6	1.5	0.0	29.6	45.0	0.52
3647	32.2	2.1	0.0	32.2	45.0	0.40
3765	25.3	0.0	-1.0	26.3	45.0	0.71
4407	29.6	1.5	0.0	29.6	45.0	0.52

*1.5 S_m = 1.5 x 30.0 ksi at 500°F.

Table 2.6.15.4-2 $P_m + P_b$ Stresses for Support Disk 1-Foot End-Drop, Thermal Case 4

Node	Principal Stresses (psi)			Stress Intensity (psi)	Allowable Stress (psi)*	Margin of Safety
	S1	S2	S3			
86	25.6	0.0	-1.1	26.7	45.0	0.69
474	32.5	2.1	0.0	32.5	45.0	0.39
1129	29.9	1.5	0.0	29.9	45.0	0.51
1444	32.5	2.1	0.0	32.5	45.0	0.39
1564	25.6	0.0	-1.1	26.7	45.0	0.69
2236	29.9	1.5	0.0	29.9	45.0	0.51
2558	32.5	2.1	0.0	32.5	45.0	0.39
2680	25.6	0.0	-1.1	26.7	45.0	0.69
3332	29.9	1.5	0.0	29.9	45.0	0.51
3647	32.5	2.1	0.0	32.5	45.0	0.39
3765	25.6	.0	-1.1	26.7	45.0	0.69
4407	29.9	1.5	0.0	29.9	45.0	0.51

*1.5 S_m = 1.5 x 30.0 ksi at 500°F.

2.6.15.5 Stress Evaluation of BWR Support Disk for Combined Thermal and 1-Foot End Drop Load Conditions

The thermal expansion loads described in Section 2.6.15.3 (and 2.6.13.3) are applied to the finite element model simultaneously with the 20 *g* end-drop loads described in Section 2.6.15.4 to produce a combined thermal expansion plus end-impact loading. The stress evaluation is performed according to the ASME Code, Section III, Subsection NG. Because stress intensity is required at the surface only, the extreme fiber stress is required. Thermal Condition 4 is used for this evaluation. Maximum nodal stresses for the combined thermal and 1-ft end-drop condition are shown in Figure 2.6.15.5-1. The allowable stress intensity range is $3S_m$. The maximum stress intensity is 52.7 ksi and the $3S_m$ allowable limit at 500°F for SA533 Type B Class 2 carbon steel is 90 ksi, which results in a margin of safety of:

$$MS = (90/52.7) - 1 = +0.71.$$

Results from the combined thermal and 1-ft end-drop condition are presented in Table 2.6.15.5-1.

Figure 2.6.15.5-1 Locations of Maximum Primary and Secondary Nodal Stress Intensities for 1-Foot End-Drop

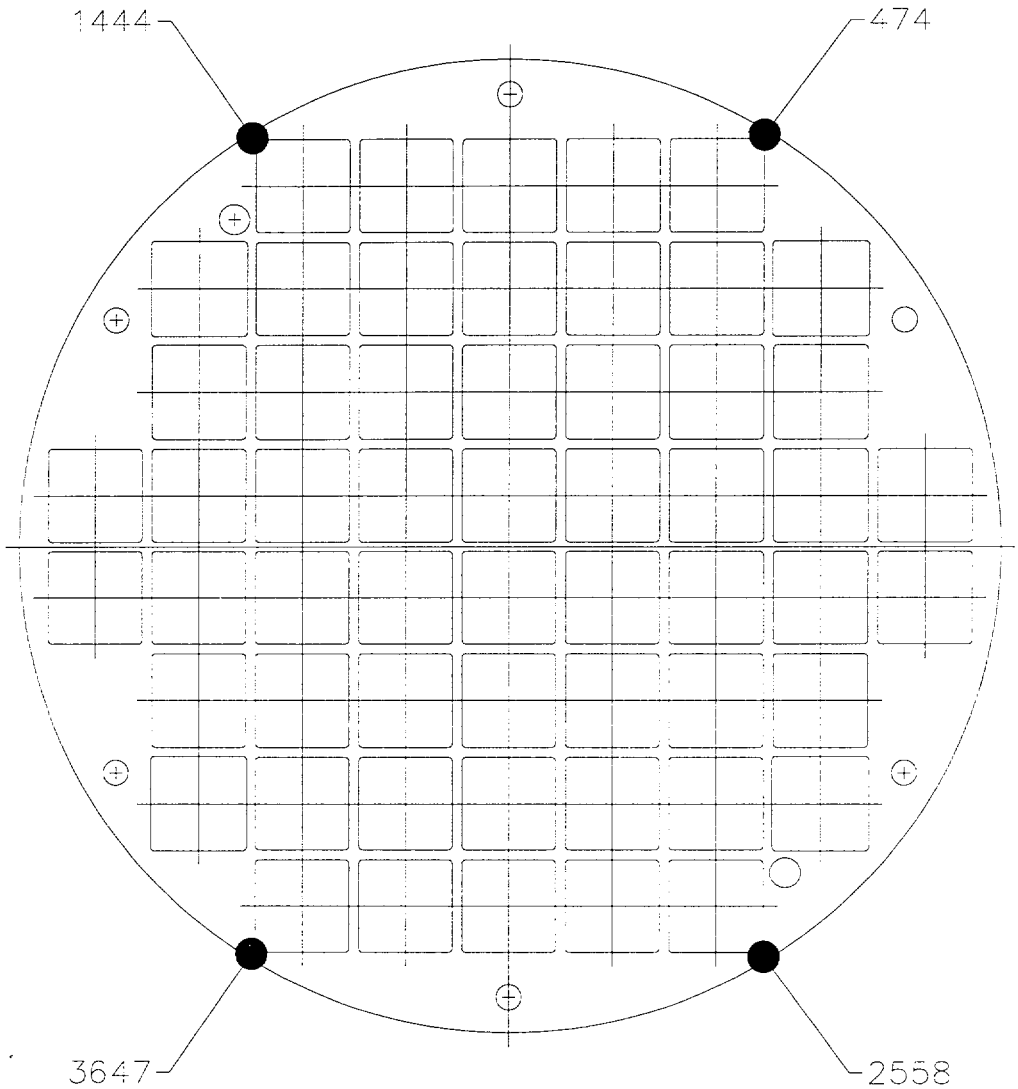

Table 2.6.15.5-1 $P_m + P_b + Q$ Stresses for Support Disk 1-Foot End-Drop, Thermal Case 4

Node	Principal Stresses (ksi)			Stress Intensity (ksi)	Allowable Stress (ksi)	Margin of Safety
	S1	S2	S3			
474	52.7	7.2	0.0	52.7	90.0	0.71
481	35.0	0.0	-3.1	38.1	90.0	1.36
1129	40.3	3.6	0.0	40.3	90.0	1.23
1444	52.7	7.2	0.0	52.7	90.0	0.71
1451	35.0	0.0	-3.1	38.1	90.0	1.36
2236	40.3	3.6	0.0	40.3	90.0	1.23
2558	52.7	7.2	0.0	52.7	90.0	0.71
2565	35.0	0.0	-3.1	38.1	90.0	1.36
3332	40.3	3.6	0.0	40.3	90.0	1.23
3647	52.7	7.2	0.0	52.7	90.0	0.71
3654	35.0	0.0	-3.1	38.1	90.0	1.36
4407	40.3	3.6	0.0	40.3	90.0	1.23

*3.0 S_m = 3.0 x 30.0 ksi at 500°F.

2.6.15.6 Stress Evaluation of BWR Support Disk for 1-Foot Side-Drop Load Condition

To determine the structural adequacy of the BWR fuel basket support disk for the 1-ft side-drop load condition, a quasi-static impact load equal to the weight of the fuel and tubes multiplied by a 20 *g* amplification factor is applied to the support disk structure. The inertial loading of the support disk is also included by means of the density input for the SA533 Type B Class 2 carbon steel. The value of 20 *g* is conservative because the Universal Transport Cask impact limiter design deceleration for a 1-ft side-drop is 16.4 *g*. The fuel assembly load is transmitted in direct compression through the tube wall to the web structure of the support disk. A conservative number of disks is assumed to transmit the load to the canister shell (See Section 2.6.15.2). The maximum in-plane loading occurs in the side-drop, which requires a detailed structural evaluation. ANSYS and the finite element model described in Section 2.6.15.2 are used to perform a finite element analysis.

2.6.15.6.1 Drop Orientations

The BWR fuel basket exhibits one-quarter symmetry. A minimal radial thickness between the corner of the fuel assembly slot in the basket and the outer radius occurs at 31.82, 49.46, 77.92 and 90° measured counterclockwise from the +X axis. To ensure that the bounding basket orientation is evaluated, basket radial orientations of 0, 31.82, 49.46, 77.92, and 90° are considered. These orientations are identified in Figure 2.6.15.6-1. The material properties are evaluated at three thermal Cases 1, 2 and 4. Allowables are evaluated at Thermal Cases 1 and 3.

2.6.15.6.2 Definition of Cross Sections for Linearized Stresses

The stress evaluation for the support disk is performed according to the ASME Code, Section III, Subsection NG, which requires comparison of the linearized stresses of cross sections of the structure against the allowable stresses. Primary membrane stress intensity is compared with S_m and primary membrane plus bending stress intensity is compared with $1.5S_m$ for the material at temperature. A conservative temperature distribution is used to determine S_m at each of the cross sections. These temperatures are obtained through thermal conduction analysis by using Thermal Case 3, where the minimum temperature of the circumference and the maximum temperature is applied at the center of the basket.

To determine the most critical cross sections, a series of cross sections is considered. To aid in the identification of these sections, Figures 2.6.15.6-2 through 2.6.15.6-5 show the point locations on a support disk. Table 2.6.15.6-1 lists the cross section versus Point 1 and Point 2, which spans the cross section of the web in the plane of the support disk. Points 1 and 2 for each cross section are shown in the previously cited figures.

2.6.15.6.3 Analysis Results for 1-Foot Side-Drop

Finite element analyses are performed for the 1-ft side-drop load conditions for the five different radial basket orientations (0, 31.82, 49.46, 77.92 and 90°) and for two Thermal Cases that would result in the use of different moduli of elasticity throughout the basket. Figures 2.6.15.6-6 through 2.6.15.6-10 show the locations of maximum nodal stress intensities (SI) for the five basket orientations.

For the normal condition of transport, the allowable stress limit is S_m, for the support disk primary membrane stress (P_m) and $1.5S_m$ for primary membrane plus bending stress ($P_m + P_b$). The cross sections with the 20 minimum margins of safety are presented in Tables 2.6.15.6-2 through 2.6.15.6-21. A summary of the minimum margins of safety is presented below.

Table Number	Basket Orientation (Deg)	Thermal Case	Stress Evaluation	Minimum Margin of Safety
2.6.15.6-2	0	1	P_m	+0.45
2.6.15.6-3	0	1	$P_m + P_b$	+0.84
2.6.15.6-4	0	2	P_m	+0.47
2.6.15.6-5	0	2	$P_m + P_b$	+0.88
2.6.15.6-6	31.82	1	P_m	+0.54
2.6.15.6-7	31.82	1	$P_m + P_b$	+0.19
2.6.15.6-8	31.82	2	P_m	+0.60
2.6.15.6-9	31.82	2	$P_m + P_b$	+0.24
2.6.15.6-10	49.46	1	P_m	+0.35
2.6.15.6-11	49.46	1	$P_m + P_b$	+0.11
2.6.15.6-12	49.46	2	P_m	+0.43
2.6.15.6-13	49.46	2	$P_m + P_b$	+0.13
2.6.15.6-14	77.92	1	P_m	+0.29
2.6.15.6-15	77.92	1	$P_m + P_b$	+0.45
2.6.15.6-16	77.92	2	P_m	+0.32
2.6.15.6-17	77.92	2	$P_m + P_b$	+0.47
2.6.15.6-18	90	1	P_m	+0.09
2.6.15.6-19	90	1	$P_m + P_b$	+0.56
2.6.15.6-20	90	2	P_m	+0.12
2.6.15.6-21	90	2	$P_m + P_b$	+0.59

The margins of safety are calculated as

MS = (stress allowable/stress intensity) - 1.

The minimum margin of safety for the side-drop (+ 0.09) occurs for the 90° basket orientation at Thermal Case 2, no thermal stresses. This margin of safety is based on a primary membrane stress of 27.4 ksi.

Figure 2.6.15.6-1 Support Disk Side-Drop Orientations

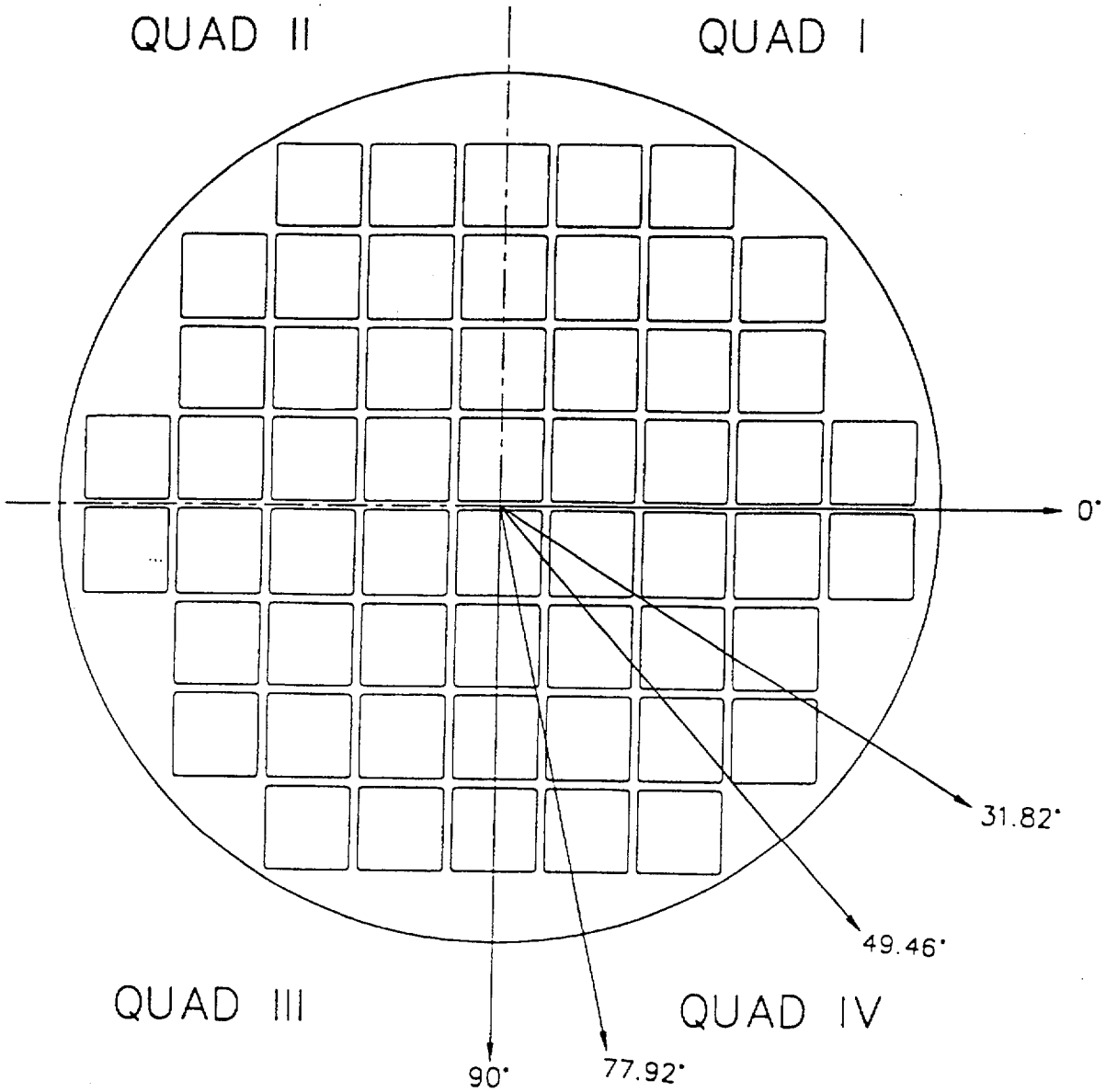

Figure 2.6.15.6-2 Locations of the Sections Used to Obtain Linearized Stresses for the Support Disk for the 1st Quadrant (X>0, Y>0)

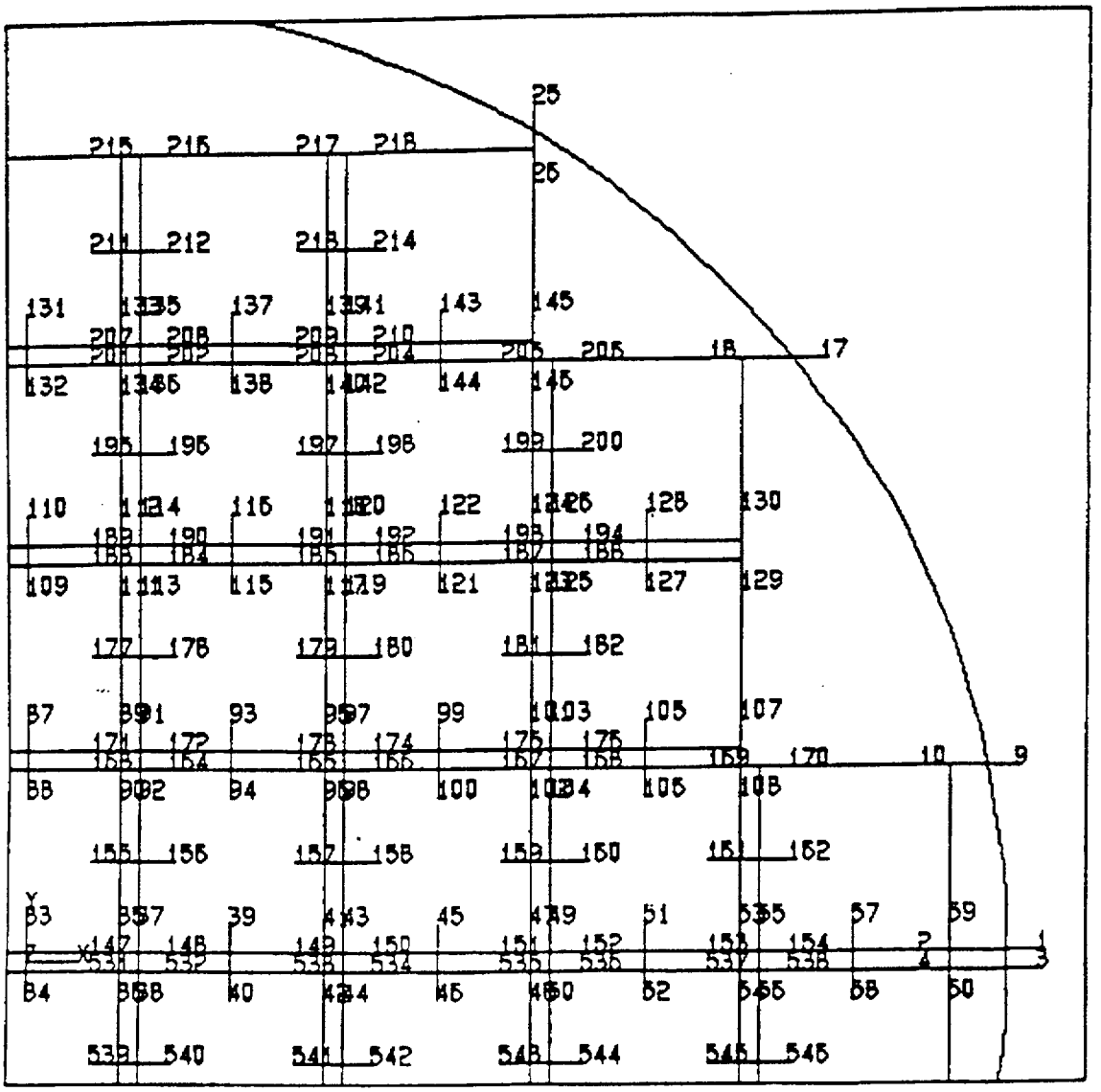

QUAD I

Figure 2.6.15.6-3 Locations of the Sections Used to Obtain Linearized Stresses for the Support Disk for the 2nd Quadrant (X<0, Y<0)

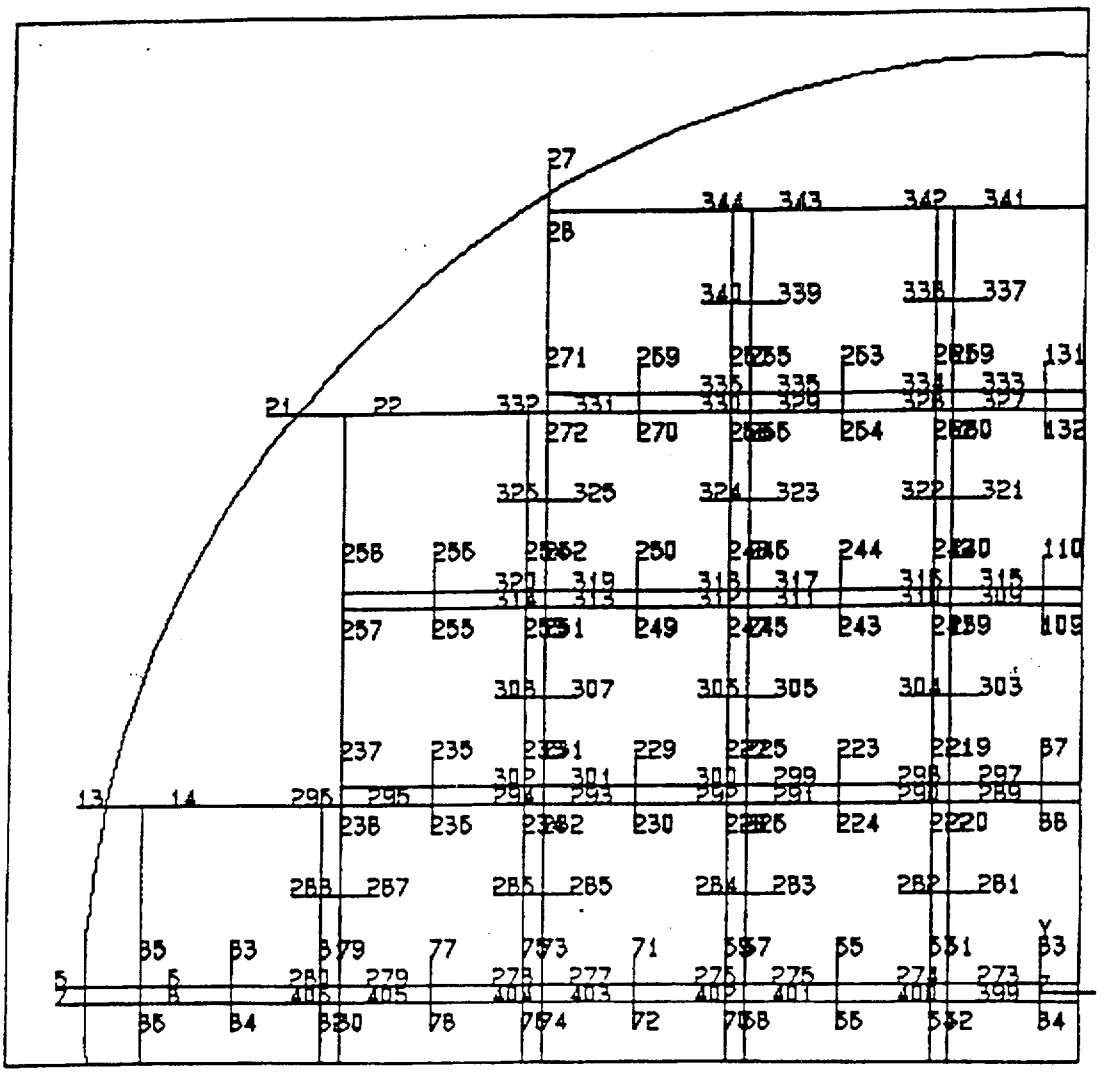

QUAD II

Figure 2.6.15.6-4 Locations of the Sections Used to Obtain Linearized Stresses for the Support Disk for the 3rd Quadrant (X<0, Y<0)

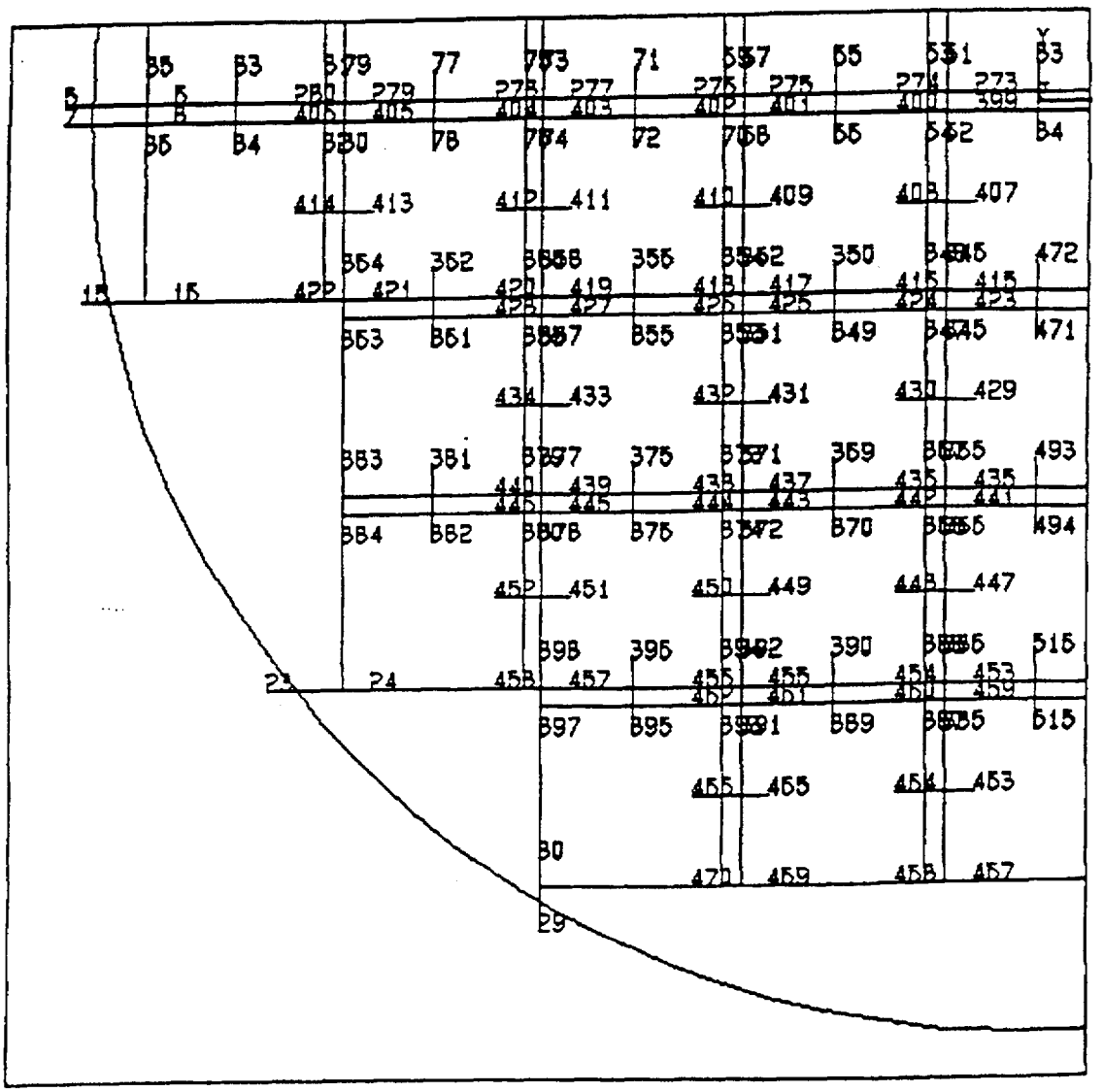

QUAD III

Figure 2.6.15.6-5 Locations of the Sections Used to Obtain Linearized Stresses for the Support Disk for the 4th Quadrant (X>0, Y<0)

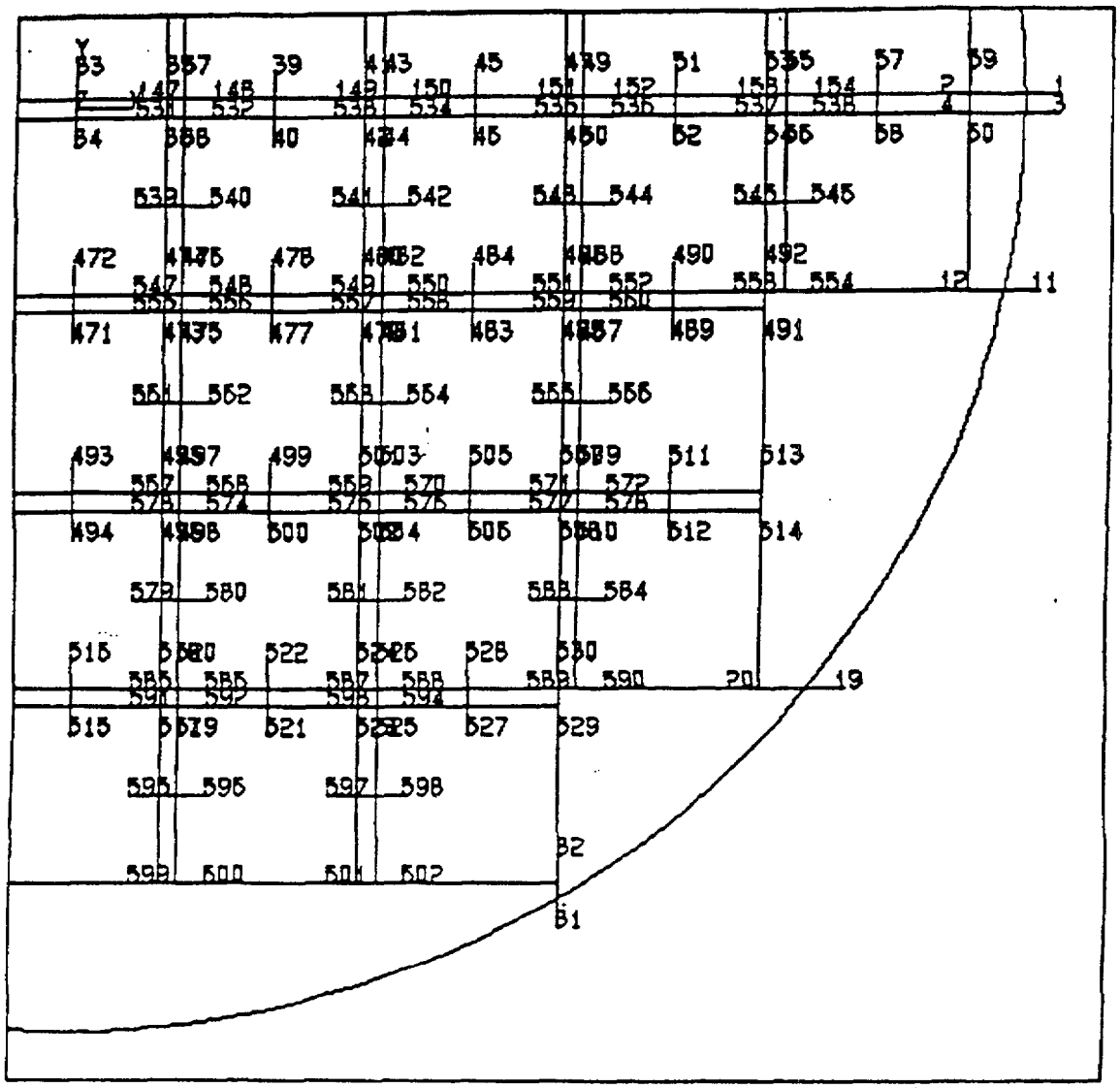

QUAD IV

Figure 2.6.15.6-6 Locations of Maximum Linearized Stress Intensities - 0° Drop Orientation

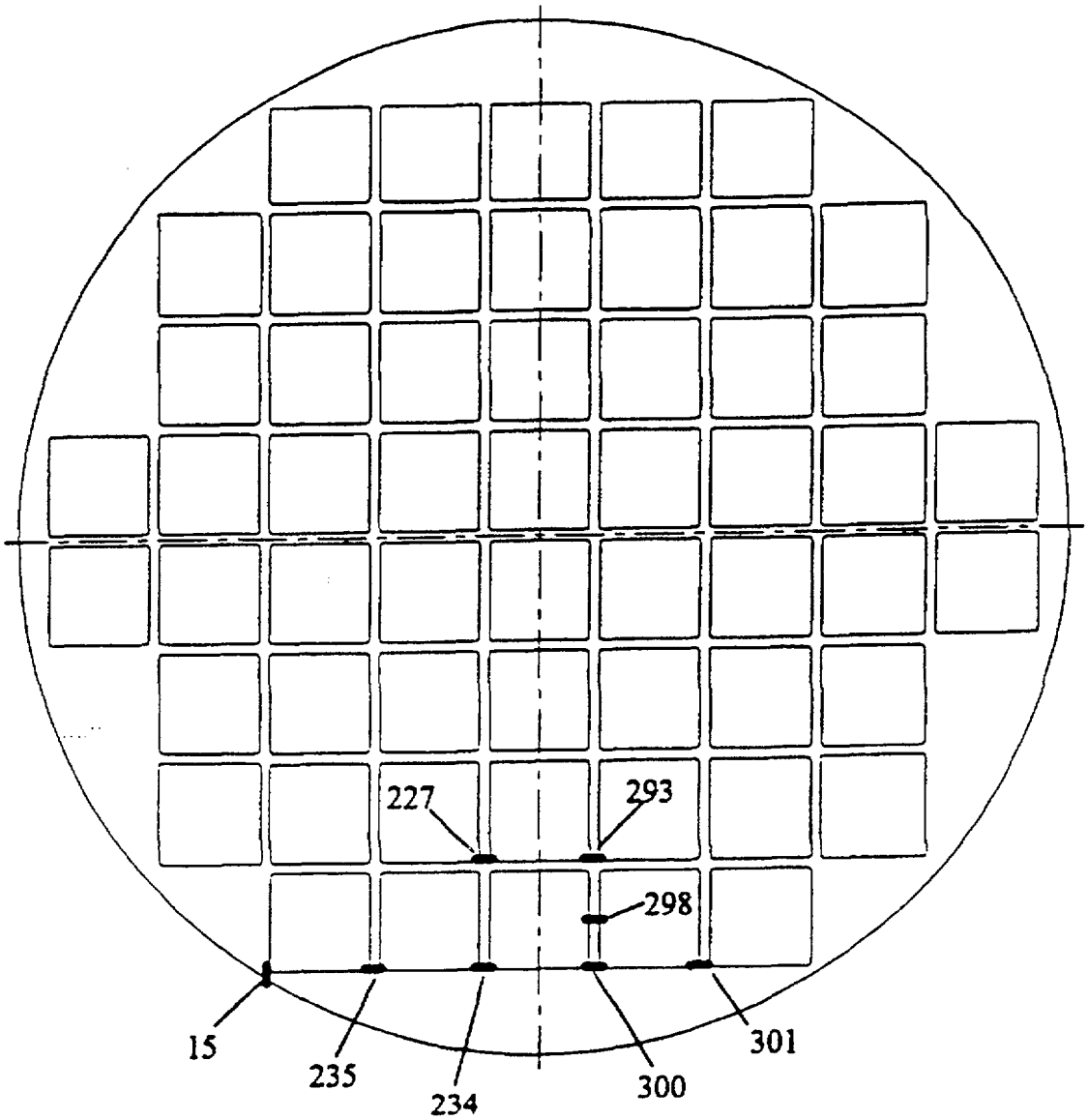

Figure 2.6.15.6-7 Locations of Maximum Linearized Stress Intensities - 31.82° Drop Orientation

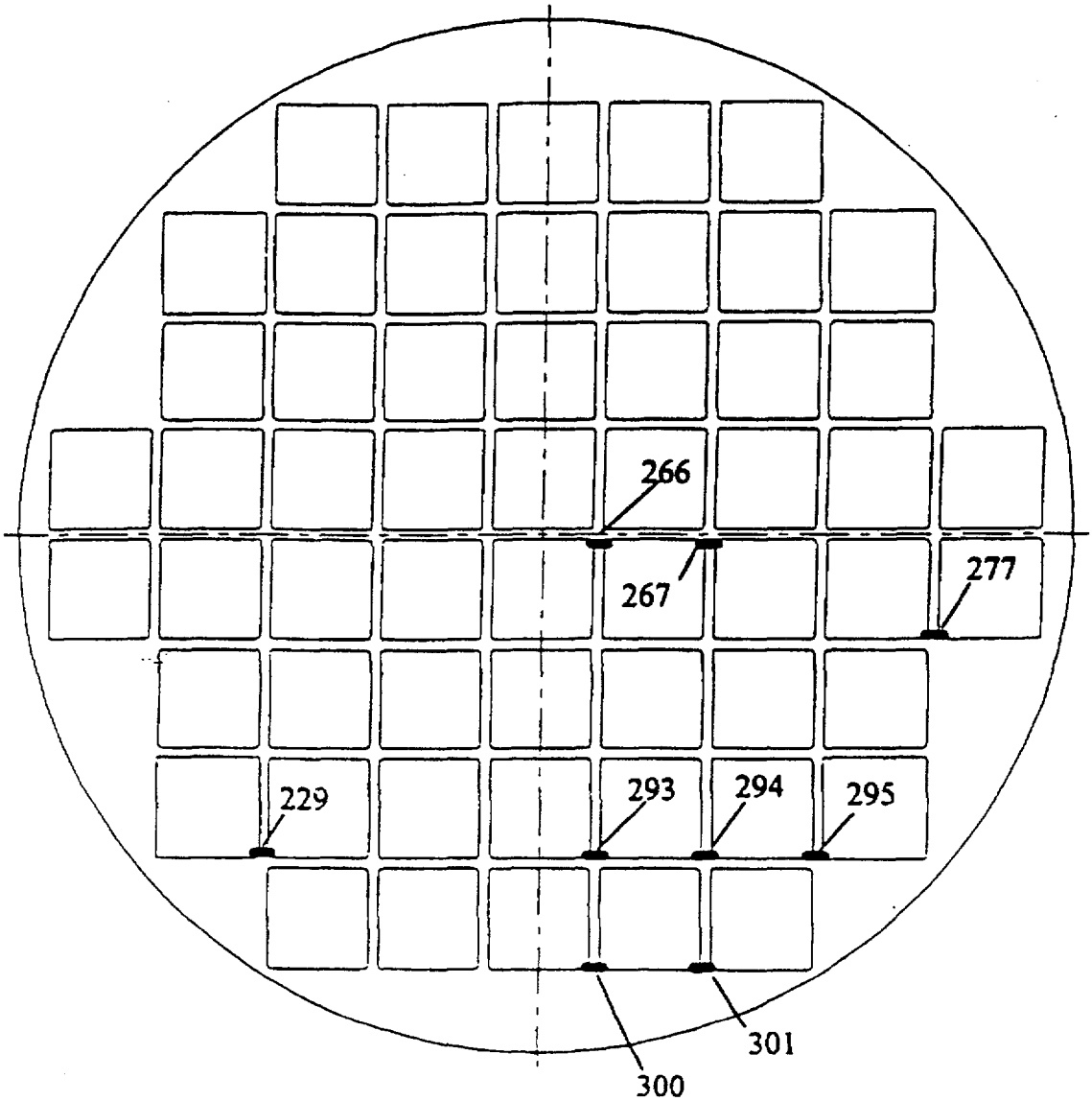

Figure 2.6.15.6-8 Locations of Maximum Linearized Stress Intensities - 49.46° Drop Orientation

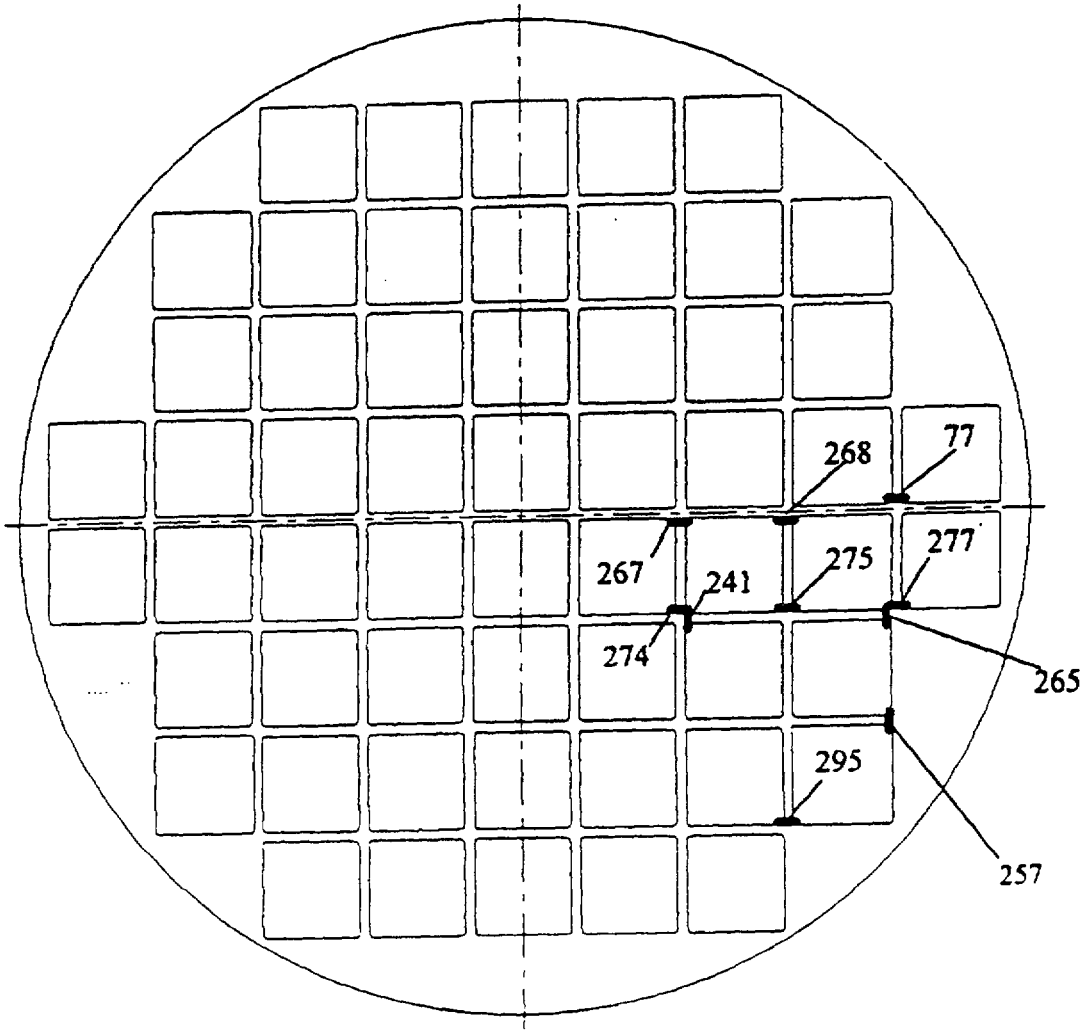

Figure 2.6.15.6-9 Locations of Maximum Linearized Stress Intensities - 77.92° Drop Orientation

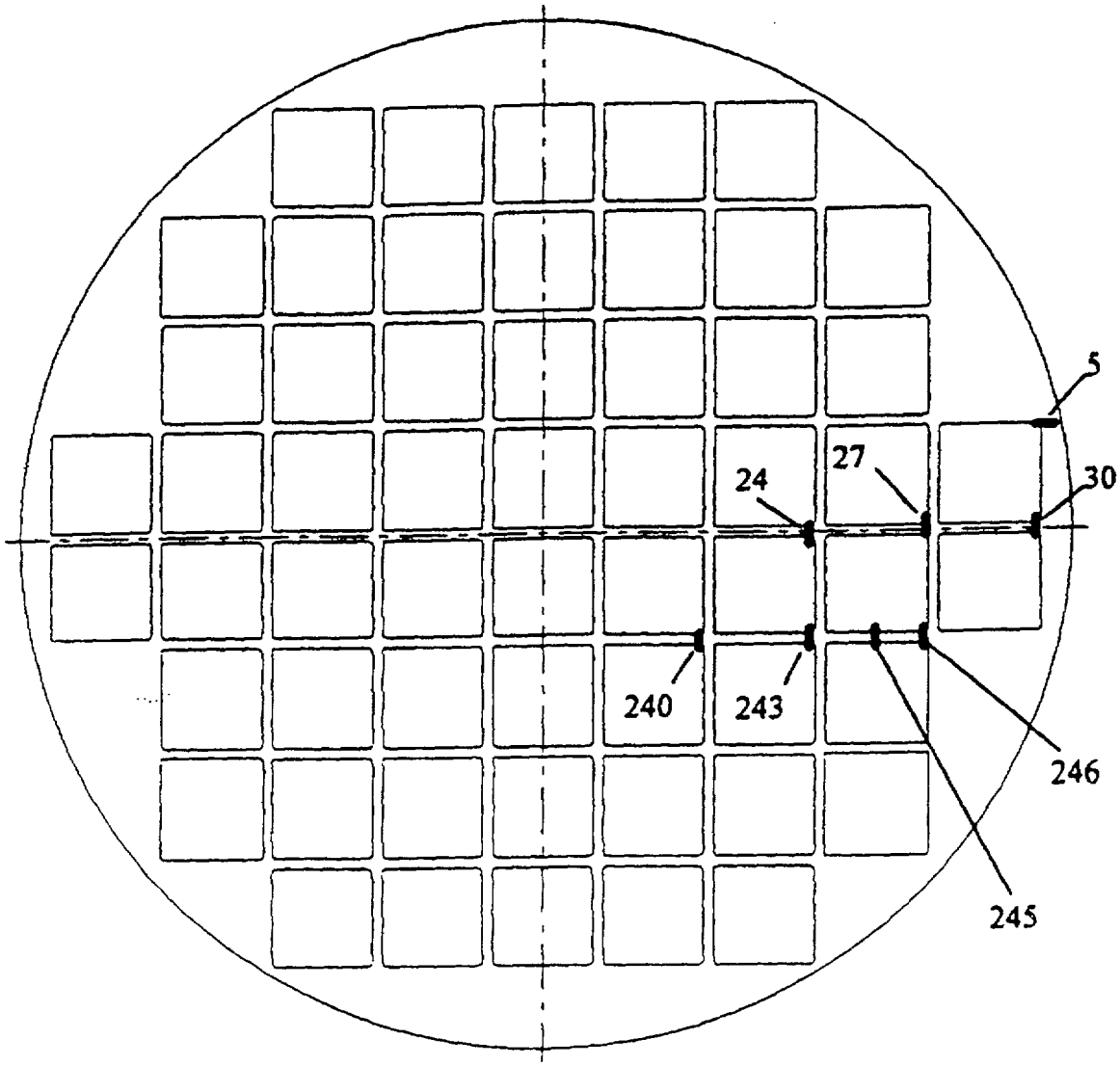

Figure 2.6.15.6-10 Locations of Maximum Linearized Stress Intensities - 90° Drop Orientation

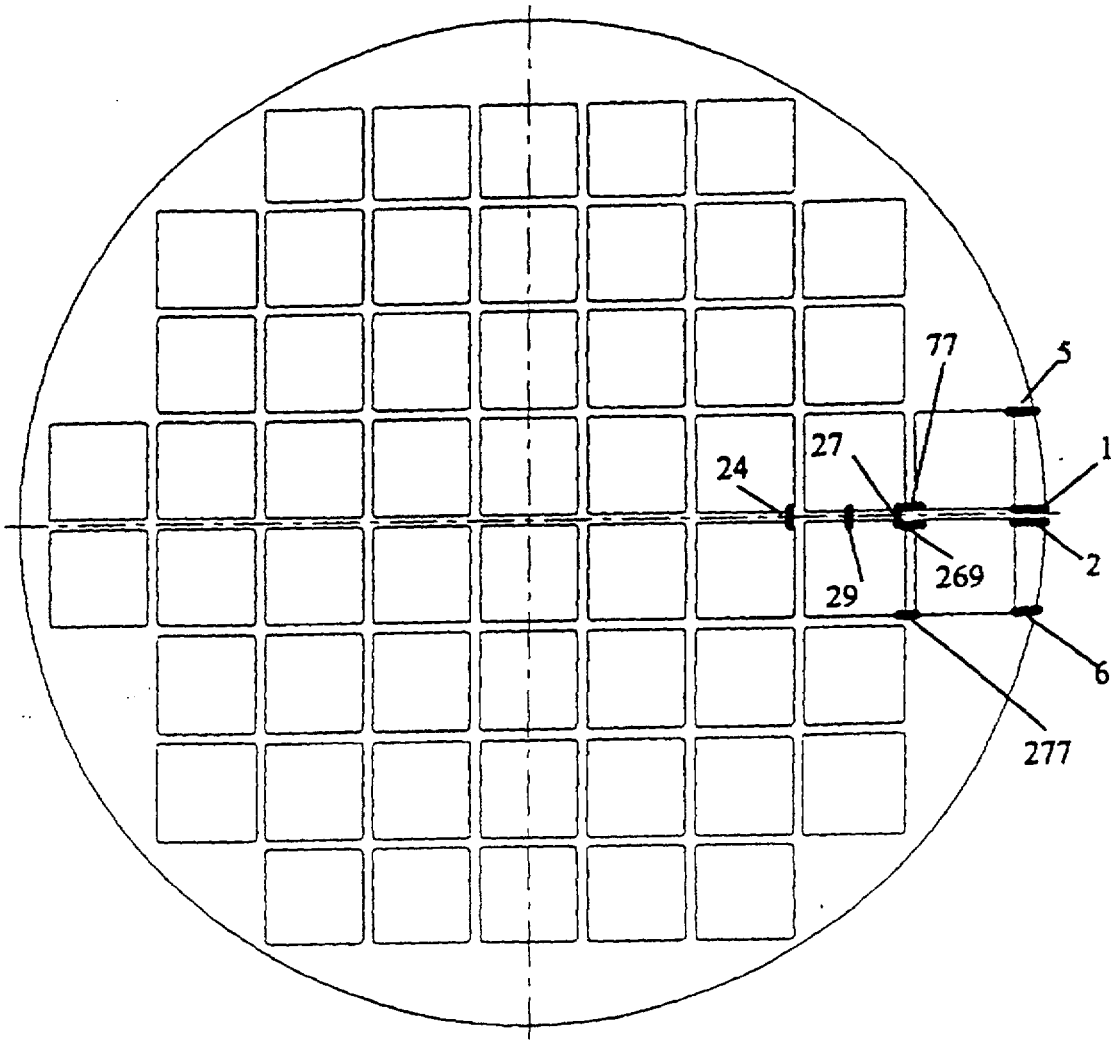

Table 2.6.15.6-1 Listing of Cross Sections for Stress Evaluation of Support Disk

Section & Line #	Point 1	Point 2	Node 1	Node 2	X 1	Y 1	X 2	Y 2
1	1	2	4724	4725	32.74	0.33	30.85	0.33
2	3	4	4726	4727	32.74	-0.33	30.85	-0.33
3	5	6	4728	4729	-32.74	0.33	-30.85	0.33
4	7	8	4730	4731	-32.74	-0.33	-30.85	-0.33
5	9	10	4732	4733	32.07	6.6	30.85	6.6
6	11	12	4734	4735	32.07	-6.6	30.85	-6.6
7	13	14	4736	4737	-32.07	6.6	-30.85	6.6
8	15	16	4738	4739	-32.07	-6.6	-30.85	-6.6
9	17	18	4740	4741	25.57	20.46	23.89	20.46
10	19	20	4742	4743	25.57	-20.46	23.89	-20.46
11	21	22	4744	4745	-25.57	20.46	-23.89	20.46
12	23	24	4746	4747	-25.57	-20.46	-23.89	-20.46
13	25	26	4748	4749	17	27.99	17	27.39
14	27	28	4750	4751	-17	27.99	-17	27.39
15	29	30	4752	4753	-17	-27.99	-17	-27.39
16	31	32	4754	4755	17	-27.99	17	-27.39
17	33	34	4756	4757	0	0.33	0	-0.33
18	35	36	4758	4759	3.14	0.33	3.14	-0.33
19	37	38	4760	4761	3.79	0.33	3.79	-0.33
20	39	40	4762	4763	6.93	0.33	6.93	-0.33
21	41	42	4764	4765	10.07	0.33	10.07	-0.33
22	43	44	4766	4767	10.72	0.33	10.72	-0.33
23	45	46	4768	4769	13.86	0.33	13.86	-0.33
24	47	48	4770	4771	17	0.33	17	-0.33
25	49	50	4772	4773	17.65	0.33	17.65	-0.33
26	51	52	4774	4775	20.78	0.33	20.78	-0.33
27	53	54	4776	4777	23.92	0.33	23.92	-0.33
28	55	56	4778	4779	24.57	0.33	24.57	-0.33
29	57	58	4780	4781	27.71	0.33	27.71	-0.33
30	59	60	4782	4783	30.85	0.33	30.85	-0.33
31	61	62	4784	4785	-3.14	0.33	-3.14	-0.33
32	63	64	4786	4787	-3.79	0.33	-3.79	-0.33
33	65	66	4788	4789	-6.93	0.33	-6.93	-0.33
34	67	68	4790	4791	-10.07	0.33	-10.07	-0.33
35	69	70	4792	4793	-10.72	0.33	-10.72	-0.33
36	71	72	4794	4795	-13.86	0.33	-13.86	-0.33
37	73	74	4796	4797	-17	0.33	-17	-0.33
38	75	76	4798	4799	-17.65	0.33	-17.65	-0.33
39	77	78	4800	4801	-20.78	0.33	-20.78	-0.33

Table 2.6.15.6-1 Listing of Cross Sections for Stress Evaluation of Support Disk (Continued)

Section & Line #	Point 1	Point 2	Node 1	Node 2	X 1	Y 1	X 2	Y 2
40	79	80	4802	4803	-23.92	0.33	-23.92	-0.33
41	81	82	4804	4805	-24.57	0.33	-24.57	-0.33
42	83	84	4806	4807	-27.71	0.33	-27.71	-0.33
43	85	86	4808	4809	-30.85	0.33	-30.85	-0.33
44	87	88	4810	4811	0	7.25	0	6.6
45	89	90	4812	4813	3.14	7.25	3.14	6.6
46	91	92	4814	4815	3.79	7.25	3.79	6.6
47	93	94	4816	4817	6.93	7.25	6.93	6.6
48	95	96	4818	4819	10.07	7.25	10.07	6.6
49	97	98	4820	4821	10.72	7.25	10.72	6.6
50	99	100	4822	4823	13.86	7.25	13.86	6.6
51	101	102	4824	4825	17	7.25	17	6.6
52	103	104	4826	4827	17.65	7.25	17.65	6.6
53	105	106	4828	4829	20.78	7.25	20.78	6.6
54	107	108	4830	4831	23.92	7.25	23.92	6.6
55	109	110	4832	4833	0	13.53	0	14.18
56	111	112	4834	4835	3.14	13.53	3.14	14.18
57	113	114	4836	4837	3.79	13.53	3.79	14.18
58	115	116	4838	4839	6.93	13.53	6.93	14.18
59	117	118	4840	4841	10.07	13.53	10.07	14.18
60	119	120	4842	4843	10.72	13.53	10.72	14.18
61	121	122	4844	4845	13.86	13.53	13.86	14.18
62	123	124	4846	4847	17	13.53	17	14.18
63	125	126	4848	4849	17.65	13.53	17.65	14.18
64	127	128	4850	4851	20.78	13.53	20.78	14.18
65	129	130	4852	4853	23.92	13.53	23.92	14.18
66	131	132	4854	4855	0	21.11	0	20.46
67	133	134	4856	4857	3.14	21.11	3.14	20.46
68	135	136	4858	4859	3.79	21.11	3.79	20.46
69	137	138	4860	4861	6.93	21.11	6.93	20.46
70	139	140	4862	4863	10.07	21.11	10.07	20.46
71	141	142	4864	4865	10.72	21.11	10.72	20.46
72	143	144	4866	4867	13.86	21.11	13.86	20.46
73	145	146	4868	4869	17	21.11	17	20.46
74	147	148	4870	4871	3.14	0.33	3.79	0.33
75	149	150	4872	4873	10.07	0.33	10.72	0.33
76	151	152	4874	4875	17	0.33	17.65	0.33
77	153	154	4876	4877	23.92	0.33	24.57	0.33

Table 2.6.15.6-1 Listing of Cross Sections for Stress Evaluation of Support Disk (Continued)

Section & Line #	Point 1	Point 2	Node 1	Node 2	X 1	Y 1	X 2	Y 2
78	155	156	4878	4879	3.14	3.46	3.79	3.46
79	157	158	4880	4881	10.07	3.46	10.72	3.46
80	159	160	4882	4883	17	3.46	17.65	3.46
81	161	162	4884	4885	23.92	3.46	24.57	3.46
82	163	164	4886	4887	3.14	6.6	3.79	6.6
83	165	166	4888	4889	10.07	6.6	10.72	6.6
84	167	168	4890	4891	17	6.6	17.65	6.6
85	169	170	4892	4893	23.92	6.6	24.57	6.6
86	171	172	4894	4895	3.14	7.25	3.79	7.25
87	173	174	4896	4897	10.07	7.25	10.72	7.25
88	175	176	4898	4899	17	7.25	17.65	7.25
89	177	178	4900	4901	3.14	10.39	3.79	10.39
90	179	180	4902	4903	10.07	10.39	10.72	10.39
91	181	182	4904	4905	17	10.39	17.65	10.39
92	183	184	4906	4907	3.14	13.53	3.79	13.53
93	185	186	4908	4909	10.07	13.53	10.72	13.53
94	187	188	4910	4911	17	13.53	17.65	13.53
95	189	190	4912	4913	3.14	14.18	3.79	14.18
96	191	192	4914	4915	10.07	14.18	10.72	14.18
97	193	194	4916	4917	17	14.18	17.65	14.18
98	195	196	4918	4919	3.14	17.32	3.79	17.32
99	197	198	4920	4921	10.07	17.32	10.72	17.32
100	199	200	4922	4923	17	17.32	17.65	17.32
101	201	202	4924	4925	3.14	20.46	3.79	20.46
102	203	204	4926	4927	10.07	20.46	10.72	20.46
103	205	206	4928	4929	17	20.46	17.65	20.46
104	207	208	4930	4931	3.14	21.11	3.79	21.11
105	209	210	4932	4933	10.07	21.11	10.72	21.11
106	211	212	4934	4935	3.14	24.25	3.79	24.25
107	213	214	4936	4937	10.07	24.25	10.72	24.25
108	215	216	4938	4939	3.14	27.39	3.79	27.39
109	217	218	4940	4941	10.07	27.39	10.72	27.39
110	219	220	4942	4943	-3.14	7.25	-3.14	6.6
111	221	222	4944	4945	-3.79	7.25	-3.79	6.6
112	223	224	4946	4947	-6.93	7.25	-6.93	6.6
113	225	226	4948	4949	-10.07	7.25	-10.07	6.6
114	227	228	4950	4951	-10.72	7.25	-10.72	6.6
115	229	230	4952	4953	-13.86	7.25	-13.86	6.6

Table 2.6.15.6-1 Listing of Cross Sections for Stress Evaluation of Support Disk (Continued)

Section & Line #	Point 1	Point 2	Node 1	Node 2	X 1	Y 1	X 2	Y 2
116	231	232	4954	4955	-17	7.25	-17	6.6
117	233	234	4956	4957	-17.65	7.25	-17.65	6.6
118	235	236	4958	4959	-20.78	7.25	-20.78	6.6
119	237	238	4960	4961	-23.92	7.25	-23.92	6.6
120	239	240	4962	4963	-3.14	13.53	-3.14	14.18
121	241	242	4964	4965	-3.79	13.53	-3.79	14.18
122	243	244	4966	4967	-6.93	13.53	-6.93	14.18
123	245	246	4968	4969	-10.07	13.53	-10.07	14.18
124	247	248	4970	4971	-10.72	13.53	-10.72	14.18
125	249	250	4972	4973	-13.86	13.53	-13.86	14.18
126	251	252	4974	4975	-17	13.53	-17	14.18
127	253	254	4976	4977	-17.65	13.53	-17.65	14.18
128	255	256	4978	4979	-20.78	13.53	-20.78	14.18
129	257	258	4980	4981	-23.92	13.53	-23.92	14.18
130	259	260	4982	4983	-3.14	21.11	-3.14	20.46
131	261	262	4984	4985	-3.79	21.11	-3.79	20.46
132	263	264	4986	4987	-6.93	21.11	-6.93	20.46
133	265	266	4988	4989	-10.07	21.11	-10.07	20.46
134	267	268	4990	4991	-10.72	21.11	-10.72	20.46
135	269	270	4992	4993	-13.86	21.11	-13.86	20.46
136	271	272	4994	4995	-17	21.11	-17	20.46
137	273	274	4996	4997	-3.14	0.33	-3.79	0.33
138	275	276	4998	4999	-10.07	0.33	-10.72	0.33
139	277	278	5000	5001	-17	0.33	-17.65	0.33
140	279	280	5002	5003	-23.92	0.33	-24.57	0.33
141	281	282	5004	5005	-3.14	3.46	-3.79	3.46
142	283	284	5006	5007	-10.07	3.46	-10.72	3.46
143	285	286	5008	5009	-17	3.46	-17.65	3.46
144	287	288	5010	5011	-23.92	3.46	-24.57	3.46
145	289	290	5012	5013	-3.14	6.6	-3.79	6.6
146	291	292	5014	5015	-10.07	6.6	-10.72	6.6
147	293	294	5016	5017	-17	6.6	-17.65	6.6
148	295	296	5018	5019	-23.92	6.6	-24.57	6.6
149	297	298	5020	5021	-3.14	7.25	-3.79	7.25
150	299	300	5022	5023	-10.07	7.25	-10.72	7.25
151	301	302	5024	5025	-17	7.25	-17.65	7.25
152	303	304	5026	5027	-3.14	10.39	-3.79	10.39
153	305	306	5028	5029	-10.07	10.39	-10.72	10.39

Table 2.6.15.6-1 Listing of Cross Sections for Stress Evaluation of Support Disk (Continued)

Section & Line #	Point 1	Point 2	Node 1	Node 2	X 1	Y 1	X 2	Y 2
154	307	308	5030	5031	-17	10.39	-17.65	10.39
155	309	310	5032	5033	-3.14	13.53	-3.79	13.53
156	311	312	5034	5035	-10.07	13.53	-10.72	13.53
157	313	314	5036	5037	-17	13.53	-17.65	13.53
158	315	316	5038	5039	-3.14	14.18	-3.79	14.18
159	317	318	5040	5041	-10.07	14.18	-10.72	14.18
160	319	320	5042	5043	-17	14.18	-17.65	14.18
161	321	322	5044	5045	-3.14	17.32	-3.79	17.32
162	323	324	5046	5047	-10.07	17.32	-10.72	17.32
163	325	326	5048	5049	-17	17.32	-17.65	17.32
164	327	328	5050	5051	-3.14	20.46	-3.79	20.46
165	329	330	5052	5053	-10.07	20.46	-10.72	20.46
166	331	332	5054	5055	-17	20.46	-17.65	20.46
167	333	334	5056	5057	-3.14	21.11	-3.79	21.11
168	335	336	5058	5059	-10.07	21.11	-10.72	21.11
169	337	338	5060	5061	-3.14	24.25	-3.79	24.25
170	339	340	5062	5063	-10.07	24.25	-10.72	24.25
171	341	342	5064	5065	-3.14	27.39	-3.79	27.39
172	343	344	5066	5067	-10.07	27.39	-10.72	27.39
173	345	346	5068	5069	-3.14	-7.25	-3.14	-6.6
174	347	348	5070	5071	-3.79	-7.25	-3.79	-6.6
175	349	350	5072	5073	-6.93	-7.25	-6.93	-6.6
176	351	352	5074	5075	-10.07	-7.25	-10.07	-6.6
177	353	354	5076	5077	-10.72	-7.25	-10.72	-6.6
178	355	356	5078	5079	-13.86	-7.25	-13.86	-6.6
179	357	358	5080	5081	-17	-7.25	-17	-6.6
180	359	360	5082	5083	-17.65	-7.25	-17.65	-6.6
181	361	362	5084	5085	-20.78	-7.25	-20.78	-6.6
182	363	364	5086	5087	-23.92	-7.25	-23.92	-6.6
183	365	366	5088	5089	-3.14	-13.53	-3.14	-14.18
184	367	368	5090	5091	-3.79	-13.53	-3.79	-14.18
185	369	370	5092	5093	-6.93	-13.53	-6.93	-14.18
186	371	372	5094	5095	-10.07	-13.53	-10.07	-14.18
187	373	374	5096	5097	-10.72	-13.53	-10.72	-14.18
188	375	376	5098	5099	-13.86	-13.53	-13.86	-14.18
189	377	378	5100	5101	-17	-13.53	-17	-14.18
190	379	380	5102	5103	-17.65	-13.53	-17.65	-14.18
191	381	382	5104	5105	-20.78	-13.53	-20.78	-14.18

Table 2.6.15.6-1 Listing of Cross Sections for Stress Evaluation of Support Disk (Continued)

Section & Line #	Point 1	Point 2	Node 1	Node 2	X 1	Y 1	X 2	Y 2
192	383	384	5106	5107	-23.92	-13.53	-23.92	-14.18
193	385	386	5108	5109	-3.14	-21.11	-3.14	-20.46
194	387	388	5110	5111	-3.79	-21.11	-3.79	-20.46
195	389	390	5112	5113	-6.93	-21.11	-6.93	-20.46
196	391	392	5114	5115	-10.07	-21.11	-10.07	-20.46
197	393	394	5116	5117	-10.72	-21.11	-10.72	-20.46
198	395	396	5118	5119	-13.86	-21.11	-13.86	-20.46
199	397	398	5120	5121	-17	-21.11	-17	-20.46
200	399	400	5122	5123	-3.14	-0.33	-3.79	-0.33
201	401	402	5124	5125	-10.07	-0.33	-10.72	-0.33
202	403	404	5126	5127	-17	-0.33	-17.65	-0.33
203	405	406	5128	5129	-23.92	-0.33	-24.57	-0.33
204	407	408	5130	5131	-3.14	-3.46	-3.79	-3.46
205	409	410	5132	5133	-10.07	-3.46	-10.72	-3.46
206	411	412	5134	5135	-17	-3.46	-17.65	-3.46
207	413	414	5136	5137	-23.92	-3.46	-24.57	-3.46
208	415	416	5138	5139	-3.14	-6.6	-3.79	-6.6
209	417	418	5140	5141	-10.07	-6.6	-10.72	-6.6
210	419	420	5142	5143	-17	-6.6	-17.65	-6.6
211	421	422	5144	5145	-23.92	-6.6	-24.57	-6.6
212	423	424	5146	5147	-3.14	-7.25	-3.79	-7.25
213	425	426	5148	5149	-10.07	-7.25	-10.72	-7.25
214	427	428	5150	5151	-17	-7.25	-17.65	-7.25
215	429	430	5152	5153	-3.14	-10.39	-3.79	-10.39
216	431	432	5154	5155	-10.07	-10.39	-10.72	-10.39
217	433	434	5156	5157	-17	-10.39	-17.65	-10.39
218	435	436	5158	5159	-3.14	-13.53	-3.79	-13.53
219	437	438	5160	5161	-10.07	-13.53	-10.72	-13.53
220	439	440	5162	5163	-17	-13.53	-17.65	-13.53
221	441	442	5164	5165	-3.14	-14.18	-3.79	-14.18
222	443	444	5166	5167	-10.07	-14.18	-10.72	-14.18
223	445	446	5168	5169	-17	-14.18	-17.65	-14.18
224	447	448	5170	5171	-3.14	-17.32	-3.79	-17.32
225	449	450	5172	5173	-10.07	-17.32	-10.72	-17.32
226	451	452	5174	5175	-17	-17.32	-17.65	-17.32
227	453	454	5176	5177	-3.14	-20.46	-3.79	-20.46
228	455	456	5178	5179	-10.07	-20.46	-10.72	-20.46
229	457	458	5180	5181	-17	-20.46	-17.65	-20.46

Table 2.6.15.6-1 Listing of Cross Sections for Stress Evaluation of Support Disk (Continued)

Section & Line #	Point 1	Point 2	Node 1	Node 2	X 1	Y 1	X 2	Y 2
230	459	460	5182	5183	-3.14	-21.11	-3.79	-21.11
231	461	462	5184	5185	-10.07	-21.11	-10.72	-21.11
232	463	464	5186	5187	-3.14	-24.25	-3.79	-24.25
233	465	466	5188	5189	-10.07	-24.25	-10.72	-24.25
234	467	468	5190	5191	-3.14	-27.39	-3.79	-27.39
235	469	470	5192	5193	-10.07	-27.39	-10.72	-27.39
236	471	472	5194	5195	0	-7.25	0	-6.6
237	473	474	5196	5197	3.14	-7.25	3.14	-6.6
238	475	476	5198	5199	3.79	-7.25	3.79	-6.6
239	477	478	5200	5201	6.93	-7.25	6.93	-6.6
240	479	480	5202	5203	10.07	-7.25	10.07	-6.6
241	481	482	5204	5205	10.72	-7.25	10.72	-6.6
242	483	484	5206	5207	13.86	-7.25	13.86	-6.6
243	485	486	5208	5209	17	-7.25	17	-6.6
244	487	488	5210	5211	17.65	-7.25	17.65	-6.6
245	489	490	5212	5213	20.78	-7.25	20.78	-6.6
246	491	492	5214	5215	23.92	-7.25	23.92	-6.6
247	493	494	5216	5217	0	-13.53	0	-14.18
248	495	496	5218	5219	3.14	-13.53	3.14	-14.18
249	497	498	5220	5221	3.79	-13.53	3.79	-14.18
250	499	500	5222	5223	6.93	-13.53	6.93	-14.18
251	501	502	5224	5225	10.07	-13.53	10.07	-14.18
252	503	504	5226	5227	10.72	-13.53	10.72	-14.18
253	505	506	5228	5229	13.86	-13.53	13.86	-14.18
254	507	508	5230	5231	17	-13.53	17	-14.18
255	509	510	5232	5233	17.65	-13.53	17.65	-14.18
256	511	512	5234	5235	20.78	-13.53	20.78	-14.18
257	513	514	5236	5237	23.92	-13.53	23.92	-14.18
258	515	516	5238	5239	0	-21.11	0	-20.46
259	517	518	5240	5241	3.14	-21.11	3.14	-20.46
260	519	520	5242	5243	3.79	-21.11	3.79	-20.46
261	521	522	5244	5245	6.93	-21.11	6.93	-20.46
262	523	524	5246	5247	10.07	-21.11	10.07	-20.46
263	525	526	5248	5249	10.72	-21.11	10.72	-20.46
264	527	528	5250	5251	13.86	-21.11	13.86	-20.46
265	529	530	5252	5253	17	-21.11	17	-20.46
266	531	532	5254	5255	3.14	-0.33	3.79	-0.33
267	533	534	5256	5257	10.07	-0.33	10.72	-0.33

Table 2.6.15.6-1 Listing of Cross Sections for Stress Evaluation of Support Disk (Continued)

Section & Line #	Point 1	Point 2	Node 1	Node 2	X 1	Y 1	X 2	Y 2
268	535	536	5258	5259	17	-0.33	17.65	-0.33
269	537	538	5260	5261	23.92	-0.33	24.57	-0.33
270	539	540	5262	5263	3.14	-3.46	3.79	-3.46
271	541	542	5264	5265	10.07	-3.46	10.72	-3.46
272	543	544	5266	5267	17	-3.46	17.65	-3.46
273	545	546	5268	5269	23.92	-3.46	24.57	-3.46
274	547	548	5270	5271	3.14	-6.6	3.79	-6.6
275	549	550	5272	5273	10.07	-6.6	10.72	-6.6
276	551	552	5274	5275	17	-6.6	17.65	-6.6
277	553	554	5276	5277	23.92	-6.6	24.57	-6.6
278	555	556	5278	5279	3.14	-7.25	3.79	-7.25
279	557	558	5280	5281	10.07	-7.25	10.72	-7.25
280	559	560	5282	5283	17	-7.25	17.65	-7.25
281	561	562	5284	5285	3.14	-10.39	3.79	-10.39
282	563	564	5286	5287	10.07	-10.39	10.72	-10.39
283	565	566	5288	5289	17	-10.39	17.65	-10.39
284	567	568	5290	5291	3.14	-13.53	3.79	-13.53
285	569	570	5292	5293	10.07	-13.53	10.72	-13.53
286	571	572	5294	5295	17	-13.53	17.65	-13.53
287	573	574	5296	5297	3.14	-14.18	3.79	-14.18
288	575	576	5298	5299	10.07	-14.18	10.72	-14.18
289	577	578	5300	5301	17	-14.18	17.65	-14.18
290	579	580	5302	5303	3.14	-17.32	3.79	-17.32
291	581	582	5304	5305	10.07	-17.32	10.72	-17.32
292	583	584	5306	5307	17	-17.32	17.65	-17.32
293	585	586	5308	5309	3.14	-20.46	3.79	-20.46
294	587	588	5310	5311	10.07	-20.46	10.72	-20.46
295	589	590	5312	5313	17	-20.46	17.65	-20.46
296	591	592	5314	5315	3.14	-21.11	3.79	-21.11
297	593	594	5316	5317	10.07	-21.11	10.72	-21.11
298	595	596	5318	5319	3.14	-24.25	3.79	-24.25
299	597	598	5320	5321	10.07	-24.25	10.72	-24.25
300	599	600	5322	5323	3.14	-27.39	3.79	-27.39
301	601	602	5324	5325	10.07	-27.39	10.72	-27.39

Table 2.6.15.6-2 P_m Stresses for Support Disk—1-Foot Side-Drop, 0° Orientation, Thermal Case 1

	P_m Stresses (ksi)					
Section	Sx	Sy	Sxy	Stress Intensity (ksi)	Allowable Stress (ksi)	Margin of Safety
300	10.6	-10.0	-.9	20.7	30.0	.45
234	8.8	-9.8	1.8	18.9	30.0	.58
293	6.9	-11.4	.1	18.3	30.0	.64
227	6.5	-11.0	.0	17.5	30.0	.72
298	-.1	-16.8	.2	16.8	30.0	.78
232	-.1	-16.2	-.3	16.2	30.0	.85
290	-.1	-14.9	.1	14.9	30.0	1.02
284	4.7	-10.0	-.1	14.7	30.0	1.04
224	-.1	-14.3	-.1	14.3	30.0	1.09
218	4.5	-9.6	.3	14.1	30.0	1.13
294	6.1	-7.7	.0	13.9	30.0	1.16
260	4.6	-8.0	-2.0	13.3	30.0	1.25
296	-1.6	-13.3	-.4	13.3	30.0	1.26
194	4.5	-8.0	2.1	13.2	30.0	1.27
281	-.1	-13.1	.1	13.1	30.0	1.29
228	5.7	-7.2	.1	13.0	30.0	1.31
301	3.7	-7.6	-3.2	13.0	30.0	1.31
230	-1.3	-12.7	.7	12.8	30.0	1.35
235	2.9	-7.3	3.7	12.6	30.0	1.38
215	-.1	-12.6	-.1	12.6	30.0	1.38

Table 2.6.15.6-3 $P_m + P_b$ Stresses for Support Disk—1-Foot Side-Drop, 0° Orientation, Thermal Case 1

	$P_m + P_b$ Stresses (ksi)					
Section	Sx	Sy	Sxy	Stress Intensity (ksi)	Allowable Stress (ksi)	Margin of Safety
234	8.2	-14.4	4.6	24.5	45.0	.84
300	10.5	-12.1	-3.7	23.8	45.0	.89
235	1.2	-18.4	5.7	22.6	45.0	.99
301	2.3	-17.3	-5.3	22.3	45.0	1.02
15	-13.0	-10.6	8.0	19.9	45.0	1.26
16	-12.5	-10.7	-7.9	19.6	45.0	1.30
231	-8.0	-17.8	3.5	18.9	45.0	1.38
293	8.3	-10.5	.4	18.8	45.0	1.40
297	-7.2	-17.3	-3.5	18.4	45.0	1.45
227	9.5	-8.7	-.3	18.2	45.0	1.48
230	-4.7	-16.9	3.6	17.9	45.0	1.51
298	-.2	-17.5	.1	17.5	45.0	1.57
232	-.3	-17.5	-.2	17.5	45.0	1.57
260	11.4	-5.4	-.9	16.8	45.0	1.67
194	12.5	-3.8	.9	16.5	45.0	1.73
296	-3.3	-15.4	-3.5	16.4	45.0	1.75
259	8.4	-7.2	.9	15.7	45.0	1.86
197	-7.0	-14.2	3.1	15.3	45.0	1.94
290	-.1	-15.0	.1	15.0	45.0	2.00
294	11.4	-3.5	-.2	14.9	45.0	2.01

Table 2.6.15.6-4 P_m Stresses for Support Disk—1-Foot Side-Drop, 0° Orientation, Thermal Case 2

	P_m Stresses (ksi)					
Section	Sx	Sy	Sxy	Stress Intensity (ksi)	Allowable Stress (ksi)	Margin of Safety
300	10.5	-9.8	-.8	20.4	30.0	.47
234	8.5	-9.6	1.8	18.4	30.0	.63
293	6.8	-11.2	.1	18.1	30.0	.66
227	6.4	-10.8	.0	17.2	30.0	.74
298	-.1	-16.6	.1	16.6	30.0	.81
232	-.1	-15.9	-.3	15.9	30.0	.89
290	-.1	-14.7	.1	14.7	30.0	1.04
284	4.7	-9.8	-.1	14.5	30.0	1.07
224	-.1	-14.1	-.1	14.1	30.0	1.13
294	6.2	-7.8	.0	14.0	30.0	1.15
218	4.4	-9.4	.2	13.8	30.0	1.17
260	4.6	-7.9	-2.0	13.2	30.0	1.28
296	-1.6	-13.1	-.4	13.1	30.0	1.29
301	3.8	-7.6	-3.2	13.1	30.0	1.29
228	5.8	-7.3	.1	13.1	30.0	1.30
194	4.5	-7.9	2.0	13.1	30.0	1.30
281	-.1	-12.9	.1	12.9	30.0	1.33
235	3.1	-7.3	3.6	12.7	30.0	1.37
230	-1.2	-12.5	.7	12.6	30.0	1.39
215	-.1	-12.4	-.1	12.4	30.0	1.43

Table 2.6.15.6-5 $P_m + P_b$ Stresses for Support Disk—1-Foot Side-Drop, 0° Orientation, Thermal Case 2

	$P_m + P_b$ Stresses (ksi)					
Section	Sx	Sy	Sxy	Stress Intensity (ksi)	Allowable Stress (ksi)	Margin of Safety
234	7.9	-14.2	4.5	23.9	45.0	.88
300	10.4	-11.9	-3.5	23.3	45.0	.93
235	1.4	-18.2	5.6	22.6	45.0	1.00
301	2.4	-17.2	-5.3	22.3	45.0	1.01
15	-13.0	-10.7	8.1	20.0	45.0	1.25
16	-12.6	-10.8	-8.0	19.7	45.0	1.29
231	-7.9	-17.7	3.5	18.8	45.0	1.40
293	8.1	-10.4	.3	18.5	45.0	1.43
297	-7.2	-17.2	-3.5	18.3	45.0	1.45
227	9.3	-8.6	-.3	17.9	45.0	1.52
230	-4.5	-16.6	3.5	17.6	45.0	1.56
298	-.2	-17.3	.1	17.3	45.0	1.61
232	-.3	-17.2	-.2	17.2	45.0	1.61
260	11.2	-5.3	-.9	16.6	45.0	1.70
194	12.3	-3.8	.9	16.2	45.0	1.78
296	-3.1	-15.1	-3.5	16.1	45.0	1.80
259	8.4	-7.1	.9	15.6	45.0	1.88
197	-6.9	-14.1	3.1	15.2	45.0	1.96
294	11.4	-3.6	-.2	15.0	45.0	2.00
290	-.1	-14.8	.1	14.8	45.0	2.04

Table 2.6.15.6-6 P_m Stresses for Support Disk—1-Foot Side-Drop, 31.82° Orientation, Thermal Case 1

	P_m Stresses (ksi)					
Section	Sx	Sy	Sxy	Stress Intensity (ksi)	Allowable Stress (ksi)	Margin of Safety
295	3.6	-10.4	6.7	19.4	30.0	.54
277	9.6	-9.2	2.0	19.3	30.0	.56
229	-11.0	4.3	5.0	18.2	30.0	.65
301	6.0	-6.6	6.2	17.7	30.0	.69
300	.6	-5.5	7.7	16.6	30.0	.81
77	7.8	-8.1	.9	16.1	30.0	.87
235	-4.9	-2.6	7.5	15.2	30.0	.97
234	-3.7	-4.4	7.5	15.0	30.0	1.00
265	-4.6	5.6	5.0	14.3	30.0	1.10
257	-.2	-2.2	6.7	13.7	30.0	1.20
273	-.1	-13.3	-.5	13.3	30.0	1.25
299	-.1	-12.9	-.9	13.0	30.0	1.31
263	-7.1	-12.6	.2	12.6	30.0	1.38
294	-.1	-8.4	4.7	12.5	30.0	1.40
73	-.1	-6.1	5.0	11.7	30.0	1.57
291	.0	-11.3	-1.4	11.6	30.0	1.59
76	6.2	-4.2	2.6	11.6	30.0	1.59
103	-8.7	-.2	3.9	11.5	30.0	1.60
292	-.1	-11.3	-1.2	11.5	30.0	1.61
276	4.3	-5.6	2.8	11.3	30.0	1.65

Table 2.6.15.6-7 $P_m + P_b$ Stresses for Support Disks—1-Foot Side-Drop, 31.82° Orientation, Thermal Case 1

Section	Sx	Sy	Sxy	Stress Intensity (ksi)	Allowable Stress (ksi)	Margin of Safety
295	-6.9	-35.9	7.8	37.8	45.0	.19
294	-19.0	-34.8	6.2	37.0	45.0	.22
293	-22.7	-33.6	5.7	36.1	45.0	.25
267	-25.7	-31.9	5.9	35.4	45.0	.27
266	-25.7	-31.8	5.2	34.8	45.0	.29
288	-26.3	-31.0	5.2	34.4	45.0	.31
274	-23.3	-32.2	4.0	33.7	45.0	.34
251	-28.9	-27.0	5.3	33.4	45.0	.35
275	-20.4	-32.0	3.8	33.1	45.0	.36
227	-23.4	-30.3	5.2	33.0	45.0	.36
287	-26.0	-30.2	4.3	32.9	45.0	.37
260	-24.9	-28.7	5.0	32.1	45.0	.40
284	-23.3	-30.4	3.7	31.9	45.0	.41
248	-28.2	-26.8	4.3	31.9	45.0	.41
74	-22.8	-30.0	3.9	31.7	45.0	.42
200	-24.7	-28.8	4.4	31.6	45.0	.42
254	-27.2	-23.3	6.0	31.5	45.0	.43
301	2.1	-24.1	8.7	31.5	45.0	.43
268	-24.2	-25.7	6.3	31.3	45.0	.44
289	-24.1	-26.8	5.7	31.3	45.0	.44

Table 2.6.15.6-8 P_m Stresses for Support Disk—1-Foot Side-Drop, 31.82° Orientation, Thermal Case 2

Section	Sx	Sy	Sxy	Stress Intensity (ksi)	Allowable Stress (ksi)	Margin of Safety
277	9.3	-8.9	2.2	18.7	30.0	.60
295	3.5	-9.8	6.5	18.6	30.0	.61
229	-10.8	4.1	4.9	17.8	30.0	.69
301	6.1	-6.5	5.9	17.2	30.0	.74
300	1.4	-5.5	7.6	16.6	30.0	.81
77	7.6	-7.8	1.0	15.6	30.0	.93
235	-4.8	-2.8	7.5	15.1	30.0	.98
234	-3.3	-4.6	7.4	14.9	30.0	1.01
265	-4.3	5.5	4.7	13.6	30.0	1.20
257	-.3	-1.4	6.7	13.4	30.0	1.24
273	-.1	-12.9	-.5	12.9	30.0	1.33
299	-.1	-12.7	-.9	12.7	30.0	1.36
294	.1	-8.2	4.5	12.3	30.0	1.44
263	-6.6	-12.2	.1	12.2	30.0	1.46
103	-8.4	-.1	3.9	11.5	30.0	1.62
73	-.2	-6.0	4.9	11.3	30.0	1.65
291	.0	-11.0	-1.3	11.3	30.0	1.66
269	-8.9	-10.2	1.4	11.1	30.0	1.70
76	5.8	-3.9	2.5	10.9	30.0	1.76
292	-.1	-10.6	-1.1	10.8	30.0	1.78

Table 2.6.15.6-9 $P_m + P_b$ Stresses for Support Disk—1-Foot Side-Drop, 31.82° Orientation, Thermal Case 2

Section	Sx	Sy	Sxy	Stress Intensity (ksi)	Allowable Stress (ksi)	Margin of Safety
295	-6.6	-34.3	7.5	36.2	45.0	.24
294	-17.9	-33.5	5.9	35.5	45.0	.27
293	-21.6	-32.6	5.4	34.9	45.0	.29
267	-24.9	-30.9	5.7	34.3	45.0	.31
266	-24.4	-30.5	5.0	33.3	45.0	.35
288	-25.3	-29.6	5.0	32.9	45.0	.37
274	-22.4	-31.3	3.9	32.8	45.0	.37
275	-19.9	-31.3	3.8	32.5	45.0	.39
227	-22.5	-29.7	5.0	32.2	45.0	.40
251	-27.9	-25.8	5.2	32.1	45.0	.40
287	-25.2	-29.2	4.2	31.9	45.0	.41
248	-27.4	-25.9	4.3	31.0	45.0	.45
234	-8.1	-27.2	9.4	31.0	45.0	.45
284	-22.3	-29.5	3.6	31.0	45.0	.45
260	-23.5	-27.8	4.7	30.8	45.0	.46
268	-23.7	-25.1	6.1	30.6	45.0	.47
200	-23.8	-27.7	4.3	30.5	45.0	.48
74	-21.7	-28.8	3.7	30.4	45.0	.48
301	2.3	-23.2	8.3	30.4	45.0	.48
208	-22.8	-28.7	3.5	30.4	45.0	.48

Table 2.6.15.6-10 P_m Stresses for Support Disk—1-Foot Side-Drop, 49.46° Orientation, Thermal Case 1

Section	Sx	Sy	Sxy	Stress Intensity (ksi)	Allowable Stress (ksi)	Margin of Safety
277	9.4	-10.8	4.7	22.2	30.0	.35
265	-8.4	9.4	5.3	20.7	30.0	.45
77	9.1	-9.4	1.6	18.8	30.0	.59
257	-3.7	2.9	8.6	18.4	30.0	.63
295	.8	-7.4	7.4	16.9	30.0	.78
246	-7.5	.2	7.5	16.8	30.0	.79
229	-8.3	3.3	5.5	16.1	30.0	.87
54	-.2	-9.4	6.4	15.7	30.0	.91
273	-.1	-15.2	-1.1	15.3	30.0	.97
262	-8.6	5.7	2.3	15.0	30.0	1.00
269	-11.6	-12.1	3.0	14.8	30.0	1.03
264	-14.3	-.1	-1.0	14.4	30.0	1.09
103	-7.2	1.8	5.2	13.8	30.0	1.18
243	-7.0	3.7	4.3	13.7	30.0	1.19
85	-12.1	-9.7	2.3	13.5	30.0	1.22
73	1.2	-7.8	5.1	13.5	30.0	1.22
259	-7.0	5.6	2.1	13.2	30.0	1.27
65	-3.3	-4.1	6.3	12.7	30.0	1.37
211	-7.9	2.2	3.8	12.6	30.0	1.39
81	-.1	-12.4	-.7	12.5	30.0	1.41

Table 2.6.15.6-11 $P_m + P_b$ Stresses for Support Disk—1-Foot Side-Drop, 49.46° Orientation, Thermal Case 1

Section	Sx	Sy	Sxy	Stress Intensity (ksi)	Allowable Stress (ksi)	Margin of Safety
275	-30.2	-36.7	6.3	40.6	45.0	.11
268	-31.7	-32.7	7.2	39.4	45.0	.14
241	-33.4	-33.1	5.8	39.0	45.0	.15
274	-29.8	-35.1	6.0	39.0	45.0	.16
267	-30.3	-34.9	5.8	38.8	45.0	.16
295	-10.8	-36.1	8.4	38.6	45.0	.17
238	-32.7	-32.0	5.5	37.9	45.0	.19
246	-35.4	-11.8	7.9	37.7	45.0	.19
243	-36.6	-20.6	4.4	37.7	45.0	.19
276	-25.6	-34.8	5.7	37.6	45.0	.20
269	-26.3	-30.2	9.1	37.5	45.0	.20
24	-35.6	-28.0	4.3	37.5	45.0	.20
266	-29.1	-33.1	5.1	36.6	45.0	.23
208	-28.0	-32.8	5.4	36.3	45.0	.24
173	-30.4	-30.2	5.0	35.3	45.0	.28
254	-32.9	-21.8	5.6	35.3	45.0	.28
27	-30.6	-23.5	7.3	35.2	45.0	.28
294	-23.0	-30.8	7.2	35.1	45.0	.28
75	-28.2	-32.0	4.4	34.9	45.0	.29
240	-34.1	-22.2	3.1	34.8	45.0	.29

Table 2.6.15.6-12 P_m Stresses for Support Disk—1-Foot Side-Drop, 49.46° Orientation, Thermal Case 2

Section	Sx	Sy	Sxy	Stress Intensity (ksi)	Allowable Stress (ksi)	Margin of Safety
277	8.5	-10.0	5.0	21.0	30.0	.43
265	-7.8	9.0	5.1	19.6	30.0	.53
257	-3.7	3.2	8.2	17.8	30.0	.68
77	8.6	-8.7	1.6	17.6	30.0	.71
246	-7.8	1.4	7.3	17.2	30.0	.74
295	.9	-7.0	7.0	16.2	30.0	.86
229	-8.2	3.1	5.4	15.7	30.0	.91
54	-.2	-9.4	6.2	15.5	30.0	.93
243	-7.4	4.3	4.1	14.2	30.0	1.11
269	-11.1	-11.2	3.1	14.2	30.0	1.11
273	-.1	-14.1	-1.1	14.2	30.0	1.12
262	-8.0	5.3	2.3	14.0	30.0	1.14
103	-7.1	1.9	5.1	13.7	30.0	1.20
264	-13.4	-.1	-1.0	13.5	30.0	1.23
85	-11.8	-8.9	2.5	13.3	30.0	1.26
73	1.0	-7.6	4.9	13.1	30.0	1.29
245	-12.3	.0	-1.4	12.6	30.0	1.39
65	-3.4	-4.0	6.2	12.5	30.0	1.40
211	-7.8	2.0	3.8	12.5	30.0	1.41
259	-6.5	5.0	2.1	12.2	30.0	1.46

Table 2.6.15.6-13 $P_m + P_b$ Stresses for Support Disk—1-Foot Side-Drop, 49.46° Orientation, Thermal Case 2

Section	Sx	Sy	Sxy	Stress Intensity (ksi)	Allowable Stress (ksi)	Margin of Safety
275	-29.5	-36.1	6.4	40.0	45.0	.13
268	-31.1	-32.0	7.0	38.6	45.0	.17
241	-32.8	-32.4	5.8	38.4	45.0	.17
274	-28.9	-34.2	6.0	38.1	45.0	.18
267	-29.5	-34.0	5.6	37.8	45.0	.19
276	-25.5	-34.4	5.9	37.3	45.0	.21
269	-26.3	-29.9	8.9	37.1	45.0	.21
246	-35.0	-10.6	7.5	37.1	45.0	.21
238	-31.8	-31.1	5.5	37.0	45.0	.22
243	-35.9	-19.3	4.2	36.9	45.0	.22
24	-34.9	-27.4	4.2	36.8	45.0	.22
295	-10.1	-34.3	8.0	36.7	45.0	.23
208	-27.2	-32.1	5.4	35.6	45.0	.27
266	-27.7	-31.7	4.9	35.0	45.0	.28
27	-30.5	-23.4	7.1	34.9	45.0	.29
173	-29.7	-29.4	5.0	34.5	45.0	.30
244	-28.4	-30.3	5.0	34.4	45.0	.31
240	-33.4	-21.1	3.0	34.1	45.0	.32
75	-27.6	-31.1	4.3	34.0	45.0	.32
254	-31.7	-20.7	5.3	33.9	45.0	.33

Table 2.6.15.6-14 P_m Stresses for Support Disk—1-Foot Side-Drop, 77.92° Orientation, Thermal Case 1

Section	Sx	Sy	Sxy	Stress Intensity (ksi)	Allowable Stress (ksi)	Margin of Safety
246	-12.1	10.0	3.6	23.3	30.0	.29
243	-11.4	8.2	1.3	19.8	30.0	.52
245	-17.6	-.1	-.7	17.7	30.0	.70
27	-10.1	6.9	2.2	17.5	30.0	.71
240	-9.6	6.9	1.1	16.6	30.0	.81
85	-7.6	5.4	4.3	15.6	30.0	.93
242	-15.2	-.1	-.6	15.2	30.0	.97
269	-10.1	5.0	.1	15.1	30.0	.99
29	-14.6	-.1	-.7	14.6	30.0	1.05
244	-14.0	-5.2	.7	14.1	30.0	1.13
237	-7.9	6.0	1.1	14.1	30.0	1.13
24	-8.7	4.8	1.1	13.6	30.0	1.21
276	-7.1	3.1	4.0	12.9	30.0	1.33
239	-12.8	-.1	-.6	12.9	30.0	1.33
254	-8.5	4.1	1.0	12.8	30.0	1.35
26	-12.7	-.1	-1.0	12.7	30.0	1.35
256	-12.6	-.1	-.3	12.6	30.0	1.39
241	-12.1	-5.7	1.0	12.2	30.0	1.45
28	-11.9	-.9	-1.2	12.0	30.0	1.49
280	-8.5	2.8	-1.9	12.0	30.0	1.51

Table 2.6.15.6-15 $P_m + P_b$ Stresses for Support Disk—1-Foot Side-Drop, 77.92° Orientation, Thermal Case 1

Section	Sx	Sy	Sxy	Stress Intensity (ksi)	Allowable Stress (ksi)	Margin of Safety
5	-23.1	-30.6	2.0	31.1	45.0	.45
30	-27.1	-3.4	7.8	29.5	45.0	.53
27	-28.4	-5.8	3.3	28.9	45.0	.56
246	-23.3	4.2	3.7	28.4	45.0	.57
24	-26.5	-10.2	2.3	26.8	45.0	.68
22	-25.6	-16.7	3.4	26.8	45.0	.68
25	-25.8	-16.1	3.1	26.7	45.0	.69
6	-8.2	-25.8	1.2	25.9	45.0	.74
244	-23.3	-14.8	5.0	25.6	45.0	.76
77	11.1	24.4	4.2	25.6	45.0	.76
241	-22.6	-15.6	5.0	25.2	45.0	.79
75	-21.2	-18.7	5.1	25.1	45.0	.79
76	11.8	23.8	3.1	24.5	45.0	.84
19	-23.1	-16.0	3.0	24.2	45.0	.86
85	.5	23.5	3.3	24.0	45.0	.88
21	-23.4	-11.0	1.7	23.7	45.0	.90
74	-19.3	-18.0	4.6	23.3	45.0	.93
238	-20.3	-15.3	4.6	23.1	45.0	.95
84	11.6	21.9	3.3	22.8	45.0	.97
275	-18.3	-16.7	5.1	22.6	45.0	.99

Table 2.6.15.6-16 P_m Stresses for Support Disk—1-Foot Side-Drop, 77.92° Orientation, Thermal Case 2

Section	Sx	Sy	Sxy	Stress Intensity (ksi)	Allowable Stress (ksi)	Margin of Safety
246	-11.8	9.9	3.5	22.8	30.0	32
243	-11.2	8.0	1.3	19.3	30.0	.55
245	-17.2	-01	-06	17.2	30.0	.74
27	-9.8	6.8	2.2	17.2	30.0	.75
240	-9.4	6.6	1.0	16.1	30.0	.86
85	-7.8	5.4	4.1	15.5	30.0	.93
269	-10.0	5.0	.1	15.0	30.0	1.00
242	-14.8	-.1	-.6	14.9	30.0	1.02
29	-14.3	-.1	-.7	14.3	30.0	1.10
244	-13.7	-4.9	.7	13.7	30.0	1.18
237	-7.7	5.7	1.0	13.6	30.0	1.21
24	-805	4.7	1.0	13.3	30.0	1.26
254	-8.4	4.1	1.0	12.7	30.0	1.36
276	-6.9	3.1	3.8	12.6	30.0	1.38
239	-12.5	-.1	-.6	12.6	30.0	1.39
256	-12.5	-.1	-.3	12.5	30.0	1.40
26	-12.4	-.1	-1.0	12.4	30.0	1.41
5	-7.7	-3.7	5.7	12.0	30.0	1.50
241	-11.8	-5.4	1.0	11.9	30.0	1.51
257	-7.1	4.1	2.0	11.9	30.0	1.53

Table 2.6.15.6-17 $P_m + P_b$ Stresses for Support Disk—1-Foot Side-Drop, 77.92° Orientation, Thermal Case 2

Section	Sx	Sy	Sxy	Stress Intensity (ksi)	Allowable Stress (ksi)	Margin of Safety
5	-23.0	-29.9	2.2	30.5	45.0	.47
30	-26.2	-3.6	7.5	28.4	45.0	.58
27	-27.9	-5.6	3.3	28.4	45.0	.59
246	-22.9	4.1	3.7	27.9	45.0	.61
24	-25.8	-9.9	2.2	26.1	45.0	.72
22	-24.8	-16.1	3.3	25.9	45.0	.73
25	-25.1	-15.6	3.0	25.9	45.0	.74
6	-8.1	-25.6	1.2	25.7	45.0	.75
244	-22.8	-14.4	4.8	25.0	45.0	.80
77	10.9	23.8	4.1	25.0	45.0	.80
241	-22.0	-15.1	4.9	24.5	45.0	.84
75	-20.5	-17.9	4.9	24.3	45.0	.85
76	11.5	23.1	3.0	23.9	45.0	.89
85	.0	22.8	3.1	23.6	45.0	.91
19	-22.1	-15.1	2.9	23.1	45.0	.94
21	-22.6	-10.6	1.6	22.8	45.0	.97
238	-19.7	-14.7	4.4	22.3	45.0	1.02
74	-18.4	-17.0	4.4	22.2	45.0	1.03
243	-22.1	-1.8	1.2	22.2	45.0	1.03
84	11.1	21.2	3.1	22.1	45.0	1.04

Table 2.6.15.6-18 P_m Stresses for Support Disk—1-Foot Side-Drop, 90° Orientation, Thermal Case 1

Section	Sx	Sy	Sxy	Stress Intensity (ksi)	Allowable Stress (ksi)	Margin of Safety
27	-13.3	14.2	.0	27.4	30.0	.09
77	-8.3	13.5	3.1	22.7	30.0	.32
269	-8.3	13.5	-3.1	22.7	30.0	.32
85	-6.5	12.7	1.2	19.4	30.0	.55
277	-6.5	12.7	-1.2	19.4	30.0	.55
29	-19.3	-.1	.0	19.3	3.0	.55
24	-11.3	7.3	.0	18.5	30.0	.62
273	.1	17.4	.4	17.4	30.0	.73
81	.1	17.4	-.4	17.4	30.0	.73
28	-16.0	.9	.0	16.9	30.0	.77
26	-16.0	-.2	.0	16.6	30.0	.81
6	-11.0	-10.3	-5.9	16.5	30.0	.81
5	-11.0	-10.3	5.9	16.5	30.0	.81
21	-9.6	5.2	.0	14.8	30.0	1.03
23	-14.3	-.1	.0	14.3	30.0	1.09
246	-7.5	6.5	-.2	14.1	30.0	1.13
54	-7.5	6.5	.2	14.1	30.0	1.13
25	-13.5	-3.1	.0	13.5	30.0	1.23
18	-8.1	4.2	.0	12.3	30.0	1.44
20	-12.2	-.1	.0	12.2	30.0	1.45

Table 2.6.15.6-19 $P_m + P_b$ Stresses for Support Disk—1-Foot Side-Drop, 90° Orientation, Thermal Case 1

Section	Sx	Sy	Sxy	Stress Intensity (ksi)	Allowable Stress (ksi)	Margin of Safety
77	-6.3	22.0	3.0	28.9	45.0	.56
269	-6.3	22.0	-3.0	28.9	45.0	.56
27	-13.3	14.2	-.4	27.4	45.0	.64
6	-17.9	-18.4	-5.8	24.0	45.0	.88
5	-17.9	-18.4	5.8	24.0	45.0	.88
85	-5.4	16.4	2.4	22.3	45.0	1.02
277	-5.4	16.4	-2.4	22.3	45.0	1.02
2	-3.9	-19.4	-.1	19.4	45.0	1.32
1	-3.9	-19.4	.1	19.4	45.0	1.32
29	-19.3	-.1	.0	19.3	45.0	1.33
24	-11.3	7.3	-1.5	18.7	45.0	1.40
273	.2	18.6	.4	18.6	45.0	1.42
81	.2	18.6	-.4	18.6	45.0	1.42
28	-16.0	.9	3.5	18.3	45.0	1.45
26	-16.6	-.2	-.1	16.6	45.0	1.71
268	-5.7	10.4	-.9	16.2	45.0	1.78
76	-5.7	10.4	.9	16.2	45.0	1.78
54	-11.7	4.0	.9	15.8	45.0	1.85
246	-11.7	4.0	-.9	15.8	45.0	1.85
21	-9.6	5.2	-1.5	15.1	45.0	1.98

Table 2.6.15.6-20 P_m Stresses for Support Disk—1-Foot Side-Drop, 90° Orientation, Thermal Case 2

Section	Sx	Sy	Sxy	Stress Intensity (ksi)	Allowable Stress (ksi)	Margin of Safety
27	-12.9	13.8	.0	26.7	30.0	.12
77	-8.0	13.4	3.0	22.3	30.0	.35
269	-8.0	13.4	-3.0	22.3	30.0	.35
85	-6.6	12.6	1.2	19.3	30.0	.56
277	-6.6	12.6	-1.2	19.3	30.0	.56
29	-18.7	-.1	.0	18.7	30.0	.60
24	-10.9	7.0	.0	17.9	30.0	.67
273	.1	17.2	.3	17.2	30.0	.74
81	.1	17.2	-.3	17.2	30.0	.74
28	-15.5	1.2	.0	16.7	30.0	.80
5	-10.7	-10.4	5.7	16.2	30.0	.85
6	-10.7	-10.4	-5.7	16.2	30.0	.85
26	-16.1	-.2	.0	16.1	30.0	.86
21	-9.3	5.0	.0	14.3	30.0	1.10
246	-7.6	6.7	-.2	14.3	30.0	1.10
54	-7.6	6.7	.2	14.3	30.0	1.10
23	-13.9	-.1	.0	13.9	30.0	1.16
25	-13.1	-2.9	.0	13.1	30.0	1.29
20	-11.9	-.1	.0	11.9	30.0	1.53
18	-7.8	4.0	.0	11.8	30.0	1.54

Table 2.6.15.6-21 $P_m + P_b$ Stresses for Support Disk—1-Foot Side-Drop, 90° Orientation, Thermal Case 2

Section	Sx	Sy	Sxy	Stress Intensity (ksi)	Allowable Stress (ksi)	Margin of Safety
77	-6.2	21.5	2.9	28.2	45.0	.59
269	-6.2	21.5	-2.9	28.2	45.0	.59
27	-12.9	13.8	-.4	26.7	45.0	.69
6	-17.1	-17.7	-5.7	23.1	45.0	.95
5	-17.1	-17.7	5.7	23.1	45.0	.95
85	-5.5	15.9	2.3	21.9	45.0	1.05
277	-5.5	15.9	-2.3	21.9	45.0	1.05
2	-3.8	-19.0	-.1	19.0	45.0	1.37
1	-3.8	-19.0	.1	19.0	45.0	1.37
29	-18.7	-.1	.0	18.7	45.0	1.40
273	.2	18.5	.3	18.5	45.0	1.44
81	.2	18.5	-.3	18.5	45.0	1.44
24	-10.9	7.0	-1.4	18.2	45.0	1.48
28	-15.5	1.2	3.4	18.0	45.0	1.50
26	-16.1	-.2	-.1	16.1	45.0	1.79
246	-11.7	4.2	-.9	16.0	45.0	1.81
54	-11.7	4.2	.9	16.0	45.0	1.81
268	-5.5	10.1	-.8	15.7	45.0	1.87
76	-5.5	10.1	.8	15.7	45.0	1.87
21	-9.3	5.0	-1.4	14.6	45.0	2.08

2.6.15.7 Stress Evaluation of BWR Support Disk for Combined Thermal and 1-Foot Side-Drop Load Conditions

The loading for the 1-ft side-drop is combined with the thermal loading for Thermal Case 2 to produce the largest stress intensities. The allowable stress intensity, 3 S_m, is evaluated at Thermal Case 3 (see Section 2.6.15.6.3). The corner-drop condition is bounded by the side and end-drops.

The 20 cross sections with the smallest margins of safety are presented in Tables 2.6.15.7-1 through 2.6.15.7-5. The margins of safety are calculated as

MS = (stress allowable/stress intensity) - 1.

The tables are identified here.

Table Number	Basket Orientation (Deg)	Thermal Case	Stress Evaluation	Minimum Margin of Safety
2.6.13.7-1	0	2	$P_m + P_b + Q$	+ 1.44
2.6.13.7-2	31.82	2	$P_m + P_b + Q$	+ 0.78
2.6.13.7-3	49.46	2	$P_m + P_b + Q$	+ 0.59
2.6.13.7-4	77.92	2	$P_m + P_b + Q$	+ 1.40
2.6.13.7-5	90	2	$P_m + P_b + Q$	+ 2.08

Table 2.6.15.7-1 $P_m + P_b + Q$ Stresses for Support Disk - 1-Foot Side-Drop, 0° Orientation, Thermal Case 2

Section	Sx	Sy	Sxy	Stress Intensity (ksi)	Allowable Stress (ksi)	Margin of Safety
14	25.5	18.4	14.5	36.9	90.0	1.44
13	24.3	17.6	-14.0	35.3	90.0	1.55
234	6.5	-14.4	5.1	23.3	90.0	2.86
232	-.2	-23.1	-.2	23.1	90.0	2.89
298	-.1	-23.1	.0	23.1	90.0	2.90
300	8.8	-11.9	-4.1	22.3	90.0	3.04
290	-.1	-21.0	.1	21.0	90.0	3.28
224	-.1	-20.6	-.2	20.6	90.0	3.37
281	-.1	-19.8	.1	19.8	90.0	3.55
145	-11.9	-14.9	6.0	19.6	90.0	3.60
111	-11.9	-14.9	6.0	19.6	90.0	3.60
215	-.1	-19.3	-.3	19.3	90.0	3.65
18	-9.3	-15.0	6.2	19.0	90.0	3.74
266	-9.3	-15.0	6.2	19.0	90.0	3.74
230	-4.1	-17.4	4.7	18.9	90.0	3.76
194	-4.1	-17.4	4.7	18.9	90.0	3.76
270	.0	-18.5	-.4	18.5	90.0	3.87
134	-15.2	-9.7	5.3	18.4	90.0	3.89
165	-15.2	-9.7	5.3	18.4	90.0	3.89
146	-12.9	-12.7	5.4	18.2	90.0	3.93

Table 2.6.15.7-2 $P_m + P_b + Q$ Stresses for Support Disk - 1-Foot Side-Drop, 31.82° Orientation, Thermal Case 2

Section	Sx	Sy	Sxy	Stress Intensity (ksi)	Allowable Stress (ksi)	Margin of Safety
18	-31.4	-37.3	15.9	50.5	90.0	.78
266	-31.4	-37.3	15.9	50.5	90.0	.78
21	-32.9	-35.4	16.0	50.3	90.0	.79
267	-32.9	-35.4	16.0	50.3	90.0	.79
238	-29.5	-36.1	13.4	46.6	90.0	.93
274	-29.5	-36.1	13.4	46.6	90.0	.93
268	-31.0	-31.6	15.0	46.3	90.0	.94
24	-31.0	-31.6	15.0	46.3	90.0	.94
137	-28.6	-33.4	14.1	45.2	90.0	.99
31	-28.6	-33.4	14.1	45.2	90.0	.99
138	-30.0	-29.1	13.7	43.3	90.0	1.08
34	-30.0	-29.1	13.7	43.3	90.0	1.08
200	-31.6	-28.0	13.0	43.0	90.0	1.09
32	-31.6	-28.0	13.0	43.0	90.0	1.09
260	-25.5	-34.1	12.1	42.6	90.0	1.11
293	-25.5	-34.1	12.1	42.6	90.0	1.11
275	-26.1	-34.0	11.9	42.6	90.0	1.11
241	-26.1	-34.0	11.9	42.6	90.0	1.11
288	-29.0	-30.8	12.1	42.0	90.0	1.14
251	-29.0	-30.8	12.1	42.0	90.0	1.14

Table 2.6.15.7-3 $P_m + P_b + Q$ Stresses for Support Disk - 1-Foot Side-Drop, 49.46° Orientation, Thermal Case 2

Section	Sx	Sy	Sxy	Stress Intensity (ksi)	Allowable Stress (ksi)	Margin of Safety
24	-38.6	-38.5	18.2	56.8	90.0	.59
268	-38.6	-38.5	18.2	56.8	90.0	.59
267	-37.6	-38.9	17.7	56.0	90.0	.61
21	-37.6	-38.9	17.7	56.0	90.0	.61
238	-37.1	-39.8	16.1	54.6	90.0	.65
274	-37.1	-39.8	16.1	54.6	90.0	.65
241	-37.1	-39.8	15.8	54.3	90.0	.66
275	-37.1	-39.8	15.8	54.3	90.0	.66
18	-34.8	-38.9	16.9	53.9	90.0	.67
266	-34.8	-38.9	16.9	53.9	90.0	.67
27	-35.5	-35.4	17.3	52.8	90.0	.71
269	-35.5	-35.4	17.3	52.8	90.0	.71
244	-34.4	-39.3	15.1	52.1	90.0	.73
276	-34.4	-39.3	15.1	52.1	90.0	.73
31	-32.8	-35.2	15.5	49.6	90.0	.82
137	-32.8	-35.2	15.5	49.6	90.0	.82
34	-33.4	-32.0	15.2	47.9	90.0	.88
138	-33.4	-32.0	15.2	47.9	90.0	.88
32	-34.5	-29.8	14.0	46.4	90.0	.94
200	-34.5	-29.8	14.0	46.4	90.0	.94

Table 2.6.15.7-4 $P_m + P_b + Q$ Stresses for Support Disk - 1-Foot Side-Drop, 77.92° Orientation, Thermal Case 2

Section	Sx	Sy	Sxy	Stress Intensity (ksi)	Allowable Stress (ksi)	Margin of Safety
31	-25.4	-25.2	12.2	37.5	90.0	1.40
137	-25.4	-25.2	12.2	37.5	90.0	1.40
24	-30.3	-18.4	11.5	37.3	90.0	1.42
268	-30.3	-18.4	11.5	37.3	90.0	1.42
138	-25.1	-23.2	11.8	35.9	90.0	1.51
34	-25.1	-23.2	11.8	35.9	90.0	1.51
27	-31.0	-11.6	10.4	35.6	90.0	1.53
269	-31.0	-11.6	10.4	35.6	90.0	1.53
25	-29.1	-17.3	10.8	35.5	90.0	1.54
76	-29.1	-17.3	10.8	35.5	90.0	1.54
244	-26.9	-22.7	10.5	35.5	90.0	1.54
276	-26.9	-22.7	10.5	35.5	90.0	1.54
74	-28.2	-18.9	10.8	35.3	90.0	1.55
19	-28.2	-18.9	10.8	35.3	90.0	1.55
2	-31.5	-5.7	10.5	35.2	90.0	1.55
30	-31.5	-5.7	10.5	35.2	90.0	1.55
75	-29.6	-15.6	10.6	35.2	90.0	1.56
22	-29.6	-15.6	10.6	35.2	90.0	1.56
37	-23.3	-24.0	11.5	35.1	90.0	1.56
139	-23.3	-24.0	11.5	35.1	90.0	1.56

Table 2.6.15.7-5 $P_m + P_b + Q$ Stresses for Support Disk - 1-Foot Side-Drop, 90° Orientation, Thermal Case 2

Section	Sx	Sy	Sxy	Stress Intensity (ksi)	Allowable Stress (ksi)	Margin of Safety
29	-29.2	.1	.0	29.2	90.0	2.08
27	-15.5	13.0	-1.2	28.7	90.0	2.14
77	-15.5	13.0	-1.2	28.7	90.0	2.14
269	-15.5	13.0	1.2	28.7	90.0	2.14
17	-28.1	-.4	-.1	28.1	90.0	2.20
26	-26.9	-.1	-.1	26.9	90.0	2.34
23	-25.5	.0	-.1	25.5	90.0	2.53
20	-24.3	.0	-.1	24.3	90.0	2.70
14	17.1	10.0	9.5	23.6	90.0	2.81
15	17.1	10.0	-9.5	23.6	90.0	2.81
3	1.2	23.6	.8	23.6	90.0	2.82
4	1.2	23.6	-.8	23.6	90.0	2.82
28	-18.9	2.2	5.1	23.4	90.0	2.84
16	14.5	9.4	8.1	20.5	90.0	3.40
13	14.5	9.4	-8.1	20.5	90.0	3.40
137	-13.7	-12.9	7.1	20.4	90.0	3.41
200	-13.7	-12.9	-7.1	20.4	90.0	3.41
31	-13.7	-12.9	7.1	20.4	90.0	3.41
33	-20.4	.1	.0	20.4	90.0	3.41
25	-17.2	-3.4	5.5	19.2	90.0	3.70

2.6.15.8 Stress Evaluation of BWR Support Disk for 1-Foot Corner-Drop Load Conditions

As is the case in the PWR basket support disks (see Section 2.6.13.8), the g-loads of the corner- and oblique-drop conditions are bounded by the g-load of the end- and side-drop conditions discussed in Section 2.6.15.6. Therefore, no separate evaluation of the 1-ft corner- and oblique-drop conditions is performed.

2.6.15.9 Stress Evaluation of BWR Support Disk for Combined Thermal and 1-Foot Corner-Drop Load Conditions

The combined thermal and 1-ft corner-drop and the combined thermal and 1-ft oblique-drop conditions are bounded by the results of combined thermal and 1-ft end- and side-drop conditions. Therefore, no separate evaluation of the combined thermal and 1-ft corner-drop condition and the combined thermal and 1-ft oblique-drop condition is performed.

2.6.15.10 Stress Evaluation of Tie Rods and Spacers for a 1-Foot End-Drop Load Condition

Tie rods and spacers are provided in the basket to maintain spacing of the support disks. Transmission of loads in different drop orientations of the BWR basket is similar to the transmission of loads in the PWR basket discussed in Section 2.6.13.10. As is the case in the PWR basket, in drop orientations other than on the end, the spacers only experience a portion of the weight of the support disks, heat transfer disks, one end weldment, and the spacers that act along the axis of the cask. Thus, the end-drop is the critical loading condition.

During an end-drop, the weight of the support disks, weldment, aluminum heat transfer disks, and spacers and end nuts is supported by the spacers on the 6 tie rods. Compressive stress over the cross-sectional area of the spacers results. With the largest weight of the two BWR fuel classes, the total weight of the basket is 18,199 lb. Because the weights of the bottom-end weldment (623 lb) and the fuel tubes (4,665 lb) are transmitted directly into the end of the canister, the remaining load acting over the area of the spacers is 12,911 lb. For the 1-ft end-drop the deceleration is 20 *g*, which results in a total end-drop load of 258,220 lb. The area in compression is $\pi(3.0^2 - 1.75^2)/4 = 4.66$ in^2. The compressive stress is 258,220/(6 x 4.66) = 9,235 psi and is considered to be a membrane stress.

The allowable membrane stress, on the basis of the ASME Code, Section III, Subsection NG [15], is 1.0 S_m. Using a conservative material temperature for the outer edge of the support disk of 500°F, S_m = 17.5 ksi. The corresponding margin of safety is

$$MS = (17{,}500/9{,}235) - 1 = +0.89.$$

Therefore, structural adequacy of the tie rod/spacer assemblies is demonstrated.

2.6.15.11 Support Disk Shear Stresses for 1-Foot Drops

ASME Code, Section III, Division 1, Subdivision NG [15], criteria define the Level A allowable for shear stress to be 0.6 S_m. The design stress intensity for SA 533 at a bounding temperature of 500°F (where maximum stresses occur) is 30 ksi. The maximum stress intensity across any section (membrane stress) for the 1-ft side-drop is 27.4 ksi for the 0° drop orientation at Thermal Condition 1. Similarly, for the end-drop, a maximum membrane stress across a section is reported at 0 ksi for the 1-ft drop. Therefore, the maximum shear stress for any normal loading condition is 27.4/2 or 13.7 ksi.

Using the allowable stresses as stated previously, the minimum margin of safety for shear is:

$$MS = [2(0.6)S_m/SI] - 1 = [2(0.6)(30)/27.4] - 1 = +.0.31$$

Therefore, structural adequacy of the BWR fuel basket support disk design for the normal conditions of transport, 1-ft side and end-drops is demonstrated for shear stress criteria.

2.6.15.12 Bearing Stress - Basket Contact with Inner Shell

For the bearing stress (S_{br}) acting along the basket support disk–canister shell interface, an angular contact of 18° is considered on the basis of the ANSYS gap element status (at a radius of 32.75 in.). The load considered to be acting on the support disks is the total contents weight (57,044 lb) times the deceleration value of 20 g, divided among 40 support disks in the basket. The bearing area is considered to be the 0.625-in. thick disk over an 18° contact area.

$$S_{br} = (57{,}044)(20)/[(0.625)(40)(\pi)(65.5)/(360/18)] = 4{,}446 \text{ psi.}$$

The allowable bearing stress is the yield stress, which for SA533 Type B, Class 2 carbon steel at a temperature of 400°F, is 63.2 ksi. The margin of safety for the support disk (not the canister) is computed as

$$MS = (63.2/ S_{br}) - 1 = +13.2.$$

2.6.15.13 Basket Weldment Analysis for 1-Foot End-Drop

The responses of the fuel assembly's top and bottom weldment plates to a 1-ft end-drop is evaluated in conjunction with the thermal expansion stress. The top and bottom weldment plates are 1.25-in thick and 1.0-in.-thick plates, respectively, of Type 304 stainless steel. The weldments support their own weight and the weight of 56 BWR fuel assembly tubes. A finite element analysis is performed for both plates, because the support for each weldment is different depending upon the location of the welded ribs for each. Both models use the SHELL63 element, which permits out-of-plane loading. Figures 2.6.15.13-1 and 2.6.15.13-2 show the finite element models for the top and bottom weldments, respectively. The load from the fuel tube is represented as point forces applied to the nodes at the periphery of the fuel assembly slots. An average point force is applied. The application of the nodal loads at the slot periphery is accurate because the tube weight is transmitted to the edge of the slot, which provides support to the fuel tubes in the end-drop condition.

The analysis demonstrates that the weldment design satisfies the primary membrane (P_m) and the primary membrane plus bending (P_m+P_b) stress criteria. An analysis including the thermal expansion stresses is also performed.

The margins of safety are calculated as

$$MS = [(P_m + P_b) / 1.5\ S_m] - 1 \quad \text{or} \quad MS = [(P_m + P_b + Q) / 3\ S_m] - 1.$$

The margins of safety evaluated for the weldments are shown in Table 2.6.15.13-1. The weldments are shown to satisfy the stress criteria in the ASME Code, Section III Division I, Subsection NG [15].

Figure 2.6.15.13-1 Finite Element Model of the Top Weldment Plate

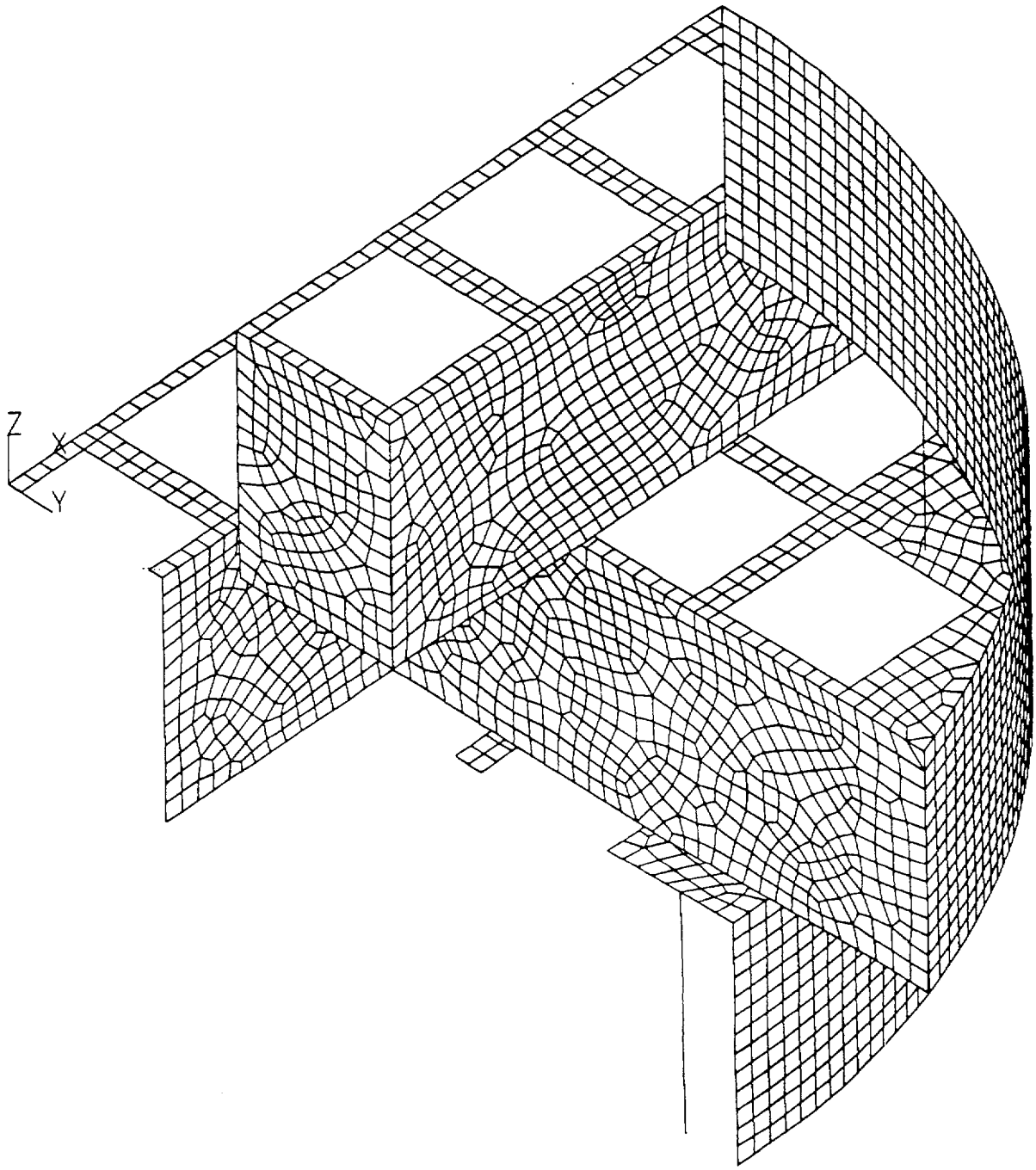

Figure 2.6.15.13-2 Finite Element Model of the Bottom Weldment Plate

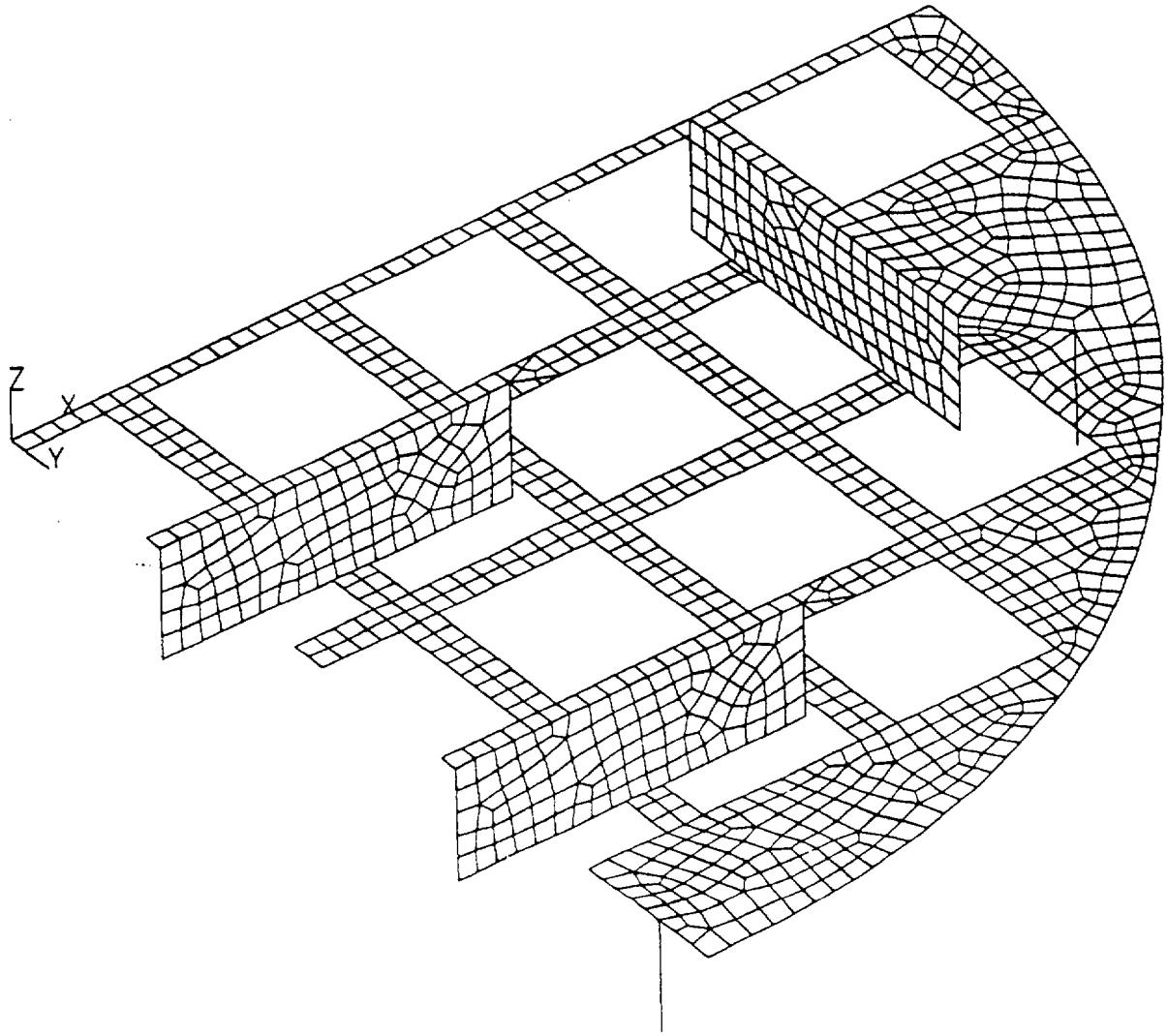

Table 2.6.15.13-1 Minimum Margins of Safety for the Top/Bottom Weldments for a 1-Foot End-Drop With and Without Thermal Stresses

Component/Condition	P_m (ksi)	Allowable S_m (ksi)	MS
Top Weldment/1-ft End-Drop	8.41	17.38	+1.07
Bottom Weldment/1-ft End-Drop	11.14	17.56	+0.58

Component/Condition	$P_m + P_b$ (ksi)	$1.5S_m$ (ksi)	MS
Top Weldment/1-ft End-Drop	16.50	26.07	+0.58
Bottom Weldment/1-ft End-Drop	18.98	26.34	+0.39

Component/Condition	$P_m + P_b + Q$ (ksi)	$3S_m$ (ksi)	MS
Top Weldment/1-ft End-Drop + Thermal	16.95	52.14	+2.08
Bottom Weldment/1-ft End-Drop + Thermal	27.26	52.68	+0.93

2.6.15.14 Support Disk Buckling Evaluation

The BWR fuel basket support disk is subjected to compressive or inertial loads during a 1-ft drop of the cask onto an unyielding surface. Depending on the cask orientation for the 1-ft drop impact, both in-plane and out-of-plane loads may be applied to the support disk. The in-plane loadings (basket side impact component) apply compressive forces on the support disk and the out-of-plane inertial loading (basket end impact component) produces bending moments in the support disk.

Buckling of the support disk is evaluated in accordance with the methods and acceptance criteria of NUREG/CR-6322. The support disk buckling evaluation for the hypothetical accident conditions is presented in Section 2.7.10.3. The characteristics of the support disk are as follows:

2.6.15.14.1 Support Disk Buckling Evaluation Input Data

Material:	SA-533, Type B, Class 2 carbon steel plate
Material yield strength for buckling:	S_y = 70.0 ksi at -40°F (Thermal Case 1) S_y = 59.3 ksi at 750°F (conservative) S_y = 60.5 ksi at 650°F (conservative)
Material modulus of elasticity for buckling:	E = 24.60 x 10^{-3} ksi at 750°F (conservative) E = 29.90 x 10^{-3} ksi at -40°F (Thermal Case 1)
Impact load amplification factor:	20 *g* for the 1-ft side or end-drop. E=25.56 x 10^{-3} ksi at 650°F (conservative)

Thermal Case 2 or 4 is bounding for Thermal Case 3.

2.6.15.14.2 Detailed Support Disk Buckling Evaluation

Conservative temperatures are used in the support disk buckling evaluation.

Methodology

The buckling evaluation of the support disk web is based on the interaction described by Equations 31 and 32 in NUREG/CR-6322 [16]. These two equations adapt the "Limit Analysis Design" approach for structural members for which stresses are beyond the yield limit of the material, i.e., for members deformed elastically as a result of both axial load and bending moment. Other equations applicable to the calculations are listed later in this section.

The maximum forces and moments are determined for the end-drop condition and for five different radial orientations of the support disk for the side-drop condition considering the thermal conditions as presented in Section 2.6.15.3. In this evaluation, thermal loading conditions (Loading Cases 1, 2 and 4) employ only the loads developed in the drop condition (no thermal stresses are considered), but the thermal cases are used to evaluate the material properties. Buckling evaluations are performed for both in-plane (about the strong axis of the web) and out-of-plane (about the weak axis of the web) forces and moments. In the in-plane buckling evaluation, the compressive forces and bending moments that occur for the 1-ft side-drop condition are considered. For the out-of-plane buckling evaluation, the compressive forces for the 1-ft side-drop condition are combined with the moment resulting from the inertial weight of the support disk in the 1-ft end-drop condition.

Detailed buckling calculations are performed in a spreadsheet format by using the methodology and equations from NUREG/CR-6322. The load amplification factors used are 20 *g* for both the 1-ft end-drop and the 1-ft side-drop conditions. The buckling evaluation is performed for each of the sections shown in Figures 2.6.15.6-2 through 2.6.15.6-5. The sections are listed in Table 2.6.15.6-1.

The buckling evaluation methodology/equations are summarized as follows:

Symbols and Units:

P = applied loads, kips
M = moment, kips-in.
P_a = allowable axial compressive load, kips
P_{cr} = critical axial compression load, kips
P_e = Euler buckling loads, kips

P_y = plastic axial load, equal to profile area times specified minimum yield stress, kips (for normal operating condition)

C_c = column slenderness ratio separating elastic and inelastic buckling

C_m = coefficient applied to bending term in interaction equation

M_m = critical moment that can be resisted by a plastically designed member in the absence of axial load, kip-in.

M_p = plastic moment, kip-in.

F_a = axial compressive stress permitted, ksi

F_e = Euler stress for a prismatic member divided by factor of safety, ksi

k = ratio of effective column length to actual unbraced length

l = unbraced length of member, in.

r = radius of gyration, in.

S_y = yield stress allowable, ksi

A = area of the ligament, in^2

Z_x = plastic section modulus with respect to the major axis, in^3

Σ = allowable reduction factor, dimensionless.

$$\frac{P}{P_{cr}} + \frac{C_m M}{M_m\left[1 - \frac{P}{P_e}\right]} \leq 1.0$$

$$\frac{P}{P_y} + \frac{M}{0.18\, M_p} \leq 1.0$$

where, $P_{cr} = 1.7 \times A \times F_a$

$$F_a = \frac{\left[1 - \frac{1}{2}\left(\frac{k \cdot l}{r \cdot C_c}\right)^2\right] \cdot S_y}{\frac{5}{3} + \frac{3}{8}\left(\frac{k \cdot l}{r \cdot C_c}\right) - \frac{1}{8}\left(\frac{k \cdot l}{r \cdot C_c}\right)^3} \quad \text{for} \quad \frac{k \cdot l}{r} < C_c = \sqrt{2 \cdot \pi^2 \frac{E}{S_y}}$$

$P_e = 1.92 \times A \times F_e$

$$F_e = \frac{\pi^2 \cdot E}{1.92\left(\frac{k \cdot l}{r}\right)^2}$$

$$P_y = S_y \text{ x } A$$

$C_m = 0.85$ for members with joint translational (sideways)

$$M_p = S_y \text{ x } Z_x$$

$$M_m = M_p \cdot \left(1.07 - \frac{\left(\frac{l}{r}\right) \cdot \sqrt{S_y}}{3160}\right) \leq M_p .$$

Load Conditions

The load conditions considered in the 1-ft drop normal condition buckling evaluation are as follows:

1. Primary loads, Thermal Case 1. (See Section 2.6.15.3)
2. Primary loads, Thermal Case 2. (See Section 2.6.15.3)
3. Primary plus secondary thermal loads, Thermal Case 4. (See Section 2.6.15.3)

For the buckling evaluation different values for the thicknesses are associated with the weak axis of the support disk web and with the strong axis of the web. The weak axis corresponds to the 0.625-in. support disk thickness and is associated with the load which would result in displacement perpendicular to the plane of the disk. The strong axis buckling would buckles the support disk web in the plane of the support disk.

Buckling of Support Disk Web Weak Axis

For weak-axis buckling the evaluation parameters are as follows (Section 17):

Parameter	Values	Parameter	Values
t	0.625 in.	S_y	60.5 ksi
b	0.66 in.	P_y	A x S_y = 24.956 ksi
A	0.4125 in^2	F_a	32.456
L	6.278 in.	C_c	91.32
I	$b\,t^3/12 = 0.0134\ in^4$	P_{cr}	22.76
r	=0.180	F_e	169.55
K	0.800	P_e	134.289
KL/r	27.837	M_p	3.899
Z	$bt^2/4 = 0.064$	M_m	3.838
E	25,560 ksi	C_m	0.85

Using the cross-sectional stresses calculated at each of the sections shown in Figures 2.6.15.6-2 through 2.6.15.6-5 for the 1-ft side-drop condition, the maximum corresponding compressive forces are combined with the maximum out-of-plane moment resulting from the 1-ft end-drop condition to obtain the conservative maximum interaction coefficients.

The terminology used in the buckling analysis is defined as follows:

$$P_1 = P/P_{cr} \qquad M_1 = \frac{C_m M}{(1 - P/P_e) M_m}$$

$$P_2 = P/P_y \qquad M_2 = \frac{M}{1.18\ M_p}$$

The X and Y directions refer to those webs that are parallel to the global X and Y directions, respectively, for the basket (X is the horizontal axis and Y is the vertical axis for the model shown in Figure 2.6.15.6-2). Section locations are identified in Figures 2.6.15.6-2 through 2.6.15.6-5 and Table 2.6.15.6-1.

The margins of safety are calculated as:

$$MS1 = \frac{1}{P_1 + M_1} - 1 \qquad \text{and} \qquad MS2 = \frac{1}{P_2 + M_2} - 1$$

For weak-axis buckling, the minimum margin of safety is +0.659 for the 90° radial basket orientation at Section 17 (thermal stresses are included).

The calculated minimum margins of safety for the drop orientations discussed in Section 2.6.15.6.1 are presented in Table 2.6.15.14-1. The location of the sections identified in the table are shown in Figures 2.6.15.6-2 through 2.6.15.6-5.

Buckling of Support Disk Web Strong Axis

For strong axis buckling the evaluation parameters are as follows:

Parameter	Value	Parameter	Value
t	0.65 in.	S_y	59.3 ksi
b	0.625 in.	P_y	A x S_y = 24.091 ksi
A	0.406 in^2	F_a	31.959
L	6.278 in.	C_c	90.491
I	$b\,t^3/12 = 0.0143\ in^4$	P_{cr}	22.071
r	=0.188	F_e	176.51
K	0.800	P_e	137.674
KL/r	26.766	M_p	3.915
Z	$bt^2/4 = 0.066$	M_m	3.87
E	24,600 ksi	C_m	0.85

Using the cross-sectional stresses evaluated for each of the sections shown in Figures 2.6.15.6-2 through 2.6.15.6-5, the maximum corresponding compressive forces in conjunction with the maximum in-plane moment produces the maximum interaction coefficients. Because the locations of the maximum force and the maximum moment may not coincide, the calculation of the interaction coefficient is conservative. The maximum magnitude of the moment is used, regardless of sign, to ensure the most severe condition.

The margins of safety are calculated by using Equations 31 and 32 from NUREG/CR-6322 as discussed earlier. For strong-axis buckling, the minimum margin of safety is + 1.552 for the 31.8° radial basket orientation at Section 295 (thermal stresses are included).

The calculated minimum margins of safety for the drop orientations discussed in Section 2.6.15.6.1 are presented in Table 2.6.15.14-2. The location of the sections identified in the table are shown in Figures 2.6.15.6-2 through 2.6.15.6-5.

Table 2.6.15.14-1 Minimum Margins of Safety from Buckling Evaluation of BWR Support Disks (Weak Axis)

Section No.	G-Load	Disk Drop Orientation	Heat Case	MS1	MS2
270	20	0	1	+2.56	+2.78
16	20	0	2	+1.68	+1.79
270	20	0	2 + thermal load	+1.22	+1.40
273	20	31.82	1	+1.93	+2.15
273	20	31.82	2	+1.57	+1.76
273	20	31.82	2 + thermal load	+1.22	+1.40
273	20	49.46	1	+1.74	+1.95
273	20	49.46	2	+1.75	+1.96
17	20	49.46	2 + thermal load	+1.18	+1.37
47	20	90	1	+3.09	+3.35
47	20	90	2	+2.56	+2.78
17	20	90	2 + thermal load	+0.66	+0.82
242	20	77.92	1	+2.22	+2.48
244	20	77.92	2	+2.66	+2.97
17	20	77.92	2 + thermal load	+0.77	+0.94

Table 2.6.15.14-2 Minimum Margins of Safety from Buckling Evaluation of BWR Support Disk (Strong Axis)

Section No.	G-Load	Disk Drop Orientation	Heat Case	MS1	MS2
298	20	0	1	+2.95	+3.303
298	20	0	2	+3.0	+3.36
298	20	0	2 + thermal load	+1.97	+2.25
295	20	31.82	1	+1.82	+1.99
295	20	31.82	2	+1.96	+2.14
295	20	31.82	2 + thermal load	+1.52	+1.69
243	20	49.46	1	+1.98	+2.13
243	20	49.46	2	+2.00	+2.16
246	20	49.46	2 + thermal load	+1.44	+1.60
244	20	77.92	1	+2.56	+2.85
244	20	77.92	2	+2.64	+2.93
244	20	77.92	2 + thermal load	+1.79	+2.03
53	20	90	1	+5.56	+6.15
53	20	90	2	+5.49	+6.08
53	20	90	2 + thermal load	+3.42	+3.82

2.6.16 Universal Transport Cask Cavity Spacers

This section documents the design analysis of the spacers used to position the Transportable Storage Canisters containing PWR or BWR fuel in the Universal Transport Cask cavity during transport of fuel. The spacers are freestanding components that are placed at the bottom of the cask cavity below the canister bottom, and are confined by the end of the canister and the bottom inner surface of the Universal Transport Cask. The spacers are designed to maintain the centers of gravity of the canisters at the required distance from the bottom inner surface of the cask.

The following requirements bound the spacer design:

1. The spacers must meet the normal conditions of transport requirements detailed in 10 CFR 71.43(f) when subjected to the free drop (10 CFR 71.71).

2. The spacers must provide spacing of the canister so that the center of gravity of the cask and contents is maintained.

For impact loading conditions, the spacer is designed to meet the requirements of 10 CFR 71.43(f) for the 1-ft drop condition (10 CFR 71.71). 10 CFR 71.43(f) requires that no substantial reduction in the effectiveness of the package be experienced in normal conditions of transport. Classical analysis is used to demonstrate compliance with these requirements.

2.6.16.1 PWR Cask Cavity Spacers

Each Transportable Storage Canister containing Class 1 or Class 2 PWR fuel is located by one spacer. Canisters containing Class 3 PWR fuel have no spacers. The PWR spacer is a weldment made of Type 304 stainless steel, ASTM A 240, 3/8-in. plate. The weldment consists of a base that is 67 in. in diameter with 6 raised cylinders of different diameters welded to it. The six different diameters are: 12, 24, 32, 50, 56, and 65 in. The lengths of the spacers used to locate the Class 1 and Class 2 fuel canisters vary. The Class 1 spacer is 18.25 in. long and the Class 2 spacer is 11.25 in. long. A sketch of the PWR spacer is provided below.

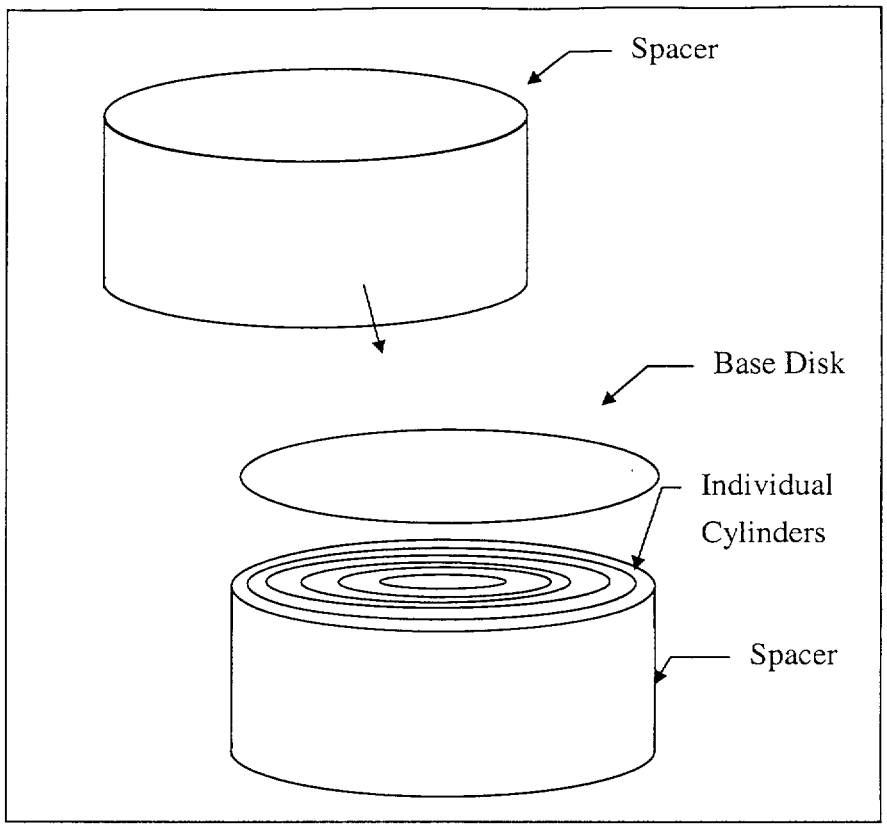

PWR Cask Cavity Spacers Accident Condition

For evaluation purposes, the PWR spacer can be viewed as separate cylinders. The cylinders are identified by numbers 1-6 with the inner most cylinder being number 1 and the outer most being 6 as shown in the following sketch.

The total load modeled is (73,000 lbs) x 60 g (conservative PWR canister weight).

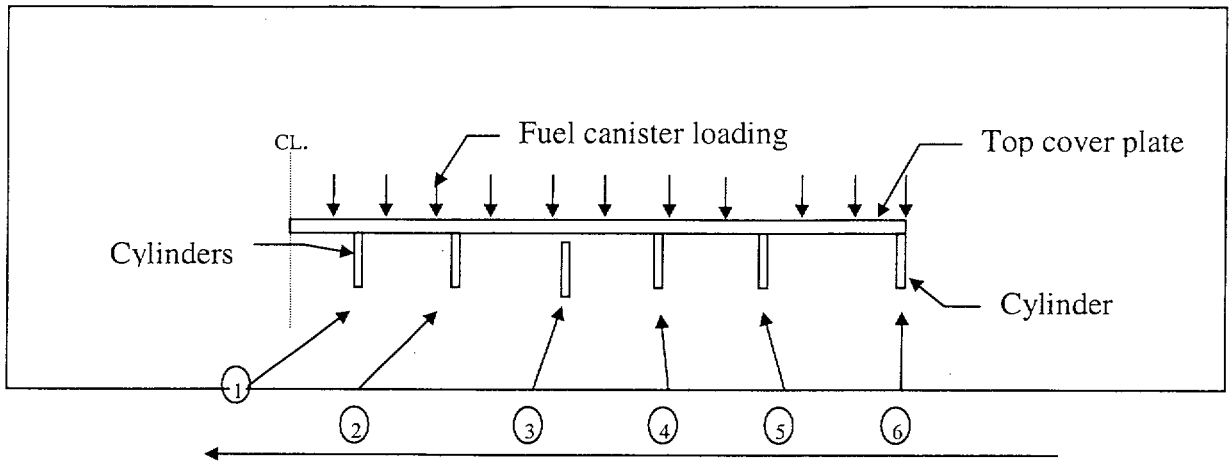

The forces exerted on each cylinder were obtained from the finite element model:

$F_1 = 0.3561\ (10)^6$ lb
$F_2 = 0.6028\ (10)^6$ lb
$F_3 = 0.8372\ (10)^6$ lb
$F_4 = 1.024\ (10)^6$ lb
$F_5 = 0.8260\ (10)^6$ lb
$F_6 = 0.7346\ (10)^6$ lb

The membrane stress experienced by each member is as follows:

$\sigma_{membrane} = F/A$

$\sigma_1 = 0.3561\ (10)^6$ lb / $2\pi(5.625 + 0.1875)(0.375)$ in^2 = 25,993 psi
$\sigma_2 = 0.6028\ (10)^6$ lb / $2\pi(11.625 + 0.1875)(0.375)$ in^2 = 21,660 psi
$\sigma_3 = 0.8372\ (10)^6$ lb / $2\pi(15.625 + 0.1875)(0.375)$ in^2 = 22,469 psi
$\sigma_4 = 1.024\ (10)^6$ lb / $2\pi(24.625 + 0.1875)(0.375)$ in^2 = 17,516 psi
$\sigma_5 = 0.8260\ (10)^6$ lb / $2\pi(27.625 + 0.1875)(0.375)$ in^2 = 12,605 psi
$\sigma_6 = 0.7346\ (10)^6$ lb / $2\pi(32.125 + 0.1875)(0.375)$ in^2 = 9,649 psi

Based on the membrane stress the lowest margin of safety is:

Allowable stress at 300°F = $0.7S_u$= 46,200 psi

$$MS = (46{,}200 \text{ psi}/25{,}993 \text{ psi}) - 1 = +0.78$$

To evaluate buckling the critical stress was determined and compared to the actual:

$$\sigma_{critical} = E((0.605 - 10^{-7}m^2)/(m(1 + 0.004\phi))$$

where:

E = modulus of elasticity for 304 SS @ 300°F---27 10^6 psi
$m = R/T$ = radius/thickness
$\phi = E/S_y$ for 304 SS = 27E6/20,000psi = 1,350 psi

$\sigma_{critical-1}$ = critical stress for each individual cylinder
$\sigma_{critical-1} = 27E6((0.605 - 10^{-7}(5.8125/0.375)^2)/((5.8125/0.375)(1 + 0.004(1350)) = 164{,}602$ psi
$\sigma_{critical-2} = 27E6((0.605 - 10^{-7}(11.8125/0.375)^2)/((11.8125/0.375)(1 + 0.004(1350)) = 80{,}894$ psi
$\sigma_{critical-3} = 27E6((0.605 - 10^{-7}(15.8125/0.375)^2)/((15.8125/0.375)(1 + 0.004(1350)) = 60{,}352$ psi
$\sigma_{critical-4} = 27E6((0.605 - 10^{-7}(24.8125/0.375)^2)/((24.8125/0.375)(1 + 0.004(1350)) = 38{,}295$ psi
$\sigma_{critical-5} = 27E6((0.605 - 10^{-7}(27.8125/0.375)^2)/((27.8125/0.375)(1 + 0.004(1350)) = 34{,}100$ psi
$\sigma_{critical-6} = 27E6((0.605 - 10^{-7}(32.3125/0.375)^2)/((32.8125/0.375)(1 + 0.004(1350)) = 29{,}257$ psi

The buckling evaluation produces a minimum margin of safety as follows:

$$MS = (38{,}295/17{,}516) - 1 = +1.19$$

The base disk of the canister spacer is evaluated to determine its ability to carry the loading of the canister. ANSYS Version 5.2 is used to construct a finite element model of the canister spacer. Plane 42 elements are used to represent the spacer. The model includes the bottom of the canister to minimize the bending experienced by the base disk. Link 1 elements are used to transmit the load from the canister bottom to the base disk.

A maximum stress intensity of 11,103 psi is calculated by ANSYS. Based on the maximum stress intensity a margin of safety is calculated as follows:

Allowable stress at 300°F = $0.7S_u$= 46,200 psi.

$$MS = (46{,}200/11{,}103) - 1 = +3.2$$

PWR Cask Cavity Spacers Normal Condition

The normal condition cask cavity spacer evaluation was performed by ratioing stresses based on the linear accident condition analysis results.

The compressive buckling load is calculated as

$$S_{1\text{-ft}} = (S_{30\text{-ft}})(20\text{ g}/60\text{ g}) = (17{,}106)(20\text{ g}/60\text{ g}) = 5{,}702\text{ psi}$$

The critical buckling allowable stress calculated earlier is 38,295 psi.

The minimum margin of safety for critical buckling is:

$$MS = \left(\frac{38.29516}{5.70216}\right) - 1 = +5.71$$

The maximum stress intensity in the canister spacer was calculated to be:

$$(SI)_{1\text{-ft}} = (SI)_{30\text{-ft}}\left(\frac{20\text{g}}{60\text{g}}\right) = 11{,}000\left(\frac{20}{60}\right) = 3{,}667\text{ psi}$$

The allowable stress (S_m) for the PWR spacer at 300°F is 20,000 psi. This results in the following margin of safety:

$$MS = \left(\frac{20{,}000\text{ psi}}{3{,}667\text{ psi}}\right) - 1 = +4.45$$

2.6.16.2 BWR Cask Cavity Spacers

Each canister containing Class 5 BWR fuel is located by one spacer. Canister containing Class 4 BWR fuel is located by 4 spacers. The lengths of the canisters containing Class 4 and Class 5 BWR fuel are 185.75 and 190.55 in., respectively. To maintain the centers of gravity of these canisters at the required distance from the bottom inner surface of the cask, spacers of 1.5 and 6

inches in length are designed to be placed at the bottom of the cask cavity below the canister bottom.

Each spacer used in the BWR cask consists of 1.5-in.-thick plate of ASTM B209 6061-T651 aluminum alloy. A sketch of the BWR spacer is provided below.

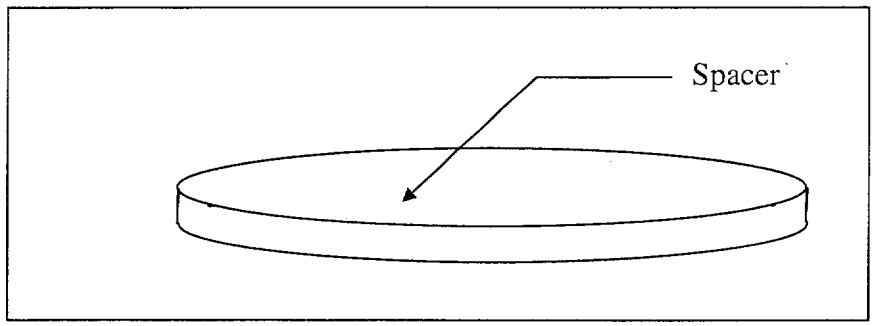

The aluminum alloy material is selected as the spacer material because it has the low weight, good thermal conductivity, and strength needed to meet the design requirements. This material is evaluated below for normal conditions of transport.

BWR Cask Cavity Spacers Accident Conditions

To apply a 1-ft end-drop load to the spacer, a total bounding load of 4,560,000 lbs (76,000 x 60 *g*) is applied.

The area of the spacer is taken to be 3,318 in^2. This results in a crushing pressure of

$$P_{cr} = (4{,}560{,}000 \text{ lb})/(3{,}318 \text{ in}^2) = 1{,}374 \text{ psi}.$$

The yield strength of 6061-T651 aluminum alloy at 300°F is 22,050 psi. Because the pressure load is less than the yield strength, the spacer will not permanently deform during the 1-ft drop. The margin of safety is

$$MS = (22{,}050/1{,}374) - 1 = +15.05$$

BWR Cask Cavity Spacers Normal Condition

The normal condition cask cavity evaluation was performed by rationing stresses based on the linear accident condition analysis results.

The compressive stress was calculated to be:

$$SI_{1\text{-ft}} = SI_{30\text{-ft}}\left(\frac{20g}{60g}\right) = 1{,}374\left(\frac{20g}{60g}\right) = 458 \text{ psi}$$

The allowable stress (S_m) for the BWR spacer at 300°F is 8,400 psi. This results in the following margin for safety:

$$MS = \left(\frac{8{,}400}{455}\right) - 1 = +17.46$$

THIS PAGE INTENTIONALLY LEFT BLANK

2.7.1.5 Lead Slump Resulting from a Cask Drop Accident

Following a drop accident, the shielding capability of the Universal Transport Cask may be reduced as a result of lead slump. The effect of the lead slump due to a bottom end-drop and a side-drop from a height of 30 feet on the dose rates is conservatively evaluated in Chapter 5.0 of this report. The dose rate as a result of the corner-drop is bounded by that for the bottom end-drop accident. The results of the evaluation are summarized in this section.

In the event of an end-drop, the lead gamma shielding could slump and fill the annular gap (if one exists) created by the cooling of the lead after fabrication. This accident could create a maximum gap of 3.05 in. at the top of the lead annulus. This gap is determined by considering the conservation of total lead volume:

$$\pi\left(r_{oa}^2 - r_i^2\right)H_a = \pi\left(r_{ob}^2 - r_i^2\right)H_b$$

where subscript "*a*" indicates quantities after slump, "*b*", before slump, *H* is the total lead height, r_i and r_o are the inner and outer lead radii, respectively. Using the transport cask geometry dimensions, the computed slump height is

$$H_b - H_a = 180.0 - 176.95 = 3.05 \text{ inches}$$

Note that the slumped lead is allowed to fill the gap between the before-drop lead outer radius and the outer shell inner radius. The parameters used in the calculation are shown in Table 2.7.1.5-1. Dose rate calculations on the basis of this 3.05-in. axial lead slump show that the peak 1 m total dose rate is 47 mrem/hr for the cask loaded with design basis PWR fuel assemblies and 64 mrem/hr for the cask loaded with design basis BWR fuel assemblies.

For a 30-ft side-drop accident, the lead may slump into the lower portion of the annulus between the inner and outer shells; thus, a reduction in the thickness of lead shielding may occur on the upper side of the cask as shown in Figure 2.7.1.5-1. An evaluation of the side-drop accident shows that the lead may sag at the opposite side by a maximum of 0.91 inch. The slump height is computed by equating the before- and after-drop cross sectional areas:

$$\frac{\pi}{2}\left(r_{oa}^2 - r_i^2\right) + 2\int_0^{\theta'} \sin^2\theta \, d\theta - \frac{\pi}{2} r_i^2 = \pi\left(r_{ob}^2 - r_i^2\right)$$

θ is the angle subtended by the top of the slumped lead, as measured from the vertical, and the integral term gives the area of that part of the upper semi-circle bounded by the slumped lead. The integral is evaluated analytically and the Excel Solver utility is used to solve the resulting transcendental equation for θ. Given θ, the resulting slump height is 37.599 inches. Table 2.7.1.5-1 provides the parameters and results of the lead slump analysis. The radial slump is:

$$r_o - r_{oa} = 38.51 - 37.599 = 0.91\,\text{inch}$$

Dose rate calculations on the basis of this 0.91-in. radial lead slump show that the peak 1 meter total dose rate is 27 mrem/hr for the cask loaded with design basis PWR fuel assemblies and 21 mrem/hr for the cask loaded with design basis BWR fuel assemblies.

The above dose rates resulting from a lead slump condition are significantly below the hypothetical accident dose rate limit of 1,000 mrem/hr at 1 meter from the surface of the cask. Thus, the hypothetical accident dose rate limits of 10 CFR 71.51 are satisfied.

2.7.1.6 Impact Limiter Analysis - Hypothetical Accident Conditions

Removable upper and lower impact limiters are provided on the Universal Transport Cask to ensure that the design impact loads on the cask are not exceeded for any of the defined impact conditions. The defined conditions are that the cask falls 1 foot (normal conditions of transport) or 30 feet (hypothetical accident conditions) and lands (a) on its side, so that both impact limiters are impacted simultaneously; (b) flat on one impact limiter at either end; or (c) oblique on one impact limiter at either end.

Detailed analysis of the impact limiters for normal conditions of transport and hypothetical accident conditions is provided in Section 2.6.7.5. The analysis is based on the assumptions that the cask impacts on an unyielding surface and that the impact limiter remains in position on the cask during all impact events. A finite element computer program, LS-DYNA [33] is used to analyze the impact limiters for an impact event to determine the dynamics of the event, the forces generated during that event, and the depth of crush. Results of the analysis are provided in Section 2.6.7.5.

As demonstrated by the results, the deceleration g-loads predicted by the LS-DYNA analysis for the 30-ft cask drop conditions are lower than the g-loads for which the Universal Transport Cask and the Transportable Storage Canister are designed.

2.10 Appendices

2.10.1 Computer Program Descriptions 2.10.1-1
2.10.1.1 ANSYS 2.10.1-1
2.10.1.2 LS-DYNA 2.10.1-2
2.10.2 Finite Element Model - Universal Transport Cask 2.10.2-1
2.10.2.1 Load Application and Boundary Conditions 2.10.2-5
2.10.2.2 Post-Processing of Results 2.10.2-13
2.10.3 Confirmatory Testing Program – UMS® Impact Limiters and Attachments 2.10.3-1
2.10.3.1 Confirmatory Testing Program Results Summary 2.10.3-1
2.10.3.2 Acceptance Criteria for Model Performance 2.10.3-3
2.10.3.3 30-Foot Top End Drop and 30-Foot Top Corner Drop Tests Performed at ORNL 2.10.3-4
2.10.3.4 30-Foot Side Drop Test Performed at SNL 2.10.3-19
2.10.3.5 Evaluation of 30-Foot Oblique Drop 2.10.3-26
2.10.3.6 Scale Model Drawings 2.10.3-26
2.10.3.7 LS-DYNA Analysis of the UMS Quarter® Scale Model 2.10.3-27
2.10.4 Dynamic Load Factor (DLF) Evaluation for PWR and BWR Support Disks 2.10.4-1

THIS PAGE INTENTIONALLY LEFT BLANK

2.10.1 Computer Program Descriptions

The structural evaluation of the Universal Transport Cask body, closure lid, canister, baskets, and impact limiters is accomplished using the ANSYS and LS-DYNA computer codes. These programs are described in the following sections.

2.10.1.1 ANSYS

The structural analysis of the main body, the closure lid, the canister, and the baskets of the Universal Transport Cask is performed by the finite element analysis method using the ANSYS structural analysis computer program [32]. The ANSYS computer program is a large-scale, general purpose computer program for the solution of several classes of engineering analyses that include: static and dynamic; elastic, plastic, creep and swelling; buckling; and small and large deflections. The matrix displacement method of analysis based on finite element idealization is employed throughout the program. The large variety of element types available gives ANSYS the capability of analyzing two-dimensional and three-dimensional frame structures, piping systems, two-dimensional plane and axisymmetric solids, three-dimensional solids, flat plates, axisymmetric and three-dimensional shells, and nonlinear problems, including gap element interfaces.

A three-dimensional model is used in the analysis of the cask for the 3 free-drop cases. Two-dimensional axisymmetric models are used to evaluate the cask lid for puncture. The interface gap elements provide the capability of realistic modeling and evaluation of the interactions between the lead layer and the surrounding stainless steel shells; between the top forging, and the lid; and between the neutron shield material and the steel in the bottom of the cask.

The ANSYS preprocessing routine (PREP7) is used to construct the finite element mesh, describe each cask component material (temperature-dependent) property, assign unique identifiers for cask components, model displacement boundary conditions and prescribe temperature, point loads, or surface tractions of appropriate element faces or nodes. The PREP7 graphics option is a valuable tool that permits the user to check the model for completeness. The ANSYS analysis option uses the PREP7 file to generate a solution file and to provide a user-oriented printout of the solution phase.

A variety of ANSYS post-processors (for example, Post1) utilizes the solution file to sort, print, or plot selected results from the ANSYS analysis. The post-processors can provide many useful

features including a maximum set of variables (such as stress components or displacements) or sectional stresses along a designated path. Additionally, the structural behavior can be viewed by model displacement and stress contour plots.

2.10.1.2 LS-DYNA

The analysis of the impact limiters is performed by the finite element analysis method using the LS-DYNA [33] computer program. The program is also used in the analysis of the Maine Yankee Damaged Fuel Can and the bail on the top of the BWR fuel assembly. LS-DYNA is an explicit general-purpose finite element program for the nonlinear dynamic analysis of three-dimensional structures. It was originally used to simulate permanent deformations of metallic objects impacting hard surfaces at high velocities. Its accuracy has been benchmarked through correlation with experimental data. LS-DYNA features include the ability to handle large deformations, finite rotation, sophisticated material models (for steel and aluminum, rubbers, foams, plastics, and composites), complex contact conditions among multiple components, and short-duration impact dynamics.

The LS-DYNA preprocessing routine (FEMB) is used to construct and modify the finite element mesh, assign material properties to parts, assign unique identifiers for model parts, model displacement boundary conditions, prescribe velocities, and create rigid impact planes. FEMB is a valuable tool that permits the user to check the model for completeness.

A variety of LS-DYNA post-processors (for example, FEMB and PostGL) utilize the solution file to plot selected results from the LS-DYNA analysis. The post-processors can provide many useful features including the ability to write AVI animation files of a drop impact event, display stress time-history contour plots of the results, and generate acceleration time-history plots of specific points of interest. LS-DYNA allows the use of the Butterworth Filter for data filtering.

2.10.3 Confirmatory Testing Program – UMS® Impact Limiters and Attachments

This section provides a description of the scale model test program, which was carried out as confirmatory support of the analysis and licensing effort for the design qualification of the NAC-UMS® Transport Cask impact limiters and attachments. More specifically, the purpose of the UMS® Scale Model Test Program was to confirm (1) the capability of the impact limiters to restrict the deceleration of the cask to the design limits used in the structural evaluation of the transport cask; and (2) the impact limiters remain attached to the cask body.

The test results confirm the impact limiter analysis and provide physical evidence that the UMS® impact limiters will function as designed to limit the deceleration applied to the cask and its contents and to remain attached to the transport cask during an accident condition impact.

The scale model test program for the NAC-UMS® impact limiters included: (1) 30-foot drops of a quarter-scale model of the UMS® cask in the top end, side, and top corner impact orientations and (2) a static compression test for the top end drop cask orientation. The total weight of the quarter-scale model and impact limiters (4,060 pounds) corresponded to the full-scale 260,000 pounds design limit of the NAC-UMS® Transport Cask.

This section presents the scale model impact limiter and attachment drawings, the test descriptions, test results, and conclusions that demonstrate the design qualification of the impact limiters and their attachments.

2.10.3.1 Confirmatory Testing Program Results Summary

Three 30-foot drop tests were performed for the UMS® transport cask scale model test program. The top end drop and top corner drop test were performed at the drop test facility at the Oak Ridge National Laboratory (ORNL) in April 1999. The side drop test was performed at Sandia National Laboratory (SNL) using a different quarter-scale model in March 2001.

Since the purpose of the UMS® Drop Test Program was to confirm the design of the UMS® transport cask impact limiters and attachments, the design of the scale model package focused on the limiters and their attachments to the cask body. The scale model body was designed to accurately represent the interface between the cask body and the impact limiters and the weight, CG and mass moment of inertia of the cask body and its contents. The use of a scale model is appropriate to perform these tests and the scale selected for the tests was a quarter-scale model.

Using a smaller scale model would present fabrication difficulties, while use of a larger scale model would increase the drop pad requirement (mass and geometric size). The drop pads at ORNL and SNL meet the requirement of the IAEA to simulate an unyielding surface for the UMS® quarter-scale model. The test data consisted of measurements of the deformations of the impact limiters, the package accelerations, and inspection of the retaining rods. Impact limiter measurements were performed before and after each test to determine the crush depth of the impact limiters. The measured crush depths are used to demonstrate that the impact limiter design calculations are bounding. The accelerations are recorded by accelerometers attached to the model body. The accelerometers are positioned and oriented so that a single accelerometer records the vertical acceleration of the model. The acceleration data obtained from the accelerometers contained contributions to the acceleration signal that were extraneous based on the frequencies of the contributions. For this reason, the acceleration data was further processed to extract accelerations, which were compared to the accelerations calculated by the LS-DYNA finite element analysis program. Additional test documentation included high-speed photography that confirmed the orientation of the cask at impact and still photographs of the scale model, impact limiters, and the impact limiter retaining rods. Post-test inspection of the retaining rods and the impact limiters confirmed that the impact limiters have a significant margin of safety for remaining attached to the cask body during and after a 30-foot drop test impact.

The LS-DYNA analyses for the quarter-scale model are presented in Section 2.10.3.9.

The quarter-scale model 30-foot drop test acceleration values and the LS-DYNA predicted (calculated) values are summarized in the following table:

UMS Cask model Drop Orientation	Quarter-Scale Drop Test Results (g)		LS-DYNA Prediction (g)		Design Basis Acceleration (g)
	Top Accelerometer	Bottom Accelerometer	Top Accelerometer	Bottom Accelerometer	
Top Corner	121	N/A	143	N/A	240
Top End	207	N/A	226	N/A	240
Side	190	198	220	213	240

The drop test measured crush depths and the LS-DYNA predicted (calculated) values are summarized in the following table:

UMS® Cask Model Drop Orientation	Quarter-Scale Drop Test Results (inch)			LS-DYNA Prediction (inch)		
	Original Thickness	Final Thickness	Measured Crush Depth	Original Thickness	Final Thickness	Total Crush Depth
Top End Drop	—	—	2.00	—	—	2.21
Top Corner Drop	—	—	2.95	—	—	3.36
Side Drop–Under the trunnion	3.50	0.63	2.87	3.47	0.38	3.09
Side Drop–Bottom impact limiter	5.13	2.38	2.75	5.13	2.39	2.74

These results of the UMS® Drop Test Program confirm the design-basis accelerations and crush depths used for the evaluation of the transport cask.

2.10.3.2 Acceptance Criteria for Model Performance

Acceptance criteria were established only for the scale model impact limiters and their attachment components, since the purpose of the scale model test program was to confirm their performance capabilities. The function of the scale model impact limiters is to limit the deceleration of the scale model package during the 30-foot drop event, while remaining firmly attached to the cask body. The impact limiter acceptance criteria requires that:

1. The crush depth be limited to prevent an impact of the cask body on the impact surface.
2. The accelerations be limited to be less than or equal to those used in the design analysis.
3. The impact limiters remain attached to the cask body and in position after the impact event.

The results of the UMS® Drop Test Program confirm:

1. The scale model body did not impact the pad surface confirming that the UMS® transport cask possesses a sufficient depth of wood to absorb all of the energy of a 30-foot drop in any orientation.
2. The maximum accelerations determined from the scale model tests are less than the design-basis values used to evaluate the UMS® transport cask components for a 30-foot drop accident.
3. The impact limiters remain attached to the transport cask body.

2.10.3.3 30-Foot Top End Drop and 30-Foot Top Corner Drop Tests Performed at ORNL

A quarter-scale model was used for the confirmatory testing of the UMS® impact limiters and attachments for the top end drop and top corner drop. These drop tests were performed at the Oak Ridge National Laboratory (ORNL) in April 1999. The quarter-scale model was only required to represent the appropriate cask body weight, center of gravity, and attachment interface materials and dimensions of the impact limiters and their attachments to the cask body. For this reason, a 20-inch diameter Schedule 160S stainless steel pipe was used to represent the cask body. To properly represent the weight and the location of the center of gravity of the cask and the mass moment of inertia, a series of weight disks (circular steel plates) were positioned inside the pipe. Three of the weight disks were 4 inches thick while a fourth was 4.5 inches thick. The actual location of the plates and the corresponding axial location of the center of gravity are shown in the model drawing 790-301, Sheets 1 through 3.

The total weight of the quarter-scale model including the impact limiters was 4,033 pounds, which closely approximates $(1/4)^3 = 1/64$ of the full-scale transport cask weight of 260,000 pounds.

The overall length of the model (without the impact limiters) is 52.31 inches, which is comprised of a 41.31-inch length of 20-inch diameter pipe welded to a 6-inch thick plate at the top end and a 5-inch thick plate at the bottom end. Both plates are Type 304 stainless steel. The top end plate was machined to represent the scaled outside diameters and axial dimensions of the upper forging and the neutron shield top plate. A 16.06-inch diameter through hole was machined in the center of the top end plate of the model body. Also, a recess was machined into the top end plate to accommodate the placement of the bolted lid. Two steel bars, scaled to represent the diameter and length of the cask lifting trunnions, were welded in the appropriate locations on the outside diameter of the top end plate.

The model lid outer diameter and the lid bolt recess diameter are quarter-scale dimensions, but the lid thickness and the number of lid bolts were not scaled. Scaling of the lid thickness and the bolts was not necessary because the purpose of the lid and bolts was only to back the upper impact limiter and to retain the dummy weights in the cavity of the model cask.

The 5-inch thick bottom end plate of the model was machined to represent the scaled outside diameters and the axial dimensions of the bottom end of the UMS® cask, including the neutron shield bottom end plate. The bottom plate thickness is not scaled, since it is only required to

provide backing area for the bottom impact limiter and to contribute to the weight and CG location of the scale model.

The four interior circular weight disks were positioned by spacers (cylinders), but were not attached (welded or bolted) to the spacers or the body of the scale model. The spacers were fabricated from 16-inch diameter Schedule 160 pipe, which provided adequate strength to maintain the position of the weight disks. The lengths of the spacers were designed to properly position the CG of the scale model package. This ensures that the load distribution to the model impact limiters for the drop tests is representative of the loading that would occur on the full-scale UMS® transport cask.

Since the top end drop and top corner drop tests involve only the top end of the model, there was no need to include a bottom impact limiter on the model for these tests. To ensure that the total scale model package weight and CG are properly represented for the top end and top corner drop tests, a steel plate corresponding to the weight of the bottom impact limiter was designed, fabricated, and bolted to the bottom end of the model.

The model impact limiters were quarter-scale representations of the full-scale impact limiters. The redwood and balsa wood used in the model limiters met the same specifications that are defined for the full-scale limiters in this SAR. The wood section shapes, joints, and bonds of the scale model impact limiters duplicate those of the full-scale impact limiters. The grain orientation of the redwood and balsa wood in the scale model impact limiters is identical to that as designed in the full-scale impact limiters. The scale model impact limiter shells were fabricated from 16 gauge (0.0625-inch thick) Type 304 stainless steel sheets and the screw tubes, which serve as the penetrations for the impact limiter retaining rods, were fabricated from 0.035-inch thick, 0.75-inch diameter tubes. Each model impact limiter is attached to the cask by sixteen quarter-scale retaining rods fabricated from ASME SA-193 Grade B8S stainless steel.

The model impact limiter shells - i.e., material thickness, geometry, and welds - are appropriately quarter-scale. The diameter of the screw tubes is quarter-scale, but the tube wall thickness is full-scale due to fabricability and material availability limitations. The use of the thicker tube is considered to be conservative, since it tends to increase the stiffness of the limiter. The axial stiffness of the model screw tube is increased by a factor of four, and the rotational stiffness of the screw tube attached to the impact limiter shell is also significantly increased. The effect of the tube thickness on the drop test results is insignificant, since the tubes are not located in the primary crush regions of the impact limiter.

2.10.3.3.1 Equipment and Instrumentation for the Tests Conducted at ORNL

The pad at ORNL functions as the essentially unyielding impact surface and is considered to meet IAEA requirements. The pad consists of concrete and armor plate, and the total weight is approximately 60 tons, which is approximately 30 times the test weight of the quarter-scale model. The 60-ton weight of the pad is considered to be conservative, since the pad rests on a 3-foot diameter column of reinforced concrete that extends vertically down 10 feet to bedrock. The armor plate, which is the impact surface of the pad, is 6-inch thick steel plate.

Lifting and dropping the model was performed with a mobile crane with a single point suspension system in conjunction with an explosive cable cutting release. This release mechanism allowed the free fall of the package to be initiated in an unimpeded fashion with minimum perturbation to the angular position of the model or its lateral position with respect to the pad surface.

To assess the model performance with respect to the acceptance criteria, a set of basic data was required to be collected throughout each test. This data included:

1. Acceleration data – to determine the maximum impact acceleration of the cask. All of the accelerometers used in the drop tests were the same model and they were calibrated to NIST traceable standards corresponding to frequencies ranging from 2K Hz to 10K Hz. Individual accelerometers were mounted on steel blocks welded to the cask model; the actual locations of the blocks are shown on Drawing 390-301, Items 23, 24, and 25. All of the accelerometers were positioned to record only the vertical acceleration component. Therefore, a combination of time histories was not required to compute the resultant vertical acceleration. The number and locations of the accelerometers were tailored to each individual drop test, as shown below.

Drop Test	Number of Accelerometers	Accelerometer Location
Top end drop	3	All three accelerometers were located 11 inches from the top end of the model and were spaced circumferentially at the 60°, 150°, and 270° positions.
Top corner drop	3	Two accelerometers were located 8 inches from the top end of the cask body and 180° apart, circumferentially. A third accelerometer was located 12.5 inches from the top end of the cask body and was at the same circumferential location as one of the other accelerometers.

The acceleration time histories were stored electronically, which permitted them to be filtered after the tests were completed. The unfiltered data consisted of acceleration (in units of gravity "g") points corresponding to time increments of 30.5 microseconds.

2. Impact limiter deformation data – to evaluate the behavior of the impact limiters, the crush depth for each orientation and the condition of the limiter attachment to the model body after each test. After each test, the impact limiters were inspected to determine the amount of deformation that had occurred (the crush depth) and to determine the condition of the retaining rods. Photographs were taken to record the post-test condition of the impact limiters and retaining rods.

3. High speed photography – to review and assess the actual angle of impact and the behavior of the cask body and impact limiters during the impact.

Two high speed cameras were used to record the behavior of the quarter-scale model as it impacted the target surface. Film speeds were 500 frames/second or greater. One camera was positioned and focused to obtain a close up view of the impact deformation. The other camera was focused to record an overall view of the impact and to verify the orientation of the cask as the impact was initiated.

2.10.3.3.2 Filter Frequency Identification for the End Drop Accelerometer Data

Accelerometers can be sensitive to high frequency vibrations in parts of the structure that could be considered to be remote from the actual location of the accelerometer. The purpose of the accelerometer is to determine the rigid body deceleration of the model body during the impact, not the high frequency vibration dynamic response of other components of the model body. High frequency vibrations typically correspond to mode shapes, which are excited by the impact.

The electronically stored acceleration time histories include the peaks corresponding to the high frequency vibration dynamic response of the spacers and weight disks inside the model body. To reduce the effects of the high frequency responses in the acceleration time histories, the acceleration time histories are filtered, i.e., a filter frequency is determined, such that acceleration time points corresponding to the high frequency vibration dynamic responses are effectively removed from the data. Since these high frequency vibration dynamic responses are a function of the loadings on the model body, separate filter frequencies are determined and applied for each of the different drop orientations. The corner drop impact orientation produces an axial loading on the cask components in a manner similar to the end drop.

While the end drop orientation does provide excitation to the weight disks and spacers, the lowest frequency of concern corresponds to the longitudinal mode, which combines the mass of the shell weldment (2,107 pounds) and the lid (157 pounds) and the bottom test weight (134 pounds). The total weight (W) of these components is W = 2,398 pounds. The mass (m) is computed as 2,398/386.4 or 6.21 lb-sec^2/inch. The equivalent axial stiffness (K) of the system is:

$$K = A \times E/L$$

Where:

A = cross sectional area of the model body = 111.5 in^2
E = modulus of elasticity of Type 304 stainless steel (70°) = 28.3 E6 psi
L = distance from the 5-inch thick bottom plate to the inner surface of the 2-inch thick model lid
= 45.3 inches

Substituting,

$$K = (111.5)(28.3+E6)/45.3 \text{ pound/inch}$$
$$K = 69.7E+6 \text{ pound/inch}$$

The corresponding natural frequency is

$$f = (1/2\pi)\sqrt{K/m}$$
$$f = 533 \text{ Hz}$$

A filter frequency of 550 Hz is used to avoid including the high frequency vibration dynamic response of the shell of the body of the model.

2.10.3.3.3 Results/Evaluation for the 30-Foot Top End Drop Test

The 30-foot top end drop was performed first. Prior to lifting the scale model package to the 30-foot drop height, the torque for the retaining rods and nuts was verified to ensure that the torque specifications were met.

Two high speed cameras were used to record the top end drop impact. In reviewing the high speed camera results, it was determined that the high speed camera recording the detailed view of the impact limiter crush had malfunctioned, causing the film to be under-exposed. The high speed camera used to record an overall view of the drop test showed that the scale model's longitudinal axis was essentially vertical and that the model impacted the drop test facility pad as targeted. The scale model remained upright during and after the impact. The high speed camera also showed that the model rebounded an estimated 18 to 24 inches back up into the air after the initial 30-foot drop impact.

2.10.3.3.3.1 Impact Limiter Deformation and Attachment Data

After the top end drop test the scale model package was lifted off the ground to remove the top end impact limiter. Removal of the top impact limiter from the cask body required that two hydraulic jacks be inserted between the impact limiter and the bottom end plate to force the impact limiter off the cask body. During the impact limiter removal, it was noted that several retaining rods were broken. The retaining rods were removed from the impact limiter and inspected, whereupon it was observed that the rods had undergone plastic buckling, having been confined to the screw tube, which is surrounded by redwood oriented in its strongest direction.

The impact limiters were then sectioned by sawing into approximately four equal quarter-sections to permit observation of the deformations of the impact limiter shells in the crushed region of the impact limiter directly under the cask. The crush depth of the four quarter sections was measured, and the average crush depth was found to be 2.04 inches. The post-test inspection of the scale model top impact limiter indicated that the "pseudo" top neutron shield plate on the model body had contacted the impact limiter and had left an indentation on the outer top surface of the impact limiter. The pretest nominal gap between the top surface of the impact limiter and the top neutron shield plate is (4.61 - 2.75) inches, or 1.86 inches. The observed average crush depth of 2.04 inches corroborates the observed indentation, since the associated model movement would have closed the 1.86 inch pretest gap and resulted in the top surface indentation as observed.

2.10.3.3.3.2 Accelerometer Data

The unfiltered accelerometer traces were electronically stored to permit filtering after the tests. The trace shown captured the initial impact of the scale model. An initial observation

of the trace is the significant "noise" vibrations associated with the accelerations. Additionally, inspection of the traces showed that the initial acceleration change was over 500 g, which occurred over three time points and the time between individual time points in the trace is 30.5 microseconds. Thus, the trace suggests that the acceleration achieves this initial value in approximately 60 microseconds and then begins to subside (from the maximum value). The impact limiter is evaluated to determine whether there is a basis for this large accelerometer response. A cursory review of the immediate load paths in the impact limiter does not support the ability to generate this type of loading. Four considerations are discussed below.

1. If the scale model retaining rods (ASME SA-193 Grade B8S) did not buckle, but instead, initiated metal flow, the load path through the rods would be an immediate load path from the scale model to the impact plane. This immediate load path could arise, since the retaining rods attach directly to the scale model lid.
   The immediate acceleration (A_{flow}) in units of gravity would be the ratio of the product of the total area of the retaining rods multiplied by the dynamic flow stress of the material to the weight of the scale model package.

   $$A_{flow} = N(\pi/4)(d)^2(\sigma_d)/W = 22.2 \text{ (g)}$$

   Where:

   σ_d = (95+50)/2 = 72.5 ksi (the average of the tensile and yield strengths at 70°F for ASME SA-193 Grade B8S)
   W = model weight acting on the retaining rods = 3,945 pounds (3,811 pounds for the model body and 134 pounds for the test weight representing the bottom impact limiter.
   N = number of retaining rods = 16 rods
   d = diameter of the retaining rod = 0.31 inch.

2. If the scale model impact limiter shell did not buckle at the 18.7-inch inner recess diameter, but instead, initiated metal flow, this section of the shell would be an immediate load path between the model lid and the impact plane. Before other sections of the model impact limiter shell can deform in the axial direction, the load must be transferred through the inner recess shell first.

   The immediate acceleration (A_{flow}) in units of gravity would be the ratio of the product of the total area of this section of the model impact limiter shell and the dynamic flow stress of the material to the weight of the scale model package.

A_{flow} = $(\pi)(18.7)(.06)(52,500)/3,945 = 46.9$ (g)

Where:

d = Thickness of the scale model impact limiter shell is 0.06 inch

σ_d = (75+30)/2 = 52.5 ksi (the average of the tensile and yield strengths at 70°F for Type 304 stainless steel)

W = model weight = 3,945 pounds (3,811 pounds for the model body and 134 pounds for the test weight representing the bottom impact limiter)

3. If the entire area of the redwood in the scale model impact limiter (outside diameter = 31 inches) would instantly initiate crushing, the force applied to the model for deceleration would be the ratio of the product of the cross-section area of the impact limiter and the intial crush strength of the redwood to the weight of the scale model package.

A_{flow} = $(\pi/4)(31)2(640)/4,078 = 118$ (g)

Where:

d = Outer diameter of the model impact limiter shell = 31 inches

σ_d = The initial crush strength of the redwood in the direction perpendicular to the grain = 640 psi

W = model weight acting on the top impact limiter bolts = 4,078 pounds (3,811 pounds for the model body, 133 pounds for the top impact limiter and 134 pounds for the test weight representing the bottom impact limiter)

4. If the redwood in the backed area of the model impact limiter (area directly under the model cask body) is considered as an elastic component only, the minimum immediate response time can be computed using the fundamental mode of the mass of the model acting on the redwood.

The total weight (W) of these components is W = 3,945 pounds (3,811 pounds for the model body and 134 pounds for the test weight representing the bottom impact limiter). The corresponding mass (m) is computed as 3,945/386.4 or 10.21 lb-sec^2/inch. The equivalent axial stiffness (K) of the system is:

$K = A \times E/L = 48.1$ E6 pounds/ inch

Where:

A = cross sectional area (backed area) of the redwood = $(\pi/4)\ (18.7)^2 = 274.6$ in^2
E = modulus of elasticity of redwood = 1.4 E6 psi
L = 8 inches (10.75 - 2.75)

The corresponding natural frequency is:

$$f = (1/2\pi)\sqrt{(K/m)}\ (Hz)$$
$$f = 345\ Hz$$

Based on this natural frequency, the accelerometer trace should indicate that for the initial peak, the acceleration varies from a positive maximum value to a negative one, corresponding to the signal period/2 or (1/345)/2 = 1,449 micro-seconds. Since the time points on the acceleration trace are 30.5 micro-seconds, there should be approximately 48 (1,449/30.5) acceleration points showing the motion from zero to the initial maximum negative value. The accelerometer traces do not demonstrate this hypothesis. Thus, the use of the elastic properties for the redwood is significantly over-conservative.

It is concluded from the foregoing four considerations, that these conservative calculations confirm that the initial acceleration values are a result of high frequency effects in the accelerometer and, therefore, filtering the acceleration data is appropriate. The filtered results do not show the steep rise time nor the associated level of accelerations that are present in the unfiltered trace. The filtered result is superimposed on the unfiltered trace in Figure 2.10.3-2. The filtered data was integrated to obtain the velocity of the model body and was shown to match the 527.4 in/sec initial velocity. The peak acceleration is shown to be 51.8 g for the full-scale UMS® package.

2.10.3.3.4 Static Crush Test for the End Drop Orientation

To further confirm the design of the UMS® impact limiters, a static crush test in a top end drop orientation was conducted. The purpose of the static test was to: 1) identify any potential initial stiffness in the impact limiter, which would corroborate the large accelerations observed on the accelerometer traces during the early part of the 30-foot top end drop impact; and, 2) indicate

any effect of the thick-walled screw tubes on the impact limiter crush force in the end drop orientation.

To provide test data for these objectives, two tests were performed:

1. Static Test 1 used an uncrushed section of the quarter-scale impact limiter design exactly as tested in the 30-foot end drop test.
2. Static Test 2 used an uncrushed section of the quarter-scale impact limiter without the 0.035-inch thick screw tubes, but otherwise identical to the end drop test limiter.

For the UMS® impact limiter design in the end drop orientation, the grain direction of the redwood is perpendicular to the direction of crush. The retaining rods and the screw tubes are equally spaced every (360°/16), or 22.5°. The static crush test used a 45°-section of a model impact limiter, which included two retaining rods and two screw tubes. Thus, the lateral circumferential edges of the test section correspond to the circumferential midpoint between two bolts. For a 45°-section, the boundary conditions at the edges require that all displacements perpendicular to the side be zero. For the thin impact limiter shell, the additional requirement of constraining certain rotation components (as would be performed in an analytical evaluation) is required. For structures developing their strength from flexure, this is a significant restraint condition, but the strength of the impact limiter shell is due to membrane stiffness not flexural stiffness. Therefore, relaxing the rotation condition at the edge of the section of the model impact limiter for this test has no effect on the results.

Additionally, the model lid must remain horizontal as it moves into the model impact limiter, just as in the case of an end drop. Two new retaining rods and associated nuts were used to connect the 45°-section of the impact limiter to a 45°-section of the model lid. The section of the model lid used in the static crush test included the recess for the lid bolts. The static test uncrushed section model used the same design and materials for the retaining rods and lid bolts as used in the scale model 30-foot end drop test.

The static test 45°-section of the scale model impact limiter was inserted into the static test fixture between the lid, which connected to the upper head of the testing machine, and a bottom plate representing the impact plane. The details of the fixture are shown in NAC Drawing 790-401, "Crush Fixture, End Drop, UMS® Testing," Sheets 1 through 3.

In the static test fixture, the lateral restraints were provided by 1-inch thick steel plates supported by 1-inch thick, triangular gussets. The sides of the fixture and the gussets were welded to the 1-inch thick base plate. All welds were fillet welds and all were located outside the region containing the 45° section of the model impact limiter. To ensure that the 45° section of the impact limiter did not move radially outward in the test fixture during the test, a curved bar (rectangular cross section of 0.18 inch by 1 inch) was fitted around the outer surface of the model impact limiter section and bolted to the lateral plates of the test fixture.

The recorded test data included the force-deflection curve for the 45°-section of the model limiter, as well as the displacements at the lateral sides of the test fixture and the radial displacement of the limiter.

The static tests were conducted at Precision Components Corporation in York, Pennsylvania, using a Tinius Olsen testing machine capable of applying 500,000 pounds of compressive load. The use of this equipment established a slow compression speed representative of a static test. Thus, the crush strengths observed in the test correspond to static crush strengths. To account for the dynamic effect in crushing the redwood, the static forces are factored by 1.058 (Section 2.6.7.5.3). Since the static test uses an 1/8th section (45°) of the quarter-scale model impact limiter, the total force (F_{total}) generated for a full quarter-scale model is determined as eight (8) times the force value observed in the static test. The corresponding acceleration for the quarter-scale model is (F_{total}/4,033), where 4,033 pounds corresponds to the minimum weight of the quarter-scale model.

The energy absorbed ($E_{limiter}$) by the model impact limiter section during the static test is computed by integrating the area under the force-deflection curve. In the end drop orientation, the crush depth of the limiter must be included in the total potential energy (E_{total}) calculation for a 30-foot drop.

$$E_{total} = (4{,}033)(360+\delta)$$

Where:

W = model weight = 4,033 pounds
D = drop height = 360 inches
δ = the crush depth.

The force applied in the static crush test was increased until the energy absorbed by the model impact limiter section ($E_{limiter}$) was equivalent to, or greater than, the total potential energy (E_{total}) of the quarter-scale model for a 30-foot drop.

2.10.3.3.4.1 Static Test Results

1. The lateral displacements of the sides of the test fixture were measured to be less than 0.001 inch and the outward radial displacement of the test article was less than 0.1 inch. These values indicate that the boundary conditions were satisfied.

2. No malfunctions of the equipment or instrumentation were experienced.

3. The force-deflection curves for the model impact limiter sections used in Static Test 1 and Static Test 2 are shown in Figures 2.10.3-3 and 2.10.3-4, respectively. These curves include the previously discussed geometry and dynamic load factors of 8 and 1.058, respectively.

4. The following crush and accelerations were determined based on Static Test 1 and Static Test 2. These values correspond to the conditions at the end of the test in which the energy absorbed by the model limiter section equals or exceeds the total potential energy of the scale model for a 30-foot drop. The force values include the geometry and dynamic load factors of 8 and 1.058, respectively.

Static Test	Crush Depth (in) (δ)	Force (kips) (F_{total})	Acceleration (g) (F_{total}/W)
1 (base line case)	3.24	701.7	174
2 (without the screw tube)	3.70	680.0	168.6

2.10.3.3.4.2 Static Test Observations

1. No initial peaks in the loading were observed for either Static Test 1 or Static Test 2. The crush forces developed in a monotonic manner increasing from zero to the maximum force reported above. During the static tests, there were no mechanical shocks observed in the equipment nor in the floor on which the testing machine was supported.

2. While the screw tubes are a source of significant strength, the initial deformation of the impact limiter does not occur in the region of the screw tubes. The calculated final accelerations for the model impact limiter design with the screw tube was only 3 percent larger than the design without the screw tubes.

3. The axial section of the model impact limiter shell at the 18.7-inch diameter next to the model lid buckled in the same general shape in the static test as in the 30-foot top end drop. Since the crush force developed in a monotonic manner and the mode of deformation between the static and dynamic drops are the same, it indicated that this section of the model impact limiter shell does not deform by plastic flow of the metal and does not contribute to large initial accelerations.

4. The crush and the accelerations reported above for the section of a model impact limiter is compared to the LS-DYNA results presented in Section 2.10.3.7. The static crush test results are compared to the LS-DYNA results in the following table:

Quarter-Scale End-Impact Static Test	Quarter-Scale Crush Depth (in)	Quarter-Scale Acceleration (g)	LS-DYNA Calculated Crush Depth (in)	LS-DYNA Calculated Acceleration (g)
Test 1	3.3	174	2.21	226
Test 2	3.7	169		

For the maximum acceleration case, the Static Test results are enveloped by the LS-DYNA analyses.

2.10.3.3.4.3 Summary of the Static Tests

The results of the static tests indicate that the initial high accelerations observed in the drop tests are a result of accelerometer high frequency effects. The filtered acceleration data more accurately reflects the response of the impact limiter in an end drop impact. Additionally, the static tests confirm that the impact limiter for the end drop has sufficient energy absorption capacity.

2.10.3.3.5 Results/Evaluation for the 30-Foot Top Corner Drop Test

The 30-foot top corner drop test was the second test to be completed using the UMS® quarter-scale model. Prior to lifting the scale model package to the 30-foot drop height, the torque for the retaining rods and nuts were confirmed to ensure that the torque specifications were met.

Only the upper impact limiter was attached to the cask model. The bottom end of the scale model used the same test weight that was used for the top end drop. This test weight is an inexpensive substitute for a bottom impact limiter and ensures that the tested package has the proper weight and CG location for the UMS® transport cask.

Two high speed cameras were used to record the top corner drop impact. One of the high speed cameras recorded a close-up view of the impact limiter crush in the region of the impact plane. The other camera recorded an overall view of the drop test and showed that the cask orientation was very close to the target angle of 23° from vertical.

2.10.3.3.5.1 Accelerometer Data

An initial observation is that significant "noise" vibrations associated with the accelerations do exist and that filtering of the accelerometer data is appropriate. The filtered result is superimposed on the unfiltered data in Figure 2.10.3-4. The results from the LS-DYNA finite element analysis program, and the maximum acceleration determined from the three accelerometer traces, are:

Location	Quarter-Scale Model Acceleration (g)	LS-DYNA Calculated Acceleration (g)
Top Impact Limiter	121	143

The acceleration determined from the quarter-scale model top corner drop test is enveloped by the LS-DYNA calculated design basis accelerations.

2.10.3.3.5.2 Summary of the Top Corner Drop Test Results

The crush depth and impact accelerations determined from the 30-foot top corner drop test of the UMS® quarter-scale model are enveloped by the LS-DYNA calculated design-basis analysis

data used in the SAR. The UMS® impact limiters are confirmed to provide adequate design margin to limit the acceleration and the crush depth of the transport cask for the 30-foot top corner drop. Thus, the UMS® cask body will not contact the impact plane during the 30-foot top corner drop.

2.10.3.3.6 Impact Limiter Deformation and Attachment Data

After the top corner drop test, the scale model package was lifted off the ground to remove the impact limiter. Similar difficulties in removing the deformed impact limiter were encountered, as with the top end drop, due to the plastic buckling of the retaining rods inside the screw tubes. Upon removing the upper impact limiter, it was observed that the three retaining rods nearest the point of impact were broken. Due to the difficulty of the process, removal of the upper impact limiter after the test may have broken these retaining rods (as in the case of the top end drop). The remaining 13 of the 16 retaining rods were intact and were still threaded into the end of the model. These results confirm that the upper impact limiter remained attached to the cask model during and after the top corner drop test.

Measurements of the model impact limiter dimensions after the top corner drop test were obtained to determine the crush depth. The measured crush depth is tabulated as follows, along with the LS-DYNA calculated crush depth. The quarter-scale model crush depth is multiplied by 4 (the scaling factor) to obtain the full-scale design crush depth. The crush depth reported in this section is the maximum crush depth for the upper impact limiter away from the trunnion cutout region.

Location	Quarter-Scale Model Impact Limiter Crush Depth (inch)	LS-DYNA Calculated Crush Depth (inch)
Top Impact Limiter	3.2	3.4

The resulting crush depth determined from the quarter-scale model top corner drop test is enveloped by the LS-DYNA calculated design-basis crush depths for the full-scale UMS® transport cask for a 30-foot top corner drop with impact limiters.

2.10.3.4 30-Foot Side Drop Test Performed at SNL

A quarter-scale model was used for the confirmatory testing of the UMS® impact limiters and attachments for a 30-foot side drop. The drop test was performed at Sandia National Laboratory (SNL) in March 2001. The quarter-scale model represents the materials and physical dimensions of the impact limiters and their attachments to the cask body in conjunction with the appropriate cask body weight, center of gravity, and attachment interface dimensions. Details of the test model are shown in the model drawing 790-308, Sheets 1 and 2.

The cask body is constructed of carbon steel. The 52.31-inch overall length of the cask body is comprised of a 38.64-inch length of 20-inch diameter schedule 120 pipe welded to an 8.36-inch thick plate at the top end. A 5.57-inch thick end plug welded to the inner shell seals the top end. At the bottom end, the 20-inch pipe outer shell is welded to a 3.3-inch thick lower end ring and 2-inch thick lower cap plate.

The top end plate is machined to represent the scaled outside diameters and axial dimensions of the upper forging and the neutron shield top plate. Two steel bars, scaled to represent the diameter and length of the cask lifting trunnions, are welded in the appropriate locations on the outside diameter of the top end plate. The 3.3-inch thick lower end ring and 2-inch thick lower cap plate are machined to represent the scaled outside diameters and the axial dimensions of the bottom end of the UMS® cask, including the neutron shield bottom end plate. The lower cap plate thickness is not scaled, since it is only required to provide backing area for the bottom impact limiter and to contribute to the weight and CG location of the scale model.

The inner shell of the cask body is constructed of a 14-inch diameter Schedule 80 pipe. The inner shell extends the length of the cask body and is flush with the top surface of the top end plate. At the lower end, the inner shell is welded to the inside surface of the lower cap plate. To properly represent the uniform axial weight distribution of the fuel and basket, the space between the inner and outer shells is filled with a uniform thickness of lead. The thicknesses of the inner and outer shells were selected to allow the cross sectional moment of inertia of the cask body cross section to correspond to $(1/4)^4$ of the full-scale design. The thickness of the top and bottom plates were adjusted to allow the model CG and polar moment of inertia to be scaled to the full-scale design. This ensures that the load distribution to the model impact limiters for the drop test is representative of the loading that would occur on the full-scale UMS® transport cask.

The total weight of the quarter-scale model, including the impact limiters, was 4,062 pounds, which closely approximates $(1/4)^3 = 1/64$ of the full-scale transport cask weight of 260,000 pounds.

The model impact limiters are quarter-scale representations of the full-scale impact limiters. The redwood and balsa wood used in the model limiters meets the same specifications that are defined for the full-scale UMS® transport cask limiters in this SAR. The wood section shapes, joints, and bonds of the scale model impact limiters duplicate those of the full-scale impact limiters. The grain orientation of the redwood and balsa wood in the scale model impact limiters is identical to that as designed in the full-scale impact limiters. The scale model impact limiter shells were fabricated from 16 gauge (0.0625-inch thick) Type 304 stainless steel sheets, and the screw tubes, which serve as the penetrations for the impact limiter retaining rods, were fabricated from 0.035-inch thick, 0.75-inch diameter tubes. Each model impact limiter is attached to the cask by sixteen quarter-scale retaining rods fabricated from ASME SA-193 Grade B8S stainless steel.

The model impact limiter shells - i.e., material thickness, geometry, and welds - are appropriately quarter-scale. The diameter of the screw tubes is quarter-scale, but the tube wall thickness is full-scale due to fabricability and material availability limitations. The use of the thicker tube is considered to be conservative, since it tends to increase the stiffness of the limiter, if it has any effect at all. The effect of the tube thickness on the drop test results is insignificant, since the tubes are not located in the primary crush regions of the impact limiter.

2.10.3.4.1 Equipment and Instrumentation for the Tests Conducted at SNL

The pad for the side drop test at the SNL functions as the essentially unyielding impact surface. The surface of the target consists of armor plate measuring 34 feet by 16 feet and has a varying thickness from 8 inches to 4 inches. The plate is attached to reinforced concrete that allows the total mass of the system to be 1,000 tons. The total mass of the target is approximately 500 times that of the quarter-scale test model, which is large compared to the ratio of 30 recommended by IAEA. The pad at SNL is considered to meet the IAEA requirements for a drop test pad.

Lifting and dropping the model was performed with a system of cables to provide sufficient restraint from lateral motion of the cask, as well as limit the motion of the cables upon release of the cask model. The cask model was attached to the cable system via a single point, and an explosive bolt mechanism was used to release the cask from the cables. This mechanism

allowed the free fall of the package to be initiated in an unimpeded fashion with minimum perturbation to the horizontal position of the cask model.

To assess the model performance with respect to the acceptance criteria, a set of basic data is collected. This data included:

1. Accelerometer data - to determine the maximum impact acceleration of the cask. All of the accelerometers used in the drop tests were the same model and they were calibrated to traceable standards. Individual accelerometers were mounted on steel blocks attached to the cask body. Three accelerometers were mounted near the top end of the cask and three were mounted near the bottom end of the cask to record the vertical accelerations during impact. Figure 2.10.3-5 is a photograph of the quarter-scale model, which shows the location of the accelerometers. The acceleration time histories were stored electronically, which permitted them to be filtered after the test was completed.

2. Impact limiter deformation data - to evaluate the behavior of the impact limiters, the crush depth and the condition of the impact limiter attachment.

3. High speed photography - to review and assess the actual angle of impact and the behavior of the impact limiters during the impact.

2.10.3.4.2 Filter Frequency Identification for the Accelerometer Data for the Side Drop

In the side drop (horizontal) orientation the load in the model body must be transferred to the impact limiters attached to the ends of the model body. The fundamental mode shape for the side drop corresponds to a beam with free-free end boundary conditions. Since the length to diameter ratio is approximately 2, the flexibility due to shear must be included. This is accomplished by computing the natural frequency due to the shear and the corresponding frequency due to flexure and then combining them.

The natural frequency for the mode shape due to shear for free–free end boundary conditions, (fs), is given by:

$$fs = \frac{\lambda}{2\pi L}\sqrt{\frac{k'G}{\rho}}$$

Blevins [50], Table 8-15, Case #1

Where:

λ = π (Blevins, Table 8-15)
L = distance between supported ends = 44.6 inches
k′ = shear coefficient = 0.54
G = shear modulus of elasticity = (28.3E+6)/((2) (1+v)) = 10.9 E+6 psi
ρ = effective mass density = 2812 /(87.2 × 44.6)/386.4 = 0.00187 lb-sec^2/in

Note that the 2,812 pounds includes the weight of the pipes and the lead. The outer shell is comprised of a 20-inch Schedule 120 pipe and the inner shell consists of a 14-inch Schedule 80 pipe.

The shear coefficient, k′, is dependent on the cross sectional shape of the model body:

$$k' = \frac{6(1+v)(1+M^2)^2}{(7+6v)(1+M^2)^2+(20+12v)M^2}$$ Blevins, Table 8-14

Where:

M = b/a
v = Poisson's ration = 0.3

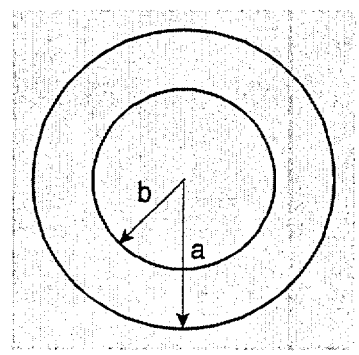

For a 20-inch diameter Schedule 120 pipe

b = 8.5 in
a = 10.0 in

Therefore:

k′ = 0.54

Substituting,

fs = 629 Hz

The natural frequency for the mode shape due to bending for the free-free end boundary conditions, (fb), is given by:

$$fb = \frac{\lambda^2}{2\pi L^2}\sqrt{\frac{EI}{\rho'}}$$ Blevins, Table 8-1

Where:

$\lambda = \pi$

$L = 44.6$ inches

Using the cross-section of both pipes, the moment of inertia is:

$$I_{20} = \frac{\pi}{64}(D_0^4 - D_i^4) = \frac{\pi}{64}(20^4 - 17^4) = 3{,}754 \text{ in}^4, \text{for the 20-inch pipe, and}$$

$$I_{14} = \frac{\pi}{64}(D_0^4 - D_i^4) = \frac{\pi}{64}(14^4 - 12.5^4) = 687 \text{ in}^4 \text{ for the 14-inch pipe}$$

The total moment of inertia is 4,441 in^4.

$E = 28.3E{+}06$ psi

ρ' = effective mass per unit length of beam

$= 2{,}812/44.6/386.4 = .163$ lb-sec^2 / in^2

Substituting,

fb = 694 Hz

In accordance with Blevins, the shear and bending mode frequencies are combined as:

1/fc = 1/fs + 1/ fb

or

fc = 330 Hz

The filter frequency is conservatively selected to be 450 Hz for the side drop.

2.10.3.4.3 Results/Evaluation for the 30-Foot Side Drop

The 30-foot side drop was the only test performed at SNL using the quarter-scale model for the transport cask. Prior to lifting the scale model package to the 30-foot drop height, the torque for the retaining rods and nuts were inspected to ensure that the torque specifications were met.

High-speed cameras were positioned at two locations with respect to the model. Cameras were positioned to view the model from the end and cameras were positioned to obtain a side view of the model impacting the pad. The lateral view confirmed that the axis of the cask model was

effectively horizontal at the time of impact. There appeared to be no rocking of the cask during the drop and the model rebound was less than six inches after the initial 30-foot drop impact.

2.10.3.4.4 Impact limiter Deformation and Attachment Data

After the side drop test, it was observed that the impact limiters remained attached to the cask body model (see Figure 2.10.3-5). The impact limiters were removed and it was observed that twelve attachment rods remained intact for the top impact limiter and nine attachment rods remained intact for the bottom impact limiter. These results indicate that both impact limiters remained attached to the cask body during and after the side drop test. Upon inspection of the rods, it was determined that the rods, which failed outside the crushed region, exhibited a tensile failure at the location where the attachment rod abruptly changed diameter (threaded undercut). The design of the square cut out in the attachment rod has been reversed to allow the thread run out to terminate at the location of the previous square cut out.

Measurements of the deformed model impact limiter dimensions were obtained after the side drop test to determine the crush depth that occurred. These dimensions are tabulated below, along with the crush depth calculated by LS-DYNA for the quarter-scale model (The description of the LS-DYNA analyses supporting these values is presented in Section 2.10.3.7).

Location	Model Drop Test Crush Depth (inch)			LS-DYNA Crush Depth Prediction (inch)		
	Original Thickness	Final Thickness	Measured Crush	Original Thickness	Final Thickness	Total Crush
Side Drop–under the trunnion	3.50	0.63	2.87	3.47	0.38	3.09
Side Drop–bottom impact limiter	5.13	2.38	2.75	5.13	2.39	2.74

2.10.3.4.4 Accelerometer Data from the 30-Foot Side Drop Test

The unfiltered accelerometer traces were electronically stored to permit filtering after the tests. Three acceleration traces were obtained near the bottom of the model and three acceleration traces were obtained near the top of the model. The acceleration time histories, both the filtered and the unfiltered data with maximum accelerations, are shown in Figure 2.10.3-6 for the top end and Figure 2.10.3-7 for the bottom end locations on the cask model. Figure 2.10.3-8 shows the acceleration trace containing the maximum acceleration for the top end along with the acceleration time history computed by LS-DYNA (as described in Section 2.10.3.9). A similar

set of curves is shown in Figure 2.10.3-9 for the bottom end of the cask that compares the maximum acceleration obtained from testing to the acceleration time history obtained from the LS-DYNA analysis in Section 2.10.3.9. The peak accelerations for the quarter-scale model are shown below.

UMS® Cask Model Drop Orientation	Model Acceleration Results (g)		LS-DYNA Acceleration Prediction (g)		Design Basis Acceleration (g)
	Top Accelerometer	Bottom Accelerometer	Top Accelerometer	Bottom Accelerometer	
Side	190	198	220	213	240

2.10.3.4.5 Energy Absorption Capacity of the Impact Limiter in the 30-Foot Side Drop

The capacity to absorb energy is the function of the impact limiter. For a side impact, the energy absorption of the impact limiter can be obtained from the 30-foot side drop test results. Similarly, the results of the static test for the end drop orientation can be used to determine the energy absorption for the end orientation. The side drop acceleration time history can be integrated twice to obtain the displacement, which can be plotted versus the force (the product of the acceleration time history and the model weight, i.e., the acceleration time history in units of g). This force versus displacement time history is shown in Figure 2.10.3-10. The area under this curve corresponds to 1.46E6 inch-pounds, which is within 1% of the total energy (TE) of the side drop test (1.47E6 inch-pounds). The total energy is obtained by multiplying the model weight of 4,060 pounds times the total distance traversed, which is 360 inches plus the average of the crush depths (2.87 + 2.75)/2. From the side drop test results, the upper impact limiter has a 0.5-inch depth of uncrushed wood remaining at the trunnion cutout and the lower impact limiter has a 2.25-inch depth of uncrushed wood remaining at the maximum crush location. Thus, the upper limiter is most limiting. Since the upper impact limiter can crush until the trunnion comes into contact with the impact plane, there is an additional 0.5-inch crush depth available. Using 750,000 pounds (which represents the total force from the top and bottom impact limiter) from the force-displacement time history curve, this potential additional 0.5-inch crush distance corresponds to 0.5×(750,000) or 375,000 inch-pounds of additional energy, which could be absorbed. Thus, for a side impact, the UMS® impact limiters have an additional energy absorption capacity of approximately 25% (375,000/1.46E6).

2.10.3.4.5 Summary of the Side Drop Test

The comparison of the maximum test accelerations to those computed by LS-DYNA is considered to be acceptable. The LS-DYNA results shows that the predicted accelerations are approximately 10% above the test values. Additionally, the design acceleration corresponding to the quarter-scale model is 240g. This indicates that, not only is there a 10% margin between LS-DYNA and the design basis acceleration, but there is considered to be additional margin between the predicted values and the test data. With respect to maximum crush depth, LS-DYNA was shown to provide a conservative prediction. Using the dynamic force-deflection curve, the UMS® impact limiter design is shown to have an additional 25% energy absorption capacity required to decelerate the transport cask. The side drop test performed at Sandia National Laboratory confirms that the UMS® impact limiters are adequate to limit the cask component accelerations well within the design basis accelerations.

2.10.3.5 Evaluation of the 30-Foot Oblique Drop

In Section 2.6.7.5.5, a parametric study was performed to show that for the NAC-STC cask, the side drop produces the maximum lateral accelerations. This is due to the low length to radius of gyration ratio for the STC cask. The following table compares the L/r of the UMS® and the NAC-STC casks. Based on this comparison, it is concluded that the side drop provides bounding accelerations over shallow oblique drops. Consequently, a separate oblique drop test is not required.

2.10.3.6 Scale Model Drawings

The drawings for the ORNL and SNL quarter-scale models are included in this section for reference.

2.10.3.6.1 ORNL Drop Test Model

The detailed dimensions, welding and materials are shown on the drawings of the model body and impact limiters used in the ORNL drop tests.

Drawing Number	Sheet	Revision	Title
790-300	1	3	Drop Test Assembly 1/4 Scale Model
790-301	1 through 3	6	1/4 Scale Cask Model, NAC- UMS®
790-401	1 through 3	2	Crush Fixture, End Drop, UMS® Testing
790-602	1	0	Lower Impact Limiter, 1/4 Scale Model, NAC-UMS®
790-603	1	0	Upper Impact Limiter, 1/4 Scale Model, NAC-UMS®

2.10.3.6.2 SNL Drop Test Model

The detailed dimensions, welding and materials are shown on the drawings of the model body and impact limiters used in the SNL drop test.

Drawing Number	Sheet	Revision	Title
790-308	1 and 2	0	1/4 Scale Cask Body 2001 Drop Confiramation NAC-UMS®
790-309	1	0	Drop Test Assembly, 2001 Drop Confirmation NAC-UMS®
790-302	1 and 2	3	Lower Impact Limiter, 1/4 Scale Model, NAC-UMS®
790-303	1 and 2	6	Upper Impact Limiter, 1/4 Scale Model, NAC-UMS®

2.10.3.7 LS-DYNA Analyses of the UMS® Quarter-Scale Model

The finite element model of the quarter-scale UMS® cask equipped with redwood impact limiters was built using LS-DYNA's Finite Element Model Builder. The top end, top corner, and side impact analyses were performed using the LS-DYNA program. The model is constructed of 8-node brick and 4-node shell elements. Using the symmetry planes that exist for the various drop orientations, the model was simplified so that only a half-model was necessary for the analyses. The finite element model used in the analyses corresponds to the quarter-scale cask body and impact limiters. The complete finite element model is shown in Figure 2.10.3-11.

The cask body section of the model consists of a single shell using an elastic material. The elastic modulus of the cask body was adjusted to allow the cross sectional modulus of the finite element model to be equal to that of the quarter-scale model. As shown in Figure 2.10.3-11, the model contains a detailed representation of the trunnion and the cut out (trunnion pocket) in the top impact limiter. The impact limiters are attached to the cask ends by beam elements corresponding to the attachment bolts for the impact limiter. The redwood and the balsa wood were modeled as an isotropic foam material. The room temperature stress-strain curves used as

input into the LS-DYNA model were obtained by dynamic crush testing of redwood and balsa wood specimens as described in Tables 2.6.7.5-3 and 2.6.7.5-4.

To account for the deformation of the Type 304 stainless steel shells and gussets, these components were modeled with an elasto-plastic material. The LS-DYNA material Type 24 was used ("Piecewise_Linear_Plasticity"). The required input data for the stainless steel consists of the stress-strain data contained in Section 2.6.7.5.

2.10.3.7.1 Boundary Conditions and Initial Conditions

LS-DYNA "Surface_to_Surface" contact interfaces are employed between the cask body and the impact limiter shells. The unyielding surface is modeled as being flat using the Rigidwall_Geometric_Flat" option in LS-DYNA. Symmetry boundary conditions are imposed on the nodes in the X-Z plane for all drops. An initial velocity of 527.4 in./sec is applied to the entire model to represent the 30-foot drops. A uniform gravitational field corresponding to 386.4 in/sec^2 is also applied in the direction of the drop.

Three drop orientations are considered in this evaluation: top end, CG over top corner, and side drop. The end drop provides the maximum axial accelerations. The corner drop results in the largest crush depth of the limiter. The side drop provides the maximum acceleration in the lateral direction of the cask.

2.10.3.7.2 Results

To obtain results from LS-DYNA, nodes of interest are used to record output data. The nodes are located on the cask body at the plane of symmetry approximately 10 inches from the impact limiters. These data nodes correspond to the location of the accelerometers mounted on the quarter-scale model. For the side drop, the nodes record the lateral acceleration, and for the end drop they record the axial acceleration. For the CG over corner orientation, the output acceleration corresponds to the direction of the drop.

The LS-DYNA output is in the form of displacement and acceleration time histories. However, the acceleration time histories contain high frequency components that do not represent the response of the cask to the external impact. Therefore, the acceleration time histories are filtered to obtain true accelerations corresponding to the impact. For this evaluation, the Butterworth low-pass filter in LS-DYNA's post-processor is used with a filter frequency of 450 Hz for the

lateral direction and 550 Hz for the axial direction (refer to Sections 2.10.3.4.2 and 2.10.3.3.2, respectively). The Butterworth filter is used in NUREG/CR-6608 to filter the acceleration of the impact tests for a steel billet in the side drop and end drop orientation.

The following table shows the maximum accelerations for the three 30-foot drop cases.

UMS® Cask Model Drop Orientation	Model Acceleration Results (g)		LS-DYNA Acceleration Prediction (g)		Design Basis Acceleration (g)
	Top Accelerometer	Bottom Accelerometer	Top Accelerometer	Bottom Accelerometer	
Top Corner	121	N/A	143	N/A	240
Top End	207	N/A	226	N/A	240
Side	190	198	220	213	240

As the table shows, the maximum predicted acceleration of 226g occurs during the top end drop. Acceleration time-history plots are provided in Figures 2.10.3-8 and 2.10.3-9 for the side drop and Figures 2.10.3-12 and 2.10.3-13 for the top end and top corner drops, respectively. In all cases, the LS-DYNA prediction is greater than the quarter-scale drop test results.

A comparison of the predicted crush depth to the actual crush depth is provided in the following table:

Location	Model Drop Test Crush Depth (inch)			LS-DYNA Crush Depth Prediction (inch)		
	Original Thickness	Final Thickness	Measured Crush	Original Thickness	Final Thickness	Total Crush
Top End Drop	[illegible]	[illegible]	2.00	[illegible]	[illegible]	2.21
Top Corner Drop	[illegible]	[illegible]	2.95	[illegible]	[illegible]	3.36
Side Drop–under the trunnion	3.50	0.63	2.87	3.47	0.38	3.09
Side Drop–bottom impact limiter	5.13	2.38	2.75	5.13	2.39	2.74

The table shows that LS-DYNA accurately predicts the amount of crush experienced during the drop tests except in regions where extreme irregular deformation occur (i.e. directly below the trunnion and corner). Figure 2.10.3-14 shows a direct comparison between the side drop test and the LS-DYNA analysis. As the figure shows, LS-DYNA provides a reasonable prediction of the crush depth that occurs in the drop accident.

Figure 2.10.3-1 Typical Filtered Acceleration Time History for the Quarter-Scale Model Top End Drop, Overlayed with the Unfiltered Data

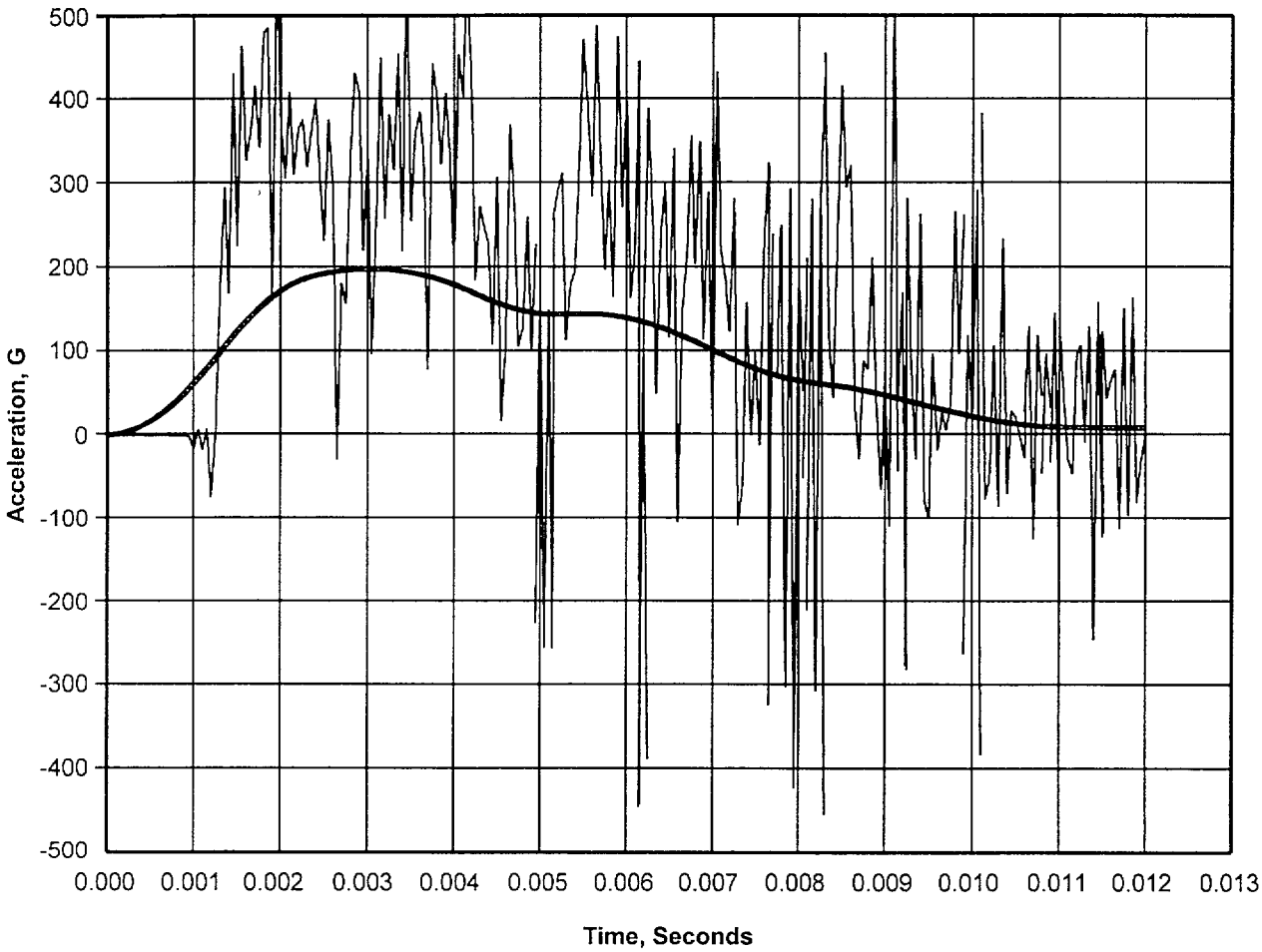

Figure 2.10.3-2 Force-Deflection Curve for Static Test 1 (End Drop Orientation) for a 45° Section of the Quarter-Scale Model Upper Impact Limiter

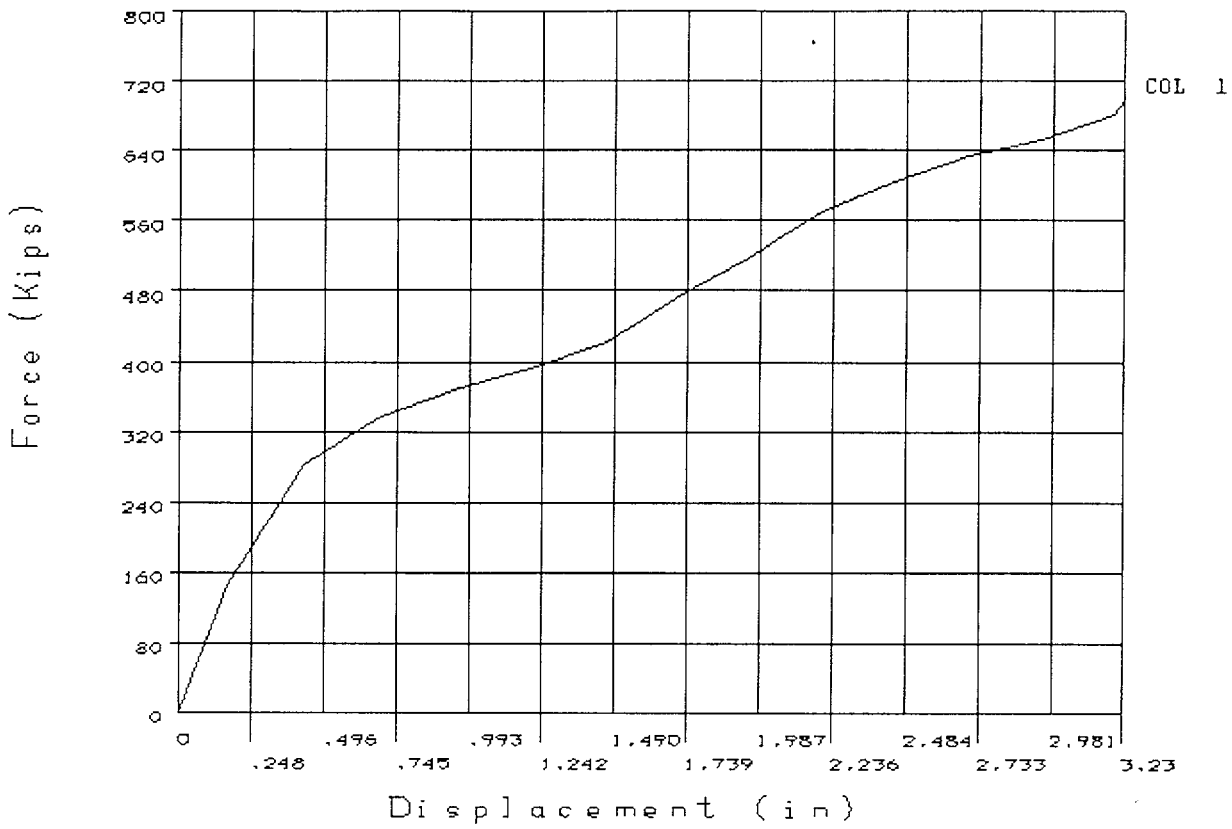

Note:

Forces correspond to a full quarter-scale model of the UMS® upper impact limiter. The forces have been factored by 1.058 to account for the dynamic crush strength of redwood.

Figure 2.10.3-3 Force-Deflection Curve for Static Test 2 (End Drop Orientation) for a 45° Section of the Quarter-Scale Model Upper Impact Limiter

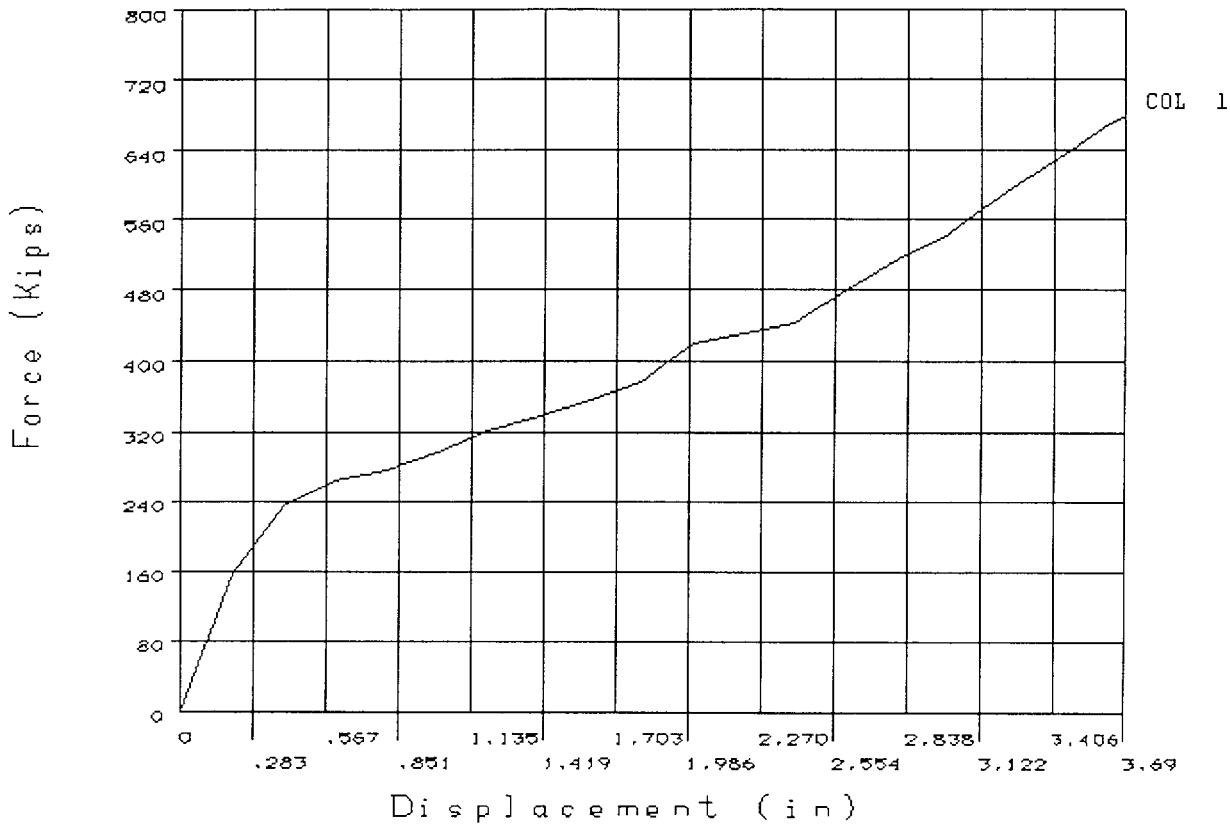

Note:

Forces correspond to a full quarter-scale model of the UMS® upper impact limiter. The forces have been factored by 1.058 to account for the dynamic crush strength of redwood.

Figure 2.10.3-4 Typical Filtered Acceleration Time History for the Quarter-Scale Model Top Corner Drop, Overlayed with the Unfiltered Data

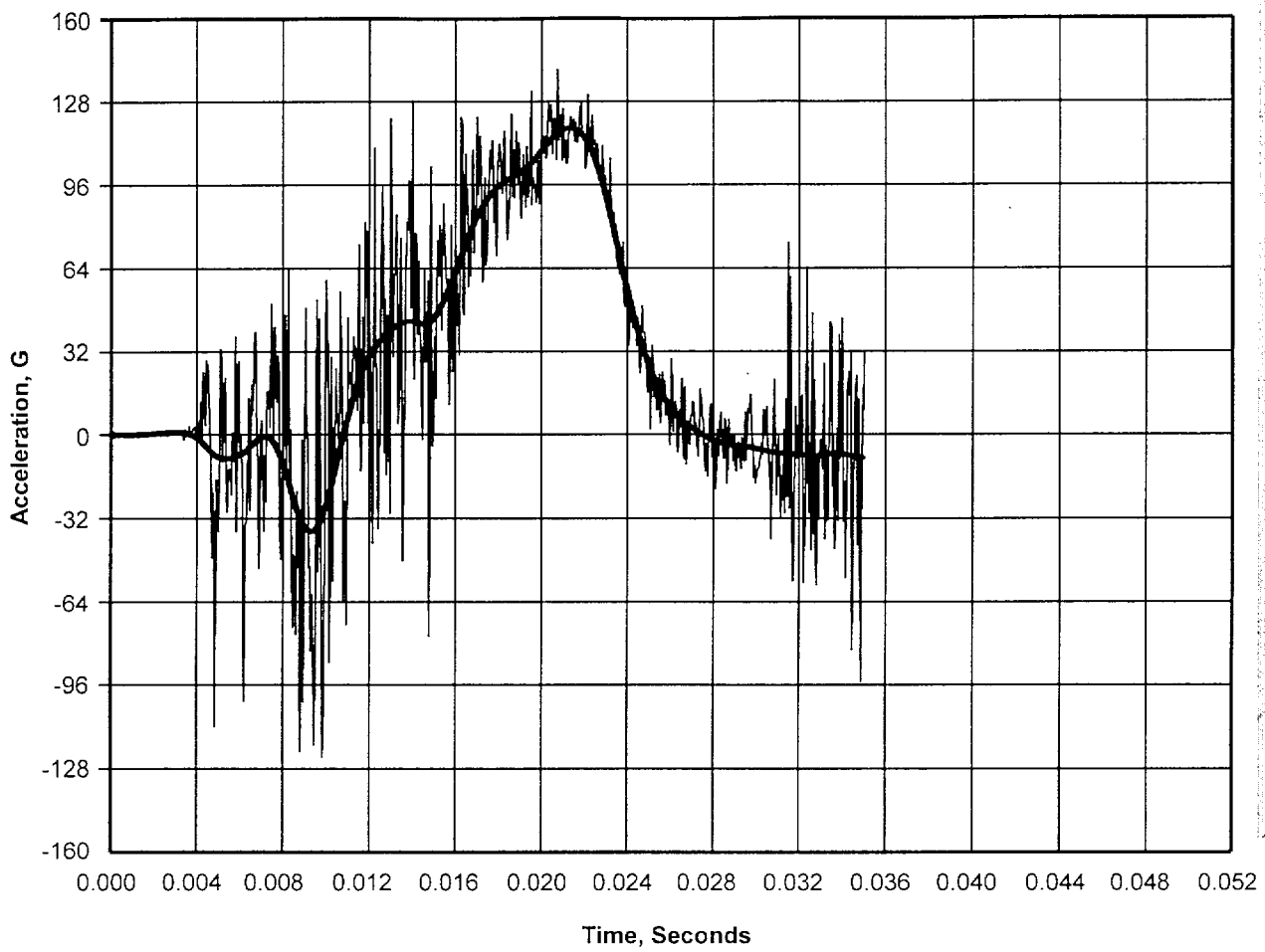

Figure 2.10.3-5 UMS® Quarter-Scale Side Drop Accelerometer Locations

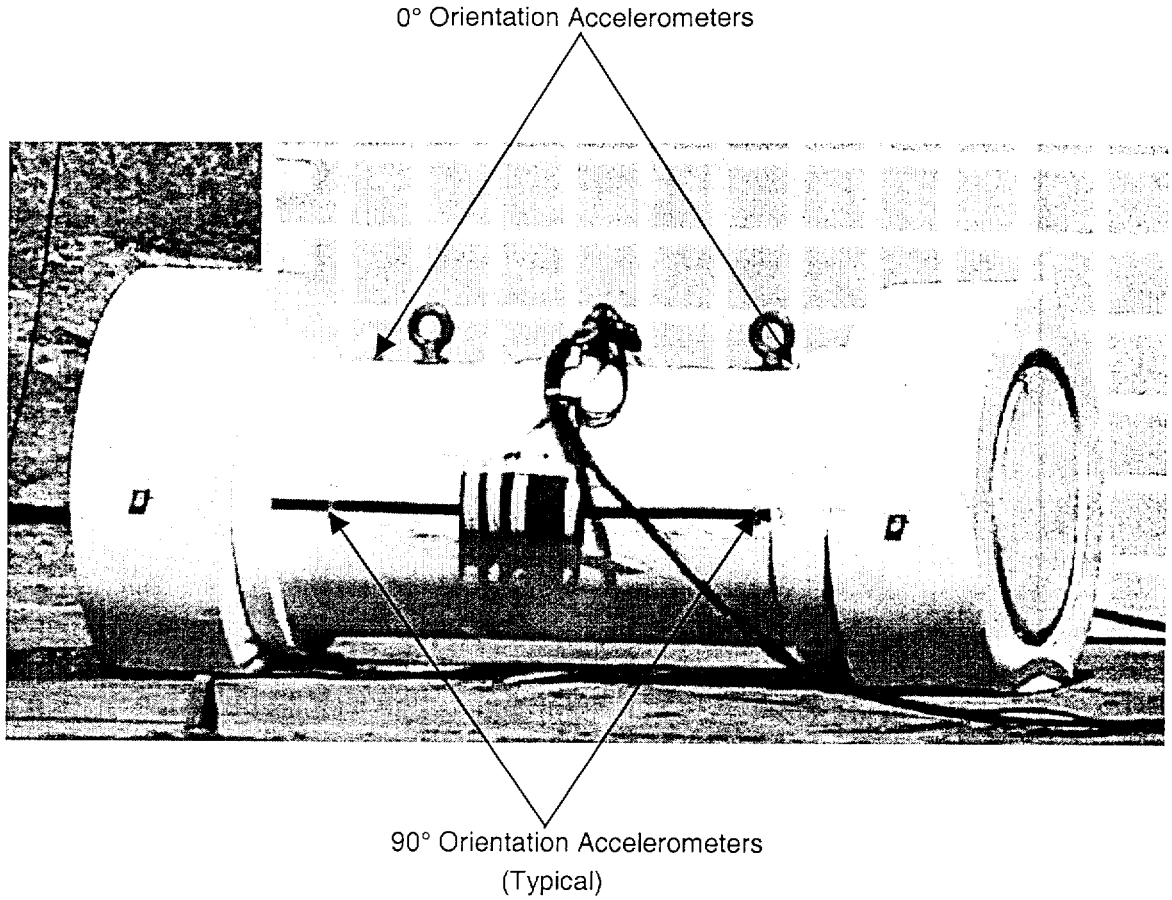

Side drop, at SNL, March 2001

Figure 2.10.3-6 Typical Filtered Acceleration (Top Accelerometer) Time History for the Quarter-Scale Model Side Drop, Overlayed with the Unfiltered Data

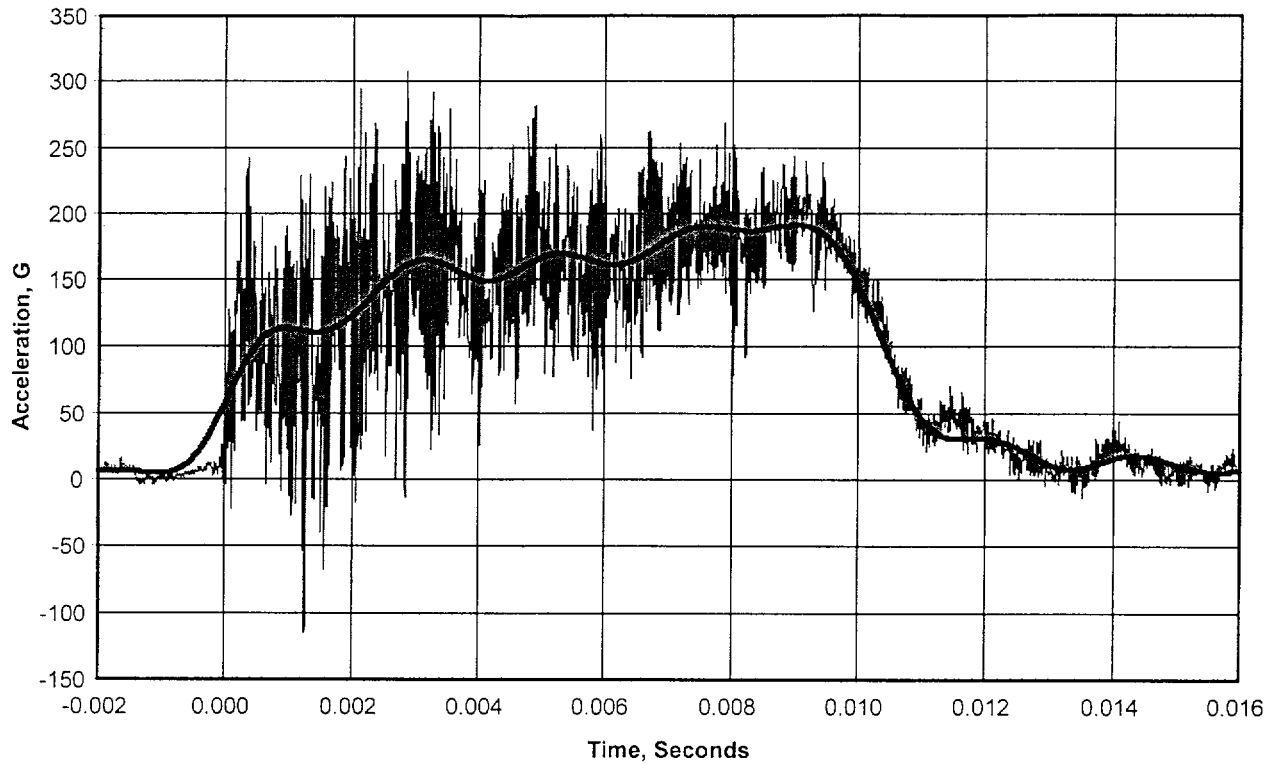

Figure 2.10.3-7 Typical Filtered Acceleration (Bottom Accelerometer) Time History for the Quarter-Scale Model Side Drop, Overlayed with the Unfiltered Data

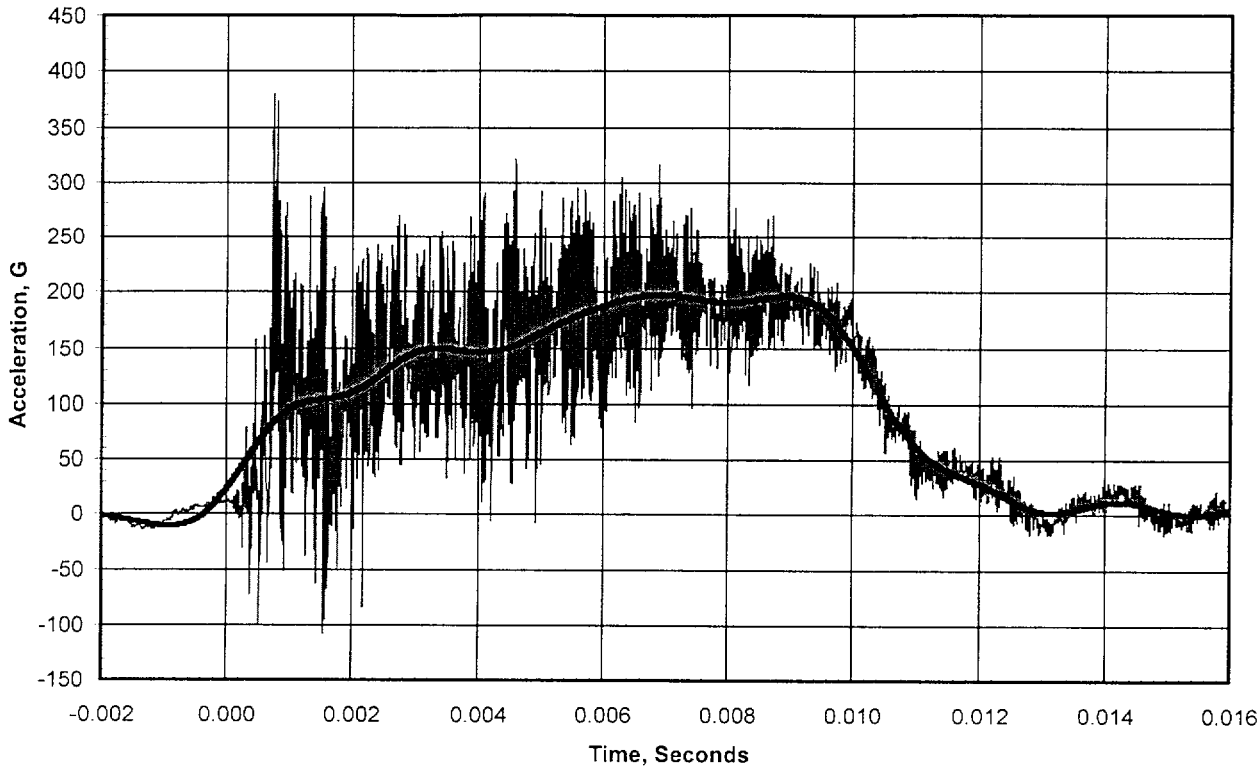

Figure 2.10.3-8 Comparison of Quarter-Scale Side Drop (LS-DYNA and Drop Test) Results (Upper Accelerometer)

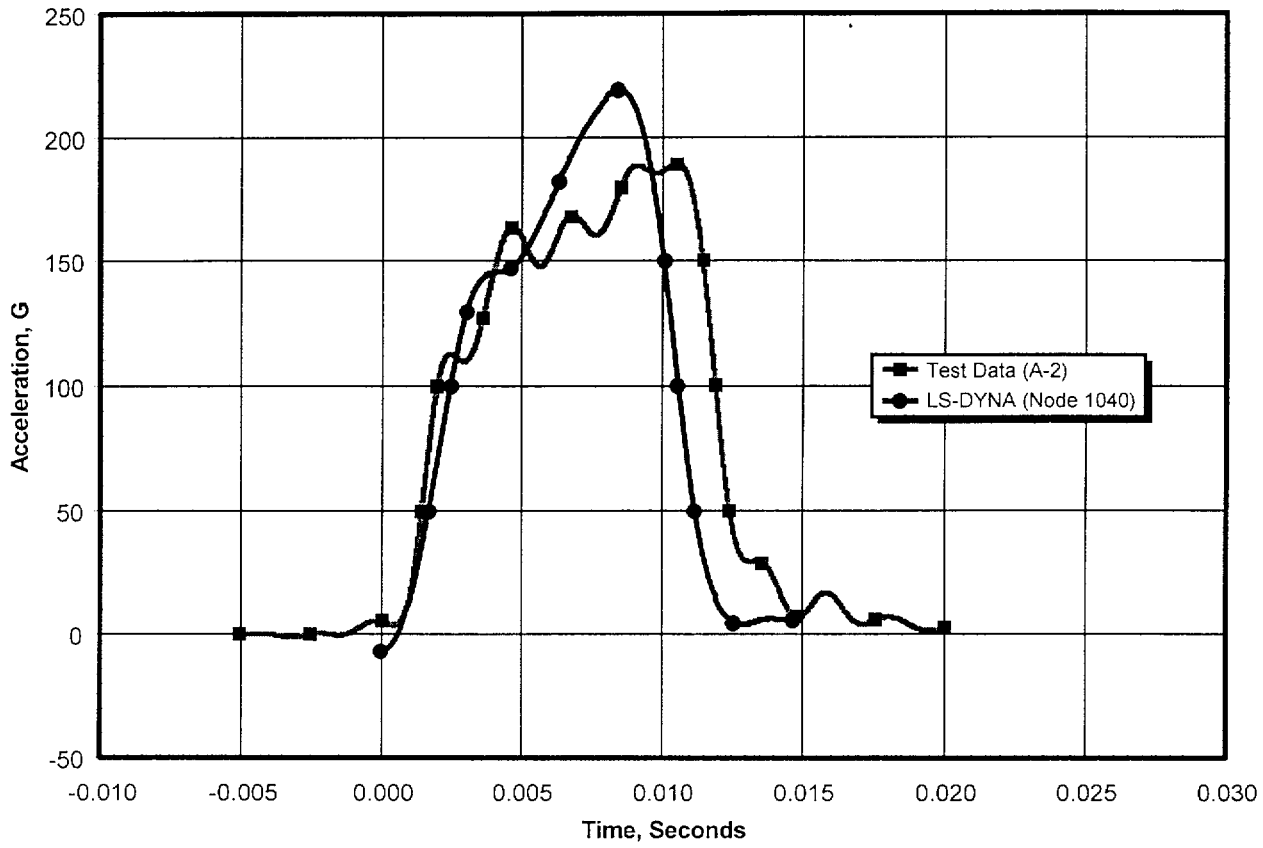

Figure 2.10.3-9 Comparison of Quarter-Scale Side Drop (LS-DYNA and Drop Test) Results (Lower Accelerometer)

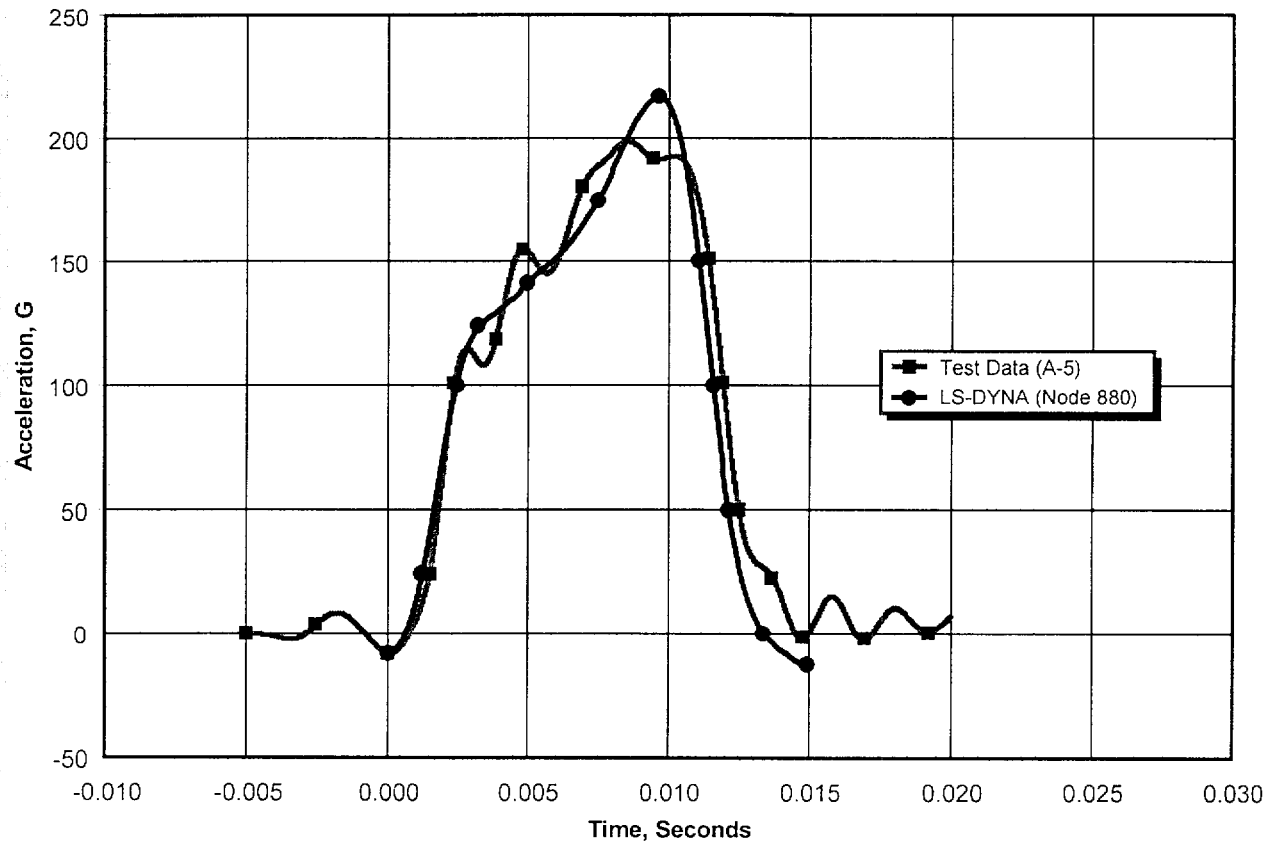

Figure 2.10.3-10 Quarter-Scale Model Side Drop Force-Displacement Curve

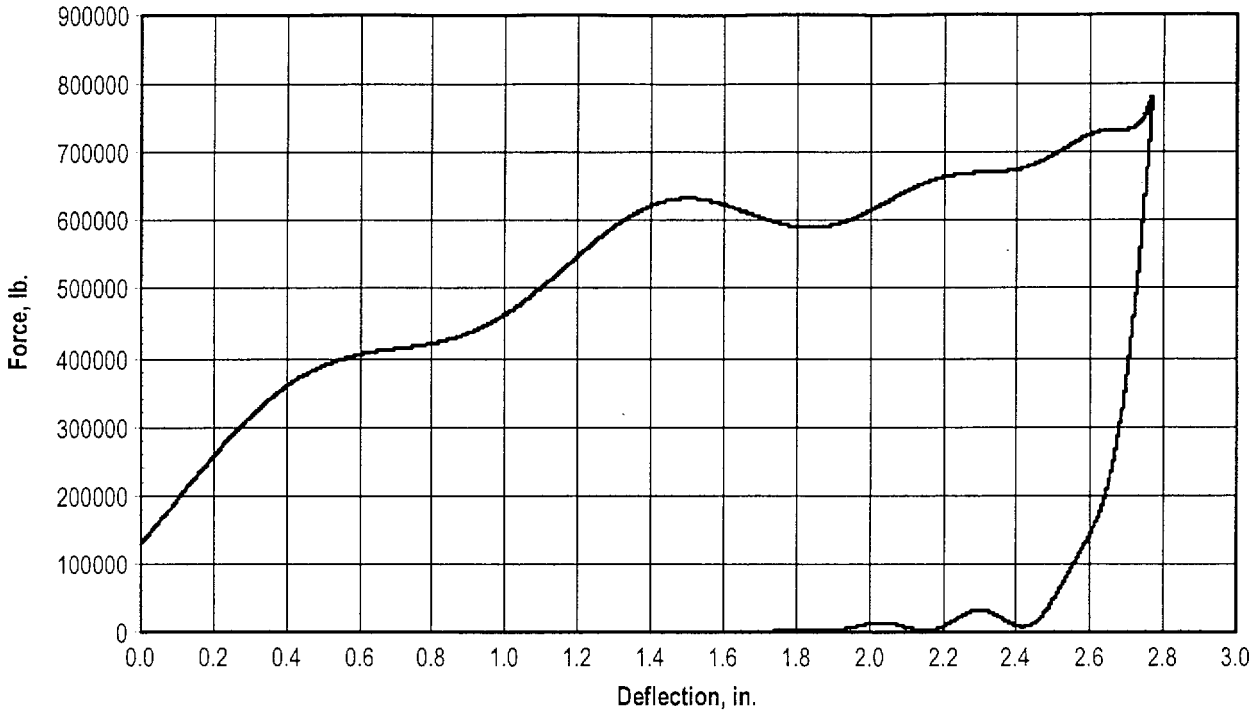

Figure 2.10.3-11 LS-DYNA Quarter-Scale Model

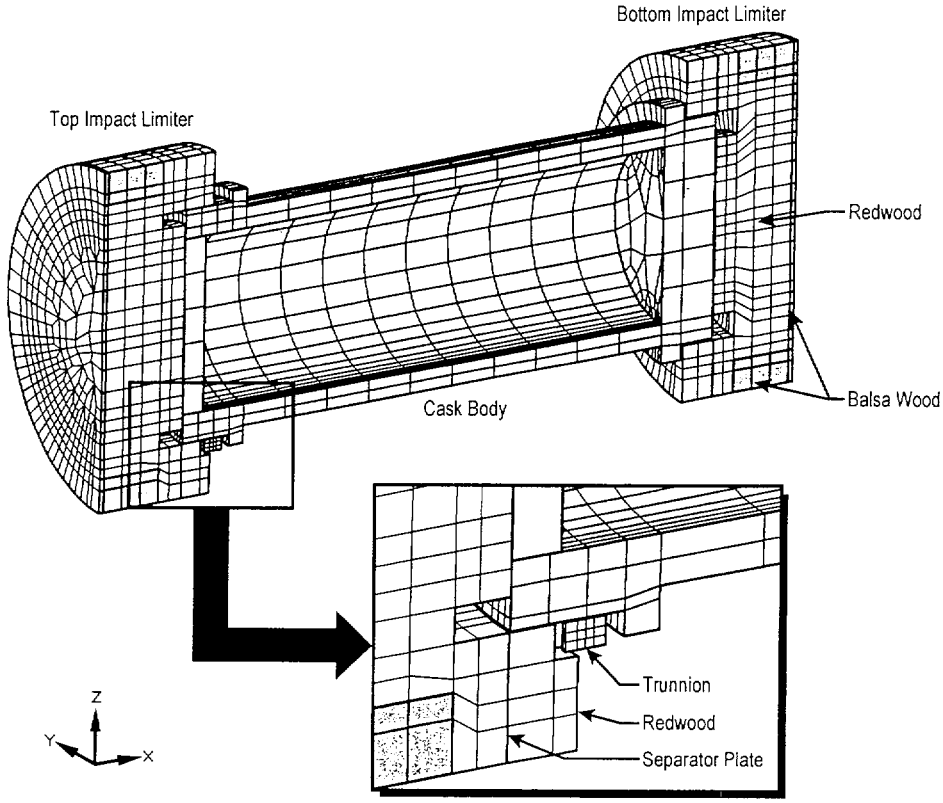

Figure 2.10.3-12 Comparison of Quarter-Scale Top End Drop (LS-DYNA and Drop Test) Results

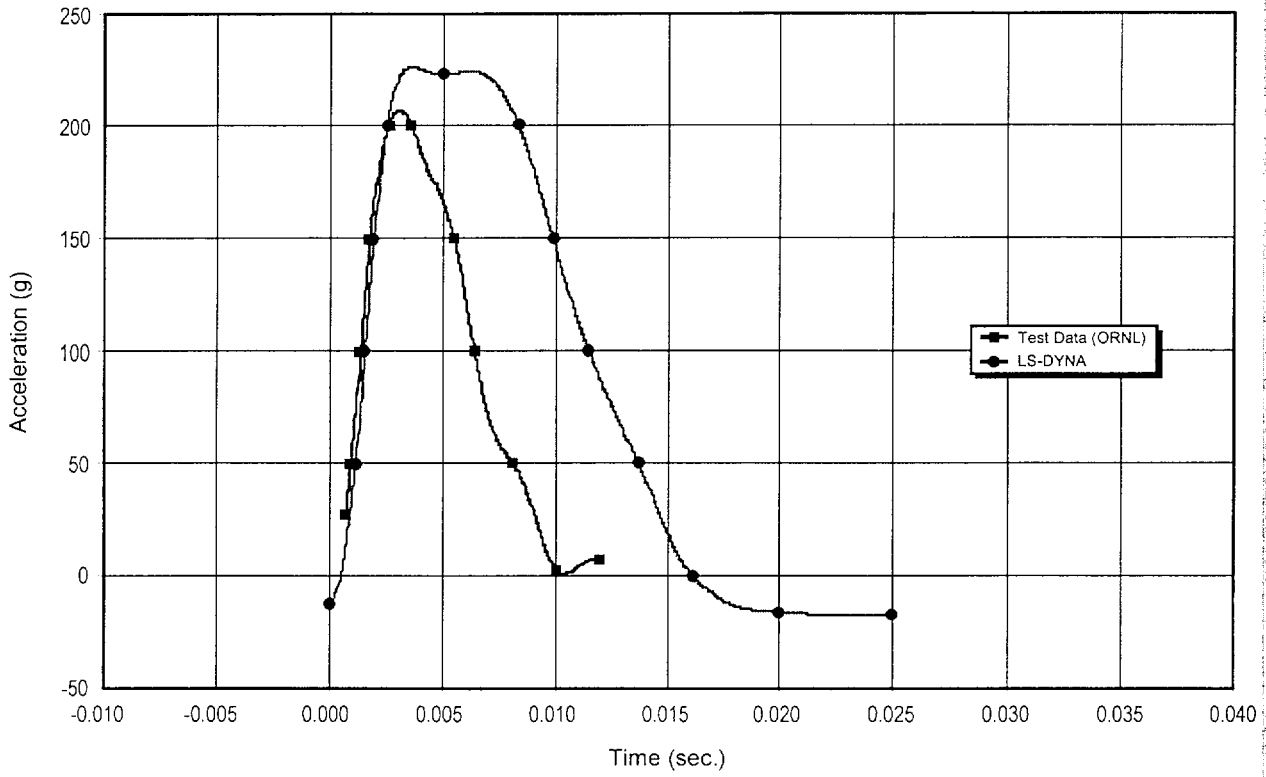

Figure 2.10.3-13 Comparison of Quarter-Scale Top Corner Drop (LS-DYNA and Drop Test) Results

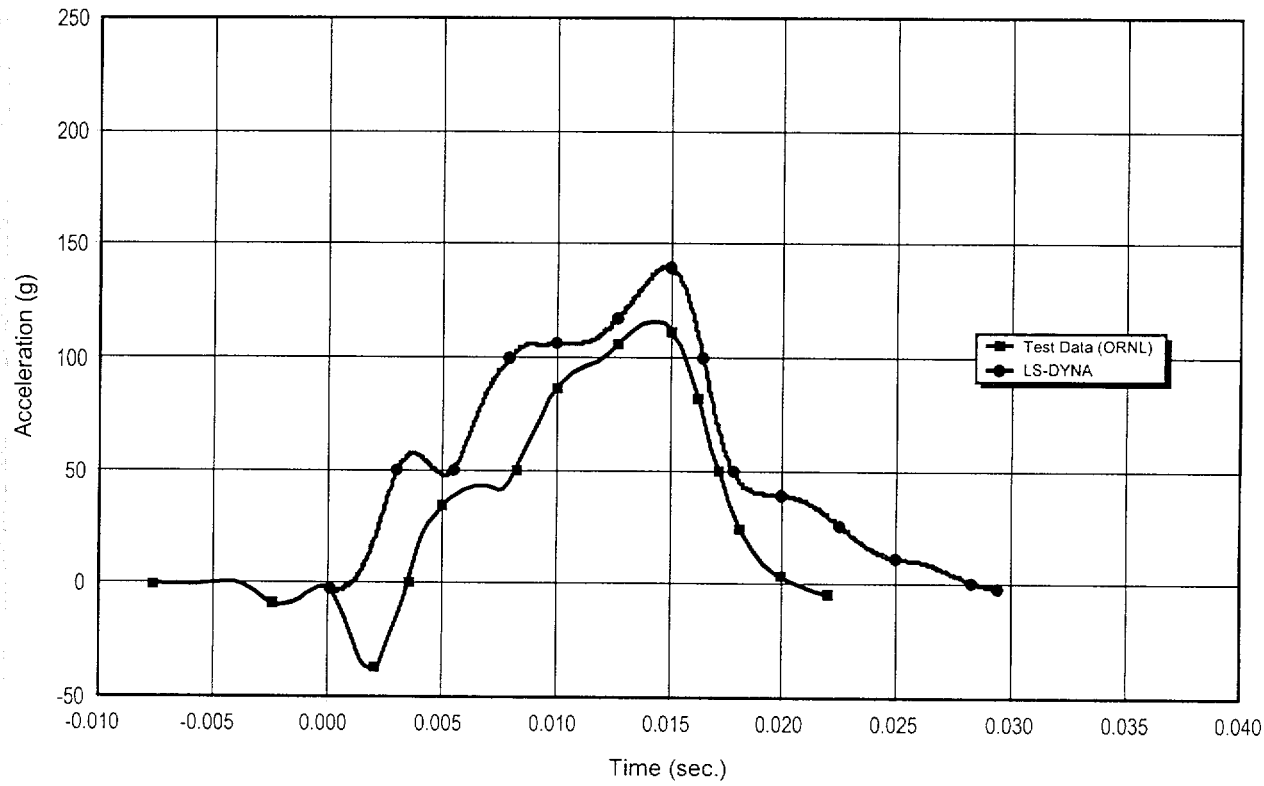

Figure 2.10.3-14 Comparison of Quarter-Scale Test Model and LS-DYNA Deformation During the Side Drop

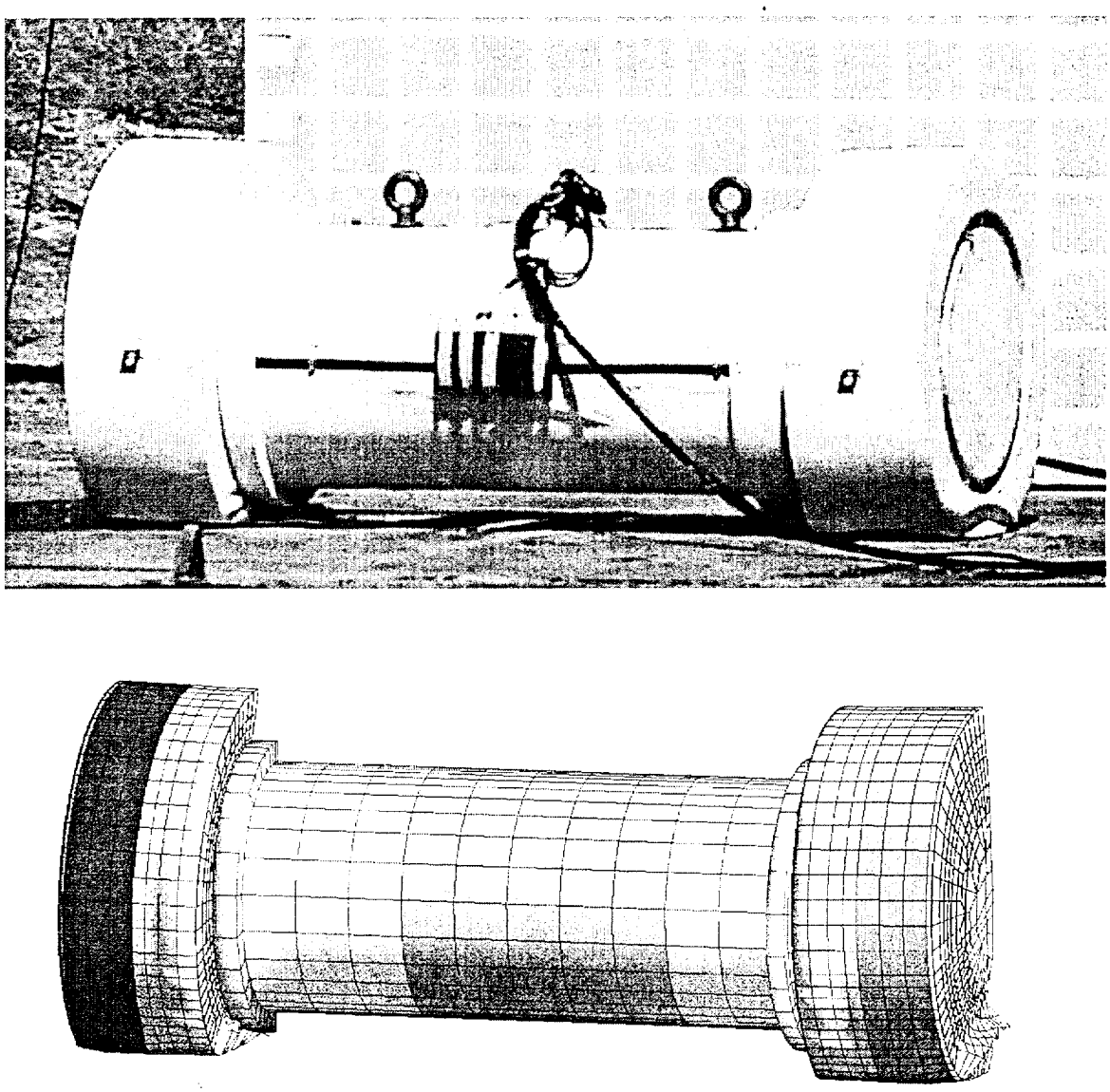

THIS PAGE INTENTIONALLY LEFT BLANK

2.11.1.1 Maine Yankee Site Specific Spent Fuel

The standard spent fuel assembly for the Maine Yankee site is the Combustion Engineering (CE) 14x14 fuel assembly. Fuel of the same design has also been supplied by Westinghouse and by Exxon. The standard 14x14 fuel assemblies are included in the population of the design basis PWR fuel assemblies for the UMS® Transport System (see Table 1.2.5). The structural evaluation for the UMS® transport system loaded with the standard Maine Yankee fuels is bounded by the structural evaluations in Sections 2.6 and 2.7 for the normal conditions of transport and hypothetical accident conditions, respectively. The Maine Yankee site specific fuel is described in Section 1.3.1.

The weight of a standard 14x14 fuel assembly with the control element assembly inserted is 1,360 lbs. This weight is bounded by the weight of the design basis PWR fuel assembly (37,608/24 = 1,567 lbs) used in the PWR support disk analysis presented in Section 2.6.13. The fuel configurations with removed fuel rods, with fuel rods replaced by solid stainless steel or Zircaloy rods, or with poison rods replaced by hollow Zircaloy rods, all weigh less than the standard 14x14 fuel assembly. The configuration with instrument thimbles installed in the center guide tube position weighs less than the standard assembly with the control element assembly installed. Consequently, this configuration is also bounded by the weight of the design basis fuel assembly. Since the weight of any of these fuel assembly configurations is bounded by the design basis fuel assembly weight, no additional analysis of these configurations is required.

A structural evaluation is required for the support disk for the configuration holding consolidated fuel. There are two consolidated fuel lattices, each constructed of 17x17 Zircaloy fuel grids and stainless steel end fittings which are connected by 4 stainless steel support rods. One of the consolidated fuel lattices has 283 fuel rods with 2 empty positions. The other has 172 fuel rods with the remaining positions either empty or holding stainless steel rods. The calculated weight for the heaviest of the two consolidated fuel lattices is 2,100 lbs.

A parametric study is performed to show that the PWR support disk holding a Maine Yankee consolidated fuel lattice is bounded by the UMS® PWR support disk stress evaluation presented in Section 2.6.13. Note that only one consolidated fuel lattice will be loaded in any single Transportable Storage Canister and that the loading position of the consolidated fuel assembly is restricted to a basket corner position (see Section 1.3.1.1).

However, Maine Yankee fuel cans holding other intact or damaged fuel can be loaded in the other three corner positions of the basket (Maine Yankee fuel cans may be loaded only in the four corner positions of the basket. See Figure 2.11.1.1-1 for corner positions). Therefore, the bounding case for Maine Yankee is the basket configuration with twenty (20) Maine Yankee fuel assemblies, three (3) fuel cans containing spent fuel, and one (1) fuel can containing consolidated fuel.

The two-dimensional ANSYS model used in the support disk evaluation (see Figure 2.6.13-2) in Section 2.6.13 is employed for the parametric study. The boundary condition of the model is modified by restraining the outer surface of the canister shell. The load from a PWR fuel assembly is modeled as a pressure load at the inner surface of each support disk slot opening. The design basis fuel pressure loading is 12.26 psi (see Section 2.6.13.2). Based on the same design parameters (slot size = 9.272 in., disk thickness = 0.5 inch, and the number of disks = 30), the pressure load corresponding to a Maine Yankee standard CE 14x14 fuel assembly is 10.3 psi. The pressure load is 11.3 psi for a Maine Yankee fuel can holding an intact or damaged fuel assembly. For a Maine Yankee fuel can holding consolidated fuel, the pressure load is 17.0 psi.

This study considers both the 1-foot (20g) and the 30-foot (60g) side drop conditions for four different drop orientations: 0°, 18.22°, 26.28°, and 45°, as shown in Figure 2.11.1.1-1. A total of five cases are considered in the study. Inertial loads are applied to the support disk in all cases. The base case considers that all 24 fuel positions hold design basis PWR fuel assemblies. The other four cases (Cases 1 through 4) represent four possible load combinations for the placement of four Maine Yankee fuel cans in the corner positions, one of which holds consolidated fuel. The remaining twenty (20) basket positions hold Maine Yankee standard 14×14 fuel assemblies. The basket loading positions are shown in Figure 2.11.1.1-1. The load combinations evaluated in the four Maine Yankee fuel can loading cases are:

Case	Basket Position 1	Basket Position 2	Basket Position 3	Basket Position 4
1	Consolidated	Damaged	Damaged	Damaged
2	Damaged	Consolidated	Damaged	Damaged
3	Damaged	Damaged	Damaged	Consolidated
4	Damaged	Damaged	Consolidated	Damaged

Table 2.11.1.1-1 provides a parametric comparison between the Base Case and the 4 cases evaluated, based on the maximum sectional stresses in the support disk. As shown in the table, the maximum stress in the UMS® basket support disk loaded with 20 standard fuel assemblies and four Maine Yankee fuel cans, including one holding consolidated fuel, is bounded by that for the support disk loaded with the design basis PWR fuel.

Additionally, a support disk analysis is performed for the Maine Yankee fuel configuration (20 standard fuel assemblies, three fuel cans containing spent fuel and one fuel can containing the consolidated fuel assembly), using the two-dimensional PWR support disk model for the governing case (45° basket orientation and thermal condition B) for the side drop condition (Section 2.6.13.6). The loading condition corresponds to Case 1 of the parametric study previously discussed. The analysis results of the P_m and $P_m + P_b$ stresses are summarized in Tables 2.11.1.1-2 and 2.11.1.1-3, respectively. The minimum margins of safety for the P_m and $P_m + P_b$ stresses are + 0.82 and + 0.24, respectively. The minimum margin of safety for the corresponding analysis for the support disk for the UMS® System design basis PWR configuration is +0.79 and +0.19 for P_m and $P_m + P_b$ stresses, respectively (see Tables 2.6.13.6-16 and 2.6.13.6-17). This comparison further substantiates the conclusion of the parametric study based on the normalized stress ratios using a two-dimensional model (Table 2.11.1.1-1).

Since no credit is taken for the structural integrity of the consolidated fuel or damaged fuel inside the fuel can, it is assumed that 100% of the fuel rods fail during an accident. For a Maine Yankee standard 14x14 fuel assembly, the volume of 176 fuel rods (100%) and 5 guide tubes will fill up 103.6 inches of the fuel can (span over 21 support disks) assuming a 50% volume compaction factor. For the consolidated fuel, the volume of 283 rods (100%) and 4 connector rods will fill up 109.6 inches of the fuel can (span over 22 support disks) assuming a 75% compaction factor. The compaction factor of 75% for the consolidated fuel considers that the number of rods in the consolidated fuel is approximately 1.5 times the number of rods in the standard Maine Yankee fuel and these rods are initially more closely spaced.

The corresponding pressure load on the support disk ligament is 15.3 psi for the 100% failed Maine Yankee damaged fuel and 22.5 psi for the consolidated fuel. Since the fuel cans holding damaged fuel and consolidated fuel are limited to the corner locations of the basket, the total load per support disk for this Maine Yankee configuration remains bounded by the total load per support disk for the UMS® System design basis configuration. To demonstrate that there is no

adverse impact on the maximum stress of the support disk, the PWR support disk analysis (Section 2.6.13.6) is reperformed for the Maine Yankee configuration (20 standard fuel assemblies, three fuel cans containing 100% failed fuel and one fuel can containing the 100% failed consolidated fuel) for the governing case of the side drop condition (45° basket drop orientation and thermal condition B). The analysis results indicate the minimum margins of safety for the P_m and $P_m + P_b$ stresses are +0.80 and +0.23, respectively. The minimum margin of safety for the corresponding analysis for the support disk for the UMS® System design basis PWR configuration is +0.79 and +0.19 for the P_m and $P_m + P_b$ stresses, respectively (Tables 2.6.13.6-16 and 2.6.13.6-17). Therefore, the maximum stress in the support disk for the Maine Yankee configuration, assuming 100% rod failure of the damaged and consolidated fuel in the fuel cans, is bounded by the maximum stress in the support disk calculated for the UMS® design basis fuel.

2.11.1.1.1 Maine Yankee Fuel Can

The Maine Yankee fuel can, shown in Drawings 412-501 and 412-502, is provided to accommodate Maine Yankee damaged fuel. The fuel can fits within a standard PWR basket fuel tube. The primary function of the Maine Yankee fuel can is to confine the fuel material within the can to minimize the potential for dispersal of the fuel material into the canister cavity volume.

The Maine Yankee fuel can is designed to hold an intact fuel assembly, a damaged fuel assembly, a fuel assembly with a burnup between 45,000 and 50,000 MWD/MTU and having a cladding oxidation layer thickness greater than 80 microns, or consolidated fuel in the Maine Yankee fuel inventory.

The fuel can is a square cross-section tube made of Type 304 stainless steel with a total length of 162.8 inches. The can walls are 0.048-inch thick sheet (18 gauge). The minimum internal width of the can is 8.52 inches. The bottom of the can is a 0.63-inch thick plate. Four holes in the plates, screened with a Type 304 stainless steel wire screen (250 openings/inch x 250 openings/inch mesh), permit water to be drained from the can during loading operations. Since the bottom surface of the fuel can rests on the canister bottom plate, additional slots are machined in the fuel can (extending from the holes to the side of the bottom assembly) to allow the water to be drained from the can. At the top of the can, the wall thickness is increased to 0.15 inch to permit the can to be handled. Slots in the top assembly side plates allow the use of a

handling tool to lift the can and contents. To confine the contents within the can, the top assembly consists of a 0.88-inch thick plate with screened drain holes identical to those in the bottom plate. Once the can is loaded, the can and contents are inserted into the basket, where the can may be supported by the sides of the fuel assembly tube, which are backed by the structural support disks. Alternately, the empty fuel can may be placed in the basket prior to having the designated contents inserted in the fuel can.

Structural evaluation of the Maine Yankee fuel can is shown below. The end drop and side drop conditions (both normal and accident conditions of transport) are considered in the evaluation.

End Drop Conditions

For the bottom end drop, the top assembly (lid), the side plates, and the tube body act against the bottom assembly. For the top end drop, the bottom assembly, tube body, and side plates act against the top assembly. Because the top assembly is heavier, the bottom end drop is the governing case for tube body compression. The can contents bear against the bottom assembly through which the loads are transferred to the TSC bottom plate.

The Maine Yankee fuel can tube body is subjected to compressive stresses. Under normal operating conditions, the tube is evaluated for a 20g acceleration. This approach addresses the transport condition 1-foot drop and bounds the storage deadweight and handling condition, including a 10% dynamic load factor. The compressive load (P) on the tube is the combined weight of the lid, side plates, and tube body times 20:

$$P = (17.89 \text{ lb} + 6.57 \text{ lb} + 78.77 \text{ lb}) \times 20 = 2{,}064.6 \text{ lb; use } 3{,}000 \text{ lb for evaluation.}$$

The compressive stress (S_c) in the tube body is:

$$S_c = \frac{P}{A} = \frac{3{,}000 \text{ lb}}{1.714 \text{ in}^2} = 1{,}750 \text{ psi}$$

where:

$$A = 8.62^2 - 8.52^2 = 1.714 \text{ in}^2$$

The margin of safety (MS) is then:

$$MS = \frac{S_m}{S_c} - 1 = \frac{16{,}700 \text{ psi}}{1{,}750 \text{ psi}} - 1 = +8.5 \text{ for normal operating conditions at 600°F.}$$

Under accident conditions, the tube is evaluated for a 60g acceleration.

The compressive load (P) is:

$$P = (17.89 \text{ lb} + 6.57 \text{ lb} + 78.77 \text{ lb}) \times 60g = 6{,}193.8 \text{ lb; use } 8{,}500 \text{ lb for evaluation.}$$

The compressive stress (S_c) in the tube body is:

$$S_c = \frac{P}{A} = \frac{8{,}500 \text{ lb}}{1.714 \text{ in}^2} = 4{,}959 \text{ psi}$$

where the margin of safety (MS) is then:

$$MS = \frac{0.7S_u}{S_c} - 1 = \frac{0.7(63{,}300) \text{ psi}}{4{,}959 \text{ psi}} - 1 = +7.9 \text{ for accident conditions at 600°F.}$$

The tube is evaluated using the Euler formula to determine the critical buckling load (P_{cr}):

$$P_{cr} = \frac{\pi^2 EI}{L_e^2} = \frac{\pi^2 (25.2 \times 10^6)(20.98)}{2(157.8)} = 16.5 \times 10^6 \text{ lb}$$

where:

$E = 25.2 \times 10^6$ psi

$I = \frac{8.62^4 - 8.52^4}{12} = 20.98 \text{ in}^4$

$L_e = 2L$ (worst case condition)

L = tube body length (157.8 in)

Because the maximum compressive load (8,500 lb under the accident condition) is much less than the critical buckling load (16.5 x 10^6 lb), the tube has adequate resistance to buckling.

The lid is analyzed for compressive stresses in a top-end drop where compressive loads are transferred through the lid structure to the TSC shield lid. The compressive load (P) is the weight of the fuel assembly plus the weight of the lid (18.01 lb; use 30 lb for analysis) times the appropriate acceleration factor.

Case 1: The Maine Yankee fuel can contents is in an intact (although damaged) Maine Yankee fuel assembly, a CF-1 fuel rod storage insert, or a consolidated fuel assembly. The compressive load for Case 1 acts directly through the support ring and the lift tee, which are directly in line with the axis of the upper end fitting posts in the top-end drop configuration.

Case 2: The Maine Yankee fuel can contents is a fuel rod storage insert with a 3/4 – 10 threaded rod that transfers the compressive load to the center of the lid directly in line with the lift tee axis.

For Case 1, the contents weight is conservatively analyzed as the consolidated fuel weight (2,100 lb); Case 2 considers the heaviest standard Maine Yankee fuel assembly (1,300 lb).

Note: Because the lid thickness is greater than the free space between the top and the Maine Yankee fuel can and the bottom of the TSC shield lid, the lid cannot become disengaged from the can.

Case 1:
For normal operating conditions, the compressive stress (σ_c) is:

$$\sigma_c = \frac{P}{A} = \frac{2130\ (20)\ \text{lb}}{7.66\ \text{in}^2} = 5{,}561\ \text{psi} \qquad \text{(using 30 lb for lid weight)}$$

where A is the combined cross-sectional area of the support ring and the lift tee:

$$A = \frac{\pi}{4}\left(\left(6.63^2 - 6.07^2\right) + 1.625^2\right) = 7.66\ \text{in}^2$$

The margin of safety (MS) is:

$$MS = \frac{S_m}{\sigma_c} - 1 = \frac{16{,}700 \text{ psi}}{5{,}561 \text{ psi}} - 1 = +2.0 \text{ (normal operating condition)}$$

For accident conditions, the compressive stress (σ_c) is:

$$\sigma_c = \frac{P}{A} = \frac{2130(60)}{7.66} = 16{,}684 \text{ psi}$$

The margin of safety (MS) is:

$$MS = \frac{0.7S_u}{\sigma_c} - 1 = \frac{0.7(63{,}300 \text{ psi})}{16{,}684 \text{ psi}} - 1 = +1.66 \text{ (accident condition)}$$

Case 2:

For normal operating conditions, the compressive stress (σ_c) is:

$$\sigma_c = \frac{P}{A} = \frac{1330(20) \text{ lb}}{2.07 \text{ in}^2} = 12{,}850 \text{ psi}$$ (using 30 lb for lid weight)

where A is the cross-sectional area of the lift tee:

$$A = \frac{\pi}{4}(1.625)^2 = 2.07 \text{ in}^2$$

The margin of safety (MS) is:

$$MS = \frac{S_m}{\sigma_c} - 1 = \frac{16{,}700 \text{ psi}}{12{,}850 \text{ psi}} - 1 = +0.30 \text{ (normal operating condition)}$$

For accident conditions, the compressive stress (σ_c) is:

$$\sigma_c = \frac{P}{A} = \frac{1330(60)}{2.07} = 38{,}551 \text{ psi}$$

The margin of safety (MS) is:

$$MS = \frac{0.7S_u}{\sigma_c} - 1 = \frac{0.7(63{,}300 \text{ psi})}{38{,}551 \text{ psi}} - 1 = +0.15 \text{ (accident condition)}$$

Side Drop Conditions

The majority of the tube body is contained within the fuel tube in the basket assembly. Because both the tube body and the fuel tube have square cross-sections, they will be in full contact (for 153.0 inches longitudinally) during the side drop and no significant bending stress will be introduced into the tube body. The last 4.8 inches of the body tube and the 5.0-inch length of the side plates will be unsupported past the fuel tube flange in the side drop configuration.

The tube body will be evaluated as a cantilevered beam with the combined weight (P) of the overhanging tube body, top assembly, and side plates multiplied by the appropriate deceleration factor and, conservatively, concentrated at the top end of the side plates.

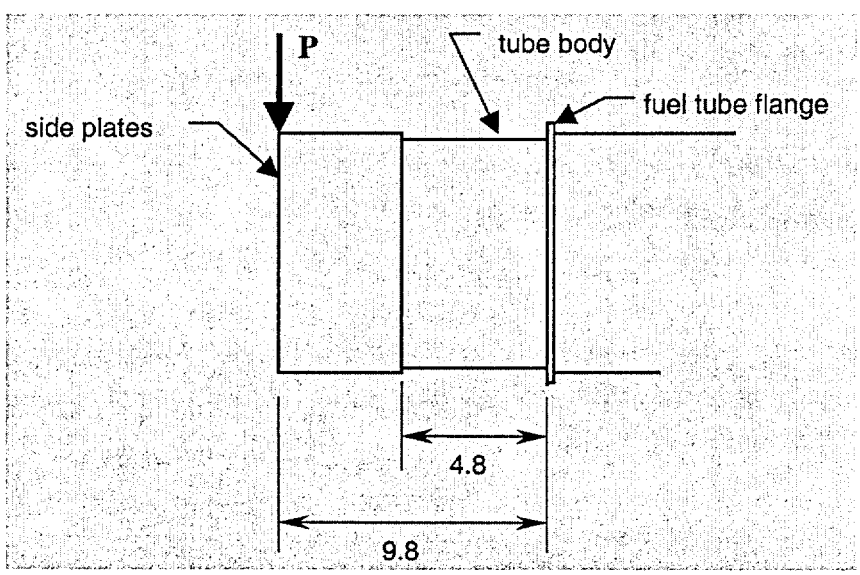

Normal condition (one-foot drop):

The maximum bending stress (f_b) is determined as follows:

$$f_b = \frac{M_{max}c}{I} = \frac{6{,}860(4.31)}{20.98} \cong 1{,}410 \text{ psi}$$

where:

M_{max} = Pg×L = 35(20)(9.8) = 6,860 lb·in.

P = 35 lb; (side plates, 6.57 lb + tube body (0.5 lb/in. × 4.8 in. = 2.4) + top assembly, 17.89 lb, equals 26.86 lb; use 35 lb for this analysis.)

g = 20 (normal condition)

L = 9.8 in. (the total overhung length of the tube body and end plates)

c = 8.62/2 = 4.31 in.

$$I = \frac{bh^3 - b_i h_i^3}{12} = \frac{8.62^4 - 8.52^4}{12} = 20.98 \text{ in}^4$$

The shear stress (τ) is:

$$\tau = \frac{Pg}{A} = \frac{35(20)}{1.714} \cong 409 \text{ psi}$$

where:

$A = 8.62^2 - 8.52^2 = 1.714 \text{ in}^2$

$$\sigma_1, \sigma_2 = \frac{1}{2}\left(f_b \pm \sqrt{f_b^2 + 4\tau^2}\right) = \frac{1}{2}\left(1{,}410 \pm \sqrt{1{,}410^2 + 4(409)^2}\right) = 1{,}520 \text{ psi and } -110 \text{ psi}$$

The stress intensity (σ_{max}) = $|\sigma_1 - \sigma_2|$ = 1,630 psi

The margin of safety (MS) is:

$$MS = \frac{1.5S_m}{\sigma_{max}} - 1 = \frac{1.5(16{,}700)\ \text{psi}}{1{,}630\ \text{psi}} - 1 = +14 \text{ for the normal condition (20g acceleration)}$$

Accident condition (30-foot drop):

The maximum bending stress (f_b) is determined as follows:

$$f_b = \frac{M_{max}c}{I} = \frac{20{,}580(4.31)}{20.98} = 4{,}228\ \text{psi}$$

where:

M_{max} = $Pg \times L = 35(60)(9.8) = 20{,}580$ lb·in.

g = 60 (accident condition)

The shear stress (τ) is:

$$\tau = \frac{Pg}{A} = \frac{35(60)}{1.714} = 1{,}225\ \text{psi}$$

$$\sigma_1, \sigma_2 = \frac{1}{2}\left(f_b \pm \sqrt{f_b^2 + 4\tau^2}\right) = \frac{1}{2}\left(4{,}228 \pm \sqrt{4{,}228^2 + 4(1{,}225)^2}\right) = 4{,}558\ \text{psi and } -330\ \text{psi}$$

The stress intensity (σ_{max}) = $|\sigma_1 - \sigma_2|$ = 4,888 psi

The margin of safety (MS) is:

$$MS = \frac{1.0\ S_u}{\sigma_{max}} - 1 = \frac{1.0(63{,}300)}{4{,}888} - 1 = +12 \text{ for the accident condition (60g acceleration)}$$

Side Drop – Consolidated Fuel

The fuel can is evaluated using the same method as in the previous section with the additional uniformly distributed weight (w) of the consolidated fuel.

Normal condition (1-foot drop):

The maximum bending stress (f_b) is determined as follows:

$$f_b = \frac{M_{max}c}{I} = \frac{17{,}409(4.31)}{20.98} \cong 3{,}577 \text{ psi}$$

where:

$$M_{max} = \left(PL + \frac{w(L-2.38)^2}{2}\right)(20g) = \left(35(9.8) + \frac{19.16(9.8-2.38)^2}{2}\right)(20g)$$

$= 17{,}409 \text{ lb} \cdot \text{in}$

2.38 in. = the distance from the top of the side plate to the bottom of the lid assembly

$$w = \frac{2{,}100 \text{ lb}}{109.6 \text{ in}} = 19.16 \text{ lb/in.}$$

2,100 lb = the consolidated fuel weight

P = 35 lb; (side plates, 6.57 lb + tube body (0.5 lb/in. × 4.8 in. = 2.4) + top assembly, 17.89 lb = 26.86 lb; use 35 lb for this analysis.)

The shear stress (τ) is:

$$\tau = \frac{(P + w(L - 2.38))g}{A} = \frac{(35 + 19.16(9.8 - 2.38))20}{1.714} \cong 2{,}068 \text{ psi}$$

$$\sigma_1, \sigma_2 = \frac{1}{2}\left(f_b \pm \sqrt{f_b^2 + 4\tau^2}\right) = \frac{1}{2}\left(3{,}577 \pm \sqrt{3{,}577^2 + 4(2{,}068)^2}\right) = 4{,}523 \text{ psi and } -946 \text{ psi}$$

The stress intensity (σ_{max}) = $|\sigma_1 - \sigma_2|$ = 5,469 psi

The margin of safety (MS) is:

$$MS = \frac{1.5S_m}{\sigma_{max}} - 1 = \frac{1.5(16{,}700) \text{ psi}}{5{,}469 \text{ psi}} - 1 = +3.58 \text{ for the normal condition (20g acceleration)}$$

Accident condition (30-foot drop):

The maximum bending stress (f_b) is determined as follows:

$$f_b = \frac{M_{max}c}{I} = \frac{52{,}226(4.31)}{20.98} = 10{,}729 \text{ psi}$$

where:

$$M_{max} = \left(PL + \frac{w(L - 2.38)^2}{2}\right)(60g) = \left(35(9.8) + \frac{19.16(9.8 - 2.38)^2}{2}\right)(60g) = 52{,}226 \text{ lb} \cdot \text{in}$$

The shear stress (τ) is:

$$\tau = \frac{(P + w(L - 2.38))g}{A} = \frac{(35 + 19.16(9.8 - 2.38))60}{1.714} \cong 6{,}202 \text{ psi}$$

g = 60 (accident condition)

$$\sigma_1, \sigma_2 = \frac{1}{2}\left(f_b \pm \sqrt{f_b^2 + 4\tau^2}\right) = \frac{1}{2}\left(10{,}729 \pm \sqrt{10{,}729^2 + 4(6{,}202)^2}\right) = 13{,}565 \text{ psi and } -2{,}836 \text{ psi}$$

The stress intensity (σ_{max}) = $|\sigma_1 - \sigma_2|$ = 16,401 psi

The margin of safety (MS) is:

$$MS = \frac{1.0\ S_u}{\sigma_{max}} - 1 = \frac{1.0(63{,}300)}{16{,}401} - 1 = +2.86 \text{ for the accident condition (60g acceleration)}$$

The welds joining the tube body to the side plates are full penetration welds (Type III NG-3352.3). Per Table NG-3352-1, the weld quality factor (n) for a Type III weld with visual surface inspection is 0.5.

The margin of safety (MS) for the welds is:

$$MS = \frac{n \cdot 1.5 \cdot S_m}{\sigma_{max}} - 1 = \frac{0.5(1.5)(16{,}700 \text{ psi})}{5{,}469 \text{ psi}} - 1 = +1.29 \text{ (normal condition)}$$

$$MS = \frac{n \cdot 1.0 \cdot S_u}{\sigma_{max}} - 1 = \frac{0.5(1.0)(63{,}300 \text{ psi})}{16{,}401 \text{ psi}} - 1 = +0.93 \text{ (accident condition)}$$

<u>100% Failed Fuel Analysis</u>

Normal Conditions:

Accident Conditions:

The Maine Yankee fuel can may hold 100% failed/damaged fuel or consolidated fuel. An evaluation is performed to demonstrate that the fuel can maintains its integrity during a tip-over accident for this condition.

The fuel can is designed to hold either Maine Yankee standard fuel assemblies (1300 lb) or consolidated fuel assemblies (2100 lb). For 100% failed fuel, the pressure load applied to the fuel can is:

standard fuel: $$P_S = \frac{1300}{8.52 \times 103.6} = 1.47 \text{ psi}$$

consolidated fuel: $$P_C = \frac{2100}{8.52 \times 109.6} = 2.25 \text{ psi}$$

where:

1300 lbs	= Maine Yankee standard fuel weight
2100 lbs	= maximum consolidated fuel weight
8.52 in	= inside width of fuel can
103.6 in	= height occupied by 100% failed standard fuel
109.6 in	= height occupied by 100% failed consolidated fuel

Therefore, the bounding pressure load on the fuel can is the consolidated fuel, 2.25 psi, multiplied by 60g (135 psi).

An ANSYS model of the Maine Yankee fuel can (8.57 in × 8.57 in) is constructed to evaluate the fuel can for a 60g loading. Note that 8.57 inches is the dimension of the fuel can based on the centerlines of its side walls.

It should be noted that the fuel tube, the BORAL plate and its cover are not included in the model. Therefore, the fuel can analysis is conservative.

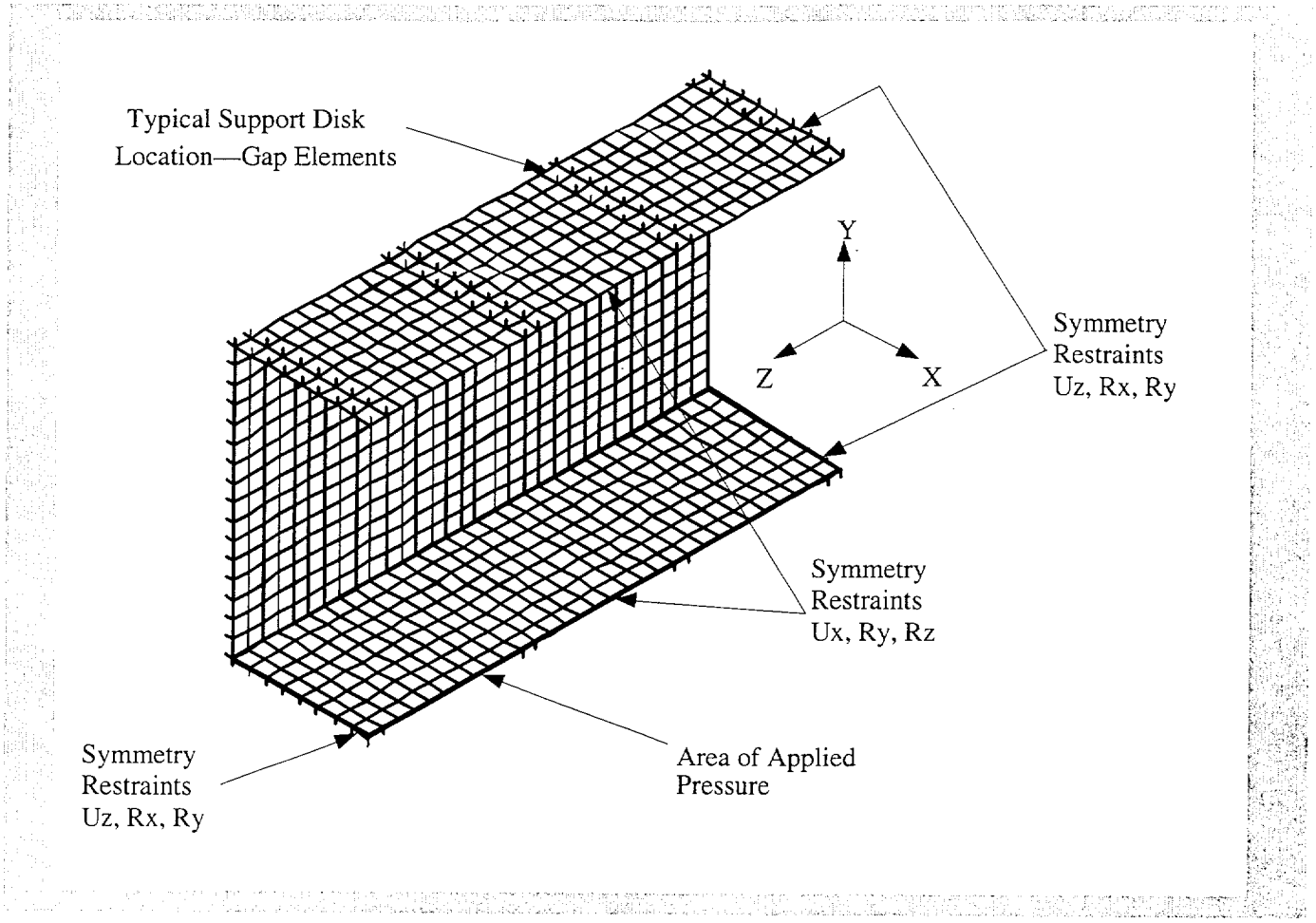

The finite element analysis results show that the maximum stress in the fuel can is 25.4 ksi, which is local to the sections of the tube resting on the support disks. At 750°F, the ultimate strength for Type 304 stainless steel is 63.1 ksi. The margin of safety is:

$$MS = \frac{63.1}{25.4} - 1 = +1.48$$

The analysis shows that the maximum total strain is 0.050 inch/inch (see Figure A-1). Defining the acceptable elastic-plastic response of the stainless steel as one-half of the material failure strain of 0.40 inch/inch at 750°F, the resulting margin of safety is:

$$MS = \frac{0.40/2}{0.05} - 1 = +3.0$$

Similarly, the margin of safety for elastic-plastic stress becomes:

$$MS = \frac{63.1 - 17.3}{25.4 - 17.3} - 1 = +4.65$$

where the yield strength of Type 304 stainless steel is 17.3 ksi at 750°F.

Figure 2.11.1.1-1 PWR Basket Drop Orientations and Case Study Loading Positions for Maine Yankee Consolidated Fuel

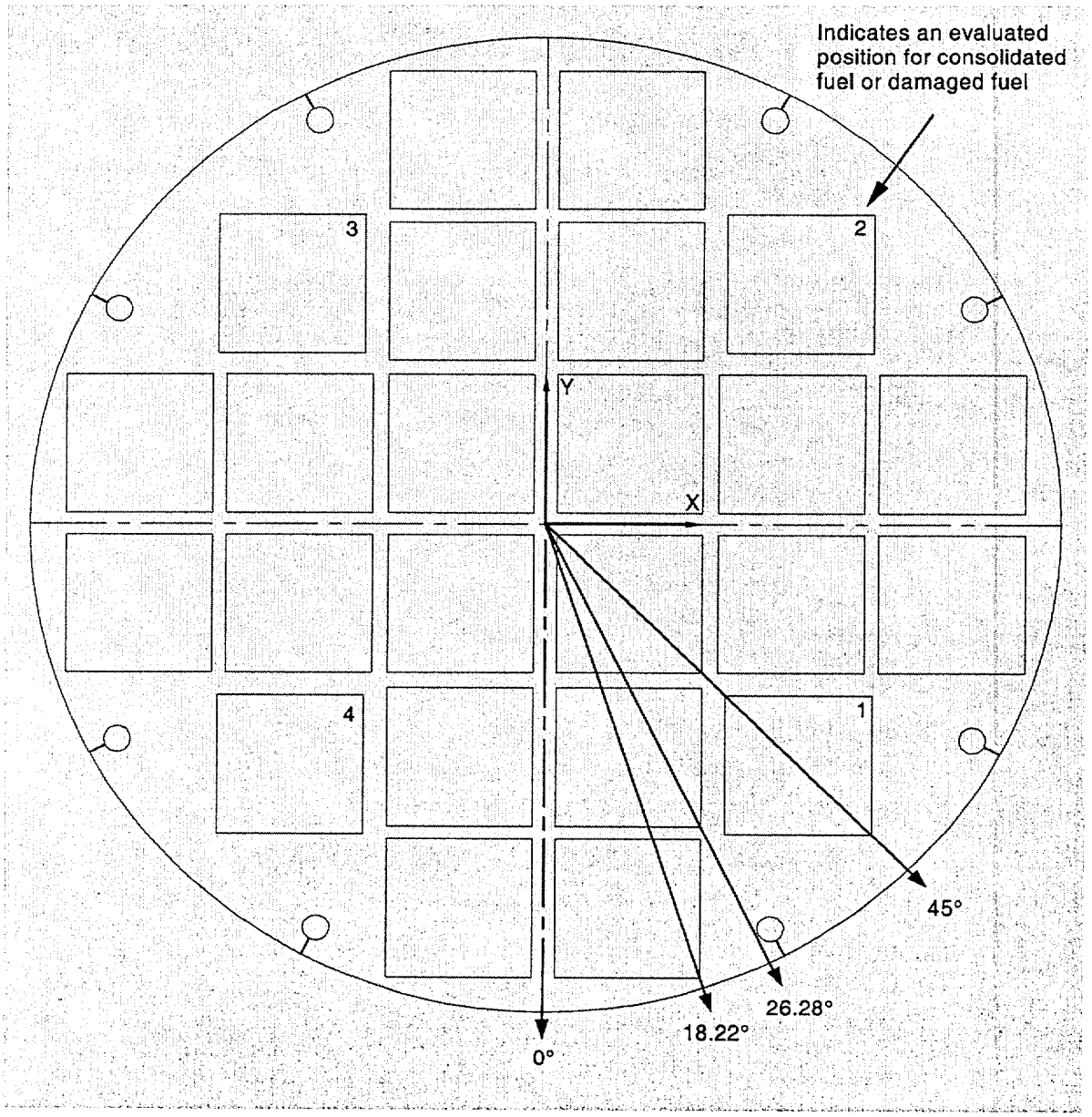

Table 2.11.1.1-1 Normalized Stress Ratios - UMS® PWR Basket Support Disk Sectional Stresses Due to Maine Yankee Consolidated Fuel to the Design Basis PWR Fuel Basket Maximum Stresses (Base Case)

Case	Support Disk Sectional Stress Intensity (ksi) – Membrane							
	Normal Conditions, 20g				Accident Conditions, 60g			
	0°	18.22°	26.28°	45°	0°	18.22°	26.28°	45°
Base Case[1]	1.00	1.00	1.00	1.00	1.00	1.00	1.00	1.00
Case 1	0.96	0.91	0.96	0.96	0.91	0.94	0.94	0.94
Case 2	0.95	0.92	0.96	0.96	0.91	0.94	0.94	0.95
Case 3	0.96	0.93	0.97	0.96	0.91	0.95	0.95	0.95
Case 4	0.95	0.93	0.97	0.96	0.91	0.95	0.95	0.96
Case	**Support Disk Sectional Stress Intensity (ksi) – Membrane + Bending**							
	Normal Conditions, 20g				**Accident Conditions, 60g**			
	0°	**18.22°**	**26.28°**	**45°**	**0°**	**18.22°**	**26.28°**	**45°**
Base Case[1]	1.00	1.00	1.00	1.00	1.00	1.00	1.00	1.00
Case 1	0.96	0.92	0.96	0.95	0.96	0.94	0.94	0.94
Case 2	0.96	0.92	0.96	0.96	0.95	0.95	0.95	0.95
Case 3	0.96	0.93	0.96	0.95	0.96	0.95	0.95	0.95
Case 4	0.96	0.93	0.97	0.97	0.96	0.98	0.98	0.97

1. Tables 2.6.13.6-16 and 2.6.13.6-17.

Table 2.11.1.1-2 P_m Stresses for Support Disk—1-Foot Side Drop, 45° Orientation, Thermal Case B, Structural Case 1

Section	Sx (ksi)	Sy (ksi)	Sxy (ksi)	Stress Intensity (ksi)	Allowable Stress (ksi)	Margin of Safety
120	9.7	-9.8	7.6	24.8	45	0.82
114	-9.9	9.7	7.6	24.8	45	0.82
35	13.9	-1.5	6.4	20	45	1.25
23	-1.4	14.1	6.3	20	45	1.25
21	-7.6	-15.9	6.6	19.5	45	1.31
37	15.8	-7.8	6.6	19.5	45	1.31
112	7.1	-5.9	6.1	17.8	45	1.52
111	-5.8	7.1	6.1	17.7	45	1.54
63	1.6	-9.8	5.5	15.9	45	1.83
96	-9.5	1.6	5.6	15.7	45	1.86
9	-0.5	-11.2	5.6	15.5	45	1.91
49	11	-0.5	5.6	15.4	45	1.92
28	-9	2.8	4.3	14.7	45	2.07
40	2.8	-8.9	4.4	14.6	45	2.07
7	3	11.6	5.5	14.3	45	2.15
104	-7	0.2	6.1	14.2	45	2.17
51	11.3	3	5.5	14.1	45	2.19
66	0.2	-7.1	6	14.1	45	2.2
72	10.6	-9.6	3.8	14	45	2.23
98	-9.7	-10.7	3.7	13.9	45	2.23
95	-3.2	-11.6	4.1	13.3	45	2.4
42	-6.3	-10.2	4.6	13.2	45	2.4
26	10.3	-6.2	4.5	13.2	45	2.4
110	13.2	-0.1	-0.5	13.2	45	2.41
64	11.3	-3.3	4.2	13.1	45	2.43
119	-0.1	-13.1	-0.5	13.1	45	2.43
94	12.1	-0.1	-0.3	12.2	45	2.7
71	-0.1	-12	-0.3	12	45	2.74
79	1	8.9	3.7	10.8	45	3.17
80	8.6	1	3.7	10.7	45	3.2
124	3.6	-6.5	1.3	10.4	45	3.34
108	-4.1	5	2.2	10.1	45	3.44
22	-2.5	-0.8	-4.9	10	45	3.5
36	-0.8	-2.6	-4.9	9.9	45	3.53
74	-0.2	-9	2.1	9.8	45	3.6
99	-9	-0.2	2.1	9.8	45	3.61
115	0.5	-4.6	3.9	9.3	45	3.82
122	-4.5	0.5	3.9	9.3	45	3.85
116	-0.1	-9.1	0	9.1	45	3.96
92	2.2	-6.8	0.2	9	45	4.02

Table 2.11.1.1-3 $P_m + P_b$ Stresses for Support Disk—1-Foot Side Drop, 45° Orientation, Thermal Case B, Structural Case 1

Section	Sx (ksi)	Sy (ksi)	Sxy (ksi)	Stress Intensity (ksi)	Allowable Stress (ksi)	Margin of Safety
37	-38.5	-45.1	12	54.2	67.5	0.24
21	-44.9	-38.5	12	54.1	67.5	0.25
23	33.4	36.6	10.2	45.3	67.5	0.49
35	36.5	33.4	10.1	45.2	67.5	0.49
34	-40.7	-41.2	3.2	44.2	67.5	0.53
20	-41	-40.8	3.2	44.1	67.5	0.53
4	37.9	41.6	3	43.3	67.5	0.56
1	41.6	37.9	3	43.3	67.5	0.56
112	-18.1	-42	3.7	42.5	67.5	0.59
111	-41.6	-18	3.6	42.2	67.5	0.6
51	30.9	34.8	9	42.1	67.5	0.6
7	34.6	31.1	9.1	42	67.5	0.61
2	-37.8	-37.2	2.6	40.1	67.5	0.68
3	-37.2	-37.8	2.6	40.1	67.5	0.68
49	-30.8	-31	8.6	39.6	67.5	0.71
9	-30.9	-30.9	8.7	39.5	67.5	0.71
64	-31	-30.4	8.2	38.9	67.5	0.73
95	-30.1	-31.2	8.2	38.8	67.5	0.74
63	-30.2	-30.7	8.3	38.8	67.5	0.74
96	-30.4	-30.5	8.3	38.8	67.5	0.74
120	0.2	-34.9	5.5	36.7	67.5	0.84
114	-34.8	0.2	5.4	36.6	67.5	0.84
42	-18.9	-33	7.6	36.3	67.5	0.86
26	-32.9	-18.7	7.5	36.1	67.5	0.87
6	32.1	33.1	1.6	34.3	67.5	0.97
48	32.9	32.3	1.6	34.2	67.5	0.98
36	-4	-32	-4.1	32.6	67.5	1.07
22	-31.7	-3.7	-4.2	32.4	67.5	1.09
80	25	25	6.5	31.5	67.5	1.14
79	24.7	25.2	6.5	31.5	67.5	1.14
72	-18	-25.2	8.8	31.1	67.5	1.17
98	-25	-17.9	8.7	30.8	67.5	1.19
40	-9.7	-29.6	4.8	30.7	67.5	1.2
28	-29.3	-9.5	4.7	30.4	67.5	1.22
108	7.8	28.1	6.3	29.9	67.5	1.26
75	13.4	19.9	-12.3	29.4	67.5	1.3
39	-18.8	-28	1.6	28.3	67.5	1.39
25	-27.9	-18.6	1.6	28.1	67.5	1.4
123	-14.5	-18.3	-11.1	27.6	67.5	1.44
115	-12.4	-27.6	-0.3	27.6	67.5	1.44

THIS PAGE INTENTIONALLY LEFT BLANK

21. ASME Boiler and Pressure Vessel Code, Section II, Part D, "Material Properties," 1995 Edition with 1995 Addenda.

22. MIL-HDBK-5F, "Metallic Materials and Elements for Aerospace Vehicle Structures," U.S. Department of Defense, November 1990.

23. Tietz, T.E., "Determination of the Mechanical Properties of High Purity Lead and a 0.05% Copper-Lead Alloy," Stanford Research Institute, Menlo Park, CA, WADC Technical Report 57-695, ASTIA Document Number 151165, April 1958.

24. NUREG/CR-0481, SAND77-1872, Rack, H.J., Knorovsky, G.A., "An Assessment of Stress-Strain Data Suitable for Finite-Element Elastic-Plastic Analysis of Shipping Containers," September 1978.

25. Baumeister, T., and Marks, L.S., Standard Handbook for Mechanical Engineers, 7th Edition, New York, McGraw-Hill Book Co., New York, N.Y., 1967.

26. NS-4-FR Fire Resistant Neutron and/or Gamma Shielding Material - Product Technical Data, Genden Engineering Services & Construction Company, Tokyo, Japan.

27. US NRC Bulletin 96-04, "Chemical, Galvanic, or Other Reactions in Spent Fuel Storage and Transportation Casks," July 1996.

28. Roark, R. J., and Young, W.C., Formulas for Stress and Strain, 6th Edition, New York, McGraw Hill, Inc., 1989.

29. Blake, A., "How to Find Deflection and Moment of Rings and Arcuate Beams," Product Engineering, January 1963.

30. Spotts, M. F., Design of Machine Elements, 2nd Edition, Prentice Hall, 1953.

31. Field Manual of the Interchange Rules as Adopted by the Association of American Railroads, Rule 88, "Mechanical Requirements for Acceptance," Washington, D.C., 1986.

32. ANSYS Revision 5.2, Computer Program, ANSYS, Inc., Houston, PA.

33. Hallquist, John 0., LS-DYNA, Version 950c, Livermore Software Technology Corporation, Livermore, CA., 1999.

34. NUREG/CR-0322, SAND 77-1589, Von Riesemann, W.A., and Guess, T.R., "The Effects of Temperature on the Energy-Absorbing Characteristics of Redwood," August 1978.

35. Technical Report 32-944, Knoell, A.C., "Environmental and Physical Effects on the Response of Balsa Wood as an Energy Dissipator," Jet Propulsion Laboratory, June 1966.

36. Technical Report 32-1295, The Wood Handbook, Jet Propulsion Laboratory.

37. NAC Services Inc., Safety Analysis Report for the NAC Storable Transport Cask (Docket Number 71-9235), Revision 8, Norcross, Georgia, August 1994.

38. Military Specification MIL-S-7998 "A Sandwich Construction Core Material, Balsa Wood," March 1970 with Amendment 1, February 1978.

39. Resnick, R., and Halliday, D, Physics, 3rd Edition, Part 1, New York, John Wiley & Sons, 1977.

40. NUREG/CR-0481, SAND77-1872, Rack, H.J., and Knorovsky, G.A, "An Assessment of Stress-Strain Data Suitable for Finite Element Elastic-Plastic Analysis of Shipping Containers," September 1978.

41. US NRC Regulatory Guide 7.9, "Standard Format and Content of Part 21 Applications for Approval of Packaging for Radioactive Material," May 1986.

42. "Guidelines for the Use of Aluminum with Food and Chemicals, 5th Edition, the Aluminum Association, Washington, D.C., April 1984.

43. UCID - 21246, "Dynamic Impact Effects on Spent Fuel Assemblies," Chun, R., Witte, M., and Schwartz, M., Lawrence Livermore Laboratory, October 1987.

44. ORNL/TM-1312, "Structural Analysis of Shipping Casks, Volume 8, Experimental Study of the Stress-Strain Properties of Lead Under Specified Impact Conditions," Evans, J.H., Volume 8, Oak Ridge National Laboratory, Oak Ridge, TN, August 1970.

45. Parker Seals "O-Ring Handbook," ORD-5700, 1992.

46. Oberg, Erik, et al, Machinery's Handbook, 25th Edition, First Printing, Industrial Press, Inc., New York, New York, 1984.

47. Clough, Ray W. and Joseph Penzien, "Dynamics of Structures," 2nd Edition, 1993.

48. Rust, James H., "Nuclear Power Plant Engineering," 1979.

49. ISG-4, Revision 1, "Cask Closure Weld Inspections," May 1999.

50. Blevins, R.D., *Formulas for Natural Frequency and Mode Shape*, Krieger Publishing Co., Malabar, Florida, 1995.

51. ARMCO Product Data Bulletin No. S-22, "17-4PH, Precipitation Hardening Stainless Steel," ARMCO, Inc., 1988.

52. ASTM B733-97, "Standard Specification for Autocatalytic (Electroless) Nickel-Phosphorus Coatings on Metal," Annual Book of ASTM Standards, Vol. 02.05, American Society for Testing and Materials, Conshohocken, PA, 1996.

53. American Society for Metals, "Metals Handbook," 1985.

54. Duncan, R.N., "Corrosion Resistance of High-Phosphorus Electroless Nickel Coatings," Plating and Surface Finishing, July 1986, pages 52-56.

55. Weaver, William Jr. and James M. Gere, "Matrix Analysis of Framed Structures," Second Edition, D. Van Nostrand Company, New York, 1980.

56. Marks' Standard Handbook for Mechanical Engineers, 9th Edition, McGraw-Hill Book Company, New York, New York.

57. NUREG-1617, "Standard Review Plan for Transportation Packages for Spent Nuclear Fuel," U.S. Nuclear Regulatory Commission, Washington, DC.

58. Sandia Report SAND90-2187 TTC-1012 UC-80, "An Analysis of Parameters Affecting Slapdown of Transportation Packages," Sandia National Laboratories, Albuquerque, NM, 1991.

59. US NRC Regulatory Guide 1.92, "Combining Modal Responses and Spatial Components in Seismic Response Analysis," Revision 1, February 1976.

THIS PAGE INTENTIONALLY LEFT BLANK

FIGURE WITHHELD UNDER 10 CFR 2.390

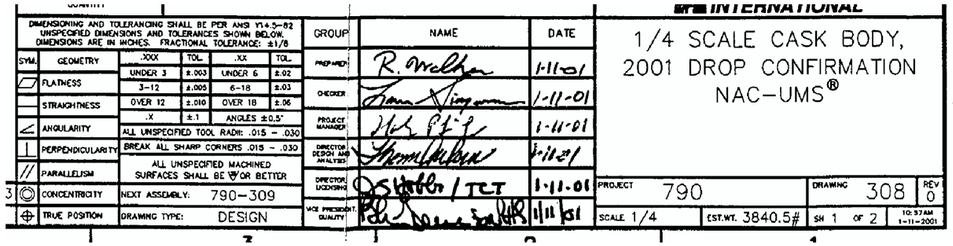

DIMENSIONING AND TOLERANCING SHALL BE PER ANSI Y14.5-82
UNSPECIFIED DIMENSIONS AND TOLERANCES SHOWN BELOW.
DIMENSIONS ARE IN INCHES. FRACTIONAL TOLERANCE: ±1/8

SYM.	GEOMETRY	.XXX	TOL.	.XX	TOL.
		UNDER 3	±.003	UNDER 6	±.02
	FLATNESS	3-12	±.005	6-18	±.03
	STRAIGHTNESS	OVER 12	±.010	OVER 18	±.06
		.X	±.1	ANGLES ±0.5°	
	ANGULARITY	ALL UNSPECIFIED TOOL RADII: .015 - .030			
	PERPENDICULARITY	BREAK ALL SHARP CORNERS .015 - .030			
	PARALLELISM	ALL UNSPECIFIED MACHINED SURFACES SHALL BE 63 OR BETTER			
3	CONCENTRICITY	NEXT ASSEMBLY: 790-309			
	TRUE POSITION	DRAWING TYPE: DESIGN			

GROUP	NAME	DATE
PREPARED	R. Walker	1-11-01
CHECKER	Tom Vingoe	1-11-01
PROJECT MANAGER	[illegible]	1-11-01
DIRECTOR DESIGN AND ANALYSIS	[illegible]	1-11-01
DIRECTOR LICENSING	[illegible] / TCT	1-11-01
VICE PRESIDENT QUALITY	[illegible]	1/11/01

INTERNATIONAL

1/4 SCALE CASK BODY,
2001 DROP CONFIRMATION
NAC-UMS®

PROJECT	790	DRAWING	308	REV 0
SCALE 1/4	EST.WT. 3840.5#	SH 1 OF 2	10:37AM 1-11-2001	

FIGURE WITHHELD UNDER 10 CFR 2.390

NAC INTERNATIONAL

1/4 SCALE CASK BODY,
2001 DROP CONFIRMATION
NAC-UMS®

PROJECT 790		DRAWING 308	REV 0
SCALE 1/4	EST.WT. 3840.5#	SH 2 OF 2	10:59AM 1-11-2001

FIGURE WITHHELD UNDER 10 CFR 2.390

DIMENSIONING AND TOLERANCING SHALL BE PER ANSI Y14.5-82
UNSPECIFIED DIMENSIONS AND TOLERANCES SHOWN BELOW.
DIMENSIONS ARE IN INCHES. FRACTIONAL TOLERANCE: ±1/8

SYM.	GEOMETRY	.XXX	TOL.	.XX	TOL.
	FLATNESS	UNDER 3	±.003	UNDER 6	±.02
		3–12	±.005	6–18	±.03
	STRAIGHTNESS	OVER 12	±.010	OVER 18	±.06
	ANGULARITY	.X	±.1	ANGLES ±0.5°	
		ALL UNSPECIFIED TOOL RADII: .015 – .030			
	PERPENDICULARITY	BREAK ALL SHARP CORNERS .015 – .030			
	PARALLELISM	ALL UNSPECIFIED MACHINED SURFACES SHALL BE ✓ OR BETTER			
	CONCENTRICITY	NEXT ASSEMBLY: N/A			
	TRUE POSITION	DRAWING TYPE: DESIGN			

GROUP	NAME	DATE
PREPARER	R. Walker	1-11-01
CHECKER	[illegible]	1-11-01
PROJECT MANAGER	[illegible]	1-11-01
DIRECTOR, DESIGN AND ANALYSIS	[illegible]	1-11-01
DIRECTOR, LICENSING	[illegible] JCT	1-11-01
VICE PRESIDENT, QUALITY	[illegible] FOR RMB	1/11/01

DROP TEST ASSEMBLY,
2001 DROP CONFIRMATION
NAC–UMS®

PROJECT	DRAWING	REV
790	309	0

SCALE 1/4 | EST.WT. NOTED | SH 1 OF 1 | 11:50AM 1-11-2001